VOL. 4 1963

POLYMER

The Chemistry, Physics and Technology of High Polymers

REPRINTED 1972 FOR
Wm. DAWSON & SONS Ltd., FOLKESTONE
WITH THE PERMISSION OF
IPC SCIENCE AND TECHNOLOGY PRESS, LTD.

Some Properties of Poly-2-vinyl Pyridine in Solution

A. J. HYDE and R. B. TAYLOR

Samples of 2-vinyl pyridine were polymerized using azo-bis-isobutyronitrile as initiator and the polymers formed fractionated to yield ten fractions. Light scattering and viscosity measurements were made on these in absolute ethanol and in a mixed solvent, the composition of which had been derived from precipitation measurements. The dependence of the various quantities derived from light scattering and viscosity measurements on molecular weight is shown. The values of ε *in the relationship* $\langle R^2 \rangle = KN^{1+\varepsilon}$ *are discussed and the 'hindered rotation' term* $(1+\cos\phi)/(1-\cos\phi)$ *in the expression for* $\langle R^2 \rangle$ *is evaluated.*

EXPERIMENTAL

INITIALLY, benzoyl peroxide was used to initiate the polymerization of 2-vinyl pyridine but since the reaction mixtures obtained were always dark coloured azo-bis-isobutyronitrile was used for all subsequent preparations. Varying amounts of initiator were used in order to obtain a range of molecular weights. One attempt was made to make a low molecular weight polymer by working with benzene as diluent.

The whole polymers formed were fractionated at 25°C by successive addition of hexane to the benzene solution of the polymers. Each polymer was separated into three fractions, each of which was freeze-dried from benzene solution. Viscosity measurements were carried out on all these fractions in ethanol solution and groups of fractions with similar limiting viscosity numbers (within 0·2) were combined forming ten lots in all. Each lot was then refractionated into three fractions of which the middle fraction was used in most of the subsequent experiments.

Viscosity measurements were made at 25°C using a Fitzsimmon's viscometer (flow time for ethanol 36 seconds). The flow times are rather small and although kinetic energy corrections are easily applied, shear effects are probably quite large and cannot be estimated without further measurements at different rates of shear.

Light scattering measurements were made using an instrument marketed by SOFICA which is based on an original design of Wippler and Scheibling[1]. Measurements were made of light scattered at eleven angles between 30° and 150° to the incident beam, from not less than four solutions of different concentrations. Solutions were clarified by filtration directly into the scattering cells through No. 5 glass sinters or by high speed centrifugation followed by transfer to the scattering cell using a dust-free pipette. The measurements were made in ethanol and a mixed solvent at room temperature (20° to 25°C). This means that the mixed solvent used was not a θ solvent for the light scattering measurements but was rather better since a subsequent experiment showed that on heating a polymer solution to a

temperature of about 30°C, the polymer precipitated. The results were treated by the usual method due to Zimm[2], except that no attempt was made to correct the extrapolated values for polydispersity.

Measurements of dn/dc were made using a Brice Phoenix differential refractometer, at room temperature, which was between 20° and 25°C, Δn being insensitive to temperature variations.

The θ solvent chosen was a mixture of *n*-propanol and *n*-heptane of refractive indices 1·3854 and 1·3876 respectively. The composition was obtained using the method described by Schultz and Flory[3]. Three polymer fractions (1, 5 and 10) of very widely separated molecular weights were used, and the composition at which precipitation occurred found for each over a wide range of polymer concentration. The procedure was to start with a concentrated solution of polymer in *n*-propanol and progessively add precipitant (*n*-heptane) till slight precipitation occurred, then to redissolve and to repeat this until solutions were quite dilute. The results obtained were then extrapolated to yield a value of the solvent composition which would just dissolve a polymer of infinite molecular weight at zero concentration, i.e. the composition of the θ solvent.

DISCUSSION

The early attempts at fractionation were carried out using the solvent–precipitant systems used by Fuoss *et al.*[4] and by Boyes and Strauss[5] for poly-4-vinyl pyridine. It was found, however, that poly-2-vinyl pyridine was generally much more soluble than its isomer and could only be precipitated using saturated hydrocarbons or water.

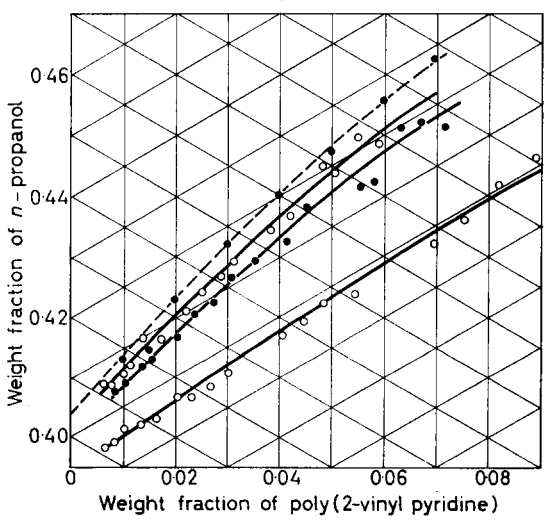

Figure 1—Part of phase diagram for system poly-2-vinyl pyridine –*n*-propanol–*n*-heptane

The curves for the precipitation of polymer from the solvent–precipitant mixtures (*n*-propanol–*n*-heptane) are shown in *Figure 1*. The lines in the ternary diagram corresponding to different molecular weights are much more closely grouped than those obtained by Schultz using polystyrene of

similar molecular weights. The broken line corresponds to the precipitation curve for infinite molecular weight polymer.

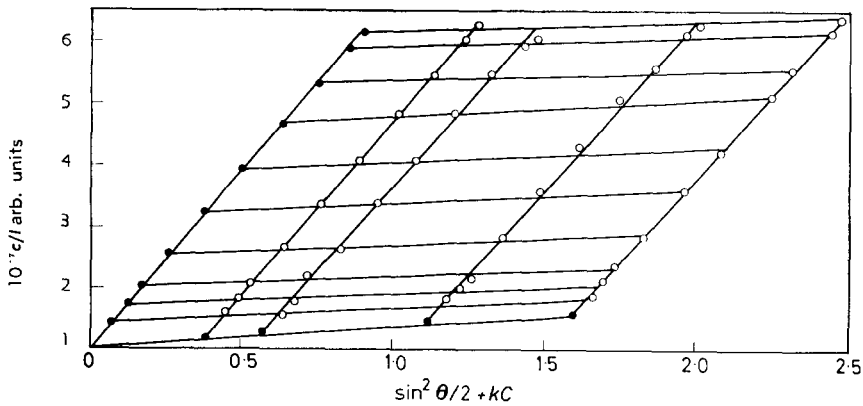

Figure 2—Zimm plot for poly-2-vinyl pyridine in ethanol

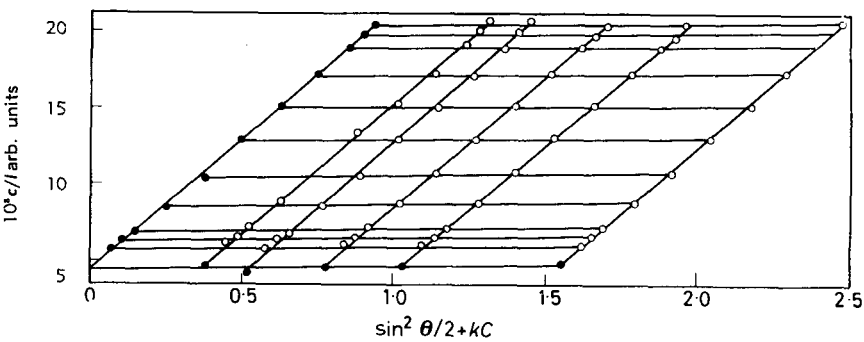

Figure 3—Zimm plot for poly-2-vinyl pyridine in mixed solvent

Zimm plots for fraction 2 in ethanol and the mixed solvent are shown in *Figures 2* and *3* and values of $\langle R^2\rangle_{z+}$ (six times the mean square $Z+$ average radius of gyration), M_w, the weight average molecular weight, and B, the second virial coefficient for the various fractions are shown, along with the limiting viscosity numbers and values of Φ, in *Table 1*.

Graphs of η_{sp}/c against c and $\log(\eta_{rel}/c)$ against c were plotted and viscosity measurements continued to concentrations sufficiently low for linear extrapolation of both graphs to be possible. Both graphs could be extrapolated in every case to the same value of the limiting viscosity number. The linear relationships found for the various quantities are:

(1) Viscosity–Molecular weight
   (a) Ethanol $[\eta] = 2{\cdot}8 \times 10^{-4} M_w^{0{\cdot}66}$
   (b) Heptane–propanol (θ solvent) $[\eta] = 1{\cdot}2 \times 10^{-3} M_w^{0{\cdot}50}$

(2) $\langle R^2\rangle_{z+}$–M_w
   (a) Ethanol $\langle R^2\rangle_{z+} = 0{\cdot}063\, M_w^{1{\cdot}25}$
   (b) Propanol–heptane $\langle R^2\rangle_{z+} = 0{\cdot}49\, M_w^{1{\cdot}08}$

(3) B–M_w, Ethanol; $B = 2{\cdot}5 \times 10^{-3} M_w^{0{\cdot}41}$

Table 1

Fraction	Ethanol				
	$M_w \times 10^{-6}$	$\langle R^2 \rangle_{z+} \times 10^{-6}$ Å^2	$B \times 10^4$	$[\eta]$ dl/g	$\Phi \times 10^{-21}$
1	4·5	13·5	1·97	6·30	1·48
2	3·17	8·75	2·10	5·60	1·83
3	2·18	5·45	2·03	4·17	1·75
4	1·69	3·72	2·36	3·45	2·04
5	1·35	3·08	3·0	3·14	2·07
6	0·85	1·50	2·81	2·51	3·0
7	0·57	1·01	4·45	1·66	2·28
8	0·474	0·770	4·65	1·50	2·58
9	0·345	0·655	5·0	1·15	1·97
10	0·086	—	19·0	0·62	3·20

Φ_{Ethanol}: Average 2·22.

Fraction	Heptane–n-propanol			
	$M_w \times 10^{-6}$	$\langle R^2 \rangle_{z+} \times 10^{-6}$ Å^2	$[\eta]$ dl/g	$\Phi \times 10^{-21}$
1	4·45	7·63	2·42	1·34
2	3·20	5·65	2·17	1·33
3	1·90	3·17	1·73	1·64
4	1·57	2·28	1·59	1·97
5	1·39	1·89	1·35	1·85
6	0·835	1·16	1·10	2·01
7	0·518	0·673	0·90	2·32
8	0·42	0·615	0·77	1·85
9	—	—	0·63	—
10	—	—	0·34	—

$\Phi_{\text{Heptane–}n\text{-propanol}}$: Average 1·79.

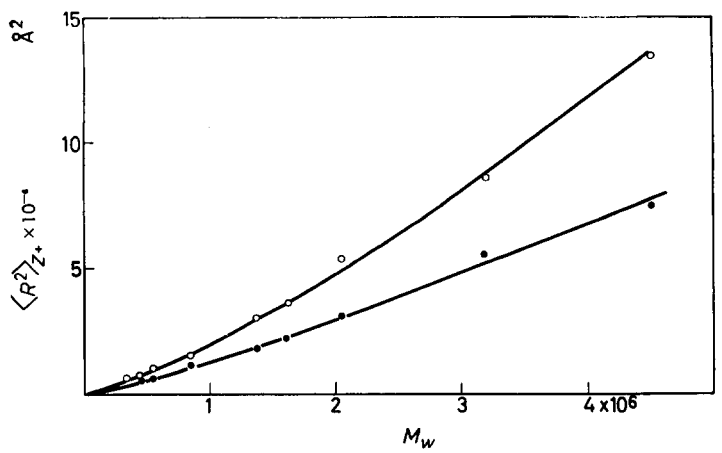

Figure 4—Plot of $\langle R^2 \rangle_{z+}$ against M_w for poly-2-vinyl pyridine in ethanol (open circles) and in mixed solvent (solid points)

The values of $\langle R^2\rangle_{z+}$ for the different polymer fractions in ethanol and the mixed solvent are shown as functions of molecular weight in *Figure 4*. The curve for ethanol is strongly concave upwards as one would expect for a good solvent. The points for the mixed solvent do not appear, however, to fall on a straight line, as they should if $R^2 \propto M$, but exhibit slight upward curvature.

Plots of $\log\langle R^2\rangle_{z+}$ against $\log M_w$ give straight lines of slopes $1{\cdot}25 \pm 0{\cdot}02$ in ethanol and $1{\cdot}08 \pm 0{\cdot}02$ in the mixed solvent. This shows that the mixed solvent is better than a θ solvent, as previously indicated. Measurements in the mixed solvent at 25°C (i.e. a θ solvent) are envisaged, when accurate temperature control of the light scattering apparatus near room temperature has been achieved.

The light scattering results for the fraction of highest molecular weight in ethanol were analysed by a method previously described[6] to find the exponent in the $\langle R^2\rangle/M$ relationship. For this fraction the exponent in the relationship $\langle r_{ij}^2\rangle = k\,(i-j)^{1+\nu}N^{\epsilon-\nu}$ is 0·1, ϵ being 0·25 according to the $\log\langle R^2\rangle_z/\log M_w$ plot. The value of ν found for the highest molecular weight fraction should be characteristic for all fractions, and graphs of $P^{-1}(\theta)$ against $(\sin^2\frac{1}{2}\theta)^{0{\cdot}9}$ were drawn in order to find $\langle R^2\rangle_N$ and M_N from which one can find an $\langle R^2\rangle/M$ relationship uninfluenced by polydispersity[7]. From a graph of $\log\langle R^2\rangle_N$ against $\log M_N$, a value of ϵ of 0·24 was obtained.

The limiting viscosity numbers of the polymer fraction when plotted in log-log form against molecular weight gave straight lines of slopes 0·66 in ethanol and 0·50 in the θ solvent.

It is rather difficult to interpret the different values of the exponents in the various relationships considered.

$$[\eta] = kM^{\alpha}$$

$$\langle r_{ij}^2\rangle = k'\,(i-j)^{1+\nu}N^{\epsilon-\nu}$$

which leads to $\langle R^2\rangle = kN^{1+\epsilon}$. ν is obtained directly from a single light scattering experiment and should be less than or equal to ϵ. ϵ is found from a plot of $\log\langle R^2\rangle$ against $\log M$, the values being obtained from light scattering. α is obtained from viscosity measurements and should be equal to $\frac{1}{2} + \frac{3}{2}\epsilon$.

For ethanol, α is 0·66 which gives a value $\epsilon = 0{\cdot}10$. However, from the $\log\langle R^2\rangle_{z+}/\log M_w$ plot, $\epsilon = 0{\cdot}25$ and from the light scattering experiment on the highest M_w fraction, $\nu = 0{\cdot}10$.

The difference between the ϵ values from viscosity and light scattering measurements seems rather large but may be due to the different averages of distances obtained in the two types of measurement, and the fact that the determination from the viscosity–molecular weight exponent is only approximate.

An attempt was made to evaluate the amount of restriction of rotation about carbon–carbon bonds in the polymer backbone using the expression

$$\langle R^2\rangle = \left\{\frac{M}{m}\right\}^{1+\epsilon}\left(\frac{1+\cos\theta}{1-\cos\theta}\right)\left(\frac{1+\cos\phi}{1-\cos\phi}\,l^2\right) \qquad (1)$$

which is a combination of the well known equation for $\langle R^2 \rangle$ involving short range interactions, with an empirical one for long range interactions (θ being the supplement of the valence angle, l the carbon–carbon bond length, $\cos\phi$ the average value of the cosine of the rotation angle measured from the trans position and m, for vinyl polymers, is half the monomer weight).

For the polymer in the mixed solvent system for which $\varepsilon = 0{\cdot}08$, $(1+\cos\phi)/(1-\cos\phi)$ has the value 7·3.

This value is in agreement with values obtained for polymers of similar structure[8]. However, if the same treatment is applied to the results for the ethanol solution for which $\varepsilon = 0{\cdot}25$, a value of 1·97 is obtained for $(1+\cos\phi)/(1-\cos\phi)$, which is much smaller than the previous value and would appear to indicate almost completely free rotation in the molecule. A similar difference is found if equation (1) is applied to polymers of similar structure investigated in several solvents by other authors[9]. From this it would seem that the effect of excluded volume cannot be simply accounted for by the introduction of the term $N^{1+\epsilon}$ into the formula for $\langle R^2 \rangle$, although the effect of short range forces should, in principle, be separable from that of long range ones.

The authors wish to thank the D.S.I.R. for the award of an equipment grant for the purchase of the light scattering apparatus and of a research studentship to one of us (R.B.T.).

Chemistry Department, The Royal College of Science and Technology, Glasgow, C.1

(*Received March 1962*)

REFERENCES

[1] WIPPLER, C. and SCHEIBLING, G. *J. Chim. phys.* 1954, **51**, 201
[2] ZIMM, B. H. *J. chem. Phys.* 1948, **16**, 1093 and 1099
[3] SCHULTZ, A. R. and FLORY, P. J. *J. Amer. chem. Soc.* 1953, **75**, 5681
[4] BERKOWITZ, J. B., YAMIN, M. and FUOSS, R. M. *J. Polym. Sci.* 1958, **28**, 69
[5] BOYES, A. G. and STRAUSS, U. P. *J. Polym. Sci.* 1956, **22**, 463
[6] HYDE, A. J. *Trans. Faraday Soc.* 1960, **56**, 591
[7] LOUCHEUX, C., WEILL, G. and BENOIT, H. *J. Chim. phys.* 1958, **55**, 540
[8] KRIGBAUM, W. R. *J. Polym. Sci.* 1958, **28**, 213
[9] NOTLEY, N. T. and DEBYE, P. J. W. *J. Polym. Sci.* 1955, **17**, 99

The Dependence of the Viscosity on the Concentration of Sodium Carboxymethylcellulose in Aqueous Solutions

D. A. I. GORING and G. SITARAMAIAH*

The Huggins coefficient, k', was measured for three fractions of sodium carboxymethylcellulose by an iso-ionic dilution technique for ionic strength I_E from 0·1 M to 0·00001 M. At I_E=0·1 M, k' was approximately 0·5. However, k' increased to values as high as 29 at lower ionic strengths. Such substantial increases of k' were produced by the increased interparticle repulsion at low ionic strength. A model of the collision doublet is proposed in which the hydrodynamic compressive force and the electrostatic repulsive force are in equilibrium. As the ionic strength is lowered, the increased electrostatic potential of the molecule causes an increase in the axial ratio of the doublet and thus produces an increment in k'. A quantitative treatment is given in which the electrostatic potential calculated from the increment in k' is compared with values computed by means of the equations for the potential of a polyelectrolyte.

THE change in the reduced viscosity with concentration of dilute solutions of high polymers has been expressed by the relationship[1]

$$\eta_{sp}/c=[\eta]+k'[\eta]^2c \qquad (1)$$

where k', the Huggins constant, depends on the nature of the polymer–polymer interactions in solution. For non-ionic polymers k' has been generally found to vary between 0·3 and 0·5[2–5]. However, with polyelectrolytes higher k' values have been reported for a number of systems[6–9].

Recently, Goring and Rezanowich[9] observed for fractions of lignin sulphonate a large increase in k' with decrease in the ionic strength, I_E. It was suggested that this trend was due to the increased electrostatic interparticle repulsion at low ionic strength. The effect was then interpreted in terms of the particle collision behaviour reported in detail by Mason *et al.*[10–14]. The constant k' is assumed to arise from the rotation of the doublet formed by the collision of spherical particles in the streamlines of the sheared solution. When the particles carry charges, the double layers interact during collision and the collision radius increases. A higher value of k' results. A diagrammatic representation of the rotating doublet is given in *Figure 1*.

The following relation was deduced between k' and half the distance of closest approach δ

$$\{(r_\eta+\delta)/r_\eta\}^6=k'/k'_0 \qquad (2)$$

in which k'_0 is the value of k' under conditions of high ionic strength when

*Holder of a Union Carbide Fellowship (1959–60) and a Mead Foundation Grant (1960–61). Present address: Borg Warner Corporation, Des Plaines, Ill., U.S.A.

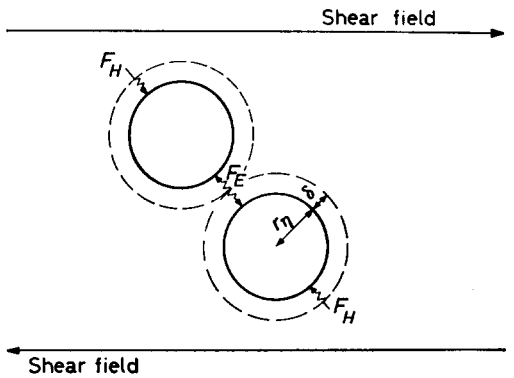

Figure 1—Collision of spheres with interacting double layers in a shear field

δ is zero. In equation (2), r_η is the radius of the equivalent sphere obtained by substituting $[\eta]$ (dl/g) in the Einstein viscosity equation

$$r_\eta = \{30M\,[\eta]/\pi N\}^{1/3} \tag{3}$$

in which M is the molecular weight and N is Avogadro's number. From equation (2), δ was computed for a series of ionic strengths. Goring and Rezanowich[9] found that the ratio of δ to the Debye width of the double layer was constant over a wide range of I_E.

In the above theory two forces are considered to act on the charged spheres. A hydrostatic compressive force tends to push the spheres into contact while the electrical repulsive force pushes them apart. The two charged spheres are separated by a distance which is set by the equilibrium between the two forces. In the present paper a theoretical extension of the original proposal is deduced from this condition of equilibrium.

It was considered of interest to test the validity of the theory by its application to the results of the current studies on the molecular size and hydrodynamic properties of sodium carboxymethyl cellulose (CMC)[15]. Intrinsic viscosities and k' values were available for a series of fractions, over a range of ionic strengths and molecular weights. A quantitative interpretation of the k' values obtained will be given here in terms of the concept outlined above.

THEORETICAL

The electrostatic repulsive force, F_E, may be obtained from an approximate equation of Verwey and Overbeek[16] for the repulsive energy, V_R, of two charged spheres separated by a distance 2δ. Written in present symbols the Verwey–Overbeek equation is

$$V_R = \tfrac{1}{2} r_\eta^2 \varepsilon \psi_k^2 \times e^{-2\kappa\delta}/(r_\eta + \delta) \tag{4}$$

where ε is the dielectric constant of the medium, ψ_k is the surface potential according to equation (4), and $1/\kappa$ is the Debye width of a double layer.

The electrostatic repulsive force, F_E, is given by

$$F_E = \tfrac{1}{2}\mathrm{d}V_R/\mathrm{d}\delta$$
$$= -\frac{\varepsilon r_\eta^2 \psi_k^2}{4}\,\frac{1}{\mathrm{e}^{2\kappa\delta}}\left[\frac{2\kappa}{(r_\eta+\delta)} + \frac{1}{(r_\eta+\delta)^2}\right] \tag{5}$$

According to Allan and Mason[17], the hydrodynamic compressive force, F_H, is

$$F_H = 2\pi\beta\eta_0 G\,(r_\eta+\delta)^2 \sin 2\phi\star \tag{6}$$

where β is a function of the axial ratio of the prolate ellipsoid equivalent hydrodynamically to the doublet, $\phi\star$ is the angle its major axis makes perpendicular to the direction of the streamlines, η_0 is the viscosity of the solvent and G is the shear rate.

Approximately all directions between 0 and $\pi/2$ for $\phi\star$ being equally likely, the average value of $\sin 2\phi\star$ becomes $2/\pi$. Allan and Mason[17] have shown that the factor β can be reduced to a value of 2·17 when the ellipsoid equivalent hydrodynamically to the doublet has an axial ratio of 2. Assuming an axial ratio of 2 and substituting $2/\pi$ for $\sin 2\phi\star$, equation (6) becomes

$$F_H = 8{\cdot}7\,\eta_0 G\,(r_\eta+\delta)^2 \tag{7}$$

Equating the compressive and repulsive forces for equilibrium (equations 5 and 7) we get

$$\psi_k^2 = \frac{34{\cdot}7\,\eta_0 G\,\mathrm{e}^{2\kappa\delta}\,(r_\eta+\delta)^4}{\varepsilon r_\eta^2\,[2\kappa\,(r_\eta+\delta)+1]} \tag{8}$$

Equation (8) can be used to compute the potential at the effective surface of the molecule.

The surface potential of a polyelectrolyte can also be calculated by means of the approximation derived by Lifson[18]. Lifson's Eq. 9 in ref. 18 written in the present symbols is

$$\psi_L = \frac{kT}{e}\sinh^{-1} f\left[1 - \frac{1+\kappa r_\eta}{2\,(\mu+\kappa)\,r_\eta}\right] \tag{9}$$

in which ψ_L is the surface potential according to Eq. 9 and e, k and T are respectively the electronic charge, the Boltzmann constant and the absolute temperature. Also $\mu^2 = \kappa^2\,(1+f^2)^{1/2}$ and $f = c/2c_s$ in which c_s is the concentration of non-polymeric monovalent salt at points far from the macromolecule where ψ_L is zero and c is the local concentration of fixed charges of the macromolecule given by

$$c = \frac{\text{Degree of substitution} \times \text{Degree of polymerization}}{(4/3)\,\pi r_\eta^3}$$

Surface potentials calculated from the viscometric data may now be compared with values derived from Lifson's Eq. 9.

EXPERIMENTAL

Three samples of CMC, Hercules Cellulose Gums 7HP, 7MP and 7LP were kindly given to us by the Hercules Powder Co., Wilmington, Delaware. The samples were fractionated by precipitation from aqueous solution with

ethanol. Three fractions, one from each series of fractionations, were chosen for viscosity measurements over a range of ionic strengths. The fractions were designated H1, M1 and L3 and were found to have the sedimentation–diffusion molecular weights (M_{sD}), degrees of substitution (*DS*) and polymerization (*DP*) shown in *Table 1*.

Table 1. Molecular weights, DS and DP for CMC fractions

Fraction	M_{sD}	*DS*	*DP*
H1	346 000	0·66	1 611
M1	163 000	0·72	743
L3	44 700	0·73	202

Viscosities were measured in aqueous sodium chloride by means of a capillary viscometer of Schurz–Immergut type[19], with four bulbs and a reservoir to permit measurement at different shear rates and concentrations. An iso-ionic dilution technique[15] was employed to obtain linear graphs of reduced viscosity versus concentration. All measurements were made at $25° \pm 0{\cdot}01°C$ and η_{sp}/c versus c graphs computed for $G = 500\ sec^{-1}$. The materials used, preparation of the fractions, as well as details of viscometry have been described in an earlier paper[15].

DISCUSSION OF RESULTS

Values of $[\eta]$ and k' derived for three fractions at different ionic strengths are given in *Table 2*. There is a marked increase of the Huggins coefficient with decrease in ionic strength. The k' value of 29·0 for fraction L3 at $I_E = 5 \times 10^{-4} M$ is the highest so far reported for CMC. Pals and Hermans[6] reported k' for CMC ranging between 0·5 and 10·0 whereas the values of Fujita and Homma[7] were between 0·4 and 4·0. Increase of k' linearly with the reciprocal of the ionic strength has been observed in the past[6,20].

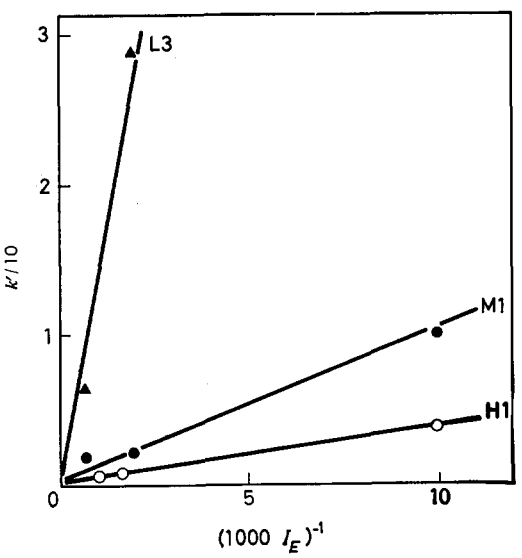

Figure 2—k' versus reciprocal ionic strengths for H1, M1 and L3

Data from the present work, plotted in *Figure 2*, confirm the linear relationship for I_E values from 0·1 to 0·0004 *M*. At lower I_E, k' falls below the straight lines shown in *Figure 2* for fractions M1 and H1.

In order to apply the analysis given in the theoretical section the molecule will be assumed to possess spherical symmetry. It is realized that this assumption is an oversimplification and it is expected that at very low I_E or molecular weight the treatment will break down because of the considerable extension of the polyelectrolyte.

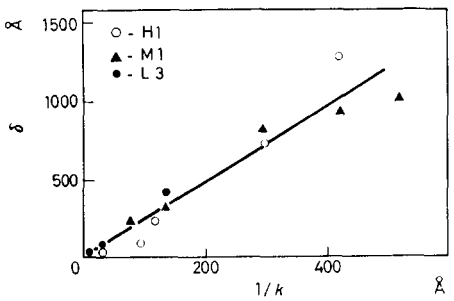

Figure 3—δ versus $1/\kappa$ for H1, M1 and L3

Proceeding, the CMC macromolecule is considered equivalent to a sphere of radius, r_η, and values of δ are computed by means of equation (2). For the calculation of δ at different ionic strengths, k'_0 values of 0·5, 0·43 and 0·44 for H1, M1 and L3 respectively were used and were obtained by extrapolation of the k' versus $1/I_E$ graphs shown in *Figure 2* to $1/I_E=0$. Meaningful calculation of δ at an ionic strength of 0·1 *M* was not possible because of the small difference between k'_0 and k' at $I_E=0{\cdot}1\ M$.

As shown in *Table 2*, δ increased with decrease in I_E. The composite graph of δ versus $1/\kappa$ (*Figure 3*) was approximately linear with a slope of 2·4. For lignin sulphonates[9] a linear relationship between δ and $1/\kappa$ was found with $\delta\kappa=1{\cdot}5$.

The electrostatic potential at the effective surface of the macromolecule was then calculated by the two methods embodied in equations (8) and (9).

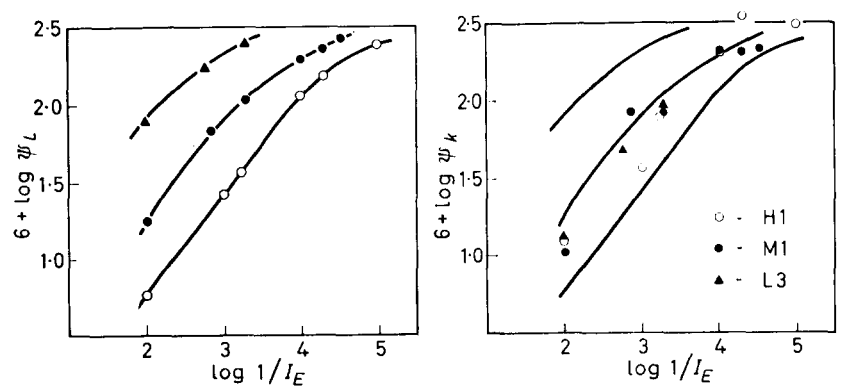

Figure 4—log ψ_k and log ψ_L versus log $1/I_E$ for H1, M1 and L3. The curves on the right are identical with those on the left

Table 2. Values of $[\eta]$, r_η, k', δ, ψ_k and ψ_L for Fractions H1, M1 and L3 at various ionic strengths

Fraction	I_E (M Na^+)	$[\eta]$ (dl/g)	r_η (Å)	k'
H1	0·1	12·3	407	0·51
	0·01	28·8	540	0·51
	0·001	62·7	700	0·65
	0·0006	68·2	720	1·1
	0·0001	91·8	795	3·7
	0·00005	105	832	8·2
	0·00001	160	957	8·9
M1	0·1	7·0	262	0·45
	0·01	11·7	311	0·46
	0·0014	19·5	369	1·9
	0·0005	27·7	415	2·2
	0·0001	39·0	465	10·5
	0·00005	48·8	501	10·6
	0·00003	51·3	510	12·8
L3	0·1	1·6	104	0·55
	0·01	2·3	118	1·1
	0·0017	3·5	135	6·5
	0·0005	3·9	141	29

Fraction	δ (Å)	$\psi_k \times 10^5$ (*e.s.u.*)	$\psi_L \times 10^5$ (*e.s.u.*)	$\frac{\psi_L}{\psi_k}$
H1	—	—	—	—
	1·6	1·3	0·6	0·4
	32	3·7	2·6	0·7
	101	8·0	3·6	0·5
	315	21·5	11·6	0·5
	494	35·2	15·4	0·4
	589	31·6	24·3	0·8
				Mean 0·6
M1	—	—	—	—
	3·1	1·1	1·8	1·7
	104	8·6	6·7	0·8
	129	8·6	10·6	1·2
	327	22·4	19·6	0·9
	354	20·9	23·1	1·1
	387	21·8	26·8	1·2
				Mean 1·2
L3	—	—	—	—
	19·4	1·4	8·4	6·2
	76	5·0	17·9	3·6
	142	9·9	26·2	2·7
				Mean 4·2

It is evident from the results given in *Table 2* that the main trend of ψ_k and ψ_L is to increase with decrease in the ionic strength. In this respect there is agreement between the two methods of deriving the potential.

The quantitative agreement between ψ_k and ψ_L at each ionic strength is best for fractions H1 and M1. With decrease in molecular weight the potential calculated from the Lifson equation increases. The data for ψ_k are more irregular and there is no consistent increase in ψ_k at the lower molecular weight. These trends are shown more clearly in the graphs of $\log \psi_k$ and $\log \psi_L$ versus $\log 1/I_E$ shown in *Figure 4*. The plot of $\log \psi_L$ versus $\log 1/I_E$ for M1 fits fairly well the $\log \psi_k$ versus $\log 1/I_E$ points for H1, M1 and L3. In effect, these results signify that for a given ionic strength, the surface potential calculated from k' is independent of the molecular weight whereas the Lifson equation predicts an increase of the surface potential with decrease in molecular weight. However, the two theories yield approximately the same potential for carboxymethylcellulose at molecular weights of 160 000 and 350 000.

The greater discrepancy between the theories for the lower molecular weight fraction, L3, may easily arise from the configurational properties of the CMC macromolecule. There is evidence that the cellulose nitrate molecule below molecular weights of 10^5 loses its spherical symmetry in solution due to the stiffness of the chain[21]. Thus at lower molecular weights, cellulose derivatives in solution would tend to deviate from the spherical shape assumed both by Lifson[18] and in the present theory. Spherical symmetry would be most nearly approximated at the higher molecular weight, i.e. for Fractions H1 and M1. It is with these fractions that agreement between ψ_k and ψ_L is closest.

It is interesting to compare the present results with those reported by Strauss[22]. Working with long-chain polyphosphates, Strauss found that the surface potential computed from the Lifson equation was lower than the ζ-potential measured electrophoretically by a factor which increased from about 4 to 50 for an increase in I_E from 0·03 *M* to 0·9 *M*. In contrast, the present results show $\psi_L \geqslant \psi_k$. Also, for any one fraction, the ratio ψ_L/ψ_k was approximately constant over a range of ionic strengths. As shown in *Table 2*, the exceptions to this occur at high ionic strength where the measurement of k' is most inaccurate.

In order to explain his discrepancy, Strauss suggested that the ζ-potential measured electrophoretically is the micropotential of the individual chain whereas the potential computed from the Lifson equation is the average potential smeared over the surface of the sphere equivalent to the polyelectrolyte. In the present study, it is probable that ψ_k is also an average surface potential since it seems unlikely that there will be interpenetration of the polyelectrolyte coils in the formation of the rotating doublet.

In conclusion, it can be claimed that the limited agreement between ψ_k and ψ_L in *Table 2* is support for the general concepts proposed in the present work. A more rigorous test of the theory is necessary using model polyelectrolytes such as spherical particles of molecular dimensions carrying charges only on their surface. Preparation and characterization of such systems is now in progress.

The authors wish to thank Dr S. G. Mason for his help in the theoretical part of the paper and also G. Suranyi for carrying out the extensive calculations.

This paper was presented at the 141st Meeting of the American Chemical Society, March (1962).

Physical Chemistry Division,
Pulp and Paper Research Institute of Canada, and
Department of Chemistry,
McGill University, Montreal, Canada *(Received April 1962)*

REFERENCES

[1] HUGGINS, M. L. *J. Amer. chem. Soc.* 1942, **64,** 2716
[2] FLORY, P. J. *Principles of Polymer Chemistry.* Cornell University Press: Ithaca, 1953
[3] KOOY, J. and HERMANS, J. J. *J. Polym. Sci.* 1955, **16,** 417
[4] CRAGG, L. H. and BIGELOW, C. C. *J. Polym. Sci.* 1955, **16,** 177
[5] JONES, M. H. *Canad. J. Chem.* 1956, **34,** 1027
[6] PALS, D. T .F. and HERMANS, J. J. *Rec. Trav. chim. Pays-Bas,* 1952, **71,** 433
[7] FUJITA, H. and HOMMA, T. *J. Polym. Sci.* 1955, **15,** 277
[8] TERAYAMA, H. and WALL, F. T. *J. Polym. Sci.* 1955, **16,** 357
[9] GORING, D. A. I. and REZANOWICH, A. *J. Colloid Sci.* 1960, **15,** 472
[10] TREVELYAN, B. J. and MASON, S. G. *J. Colloid Sci.* 1951, **6,** 354
[11] MANLEY, R. ST J. and MASON, S. G. *J. Colloid Sci.* 1952, **7,** 354
[12] MANLEY, R. ST J. and MASON, S. G. *Canad. J. Chem.* 1955, **33,** 763
[13] MANLEY, R. ST J. MASON, S. G. *Proc. Roy. Soc. A,* 1956, **238,** 117
[14] BARTOK, W. and MASON, S. G. *J. Colloid Sci.* 1958, **13,** 293
[15] SITARAMAIAH, G. and GORING, D. A. I. *J. Polym. Sci.* 1962, **58,** 1107
[16] VERWEY, E. J. W. and OVERBEEK, J. TH. G. *Theory of the Stability of Lyophobic Colloids,* p 152. Elsevier: Amsterdam, 1948
[17] ALLAN, R. S. and MASON, S. G. *Proc. Roy. Soc. A,* 1962, **267,** 62
[18] LIFSON, S. *J. chem. Phys.* 1957, **27,** 700
[19] SCHURZ, J. and IMMERGUT, E. H. *J. Polym. Sci.* 1952, **9,** 281
[20] SCHNEIDER, N. S. and DOTY, P. *J. phys. Chem.* 1954, **58,** 762
[21] HUQUE, M. M., GORING, D. A. I. and MASON, S. G. *Canad. J. Chem.* 1958, **36,** 952
[22] STRAUSS, U. P. *J. Amer. chem. Soc.* 1958, **80,** 6498

Radiochemical Investigation of Polymer Unsaturation. Reaction of Butyl Rubber with Radiochlorine

I. C. McNeill*

The reaction between chlorine and butyl rubber is of interest for two reasons: because of the industrial importance of the reaction, the mechanism of which has not been fully understood, and because of the possibility of using it as a method for the determination of unsaturation. By the use of (^{36}Cl)-chlorine, it has been possible to study the reaction on a conveniently small scale, the radiochlorine being manipulated quantitatively by a vacuum line technique. It has been shown that the reaction with chlorine is freer from side effects than the iodine chloride reaction. Two atoms of chlorine are incorporated in the polymer for each double bond originally present. These are incorporated not by addition but by a substitution process which is probably not free-radical in nature. A mechanism is proposed for the reaction. Radiochlorine is demonstrated to be potentially a useful reagent for investigating very low unsaturations in polymers.

SMALL amounts of unsaturated centres in polymer chains are important for a number of reasons. They may form centres for crosslinking reactions, as in the vulcanization of rubbers, points at which modification of the polymer can be brought about by reactions such as grafting, points of weakness towards oxidative attack, or centres at which degradation may be initiated. Their presence in very small amounts may also provide evidence for particular mechanisms of initiation, termination or transfer. There is therefore some interest in being able to measure accurately the number of double bonds present in a polymer. Satisfactory methods are available for the determination in polymers of unsaturations down to about 0·5 mole per cent. Below this level the accuracy of ordinary chemical methods becomes inadequate. Thus while there is considerable interest in unsaturations far below 0·5 mole per cent, there are no satisfactory quantitative methods for investigating these. Radiochemical techniques should enable this difficulty to be resolved—the use of a reagent labelled with a suitable radioactive isotope should enable very low double bond contents to be determined; for higher unsaturations it would permit determinations to be carried out on extremely small samples of polymer.

Much of the published work on the determination of polymer unsaturation has been carried out using butyl rubbers, which normally have unsaturations in the range 1 to 5 mole per cent. The most satisfactory of the variety of procedures which have been described for the determination of unsaturation in butyl rubbers[1–6] appear to be the iodine/mercuric acetate method of Gallo, Weise and Nelson[1], and the iodine chloride method of Lee, Kolthoff and Johnson[2]. The former method yields reproducible results provided time of reaction and concentration of reagent are strictly standardized. It suffers from the disadvantage, however, that

*Present address: Chemistry Department, The University, Glasgow, W.2, Scotland.

the nature of the reaction is not well understood, and that in order to calculate unsaturation values an empirical assumption must be made that three iodine atoms are consumed per double bond. The reaction of isoprene butyl rubber and butadiene butyl rubber with iodine chloride in carbon tetrachloride solution has been the subject of a very careful study[2], in which it was shown that the reaction with double bonds of the butadiene type is straightforward addition of a molecule of ICl. Where there are substituents in the vicinity of the double bond, however, the reaction is complicated with side effects and is believed to proceed in these stages:

(*i*) initial addition of ICl

(*ii*) splitting out of HI, which then reacts with a molecule of ICl to give HCl and I_2

(*iii*) slow addition of ICl to the double bond resulting from stage (*ii*).

In spite of the complexity of the reaction, Lee, Kolthoff and Johnson were able to devise a reliable procedure for the determination of unsaturation using the iodine chloride reagent.

Although either of the above mentioned methods could in theory provide a basis for the development of a radiochemical procedure for unsaturation determination (using e.g. iodine-131 or chlorine-36), from the above considerations neither was regarded as ideal.

Little attempt has been made in the past to use chlorine for the quantitative estimation of double bonds in polymers, partly because of difficulties in handling chlorine, and also because of the readiness with which chlorine will react with hydrocarbons by free radical substitution processes. Chlorine is an attractive reagent, however, from the radiochemical point of view, since there is a suitable isotope available, and the preparation of radiochlorine is readily accomplished[7]. Quantitative manipulation of chlorine can now be carried out on a vacuum line without difficulty, using greaseless stopcocks.

In the development of a radiochemical method for investigating polymer unsaturation, using radiochlorine as reagent, butyl rubbers were selected for study for a number of reasons. First, the reaction is itself of considerable interest, partly because of its industrial importance in the preparation of chlorobutyl. The mechanism has not been elucidated. Secondly, butyl rubbers have unsaturations just high enough to be determined unambiguously by conventional techniques. Thirdly, unsaturation of the isoprene type has proved more difficult to determine than the butadiene type, because of side reactions. The reaction with butyl rubber is therefore a searching test of chlorine as a potential reagent for estimating double bonds in polymers.

EXPERIMENTAL

(1) *Design and operation of the radiochlorine gas apparatus*

This is illustrated in *Figure 1*. Stopcocks 1 to 4 are greaseless stopcocks (G. Springham and Co. Ltd) with Viton A Fluorocarbon diaphragms. The system is evacuated through stopcock 2 and the liquid air trap F. Radiochlorine, produced as previously described[7] by decomposition of palladous (^{36}Cl) chloride in bulb E, is collected in D, which is cooled in liquid air (stopcock 1 closed). The bulb E is then removed by drawing off the tube

at I. Chlorine is transferred from D to A by thawing D, opening stopcocks 1, 3 and 4, and cooling the tail of the bulb A in liquid air. Bulb A is then thawed to room temperature. A definite fraction of the weight of chlorine in A may be removed by opening stopcock 4 (stopcock 3 closed) and allowing the chlorine in A to expand into B. If stopcock 4 is now closed, B contains a weight of chlorine given by the original weight in A multiplied by the 'delivery fraction' volume B/(volume A + volume B), which can be distilled into a reaction tube C or into D for storage, as desired. Further portions of the chlorine in A may be removed by repeating these operations, the amount removed at each stage being a constant fraction of that present in bulb A before expansion into B.

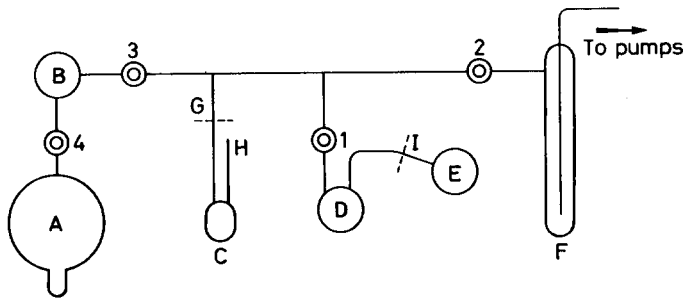

Figure 1—Vacuum apparatus for the quantitative manipulation of radiochlorine

(2) *Method of filling reaction tubes*

Reaction tubes were of 20 ml capacity and had two arms (C, *Figure 1*). One arm of the tube is fused on to the apparatus at G and the solution for reaction is added through the other arm using a hypodermic syringe. The latter arm is then sealed by drawing off the end at H. The solution in C may then be degassed, if required, by the usual freezing and thawing technique. Radiochlorine from the bulb system is then distilled into the frozen solution. The reaction tube is finally removed by drawing off at G and thawed to the reaction temperature. Further reaction tubes are attached at G, and the procedure repeated as required.

(3) *Calibration of the radiochlorine gas apparatus*

The apparatus is calibrated for use by determination of the delivery fraction. This may be carried out by two methods. First, successive portions of inactive chlorine are collected in reaction tubes, cooled to liquid air temperature, containing excess of 0·1 M aqueous potassium iodide. The tubes are sealed off at G and thawed to room temperature, and the liberated iodine is estimated by titration against standard 0·1 N sodium thiosulphate. The ratio of titres from successive samples is equal to the fraction volume A/(volume A + volume B), from which the delivery fraction may be calculated. Results for a series of four successive operations are given in *Table 1*. Secondly, the delivery fraction may be determined radiochemically. With radiochlorine initially in bulb A, successive portions of chlorine (about 1 to 3 mg) are collected in reaction tubes containing 5 ml

Table 1. Calibration of the radiochlorine gas apparatus

Operation No.	*Thiosulphate titre*	*Counts per minute*	*Delivery fraction*
1	1·75	—	
2	1·40	—	0·200
3	1·11	—	0·203
4	0·88	—	0·207
A	—	557	
B	—	447	0·197

(degassed) of 5 per cent v/v solution of styrene (BDH) in AR carbon tetrachloride. The sealed tubes are thawed to room temperature and left in the dark for more than two hours. The contents of each tube are then made up to 25 ml with carbon tetrachloride and 10 ml portions of these solutions are counted in a liquid counter (see below). The ratio of counts from successive samples, corrected for background, gives again the ratio volume A/(volume A+volume B). The values of the delivery fraction obtained by the two methods are in good agreement (*Table 1*).

(4) *Counting technique*

10 ml portions of solutions were counted in a halogen-quenched liquid counter (20th Century Electronics, type M6H), using a Dynatron type 200 scaling unit, along with a type 1014 probe unit. For each solution, duplicate 10 ml portions were also counted.

Observed counts on samples were generally of the order of 100 to 1 000 counts/min. Due correction was made for counter dead time and for background.

(5) *Determination of specific activity of radiochlorine*

The specific activity of each batch of radiochlorine was determined from two successive operations of the apparatus. The first sample was collected in aqueous potassium iodide, as already described, and the chlorine estimated by titration of liberated iodine with standard sodium thiosulphate. The second sample was collected in 5 per cent v/v styrene in carbon tetrachloride and made up to standard volume for counting. The weight of chlorine in the latter sample was calculated from the former result multiplied by (1 − delivery fraction). The specific activity of the radiochlorine could then be expressed as counts/min per mg chlorine, as counted in carbon tetrachloride solution. Specific activities of the radiochlorine used in these experiments were in the range 2 000 to 3 500 counts/min per mg chlorine.

(6) *Purification of butyl rubbers*

Three rubbers were kindly supplied by Polymer (UK) Ltd. All contained an antioxidant, which was removed by the following procedure. One gramme of rubber was dissolved in 100 ml of *n*-hexane (BDH) and precipitated by pouring the solution into one litre of methanol, with vigorous stirring. The precipitated rubber was washed with methanol, dried

in air for 48 hours, and finally heated to 100°C for two hours in an evacuated system to remove all traces of solvent and precipitant.

(7) *Reaction of butyl rubbers with radiochlorine*

20 mg rubber samples were dissolved in 10 ml AR carbon tetrachloride (overnight) and the solutions were in turn transferred to reaction vessels attached to the vacuum system (*Figure 1*) using a hypodermic syringe. The amount of liquid in each reaction vessel was made up to $15 \pm 0{\cdot}5$ ml by adding washings from the flask and syringe. Reaction vessels were sealed at H (*Figure 1*), the solutions thoroughly degassed, and radiochlorine transferred as previously described. After the reaction vessels had been sealed off at G and thawed to room temperature, they were immersed in a bath at $20° \pm 1°C$, with exclusion of light, for the desired times of reaction.

(8) *Preparation of rubber solutions for counting*

The solutions after reaction contained reacted polymer, unreacted radiochlorine and radioactive hydrogen chloride. Before counts could be made on the polymer, it was necessary to remove the other radiochlorine-containing materials. Immediately after each reaction vessel was opened, the solution was shaken with 10 ml aqueous 0·1 N sodium thiosulphate. The carbon tetrachloride layer was run off and the aqueous layer was shaken with 3 to 4 ml carbon tetrachloride. The organic layer was run off and added to that previously collected; the aqueous layer was discarded. The carbon tetrachloride solution was shaken with a fresh portion of thiosulphate and the above procedure repeated. Finally the solution was made up to 25 ml with carbon tetrachloride.

(9) *Solvent background*

Tests were made on 15 ml portions of benzene, chloroform and carbon tetrachloride, which were reacted with 1 mg of radiochlorine for 48 hours: the reacted solutions were treated in exactly the same way as rubber solutions, and the activity determined. Of the reacted solvents, only carbon tetrachloride showed negligible activity and this solvent was therefore used in all chlorination experiments.

(10) *Iodine chloride experiments*

Unsaturations of the butyl rubbers were determined by the procedure of Lee, Kolthoff and Johnson[2]. A typical extrapolation is shown in *Figure 3*; the results are given in *Table 2*.

(11) *Iodine–mercuric acetate experiments*

Unsaturations were determined by the method of Gallo, Weise and Nelson[1], the reaction time being limited strictly to 30 minutes. The results are quoted in *Table 2*.

RESULTS AND DISCUSSION

Choice of solvent

Chlorine reacts with many common solvents, particularly in the presence of air. For quantitative work on reaction of chlorine with a polymer dis-

Table 2. Unsaturations of three butyl rubbers by the iodine chloride and iodine–mercuric acetate methods

Polymer	*Unsaturation (moles %)*		
	Iodine chloride	*Iodine–mercuric acetate*	*Mean value*
1	1·80	1·69	1·75
2	1·38	1·40	1·39
3	0·53	0·51	0·52

solved in a solvent, the side reaction with the solvent must either be negligible or sufficiently limited to permit a correction to be made. When radiochlorine is used, the possibility of exchange of activity between the chlorine and a chlorinated solvent must also be examined. Test experiments showed that benzene and chloroform were unsuitable as solvents but that carbon tetrachloride was completely satisfactory.

Choice of reaction conditions

In view of the well known tendency of chlorine to react by free radical processes in the presence of air, the exclusion of air in the reaction with butyl rubber was considered essential. Baldwin, Buckley, Kuntz and Robison[8], who chlorinated butyl samples for 16 hours in chloroform using sulphuryl chloride, without exclusion of air and light, claim that the presence or absence of air or antioxidant has little or no effect on the reaction. These workers, however, noticed a pronounced drop in the viscosity of butyl rubber solutions after chlorination, which they interpreted as due to a molecular weight drop resulting from free radical attack of a chlorine atom on a methyl hydrogen followed by chain scission. The present experiments were carried out in conditions designed to reduce or eliminate any such free radical reaction: an inert solvent was used, reaction mixtures were thoroughly degassed to remove air, chlorine was distilled and tubes were sealed off under high vacuum, and reaction was carried out for short times with exclusion of light.

Results

Lee, Kolthoff and Johnson, in their study of the reaction of iodine chloride with butyl rubber, tested the effect of varying the halogen content of reaction mixtures and the duration of reaction; the amount of halogen used up in reaction was found to be acutely sensitive to both excess of halogen and time.

A similar approach has been used in the radiochlorine method. *Table 3* shows, for three samples of different unsaturations, the effect of varying the concentration of chlorine, all other variables being kept constant. The observed behaviour shows a similarity to the iodine chloride reaction in that the plot (*Figure 2*) of chlorine content of polymer against chlorine content of reaction mixture has an initial steeply sloping linear part and a second linear but less steeply sloping part. Following the method of Lee, Kolthoff and Johnson, the two linear portions may be extrapolated to an

Table 3. Reaction of butyl rubbers with radiochlorine, under vacuum, in carbon tetrachloride solution

Wt % Cl *in reaction mixture*	*Moles* % Cl *in reaction mixture*	*Moles* Cl *per mole double bond*	*Counts/min per 100 mg reacted polymer*	*Wt* % Cl *in polymer*	*Moles* % Cl *in polymer*	*Atoms* Cl *in polymer per original double bond*
Polymer 1. Unsaturation 1·75 mole %. 10 minutes reaction at 20°. (Radiochlorine specific activity = 2 585 counts/min per mg Cl, in carbon tetrachloride solution)						
18·9	14·9	8·51	6730	2·60	2·05	2·34
12·7	10·0	5·62	6328	2·45	1·93	2·21
10·2	8·05	4·60	6178	2·39	1·89	2·15
8.27	6·52	3·73	5750	2·22	1·75	2·00
5·93	4·67	2·67	5000	1·93	1·52	1·74
3·91	3·08	1·76	4430	1·72	1·35	1·54
2·68	2·12	1·21	3625	1·40	1·11	1·26
1·35	1·07	0·608	1768	0·683	0·538	0·615
Polymer 2. Unsaturation 1·39 mole %. 10 minute reaction at 20°. (Radiochlorine S.A. = 3 300 counts/min per mg Cl)						
16·4	12·9	9·35	6430	1·95	1·54	2·23
13·5	10·6	7·68	6290	1·91	1·51	2·18
10·1	7·98	5·78	6163	1·87	1·48	2·14
7·34	5·79	4·20	5700	1·73	1·37	1·98
2·98	2·35	1·70	4280	1·30	1·03	1·49
1·45	1·14	0·826	2070	0·628	0·495	0·718
0·99	0·780	0·565	1318	0·399	0·315	0·456
2 hours reaction at 20°. (Radiochlorine S.A. = 2 700 counts/min per mg Cl)						
15·0	11·8	8·56	5827	2·15	1·69	2·45
10·0	7·89	5·72	5278	1·96	1·55	2·24
2·43	1·92	1·39	3312	1·23	0·97	1·41
16 hours reaction at 20°. (Radiochlorine S.A. = 2 700 counts/min per mg Cl)						
14·9	11·7	8·49	8903	3·30	2·60	3·77
9·26	7·30	5·29	7004	2·60	2·05	2·97
7·67	6·05	4·38	6280	2·33	1·84	2·67
6·11	4·82	3·49	6200	2·30	1·82	2·63
1·95	1·54	1·11	2833	1·05	0·83	1·20
Polymer 3. Unsaturation 0·52 mole %. 10 minute reaction at 20°. (Radiochlorine S.A. = 2 585 counts/min per mg Cl)						
15·3	12·1	23·0	1948	0·754	0·594	2·26
13·1	10·3	19·6	1637	0·633	0·500	1·91
8·88	7·00	13·3	1696	0·656	0·518	1·97
6·78	5·35	10·2	1355	0·524	0·413	1·58
5·39	4·25	8·10	1250	0·483	0·382	1·46
1·73	1·37	2·61	841	0·325	0·256	0·98

Table 4. Extrapolated results from *Figure 2*

Polymer	*Unsaturation*	*Wt* % Cl *in polymer*	*Atoms* Cl *per original double bond*
1	1·75	2·22	2·00
2	1·39	1·76	2·02
3	0·52	0·59	1·77

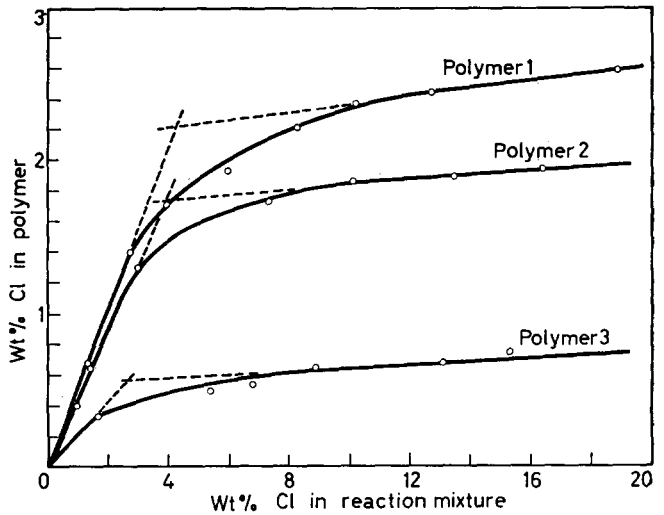

Figure 2—Reaction of radiochlorine with three butyl rubbers with different unsaturations: Polymer 1: 1·75, Polymer 2: 1·39, Polymer 3: 0·52 mole per cent

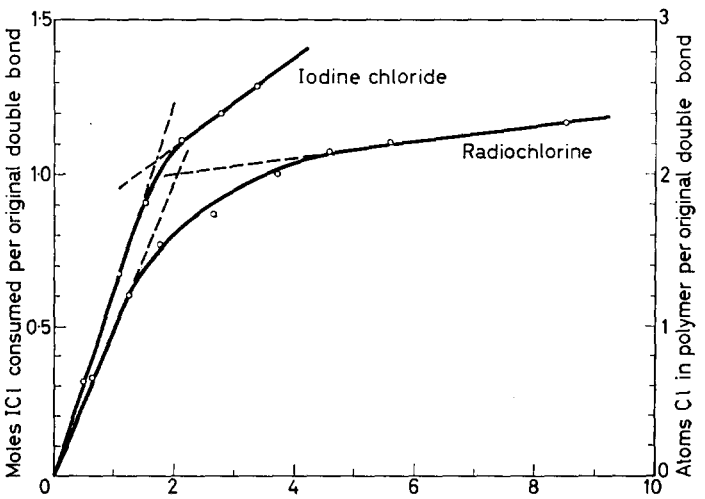

Figure 3—Comparison of the reaction of butyl rubber (Polymer 1: 1·75 mole per cent unsaturation) with radiochlorine and with iodine chloride

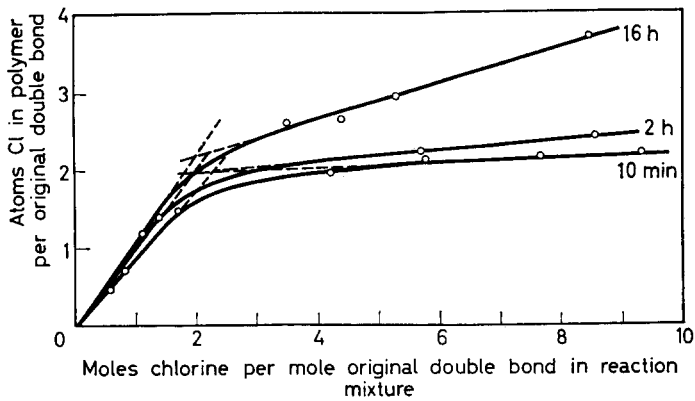

Figure 4—Effect of varying time of reaction of butyl rubber (Polymer 2: 1·39 mole per cent unsaturation) with radiochlorine

intersection, which corresponds to the reaction of almost exactly two chlorine atoms per original double bond. *Table 4* lists the extrapolated values for the three polymers. In *Figure 3*, the reaction plots for the iodine chloride and radiochlorine reactions with the same polymer are compared. Clearly the radiochlorine reaction is much less sensitive to excess halogen than is the reaction with iodine chloride.

Sensitivity to time of reaction has also been investigated. *Figure 4* shows the effect of varying time of reaction from 10 minutes to 16 hours for polymer 2. Satisfactory extrapolated values are obtained for the 10 minute and 2 hour plots, but somewhat high results are obtained after 16 hours.

It is clear from these experiments that reaction of chlorine with double bonds of the isoprene type proceeds without serious complication from side reactions. The radiochlorine procedure described may be used as a microanalytical method for the determination of polymer unsaturations greater than one mole per cent; it is also potentially applicable to the study of very low unsaturation contents of polymers, using larger samples, provided due precautions are taken to ensure that results are not vitiated by reaction of chlorine with impurities such as monomer present in the polymer.

Nature of the reaction between chlorine and butyl rubber

From consideration of the results of this and previous work, it is now possible to put forward suggestions as to the mechanism of the reaction between chlorine and butyl rubber in the absence of air and light. The following evidence is now available:

(*i*) Two chlorine atoms become incorporated in the polymer for every double bond originally present (*Figures 2* and *3*, *Table 4*).

(*ii*) The incorporation of the first chlorine atom is very rapid, that of the second less so (*Figure 2*).

(*iii*) Chlorine does not react by addition, since, even with prolonged

reaction and excess polymer only 50 per cent, or less, of the chlorine initially present appears in the reacted polymer (*Figure 4*).

(*iv*) There is evidence for allylic chlorine in butyl rubber[8].

(*v*) There is a possibility that some 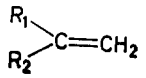

structures arise in the polymer in the reaction[8].

(*vi*) Isobutene monomer reacts with chlorine (1 mol.) by the reaction[9]

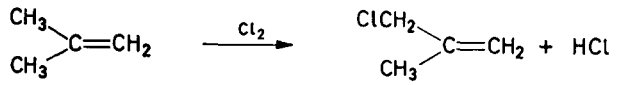

The following mechanism is proposed to account for these facts. In view of the absence of appreciable side reactions except with large excesses of chlorine and prolonged reaction, a free radical mechanism is unlikely. By analogy with the isobutene reaction, chlorine is assumed to enter the polymer mainly by substitution at the methyl group.

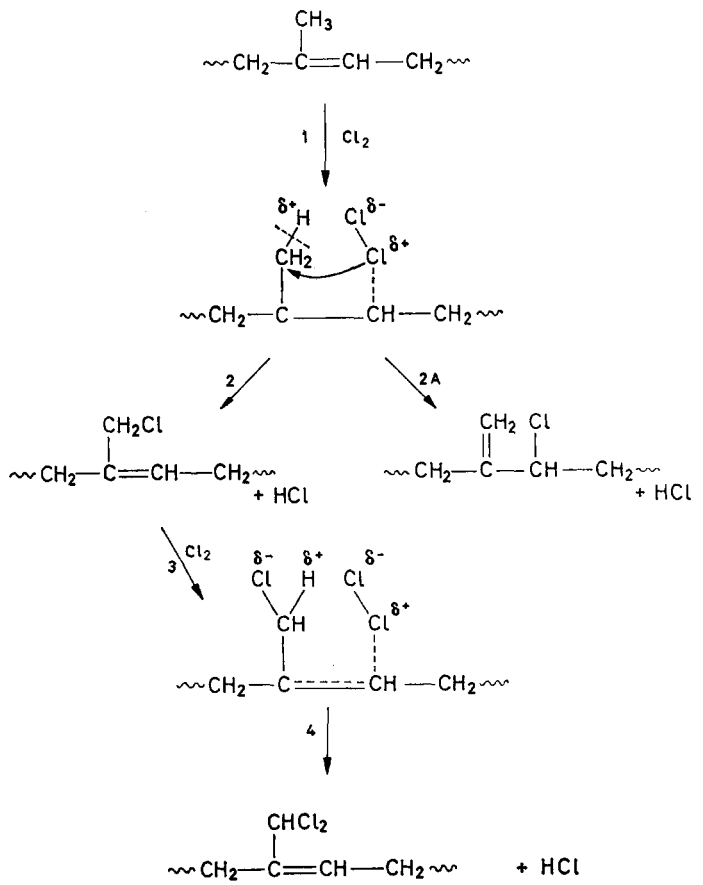

It is suggested that reaction 3 is slower than reaction 1 because of the bulk of the chlorine atom, preventing access of the chlorine molecule to the double bond. Further reaction of the dichloro product may be very slow for the same reason.

I am indebted to Mr G. R. Martin for helpful discussion, to Polymer (U.K.) Ltd, for providing the butyl rubbers used in this work, and to the University of Durham for the award of an I.C.I. Fellowship, during the tenure of which this work was carried out.

Londonderry Laboratory for Radiochemistry,
University of Durham,
South Road, Durham

(*Received April 1962*)

REFERENCES

[1] GALLO, S. G., WEISE, H. K. and NELSON, J. F. *Industr. Engng Chem. (Industr.)*, 1948, **40,** 1277
[2] LEE, T. S., KOLTHOFF, I. M. and JOHNSON, E. *Analyt. Chem.* 1950, **22,** 995
[3] REHNER, J. *Industr. Engng Chem. (Industr.)*, 1944, **36,** 118
[4] REHNER, J. and GRAY, P. *Industr. Engng Chem. (Anal.)*, 1947, **17,** 367
[5] BUCKWATER, H. M. and WAGNER, E. C. *J. Amer. chem. Soc.* 1930, **52,** 5241
[6] MCNALL, L. R. and EBY, L. T. *Analyt. Chem.* 1957, **29,** 951
[7] MCNEILL, I. C. *J. chem. Soc.* **1961,** 639
[8] BALDWIN, F. P., BUCKLEY, D. J., KUNTZ, I. and ROBISON, S. B. *Rubber Plastics Age,* 1961, **42,** 500
[9] MAYER, G., KURIACOSE, J. C. and ESCHARD, F. *Bull. Soc. chim. Fr.* **1961,** 624

The Low Frequency Dielectric Relaxation of Polyoxymethylene (Delrin) using a Direct Current Technique

G. WILLIAMS

The dielectric measurements on polyoxymethylene previously reported have been extended to the low frequency range 10^{-2} to 10^{-4} c/s using a direct current method. Measurements have been made over the temperature range 20° to −110°C. Two regions of absorption are observed and discussed in relation to the dielectric and dynamic mechanical results obtained at higher frequencies.

THE investigation of polyoxymethylene in the frequency range 10^2 c/s to 10^{10} c/s showed that the single broad relaxation absorption was very temperature dependent in the low temperature range. It is the purpose of the present work to extend the measurements to the very low frequency and low temperature range in order to see if the dielectric absorption is discontinuous near the apparent glass transition (−87°C) and also to make a more direct comparison of the temperature of maximum dielectric absorption with that obtained by dynamic mechanical measurements[1] at 0·186 c/s.

EXPERIMENTAL

The polyoxymethylene used in this experiment was Du Pont 'Delrin' 500 which has a number average molecular weight in the range 3×10^4 to 5×10^4. This was the same material as investigated previously.

The sample was 51 mm in diameter and 1·52 mm thick. Measurements were made in a three-terminal cell in order to eliminate surface conduction across the edge of the sample.

A step voltage applied to the sample produced a transient charging current. After equilibrium had been attained, removal of the voltage produced a discharge current. The currents were measured using a modified E.I.L. 37B d.c. amplifier. *Figure 1*(a) shows a schematic diagram of the experimental arrangement. The battery V and three-terminal cell are connected in series with a calibrated Victoreen resistor R_1 of either 10^{10} or 10^{12} ohms. The current flowing in the sample is measured by the d.c. amplifier as a voltage appearing across R_1. The voltage V must drop across the sample only and this is achieved by a feedback arrangement in the amplifier so that the voltage across R_2 is equal and opposite to that across R_1. The time constant of the response of the amplifier depends upon the stray capacitance between A and B. The time constant of the commercial instrument was eighteen seconds. This was reduced to 0·6 second by means of the following modifications. R_1 was mounted externally to the amplifier in a screened box. The capacitance between A and B was

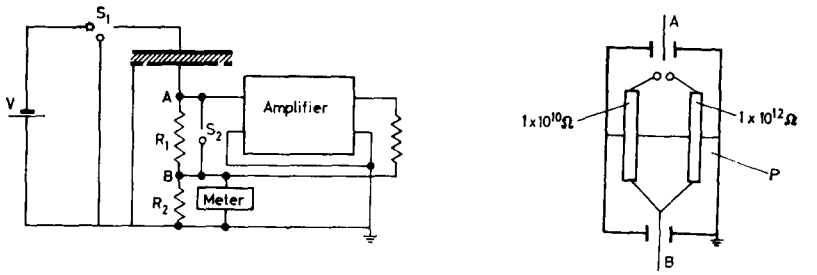

Figure 1

reduced using an earthed plate P as shown in *Figure 1*(b). The shorting switch S_2 was employed to zero the amplifier meter and to protect the amplifier against large transient currents at short times. S_2 was a manual make-and-break device so that there was zero capacitance associated with it in the open condition. Step voltages in the range 60 to 240 V were applied to the sample to confirm that the super-position principle was obeyed and that other non-linear effects were absent. The charging and discharging currents for the polyoxymethylene sample were in the range 10^{-11} to 10^{-14} A, and were measured over the time range of 10 to 900 seconds, depending upon the response of the dielectric. The currents could be measured to an accuracy of three per cent.

The dielectric loss factor $\varepsilon''_{(\omega)}$ at a frequency $\omega=(2\pi f)$ is given by[2,3]

$$\varepsilon''_{(\omega)}=\frac{1}{C_a}\left[\frac{G}{\omega}+\int_0^\infty \phi(t)\sin\omega t\,dt\right] \tag{1}$$

C_a is the capacitance of the electrodes when the sample is replaced by air, G is the steady conductivity of the sample. $\phi(t)$ is the current per unit voltage flowing in the sample at a time t after the application of the step voltage. The steady conductivity current was obtained as the difference between the charging and discharging currents. The dielectric loss factors given below were obtained from the approximate solution of the integral of equation (1) where $\phi(t)$ was the reversible charge–discharge current and thus did not contain the steady conductivity contribution. The solution of the transient part of equation (1) has been given by Hamon[4] and has been recently confirmed[5] for the special case of a Cole–Cole distribution of relaxation times. The loss factors are thus derived using the relations

$$\varepsilon''_{(\omega)}=\frac{\phi(t=0{\cdot}63/\omega)}{\omega C_a};\quad \omega=\frac{0{\cdot}63}{t} \tag{2}$$

These relations are valid if the double logarithmic plot $\phi(t)$ against time has a slope β in the range $0{\cdot}1<\beta\leqslant 1{\cdot}2$.

The cell was placed in a Dewar flask and using methanol–carbon dioxide mixtures down to $-76°C$ and methanol–liquid nitrogen mixtures down to $-110°C$, the low temperatures were obtained and maintained to $\pm 0{\cdot}1°C$.

RESULTS AND DISCUSSION

Figure 2 shows the double logarithmic current/time curve for polyoxymethylene at different temperatures. The current values given are normalized to 120 V. All currents are average charge–discharge values, where the charging current has been corrected for the steady direct current observed. In all cases, the charge–discharge currents were within two to five per cent of each other depending upon the magnitude of the current observed. The two significant features of *Figure 2* are that the current/time slopes are temperature dependent and the magnitude of the current at short times (10 seconds, say) decreases with decreasing temperature to a steady value between about $-35°$ to $-55°C$ then increases rapidly to a maximum in the region of $-80°$ then decreases again at lower temperatures.

First let us consider the temperature dependent slopes since the transformation of equation (1) to equations (2) depends on the value of β.

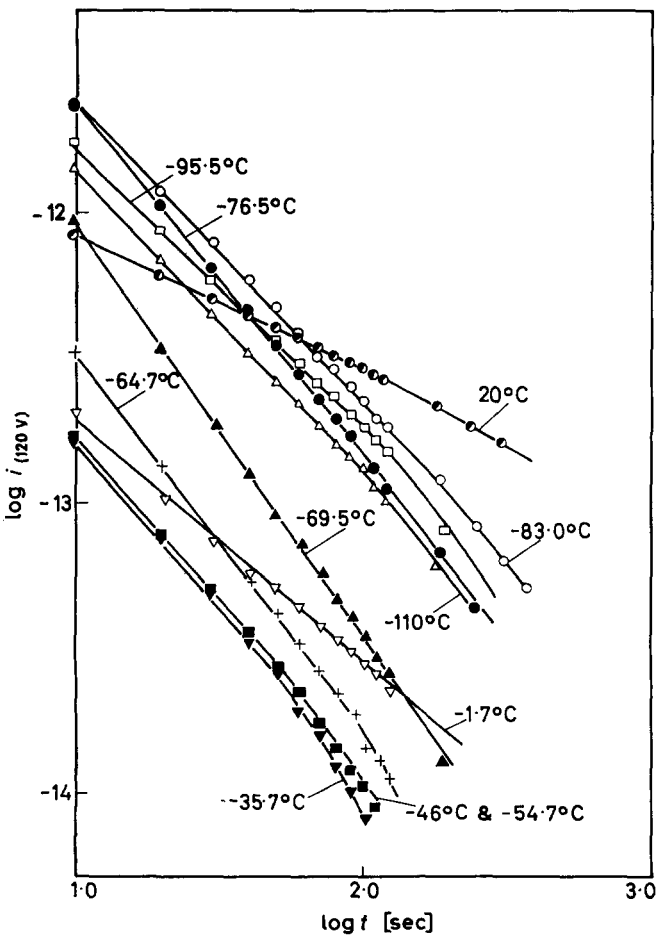

Figure 2

In all cases the current/time plots curve to larger slopes at the longest times measured but since the plots at times less than 100 sec are linear, the values of β in *Table 1* refer to initial slopes.

Table 1. β as a function of temperature

T°C	β	T°C	β
20	0·46	−64·7	1·30
−1·7	0·83	−69·5	1·43
−35·7	1·11	−76·5	1·20
−46·0	1·14	−83·0	1·04
−54·7	1·14	−95·5	1·00
		−110	1·00

It is seen that β first increases with decreasing temperature down to about −70°C then decreases to unity. The significance of this variation will be discussed after the magnitude of the temperature dependent current has been described. The transformation of the current/time data into dielectric absorption data given by equations (2) can only be applied where $0{\cdot}1 < \beta \leqslant 1{\cdot}2$, thus equations (2) have to be modified as described by the author[5] for the values in the temperature range −64°C to 70°C.

The dielectric loss factors were evaluated using equations (2) or modifications of them, and *Figure 3* shows the plot of ε'' against frequency.

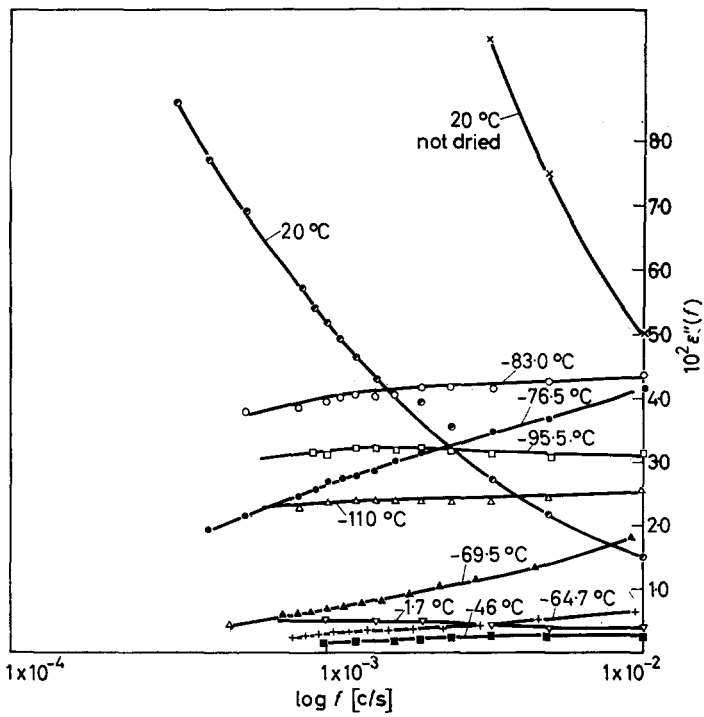

Figure 3

The results for $-35{\cdot}7°$ and $-54{\cdot}7°$ are omitted since they are almost identical with those for $-46{\cdot}0°C$. It is seen that at room temperature the loss factor increases slowly with decreasing frequency, far slower than that for a single relaxation time. Also shown in *Figure 2* are the room temperature results for the sample before drying. The loss factors of the wet sample are larger than those of the dried sample, thus the relaxation observed is either of Maxwell–Wagner type due to absorbed water or results from the effect of water on a relaxation process which occurs in the absolutely dry polymer. A slight reduction in temperature to $-1{\cdot}7°C$ reduces the loss factor to very small values. Since Maxwell–Wagner losses are due to the presence of conducting particles in a poorly conducting medium, and conductivity is exponentially dependent on temperature, the drastic reduction in the loss factor on lowering the temperature suggests that the room temperature loss mechanism is of Maxwell–Wagner type and arises from impurities and water particles in the polymer.

The loss factors are at very small values at temperatures in the range $-10°$ to $-60°C$ at about $2{\cdot}5$ to 10^{-3}. Since these very small loss factors are easily measured, it serves to emphasize the accuracy to which very small loss factors can be determined using the d.c. amplifier technique.

At $-70°C$ and $-76°C$ the loss factor values are much larger and it is seen that the measurements refer to the low frequency side of a relaxation absorption. At $-83°C$ the loss is near its maximum value for this frequency range, and is only slightly dependent on frequency. At $-95{\cdot}5°$ and $-110°$ the loss is independent of frequency and is decreasing with decreasing temperature. The curves are very broad at these low temperatures and it is not possible to define the average frequency of maximum loss.

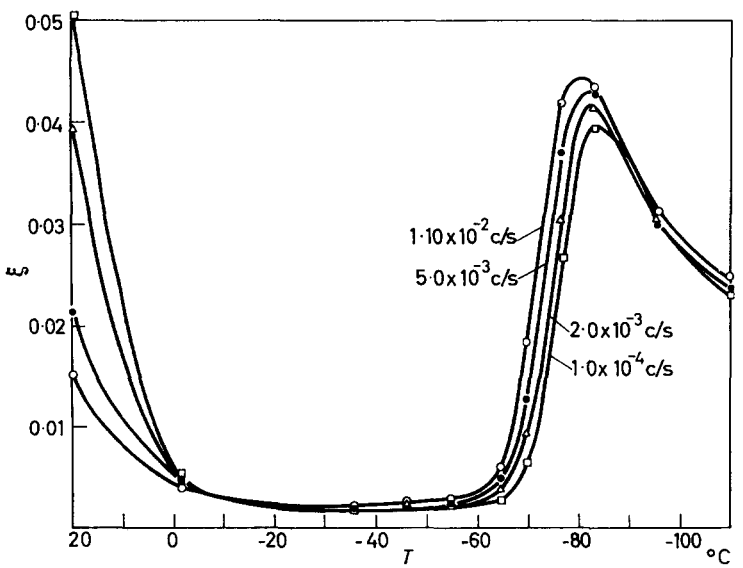

Figure 4

If, however, we plot the loss factor at constant frequencies against temperature the relaxation maxima are clearly seen. The results are shown in *Figure 4*. At temperatures above zero, the Maxwell–Wagner type absorption predominates. There is a plateau in the loss between $-20°$ and $-60°C$ then the main relaxation absorption appears. This absorption which is centred around $-80°C$, is the main dipolar relaxation mechanism previously described and is due to reorientation occurring in the amorphous regions of the partly crystalline polymer. The asymmetry of the absorption at lower temperatures was also observed at higher frequencies and is due to a temperature dependent distribution of relaxation times.

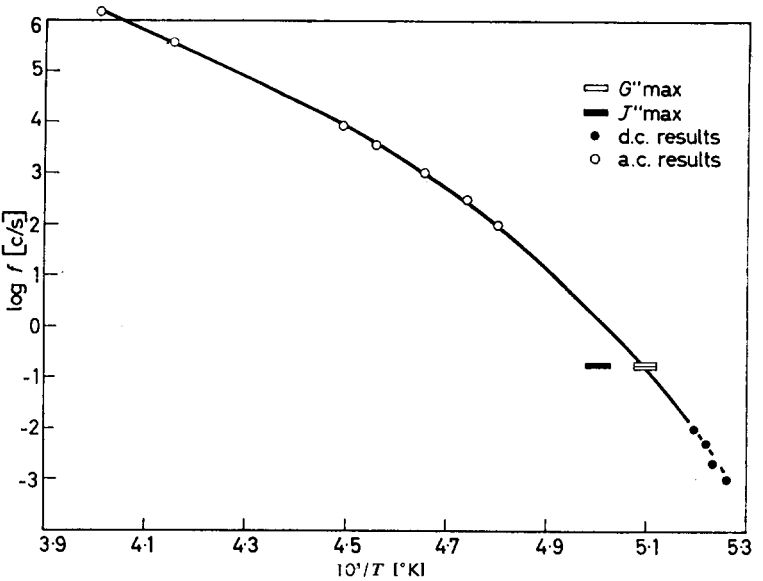

Figure 5

In *Figure 5* the temperatures of maximum dielectric loss for given constant frequencies are plotted against frequency. The open circles correspond to the higher frequency results previously obtained. The filled circles correspond to the points derived from *Figure 4*. The d.c. values are seen to lie on the smooth extrapolation of the higher frequency data. The open and filled bar points in *Figure 5* correspond to the imaginary components of the complex shear modulus G'' and compliance (J''). It is seen that the G'' point lies on the dielectric curve, but the J'' point is about four degrees higher in temperature. Since the mechanical and dielectric relaxation processes should be compared as ε'' to J'' a discrepancy is present between the two types of measurement. However, it is rare that mechanical and dielectric maxima compare within ten degrees. It is of interest to note that the plots of G'', J'' and ε'' against temperature were compared and it was found that the G'' and ε'' plots when normalized had almost identical shapes. The J'' plot was more symmetrical at lower temperatures as expected. Thus the present data show a better comparison between G'' and ε'' data than is obtained from J'' and ε'' data.

The values of β given in *Table 1* can now be explained. At room temperature the measurements refer to the high frequency side of a Maxwell–Wagner type absorption. Between $-20°$ and $-68°$ β is unity since polyoxymethylene has a small frequency and temperature independent loss around $2{\cdot}5 \times 10^{-3}$. Between $-65°$ and $-78°$C the measurements refer to the low frequency side of the main dipole relaxation and if the dielectric conformed exactly to a Cole–Cole type distribution it has been shown[5,6] that the slope is given by

$$\beta = (1 + n)$$

where n is the Cole–Cole parameter. It is seen from *Table 1* that β is $1{\cdot}3 \pm 0{\cdot}1$ in this range, thus we calculate the Cole–Cole parameter n as $0{\cdot}3 \pm 0{\cdot}1$. From the Cole–Cole 'n' value we may estimate[7] the Fuoss–Kirkwood distribution parameter γ as $0{\cdot}2 \pm 0{\cdot}1$. These rough estimates of the distribution are in agreement with the values obtained previously in this temperature range[1] and serve to emphasize the breadth of the loss factor/frequency curves at lower temperatures. At temperatures lower than $-80°$C the β values are near unity. Since the distribution is so broad at these temperatures it is not possible to conclude from the β value that γ is zero, but with the results at higher temperatures we strongly suggest that at temperatures below about $-85°$C the distribution is very broad leading to loss factor/frequency curves which are nearly independent of frequency over several decades. The apparent glass transition has been determined from specific volume/temperature measurements[8] and is found to be $-87° \pm 2°$C at a cooling rate of $0{\cdot}1°$C per minute. Since the specific volume measurements are not made at precise thermal equilibrium at each temperature it is not possible to say that a true thermodynamic glass temperature exists for polyoxymethylene. It is, however, significant that the dielectric measurements which correspond to the same time scale show a relaxation maximum in the temperature range $-82°$ to $-84°$C. Inspection of *Figure 5* shows that if measurements are made to still lower frequencies, since the plot is curved and the $(1/T)$ scale is an expanding one at lower temperatures, the ultimate temperature of maximum loss at the lowest measurable frequencies is predicted to be $-87° \pm 2°$C. Also in this temperature range it is predicted that the distribution of relaxation times becomes very broad.

CONCLUSION

Using a d.c. method the very low frequency dielectric behaviour of polyoxymethylene has been examined. Two main regions of absorption were observed. At higher temperatures the loss increases with decreasing frequency, but no maximum is observed. Since this absorption depended upon the moisture content of the sample it is presumed to be due to water or impurities in the polymer. At low temperatures the main dipole relaxation process is observed and is found to be a continuation of the results obtained previously. It is found that the position of the low temperature mechanical loss agrees well with the present results. The temperature of maximum loss at the lowest frequencies measured is in good agreement with the apparent glass transition obtained from specific volume measurements.

The author acknowledges the assistance and advice of Dr D. W. Ovenall and Mr D. G. Moss of this Laboratory and also discussions with Mr Desty of B.P. Research Laboratories on the modification of the electrometer apparatus. This work forms part of the research programme of the National Physical Laboratory, and is published by permission of the Director of the Laboratory.

Basic Physics Division,
National Physical Laboratory,
Teddington, Middlesex

(*Received April 1962*)

REFERENCES

[1] READ, B. E. and WILLIAMS, G. *Polymer, Lond.* 1961, **2,** 239
[2] GROSS, B. *Phys. Rev.* 1941, **59,** 748
[3] FRÖHLICH, H. *Theory of Dielectrics.* Oxford University Press: London, 1949
[4] HAMON, B. V. *Proc. Instn elect. Engrs,* 1952, **99,** Pt IV (Monograph 27)
[5] WILLIAMS, G. *Trans. Faraday Soc.* 1961, **57,** 1979
[6] COLE, R. H. and COLE, K. S. *J. chem. Phys.* 1942, **10,** 98
[7] BÖTTCHER, C. J. F. *Theory of Electric Polarization,* p 373. Elsevier: Amsterdam and London, 1952
[8] READ, B. E. Private communication

Viscosity/Temperature Relationships for Dilute Solutions of High Polymers

R. J. FORT, R. J. HUTCHINSON, W. R. MOORE and Miss M. MURPHY

Values of Q and A in the expression $\eta = Ae^{Q/RT}$ have been obtained for dilute solutions of polyisobutylene, polyvinyl acetate, polymethyl methacrylate, cellulose trinitrate and cellulose triacetate in representative solvents. The apparent activation energy of viscous flow Q is given by

$$Q = Q_0 + K_e Mc$$

where Q_0 is the value for the solvent, M and c are the molecular weight and concentration of polymer and K_e depends on polymer and solvent. Values of K_e for the cellulose triesters are much larger than for the other polymers and it is suggested that this is due to their greater chain stiffness and extension. For the polymers with flexible chains

$$A = A_0 + K_a M^{\beta} c$$

over a limited molecular weight range but with the cellulose triesters

$$A = A_0 \exp(-K_a' M^{\alpha} c)$$

where A_0 is the value for the solvent and K_a, K_a', α and β depend on polymer and solvent. Application of rate theory suggests that the entropy of activation of viscous flow decreases with increasing c and M for solutions of flexible chain polymers but that the reverse is true for solutions of stiff, extended cellulose derivative chains. Equations are derived relating the intrinsic viscosity to K_e, K_a or K_a', α or β, M and T.

INVESTIGATIONS of viscosity/temperature relationships for dilute solutions of high polymers seem to have been largely restricted to the effects of temperature changes on viscosity numbers or intrinsic viscosities and on parameters derived from these. Although a number of studies have been made of the effects of temperature changes on the actual viscosities of concentrated solutions[1] few comparable studies have been made with dilute solutions and these have been concerned with cellulose derivatives. Studies of the temperature dependence of viscosities of dilute solutions of ethyl cellulose[2] and of an incompletely substituted cellulose nitrate[3] show that both the pre-exponential term A and the apparent activation energy of viscous flow Q in the expression

$$\eta = A\, e^{Q/RT} \tag{1}$$

where η is the viscosity, depend on both the concentration c and the molecular weight M of the polymer. For concentrations in the range 0·1 to 0·4 g/dl it is generally found that

$$A = A_0 \exp(-K_a M^{\alpha} c) \tag{2}$$

and

$$Q = Q_0 + K_e Mc \tag{3}$$

where A_0 and Q_0 are values for the pure solvents and K_a, K_e and α are constants whose values depend on solvent and polymer.

Extension of such studies to dilute solutions of other polymers shows that the variations of A and Q with c and M obtained when dilute solutions of more flexible and less polar polymers are used differ markedly from those obtained with comparable solutions of cellulose derivatives. Differences in the values of $(A-A_0)$ and $(Q-Q_0)$ for one per cent solutions of different polymers of comparable molecular weight have been reported[4]. This paper reports more detailed studies of the variations of A and Q with c and M obtained using dilute solutions of fractions of polyisobutylene, polyvinyl acetate, polymethyl methacrylate, cellulose trinitrate and cellulose triacetate. Polyisobutylene was chosen as an example of a non-polar, flexible polymer and polyvinyl acetate and polymethyl methacrylate as examples of flexible polar polymers with possibly differing flexibility[5]. Cellulose trinitrate was used in order that results could be compared with those for the incompletely substituted nitrate[3]. The chains of the latter, although stiff, are believed to possess some degree of flexibility and the chain stiffness of cellulose nitrate has been found to increase with increasing degree of substitution[6]. The triacetate was used as an example of a triester which is believed to be less stiff than the trinitrate[7].

EXPERIMENTAL

Materials

Polyisobutylene—Three sub-fractions were used, obtained by stepwise precipitation on addition of methanol to one per cent solutions of the polymer in benzene. Their number average molecular weights, obtained osmotically in cyclohexane at 25°C, were 485 000, 250 000 and 90 000. Cyclohexane was used as solvent in viscosity determinations.

Polyvinyl acetate—Six sub-fractions were used, with number average molecular weights 340 000, 217 000, 148 000, 141 000, 61 000 and 40 000. Methods of fractionation and characterization of these fractions have been described[8]. Acetone, dioxan, chloroform, toluene and methanol were used as solvents in viscosity determinations.

Polymethyl methacrylate—Six sub-fractions were used, with number average molecular weights 406 000, 325 000, 314 000, 297 000, 122 000 and 48 000. Methods of fractionation and characterization of fractions have been described[9]. Acetone, toluene, benzene and chloroform were used as solvents in viscosity determinations.

Cellulose trinitrate—Four sub-fractions, the preparation and characterization of which have been described[6], were used. Their number average molecular weights were 175 000, 148 000, 130 000 and 90 000. The nitrogen content of each was $13{\cdot}8 \pm 0{\cdot}1$ per cent. Acetone was used as solvent in viscosity determinations.

Cellulose triacetate—Three sub-fractions were used, obtained by non-degradative acetylation[10] of sub-fractions of a secondary cellulose acetate which were obtained by methods previously described[11]. The acetic acid yield of each was $62{\cdot}5 \pm 0{\cdot}1$ per cent and their number average molecular weights, obtained osmotically in chloroform at 25°C, were 107 000, 69 000 and 56 000. Chloroform was used as solvent in viscosity determinations.

All solvents were purified and dried by appropriate methods and fractionally distilled just before use. Solutions were prepared at 20°C one week before use and allowed to stand in the dark at room temperature until required.

Viscosity determinations

Viscosities of the pure solvents and of solutions in the concentration range 0·1 to 1·0 g/dl at 20°C were measured at several temperatures in the range 18° to 70°C, the range used depending on the solvent. Capillary viscometers were used and were of such dimensions as to eliminate shear effects. The viscometers used were calibrated over the temperature range used and kinetic energy corrections were made where applicable. Measurements were made in thermostatically controlled water baths, the temperatures of which could be maintained to $\pm 0{\cdot}02°$ of any temperature in the range used. The viscometers were fitted with small glass bulbs containing glass wool soaked with solvent to prevent evaporation at the higher temperatures used. All solutions were filtered before use. Viscosities of the pure solvents at the different temperatures were in good agreement with published values[12,13].

RESULTS

Figure 1 shows typical plots of $\log \eta$ against $1/T$. All are linear over the temperature range used. Values of Q and A were obtained from such plots

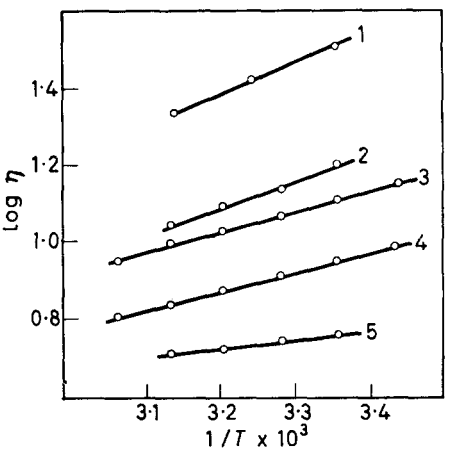

Figure 1—Log η as a function of $1/T$. 1, polyisobutylene, $\overline{M}_N$ 250 000, 1 per cent in cyclohexane. 2, cellulose trinitrate, $\overline{M}_N$ 175 000, 0·4 per cent in acetone. 3, polyvinyl acetate, $\overline{M}_N$ 148 000, 1 per cent in chloroform. 4, cellulose triacetate, $\overline{M}_N$ 107 000, 0·4 per cent in chloroform. 5, polymethyl methacrylate, $\overline{M}_N$ 406 000, 1 per cent in acetone

by the method of least squares. *Figure 2* shows typical plots of Q against c for solutions of the polymers with flexible chains. These are linear with intercepts Q_0 in good agreement with published values for the solvents[14]. Q appears to be independent of c for polyvinyl acetate in toluene. Q decreases with increasing concentration in all cases involving polymethyl methacrylate and the same is true for polyvinyl acetate in methanol. In all other cases Q increases with increase of c. *Figure 3* shows Q as a function of c for solutions of the cellulose triester fractions. The plots are linear

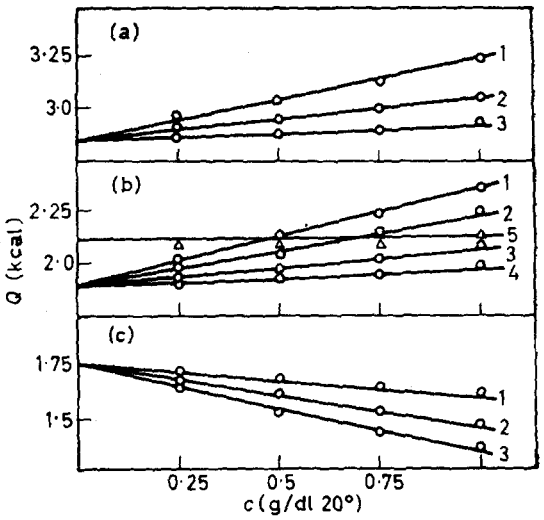

Figure 2—Apparent activation energy of viscous flow as a function of concentration. (a) polyisobutylene–cyclohexane. 1, $\overline{M}_N$ 485 000; 2, $\overline{M}_N$ 250 000; 3, $\overline{M}_N$ 90 000. (b) polyvinyl acetate. 1, 2, 3 and 4 refer to fractions of $\overline{M}_N$ 217 000, 141 000, 61 000 and 43 000 respectively in chloroform; 5 refers to $\overline{M}_N$ 217 000 in toluene. (c) polymethyl methacrylate–acetone. 1, $\overline{M}_N$ 48 000; 2, $\overline{M}_N$ 297 000; 3, $\overline{M}_N$ 406 000

and the rates of increase of Q with c are considerably greater than those obtained with the polymers with flexible chains. In all cases, however, we may write

$$Q = Q_0 + k_e c \tag{4}$$

where k_e depends on solvent, polymer and molecular weight and may be positive, negative or zero. *Figures 4* and *5* show typical plots of k_e against $\overline{M}_N$. These are linear so that, in each case,

$$k_e = K_e M \tag{5}$$

and

$$Q = Q_0 + K_e M c \tag{3}$$

where K_e, values of which are given in *Table 1*, depends on the polymer and the solvent.

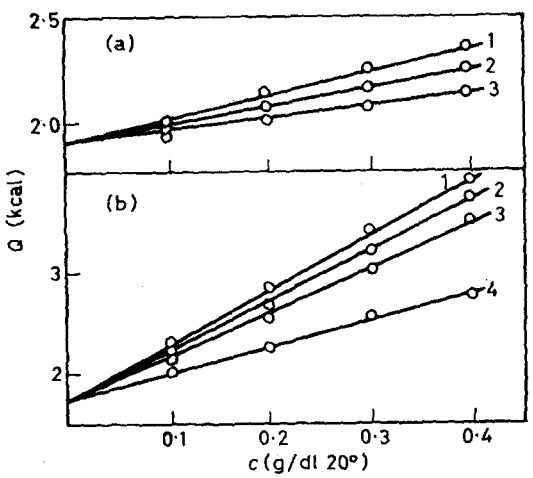

Figure 3—Apparent activation energy of viscous flow as a function of concentration. (a) cellulose triacetate–chloroform. 1, $\overline{M}_N$ 107 000; 2, $\overline{M}_N$ 69 000; 3, $\overline{M}_N$ 56 000. (b) cellulose trinitrate–acetone. 1, $\overline{M}_N$ 175 000; 2, $\overline{M}_N$ 148 000; 3, $\overline{M}_N$ 130 000; 4, $\overline{M}_N$ 90 000

Figure 6 shows typical plots of A against c for the polymers with flexible chains. All seem to be linear and to extrapolate to values of A_0 in good agreement with published values where these are available[14]. We may write

$$A = A_0 + k_a c \tag{6}$$

where k_a depends on polymer, solvent and M. In the cases involving the cellulose triesters A is not a linear function of c but, as shown in *Figure 7*

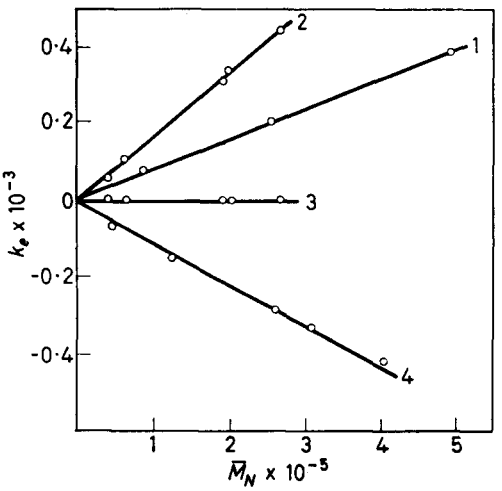

Figure 4—k_e as a function of $\overline{M}_N$. 1, polyisobutylene–cyclohexane. 2, polyvinyl acetate–chloroform. 3, polyvinyl acetate–toluene. 4, polymethyl methacrylate–acetone

and in agreement with other results for cellulose derivatives[2,3], $-\log A$ seems to be directly proportional to c so that

$$-\log A = -\log A_0 + k'_a c \tag{7}$$

where k'_a depends on polymer, solvent and M.

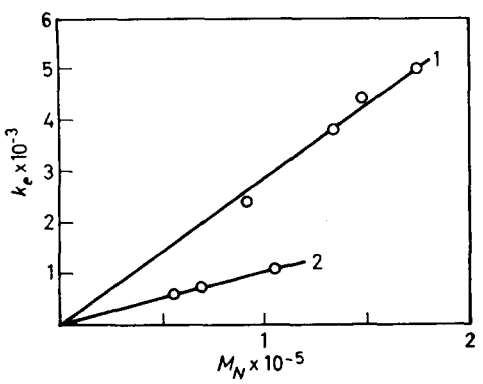

Figure 5—k_e as a function of $\overline{M}_N$. 1, cellulose trinitrate–acetone. 2, cellulose triacetate–chloroform

k_a is not a linear function of M but, as shown in *Figure 8*, a plot of $\log k_a$ against $\log \overline{M}_N$ is linear over the molecular weight range covered for polyisobutylene. The same seems to be true for polyvinyl acetate and polymethyl methacrylate up to molecular weights of about 300 000. The

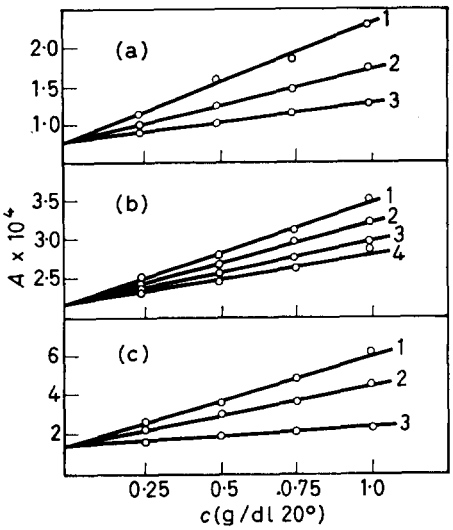

Figure 6—A as a function of concentration. (a) polyisobutylene–cyclohexane. 1, $\overline{M}_N$ 485 000; 2, $\overline{M}_N$ 250 000; 3, $\overline{M}_N$ 90 000. (b) polyvinyl acetate–chloroform. 1, $\overline{M}_N$ 217 000; 2, $\overline{M}_N$ 141 000; 3, $\overline{M}_N$ 61 000; 4, $\overline{M}_N$ 43 000. (c) polymethyl methacrylate–acetone. 1, $\overline{M}_N$ 406 000; 2, $\overline{M}_N$ 297 000; 3, $\overline{M}_N$ 48 000

plots tend to curve upward at higher molecular weights. For the molecular weight ranges within which the plots are effectively linear we may write, to a first approximation,

$$k_a = K_a M^{\beta} \tag{8}$$

and

$$A = A_0 + K_a M^{\beta} c \tag{9}$$

where the constants K_a and β depend on polymer and solvent. k'_a is not directly proportional to M but, as shown in *Figure 9*, a plot of $\log k'_a$ against $\log \overline{M}_N$ is approximately linear. Slight curvature is possible but, again, to a first approximation,

$$k'_a = K'_a M^{a} c \tag{10}$$

and

$$-\log A = -\log A_0 + K'_a M^{a} c \tag{11}$$

or

$$A = A_0 \exp(-K'_a M^{a} c) \tag{2'}$$

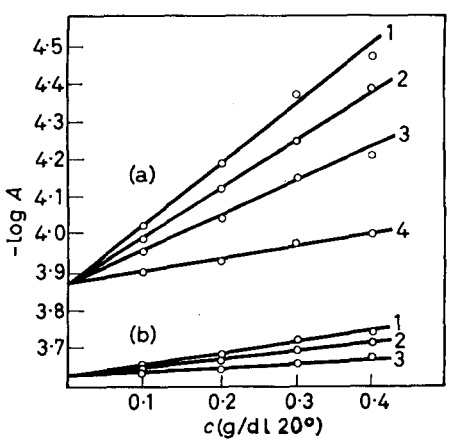

Figure 7— $-\log A$ as a function of concentration. (a) cellulose trinitrate–acetone. 1, $\overline{M}_N$ 175 000; 2, $\overline{M}_N$ 148 000; 3, $\overline{M}_N$ 130 000; 4, $\overline{M}_N$ 90 000. (b) cellulose triacetate–chloroform. 1, $\overline{M}_N$ 107 000; 2, $\overline{M}_N$ 69 000; 3, $\overline{M}_N$ 56 000

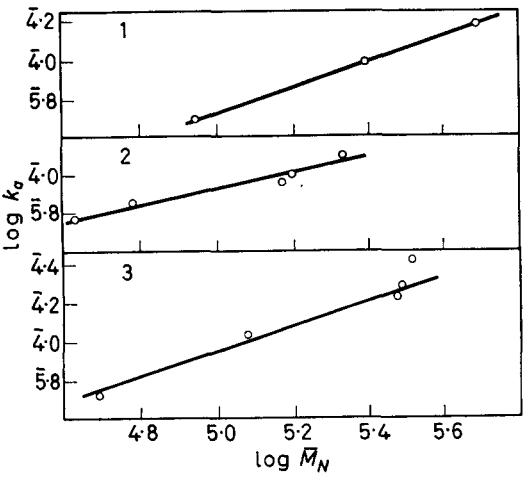

Figure 8—log k_a as a function of log $\bar{M}_N$. 1, polyisobutylene–cyclohexane. 2, polyvinyl acetate–chloroform. 3, polymethyl methacrylate–acetone

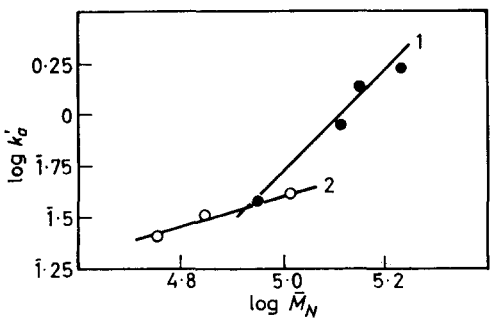

Figure 9—log k_a' as a function of log $\bar{M}_N$. 1, cellulose trinitrate–acetone. 2, cellulose triacetate–chloroform

where K_a' and α depend on polymer and solvent. Values of K_a, K_a', α and β are given in *Table 1*.

Table 1. Values of K_a, K_a', α and β

Polymer	*Solvent*	K_e	K_a	K_a'	α	β
Polyisobutylene	Cyclohexane	$7{\cdot}8\times10^{-4}$	$1{\cdot}55\times10^{-4}$			0·71
	Toluene	Nil	$1{\cdot}77\times10^{-4}$			0·51
	Chloroform	$2{\cdot}0\times10^{-3}$	$8{\cdot}7\times10^{-4}$			0·59
Polyvinyl acetate	Acetone	$1{\cdot}5\times10^{-3}$	$2{\cdot}0\times10^{-4}$			0·63
	Dioxan	$1{\cdot}5\times10^{-3}$	$2{\cdot}6\times10^{-4}$			0·58
	Methanol	$-2{\cdot}1\times10^{-3}$	$1{\cdot}1\times10^{-4}$			0·57
	Acetone	$-1{\cdot}2\times10^{-3}$	$1{\cdot}0\times10^{-4}$			0·77
Polymethyl methacrylate	Benzene	$-2{\cdot}1\times10^{-4}$	$3{\cdot}9\times10^{-5}$			0·80
	Toluene	$-6{\cdot}1\times10^{-4}$	$5{\cdot}2\times10^{-5}$			0·82
	Chloroform	$-3{\cdot}5\times10^{-4}$	$1{\cdot}27\times10^{-4}$			0·79
Cellulose nitrate	Acetone	$2{\cdot}75\times10^{-2}$		$4{\cdot}7\times10^{-14}$	2·6	
Cellulose triacetate	Chloroform	$1{\cdot}0\times10^{-2}$		$2{\cdot}1\times10^{-6}$	0·62	

DISCUSSION

K_e represents the contribution to Q made by unit polymer concentration and molecular weight. Marked differences are seen between values for systems involving the two types of polymers. For those in which flexible chains are concerned K_e may be positive, zero or negative and, if not zero, its magnitude is ten to a hundred times smaller than values for the systems

involving the cellulose triesters where K_e is positive and of similar magnitude to values for other systems involving cellulose derivatives[2,3].

Such marked differences may possibly be related to differences in chain flexibility and extension. Chains of cellulose derivatives are stiff and adopt extended forms even in poor solvents[7]. Those of flexible chain polymers adopt much more coiled and contracted forms even in good solvents. Stiff, extended chains, which may overlap or interfere hydrodynamically at the concentrations used might be expected to cause greater interference with the flow of the solvent and make greater contributions to Q.

This correlation of K_e with chain stiffness and extension is supported by comparisons of the values for the trinitrate and triacetate systems and of those for the trinitrate and an incompletely substituted nitrate in acetone[3]. Cellulose triacetate chains are believed to be less stiff than those of the trinitrate and to adopt somewhat less extended forms in solution[7]. The lower value of K_e in *Table 1* for the triacetate system might therefore be expected. Chain stiffness and extension in a given solvent increase with increasing degree of substitution of cellulose nitrate[6] and the value of K_e for the incompletely substituted nitrate is close to that for the triacetate in chloroform.

The variation of K_e with solvent in systems involving the incompletely substituted nitrate may also support the view that K_e and chain extension are related. The value of the exponent a in the Mark–Houwinck equation

$$[\eta] = KM^a \tag{12}$$

where $[\eta]$ is the intrinsic viscosity and K and a are constants for a particular polymer–solvent system, may be regarded as a measure of chain extension, larger values implying greater extension. *Table 2* gives values of K_e and a for the incompletely substituted nitrate.

Table 2. Values of K_e and a for a 12·2% N nitrate[3]

Solvent	$K_e \times 10^2$	a (25°C)
Acetone	1·1	0·80
Cyclohexanone	2·0	0·81
Methyl acetate	1·4	0·835
n-Butyl acetate	2·7	0·91

Although other factors seem to be operative, K_e tends to increase as a increases. It may be noted that the value of K_e for butyl acetate, for which a is 0·91, is very close to that for the trinitrate in acetone with an exponent a of 0·92 at 25°C[6].

The variation of K_e with solvent in the polyvinyl acetate and polymethyl methacrylate systems might also be connected, at least partly, with differences in chain extension resulting from differing solvent power. The order of solvent power for polyvinyl acetate[5,8] is chloroform > dioxan > acetone > toluene > methanol and K_e decreases in this order. The zero value with toluene and the negative one with methanol might be connected with association of polymer which is believed to occur in these solvents[9] but it is not clear how this could lead to no change or a reduction in Q as c

and M are increased. Association is also unlikely to be responsible for all the negative values of K_e in the polymethyl methacrylate systems since chloroform can be regarded as a good solvent in which association is improbable. The other solvents are poorer with order of solvent power benzene > toluene > acetone[5,9] and negative values of K_e increase as solvent power decreases, the value of K_e for benzene being very small and that for acetone relatively large. The chains may be tightly coiled or associated in these poorer solvents and this may, in some way, lead to decreases in Q as c and M increase. This cannot, however, be the case with chloroform in which the chains are believed to be solvated and relatively extended. It is not clear why Q is reduced in this case or in those where tight coiling or association may occur.

Even more marked differences between the two types of polymer are seen in the variation of the pre-exponential term A with c and M. With flexible chain polymers A is a linear function of c and, over a limited molecular weight range, approximately proportional to a power of M, this power varying from about 0·5 to about 0·8. Values of β are somewhat greater and those of K_a somewhat less for the polymethyl methacrylate systems perhaps because of their slightly greater chain stiffness[5]. With cellulose triesters, as in other cases involving cellulose derivatives[2,3], $-\log A$ is linearly related to c and to a power of M. Values of K_a for the polyvinyl acetate systems seem to increase with increasing solvent power but this does not seem to be so with the polymethyl methacrylate systems.

The significance of the constants K_a, K'_a, α and β is not very clear but they would seem to be related to the entropy of activation of viscous flow ΔS. In terms of rate theory[15]

$$\eta = (N\mathbf{h}/V)\, e^{-\Delta S/R} e^{Q/RT} \tag{13}$$

where N is the Avogadro number, $\mathbf{h}$ Planck's constant and V the molar volume of the liquid. From equations (1) and (13)

$$A = (N\mathbf{h}/V)\, e^{-\Delta S/R} \tag{14}$$

For the dilute solutions considered V will differ little from the value for the solvent and the value of A will depend primarily on that of ΔS. Flexible chains presumably lead to a decrease in ΔS while the cellulose derivatives lead to an increase. From equation (14)

$$-\log A = -\log (N\mathbf{h}/V) + \Delta S/R \tag{15}$$

$-\log A$ is a linear function of c for the concentration and molecular weight ranges applying to the cellulose triesters so that within these ranges ΔS would seem to be directly proportional to c, at least to a first approximation.

Barrer[14] has pointed out that the entropy of activation of viscous flow is made up of two parts:

(*1*) A positive component proportional to Q/T

(*2*) A negative component not primarily dependent on Q and resulting from synchronization between intermolecular movements necessary for a successful unit act of flow.

If Q/T is small the positive component may be less important than the negative so that ΔS is negative. This usually applies with pure liquids, only those with high values of Q having positive values of ΔS.

The marked increases in Q with increasing c and M for the systems involving the cellulose derivatives with stiff, extended chains would lead to corresponding increases in the positive component of ΔS which may be large enough to offset any increases in the negative component so that ΔS may increase with c and M. The contribution of the negative component presumably increases with c and M for systems involving flexible chains and in cases where K_e is positive such increases must be greater than the small ones of the positive component. It may be significant that the values of A for lower molecular weight fractions of the incompletely substituted cellulose nitrate increase[3] with c like those for systems involving flexible chains. k_e is relatively small in these cases and the negative component may increase more rapidly with c than the positive component. When K_e is negative the positive component will decrease as c and M increase and increases in the negative component might be expected to lead to reductions in ΔS. Although the physical significance of the negative component of ΔS is not very clear the presence of polymer may lead to increased synchronization of intermolecular movements but it is not clear whether these involve polymer and solvent or solvent only. Different synchronization might be required in the flow of solvent through or past the contracted semipermeable coils of flexible chains than in flow past the stiff extended chains of cellulose derivatives.

It is possible, from equations (1), (3) and (9), to derive an expression relating the intrinsic viscosity of a flexible chain polymer to its molecular weight and the temperature. The specific viscosity, $(\eta-\eta_0)/\eta_0$, may be written, from equation (1), as

$$\eta_{sp}=(A\ e^{Q/RT}-A_0\ e^{Q_0/RT})/A_0\ e^{Q_0/RT} \tag{16}$$

Substituting from equations (3) and (9) in (16) and simplifying gives

$$\eta_{sp}=[1+(K_aM^\beta c)]\ e^{K_eMc/RT}-1 \tag{17}$$

which, on expansion and neglect of terms beyond c^2, gives

$$\eta_{sp}/c=K_eM/RT+K_aM^\beta/A_0+K_e^2M^2c/2R^2T^2+K_aK_eM^{1+\beta}c/A_0RT \tag{18}$$

from which

$$[\eta]=\lim_{c\to 0}\eta_{sp}/c=K_eM/RT+K_aM^\beta/A_0=K_1M+K_2M^\beta \tag{19}$$

where

$$K_1=K_e/RT \text{ and } K_2=K_a/A_0$$

For cellulose derivatives, in a similar way[2,3], it may be shown that substitution from equations (3) and (11) in (16), simplifying and expansion, lead to:

$$[\eta]=K_eM/RT-K'_aM^a=K_1M-K'_aM^a \tag{20}$$

Values of K_1 and K_2 at 25°C are given in *Table 3*.

Table 3. Values of K_1 and K_2

Polymer	*Solvent*	K_1	K_2
Polyisobutylene	Cyclohexane	$1{\cdot}3\times10^{-6}$	$2{\cdot}1\times10^{-4}$
	Toluene	Nil	$10{\cdot}9\times10^{-4}$
	Chloroform	$3{\cdot}5\times10^{-6}$	$4{\cdot}0\times10^{-4}$
Polyvinyl acetate	Acetone	$2{\cdot}5\times10^{-6}$	$1{\cdot}4\times10^{-4}$
	Dioxan	$2{\cdot}5\times10^{-6}$	$3{\cdot}4\times10^{-4}$
	Methanol	$-3{\cdot}6\times10^{-6}$	$13{\cdot}4\times10^{-4}$
Polymethyl methacrylate	Acetone	$-2{\cdot}0\times10^{-6}$	$6{\cdot}3\times10^{-5}$
	Benzene	$-3{\cdot}5\times10^{-7}$	$3{\cdot}8\times10^{-5}$
	Toluene	$-1{\cdot}0\times10^{-6}$	$3{\cdot}0\times10^{-5}$
	Chloroform	$-5{\cdot}9\times10^{-7}$	$5{\cdot}6\times10^{-5}$
Cellulose trinitrate	Acetone	$4{\cdot}6\times10^{-5}$	
Cellulose triacetate	Chloroform	$1{\cdot}7\times10^{-5}$	

Equations (19) and (20) are approximations and only likely to apply over the molecular weight ranges for which linear plots of $\log k_a$ and $\log k'_a$ against $\log \overline{M}_N$ were assumed to hold. Within these ranges, however, substitution of appropriate values of M in equations (19) and (20) leads to values of $[\eta]$ which are in reasonable agreement with experimental ones. In equation (19) values of K_2 are generally considerably larger than those of K_1 so that the second term on the RHS is the more important. Equation (19) may be written as

$$[\eta]=(K_1M^{1-\beta}+K_2)\,M^{\beta} \tag{21}$$

$K_1M^{1-\beta}$ is of the same order as K_2 so that equation (21) is similar to equation (12). The second term on the RHS of equation (20) will be small unless M is large and up to relatively high values of M equation (20) will approximate to a Staudinger expression. Similar variations of $[\eta]$ with M have been suggested for other cellulose derivatives[11,16,17].

It must be emphasized that the relationships obtained will only be applicable to the dilute solutions and molecular weight ranges considered. More complicated dependence of Q and A on both c and M is to be expected at higher concentrations and molecular weights.

We are grateful to Bradford City Council for a research scholarship to R.J.F.

Polymer Research Laboratories,
Department of Chemical Technology,
Bradford Institute of Technology,
Bradford, Yorkshire

(*Received April 1962*)

REFERENCES

[1] See: Fox, T. G, Gratch, S. and Loshaek, S. in *Rheology* (Ed. F. R. Eirich), Vol. I, p 463. Academic Press: New York, 1956
[2] Moore, W. R. and Brown, A. M. *J. Colloid Sci.* 1959, **14**, 1
[3] Moore, W. R. and Edge, G. D. *J. Polym. Sci.* 1960, **47**, 469

[4] MOORE, W. R. *Nature, Lond.* 1961, **191,** 1292
[5] DAOUST, H. and RINFRET, M. *J. Colloid Sci.* 1952, **7,** 11
[6] MOORE, W. R. and PEARSON, G. P. *Polymer, Lond.* 1960, **1,** 144
[7] IMMERGUT, E. H. and EIRICH, F. R. *Industr. Engng Chem.* (*Industr.*), 1953, **45,** 2500
[8] MOORE, W. R. and MURPHY, M. *J. Polym. Sci.* 1962, **56,** 519
[9] MOORE, W. R. and FORT, R. J. *J. Polym. Sci.* In press
[10] HOWLETT, F. *Shirley Inst. Mem.* 1941–3, **18,** 241
[11] MOORE, W. R. and TIDSWELL, B. M. *J. appl. Chem.* 1958, **8,** 232
[12] TIMMERMANS, J. *Physicochemical Constants of Pure Organic Compounds.* Elsevier: Amsterdam, 1950
[13] *International Critical Tables.* McGraw-Hill: New York, 1926.
[14] BARRER, R. M. *Trans. Faraday Soc.* 1943, **39,** 48
[15] EYRING, H. *J. chem. Phys.* 1936, **4,** 283
[16] MOORE, W. R. and BROWN, A. M. *J. appl. Chem.* 1958, **8,** 363
[17] BADGLEY, W. J. and MARK, H. *J. phys. Colloid Chem.* 1947, **51,** 58

Infra-red Spectra and Chain Arrangement in Some Polyamides, Polypeptides and Fibrous Proteins

E. M. BRADBURY* and A. ELLIOTT†

The weak amide bands which Miyazawa has recently interpreted in polypeptide spectra as arising from interaction between molecular vibrations in amide groups have been examined in a homologous series of polyamides. This has enabled the contributions from inter- and intra-molecular interactions to be clearly distinguished. The diagnostic value of these weak bands is critically considered in the light of the more accurate interaction constants now available. It is concluded that in steam-stretched hair the arrangement of chains connected by hydrogen bonds is antiparallel. *Suggestions as to the structure of polymorphic nylons based on ω-amino acids are made; these forms may be distinguished by their infra-red spectra.*

IN polypeptides (CO·NH·CHR) and in some polyamides [for instance in nylon 6 $\{CO{\cdot}NH{\cdot}(CH_2)_5\}_n$ and its homologues] the sequence of atoms in the chains is polar and there is in consequence a distinction between 'parallel' and 'antiparallel' chain arrangements within a crystal. In nylon 6 an antiparallel arrangement has been found in a careful analysis of the X-ray diffraction pattern of the crystal forms known as α and β by Holmes, Bunn and Smith[1]. The α and β forms (not to be confused with α and β synthetic polypeptides) both have extended antiparallel chains in the hydrogen-bonded sheets, and differ only in the way in which these sheets pack together.

Recently Kinoshita[2] has investigated the X-ray diffraction patterns of a number of polyamide series. He has found that when the fibre-axis repeat distance is plotted against the number of CH_2 groups in the monomer unit, *two* nearly straight lines are obtained. The one corresponds to fully extended chains and includes the (α, β) form of nylon 6. The other indicates a slightly contracted chain and includes nylon 7.7, whose structure he has determined (Kinoshita[3]). In this structure (the γ form) the planes of the amide groups make an angle of about 30° to the chain axis; the unit cell is pseudo-hexagonal with only one chain running through it. The form of the chain is such that the hydrogen bonds are more linear than they would be with a fully extended chain. In nylon 7.7 there is no difference between parallel and antiparallel arrangements. Since the chain contraction is the same for all the polyamides on the linear plot which includes nylon 7.7, their chain conformation has provisionally been given the designation γ by Kinoshita.

Nylon 6, 8 and 10 can exist in either the (α, β) or the γ form according to the method of preparation, but the homologous nylon 4 is known only in the (α, β) form. It is interesting that Kinoshita's curves can be extended to include the two forms of nylon 2, usually known as polyglycine I and II

*Present address: College of Technology, Portsmouth, England.
†Present address: Biophysics Department, King's College, Strand, London W.C.2.

(Elliott and Malcolm[4]; Crick and Rich[5]). Polyglycine I must correspond to the (α, β) form of nylon 6 etc. but the question whether polyglycine II properly belongs to the γ series requires consideration.

Polypeptides in the near-extended form are usually assumed to be in an antiparallel arrangement, for this would be more favourable for hydrogen bond formation (Huggins[6]; Pauling and Corey[7]). The consequent doubling of the *a* axis (direction of hydrogen bonding) has been observed in β-keratin by Astbury and Street[8] and in poly-β-*n*-propyl-L-aspartate by Bradbury, Brown, Downie, Elliott, Fraser, Hanby and McDonald[9]. Curiously, it has not been found in poly-L-alanine (Brown and Trotter[10]).

In some important recent papers the effect of interaction between the vibrations in amide groups has been discussed and certain weak bands in the infra-red (i.r.) spectra of polypeptides (known for some years) have been explained as arising from such interactions (Miyazawa[11]; Miyazawa and Blout[12]). The interactions are different in parallel and in antiparallel arrangements and should therefore have diagnostic value.

In a crystalline polymer with one chain with a twofold screw axis in the unit cell, the normal modes of vibration of the repeat unit are double those of the monomer unit. This arises from coupling or interaction between the normal modes of the two monomeric units in the repeat unit of the chain. The normal modes of the system are those in which the motions in these monomer units are either in phase or out of phase and there is a (usually) small difference in frequency between them. The motions have transition moments which are along and normal to the chain axis, respectively. If the transition moment of a normal mode of one of the individual monomer units is in either of these directions then one of the combined modes will be i.r. inactive. Instead of a splitting of the absorption bands, each one will be displaced as a result of interaction.

When there are two molecular chains in the unit cell (for instance, when there is a regular alternation of chain sense along one of the crystal axes), coupling occurs between motions in the chains, giving four normal modes if the individual chains themselves each have two monomer units in the repeat length. Miyazawa has given diagrams of the molecular motion for parallel and for antiparallel chain arrangements, and has derived equations for the frequencies of the absorption bands (below).

If δ is the phase angle between the motions in adjacent amide groups within one chain and δ' the corresponding angle for amide groups connected by a hydrogen bond then the normal modes within the unit cell may be specified by the values of δ and δ', which are restricted to 0 and π. The two bands of the parallel chain arrangement are designated $\nu//(0, 0)$ and $\nu\perp(\pi, 0)$, the first angle in the parenthesis being δ. (In the parallel chain arrangement δ' must always be zero because all unit cells must be identical.) The frequencies of the two bands are given by

$$\nu//(0, 0) = \nu_0 + D_1 + D_1' \tag{1}$$

$$\nu\perp(\pi, 0) = \nu_0 - D_1 + D_1' \tag{2}$$

Here ν_0 is the frequency of the motion when unaffected by coupling, and D_1 and D_1' are interaction constants for intra- and inter-chain effects respectively.

For antiparallel chains there are four bands, of which one [$\nu(0, 0)$] is always i.r. inactive. The frequencies of the other three are:

$$\nu//(0, \pi) = \nu_0 + D_1 - D_1' \tag{3}$$

$$\nu\perp(\pi, 0) = \nu_0 - D_1 + D_1' \tag{4}$$

$$\nu\perp(\pi, \pi) = \nu_0 - D_1 - D_1' \tag{5}$$

The last band has a finite intensity only when the transition moments of the individual monomer units are out of the plane of the hydrogen-bonded sheet. It is of zero intensity for fully extended, planar chains.

In near-extended polypeptide structures, the transition moment of the Amide I band (mainly C=O stretching) is nearly perpendicular to the chain axis, hence the $\nu\perp(\pi, 0)$ of an antiparallel arrangement is a strong perpendicular band, whereas $\nu//(0, \pi)$ is a weak parallel band, and $\nu\perp(\pi, \pi)$ should be very weak. Miyazawa has very plausibly assigned the strong perpendicular band at *ca.* 1 630 cm^{-1} and the weak parallel band at *ca.* 1 690 in polypeptide spectra to the first two of these three modes.

The interaction constants D_1 and D_1' have been calculated by Miyazawa and Blout from data on several materials (particularly polyglycine and nylon 66), it being assumed that the interaction constants are the same in these materials. This gives the approximate magnitude of the constants, but small changes in ν_0 will cause disproportionately large changes in D. It appeared to us that a possibly more accurate method could be based on measurements of homologous series of polyamides in which the members form, or may be expected to form, antiparallel sheets. Such a series is formed by the polyamides from ω-amino acids with odd numbers of CH_2 groups, nylons 2, 4, 6 etc.

EXPERIMENTAL

Oriented specimens of the polyamides were made by dissolving the polymer and casting at about 60°C on silver chloride. When nearly dry, the sheet was rolled in a small jeweller's rolling mill. The specimen was subsequently heated to remove the solvent.

Nylon 6 (which usually occurs in the α, β form) has been converted to the γ form by treating with aqueous potassium iodide containing iodine. The iodine is subsequently removed by sodium thiosulphate. This remarkable process leaves the polymer in its initial state of orientation (Kinoshita[2]; Ueda and Kinura[13]). The change may be reversed by treatment with aqueous phenol, with loss of orientation. Nylons 8 and 10 tend to be in the γ-form, but may be obtained in the (α, β) form by the phenol treatment. These facts suggested that we might obtain oriented specimens of nylons 8 and 10 in the γ form from dichloracetic acid and in the (α, β) form from *m*-cresol, and this proved to be so. Nylons 2, 4 and 6 in the (α, β) are obtained from dichloracetic acid. Of these, only nylon 6 has been obtained in the γ form, by the iodine treatment.

The i.r. spectra were recorded on a Grubb–Parsons S3 spectrometer with rocksalt prism. This had been converted to a double-beam system (in time) by fitting with a microscope and rocking stage. The associated electronics were designed by Dr M. A. Ford of Perkin–Elmer Ltd, Beaconsfield.

The complete instrument is an improved version of one described by Ford, Price, Seeds and Wilkinson[14]. A selenium polarizer was used with oriented specimens[15].

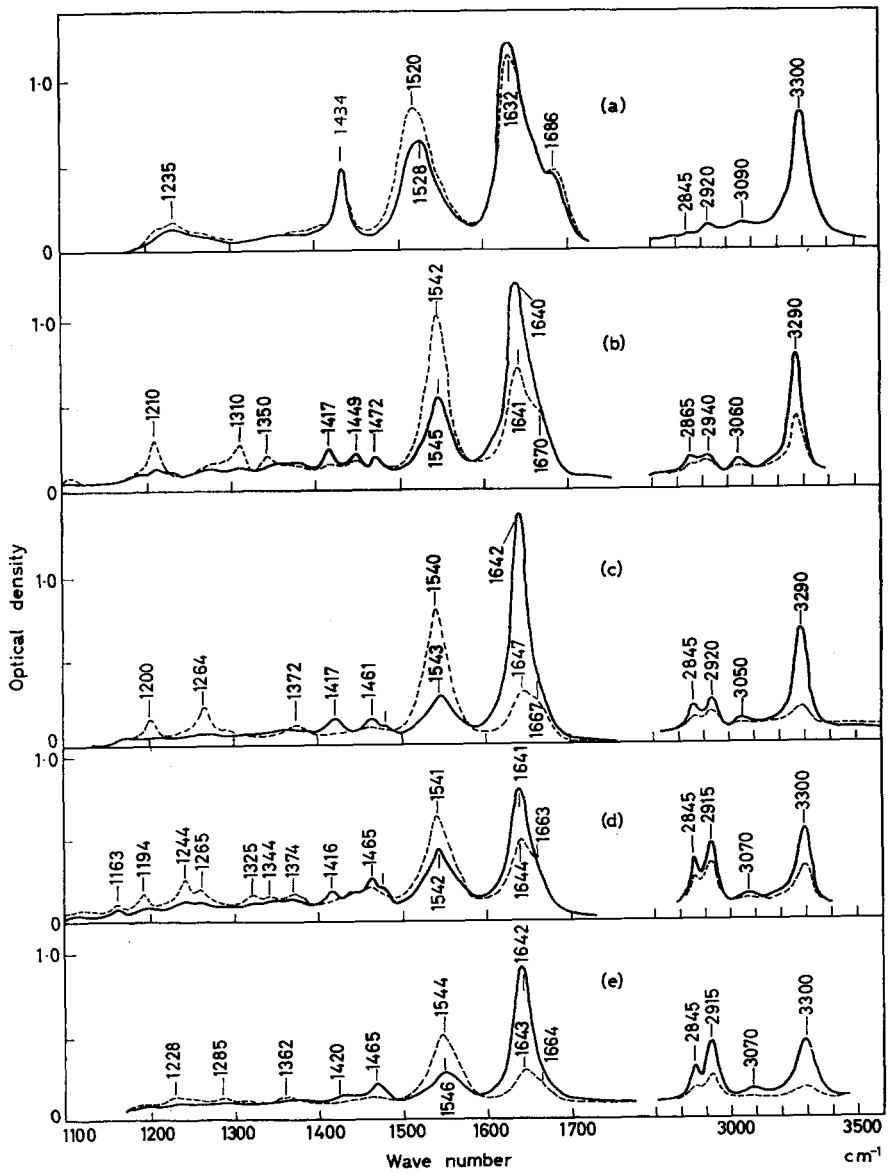

Figure 1—Infra-red spectra of oriented polyamides in (α, β) form. Full line—*E* vector perpendicular to fibre axis. Broken line—*E* vector parallel to fibre axis. (a) Nylon 2 (polyglycine)—3μ region shown for unoriented polymer. (b) nylon 4, (c) nylon 6, (d) nylon 8, (e) nylon 10

RESULTS AND DISCUSSION

The spectra of the ω-amino acid nylons 2 to 10 in the (α, β) form are shown in *Figure 1* and those of 6 to 10 in the γ form are shown in *Figure 2.*

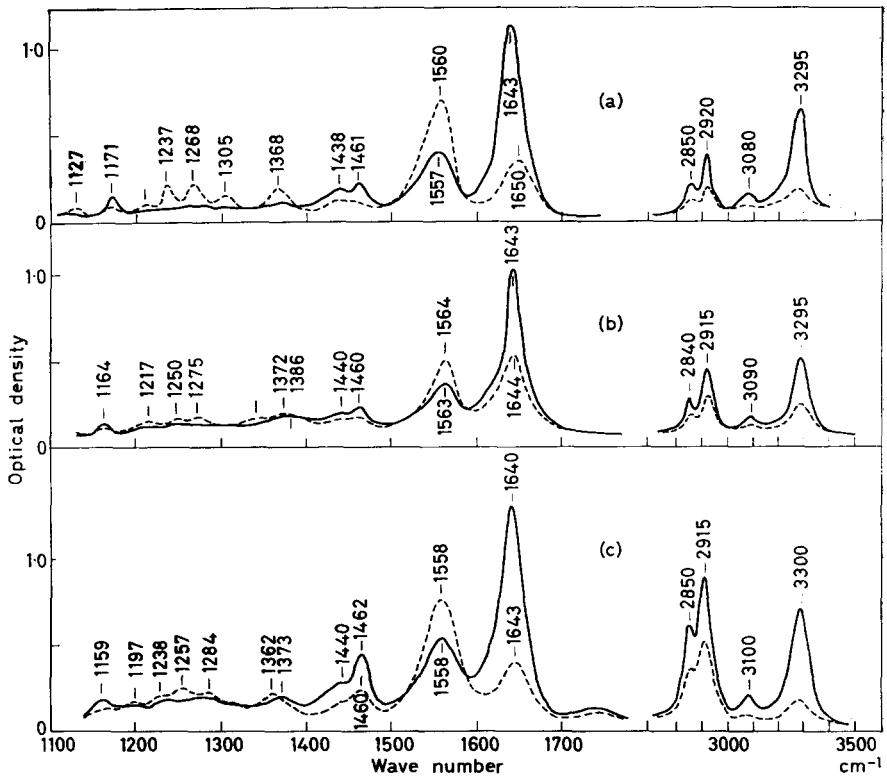

Figure 2—Infra-red spectra of oriented polyamides in γ form. Full and broken lines as in *Figure 1.* (a) nylon 6, (b) nylon 8, (c) nylon 10

Marked differences in the spectra of the two forms are seen. The Amide I band is clearly double in the (α, β) form in nylons 2 to 10. The doubling is most clearly seen in the spectrum with the *E* vector parallel to the fibre axis. The separation diminishes towards the higher members of the series. The corresponding components of polyglycine I (nylon 2) are well separated and are the bands which Miyazawa identifies with $\nu\perp(\pi, 0)$ and $\nu//(0, \pi)$. The separations of the two components are plotted against the series number in *Figure 3.* No splitting of Amide I can be seen in the spectrum of the γ form, and the Amide II band is at about 1 560 cm^{-1}, some twenty wave numbers higher than in the (α, β) form.

Antiparallel chains—Amide I band

One member of the polyamide series in the α, β form (nylon 6) is known to have an antiparallel chain arrangement and the others so clearly belong to the same series that they may confidently be assumed to be the same in

this respect. Let us consider the composite nature of the Amide I band of the (α, β) form. The polarization and (at least approximately) the relative intensities are as expected for $\nu\perp(\pi, 0)$ and $\nu//(0, \pi)$ and we feel sure that this is the correct assignment. The value of D'_1 the constant for interaction across the hydrogen bond should be the same throughout the series, but D_1 should diminish rapidly with increasing series number, since the distance between consecutive amide groups within the chain increases in this way.

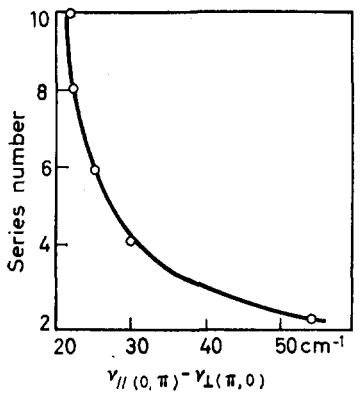

Figure 3—Separation of Amide I components plotted against polyamide series number

The separation in *Figure 3* is tending to an asymptotic value of about 22 cm^{-1} and from equations (3) and (4) D'_1 is -11 cm^{-1}. The values of ν_0 and of D_1 may be calculated from the observed frequencies and are given in *Table 1*. It is clear that, if Miyazawa's equations are of the correct form, ν_0 is varying somewhat through the series. This is independent of the values of D_1 for ν_0 is simply the average frequency of the two components.

Our results for the polyglycine interaction coefficients differ somewhat from those of Miyazawa and Blout, and make the intra-chain interaction the more important. Miyazawa and Blout's estimation depends on the assumption that ν_0 and D'_1 for polyglycine are the same as for nylon 66 and in view of the fact that ν_0 changes within a homologous series this could be true only by chance. For instance, within the range of polypeptides known to be in the β form the value of ν_0 varies from 1 659 in polyglycine to 1 669½ cm^{-1} in poly-β-*n*-propyl-L-aspartate and in the polyamides it is as low as 1 652 cm^{-1}. The errors introduced could be as large as the interaction constants themselves.

Amide II *band*

This band (connected largely with in-plane deformation of the NH bond) should be split in the same way as Amide I, though since the directions of the transition moments in the individual amide groups are different for the two motions, the relative intensities of the three active components will be very different. Miyazawa and Blout have not identified either of the weaker bands in Amide II in the spectra of extended polypeptides. In the α-helix *two* components are expected and these have been identified as the parallel band at 1 546 and the perpendicular (weak) band at 1 516 cm^{-1}.

The value of ν_0 is determined by the position of Amide II (1 535 cm^{-1}) in a partially *N*-deuterated specimen in the α-helix form[11]. In this case, there is no regular interaction with neighbouring amide groups (most of which contain ND groups and so have no Amide II mode) and the frequency is that of Amide II in a hydrogen-bonded but not interacting amide group. A similar technique has been employed by Hiebert and Hornig[16] and by Abbott and Elliott[17]. In the work of the last-named authors, the components of the Amide II band along the *a*, *b* and *c* crystal axes were found to be 1 555, 1 538 and 1 562 cm^{-1}. In the partially *N*-deuterated form, they were 1 547, 1 543 and 1 547 cm^{-1}, clearly indicating the approach to a common frequency as the interaction with neighbouring groups became less. In order to determine the uncoupled frequency ν_0 for Amide II we have measured the i.r. spectrum of several polyamides *N*-deuterated to the extent that the ND stretching band is much stronger than the residual NH band. The frequencies of the residual Amide II band are identified with ν_0 and given in *Table 3*.

In the (α, β) form there is little variation in ν_0 throughout the series. In the γ form, however, the frequency of ν_0 is higher by about 20 cm^{-1}. Also, an interesting effect is observed when a well-deuterated specimen is allowed to exchange with water vapour in the atmosphere. A band at 1 550 cm^{-1} appears and this we attribute to the disordered part of the polymer, which is always more accessible to water or heavy water than the crystalline part. These facts are evidence that for Amide II the value of the uncoupled frequency ν_0 depends on the conformation. If our conclusions are correct then other factors are present than are considered in Miyazawa's theory. For example, differences in hydrogen bonding and perhaps slight departures from planarity of the amide group may well affect the value of ν_0. The Amide II band appears to be much more sensitive to such influences than Amide I.

The existence of a band at *ca.* 1 550 cm^{-1} attributed to a disordered fraction also explains the displacement of the perpendicular peak with respect to the parallel peak (see *Figures 1* and *2*). The perpendicular component is composite; it is made up of a contribution from $\nu//$ because of imperfect orientation of the crystallites, a contribution from disordered material and the interaction band $\nu\perp$. The disordered material contributes equally to the band observed both in perpendicular and parallel positions of the polarizer but has a correspondingly larger effect in the perpendicular position. This band, whose frequency is midway between that of the (α, β) and γ forms produces a displacement of the perpendicular peak towards higher frequencies in the (α, β) form and towards lower frequencies in the γ form, as observed. Similar factors may be operating in the case of Amide I, where small displacements are observed.

Discrimination between structures with parallel and with antiparallel chains

β-keratin—Miyazawa's work on interaction bands has made it possible to distinguish between parallel and antiparallel arrangements of near-extended polypeptide chains. Some years ago Pauling and Corey[7] suggested that a polypeptide chain with a chain repeat distance of 6·5 Å would form better (more linear) hydrogen bonds in a parallel than in an antiparallel

arrangement, and that β-keratin (repeat 6·6 Å) might be an example of a parallel pleated sheet. Miyazawa and Blout have claimed to find evidence of this in the spectrum of β-keratin (Parker in Bamford, Elliott and Hanby[18]). We disagree with their interpretation for the following reasons.

(*1*) The parallel band which they identify as $\nu//(0,0)$ is said to have a frequency 1 645 cm^{-1}. We have recently measured a number of spectra of horse hair and find in every case a band, possibly parallel but more probably non-dichroic at 1 660 cm^{-1}. We find no evidence of a peak at or near 1 645 cm^{-1} (see *Figure 4*). We should always expect $\nu//(0,0)$ to be quite weak. If the Amide I transition moment is similarly situated in β-keratin and in some simple compounds containing amide groups[17,19] it will make an angle of about 20° to the C=O bond (in the plane of the amide group), inclined towards the CN bond. With a polypeptide chain contracted to a repeat length 6·6 Å (for β-keratin) the Amide I transition moment will then be inclined at about 80° to the chain axis. The ratio of intensities $\nu\perp(\pi,0)$ to $\nu//(0,0)$ in a sample where the chains have their axes all aligned along the fibre axis (but not otherwise oriented) will be[19] $\frac{1}{2}\tan^2 80°$, about 16. Even with a generous margin for error in the transition moment direction it is evident that the 1 660 cm^{-1} band is too strong to be $\nu//(0,0)$. It could be caused by α-helices too poorly developed and crystallized to be recognized in the X-ray diffraction pattern of stretched hair, or from a random arrangement of polypeptide chains.

(*2*) There is a distinct indication in Parker's spectrum of a very weak, parallel band at about 1 690 cm^{-1}, just where it would be expected if the arrangement were *antiparallel*. We have examined the spectrum of steam-stretched horse air and are convinced that there is in fact such a band (*Figure 4*). It becomes more prominent if the specimen is exposed to heavy water vapour. This exchanges with the NH bond of the peptide link, the

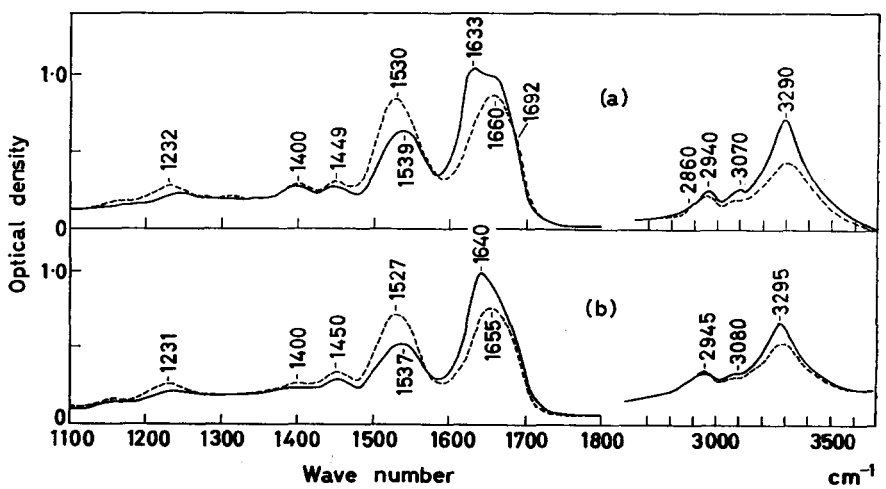

Figure 4—Infra-red spectra of keratins. Full and broken lines as in *Figure 1*. (a) Section of steam-stretched horse hair (105 per cent extension). (b) Section of swan wing feather rachis

attack being most rapid in the largely random or disordered parts of the protein which are responsible for the band centred approximately at 1 660 cm^{-1}. The frequency of this band is lowered by about 10 cm^{-1} on deuteration, and the band at 1 690 cm^{-1} is more clearly seen. (The more highly ordered parts with which this band is associated do not readily become deuterated and in consequence it does not move to a lower frequency.)

Table 1. Wave numbers of Amide I band observed in poly-ω-amino acids (α, β form) and values of D_1 and ν_0 (cm^{-1})

Polymer	$\nu \perp (\pi, 0)$	$\nu // (0, \pi)$	ν_0	D_1
Nylon				
2	1 632	1 686	1 659	16
4	1 640	1 670	1 655	4
6	1 642	1 667	1 654½	1½
8	1 641	1 663	1 652	0
10	1 642	1 664	1 653	0

The intermolecular interaction constant D_1' is taken as −11 cm^{-1} throughout.

Assuming that the interaction constants for polyglycine given in *Table 1* are applicable to other polypeptides, we should expect a parallel arrangement of chains to give components for Amide I at 1 632 and 1 664 cm^{-1}. The band at *ca.* 1 690 cm which is to be seen in *Figure 4* may therefore be attributed with some confidence to an antiparallel arrangement, though it remains a possibility that some chains are arranged in a parallel way. A weak band at 1 664 cm^{-1} could easily escape detection.

The deduction that chains arranged antiparallel are present in steam-stretched hair is in accord with the observation of Astbury and Street[8] that the unit cell of β-keratin contains two chains linked by hydrogen bonds.

We would now like to suggest that there is evidence for a component with a *parallel* as well as with an antiparallel chain arrangement in the spectrum of poly-β-*n*-propyl-L-aspartate which forms a cross-β structure (Bradbury, Brown, Downie, Elliott, Fraser, Hanby and McDonald[9], *Figure 1*). The antiparallel arrangement is shown by the presence of the $\nu \perp (\pi, 0)$ and $\nu // (0, \pi)$ bands at 1 637 and 1 702 cm^{-1} respectively. There is a very weak band at 1 676 cm^{-1} of the same perpendicular dichroic character as the 1 702 cm^{-1} band which we believe to be the $\nu // (0, 0)$ band of a parallel arrangement (the band appears as a perpendicular one because of the cross-β arrangement). This band is clearly not associated with the α-helix form of the polymer, which is known to absorb at 1 662 cm^{-1}. With the identification of three interaction bands in the spectrum of the one polymer, the constant ν_0, D_1 and D_1' can be calculated from Miyazawa's expressions. They are found to be 1 669½, 19½ and −13 cm^{-1}, respectively. When these are compared with the values in *Table 1* for polyglycine it is seen that the greatest variation is in ν_0. We note that for both polypeptides the intra-chain constant is the larger.

It is not altogether unexpected that evidence of a parallel chain arrangement should be found in poly-β-*n*-propyl-L-aspartate. We have commented elsewhere (Bradbury *et al.*[9]) that with the observed chain repeat length of

6·79 Å there is little difference between the linearity of the N—H...O atoms in parallel and in antiparallel hydrogen-bonded sheets. Some evidence of an occasional interruption of the regular alternation of chain sense in this polymer was seen in the diffuseness of some of the X-ray reflections, and it could well happen that there are some groupings in the 'parallel' arrangement sufficiently large to give the characteristic band $\nu//(0, 0)$.

Feather keratin—We have sought by similar methods to decide whether an antiparallel chain arrangement can be shown to occur in feather rachis keratin. The spectrum in the 6μ region was published by Ambrose and Elliott[20]; we reproduce in *Figure 4* a spectrum of swan quill made with a somewhat improved technique. No band can be detected at or near 1 690 cm^{-1}. We have exposed the quill section to heavy water vapour; the NH groups exchange quite quickly but this technique, effective with stretched hair keratin, has failed to show the 1 690 cm^{-1} band. This negative evidence is not conclusive for the absence of an antiparallel arrangement, however, for the intensity of the $\nu//(0, \pi)$ band might be very low.

The γ-structure—As mentioned above, the contracted form of nylons 6, 8 and 10 is provisionally called the γ-form because of certain resemblances to nylon 7.7 whose structure is known and is also so designated. The diffraction patterns of all these γ forms are very similar, as are their unit cells (apart from differences in the length of the chain axis).

We have found that the i.r. spectrum of nylon 7.7 resembles that of the other γ forms both in having an apparently single Amide I band and also in having an Amide II band of about 20 cm^{-1} higher frequency than is usual in nylons. There is therefore a strong family resemblance among the γ structures.

On comparing the spectra in *Figures 1* and *2* it will be seen that in the γ form the dichroism of the Amide II band (relative to that of Amide I) is less than in the (α, β) form and such a change would be expected if the chains in the γ forms of nylons 6, 8 and 10 have a similar conformation to that of nylon 7.7 as determined by Kinoshita. In nylon 7.7 the chains are not polar, but since there is only one chain in the unit cell the amide groups connected by a hydrogen bond must be equivalent. They therefore stand in the same relation to one another as do the hydrogen-bonded amide groups in any *parallel* arrangement of nylon chains. This suggests that the chains in the γ form of nylon 6, 8 and 10 connected by hydrogen bonds might be *parallel* chains, and they are so shown in Kinoshita's diagrammatic representation of the γ-structure in nylon 8.

With the interaction constants given in *Table 1* the frequencies of the $\nu//(0, 0)$ and $\nu\perp(\pi, 0)$ Amide I bands of a parallel arrangement may be calculated; they are given in *Table 2*. The $\nu\perp(\pi, 0)$ values are in reasonable agreement with the observed values of $\nu\perp$. The frequencies of $\nu//(0, 0)$ are expected to be only a few wave numbers higher; no separate band is seen but in the parallel direction of the *E* vector the maximum absorption is found at a slightly higher wave number. Much of this absorption, of course, comes from the $\nu\perp(\pi, 0)$ band in the poorly oriented part of the polymer. The criterion is too blunt to claim that the results confirm a parallel chain arrangement, but they do not contradict it.

Table 2. Calculated wave numbers of Amide I band in hypothetical structures and observed values of γ form (cm^{-1})

Polymer	Parallel-chain H-bonded sheet		Random chain sense				γ form (obs.)	
			2-fold screw		3-fold screw			
	$\nu//(0,0)$	$\nu\perp(\pi,0)$	$\nu//(0,0)$	$\nu\perp(\pi,0)$	$\nu//(0,0)$	$\nu\perp(\pi,0)$	$\nu//$	$\nu\perp$
Nylon								
2	1 664	1 632	1 675	1 643	1 675	1 651		(1648)*
4	1 648	1 640	1 659	1 651	1 659	1 653		Not obs.
6	1 645	1 642	1 656	1 653	1 656	1 654	1 650	1 643
8	1 641	1 641	1 652	1 652	1 652	1 652	1 644	1 643
10	1 642	1 642	1 653	1 653	1 653	1 653	1 643	1 640

*Polyglycine II, which probably does not belong to the γ series. No separate components ascribable to $\nu//(0,0)$ have been observed.

Table 3. Values of ν_0 (residual Amide II band in partially *N*-deuterated samples)

Polymer	ν_0 (cm^{-1})	
	α, β form	γ form
Nylon 2	1 540	—
4	1 544	—
6	1 542	1 566
8	1 542	1 566
10	1 542	1 563

The pseudo-hexagonal packing might suggest that the sheet structure usually characteristic of polyamides is destroyed, and the hexagonal structure suggested by Crick and Rich[5] for polyglycine II comes to mind. In this structure each chain has a threefold screw axis and all the hydrogen bonds are between chains. Since Crick and Rich[5] state that hydrogen bonds appear to form equally well between parallel and between antiparallel chains it is unlikely that a strictly parallel arrangement will be found. Only a powder diffraction picture has been obtained and it is not certain whether there is one chain or more in the unit cell. A random chain sense is therefore a possibility. In such a case the interaction constant D'_1 would be zero, for no regular relations would exist among the inter-chain coupled amide groups. The frequencies of the vibrations modified by intra-chain coupling should be given by expressions similar to those given by Miyazawa[11] for the α-helix, except that there is no term for interaction between third neighbours (which in the α-helix are hydrogen-bonded). For the parallel band

$$\nu// = \nu_0 + D_1 \tag{6}$$

and for the perpendicular band

$$\nu\perp = \nu_0 + D_1 \cos\chi \tag{7}$$

Here χ is the axial rotation between successive groups, and is 120° in polyglycine II. From the constants for polyglycine (*Table 1*) we find $\nu\perp = 1\,651\ cm^{-1}$. The value for $\nu\perp$ agrees well enough with the observed value $1\,648\ cm^{-1}$ for polyglycine II (Elliott and Malcolm[4]). The band $\nu//$ has not been observed; it would be expected to be quite weak, since the transition moment of the Amide II band in polyglycine II is more nearly perpendicular to the chain axis than it is in extended chain (β-polypeptide) structures.

Although the structure suggested for polyglycine II receives support from this calculation, it is clear that the same kind of structure cannot apply to the γ forms. For the higher members of the series, the frequency of Amide I should approach ν_0 both for $\nu//$ and for $\nu\perp$ and comparison of *Tables 1* and *2* shows that this is not so. Any *random* arrangement of chain sense would lead to the same unacceptable result.

An arrangement of chains in which the hydrogen bonds are formed between a regular antiparallel chain arrangement for the γ form should give the same frequencies as those of the (antiparallel) α and β forms of the polyamides, with a marked splitting of Amide I. Since this is also contrary to observation we are forced to conclude that a parallel chain sense in the hydrogen-bonded sheet is the only one which will fit the observations. We can escape this conclusion only by supposing that the interaction constants (and perhaps ν_0) are different in the extended α, β and contracted γ forms, a possibility which cannot be excluded.

The objection to the parallel hydrogen-bonded sheet lies in Kinoshita's observation that there is apparently only one chain in the unit cell. Since there are antiparallel chains in the α, β form in nylon 6 from which an oriented γ structure can be made, there must be antiparallel sheets in the γ form also. If the hydrogen bonds form within parallel sheets, then the sheets themselves must alternate in chain sense and the inter-sheet distance should be doubled. It could happen, by chance, that the reflections indicating this doubling are too weak for detection. Clearly the problem must await further work on the diffraction pattern of the γ form.

CONCLUSION

Our measurements on the poly-ω-amino acid series provide strong support for Miyazawa's assignments of the Amide I bands in polypeptide spectra. They show, however (as we have suggested elsewhere[21]), that the more important interaction of adjacent amide groups is the intra-chain one, and this may make it necessary to take account of next nearest as well as nearest neighbours. As far as the Amide I band is concerned, a satisfactory situation exists for the polyamide series, for β-keratin and for polyglycine I and II, and for both a parallel and an antiparallel chain arrangement in poly-β-*n*-propyl-L-aspartate. For the Amide II band it would appear that the change in frequency from one conformation to another is affected by factors other than chain interaction.

We wish to thank Mr C. G. Cannon of British Nylon Spinners Ltd, for the polyamides used in our experiments, and Mr H. A. Willis of Imperial Chemical Industries Ltd, for specimens of nylon 6 monofil.

Research Laboratory,
Courtaulds Ltd,
Maidenhead, Berkshire

(Received May 1962)

NOTE ADDED JUNE 1962

We have commenced an examination of the X-ray diffraction pattern of the γ form of nylon 6 (jointly with Mr L. Brown of Courtaulds' Coventry laboratories) and find that the unit cell is not, in fact, pseudo-hexagonal. The fifteen reflections so far observed fit a body-centred orthorhombic cell with $a = 4{\cdot}82$ Å, $b = 7{\cdot}82$ Å, $c = 16{\cdot}70$ Å (fibre axis), with two chains running through the unit cell. The distance between like chains, 4·82 Å, corresponds exactly to the separation of chains within a hydrogen-bonded sheet. The distance between unlike chains, 4·59 Å, on the other hand is too short. These results, as well as consideration of the breadth of the X-ray reflections, suggest strongly that the hydrogen bonds are formed between *parallel* chains. The results of X-ray diffraction do not contradict our tentative conclusions from i.r. spectra, but afford them strong support. A fuller account will be presented later.

REFERENCES

[1] HOLMES, D. R., BUNN, C. W. and SMITH, D. J. *J. Polym. Sci.* 1955, **17,** 159
[2] KINOSHITA, Y. *Makromol. Chem.* 1959, **33,** 1
[3] KINOSHITA, Y. *Makromol. Chem.* 1959, **33,** 21
[4] ELLIOTT, A. and MALCOLM, B. R. *Trans. Faraday Soc.* 1956, **52,** 528
[5] CRICK, F. H. C. and RICH, A. *Nature, Lond.* 1955, **176,** 780
[6] HUGGINS, M. L. *Chem. Rev.* 1943, **32,** 195
[7] PAULING, L. and COREY, R. B. *Proc. Nat. Acad. Sci., Wash.* 1953, **39,** 253
[8] ASTBURY, W. T. and STREET, A. *Phil. Trans. A,* 1931, **230,** 75
[9] BRADBURY, E. M., BROWN, L., DOWNIE, A. R., ELLIOTT, A., FRASER, R. D. B., HANBY, W. E. and MCDONALD, T. R. R. *J. molec. Biol.* 1960, **2,** 276
[10] BROWN, L. and TROTTER, I. F. *Trans. Faraday Soc.* 1956, **52,** 537
[11] MIYAZAWA, T. *J. chem. Phys.* 1960, **32,** 1647
[12] MIYAZAWA, T. and BLOUT, E. R. *J. Amer. chem. Soc.* 1961, **83,** 712
[13] UEDA, S. and KIMURA, T. *Chem. High Polymers (Tokyo),* 1958, **15,** 243 (in Japanese)
[14] FORD, M. A., PRICE, W. C., SEEDS, W. E. and WILKINSON, G. R. *J. opt. Soc. Amer.* 1958, **48,** 249
[15] ELLIOTT, A., AMBROSE, E. J. and TEMPLE, R. B. *J. opt. Soc. Amer.* 1948, **38,** 212
[16] HIEBERT, G. L. and HORNIG, D. F. *J. chem. Phys.* 1952, **20,** 918
[17] ABBOTT, N. B. and ELLIOTT, A. *Proc. Roy. Soc. A,* 1956, **234,** 247
[18] BAMFORD, C. H., ELLIOTT, A. and HANBY, W. E. *Synthetic Polypeptides,* p 405. Academic Press: New York, 1956
[19] SANDEMAN, I. *Proc. Roy. Soc. A,* 1955, **232,** 105
[20] AMBROSE, E. J. and ELLIOTT, A. *Proc. Roy. Soc. A,* 1951, **206,** 206
[21] ELLIOTT, A., BRADBURY, E. M., DOWNIE, A. R. and HANBY, W. E. Symposium on Poly-amino acids, Wisconsin, June, 1961

The Crystallization of Polyethylene I

W. BANKS, M. GORDON*, R.-J. ROE† and A. SHARPLES

The crystallization of polyethylene fractions of varying molecular weight has been studied by the dilatometric method, and a procedure developed to enable the primary and secondary processes to be analysed separately. The value of the Avrami exponent, n, calculated on the basis of this method, varies with molecular weight and temperature, and is often significantly different from the integers required by theory. Modifications to the assumptions on which the theory is based are proposed to account for this observation. A reversal in crystallization behaviour occurs at a molecular weight of ca. *60 000 and as this is near to the point where melt viscosity also undergoes a change, it is suggested that viscosity is an important factor governing crystallization rate. It thus follows that crystallization is determined by the same molecular weight average as that determining melt flow. The secondary crystallization has a rate which is less than one order slower than that for the primary process and also has a similar temperature dependence to the latter, in that the rate decreases as the temperature is raised.*

NUMEROUS studies have been reported of the crystallization of high polymers, and the picture which has generally been used to account for the observed facts is that nuclei appear randomly in space in the supercooled melt, and subsequently grow at a constant linear rate, in one, two, or three dimensions, to form rods, discs, or spheres[1,2]. The disappearance of the liquid phase can be related to the time of crystallization, t, by an equation developed by Avrami[3] and others[1,2,4], which has the form

$$W_1/W_0 = \exp(-zt^n) \qquad (1)$$

where W_1/W_0 is the weight fraction of liquid phase remaining, and z is a function of nucleation and growth rates which is constant for a given temperature. n is an integer having a value between 1 and 4 depending on whether nucleation is instantaneous or sporadic, and also on the number of dimensions in which growth occurs. Thus, in the normally postulated case of sporadic nucleation and spherical growth, n is equal to 4.

With some polymers (e.g. nylon 6.6[5] and polyethylene[6]) the crystallization is complicated by an additional process, normally referred to as secondary crystallization, which is considered to involve either 'further growth or improvement of the degree of the crystalline order' or 'filling up the holes remaining after primary crystallization'[6]. The time dependence in this case has a different form from that of the primary crystallization, and difficulty in resolving the two processes has previously rendered unsatisfactory any kinetic analysis. Consequently, in spite of the wide interest in the bulk crystallization of polyethylene, the large secondary effect (sometimes greater than 40 per cent of the total) has in the past necessitated the use of arbitrary assumptions concerning the mechanism, in order to enable any analysis to be made[7].

*Present address: Chemistry Department, Imperial College of Science and Technology, London S.W.7.

†Present address: Chemistry Department, Duke University, Durham, North Carolina.

In this paper a method is proposed for resolving the two processes, and it is applied to the data obtained for a range of polyethylene samples of different molecular weight and distribution. In addition, as the dilatometric method normally used for studying polymer crystallization is capable of high degrees of accuracy, the validity of the Avrami equation, and hence the assumptions on which it is based, are critically considered in the light of the results obtained.

EXPERIMENTAL

Materials

Representative samples from two series of fractions were used, derived from Phillips type polyethylenes. Degrees of polymerization, $\overline{P}_v$ (determined from viscometric measurements[8]) and melting points are given in *Table 1*, both for these fractions, and for commercial whole polymers. The blend was prepared in order to assess the effect of distribution on crystallization behaviour, uncomplicated by the presence of other variables, such as short chain branching. It consisted of 48·94 per cent by weight of fraction 5902 mixed with 51·06 per cent fraction 5907 to give a product whose intrinsic viscosity average degree of polymerization was the same as that for fraction 5905.

Table 1

Sample	$\overline{P}_v$	T_m°C	*Comments*
1	380	—	Fraction from Phillips type polyethylene A
3	670	135·9	Fraction from Phillips type polyethylene A
5	1 030	136·0	Fraction from Phillips type polyethylene A
5908	350	135·5	Fraction from Phillips type polyethylene B
5907	1 800	136·1	Fraction from Phillips type polyethylene B
5905	7 300	136·6	Fraction from Phillips type polyethylene B
5902	14 800	136·8	Fraction from Phillips type polyethylene B
5901	18 500	136·8	Fraction from Phillips type polyethylene B
B	7 300	136·6	Blend of 5902 and 5907
M	3 100	136·2	Marlex type polyethylene
PM	26 000	137·6	Polymethylene
EBC	4 000	133·4	Ethylene butene copolymer, MI=0·28, 2·2 ethyl groups/1 000 C atoms

Dilatometry

The dilatometers used were considerably smaller than the conventional type; measuring capillaries were 0·04 cm in diameter, and 80 to 100 mg plugs of polymer, previously moulded to shape, were confined by *ca.* 0·4 ml mercury. Liquid expansion coefficients were in excellent agreement with those given in the literature[9]. Crystallinities were determined by Swan's equation[9]. The high temperature dependence of the crystallization necessitated a high degree of temperature stability, and the thermostats used were designed to give variations of less than 0·02°C. Owing to the small size of the dilatometers the time to reach equilibrium after transference from the melting bath was never greater than two minutes.

In one series of experiments at constant temperature, the position of the polymer in the dilatometer (and hence the ratio of surface to volume) was

changed, with no effect on the subsequent kinetics, from which it is concluded that surface nucleation is not important[11]. Thermal memory, i.e. the dependence of crystallization rate on temperature of pre-melting[1,11], was found to be absent, since melting for 15 minutes at any temperature between 137°C (less than 1°C above the melting point) and 210°C produced the same isotherm on subsequent crystallization. Melting points were determined on samples which had been crystallized for up to 30 000 minutes, the temperature of crystallization being such that the half-life of the Avrami stage was *ca.* 30 minutes. The error in the melting point was considered to be less than 0·10°C.

ANALYSIS OF DATA

The weight fraction of amorphous material remaining at time t is related to the volume of the crystallizing system, V_t, by the equation[2]

$$W_t/W_0=(V_t-V_\infty)/(V_0-V_\infty) \tag{2}$$

where V_0 and V_∞ are the initial and final volumes. Thus, during the primary crystallization process it follows from equation (1) that

$$(V_t-V_\infty)/(V_0-V_\infty)=\exp(-zt^n) \tag{3}$$

As relative volumes are determined experimentally from dilatometric column heights, h_t, equation (3) is normally written

$$(h_t-h_\infty)/(h_0-h_\infty)=\exp(-zt^n) \tag{4}$$

Several methods have been evolved[2,10] for analysing data on the basis of equation (4) but the general objection which can be made is that the use of logarithms in the time axis has made any test for goodness of fit an insensitive one. Hoffman, Weeks and Murphey[11] have suggested an alternative approach which avoids this difficulty, but it is based on an approximation which leads to large errors at high values of t.

The method proposed here is as follows. Equation (4) can be differentiated to give

$$n=t\,(\mathrm{d}h_t/\mathrm{d}t)/(h_\infty-h_t)\ln\{(h_0-h_\infty)/(h_t-h_\infty)\} \tag{5}$$

and as $\mathrm{d}h_t/\mathrm{d}t$ can be calculated from successive pairs of results, n can be obtained for every stage of the crystallization as a function of the crystallinity, or some related quantity such as $(h_t-h_\infty)/(h_0-h_\infty)$. The rate constant, z, can then be calculated from the half-life, $t_{\frac{1}{2}}$, and the average value of n, as follows

$$z=\ln 2/t_{\frac{1}{2}}^n \tag{6}$$

Resolution of primary and secondary crystallizations

In general, these two processes may be considered to occur either consecutively or concurrently. In either case equation (5) cannot be applied without making further assumptions, and it is this factor which has led to difficulties in the past. Here it is initially assumed that the processes are consecutive so that the problem now becomes that of choosing a suitable value of h_∞ to characterize the completion of the primary crystallization. This is achieved by adjusting h_∞ until values of n, calculated from equation

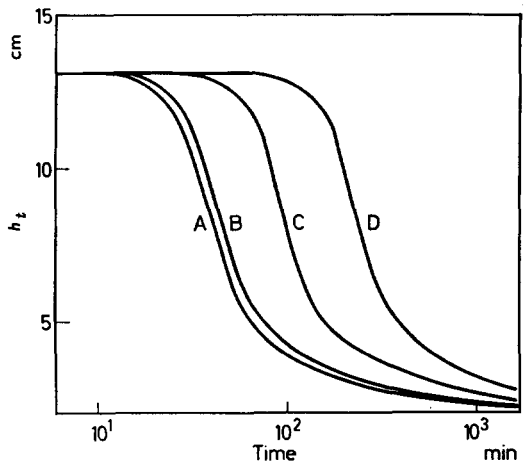

Figure 1—Crystallization of fraction 5907. (A) 128·26°C, (B) 128·70°C, (C) 129·45°C, (D) 130·00°C

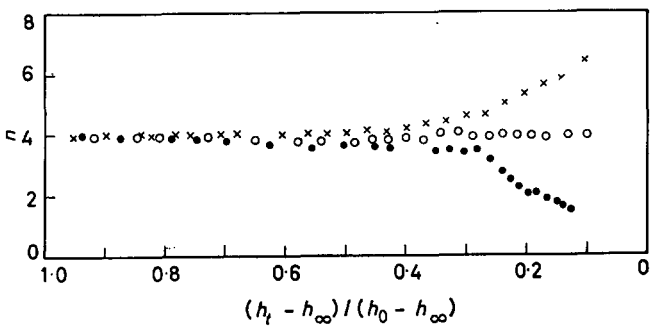

Figure 2—Results from (D) *Figure 1* plotted according to equation (5) using three arbitrarily chosen values of h_∞. (x) $h_\infty = 4{\cdot}00$ cm, (o) $h_\infty = 5{\cdot}00$ cm, (•) $h_\infty = 6{\cdot}00$ cm

(5), remain constant for the maximum period of time. The method is illustrated by some data for fraction 5907. The results are first plotted in *Figure 1* in the form of h_t versus $\log t$, and it can be seen that there is no obvious break to indicate a transition from one process to the other. In *Figure 2*, three values of h_∞ are chosen for one of the runs, and used in equation (5) to enable plots to be made of n versus $(h_t - h_\infty)/(h_0 - h_\infty)$. It is evident that the correct choice of h_∞ ($= 5{\cdot}00$ cm) is a critical one, and this in itself provides indirect support for the method. However, more direct confirmation arises from a consideration of the melting behaviour of the material at different stages in the crystallization. Details of the experiments are given elsewhere[12] but the relevant feature is that melting point remains almost constant for varying extents of crystallization until a point is reached corresponding to the correctly chosen value of h_∞, after which a continual increase is observed. It can thus be concluded that during the primary process, before h_∞ is reached, the size or degree of perfection of the crystallites remains unchanged, and only the amount of crystalline

material increases. After h_∞ a new process commences, which increases the size or perfection of the existing crystallites and hence their melting point.

The assumption that two entirely different processes are involved, and that they occur consecutively, thus seems to be reasonable, and in fact it has been observed that for some polymers the plots show two distinct regions[5, 6]. In the present results, no discontinuity is apparent, and it is always necessary to use the method described above to determine h_∞. Matsuoka[13], however, has found that even with polyethylenes, separation into two regions can occur if the pressure on the system is increased.

RESULTS

(1) *The primary crystallization*

(a) *The value of n*—Crystallization parameters for three typical samples are given in *Table 2*, and results for an individual run are given in *Figure 3*.

Table 2. Avrami parameters for the crystallization of polyethylene samples

Sample	T_m °C	*Temp. of crystallization* °C	*n*	*z* (*time in min*)	χ_∞ %	χ_f %
5901	136·8	125·36	3·12 ± 0·08	$1{\cdot}45\times10^{-4}$	34·2	58
		125·75	3·14 ± 0·11	$5{\cdot}51\times10^{-5}$	35·0	58
		126·85	3·08 ± 0·07	$3{\cdot}27\times10^{-6}$	33·6	58
		127·56	2·97 ± 0·06	$8{\cdot}68\times10^{-7}$	34·1	58
		127·76	2·96 ± 0·08	$3{\cdot}30\times10^{-7}$	33·6	58
		128·49	2·75 ± 0·10	$1{\cdot}04\times10^{-7}$	35·3	58
		128·60	2·70 ± 0·07	$9{\cdot}01\times10^{-8}$	37·9	58
5905	136·6	126·62	3·52 ± 0·06	$4{\cdot}69\times10^{-6}$	46·0	71
		127·50	3·48 ± 0·06	$5{\cdot}62\times10^{-7}$	46·5	71
		128·49	3·48 ± 0·14	$3{\cdot}66\times10^{-8}$	45·4	71
		129·48	3·54 ± 0·10	$1{\cdot}18\times10^{-9}$	46·5	71
		130·50	3·50 ± 0·15	$3{\cdot}42\times10^{-12}$	46·7	71
		131·02	3·54 ± 0·09	$5{\cdot}62\times10^{-14}$	46·8	71
5907	136·1	128·26	3·47 ± 0·11	$7{\cdot}48\times10^{-6}$	54·7	79
		128·70	3·54 ± 0·11	$1{\cdot}86\times10^{-6}$	55·0	79
		129·45	3·50 ± 0·05	$8{\cdot}30\times10^{-8}$	55·5	79
		130·00	3·87 ± 0·06	$5{\cdot}65\times10^{-10}$	55·8	79
		130·34	3·77 ± 0·08	$9{\cdot}52\times10^{-11}$	55·7	79

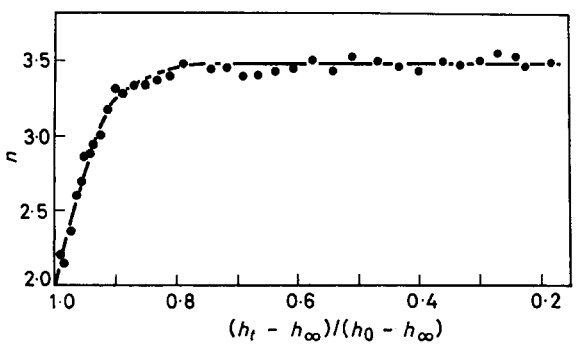

Figure 3—Primary crystallization of fraction 5905 at 127·50°C

Several features are apparent. First, in *Figure 3* it can be seen that n increases initially from a value of about two to a final steady value. This effect is present in a number of cases, and as it has been proposed in the past that spherulitic structures commence their growth in the form of rods[14], it is reasonable to suppose that the value of $n \approx 2$ observed here corresponds to initial rodlike growth from sporadically formed nuclei. The fact that this initial change is present to varying extents in different cases, suggests that the final size of the growing bodies varies from sample to sample, and that where this is large, the early stage of rodlike growth constitutes only a small fraction of the total. As the trend is for this effect to decrease with decreasing molecular weight (cf. *Figure 2*) it can be deduced that spherulite size increases in the same direction.

Secondly, the constant value of n which characterizes the majority of the crystallization, is often significantly different from the integral values of 1, 2, 3 or 4 required by previous theories. Although fractional values of n have been recorded in the past[15,16], the tendency has been to assume that the process is characterized by the nearest integer. The results in *Table 2* show that certainly in the present case there is no justification for this procedure, as the differences from integral values are frequently greater than the experimental errors involved. In general n varies from 2·0 to 4·0, depending on molecular weight and temperature of crystallization, and it can be seen from *Figure 4* and *Table 2* that although there is no obvious correlation with temperature, there is a tendency for a maximum to be reached in the dependence on degree of polymerization. This becomes more obvious if the fractions only are considered, when it can be seen that this maximum occurs in the region of $\bar{P}_v = 2\,000$. The results for other samples presumably deviate owing to the presence of other variables, such as branching and polydispersity. The effect of the latter only can be seen from the results for the blend, which has values of n well outside those recorded not only for the lower molecular component (5907), but also for

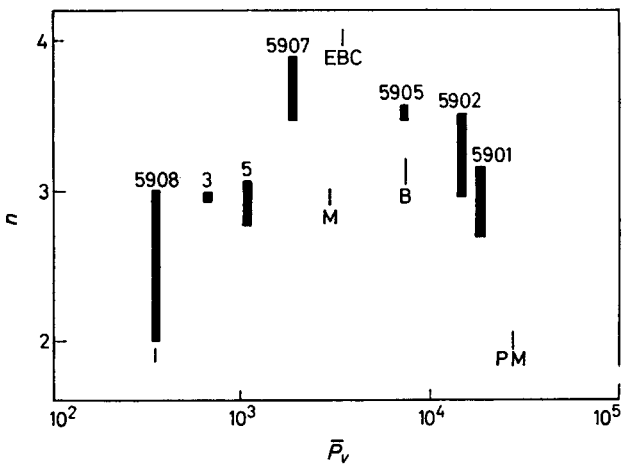

Figure 4—Values of the Avrami exponent, n, for different temperatures of crystallization, plotted as a function of degree of polymerization. (The thick lines refer to fractions)

the fraction of identical viscosity average degree of polymerization (5905). It is thus evident that the behaviour of the blend is very little affected by the presence of the large amount (51 per cent) of the low molecular weight component, from which it may be deduced that the operative molecular weight average must be higher than the intrinsic viscosity average used here.

(b) *Temperature dependence of rate*—The temperature dependence of the primary crystallization process for polyethylene is extremely high, as is indicated by the fact that the time scale of the observations can change from minutes to days over a temperature range of only 3°C. Consequently, as the data are necessarily derived from measurements taken within this narrow range, it is important to realize that any conclusions which are reached may not apply to crystallizations carried out at lower temperatures.

The overall rate constant, z, depends on both nucleation and growth rates, but as growth is generally found to involve secondary nucleation, the temperature dependence of z is governed by that for the nucleation rate[2]. The relation normally proposed is of the form[2]

$$\log z = A - 4B/\Delta T^2 \tag{7}$$

although the following alternative has been suggested[2]

$$\log z = A - 4B/\Delta T \tag{8}$$

where A and B are constants and ΔT is the difference between the temperature of crystallization, T_c, and the melting point, T_m. In the present case where the Avrami exponent, n, varies it is likely, for reasons given later, that equations (7) and (8) should be modified to:

$$\log z = A - nB/\Delta T^2 \tag{9}$$

and

$$\log z = A - nB/\Delta T \tag{10}$$

Previously[2,11], T_m has been treated as an adjustable parameter, owing to the uncertainty attached to the experimentally obtained values. In the present study, a kinetic method was used[12] to determine T_m, and the values obtained are considered to represent the true values to within $\pm 0{\cdot}1$°C. With this accuracy, more satisfactory use can be made of the crystallization data in deciding on the correct temperature relationship. In *Figure 5*, where results for fraction 5901 are plotted according to equations (7) to (10), it can be seen that the data are best fitted by equation (9). A similar conclusion can be drawn for all the samples from which it follows that growth proceeds by three-dimensional secondary nucleation[2].

The values of the parameter B are plotted in *Figure 6* against degree of polymerization, and again if fractions only are considered, a reversal in trend is apparent in the region of $\bar{P}_v \approx 2\,000$. The blend also has a value very close to that for its high molecular weight component (5902). Most striking is the *extent* of variation of B in view of the fact that previous workers have found this parameter to be constant[7]. The significance of this point theoretically is that the critical free energy of the secondary nucleation relative to that of the primary process, must also be changing with molecular weight[2].

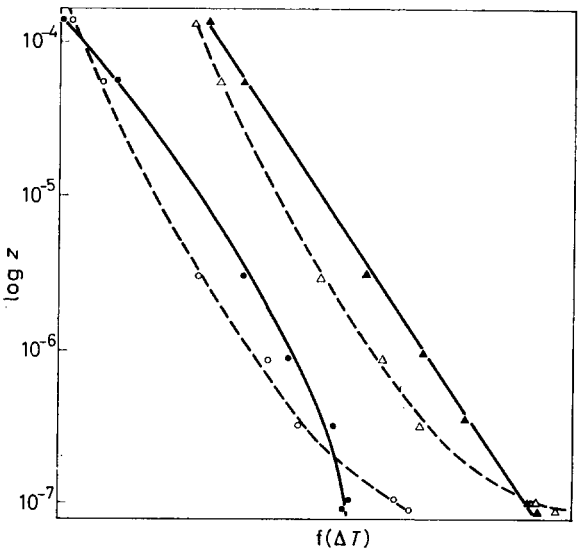

Figure 5—Temperature dependence of rate constant, z, for sample 5901, fitted according to equations (6) to (9). (△) Equation (6), (o) equation (7), (▲) equation (8), (•) equation (9)

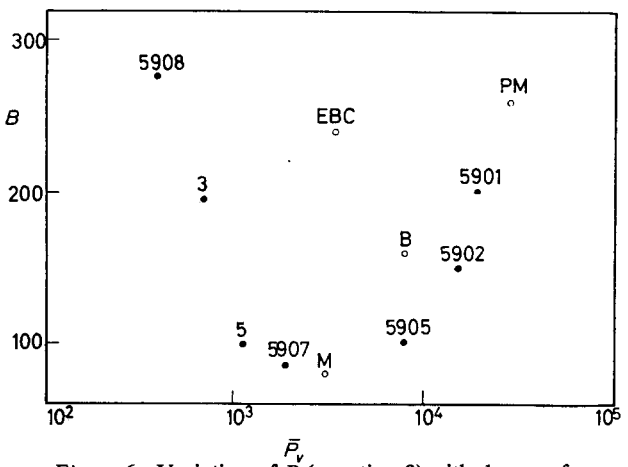

Figure 6—Variation of B (equation 8) with degree of polymerization

(c) *Molecular weight dependence of rate*—It has previously been reported that polymers in general (e.g. ref. 7) crystallize with increased rates at lower molecular weights. The choice of a suitable standard of comparison is in fact not a straightforward one, as can be seen from equation (9) which shows that z also varies with n, B and ΔT. It is considered, however, that the characteristic features of the dependence, for the limited temperature range studied here, are satisfactorily illustrated by the plot used in

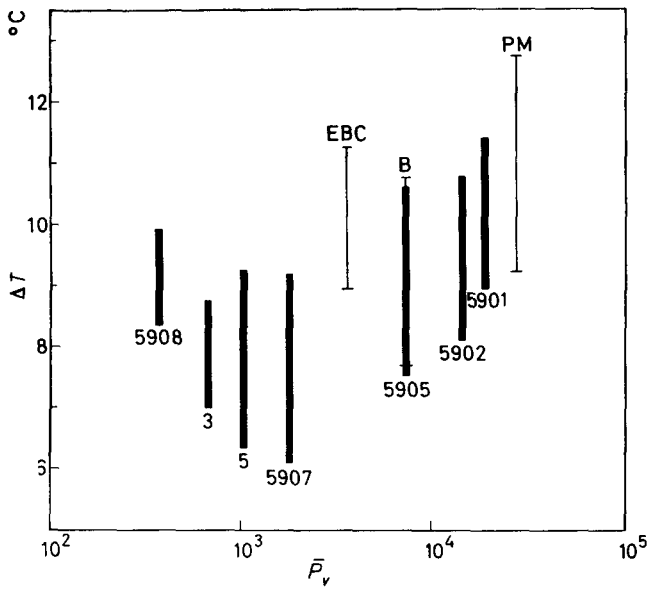

Figure 7—Temperature range below melting point for which 10 min $< t <$ 250 min, plotted as a function of degree of polymerization. (The thick lines refer to fractions)

Figure 7. The trend noted above is confirmed, down to $\bar{P}_v \approx 2\,000$, but below this value there is again a reversal in behaviour, and the rate now starts to decrease as the molecular weight is further reduced. The behaviour of the blend is again nearer to that of the high molecular weight component.

(2) *The secondary crystallization*

Although no detailed picture exists for this process it has been established[17] that crystallinity increases with time according to the following empirical relation

$$\chi_t = C + D \log t \tag{11}$$

where χ_t is the crystallinity, C and D are constants, and t has its origin at the beginning of the secondary process. The choice of a suitable origin is critical if the best fit is to be obtained, and here it was found that values giving optimum agreement corresponded to values of χ within two or three per cent of those for χ_∞, thus confirming the sharp transition between the primary and secondary processes. χ_∞ is thus used here to indicate the value of χ at which the secondary process commences. Although there is a progressive decrease in the rate of this secondary process, there is no experimentally accessible time where the crystallization can be considered to be complete. Consequently, the values of χ_f, the 'final' degree of crystallinity, are arbitrarily taken at a time 150 times greater than that required to complete the primary stage.

As can be seen from *Figure 8* the results conform to equation (11) over a limited range, but show deviations as the final value of the crystallinity,

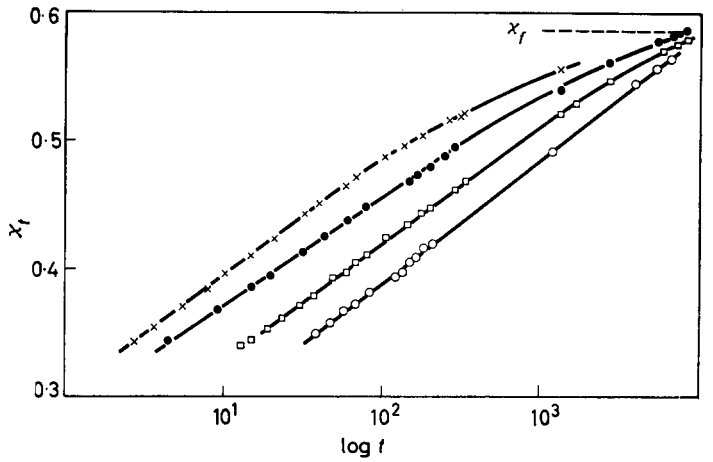

Figure 8—Secondary crystallization process for fraction 5901. (x) 125·00°C, (•) 125·75°C, (□) 126·85°C, (o) 127·76°C

χ_f, is approached. This is to be expected, as equation (11) is necessarily an approximation in that it predicts that crystallinity should increase without limit as t increases. A more fundamental equation is that derived by Hirai and Eyring[18,19] to account for the shrinkage of glasses

$$\tanh\left(\frac{a}{2}\frac{V_\infty - V_f}{V_f} \cdot \frac{\chi_f - \chi_t}{\chi_f - \chi_\infty}\right) = \left[\tanh\frac{a}{2}\left(\frac{V_\infty - V_f}{V_f}\right)\right] e^{-t/\tau} \qquad (12)$$

where $a \approx V_m/6RT\Delta\beta$, V_m is the molar volume of the contracting molecular unit, $\Delta\beta$ is the difference in compressibilities between the liquid and glassy stages, τ is a relaxation time, and $_\infty$ and $_f$ refer to the beginning and end of the secondary process. At intermediate values of χ_t this approximates to

$$\frac{a(V_\infty - V_f)}{V_f} \cdot \frac{\chi_f - \chi_t}{\chi_f - \chi_\infty} \approx 2{\cdot}3 \log (t/2\tau)$$

which can be written as

$$\chi_t = \chi_f + \frac{2{\cdot}3(\chi_f - \chi_\infty)V_f}{a(V_\infty - V_f)} \log t - \frac{2{\cdot}3(\chi_f - \chi_\infty)}{a(V_\infty - V_f)} V_f \cdot \log 2\tau \qquad (13)$$

and this is of the same form as equation (11). Equation (13) predicts that the value of D should be independent of temperature for the small temperature range studied, a feature which was observed to hold experimentally for all the samples studied (cf. *Figure 8*). The variation with molecular weight also is small, and accountable for in terms of the changes in $(\chi_f - \chi_\infty)V_f/(V_\infty - V_f)$, which is to be expected if V_m is interpreted as the volume of a chain segment. The value of V_m calculated from the result for D corresponds to a chain segment of roughly 60 —CH_2— units which is certainly likely to be of the right order of magnitude. However, although this approach is able to account for the approximate validity of equation (11) and also to lead to a reasonable value for the parameter D, there must

be reservations to the inference that the assumptions on which the Hirai and Eyring treatment is based are entirely applicable here. In the first instance equation (12) fits the observed data no better than does the approximate form (equation 11) at very large values of t, indicating that some other process eventually intervenes. Secondly, the rate of the process, a practical assessment of which can be obtained from $t_{\frac{1}{2}}$ *or* τ ($t_{\frac{1}{2}} \approx 2\tau/e^4$), increases as the temperature decreases, whereas for a relaxation phenomenon the reverse should apply. In fact $t_{\frac{1}{2}}$ has a temperature coefficient which is very close to that for the primary crystallization, as can be seen from *Table 3*. It is also apparent that the absolute values of $t_{\frac{1}{2}}$ for the two stages are separated by less than one order, which suggests that the slow volume contraction observed by Kovacs[17] at much lower temperatures, where the primary crystallization is effectively instantaneous, is a different process.

Table 3. Half-lives for the primary and secondary processes in polyethylene fraction 5901

T_c °C	$t_{\frac{1}{2}}$ (*primary*) *min*	$t_{\frac{1}{2}}$ (*secondary*) *min*	*Ratio*
125·36	15·1	80	5·3
125·75	20·2	115	5·7
126·85	53·6	290	5·4
127·50	97·1	530	5·5
127·76	137	700	5·1
128·49	303	1 300	4·3
128·70	355	1 500	4·2

(3) *Crystallinity*

The reversal in trend of the crystallization rate parameters at $\overline{P}_v \approx 2\,000$ raises the question of whether the amount of crystalline material shows a similar dependence on molecular weight. Previous workers[7] have noticed that crystallinity increases as molecular weight is decreased, and this is confirmed in *Figure 9*, where χ_f, the crystallinity at the end of the secondary stage, is plotted as a function of $\overline{P}_v$. A reversal again occurs, however, and χ_f can be seen to decrease at lower molecular weights. A similar relation also holds for χ_∞, the crystallinity at the end of the primary stage, which

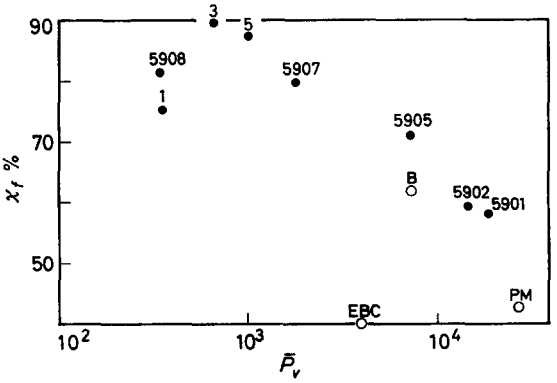

Figure 9—Plot of crystallinity at the end of the secondary process, as a function of degree of polymerization

is between 20 and 25 per cent less than χ_f, and varies slightly with temperature of crystallization. The conditions of crystallization used in these experiments are favourable to the formation of the maximum amount of crystalline material, and it can be seen that in fraction 3, approximately 90 per cent is formed.

The blend is again nearer in behaviour to the higher molecular weight component, so that if comparisons are made on the basis of viscosity average molecular weight, increasing polydispersity leads to a reduction in crystallinity. The result for the ethylene–butene copolymer shows that short chain branching, as expected, has a similar effect.

DISCUSSION

The results indicate that although the secondary crystallization in polyethylene can be as high as 40 per cent of the total, it overlaps the primary process only to a very small extent, so that the method proposed for analysing the data is considered to yield unambiguous parameters for each stage. The Avrami exponent, n, has values determined by this method which are often significantly different from the integers required by theory, and although fractional but changing values of n can be accounted for by the simultaneous occurrence of two different Avrami processes (e.g. with predetermined and sporadic nucleation) the values observed here are both fractional and constant, so that no such simple explanation applies. Consequently it is necessary to examine the assumptions which have been used in the past to derive the Avrami equation.

The occurrence in some cases of initial values of $n \approx 2$ (*Figure 3*) suggests that growth starts in the form of rods, from nuclei that appear sporadically, and not instantaneously. The fact that n in general approaches but never exceeds four confirms that sporadic nucleation is the more likely possibility, followed by three-dimensional growth, modified in some way so as to reduce n in certain cases. The normal equation for sporadic nucleation and spherulitic growth is derived by assuming first that the density of the spherulite is the same at every stage of its growth, and secondly that growth and nucleation rates are constant[2]. The more detailed form of equation (1) is then[2]

$$W_l / W_0 = \exp(-N_v \pi G^3 \rho_s t^4 / 3\rho_l) \tag{14}$$

so that

$$z = N_v \pi G^3 \rho_s / 3\rho_l \tag{15}$$

where N_v is the nucleation rate per unit volume, G is the linear growth rate, and ρ_s and ρ_l are the densities of the solid and liquid phases. Modification of either of the two assumptions given above can lead to a form of equation (14) where the power of t (i.e. the Avrami exponent n) is reduced to a constant fractional value, as observed. The dilatometric method of following the crystallization process is not capable of yielding separate information on growth and nucleation rates, so that a detailed discussion of the possible modifications is deferred to the second part of this work, which involves direct microscopic observations of these quantities. It is possible to note at this stage, however, that these modifications lead to

versions of equations (14) and (15), of the form

$$W_t/W_0 = \exp(-\text{const.}\, N_v G^{n-1} t^n) \tag{16}$$

and

$$z = \text{const.}\, N_v G^{n-1} \tag{17}$$

which, apart from accounting for fractional values of the Avrami exponent, are relevant in connection with the observed temperature dependence of z. It has been shown that[2]

$$\log N_v = A_1 - B_1/\Delta T^2 \tag{18}$$

where A_1 and B_1 are constants, and ΔT is the difference between melting and crystallization temperatures. If it is assumed[2] that growth proceeds by secondary nucleation then

$$\log G = A_2 - B_2/\Delta T^2 \tag{19}$$

Hence

$$\log z = \text{const.} + A_1 - (B_1/\Delta T^2) + (n-1)\,A_2 - (n-1)\,B_2/\Delta T^2) \tag{20}$$

Microscope observations[19] of growth rate show that $(n-1)\,A_2$ is negligible compared with the other variable terms in equation (20) so that, if it is assumed that $B_1 = B_2$ (i.e. that primary and secondary nucleation processes have a similar temperature dependence), then

$$\log z = \text{const.} - B_1 n/\Delta T^2 \tag{21}$$

which is the relation found to hold experimentally (equation 8 and *Figure 5*) in the present experiments.

This lends support to the general picture suggested above, namely that the Avrami mechanism is still operative, with three-dimensional growth from sporadically formed nuclei, but that one of the assumptions on which it is based is modified. The extent of the deviation from $n=4$ varies from sample to sample, and also with temperature, which suggests that the nature of the spherulite growth is similarly changing. This is confirmed by microscope observations[2, 19] and also by the fact that quite large variations are observed in B_1 (equations 9 and 21), which is dependent on the critical free energy involved in secondary nucleation, and hence on the nature of the growing surface.

The reversal in behaviour which occurs in the region of $\overline{P}_v = 2\,000$ has no obvious explanation in terms of the above picture. It does occur, however, at a molecular weight which, from viscosity measurements, is near the critical point below which chain entanglements cease to be of importance[20]. Consequently although it has generally been accepted in the past[2] that the rate controlling step in spherulite growth is unlikely to be determined by diffusion to the growth surface, it would seem from the present results that the viscosity of the liquid polymer in the neighbourhood of this surface is an important factor regulating growth rate. Confirmation of this point derives from the fact that the behaviour of the blend in the above experiments is very close to that for the higher molecular component. The dependence of melt viscosity on molecular weight (above the critical molecular weight) is a 3·4 power law[21], so that if viscosities can be assumed to be additive, the appropriate average is not the intrinsic viscosity average previously used but that defined by

$$\overline{M}_{\text{m.v.}} = (\Sigma\, W_i M_i^{3\cdot4})^{1/3\cdot4}$$

where W_i is weight fraction of the ith component. $\bar{P}_{m.v.}$ for the blend can thus be calculated to be 12 000, compared with 14 800 and 1 800 for the two components and 7 300 for the intrinsic viscosity average value. The dominance of the high molecular weight component is thus explained, and it is evident that the molecular weight average which determines crystallization behaviour is the same as that which determines melt flow.

We are grateful to B.P. Ltd for financial assistance in this project.

Arthur D. Little Research Institute,
Inveresk, Musselburgh, Midlothian

(*Received May 1962*)

REFERENCES

[1] MORGAN, L. B. *Phil. Trans.* 1954, **247**, 13
[2] MANDELKERN, L. *Growth and Perfection of Crystals*, pp 467–497. Chapman and Hall: London, 1958
[3] AVRAMI, M. *J. chem. Phys.* 1939, **7**, 1103
[4] EVANS, U. R. *Trans. Faraday Soc.* 1945, **41**, 365
[5] HARTLEY, F. D., LORD, F. W. and MORGAN, L. B. *Ric. sci. A*, 1955, **25**, 577
[6] RYBNIKAR, F. *J. Polym. Sci.* 1960, **44**, 517
[7] BUCKSER, S. and TUNG, L. H. *J. phys. Chem.* 1959, **63**, 763
[8] WESSLAU, H. *Makromol. Chem.* 1956, **20**, 111
[9] SWAN, P. R. *J. Polym. Sci.* 1960, **42**, 525
[10] GRIFFITHS, J. H. and RANBY, B. G. *J. Polym. Sci.* 1959, **38**, 107
[11] HOFFMAN, J. D., WEEKS, J. J. and MURPHEY, W. M. *J. Res. Nat. Bur. Stand. A*, 1959, **63**, 67
[12] BANKS, W., GORDON, M., ROE, R.-J. and SHARPLES, A. To be published
[13] MATSUOKA, S. *J. Polym. Sci.* 1960, **42**, 511
[14] KELLER, A. *Makromol. Chem.* 1959, **34**, 1
[15] HATANO, M. and KAMBARA, S. *Polymer, Lond.* 1961, **2**, 1
[16] INOUE, M. *J. Polym. Sci.* 1961, **55**, 753
[17] KOVACS, A. J. *Ric. sci. A*, 1955, **25**, 666
[18] HIRAI, M. and EYRING, H. *J. appl. Phys.* 1958, **29**, 810
[19] BANKS, W., HAY, J. N., SHARPLES, A. and THOMSON, G. To be published
[20] FOX, T. G and LOSHAEK, S. *J. appl. Phys.* 1955, **26**, 1080

Polymerization of tert-*Butyl Acrylate in the Presence of* n-*Butyl Lithium and Titanium Tetrachloride*

E. A. H. HOPKINS and M. L. MILLER

The use of a Ziegler-type catalyst for the polymerization of tert-*butyl acrylate is reported. By the proper choice of catalyst components, conditions and procedures, high yields of stereoregular, crystalline poly*(tert-*butyl acrylate*) *are obtained. The optimum conditions for this polymerization are noted.*

ESTERS normally inactivate Ziegler-type catalysts unless complexing solvents are used[1]. We have found, however, that *tert*-butyl acrylate can be polymerized in petroleum ether in good yield to highly crystalline polymer by the Ziegler-type catalyst, *n*-butyl lithium plus titanium tetrachloride. This polymerization is in marked contrast to polymerization of the less bulky esters, methyl methacrylate and vinyl acetate which are polymerized to crystalline polymer by Ziegler catalysts only if polymerization is carried out in the presence of diethyl ether, tetrahydrofuran or similar complexing agents[2,3]. The beneficial effect of the *tert*-butyl group may result from its ability to shield the ester carbonyl and prevent inactivation of the catalyst. Other polar monomers with bulky groups which have been polymerized to stereoregular polymer by active Ziegler catalysts are: vinyl carbazole[4] and *N,N*-dialkyl acrylamides[5].

The object of the work reported here was to study the polymerization of *tert*-butyl acrylate with a Ziegler-type catalyst.

EXPERIMENTAL

Materials

tert-Butyl acrylate was prepared by the method of McCloskey, Fonken, Kluiber and Johnson[6] (b.pt 117°C, 760 mm of mercury, d_4^{30} 0·8711, n_D^{25} 1·4080). The monomer was stored over calcium hydride at 7°C for at least four days and then distilled under vacuum into glass ampoules provided with break tips. The petroleum ether was ACS reagent grade, b.pt 30° to 60°C. *n*-Butyl lithium was supplied by the Foote Mineral Company as a 15·5 per cent solution in mixed hydrocarbons (1/3 pentane, 2/3 hexane). The solution was analysed by the double titration method of Gilman and Haubein[7] and by the single titration method of Frankel, Rabani and Zilkha[8]. Titanium tetrachloride was Fisher's 'purified' from Fisher Scientific Company.

Polymerization

All glassware was dried at 150°C and cooled in an inert atmosphere. 150 ml of petroleum ether was introduced into a 250 ml flask which was fitted with a serum stopper, a stirring bar, and a side tube to which the ampoule containing monomer was attached by Tygon plastic tubing.

The petroleum ether was boiled five minutes under vacuum and then 'prepurified' nitrogen was admitted. Unless otherwise specified polymerization was carried out as follows.

The catalyst components were injected through the serum stopper, first 9·6 mmoles of *n*-butyl lithium followed by 3·2 mmoles of titanium tetrachloride. The catalyst was aged ten minutes at room temperature and then cooled in an ice bath for ten minutes. 2½ to 5 ml of monomer, containing approximately 4 mg of calcium hydride, was added at the rate of 0·78 g/min and the polymerization allowed to proceed at 0°C for 40 minutes. In early experiments the polymerization was quenched by the addition of a 1 : 1 (v/v) solution of methanol in water. When this method of quenching was used the polymers, although recoverable and useful, were difficult to handle and had a high percentage of ash. If absolute methanol was added to the polymerizing mixture before the introduction of air, the polymers were easier to extract and the ash was reduced from ten per cent to a few tenths of one per cent. The coagulated polymer was filtered, washed with aqueous methanol, dried under vacuum at 50°C and extracted repeatedly with boiling acetone to remove amorphous polymer. The polymer that failed to dissolve in acetone was examined for crystallinity by X-ray diffraction and for metals by ultra-violet emission spectroscopy. The molecular weight was estimated from the viscosity in chloroform at 30°C[9].

RESULTS

The effect of the following variables on the polymerization was examined: (*a*) variation in the metal alkyl component of the catalysts; (*b*) variation in the concentration of catalyst; (*c*) order of addition of catalyst components; (*d*) variation in the time of catalyst ageing; (*e*) the rate of addition of the monomer; (*f*) the temperature of polymerization, and (*g*) the use of additives.

The organometallic compounds tested as catalyst components were: *n*-butyl lithium, amyl sodium, diethyl aluminium chloride, tri-*n*-butyl aluminium, diethyl cadmium and diethyl zinc. In all tests, except those with amyl sodium a 3/1 mole ratio of metal alkyl to titanium tetrachloride was used. With amyl sodium a 5·3/1 ratio was used. Catalysts made with *n*-butyl lithium polymerized 86 per cent of the monomer (molecular weight 1×10^6) and catalysts made with tri-*n*-butyl aluminium, 61 per cent (molecular weight $2{\cdot}5 \times 10^4$). Other metal alkyls tested produced lesser amounts of polymer.

The order in which the catalyst components were added to the reaction vessel had an effect on the percentage of monomer polymerized. When titanium tetrachloride was added to *n*-butyl lithium, the percentage conversion was higher than when the reverse order of addition was used.

Experiments were run to test the effect of a number of variables on polymerizations initiated by *n*-butyl lithium plus titanium tetrachloride. Experiments were run to test the effect of the length of time that elapsed between the initial contact of the titanium tetrachloride with the butyl lithium and the beginning of the introduction of the *tert*-butyl acrylate. We refer to this time as the ageing time. The total ageing time included the time required to cool the catalyst dispersion to the polymerization temperature as well as the time used in the initial ageing at room tempera-

Table 1. Effect of length of time catalyst was aged on conversion to polymer

Temperature of catalyst preparation, °C	*Minutes at room temp.*	*Minutes at °C*	*Total time*	*Percentage conversion*	*% of polymer insoluble in acetone*
0	0	0	0	58·0	58·5
25	5	5	10	72·0	35·1
25	10	10	20	86·0	90·5
25	15	10	25	5·0	7·5

ture. *Table 1* gives the percentage of monomer which was converted to polymer and the percentage of the polymer that was insoluble in boiling acetone (crystalline polymer) in experiments in which the catalyst was prepared and aged at different temperatures and for different times. The highest yield of polymer and the highest yield of crystalline polymer resulted when the catalyst was aged ten minutes at room temperature and transferred to an ice bath at 0°C where it stood for ten minutes.

Table 2. Effect of temperature of polymerization on percentage of monomer polymerized*

Time of catalyst ageing, min	*Time of polymerization, min*	*Temperature of polymerization, °C*	*Percentage conversion*
10–room temp. 20–to cool	360	−70	11
10–room temp. 10–to cool	40	0	39
10–room temp.	40	room	< 5

*Rate of addition of monomer 0·2 g/min.

The effect of the temperature of polymerization was examined in the series of experiments listed in *Table 2*. This table shows that polymerization at 0°C gives higher conversion than polymerization at either −70° or +25°C. The percentage conversion to polymer was increased by an increase in the rate of addition of monomer to the catalyst dispersion. *Figure 1*, which plots the percentage of the monomer polymerized against the rate

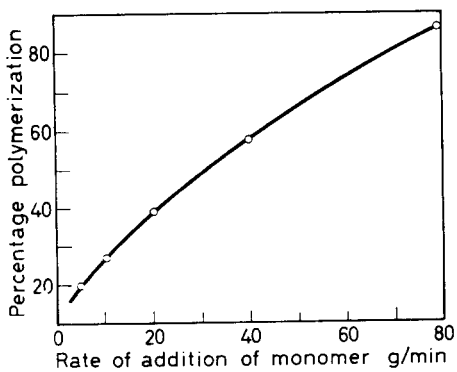

Figure 1—Effect of rate of addition of monomer on percentage polymerization

at which the monomer was added, shows that the faster the monomer was added the higher the conversion to polymer. A faster rate of monomer addition also increased the percentage of polymer that was insoluble in acetone. When the rate of addition of monomer was 0·78 g/min, 90·5 per cent of the polymer was insoluble in acetone. When the rate was 0·05 g/min, 63·7 per cent of the polymer was insoluble in acetone.

Table 3. Effect of inclusion of calcium hydride and air on polymerization

Conc. of $TiCl_4$ *mmoles/ml* $\times 10^2$	*Additive*	*Percentage polymerization*	*% of polymer insoluble in acetone*
1·1	None	3	
1·1	4 mg CaH_2 Trace of air	86	90·5
2·2	None	95	82·4

An increase in the concentration of titanium tetrachloride from $1{\cdot}1 \times 10^{-2}$M to $2{\cdot}2 \times 10^{-2}$M, with a fixed ratio of *n*-butyl lithium to titanium tetrachloride of 3/1 increased the percentage conversion from 3 to 95 per cent.

When a small amount of calcium hydride, either with or without traces of air, was added with the monomer, the yield of crystalline polymer increased. This increase was especially marked when the concentration of catalyst was low, *Table 3*.

The acetone-insoluble polymer had a high molecular weight and a degree of crystallinity (shown by X-ray diffraction) that was as high as the crystallinity of poly(*tert*-butyl acrylate) polymerized with lithium or *n*-butyl lithium[9] alone.

CONCLUSIONS

From the foregoing it can be seen that the polar monomer, *tert*-butyl acrylate, can be converted to stereoregular polymer with a Ziegler-type catalyst. The polymerization is reproducible, as shown in *Table 4*, and

Table 4. Reproducibility of results

g monomer used	*Percentage conversion*	*% of polymer insoluble in acetone*	*% ash*	*Infra-red absorption*	*X-ray diffraction*	*Mol. wt (viscosity average)* $\times 10^{-6}$
3·48	97	75	0·3	stereo-regular	crystalline	1·0
3·48	96	73	0·1	stereo-regular	crystalline	1·1

there is a good yield of highly crystalline polymer with a high molecular weight.

The authors wish to acknowledge the assistance of Mr J. Skogman in the preparation of the monomer.

Polymer Chemistry Section,
American Cyanamid Co.,
Stamford, Conn., U.S.A.

(Received May 1962)

REFERENCES

[1] NATTA, G. *J. Polym. Sci.* 1960, **48,** 219
[2] *Australian Patent No. 225 990* (1957)
[3(a)] *British Patent No. 819 291* (1959)
(b) *British Patent No. 832 319* (1960)
[4] SOLOMON, O. F., DIMONIE, M., AMBROZH, K. and TOMESKU, M. *J. Polym. Sci.* 1961, **52,** 205
[5] ATTFIELD, D. J., BUTLER, K., RADCLIFFE, A. T., THOMAS, P. R., THOMPSON, R. A. and TYLER, G. J. *Chem. & Ind.* **1960,** 263
[6] MCCLOSKEY, A. L., FONKEN, G. S., KLUIBER, R. W. and JOHNSON, W. S. *Org. Synth.* 1954, **34,** 26
[7] GILMAN, H. and HAUBEIN, A. H. *J. Amer. chem. Soc.* 1944, **66,** 1515
[8] FRANKEL, M., RABANI, J. and ZILKHA, A. *J. Polym. Sci.* 1958, **28,** 387
[9] MILLER, M. L. and RAUHUT, C. E. *J. Polym. Sci.* 1959, **38,** 63

The Radiation Chemistry of Some Polyamides. An Electron Spin Resonance Study

C. T. GRAVES and M. G. ORMEROD

Electron spin resonance spectroscopy was used to study the nature, concentration and kinetics of disappearance of the free radicals produced in polyamides by gamma irradiation at 77°K. At 77°K, two radical species predominated, one of which has been identified as $-CH_2-CO-NH-\dot{C}H-CH_2-$. *At room temperature the radicals decay leaving a more stable species which is probably a radical stabilized on a radiation-induced double bond. G values for these radicals have been calculated and the kinetics of their decay studied. We have related our electron spin resonance data to the radiation chemical studies of other workers. This has enabled us to present a scheme for the radiation-induced reactions in polyamides.*

ALTHOUGH chemical changes induced by ionizing radiation can be measured using a variety of techniques—e.g. infra-red (i.r) and ultra-violet (u.v.) spectroscopy, viscometry, light scattering measurements and analysis of the evolved gases—few definite conclusions have been reached about the intervening mechanisms by which they occur. It is therefore of interest to examine the unstable intermediates whose reactions give rise to the final products.

If irradiation is carried out at a sufficiently low temperature, the free radicals initially formed by the radiation are stabilized and can be examined. Subsequent warming of the sample allows radical reactions to occur and these can be followed by using electron spin resonance (e.s.r.) techniques. This method has been used successfully with several polymers[1,2]—in particular, polyethylene[3–5], polyvinyl chloride[2,6,7] and polysiloxanes[8].

We have used e.s.r. to investigate the radiation-induced free radicals in a range of drawn and undrawn polyamides differing in the number of $-CH_2-$ groups between the amide groups. Radical identification has been facilitated by studying the variation with the direction of the magnetic field of the e.s.r. spectrum of an oriented sample. Our data have been related to previous radiation chemical studies.

EXPERIMENTAL

An X-band, 400 kc/s modulation frequency spectrometer, which has been described more fully elsewhere[5,8], was used for the measurements at 77°K and at 195°K. The room temperature measurements were made on a similar X-band, 105 kc/s modulation frequency spectrometer which was built by L. G. Stoodley of this laboratory. All spectra are shown as the first derivative of the absorption intensity.

The polyamide samples were irradiated at 77°K *in vacuo* in glass tubes. Their e.s.r. spectra were observed at 77°K without prior warming. They were then warmed to room temperature and the decay of the free radicals followed.

Concentrations of free radicals were determined by numerical integration of derivative curves and by comparison with the signal from a molybdenum disulphide sample which had been calibrated against α,α'-diphenyl-β-picryl hydrazyl. Radical concentrations are expressed as the number formed per 100 eV of absorbed energy. This is known as the G value.

The source of radiation was a 2 kilocurie ^{60}Co γ source (dose rate = 600 kilorad h^{-1}).

The polyamides studied which were supplied by British Nylon Spinners Ltd were nylons 6; 6.6; 6.8; 6.10; 11. Drawn samples of nylon 6.10; 8; 6.8; 6.6; 7; were also used. These were placed in sample tubes in a random fashion so as to avoid any orientation effects. For studies of radical anisotropy an oriented sample of nylon 6.10 was mounted so that measurements could be made with the magnetic field either along the fibre axis or at right angles to it.

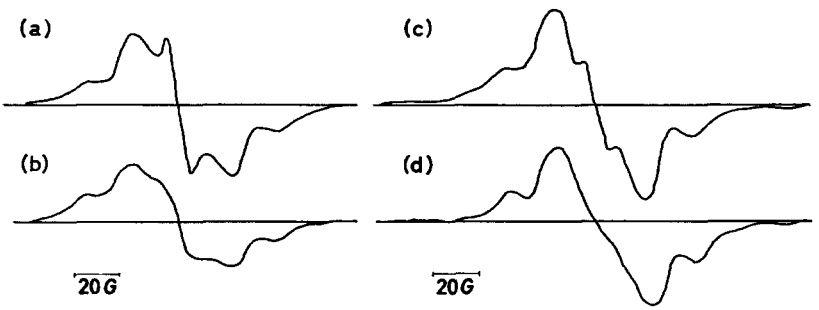

Figure 1—E.s.r. spectra from some polyamides irradiated and studied at 77°K: (a) Nylon 6.6 undrawn, (b) Nylon 6.6 drawn, (c) Nylon 6.8 undrawn, (d) Nylon 6.8 drawn

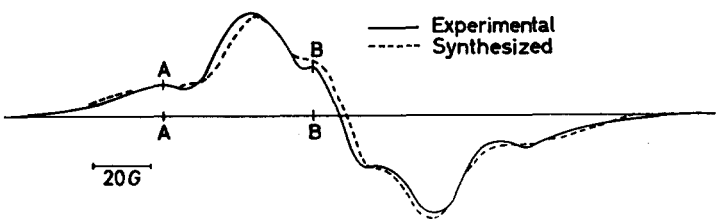

Figure 2—E.s.r. spectrum of nylon 11 undrawn, irradiated and studied at 77°K

RESULTS

After γ irradiation to a dose of about 10 MR and observation at that temperature, all the polyamides gave an e.s.r. spectrum which was stable at 77°K. It consisted of a quartet with a hyperfine splitting of about 21 gauss and a superimposed singlet, the relative proportions differing according to the specimen. There were also some weak lines in the wings of the spectra indicating the presence, in low concentrations, of another type of radical. Typical spectra are shown in *Figure 1*.

It is possible to synthesize the spectra at 77°K by assuming gaussian line shape, a line width of 13 gauss for the quartet, and a line width of 11 gauss for the singlet. This is shown for undrawn nylon 11 in *Figure 2*. From the distances AA and BB marked in the figure the relative sizes of the quartet and the singlet were estimated for all the nylons and hence their relative areas could be calculated. These results are in *Table 1*. It can be seen that the only effect of drawing the nylons is to reduce the intensity of the singlet. On warming to 195°K the weaker lines disappeared (*Figure 3*).

Table 1

NYLON	G_{TOTAL}	$G_{QUARTET}$	$G_{SINGLET}$
Undrawn			
6	0·7	0·5	0·2
6·6	1·0	0·7	0·3
6·8	1·4	1·1	0·3
6·10	1·4	1·0	0·4
11	1·1	0·8	0·3
Drawn			
7	1·1	0·9	0·2
8	1·0	0·8	0·2
6·6	1·3	1·1	0·2
6·8	1·5	1·3	0·2
6·10	0·9	0·8	0·1

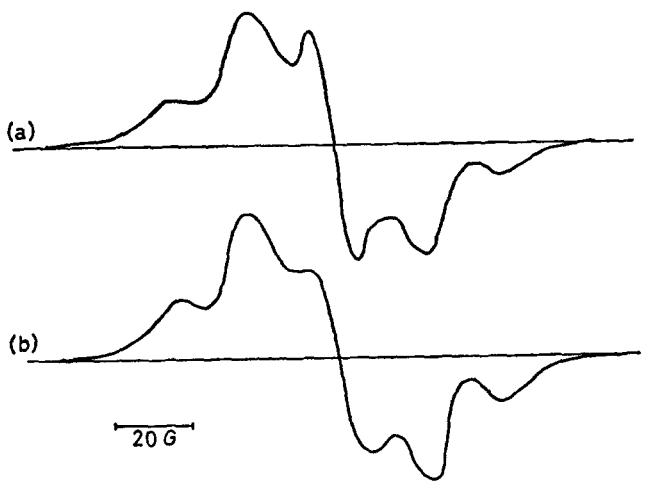

Figure 3—E.s.r. spectra of two polyamides irradiated at 77°K and studied at 195°K: (a) Nylon 6.6 undrawn, (b) Nylon 7 drawn

On warming the samples to room temperature, the quartet and the singlet decay at different rates. At the same time a single broad line appears (*Figure 4*). These spectra are similar to those reported by other workers[9,10].

The overall radical decay at room temperature has only been plotted for one sample—undrawn nylon 6.8—and is shown in *Figure 5*. In order to compare relative radical stabilities in different samples, we plotted the

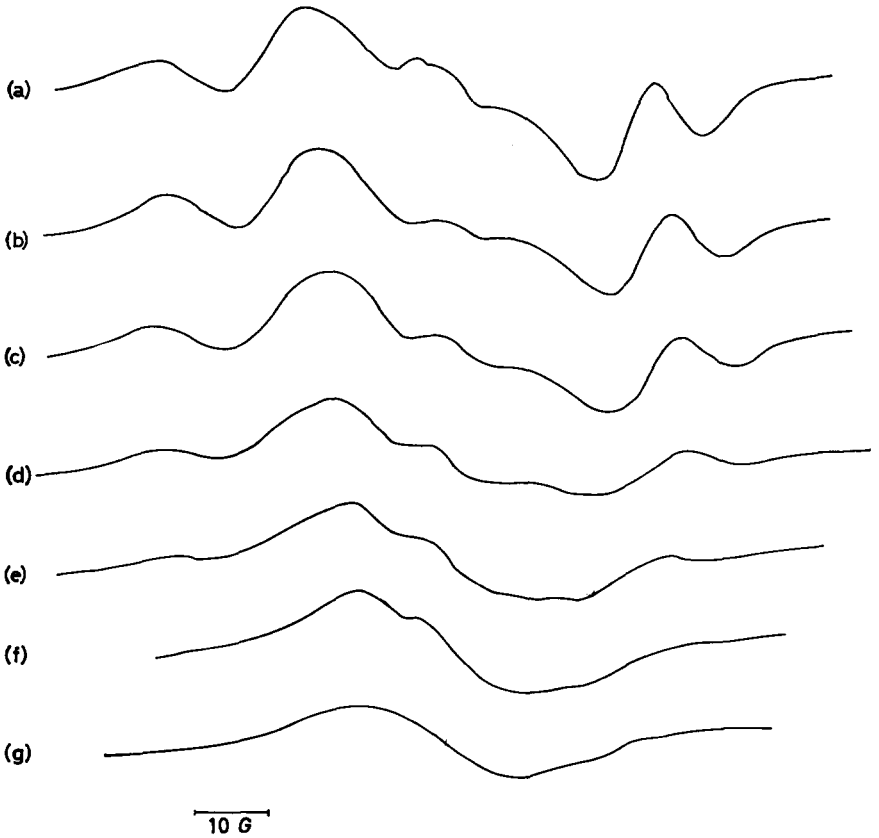

Figure 4—Room temperature (20°C) decay of the e.s.r. spectrum of nylon 6.8 undrawn irradiated at 77°K: (a) After 2 min, (b) After 16 min, (c) After 150 min, (d) After 455 min, (e) After $1{\cdot}44\times10^{3}$ min, (f) After $4{\cdot}32\times10^{3}$ min, (g) After $1{\cdot}73\times10^{4}$ min

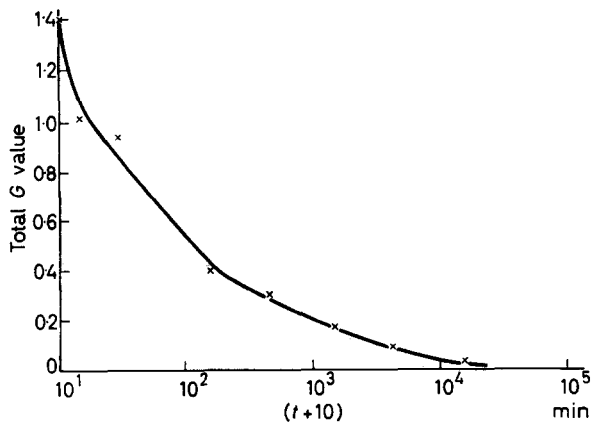

Figure 5—Total radical decay at room temperature (20°C) of nylon 6.8 undrawn irradiated at 77°K

decay of the outer lines of the quartet, since they are unaffected by the singlet. The results of these plots are shown in *Figure 6*. Neither the total radical concentration nor the quartet concentration showed a first or second order decay. The scales used in the figures were adopted for convenience. Radical stability was about the same in all the polyamides.

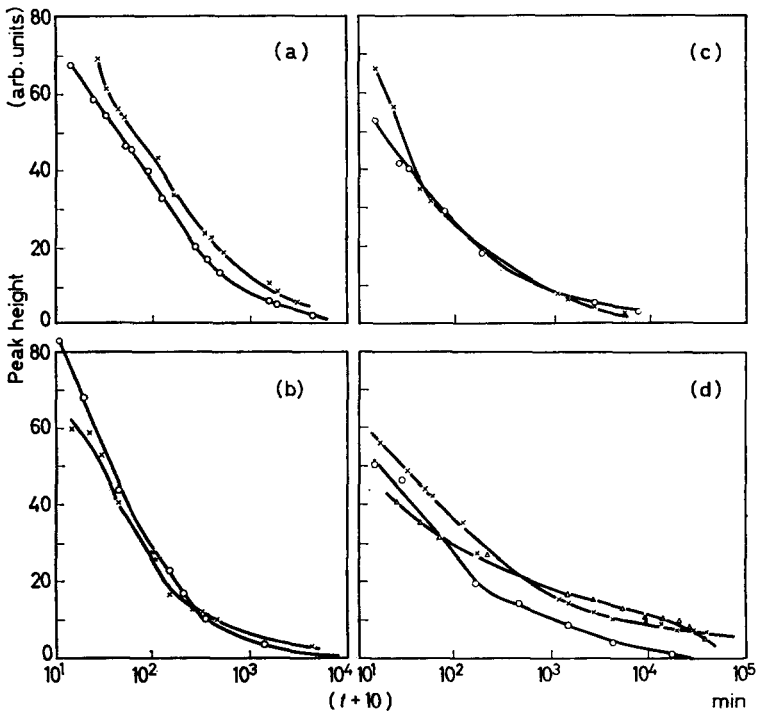

Figure 6—Room temperature (20°C) decay of the outer lines of the quartet in the e.s.r. spectrum of each polyamide irradiated at 77°K: (a) × Nylon 7 drawn, ○ Nylon 8 drawn; (b) × Nylon 6.8 undrawn, ○ Nylon 6.8 drawn; (c) × Nylon 11 undrawn, ○ Nylon 6 undrawn; (d) × Nylon 6.6 drawn, ○ Nylon 6.10 undrawn, △ Nylon 6.10 drawn

RADICAL IDENTIFICATION

Unambiguous radical identification in solids is best made by studying single crystals, and using the property that, while the hyperfine splittings due to β-hydrogen atoms are isotropic with magnetic field direction, the α-hydrogen splittings are markedly anisotropic[11]. Similar studies can be made with polymers by orienting them by cold drawing prior to irradiation, as has been done with polyethylene[12].

Using this technique Gordy and Shields[13] have studied the doublet found in silk irradiated at room temperature. They concluded that the radical was —NH—$\dot{C}$H—CO—. Similar radicals have been observed in single crystals of acetyl-glycine[14] and glycyl-glycine[15]. The only effect of the —NH— group is a line broadening due to unresolved coupling with the ^{14}N nucleus.

From these results it appears that the most stable radical species is that adjacent to the amide group. This is an agreement with Burrell's work[16] on polycrystalline amides studied at 77°K. It is therefore to be expected that the radical

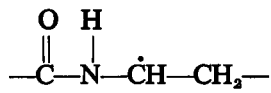

will be found in irradiated nylon, and it seems reasonable to associate the observed quartet with this radical since four lines would arise from the unpaired spin coupling with the α-hydrogen and the two β-hydrogens.

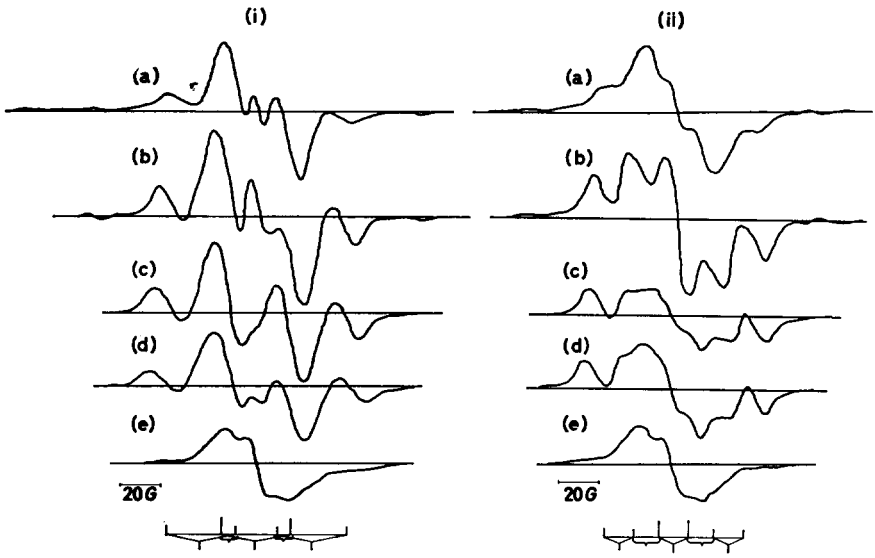

Figure 7—E.s.r. spectra of an oriented specimen of nylon 6.10 irradiated at 77°K and studied at different temperatures: (i) *H* parallel to the fibre direction, (ii) *H* perpendicular to the fibre direction; (a) 77°K, (b) 195°K, (c) After 2 min at 20°C, (d) After 4 h at 20°C, (e) After 11 days at 20°C

In order to check this radical identification an oriented sample of nylon 6.10 was studied. The spectra obtained after irradiating at 77°K and viewing at 77°K, 195°K and room temperature are shown in *Figure 7*. The change in spectrum between 77°K and 195°K is irreversible and is probably due to the decay of another radical species (perhaps $-CH_2-\dot{C}H-CH_2-$) present in low concentration which gives rise to the previously mentioned lines in the wings of the spectrum at 77°K. The lines that are to be expected from a radical containing one α- and two β-hydrogens are also shown in *Figure 7*. These lines are calculated on the assumption that a β-hydrogen gives a hyperfine splitting of 26 gauss and that an α-hydrogen gives a splitting of 32 gauss when the fibre axis is parallel to the magnetic field and 14 gauss when it is perpendicular. These data have been taken from previous work on the radical $-CH_2-\dot{C}H-CH_2-$ in polyethylene[12,17].

The presence of the singlet in the centre tends to obscure the quartet spectrum, but it can be seen that the experimental results agree with those predicted. At low temperatures the lines which have been coupled together in *Figure 7* cannot be resolved from one another owing to their proximity and to the large line width. At room temperature, with the magnetic field perpendicular to the fibre axis, all the lines can be resolved. Our e.s.r. data cannot distinguish between the radicals —CO—NH—$\dot{C}$H—CH_2— and —CH_2—$\dot{C}$H—CO—NH—CH_2— since both have one α- and two β-hydrogens. However, Burrell's work on substituted amides[16] shows that it is the hydrogen adjacent to the —NH— group which is usually removed. We therefore assign the quartet to the radical —CO—NH—$\dot{C}$H—CH_2—.

The assignment of the central singlet is more difficult. It is not a radical formed by scission of a ≡C—H, ≡C—C≡, or =N—H bond since any such radical would couple with one or more hydrogen atoms, or, in the case of —$\dot{N}$—, with the nitrogen nucleus. The unpaired species is either the result of a reaction of the polymer with hydrogen atoms formed by irradiation or it is an ion. Since the singlet takes several hours to decay at room temperature we think it unlikely that it arises from an ion. We suggest that it is due to the addition of a hydrogen atom to the carbonyl group to give the radical

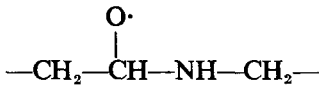

In most polymers with a carbon backbone, radiation forms vinylene double bonds. With polyethylene and polypropylene it has been shown that at room temperature radicals tend to become stabilized on these double bonds to give a comparatively stable allylic radical[3,18]. It has been suggested that the double bond —CO—N=CH— is formed in polyamides[19]. It seems probable that the broad stable singlet which is formed in irradiated polyamides after standing at room temperature is the radical

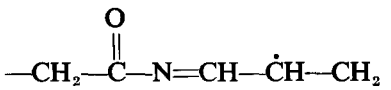

which resonates with the structures

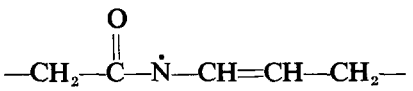

and

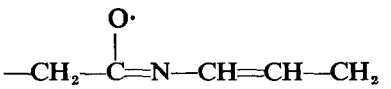

Any hyperfine splittings will be small owing to the extended conjugation of the unpaired spin and will probably be smaller than the line width. Hence only a single broad line will result. Similar broad lines have been observed in highly irradiated polymers and have been assigned to polyene radicals[25].

DISCUSSION

Comparatively few studies have been made of the radiation chemistry of polyamides. Early workers were in disagreement as to whether they crosslinked or degraded under radiation[20–22]. From later work it seems that crosslinking and degradation occur simultaneously[21,22].

Marjury and Pinner[23] obtained a G value for the net number of crosslinks formed in polycaprolactum (nylon 6) of number molecule weight 20 000 of 0·35. They also found that $-NH_2$ end groups are formed with a G value of 0·6 while at the same time there is a decrease in the number of carboxylic groups. If it is assumed that for every $-NH_2$ group formed one main chain fracture occurs, one obtains a value of 0·6 for G (degradation). With this value and assuming a random distribution for the polymer, it can be calculated that $G_{(\text{crosslinks})} = 0{\cdot}5$.

Zimmerman[23] has studied the change in viscosity with radiation dose in nylon 6.6 and in a 6.6/6/6.10 terpolymer of low crystallinity. He found that the terpolymer crosslinked more readily and that temperature also had a marked effect. From these facts he suggested that degradation is due to a radical reaction, such as disproportionation, and that it is difficult for crosslinks to form in crystalline regions, probably due to the hydrogen bonding.

Our e.s.r. data have shown the presence of radicals formed at 77°K with a G value of about one. It is believed that in polyethylene crosslinks are formed by the combination of two radicals and that the radicals meet one another by a slow migration due to a hydrogen transfer reaction[3,5], i.e. $RH + R\cdot \longrightarrow R\cdot + RH$. It is probable that radicals can migrate through nylon in the same way. At room temperature there is no evidence for radicals of the type $-CH_2-\dot{C}H-CH_2-$ which are to be expected if the radicals are migrating. Since $-CO-NH-\dot{C}H$ is the more stable radical, the reactions

$$-NH-\dot{C}H- + -CH_2-CH_2- \longrightarrow -NH-CH_2- + -CH_2-\dot{C}H- \quad (1)$$

$$-CH_2-\dot{C}H- + -CH_2-CH_2- \longrightarrow -CH_2-CH_2- + -CH_2-\dot{C}H- \quad (2)$$

$$-CH_2-\dot{C}H- + -NH-CH_2- \longrightarrow -CH_2-CH_2- + -NH-\dot{C}H- \quad (3)$$

will occur in order of difficulty (1) > (2) > (3), so that reaction (1) will occur much less readily than the other reactions. The concentration of $-CH-NH-\dot{C}H-$ radicals will be in sufficient excess to prevent the observation of $-CH_2-\dot{C}H-CH_2-$ radicals.

There is evidence that main chain fracture in polyamides is a radical disproportionation reaction[24]. It has also been shown that $-NH_2$ end groups are formed[23]. It seems that the main radical species present, $-CO-NH-\dot{C}H-CH_2-$ will react to give a chain fracture and an $-NH_2$ group—possibly by a series of reactions of the type shown below

$$-CH_2-CO-NH-\dot{C}H-CH_2- \longrightarrow -CH_2-\dot{C}O + HN{=}CH-CH_2-$$

$$—CH_2—CO + \text{Polymer} \longrightarrow —CH—\overset{\overset{O}{\|}}{C}—H + \text{polymer radical} \quad (5)$$

$$HN{=}CH—CH_2—CH_2— \longrightarrow H_2N—CH{=}CH—CH_2— \quad (6)$$

If this scheme is correct, a chain fracture does not result in the destruction of a radical—the number of crosslinks eventually formed will be independent of the amount of degradation.

Summarizing the above arguments we suggest that the following reaction scheme takes place upon irradiating polyamides:

$$—CH_2—CO—NH—CH_2—CH_2— \overset{h\nu}{\sim\!\!\sim\!\!\longrightarrow} —CH_2—CO—NH—\dot{C}H—CH_2— + H\cdot$$

$$\sim\!\!\sim\!\!\longrightarrow CH_2—\dot{C}H—CH_2— + H\cdot$$

$$+ \text{ a few other radicals}$$

$$\sim\!\!\sim\!\!\longrightarrow —CH_2—CO—N{=}CH—CH_2— + H_2$$

$$2\dot{H} \longrightarrow H_2 \quad (7)$$

$$H\cdot\star + \text{Polymer} \longrightarrow H_2 + \text{polymer radical (H}\cdot\star \text{ represents a 'hot' H atom)} \quad (8)$$

$$H\cdot + —CH_2—CO—NH—CH_2— \longrightarrow —CH_2—\overset{\overset{O}{\diagdown}}{CH}—NH—CH_2— \quad (9)$$

$$\text{Radicals} \xrightarrow{\text{disproportionate}} \text{fractures}$$

$$\text{or} \xrightarrow{\text{migrate}} \text{crosslinks}$$

$$\text{or} \xrightarrow{\text{migrate}} —CH_2—CO—N{=}CH—\dot{C}H—CH_2—$$

These reactions give $G_{(\text{crosslinks})} = \frac{1}{2}G_{(\text{radicals})} \approx 0{\cdot}5$. The number of chain fractures depends on the relative rates of the disproportionation reaction (4) and the hydrogen transfer reaction (1). If the rate of reaction (1) is slowed down then there is a greater probability that reaction (4) will occur, which explains why it is more difficult to crosslink a more crystalline polyamide. Temperature should also have an effect which will depend upon the relative activation energies of the two reactions.

One might expect that the relative rates of the reactions (8) and (9) above would depend upon the number of methylene groups between the amide groups in the polymer, i.e. the fewer the number of amide groups, the fewer the number of $—\overset{\overset{O\cdot}{|}}{\underset{\underset{H}{|}}{C}}—NH—$ radicals formed. In practice this is not found to be so. This might be because an insufficient range of polyamides was studied.

Finally it should be noted that the radicals in these polyamides are long-lived—on average it takes 160 h at 20°C for the radical concentration to be reduced by 95 per cent. If oxygen is let into an evacuated sample

after irradiation it will react with any remaining radicals thus preventing them from reacting with one another. This may account for some of the discrepancies found by early workers[20–22]. Any future studies on the radiation chemistry of these compounds should allow for this effect.

CONCLUSIONS

A range of drawn and undrawn nylons with ratios of methylene groups to amide groups varying from 5:1 to 10:1 when irradiated at 77°K gave essentially the same radicals. It was not possible to obtain a simple correlation between this ratio and the corresponding G values. The identification of the spectra was greatly facilitated by the study of an oriented specimen, again demonstrating the value of this technique in polymer studies.

The overall G values vary from 0·7 to 1·4. The e.s.r. spectrum consists of two major components:

(*a*) a quartet due to the removal of a hydrogen α to the amide group, and
(*b*) a singlet which is probably due to hydrogen addition to a carbonyl group, but whose interpretation is not certain.

There is also evidence of the existence of signals due to other radicals. The singlet was less intense in the drawn samples than in the undrawn.

The radicals are stable at 77°K, and decay at room temperature at a rate which is an order of magnitude slower than the decay of free radicals in polyethylene[35]. This confirms the view that a radical associated with the amide group is more stable than an alkyl radical. During this decay some of the original radicals become stabilized on radiation-induced double bonds.

Previous work[24] has shown that the final radiation-induced products depend on the post-irradiation storage temperature. We believe this to be due to the competition between disproportionation, which gives rise to scissions, and migration which gives rise to crosslinks.

We wish to thank Professor A. Charlesby with whom we had several discussions, Mr L. G. Stoodley who built the e.s.r. spectrometers, and British Nylon Spinners Ltd who supplied the nylon samples.

Physics Branch,
Royal Military College of Science,
Shrivenham, Swindon, Wiltshire

(*Received June 1962*)

REFERENCES

[1] TSVETKOV, YU. D., MOLIN, YU. N. and VOEVODSKII, V. V. *Vysokomol. Soedineniya,* **1959,** No. 1, 1805
[2] CHARLESBY, A. and ORMEROD, M. G. *Fifth International Symposium on Free Radicals, Uppsala, 1961.* Almqvist and Wiksell: Stockholm, 1961
[3] KORITSKII, A. T., MOLIN, YU. N., SHAMSHEV, V. N., BUBEN, N. YA. and VOEVODSKII, V. V. *Vysokomol. Soedineniya,* **1959,** No. 1, 1182
[4] LAWTON, E. J., BALWIT, J. S. and POWELL, R. S. *J. chem. Phys.* 1960, **33,** 395
[5] CHARLESBY, A., LIBBY, D. and ORMEROD, M. G. *Proc. Roy. Soc. A,* 1961, **262,** 207
[6] LOY, B. R. *J. Polym. Sci.* 1961, **50,** 245

[7] LAWTON, E. J. and BALWIT, J. S. *J. phys. Chem.* 1961, **65,** 815
[8] ORMEROD, M. G. and CHARLESBY, A. In press
[9] OHNISHI, S., IKEDA, Y., KISHIWAGA, M. and NITTA, I. *Polymer, Lond.* 1961, **2,** 119
[10] BALLANTINE, D. S. and SHINOHARA, Y. *Fifth International Symposium on Free Radicals, Uppsala, 1961.* Almqvist and Wiksell: Stockholm, 1961
[11] GOSH, D. K. and WHIFFEN, D. H. *Mol. Phys.* 1959, **2,** 285
[12] LIBBY, D. and ORMEROD, M. G. *J. Phys. Chem. Solids,* 1961, **18,** 316
[13] GORDY, W. and SHIELDS, H. *Proc. Nat. Acad. Sci., Wash.,* 1960, **46,** 1129
[14] MIYAGAWA, I., KURITA, Y. and GORDY, W. *J. chem. Phys.* 1960, **33,** 1599
[15] KATAYAMA, M. and GORDY, W. *J. chem. Phys.* 1961, **35,** 117
[16] BURRELL, E. J. *J. Amer. chem. Soc.* 1961, **83,** 574
[17] LIBBY, D., ORMEROD, M. G. and CHARLESBY, A. *Polymer, Lond.* 1960, **1,** 212
[18] FISCHER, H. and HELLWEGE, K. H. *Fifth International Symposium on Free Radicals, Uppsala, 1961.* Almqvist and Wiksell: Stockholm, 1961
[19] ZIMMERMAN, J. *J. appl. Polym. Sci.* 1959, **2,** 181
[20] CHARLESBY, A. *Nature, Lond.* 1953, **171,** 107; 1953, **171,** 167
[21] LAWTON, E. J., BUECHE, A. M. and BALWIT, J. S. *Nature, Lond.* 1953, **172,** 76
[22] LITTLE, K. *Nature, Lond.* 1952, **170,** 1075; 1954, **173,** 680
[23] MARJURY, T. G. and PINNER, S. H. *J. appl. Chem.* 1958, **8,** 168
[24] ZIMMERMAN, J. *J. Polym. Sci.* 1960, **46,** 151
[25] OHNISHI, S., IKEDA, Y., SOGIMOTO, S. and NITTA, I. *J. Polym. Sci.* 1960, **47,** 503

Proton Magnetic Relaxation in Polyamides

D. W. McCall and E. W. Anderson

Proton magnetic relaxation studies of three polyamides have been carried out. Nuclear magnetic resonance relaxation times, T_1 and T_2, have been measured over a wide range of temperature and the transitions observed have been correlated with dielectric and mechanical loss transitions. The low temperature transition involves the entire specimen and is interpreted in terms of molecular reorientations about the long chain axes. The high temperature transition is associated with the onset of liquid-like motions in the non-crystalline regions. Between 130° and 190°C it is possible to decompose the resonances into a broad and a narrow component and to deduce a 'rigid fraction'.

PROTON magnetic resonance in polyamides has been studied extensively by workers in many laboratories. Therefore, it is disappointing that the experimental characterization is incomplete and the interpretation in terms of molecular mechanisms is in question. For example, we are not aware of any extensive study of T_1, the spin-lattice relaxation time, as a function of temperature or composition. Also, the decomposition of the resonance into narrow and broad components (i.e. amorphous and crystalline, in the usual discussion) is in dispute. In the present paper we shall present some new data; specifically, T_1 versus temperature and some T_2 results at high temperatures where resonance widths are difficult to measure. (Recall that T_2, the spin–spin relaxation time, is about equal to $1/\gamma\delta H$.) The transitions observed will be correlated with dielectric and mechanical observations, and molecular mechanisms will be proposed. In addition, we shall argue that the resonances can be justifiably decomposed into two components (at least above 130°C) and show how saturation measurements can be used to support this contention.

EXPERIMENTAL

Most of the data were acquired by pulse techniques. The spectrometer has been described in detail by Schwartz[1] but the transmitter described by Schwartz has been replaced by an Arenburg Ultrasonic Laboratory pulsed oscillator. A new probe has been constructed entirely of Teflon, and heating or cooling is accomplished by means of flowing nitrogen gas. This probe was machined from two Teflon blocks and is constructed such that the conditioned nitrogen passes up past the specimen tube and then down through an outer jacket which nearly surrounds the inner chamber. With this double jacket arrangement we have covered the temperature range $-185°$ to $+300°$C.

This spectrometer is not ideally suited to the study of resonances in solid materials. The receiver takes about 20 μsec to recover from the transmitter pulse and thus signals that decay in this period cannot be observed. We take $T_2 = t_{1/2}/\ln 2$ where $t_{1/2}$ is the half-time of the decay observed after the receiver has recovered. This procedure ties in with steady state results fairly well; $T_2 = 2/\gamma\delta H$ where δH is the steady state (peak-to-peak derivative) resonance width. *Figure 1* shows a typical decay following

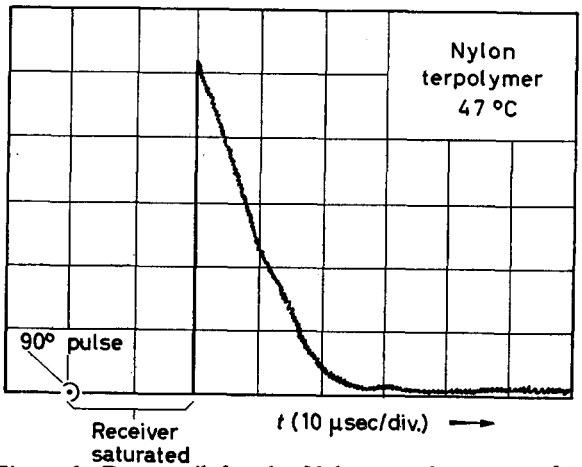

Figure 1—Decay tail for the Nylon terpolymer at 47°C. A 90° pulse (~2·5 μsec duration) begins at the first division mark. The receiver is saturated for about 20 μsec and then the nuclear signal appears after the third division mark

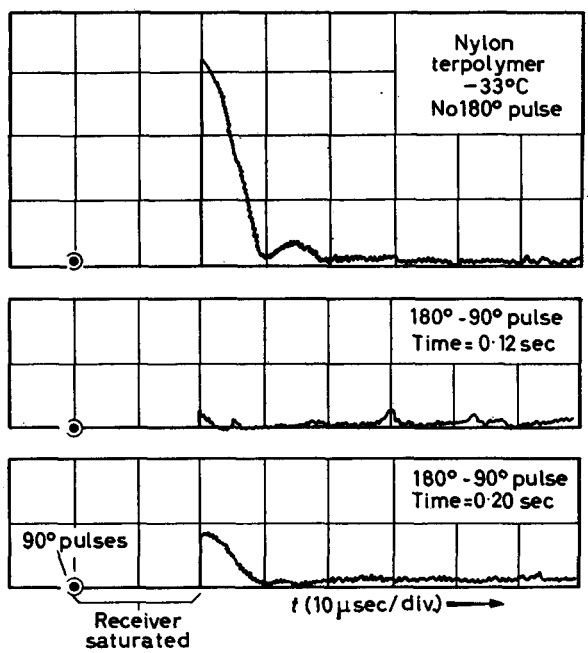

Figure 2—Decay tails for the Nylon terpolymer at −33°C. The 90° pulses (~2·5 μsec duration) begin at the first division marks. The receiver is saturated for about 20 μsec and then the nuclear signals appear after the third division marks. In the first trace there is no 180° pulse. In the middle trace the 180° pulse precedes the 90° pulse by 0·12 sec and in the bottom the 180° pulse precedes the 90° pulse by 0·20 sec

a 90° pulse (duration ~2·5 μsec). The time scale is 10 μsec/division and the pulse is marked by the spot on the baseline at one division. The receiver is saturated for the next 20 μsec and the nuclear signal appears following the fourth division mark. T_2 here is approximately 9/0·692 ~ 13 μsec.

To measure T_1, a 180° pulse is applied at time t before the 90° pulse and t is adjusted until the decay tail disappears. Then $T_1 = t_{\text{null}}/\ln 2$. *Figure 2* shows a typical case. At the top we see the 90° tail. In the two lower traces we see the same tail but the 90° pulse has been preceded by a 180° pulse. For this case $t_{\text{null}} \simeq 0{\cdot}12$ second and $T_1 \simeq 0{\cdot}17$ second. It is sometimes apparent that the specimens exhibit a distribution of T_1s but the differences are small, and we have not investigated this effect in detail.

The low temperature resonance widths were taken from the earlier study of Slichter[2] for Nylon 6–6 and Nylon 6–10. The terpolymer was not studied by Slichter. This material was measured by standard techniques employing a Varian variable frequency spectrometer operated at 15 Mc/s.

Steady-state saturation studies were carried out above 100°C. A Varian DP60 spectrometer was employed, together with a modified variable temperature probe. Details of this probe were kindly made available to us by Professor P. R. Shafer, Dartmouth College. This temperature region (i.e. above 100°C) is believed to be favourable to the decomposition of the resonance into a broad and a narrow component. The r.f. field (H_1) was calibrated by subsequent measurement of T_1 and T_2 by pulse methods. With no attenuation, $H_1 \simeq 0{\cdot}1$ gauss.

The materials, Nylon 6–6, Nylon 6–10, and the terpolymer (consisting mainly of Nylon 6–6 co-polymerized with Nylon 6–10 and Nylon 6) are du Pont products. The same polymers were previously studied in an investigation of dielectric behaviour[3]. The specimens were conditioned under vacuum for 24 h at about 100°C and then sealed under vacuum. This drying treatment is similar to that employed earlier in the dielectric study. When the specimens are heated through the melting point, they foam, darken slightly, and on subsequent cooling, usually break their glass tubes. We have not studied this foamed material extensively, but it would appear that some sort of irreversible change has occurred on melting.

PROTON RELAXATION TIMES

The spin-lattice relaxation time, T_1, and the spin–spin relaxation time, T_2, are expected to behave in the following way[4]. At low temperatures T_2 is very short and independent of temperature whereas T_1 is very long and dependent upon temperature. As the temperature is raised the molecules begin to move and, when the molecular correlation time, τ_c, is roughly equal to T_2 (i.e. the low temperature T_2), T_2 begins to increase with increasing temperature. T_1 continues to decrease with increasing temperature until $\tau_c \sim 1/\omega$, where ω is the angular resonance frequency (i.e. $2\pi\nu$). T_1 will be at a minimum at this temperature and will increase on further heating. When τ_c is very short, as in a mobile liquid, $T_1 \simeq T_2$.

In the polyamides studied in this work we observed two T_1 minima and at least two (and probably three) regions of increasing T_2, see *Figures 3, 4* and *5*. We shall try to identify these features with transitions observed by

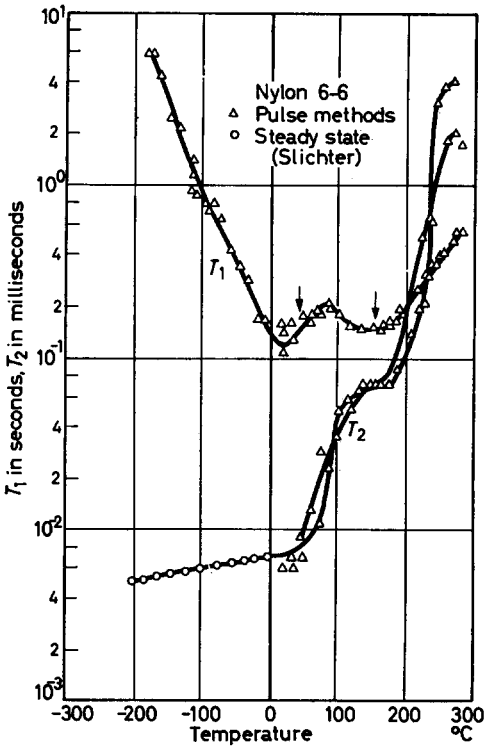

Figure 3—T_1 (sec) and T_2 (msec) for Nylon 6–6 as a function of temperature. The two arrows indicate predicted temperatures for T_1 minima based on dielectric relaxation studies

dielectric and mechanical techniques and interpret the transitions in terms of molecular motions. As will be seen, the identifications with previous measurements are easy and satisfying whereas the molecular interpretations are less definite.

Figure 3 shows the temperature dependence of T_1 and T_2 for Nylon 6–6. (When a distribution of T_2s is present, our technique sees mainly the longer times.) T_2 begins to increase just above −200°C and continues to increase gradually until the temperature has reached 50°C. This increase in T_2 must be associated with the T_1 minimum at 20°C. T_2 then increases rather abruptly between 50° and 120°C and a T_1 minimum corresponding to this increase is observed at 155°C. (Two sets of data representing different specimens are shown in the high temperature portion of *Figure 3*.) Finally, T_2 increases further above 200°C but no T_1 minimum is detected.

Figure 4 shows similar results for Nylon 6–10. T_2 increases from its low temperature value gradually and a corresponding T_1 minimum is observed at 17°C. Then a rather abrupt increase in T_2 occurs, beginning at about 50°C, with a corresponding T_1 minimum appearing at 150°C. Finally, T_2 increases sharply above 200°C but no T_1 minimum is observed. The principal difference between the results for Nylon 6–6 and Nylon 6–10 is to be seen in the T_2 plot near 150°C. T_2 is almost constant in this region for Nylon 6–6 but continues to increase in Nylon 6–10.

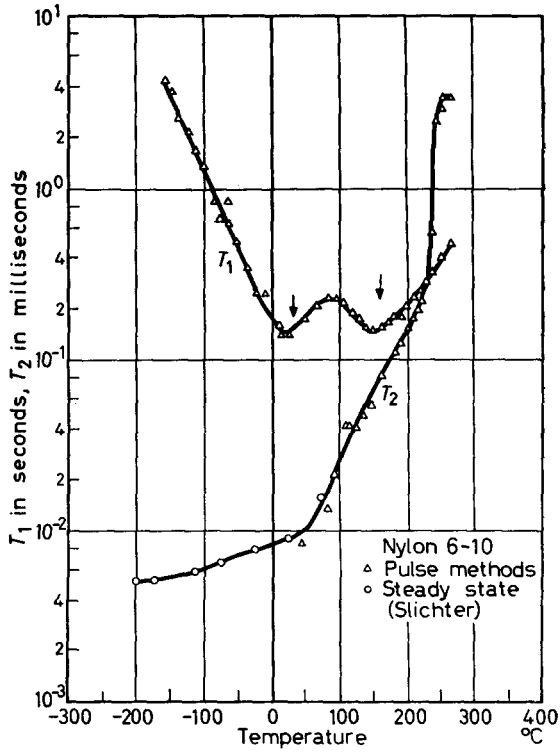

Figure 4—T_1 (sec) and T_2 (msec) for Nylon 6–10 as a function of temperature. The two arrows indicate predicted temperatures for T_1 minima based on dielectric relaxation studies

Figure 5 shows similar results for the terpolymer. Again we see the gradual low temperature increase in T_2 and the associated T_1 minimum near 10°C. This is followed by a relatively sharp increase in T_2 between 40° and 150°C and the corresponding T_1 minimum occurs at 140°C. T_2 increases relatively more slowly between 150° and 230°C but no associated T_1 effect is observed. The terpolymer appears to melt in the neighbourhood of 140°C.

In view of the obvious similarities between *Figures 3*, *4* and *5* a single discussion should suffice. The low temperature transition has been observed by several workers and has been designated as the γ transition. Recalling that the frequency of molecular motion must be equal to the resonance frequency at the temperature of the T_1 minimum, we can predict this temperature on the basis of the dielectric loss data. *Table 1* shows a comparison based on Curtis's[5] data. The agreement is excellent.

Similarly, the higher temperature transition beginning at about 50°C has been observed by a large number of workers. It seems clearly established that only the amorphous regions of the polymers are involved[3,5]. This transition is sometimes designated the α transition. Again, dielectric loss data can be used to predict the temperature of the T_1 minimum and these predictions, based on the data of McCall and Anderson[3], are given in *Table 1*. The agreement is quite good.

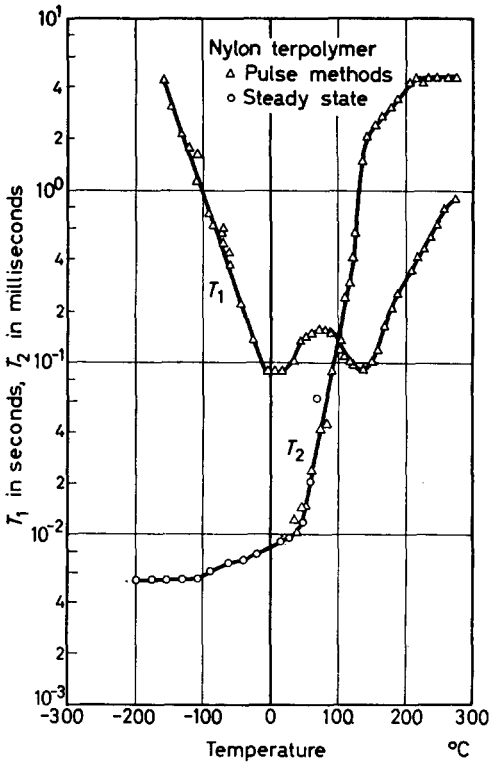

Figure 5—T_1 (sec) and T_2 (msec) for the Nylon terpolymer as a function of temperature

Table 1. Temperatures of T_1 minima

Polymer	*Observed* °C	*Predicted* °C
Nylon 6–6	20	35
Nylon 6–6	155	157
Nylon 6–10	17	23
Nylon 6–10	150	158

If the transition phenomena could be characterized properly by a single molecular correlation time, one could analyse the temperature dependencies of T_1 and T_2 in terms of activation energies. Such an analysis yields 1 to 2 kcal/mole for the low temperature process and 7 to 8 kcal/mole for the high temperature process. These activation energies are much too small for reasons discussed by Powles[6]; a distribution of correlation times leads to low results. The dielectric data yield about 10 kcal/mole for the low temperature process[5] and about 40 kcal/mole for the high temperature process[3]. A valid estimate of the activation energies from proton resonance measurements could be made if T_1 minima were measured at various frequencies.

The increase in T_2 observed above 200°C in Nylons 6–6 and 6–10 is associated with the crystalline melting transition. The absence of a T_1 minimum could be the result of the discontinuous change in correlation frequency which is expected at a first order transition. However, the continuity of the T_1 curve through this region suggests a continuous change in correlation times. A 30 per cent increase in resonance intensity occurs at about 245°C for Nylon 6–6 and about 230°C for Nylon 6–10 indicating that below these temperatures the resonance tail from the crystalline regions has decayed considerably before our receiver has recovered from the pulse. Thus, the T_1s and T_2s shown in *Figures 3*, *4* and *5* at high temperatures refer predominantly to the non-crystalline parts of the samples and are only indirectly affected by the melting transition. (The increase in intensity is about 25 per cent for the terpolymer and is observed near 130° to 140°C.)

Yet another transition is observed dielectrically near room temperature at 10 kc/sec but no evidence of this relaxation process is observed in the proton resonance curves presented here. Curtis[5] has shown that this transition is caused by a small residual concentration of water (less than 1 per cent) and thus we would not expect to detect this transition. This is a good example of a process for which the dielectric techniques are much more sensitive than resonance techniques.

RESONANCE DECOMPOSITION

Several years ago Wilson and Pake[7] made the important observation that in favourable circumstances one can measure the degree of crystallinity by means of nuclear magnetic resonance. In the polyamide systems, however, the procedure has not been generally accepted. In this section we shall examine this problem and argue that decomposition of the resonance into two components is sensible. For this discussion we shall employ the terminology of steady-state resonance.

In applying the Wilson–Pake treatment it is important that the crystalline material exhibit as broad a resonance as possible while the amorphous material exhibits as narrow a resonance as possible. Linear polyethylene and Teflon are good examples of this type of polymer; the amorphous resonances are quite narrow while the crystalline resonances exhibit their rigid lattice widths. In polyamides, on the other hand, both components of the resonance have narrowed during the low temperature transition, and we must separate the amorphous curve from a crystalline resonance that is only about half its rigid lattice width. We expect that the temperature range above the α transition but below the onset of melting will be best suited to our purposes.

Figure 6 shows a series of resonance derivative curves for Nylon 6–6 at various r.f. field intensities at 110°C. From the saturation behaviour it is apparent that the broad portion of the spectrum saturates at much higher levels than the narrow portion. We interpret this to demonstrate that the observed signal is a superposition of two resonances. Mobile regions in the polymer are associated with the narrow resonance and relatively rigid regions of the polymer are associated with the broad resonance. Decomposition of the resonances (indicated by dashed lines in *Figure 6*) is

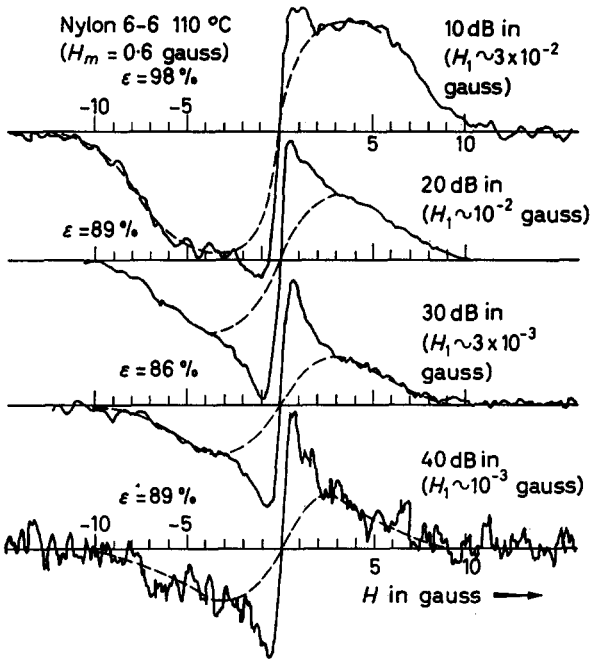

Figure 6—Resonance derivative curves for Nylon 6–6 at 110°C at various r.f. levels

Table 2

Polymer	*Rigid fraction (n.m.r.)*, %	*Rigid fraction (diel.)*, %	*Crystallinity (dens.)*, %
Nylon 6–6	60	70	53
Nylon 6–10*	55	—	36
Nylon 6–10*	—	70	60

*The Nylon 6–10 samples differed in density, 1·11 in the dielectric studies and 1·08 in the present studies.

admittedly an intuitive operation but the intensity ratios deduced are not significantly affected by varying the shape of the decomposition curve. The method employed here leads to maximum 'rigid fractions'. The 'rigid fraction' is computed as the ratio of the first moment of the broad derivative curve to the first moment of the total derivative curve. At each temperature we measured a series of curves and extrapolated the apparent 'rigid fraction' (which we sometimes call ε) to low r.f. level. This is important.

'Rigid fractions' for Nylons 6–6 and 6–10 are plotted as functions of temperature in *Figure 7*. It is seen to decrease with increasing temperature, level off near 130°C, and decrease again above 190°C. The plateau 'rigid fraction' is about 60 per cent for Nylon 6–6 and 55 per cent for Nylon 6–10 and these are compared with 'degrees of crystallinity' computed from room temperature densities[8] (1·15 for Nylon 6–6 and 1·08 for Nylon 6–10) in *Table 2*. 'Rigid fractions' computed on the basis of dielectric relaxation measurements[3] are also included.

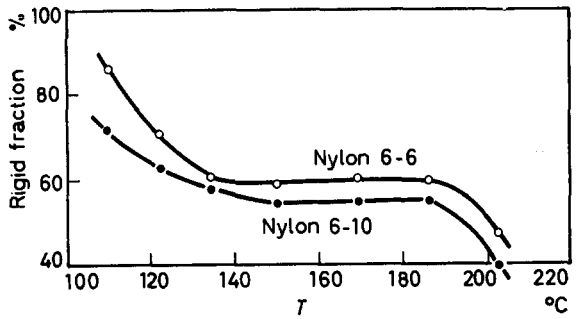

Figure 7—'Rigid fraction' for Nylons 6–6 and 6–10 as a function of temperature

We suggest that there is a non-trivial correlation between 'rigid fraction' and crystallinity as determined from the density. The plateau region of *Figure 7* suggests that the temperatures of melting and the α transition are sufficiently different that the association of the 'rigid fraction' with the degree of crystallinity is sensible. Only a rough correlation can be supported and even this is a controversial matter. The problem has been discussed previously[9,10].

It is of some interest to consider possible reasons for the fact that resonances of polyamides have not been decomposed by a number of previous workers. First of all, as noted above, the situation is difficult owing to partial narrowing of the broad component. Secondly, only recently has instrumentation been available which offers adequate signal to noise at modulation levels that do not broaden the narrow component artificially. Thirdly, the dielectric data that were helpful in choosing a favourable temperature range are of recent origin. Illers and Kosfeld[11] decomposed their curves in the same manner as we have used here. However, Jones[12] states that such a decomposition is not indicated by his data. The highest temperature curve reported by Jones was taken at 105°C, and this is at the low end of the range that we consider reasonable for decomposition.

MOLECULAR INTERPRETATION

The low temperature relaxation has been discussed in detail by Curtis[5]. Both mechanical and dielectric loss maxima are observed. Curtis states that the mechanical and dielectric relaxation times do not match exactly*. The slight mismatch in absolute values can be explained as follows. The frequency of maximum loss, either dielectric or mechanical, is the *macroscopic* relaxation frequency. This is related through a theoretical model to the molecular correlation frequency by a factor of order unity. It would not be surprising if this factor were different for the various experiments. *Figure 8* is a composite Arrhenius plot (for Nylon 6–6) composed of

*Curtis[5] also states that the dielectric activation energies are about 13 kcal/mole for the low temperature process compared with 9 kcal/mole as found by mechanical studies. More recently Curtis has stated that this discrepancy was the result of a computational error and both methods yield 9 kcal/mole (private communication).

dielectric and mechanical frequencies of maximum loss and magnetic resonance points deduced from the T_1 minima*.

T_2 increases by about a factor of two during this low temperature transition which suggests strongly that the chains begin to reorient about their long axes. This is probably an activated motion consisting of rapid reorientation between potential minima. The correlation frequency is the number of reorientations per second. We cannot say what the explicit reorientation mechanism involves; we only know that motion does occur at the average correlation frequency. Proton resonance does make it clear that the entire specimen is involved and is consistent with the model that allows reorientation about the long chain axes only†.

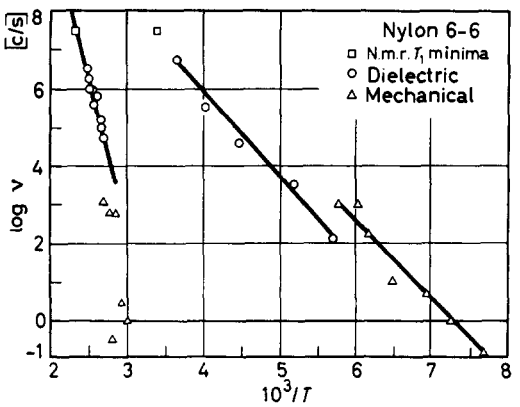

Figure 8—Arrhenius plots for the relaxation frequencies of Nylon 6–6

The high temperature relaxations with T_1 minima in the neighbourhood of 150°C correspond to dielectric and mechanical loss processes studied by many workers. Activation energies are greater than 40 kcal/mole and the process is definitely associated with only a portion of the specimens. We interpret this transition as a glass transition in the amorphous regions. In other words the molecules simply change their average rate of motion continuously as the temperature is changed. There is no abrupt change in order and above the transition the amorphous material can be considered to be a viscous liquid. The presence of crystalline material will obviously affect the molecular freedom in the amorphous regions. The increase in T_2 observed at high temperature is interpreted as the effect of crystalline melting on the mobility of molecules in the amorphous regions. Motional processes occurring in the crystalline regions have been discussed in detail by Slichter[2, 14].

The molecular motions signalled by the resonance narrowing above 50°C must be quite general as local magnetic fields must be averaged to less than one per cent of their rigid lattice values in times of the order of

*The data exhibited in *Figure 8* were drawn mainly from the literature[5, 13]. Primary references are given in Curtis's paper[5].

†Dr D. Hyndman has suggested that studies of drawn fibres could do much to characterize the motion.

milliseconds[10]. It is difficult to conceive a specific motion that would be capable of such complete averaging. T_2 does not change drastically on passing through the melting point so we suggest that the motions of molecules in the amorphous regions are similar to motions of molecules in the liquid phase.

The use of the term glass transition to describe the α transitions is open to question. Our tentative molecular interpretation is the same for amorphous transitions in either semi-crystalline or glassy polymers but further investigation is needed.

We are indebted to Drs D. C. Douglass and W. P. Slichter for extensive aid in connection with the development of this paper. We have profited from valuable discussions with Drs D. Hyndman and W. O. Statton. We are indebted to Dr Paul McMahon for pointing out an error that existed in our original manuscript.

Bell Telephone Laboratories Inc.,
Murray Hill, New Jersey, U.S.A.

(*Received June 1962*)

REFERENCES

[1] SCHWARTZ, J. *Rev. sci. Instrum.* 1957, **28,** 780
[2] SLICHTER, W. P. *J. appl. Phys.* 1955, **26,** 1099
[3] MCCALL, D. W. and ANDERSON, E. W. *J. chem. Phys.* 1960, **32,** 237
[4] BLOEMBERGEN, N., PURCELL, E. M. and POUND, R. V. *Phys. Rev.* 1948, **73,** 679
[5] CURTIS, A. J. *J. Res. Nat. Bur. Stand. A,* 1961, **65,** 185
[6] POWLES, J. G. *I.U.P.A.C. Symposium, Wiesbaden, 1959,* Vol. IA, p 10
POWLES, J. G. *Polymer, Lond.* 1960, **1,** 219
[7] WILSON, III, C. W. and PAKE, G. E. *J. Polym. Sci.* 1953, **10,** 503
[8] STARKWEATHER, H. W. and MOYNIHAN, R. E. *J. Polym. Sci.* 1956, **22,** 363
[9] SLICHTER, W. P. and MCCALL, D. W. *J. Polym. Sci.* 1957, **25,** 230
[10] MCCALL, D. W. and ANDERSON, E. W. *J. Polym. Sci.* In press
[11] ILLERS, K. H. and KOSFELD, R. *Makromol. Chem.* 1960, **42,** 44
[12] JONES, D. W. *Polymer, Lond.* 1960, **1,** 203
[13] SAUER, J. A. and WOODWARD, A. E. *Rev. mod. Phys.* 1960, **32,** 88
[14] SLICHTER, W. P. *J. Polym. Sci.* 1959, **35,** 77

Intermolecular Forces and Chain Flexibilities IV—Internal Pressures of Polyethylene Glycol in the Region of its Melting Point

G. ALLEN* and D. SIMS†

Experimental support for the suggestion (Part III), that the freezing-in of chain conformations is a major factor contributing to the low values of internal pressure found in polymeric glasses compared with the glass transition regions for corresponding rubbers, is advanced as a result of tests on a commercial sample of polyethylene glycol. The reliability of the results is considered.

IN PART III[1] it was shown that the internal pressure (P_i) of a polymeric glass is much lower than the value observed in the glass transition region for the corresponding rubber. It was suggested that the freezing-in of chain conformations is a major factor contributing to this behaviour and this contention was supported by an analysis of a crude lattice model. Experimental support for this hypothesis can be obtained from studies of crystalline polymers since there is also a transformation from rigid to mobile chains on melting and thus a corresponding increase in P_i is to be expected.

A commercial sample of polyethylene glycol (carbo-wax 1540; $M_n = 1\,500$) was selected for this study because it is highly crystalline at room temperature and melts conveniently at $\sim 50°C$ to give a mobile oil. Before use, the sample was refined by zone melting‡ and two consecutive sections cut from the purified end of the fused rod were retained for further investigation. The first specimen was studied in an apparatus previously described[1,2], coefficients of thermal pressure $\gamma_v = (\partial P/\partial T)_v$ and thermal expansivity being measured over the range 0° to 80°C. The second specimen was studied at the Explosives Research and Development Establishment using an apparatus in which the coefficients of thermal expansivity and isothermal compressibility were measured below the melting point. The thermal histories of the specimens were changed by melting and recasting them at different rates of cooling. Unfortunately, rapid rates of cooling could not be used because quenching invariably led to the formation of cracks and voids in the crystalline rods. In each experiment the transition was approached from lower temperatures. The results are summarized in *Table 1* and *Figure 1*; the values of P_i are estimated to be accurate to ± 2 per cent above and ± 3 per cent below the melting point.

The reliability of the data may be judged from the fact that above the melting point our data compare well with the results reported by Malcolm

*University of Manchester.

†Ministry of Aviation.

‡Kindly performed by Dr J. H. Beynon and his colleagues, I.C.I. Dyestuffs Division, Blackley, Manchester.

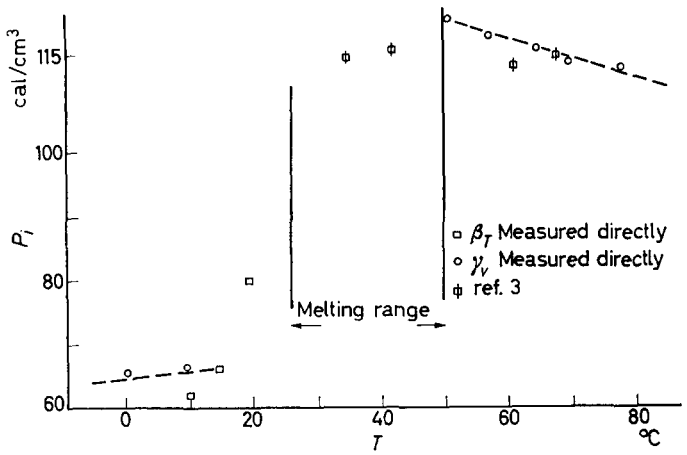

Figure 1—Internal pressure of polyethylene oxide

Table 1. Physical constants of polyethylene glycol 1 540*

T°C	$10^4\ \alpha\ deg^{-1}$	$10^5\ \beta_T$ atm^{-1}	γ_v atm/deg
0·3	2·53		10·0
9·7	2·54		9·8
10·0†	2·54	2·73	(9·0)
15·0†	2·77	2·96	(9·4)
20·0†	3·28	2·82	(11·2)
33·5‡			15·4
42·0‡			15·1
51·4	8·28		15·4
57·5	8·26		14·8
61·0‡			14·3
65·2	8·25		14·2
68·0‡			13·8
70·4	8·24		13·7
78·5	8·22		13·2

*Melting range 25° to 50°C.
†β_T measured directly.
‡Malcolm and Ritchie's data recalculated using our values for α.

and Ritchie[3] for a polyethylene glycol of similar molecular weight. In view of the fact that these latter measurements were made in a simpler cell in which mercury was not used as a containing fluid and hence no correction for its dilation was required, the agreement is very satisfactory. Malcolm and Ritchie also report data for the supercooled melt showing that P_i is not markedly temperature dependent in accordance with normal trends[2] observed in liquids and rubbery polymers. However, our data show that crystalline polyethylene glycol has a much lower internal pressure, as predicted above.

There is, admittedly, some scatter in our data obtained below the melting point and this is probably due to slightly different degrees of crystallinity induced by the various thermal histories of the specimens and

to slight differences in the composition of the two sections originally cut from the fused rod. Nevertheless there is a significantly large increase in P_i on raising the temperature of the specimen through the melting region. The magnitude of the increment is somewhat larger ($\Delta P_i \approx 60$ cal/cm^3) than for polyvinyl acetate in its glass transition region ($\Delta P_i \approx 40$ cal/cm^3). This is due mainly to the higher internal pressure of the polyethylene glycol melt relative to that of rubbery polyvinyl acetate. In fact the internal pressures of crystalline polyethylene glycol and the two glasses (polyvinyl acetate and polymethyl methacrylate) previously studied are very similar, with $P_i = 65 \pm 5$ cal/cm^3.

One of the authors (David Sims) thanks the D.S.I.R. for the award of a research studentship during part of the work. Dr Malcolm's kindness in forwarding unpublished data is also acknowledged.

Chemistry Department,
The University,
Manchester, 13
Ministry of Aviation,
Explosives Research and Development Establishment,
Waltham Abbey, Essex

(*Received June 1962*)

REFERENCES

[1] ALLEN, G., SIMS, D. and WILSON, J. G. *Polymer, Lond.* 1961, **2**, 375
[2] ALLEN, G., GEE, G., MANGARAJ, D., SIMS, D. and WILSON, J. G. *Polymer, Lond.* 1960, **1**, 467
[3] MALCOLM, G. N. and RITCHIE, G. L. D. *J. phys. Chem.* In press

Gas Discharge Etching as a New Approach in Electron Microscopy Research into High Polymers

B. J. SPIT

Fragments of the cellulose fibres Fortisan and Fiber G were etched in a low voltage gas discharge. The transverse striation obtained is discussed. Two samples of high impact polystyrene were also etched. The differences in impact resistance can be correlated with the electron microscopy image.

RECENTLY in several papers attention has been drawn to the possibility of etching in a low voltage gas discharge. Jakopić[1] has used a high frequency discharge in oxygen and has described some results on latex particles and filler material in rubber. Spit[2] used a direct current supply for the discharge and has given some results obtained with different gases on cellulose material. Anderson and Holland[3], working with a discharge in argon, reported a cross striation on nylon fibres, while Dlugosz[4] applied this method in an investigation showing two components in a high polymer mixture. Harris and Magill[5], Keller[6] and Moscou[7] have also used gas discharge etching for thinning thick specimens.

The growing interest in this method makes a more detailed discussion of our previous results valuable. New investigations carried out on the regenerated cellulose fibres Fortisan, Fiber G and a preliminary result with high impact polystyrene have given a better impression of the applicability of this method.

MATERIALS AND METHOD

The materials used in this investigation were the cellulose fibres: Fortisan*, Fiber G, and a core skin yarn. Further we studied two samples of high impact polystyrene. These samples originate from different manufacturers and have respectively a high and low impact value. Thin transverse sections of the fibres, embedded in Araldite, were cut on a Reichert microtome with a diamond knife (51°). The polystyrene samples were cut without embedding. The sections were etched in oxygen in a direct current discharge on the anode side and shadowed with platinum or tungsten oxide.

Only in a few special cases were we able to get longitudinal sections. Mostly they were rather thick and not fully expanded.

Fortisan and Fiber G were also disintegrated in a Bühler homogenizer. Fibrillar fragments were mounted on a carbon coated grid and etched. The etch apparatus used and the circumstances during etching have been described[2].

*Fortisan was kindly supplied by Professor K. Hess of the 'Eiweisz und Mehlinstitut', Hannover, Germany.

RESULTS WITH CELLULOSE FIBRES

After etching, transverse sections of regenerated cellulose fibres show that the surface has been partly etched away. The surface has obtained relief as shown in *Figures 2* and *3*, for Fortisan. This fibre contains many irregularly shaped voids. *Figure 3* is a positive printed micrograph hence the fibre appears against a black background of surrounding Araldite, the voids in the fibre show up as white spots. *Figure 2* is a negative printed micrograph and hence voids in the fibre appear as black dots in it and the embedding medium (at the bottom left hand corner) is white.

After etching, the cellulose material between the voids has split up. This means that there is a different sensitivity of the cellulose material with respect to the ion bombardment.

As will be discussed below we have correlated this with the amorphous and crystalline state of the material which makes up the fibre. Previously we already made it clear that the etch pattern obtained is a function of the duration of etching. Now we have found that the etch figures also vary

Figure 1—Portion of an etched transverse section of a core skin yarn. Shadowed with tungsten oxide

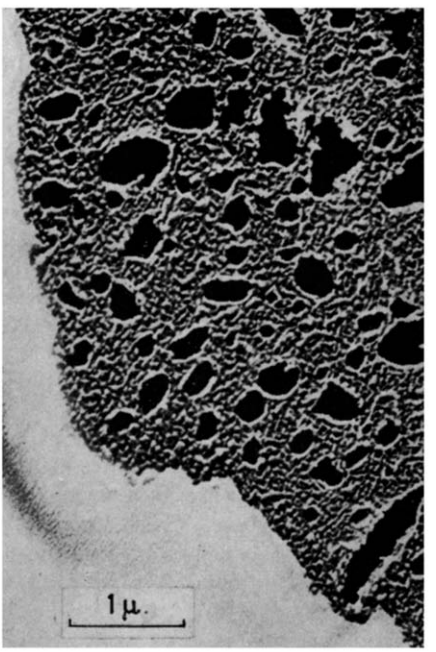

Figure 2—Portion of an etched transverse section of Fortisan. Shadowed with tungsten oxide

with the type of fibres, which is demonstrated in *Figure 1* for a core skin yarn as compared with *Figure 2* for Fortisan. *Figure 1* is also a negative printed micrograph. At the bottom left hand corner in this figure one sees the porous core material surrounded by a densely packed skin layer. The black and white areas at the top of the picture are respectively a hole in

the section and the embedding material. The etch pattern from core and skin as well as that of Fortisan differ. These phenomena lead to the conclusion that the etch pattern is typical of the submicroscopical structure of the fibre. As many fibres have obtained an axial orientation in accordance with their stretching during manufacture, we can expect that the etching of longitudinal sections will yield more interesting results.

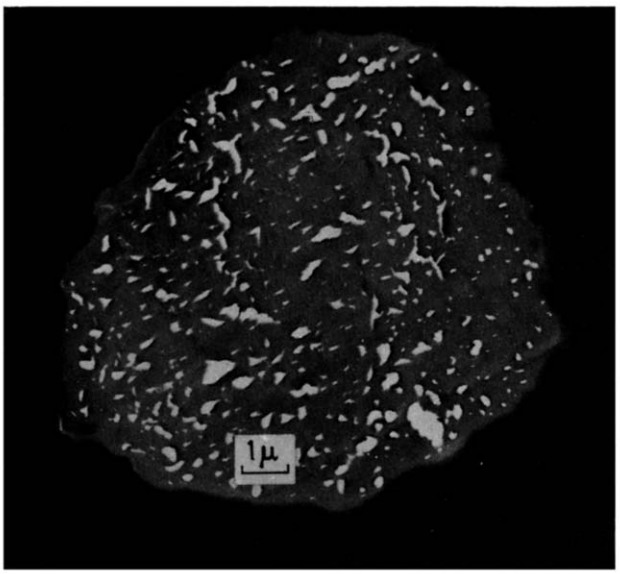

Figure 3—Transverse section of Fortisan embedded in Araldite

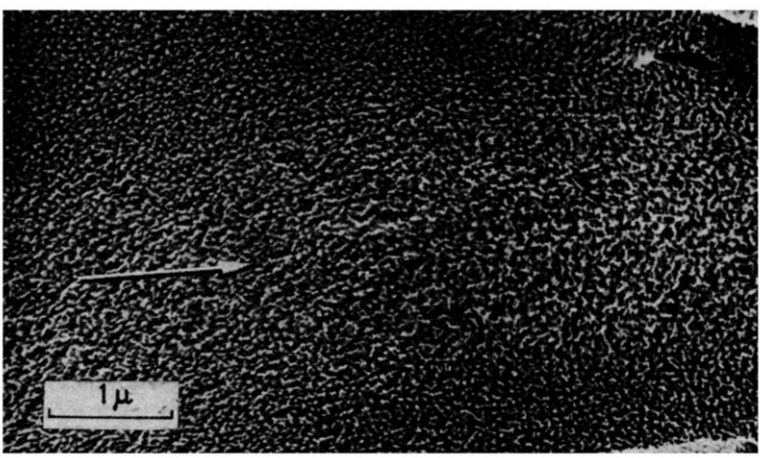

Figure 4—Etched longitudinal section of a core skin yarn. Arrow indicates fibre axis

Attempts in this direction suceeded only seldom. With the core skin yarn we got a picture like *Figure 4* (negative print). Here again the core has a coarser texture than the skin. To solve the problem of cutting good longitudinal sections we decided to disintegrate the fibres in a homogenizer. This was done with the fibres Fortisan and a third fibre known as Fiber G. After having etched the fibre fragments we observed a cross striation as shown in *Figures 5* and *6*; the arrow in the figures indicates the fibre axis. These etch patterns are totally different from the etch pattern obtained in the longitudinal section of the core skin yarn in *Figure 4*. In a previous publication we showed that, after etching, microfibrils of native cellulose split up into lumps at more or less regular distances. If these lumps are

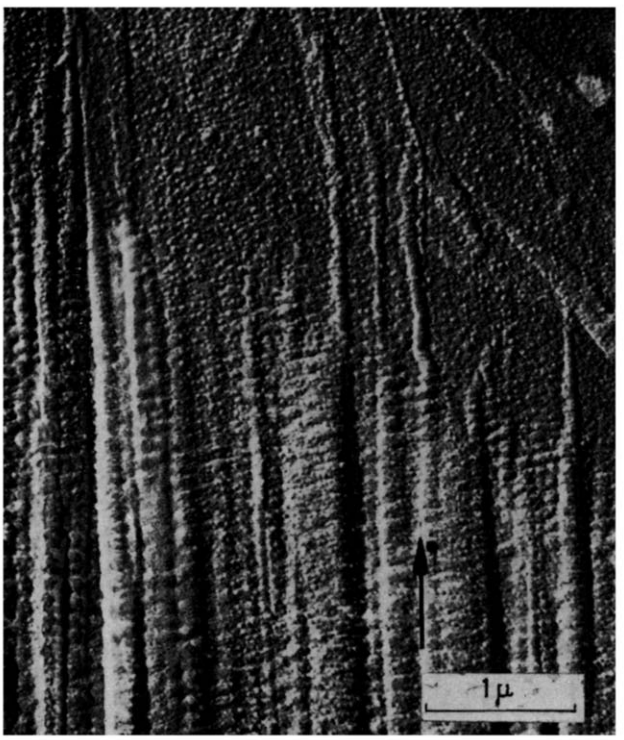

Figure 5—Blendered microfibrils of Fortisan after etching in a gas discharge six minutes at 3 mA. Arrow indicates fibre axis

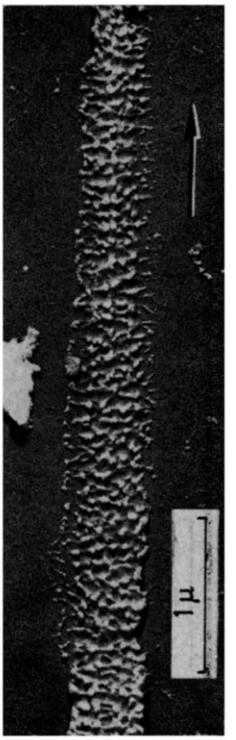

Figure 6—Blendered microfibrils of Fiber G after etching in a gas discharge. Arrow indicates fibre axis

laterally located we get a cross striation in bundles of microfibrils. The same is visible in the fibre fragments of Fiber G (*Figure 6*) and Fortisan (*Figure 7*). It is pointed out that these micrographs are reminiscent of the diagram given by Hess *et al.*[8] about the sequence of amorphous and crystalline parts in regenerated cellulose fibres. In view of this diagram,

based on iodine-stained Fortisan, it is of particular interest to measure the distances between these lumps.

Emphasizing that we have used the same Fortisan material, measurements for this fibre in *Figure 5* give values ranging from 300 Å to 700 Å. In other fragments a basic periodicity of about 1 000 Å remains as in *Figure 7* (arrow indicates fibre axis). The shadow on the edge of the fibre

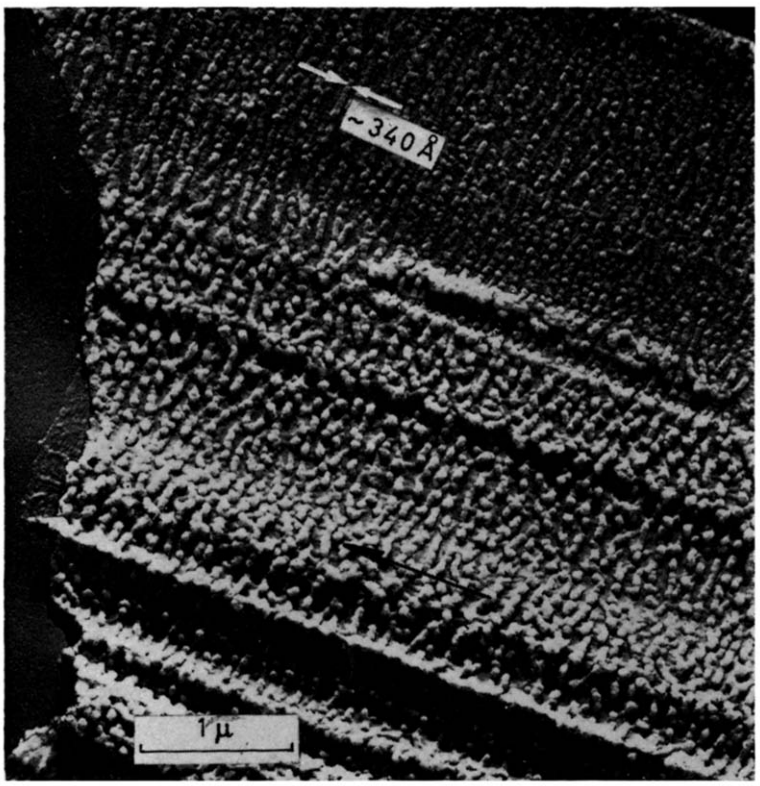

Figure 7—Fragment of blendered Fortisan after gas discharge etching. Arrow indicates fibre axis

fragment in the upper left hand part of the picture is smaller than the one in the lower part. This means that the fragment is not lying absolutely flat on the substrate. This causes a different appearance of the upper and lower parts of the micrograph. The flat upper part shows a fairly regular structure. The relationship necessary between the etch figures obtained in the transverse (*Figure 2*) and longitudinal plane (*Figures 5* and *7*) of the Fortisan fibre is discussed further on. It is noted here that all our pictures of Fortisan and Fiber G leave no doubt as to the microfibrils possessing an axial and a lateral orientation, the latter extending over reasonable areas.

RESULTS WITH HIGH IMPACT POLYSTYRENE*

In high impact polystyrene, a mixture of polystyrene and rubber, it is interesting to know in which manner the two polymers in this material occur. Therefore we chose a sample (1) with a high impact and a sample (2) with a low impact value, from different manufacturers. The results are a remarkable example of valuable information to be gained from the application of electron microscopy.

Figures 8 and *9* are positive printed micrographs of sections cut from both samples. A very smooth picture without structural details was obtained, especially in the case of *Figure 9*. Sample 1 in *Figure 8* demonstrates a large island 2·5 μ long lying in a matrix.

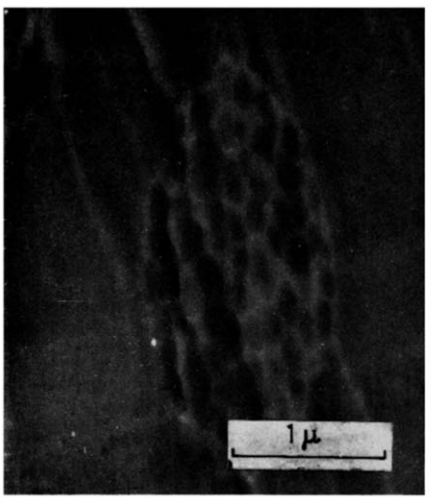

Figure 8—Section of high impact polystyrene. Sample 1

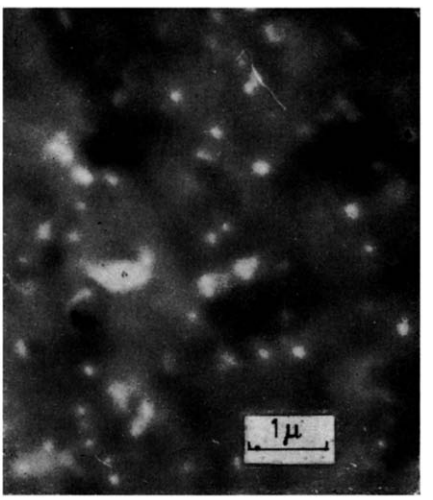

Figure 9—Section of high impact polystyrene. Sample 2

This island is filled up with a number of small particles. *Figure 10* (reversed-printed) shows a part of such an island after gas discharge etching for comparison with *Figure 8*. The particles in the island are now more conspicuous, as the material surrounding them is partly etched away. Obviously there is a selective attack. The main matrix surrounding the island and the particles in the island are more resistant to the gas discharge than the material surrounding the particles in the island. On the basis of these data we may conclude that in this sample polystyrene particles are surrounded by rubber and form an egg-shaped body (the island). This body in its turn is embedded in polystyrene. On impact a shock wave travelling through this material will be damped by these islands.

With sample 2 we got the *Figures 9* and *11*. *Figure 9* shows dispersed white blobs which correspond with the black globules in the reversed-printed *Figure 11*. In this last figure these globules, about 0·2 μ in size, are partly etched away. The rubber must be localized in these small

*Carried out in collaboration with Dr J. Isings of the Central Laboratory T.N.O., Delft.

globules. It is clear that these individual rubber globules embedded in polystyrene give little damping, as the shock waves run between the rubber globules.

Finally these micrographs demonstrate that the two materials went through different manufacturing processes.

To confirm the explanation given of the impact properties further work is being prepared.

DISCUSSION

The effects of attack obtained by etching in a gas discharge with oxygen are totally different in the two cases. The etching of cellulose can be described as the corroding action as effected by active oxygen in relation to local differences in physical modifications, whereas with impact polystyrene the way corrosion acts depends on the various chemical components of the material. The attack on cellulose can be related to ordered or 'crystalline' and unordered or 'amorphous' parts in the axial direction of

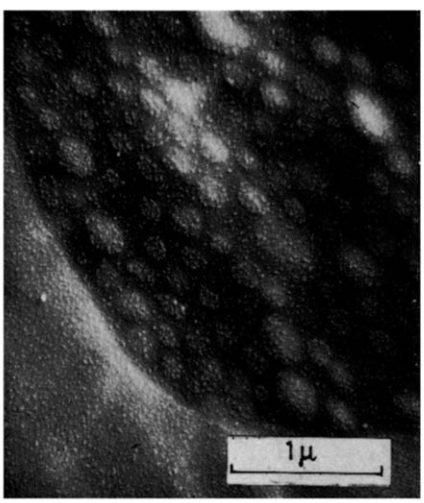

Figure 10—Section of high impact polystyrene. Sample 1 after gas discharge etching. Shadowed with platinum

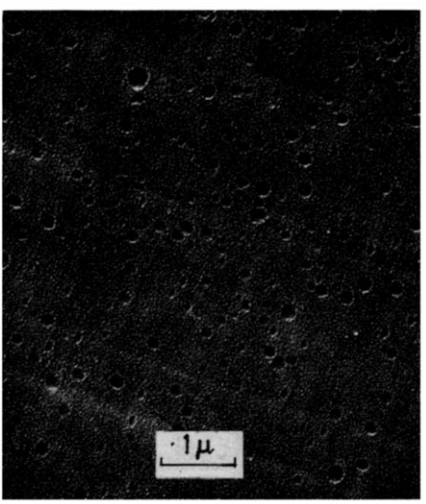

Figure 11—Section of high impact polystyrene. Sample 2 after gas discharge etching. Shadowed with platinum

microfibrils. Furthermore it seems reasonable to believe that the crystalline parts are more stable under bombardment.

Looking at the etched fibre fragments of Fortisan and Fiber G (*Figures 5* and *6*) the material left there represents the crystalline fraction, extending laterally to several hundred Ångstrom units. Considering the surface of a transverse section of Fortisan (*Figure 2*) it is obvious that amorphous and crystalline regions occur in the surface of this section. These regions have the same dimensions as the lateral ordered crystalline parts. In agreement with this, one sees in *Figure 2* that the material between the voids is split up into points and 'threads'.

It is noted that the etch figure obtained is a function of the difference in the speed of etching as related to the amorphous or crystalline nature of the material. Secondly by stronger etching the attack could be extended beyond the first layer of amorphous or crystalline material. Lastly it is possible that the section is not cut fully normal to the fibre axis and in view of the inexact alternation of crystalline and amorphous parts, the etch figures become very complicated and craters can be formed.

In the micrographs of Hess *et al.*[8] of iodine-stained Fortisan, clearly depicted repetition of the stained zones can be observed and hence measured. Our measured distances between the lumps in *Figure 5* do not agree with the measurement in Hess's pictures.

Dlugosz and Michie[9] have discussed the appearance of elongated particles after ultrasonic irradiation of acid-swollen Fortisan. These authors found particle sizes compatible with those of Morehead[10], namely length 334 Å and width 50 Å. It is striking that our remaining lateral ordered parts (*Figure 7*) have the same width as the length of these particles (denoted in *Figure 7*). This bears out the opinion of Dlugosz and Michie that the particles exist before acid treatment. Both experiments make it probable that these particles form a basic structure of the fibre. Between this structure smaller more or less ordered areas can be seen to occur here and there in *Figure 5*. After acid treatment these smaller areas are dissolved and the larger lateral ordered areas split up into the smallest microfibril dimension of 50 Å. This construction makes it understandable that Fortisan after blendering splits up into ribbon-shaped fragments. Both acid-swollen and gas-discharge etching experiments tend to the Hess–Kiesig model for the fibres Fortisan and Fiber G.

Finally Anderson and Holland[3], working with a discharge in argon, found in drawn nylon 6.6 fibres a structure perpendicular to the axis of draw. We believe that this structure too can be explained as lateral ordering from etch-stable areas in the fibrils.

I am indebted to S. C. van der Knaap and Miss T. ter Lintel Hekkert for their help in carrying out the experiments.

Technical Physics Department T.N.O. and T.H.
Microstructure Section,
Delft, The Netherlands

(*Received June 1962*)

REFERENCES

[1] JAKOPIC, E. *Proceedings of the European Regional Conference on Electron Microscopy, Delft 1960*, Vol. I, p 559. Delft, 1961
[2] SPIT, B. J. *Proceedings of the European Regional Conference on Electron Microscopy, Delft 1960*, Vol. I. p 564. Delft, 1961
[3] ANDERSON, F. R. and HOLLAND, V. F. *J. appl. Phys.* 1960, **31**, 1516
[4] DLUGOSZ, J. 'Electron microscopy', *Fifth International Congress for Electron Microscopy, Philadelphia 1962*, Vol. I, BB 11. Academic Press: New York, 1962
[5] HARRIS, P. H. and MAGILL, J. H. *Polymer, Lond.* 1962, **3**, 252

[6] KELLER, A. 'Electron microscopy', *Fifth International Congress for Electron Microscopy, Philadelphia 1962*, Vol. I, BB 3. Academic Press: New York, 1962
[7] MOSCOU, L. 'Electron microscopy', *Fifth International Congress for Electron Microscopy, Philadelphia 1962*, Vol. I, BB 5. Academic Press: New York, 1962
[8] HESS, K., GÜTTER, E. and MAHL, H. *Kolloidzschr.* 1958, **158,** 115
[9] DLUGOSZ, J. and MICHIE, R. J. C. *Polymer, Lond.* 1960, **1,** 41
[10] MOREHEAD, F. F. *Text. Res. (J.)*, 1950, **20,** 549

The Crystallization of Polydecamethylene Terephthalate

A. SHARPLES and F. L. SWINTON*

A study has been made of the crystallization of polydecamethylene terephthalate at various temperatures. The interpretation of the results is uncomplicated by the presence of any detectable secondary stage but the process nevertheless shows several unusual features. First, although the majority of the crystallization conforms to an Avrami relation, the values of the exponent, n, are fractional, whereas current theory requires integral values. Secondly, an additional process intervenes towards the end of the crystallization to cause a decrease in the normal rate. It is possible that this is related to an observed decrease in the nucleation rate. Finally, a pronounced change in behaviour takes place about 15°C below the melting point causing a 30 per cent decrease in the density change during crystallization to occur for a temperature lowering of only 0·5°C. The kinetic behaviour also changes on passing through this point.

IN GENERAL, the crystallization of high polymers is considered to involve the formation of nuclei in the supercooled melt, followed by the growth of these centres to form rods, discs or spheres. The decrease in volume of the system resulting from the formation of the more dense, crystalline phase, can be related to time by an equation of the form[1–3]

$$(V_t - V_\infty)/(V_0 - V_\infty) = \exp(-zt^n) \qquad (1)$$

where V_t is the volume of the system at time t, z is constant for a given temperature, and n is an integer having a value of 1, 2, 3 or 4. Usually a process referred to as secondary crystallization[4] intervenes to complicate the interpretation of the data, and although methods have been proposed to allow for this effect[5], it was considered desirable to study the behaviour of a polymer where it is absent, especially in view of the fact that recent results on polyethylene[5] have indicated that the integral values of n predicted by existing theory are not always obtained.

Polydecamethylene terephthalate shows no detectable secondary crystallization, and an account of its behaviour is given below.

EXPERIMENTAL

Materials

The polymer was prepared by the method of Flory, Bedon and Keefer[6]. The equilibrium melting temperature obtained by dilatometry using slow (1°C/24 h) rates of heating was found to be 137·5°C, in good agreement with Flory's value of 138°C, although the values of $0{\cdot}968_6$ cm^3/g for the specific volume of the liquid polymer at 150°C is in rather poor agreement with that of 0·956 cm^3/g quoted by Flory.

The melt viscosity of the liquid polymer was measured at 255°C and was found to be 740 poise. According to Flory *et al.*[6] this indicates that the number average molecular weight is greater than 10 000, and that the true equilibrium melting point will not be depressed to any extent by the number of chain ends present in the melt.

*Present address: Chemistry Department, Royal College of Science and Technology, Glasgow, C.1.

Dilatometry

Molten polydecamethylene terephthalate has the property of wetting glass, so that when the temperature is lowered and the polymer crystallized, the resultant volume contraction invariably shatters the containing tube if this is made of glass. The dilatometers used in the present study were consequently constructed with stainless steel bodies, connected to the measuring capillaries through flanged joints, which were lightly greased with high melting silicone grease to render them vacuum-tight. The measuring capillaries were made of 2 mm internal diameter precision-bore Veridia tubing.

The dilatometers were filled with weighed amounts of polymer and mercury in the usual way, under vacuum[4]. Approximately 10 g of dried polymer was used for each dilatometer, and the height of the mercury column as a function of time and temperature was measured to $\pm 0{\cdot}01$ mm using a 1 m cathetometer manufactured by the Precision Tool and Instrument Co. The crystallizations were carried out in an oil thermostat of conventional design, the temperature control of which was $\pm 0{\cdot}03$°C at the experimental temperatures. Before each crystallization run, the sample was melted at 180° to 190°C for 30 min. As an indication of the extent of the volume change measured, the specific volume of the polymer at 120·00°C before crystallization is $0{\cdot}9527_0$ cm³/g, while after crystallization at this temperature the value is $0{\cdot}9113_6$ cm³/g.

Microscopy

Measurements of nucleation and growth rates were made using a 10 × micrometer eyepiece and a $\frac{2}{3}$ in. objective. Temperature control was effected with a Köfler hot-stage, thermostatted to $\pm 0{\cdot}1$°C. Films of polymer approximately 10μ thick were prepared by pressing the molten material between glass slides and cover slips, but even when precautions were taken to avoid degradation, the resultant nucleation densities were very variable, and often were so high that an unresolvable birefringent mass was formed[7]. The results reported were obtained using a sample with resolvable spherulitic structure prepared under similar conditions to those involved in the dilatometry. Approximately 1 mg was heated on an open glass slide *in vacuo* at 170°C for 15 min. The sample was then cooled, a cover slip was placed in position, and the slide was reheated to 200°C prior to pressing to form a suitable film. Subsequent measurements were made by first melting at 160°C for 5 min and then lowering the temperature to that required for crystallization. Prior melting at 140°C and 300°C produced identical results. The mean thickness of the specimen was determined from the known weight and the measured area. Variation in thickness across the specimen was assessed by differential focusing under high magnification, and was found to be less than 20 per cent. This was considerably less than the variation in nucleation density observed to occur from one sample to another.

RESULTS

Dilatometry

Relative values of the volume change occurring in a crystallizing polymer can in practice be determined from dilatometric heights, so that equation (1) can be written

$$(h_t - h_\infty)/(h_0 - h_\infty) = \exp(-zt^n) \qquad (2)$$

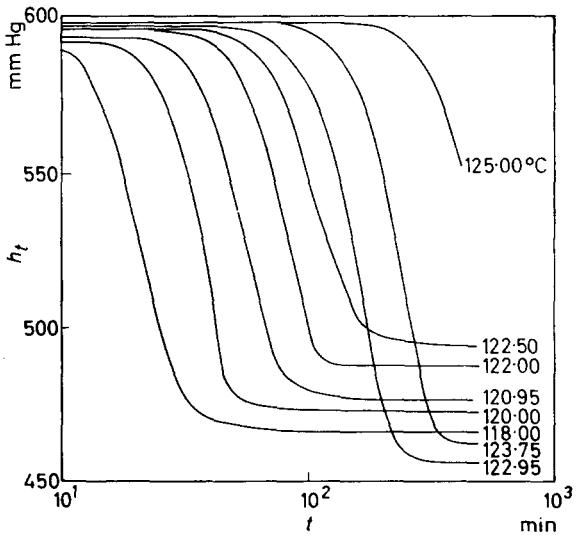

Figure 1—Crystallization of polydecamethylene terephthalate at various temperatures. Dilatometric height versus log (time)

where h_t is the dilatometric height at time t. Results for h_t obtained during the crystallization of polydecamethylene terephthalate at various temperatures, are plotted[3] in *Figure 1* against log t and it is immediately apparent that, for example at 118°C, the final value, i.e. h_∞, is constant (to within 0·1 per cent of the total change, $h_0 - h_\infty$) for a period of time one order greater than that involving the primary crystallization. Thus, secondary crystallization[4], which involves a continual, slow decrease in volume after the completion of the primary stage, is effectively absent from this polymer.

The unexpected feature of the results is the anomalous volume change which takes place at *ca.* 122·8°C. This can be seen more readily in *Figure 2*, where the change in dilatometer height occurring during crystallization is plotted as a function of crystallization temperature. Above 122·95°C and below 122·50°C the volume change increases with decreasing temperature, as is to be expected from the different expansion coefficients of liquid and

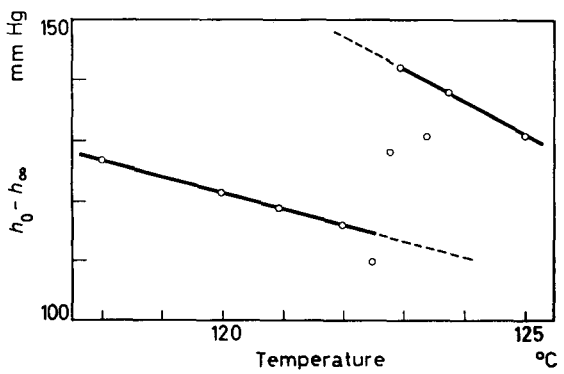

Figure 2—Volume change occurring during crystallization, plotted as a function of temperature

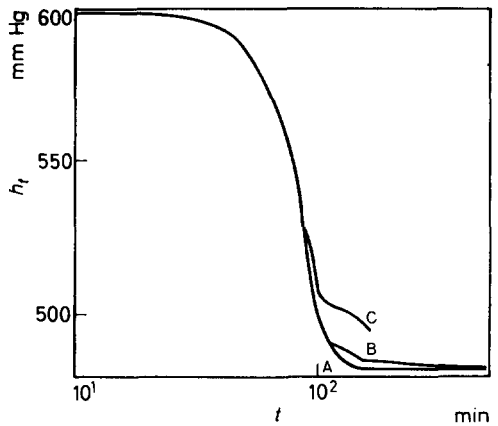

Figure 3—Intervention of process causing decrease in crystallization rate—122·00°C. B and C: experimental plots. A: theoretical plot, assuming continuation of early stages of B and C according to equation (2)

solid phases. Between these two temperatures, however, there is a displacement of about 30 per cent. No obvious explanation or precedent is available to account for this effect, but it immediately raises the question of whether the kinetics are also affected on passing through this transition.

In the first instance it was noted that an obvious discontinuity is present at all temperatures in the crystallization plots. This is illustrated by the results for 122·00°C (*Figure 3*). Deviations from the extrapolated curve A are apparent in two successive experiments, B and C, and it is evident that some process intervenes in an irreproducible manner to slow down the normal course of crystallization. In most of the isotherms the discontinuity does not occur until the crystallization is about 80 per cent complete as

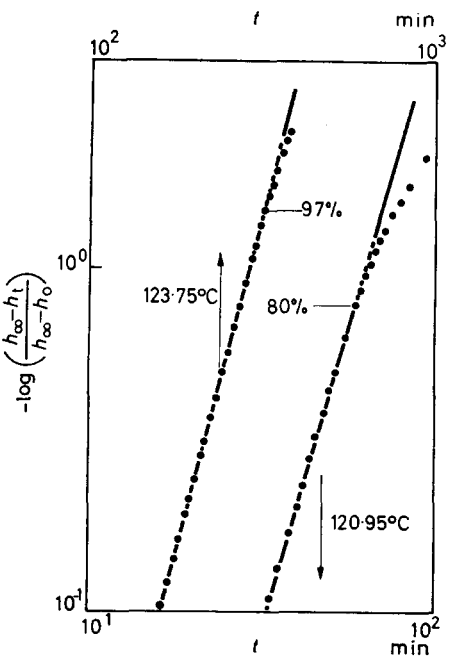

Figure 4—Avrami plots showing conformity to equation (2) for majority of crystallization

Table 1. Crystallization rate parameters for polydecamethylene terephthalate

Crystallization temperature °C	*n*	*z (time, min)*	*Range of agreement per cent*
125·00	3·76 ± 0·05	$7{\cdot}00\times10^{-11}$	—
123·75	3·79	$1{\cdot}00\times10^{-9}$	97
123·40	3·87	$1{\cdot}13\times10^{-9}$	98
122·95	3·60	$1{\cdot}25\times10^{-8}$	97
122·80	3·74	$8{\cdot}04\times10^{-9}$	94
122·50	3·59	$5{\cdot}65\times10^{-8}$	57
122·00	3·97	$3{\cdot}44\times10^{-8}$	90 and 59
120·95	3·49	$1{\cdot}40\times10^{-6}$	80
120·00	3·08	$3{\cdot}23\times10^{-5}$	75
118·00	2·66	$1{\cdot}35\times10^{-3}$	80

can be seen from *Table 1* and in fact the slight deviations observed for the results at 122·95°C and above only occur in the last 2 to 3 per cent of the crystallization and are barely outside the limits of experimental error.

Before this discontinuity occurs, the results at all temperatures accurately fit the version of the Avrami relation given in equation (2). Two typical sets of data are plotted in *Figure 4* in the form of

$$\log\{-\log[(h_t-h_\infty)/(h_0-h_\infty)]\} \text{ versus } \log t.$$

For the results at 123·75°C, agreement is found for 97 per cent of the crystallization, while at 120·95°C the discontinuity occurs after 80 per cent crystallization. The values of the Avrami exponent n, however (equation 2), frequently differ signficantly from the integral values required by theory, as can be seen in *Table 1*. A similar effect has been reported for the crystallization of polyethylene[5] where the values of n were found to range from 2·0 to 4·0. For the temperatures covered in the present study, the range is from 2·7 to 4·0 (*Table 1*).

The temperature dependence of the crystallization rate has been shown by Mandelkern[3] and others to take the form

$$\log z = A - 4B/\Delta T^2 \tag{3}$$

where A and B are constants, and ΔT is the difference between melting and crystallization temperatures. In the case where n varies with temperature it has been proposed[5] that this should be modified to

$$\log z = A - nB/\Delta T^2 \tag{4}$$

and in *Figure 5* the results from *Table 1* are plotted on this basis. The agreement with equation (4) is good, confirming that the observed variations in n are real, and require to be accounted for[5]. Alternative plots (e.g. equation 3) which do not allow for changing n, show very poor agreement. The parameter B, which is a measure of the critical free energy involved in secondary nucleation[3], decreases on passing through the temperature at which the crystallinity changes (122·80°C, *Figure 2*) indicating a transition in the nature of the growing surface. This, however, is the only aspect of the kinetics which can be considered unambiguously to change on passing through the transition temperature.

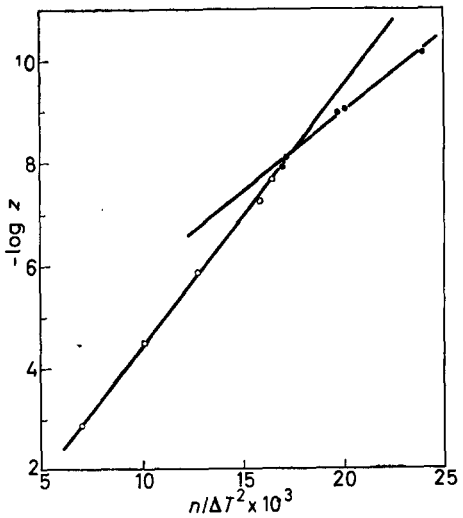

Figure 5—Temperature dependence of crystallization rate (dilatometry experiments). ● Results for 122·80°C and above. ○ Results for 122·50°C and below

Microscopy

The dilatometric method yields information only on the combined effect of nucleation and growth during crystallization. The microscopy experiments were designed to determine whether the behaviour reported in the previous section could be accounted for in terms of anomalies in the separately observed nucleation and growth rates. A major difficulty was encountered, however, in that the nucleation density was found to vary from sample to sample, an effect which has previously been observed for polyethylene[7]. As with this latter polymer, the nucleation density is frequently so great as to produce a birefringent structure which is not resolvable microscopically at any stage during its growth. The particular sample studied was chosen because it yielded resolvable nuclei and because the method of preparation (given in the experimental section) is not likely to have caused any degradation. The absolute values of the nucleation rate, however, are subject to an unknown error.

The appearance of the spherulitic structures formed during crystallization is similar to that for the spherulitic aggregates observed in nylon[8], and remains constant over the measurable temperature range of 120·0°C to 126·0°C. Apart from the effect discussed later, both nucleation and radial growth rates (N and G) are also constant at a given temperature, and the values obtained are given in *Table 2*. It has previously been shown that for sporadic nucleation and spherulitic growth, as is observed here, the constant z in equation (2) is related to G and N by

$$z = \pi \rho_c N G^3 / 3 \rho_l X_w \tag{5}$$

where ρ_l and ρ_c are the densities of the liquid and crystalline phases and X_w is the weight fraction of crystalline material within the spherulites. The derivation of this equation, however, also leads to a value of $n=4$ in equation (2), and consequently the deviations from this value observed in the present case (*Table 1*) indicate that one of the assumptions involved

Table 2. Microscopy data for polydecamethylene terephthalate

Temperature of crystallization	$G \times 10^6$ *cm/min*	$N \times 10^{-6}$/cm³/min	t_s *(min)*	$t_{\frac{1}{2}}$ *(min) from dilatometry*
126·0	1·53	0·246	—	
125·0	3·73	0·800	127	457
123·9	6·55	1·90	88	241
123·7	6·60	1·86	82	210
123·0	9·50	3·33	52	143
121·9	15·4	11·0	23	70
121·0	20·7	22·6	16	45
120·0	33·2	54·6	10	25

(possibly the one implying that the density of growing spherulites is constant) is not valid. Consequently a comparison of the values of z obtained dilatometrically from equation (2), and microscopically from equation (5) is not justifiable on an absolute basis, although the relative changes with temperature may be comparable. In *Figure 6*, values of z from microscopy data are plotted for various temperatures on the basis of equation (3). The solid lines represent the dilatometric data from *Figure 5*, and it can be seen that the change in behaviour at 122·8°C is confirmed, although the absolute values are displaced by a factor of 200 to 300 per cent. This displacement may be due to the arbitrary nature of the nucleation rate, or to the unknown factor causing n to be less than its predicted value of 4.

A feature of the nucleation process which has previously been reported[9] is that although the rate is constant for a considerable period of time, it eventually decreases and finally falls to zero, leaving a fixed number of nuclei which is determined by the temperature of crystallization. The time at which nucleation stops t_s is well within the time scale of the overall crystallization process as can be seen from *Table 2* where the observed values of t_s are compared with those calculated for the half-life, $t_{\frac{1}{2}}$, from

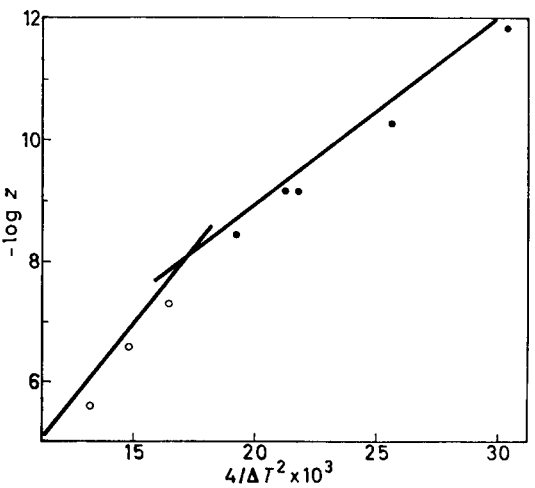

Figure 6 — Temperature dependence of crystallization rate (microscopy experiments). ● Results for 123·0°C and above. ○ Results for 121·9°C and below. Solid line indicates dilatometric plot from *Figure 5*

dilatometry data. Owing to the arbitrary nature of the nucleation experiments, the absolute values of t_s are likely to have a considerable error attached to them. Relatively, however, the change with temperature follows that of $t_{\frac{1}{2}}$ very closely, and again indicates a change in behaviour at *ca.* 122·8°C.

DISCUSSION

In spite of the absence of any complicating secondary process, the crystallization of polydecamethylene terephthalate nevertheless shows several unusual features. First, fractional values of the Avrami exponent n (equation 2) which have previously been observed for polyethylene[5], are also found in the present case (*Table 1*), and as existing theory[2,3] requires integral values of 1, 2, 3 or 4, it is evident that some aspect of the present mechanism requires modification. It is possible that more careful analyses of existing data for other polymers, where the presence of secondary crystallization in general renders interpretation more difficult, may reveal that integral values of n are the exception rather than the rule. No detailed explanation can be proposed to account for this behaviour, but the microscopy data suggest that the usual picture of sporadic nucleation followed by spherulitic growth at a constant radial rate may be basically correct, and that some process is superimposed to reduce n from its expected value of 4 for this system. One likely possibility[5] is that the density of the growing spherulites is not constant with time, as is normally assumed.

Secondly, there is evidence from the dilatometry experiments that the crystallization is interrupted by some process which causes a slowing down of the normal rate. It is important to note, however, that this effect does not prevent the attainment of the expected value for the final density, as the data for the earlier stage of crystallization conform to an Avrami plot (equation 2) best if the *experimentally observed* value of h_∞ is used. It would seem at first sight that this effect is explicable in terms of the stopping of nucleation, which is observable microscopically, and which is naturally expected to lead to a decrease in rate. Comparison of the observed time of stopping with the time at which the decrease in rate occurs in the dilatometric experiments is unfortunately not justifiable owing to the arbitrary nature of the nucleation data, so that this obvious test is not possible. The quantitative form of the dilatometric rate plots is informative, however, and is such that the decrease in rate (*Figure 3*) is much too sharp to be accounted for solely by cessation of nucleation. Consequently, although these two effects may be related (and obviously, as is noted above, some decrease in overall rate is bound to occur if the reduction in nucleation rate takes place within the time scale of the bulk crystallization), some additional factor must also be operative.

Thirdly, in the region of 122·80°C, a pronounced change occurs in the density of the crystallized product (*Figure 2*). For example, the density increase resulting from crystallization is *ca.* 30 per cent greater at 122·95°C than at 122·50°C. At the same time the temperature dependence parameter for the rate of crystallization (*Figure 5*) also changes indicating an alteration in the nature of the growing spherulites. No difference is detectable in the qualitative appearance of the spherulites above and below this

temperature, but the change is reflected quantitatively in the microscopically observed rate constant (*Figure 6*).

Changes in kinetic behaviour on decreasing the crystallization temperature have previously been observed for polyethylene terephthalate[10], and explained on the assumption that sporadic and predetermined nucleation occur simultaneously to varying extents, depending both on temperature of crystallization, and on time and temperature of melting. However, the existence of two simultaneously occurring Avrami processes, each with a different value of n, such as would be expected if nuclei are formed both sporadically and from pre-existing sites, leads to a changing value of n, whereas in the present case, n, although fractional, is also constant.

The most pronounced change is not that occurring in the kinetics but in the value for the final density of the crystallized product. In general this effect (*Figure 2*) could arise from one of three causes; incomplete crystallization, a modification of crystal form, or a change in the fraction of crystalline material within the spherulite. Incomplete crystallization is unlikely because it would require that the value of h_∞ (equation 2) to give the best fit for the data should be less than the observed value. In fact, as is noted above, the experimentally observed value gives the optimum agreement. Simple modification of crystal form is also unlikely to account for the large effect observed, but the following explanation proposed by Morgan[11] is a possibility.

This assumes that crystallization at higher temperatures involves only the polar groups in the chain, and that it is not until temperatures below 122·8°C are reached that the ten-carbon paraffinic segments take part in the process, imposing more restrictive conditions that result in a reduced extent of crystallization within the growing spherulite. This hypothesis would also predict a change in the nature of the growing surface on passing through the transition temperature, and this is consistent with the observed change in the temperature dependence parameter[3], B (equation 4, *Figure 5*). It suffers, however, from one serious objection, in that at the higher temperatures where the density change on crystallization is at a maximum, this change should still be less than, for example, in polyethylene terephthalate where the entire chain is presumably capable of being involved in crystallization. In fact, at 122·95°C the density increase on crystallization is 5·1 per cent, whereas the maximum figure observed for polyethylene terephthalate[10] is 2·6 per cent.

The effects discussed above, and the results reported recently for polyethylene[5], suggest that the existing picture of polymer crystallization may require modification. The postulate of nucleation and spherulitic (or occasionally rodlike) growth may be generally correct, but the additional assumptions that the growth and nucleation rates are constant, and that the density of the growing crystalline regions is similarly independent of time, require to be examined in greater detail than has previously been the case.

Arthur D. Little Research Institute,
Inveresk, Musselburgh, Midlothian

(*Received July 1962*)

REFERENCES

[1] AVRAMI, M. *J. chem. Phys.* 1940, **8**, 212
[2] MORGAN, L. B. *Phil. Trans.* 1954, **247**, 13
[3] MANDELKERN, L. *Growth and Perfection of Crystals*, pp 467–497. Chapman and Hall: London, 1958
[4] KOVACS, A. J. *Ric. sci. A*, 1955, **25**, 666
[5] BANKS, W., GORDON, M., ROE, R.-J. and SHARPLES, A. *Polymer, Lond.* 1963, **4**, 61
[6] FLORY, P. J., BEDON, H. D. and KEEFER, E. H. *J. Polym. Sci.* 1958, **28**, 151
[7] BANKS, W., HAY, J. N., SHARPLES, A. and THOMSON, G. *Nature, Lond.* 1962, **194**, 542
[8] KHOURY, F. *J. Polym. Sci.* 1958, **33**, 389
[9] SHARPLES, A. *Polymer, Lond.* 1962, **3**, 250
[10] HARTLEY, F. D., LORD, F. W. and MORGAN, L. B. *Phil. Trans.* 1954, **247**, 23
[11] MORGAN, L. B. Conference on Physics of High Polymers, University of Bristol, 1961

Studies of 2-Cyano-2-propylazoformamide II—Measurements of Rate of Dissociation

J. C. BEVINGTON and ABDUL WAHID

At 100°C, the velocity constant for the dissociation of 2-cyano-2-propylazoformamide in solution in aromatic hydrocarbons is $1{\cdot}9 \times 10^{-5}$ sec^{-1}; the activation energy is 34·5 kcal/mole. The limiting efficiency of the azoformamide as an initiator for the polymerization of styrene is about 60 per cent.

2-CYANO-2-PROPYLAZOFORMAMIDE, $(CH_3)_2C(CN)\cdot N:N\cdot CO\cdot NH_2$, can be used conveniently as an initiator of radical polymerizations at temperatures of about 100°C. Experiments involving the azo compound labelled in its methyl groups with carbon-14 have been reported already[1]. Measurements of the rates at which 2-cyano-2-propyl groups become incorporated in polystyrene indicate that at 100°C the velocity constant for the dissociation of the azo compound into *available* radicals is $1{\cdot}08 \times 10^{-5}$ sec^{-1}. This velocity constant is equal to $k_d f$ where k_d is the velocity constant for dissociation of the azo compound into radicals and nitrogen, and f is the efficiency of initiation of polymerization.

The velocity constant k_d has now been determined at temperatures in the range 100° to 120°C for solutions of the azo compound in toluene, xylene and chlorobenzene. Three procedures have been used; these involved: (*a*) determination of undecomposed azo compound in reaction mixtures by the method of isotope dilution analysis, (*b*) spectrophotometric determination of the azo compound remaining in reaction mixtures, and (*c*) measurements of the volume of nitrogen evolved during the decomposition.

EXPERIMENTAL METHODS AND RESULTS

For experiments involving isotope dilution analysis, degassed solutions of ^{14}C-2-cyano-2-propylazoformamide at a concentration of 4×10^{-3}M in toluene were used; the solutions contained about 30 mg of the labelled azo compound. After treatment at 100°C, a known weight (about 200 mg) of unlabelled azo compound was dissolved in the reaction mixture which was then cooled strongly to precipitate the azo compound; the recovered material was purified by repeated crystallization and assayed by gas counting. Results are presented in *Figure 1*; the decomposition follows a first order kinetic law and k_d is $1{\cdot}8 \times 10^{-5}$ sec^{-1}.

In the experiments in which the decomposition was followed spectrophotometrically, degassed solutions of the azo compound were used. Optical densities of solutions were measured at 370, 380 and 390 mμ using a 1 cm quartz cell in a Unicam spectrophotometer; there was no interference resulting from absorption by products of the decomposition and, for the azo compound, Beer's law was obeyed. Both the azo compound and an unstable intermediate in its decomposition absorb strongly between

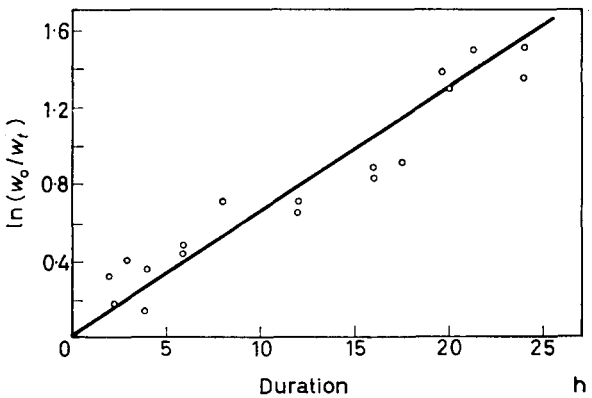

Figure 1—Results of isotope dilution analyses; w_0 denotes initial weight of azoformamide; w_t, the weight remaining after treatment at 100°C

280 and 320 mμ; optical densities at these wavelengths could not be used directly for determination of the azo compound remaining in reaction mixtures. Results of experiments at 100°C are shown in *Figure 2*. In the hydrocarbons, k_d is $2{\cdot}1 \times 10^{-5}$ sec^{-1}; in chlorobenzene, k_d is $1{\cdot}5 \times 10^{-5}$ sec^{-1}. The values of k_d for decomposition in toluene at 110°C and in xylene at 120°C are $6{\cdot}8 \times 10^{-5}$ sec^{-1} and $2{\cdot}4 \times 10^{-4}$ sec^{-1} respectively; for decomposition in the aromatic hydrocarbons, the energy of activation is 34·5 kcal/mole.

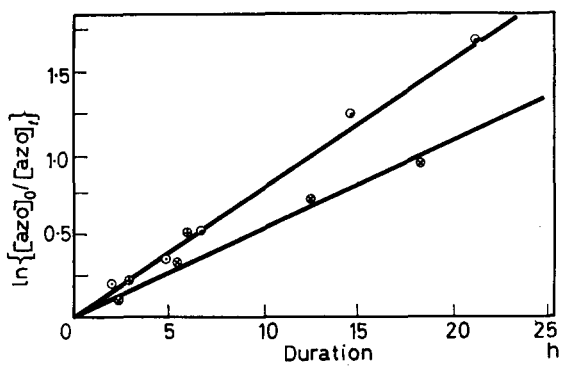

Figure 2—Results of spectrophotometric analyses; $[azo]_0$ denotes initial concentration of azoformamide; $[azo]_t$, the concentration remaining after treatment at 100°C. Initial solutions: ⊕ $7{\cdot}8 \times 10^{-3}$M in toluene, ◑ $8{\cdot}0 \times 10^{-3}$M in toluene, ○ $9{\cdot}9 \times 10^{-3}$M in xylene, ⊗ $8{\cdot}0 \times 10^{-3}$M in chlorobenzene

A simple gas burette was used for the manometric measurements. A value of $1{\cdot}22 \times 10^{-5}$ sec^{-1} was obtained for k_d for azo*iso*butyronitrile in benzene at 60°C; this is close to the accepted value[2] indicating that the experimental procedure was satisfactory. Prolonged experiments at 100°C

showed that, within experimental error, one mole of gas is evolved during the decomposition of one mole of the azoformamide; mass spectrometric analysis showed that the gas was nitrogen with traces of carbon monoxide. *Figure 3* shows the results of experiments involving 4×10^{-3} M solutions of the azoformamide in toluene; the line corresponds to a first order process having a velocity constant of $1{\cdot}8 \times 10^{-5}$ sec^{-1}. The results show more scatter than with azo*iso*butyronitrile; this effect is attributed to difficulties associated with the use of a higher temperature for the azoformamide, and with the comparatively low solubility of this substance.

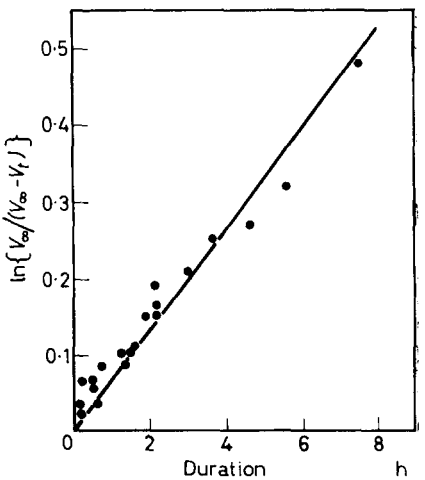

Figure 3—Results of manometric measurements; V_∞ denotes corrected volume of nitrogen calculated for complete decomposition; V_t, the corrected volume of gas evolved after treatment at 100°C

DISCUSSION

The primary dissociation of 2-cyano-2-propylazoformamide may be represented by the equation

$$(CH_3)_2C(CN)\cdot N:N\cdot CO\cdot NH_2 \longrightarrow (CH_3)_2C(CN)\cdot + NH_2\cdot CO\cdot + N_2$$

The evolved gas contains traces of carbon monoxide so evidently the further dissociation

$$NH_2\cdot CO\cdot \longrightarrow NH_2\cdot + CO$$

may occur to a small extent. It has been established[3] that 2-cyano-2-propyl radicals generated by dissociation of azo*iso*butyronitrile may react in the form $(CH_3)_2C:C:N\cdot$; this effect is likely to occur also for radicals formed from the azoformamide. The unstable intermediate already mentioned may be the compound $(CH_3)_2C:C:N\cdot CO\cdot NH_2$ analogous to the ketene-imine formed during the decomposition of the azonitrile.

Those radicals which are formed in the primary dissociation of the azoformamide and which escape geminate recombination, are available for initiating polymerizations and other reactions. The measurements of rates of decomposition reported here refer to the primary dissociation; they are in no way affected by the nature of the products formed in the system.

The spectrophotometric measurements indicate that, at 100°C, there are only small differences between the rates of dissociation of the azo compound in the aromatic hydrocarbons, although the rate in chlorobenzene is significantly smaller. Differences such as this are found for many other

similar dissociations and can be attributed largely to changes in the heat contents and entropies of initial and transition states resulting from solvation. The three methods of measurement give slightly different values for k_d for 2-cyano-2-propylazoformamide in toluene but probably k_d can be taken as close to $1{\cdot}9 \times 10^{-5}$ sec^{-1} at 100°C. This is considerably greater than the value of $1{\cdot}08 \times 10^{-5}$ sec^{-1} found for the velocity constant for the dissociation into available radicals in styrene. It is probable that the rate of the primary dissociation in styrene is close to that in other aromatic hydrocarbons, and so the efficiency of initiation for styrene is about 60 per cent. This efficiency is close to that found[4] for azo*iso*butyronitrile; it seems that for both the azoformamide and the azonitrile, there is appreciable geminate recombination of radicals and that scavengers cannot suppress this process.

Department of Chemistry,
University of Birmingham

(*Received July 1962*)

REFERENCES

[1] BEVINGTON, J. C. and WAHID, ABDUL. *Polymer, Lond.* 1962, **3**, 585
[2] VAN HOOK, J. P. and TOBOLSKY, A. V. *J. Amer. chem. Soc.* 1958, **80**, 779
[3] TALÂT-ERBEN, M. and BYWATER, S. *J. Amer. chem. Soc.* 1955, **77**, 3710
[4] BEVINGTON, J. C. *Trans. Faraday Soc.* 1955, **51**, 1397

Book Review

Kunststoffe, Struktur, physikalisches Verhalten und Prüfung
Two volumes. Edited by RUDOLF NITSCHE† and KARL A. WOLF

Volume I: *Struktur und physikalisches Verhalten der Kunststoffe*
Edited by K. A. WOLF in collaboration with numerous experts.
Springer-Verlag: Berlin–Göttingen–Heidelberg, 1962.
(xvi+974 pp.; 582 illus.; 6¾ in. by 10 in.), DM 168.

THIS large volume is the first of two designed to survey present knowledge about the structure, physical properties and testing of plastics. It is also Volume 6 of the series: 'Chemistry, Physics and Technology of Plastics in Individual Applications'. The second volume will deal with testing while the first consists of 48 essays by many authors on every conceivable aspect of the physics of plastics.

It can be seen that, since the average length of an essay is 20 pages, it is impossible for the authors to go into great detail in any of the subjects. Consequently, this is not a book for specialists in any of the fields; it must be regarded as an introductory work for those beginning a study of the subject.

Because this book is in German, English-speaking readers will probably prefer other textbooks when they are starting on the subject but those who can read German fluently may find it convenient to have so many topics treated in one place.

It is impossible to do justice to the quality of a work of this scope and magnitude in a short review but the treatment does appear to be rather uneven. Perhaps this is almost inevitable when so many different authors are involved. This unevenness can be illustrated by considering five essays from the section on the experimental study of the physical properties of polymers.

The article on flow properties by SLIWKA seems rather academic and out-of-date; it is unlikely to assist beginners to get a grasp of what is currently known or to introduce them to modern work. The article on dynamic mechanical properties by HEIJBOER, SCHWARZL and THURN is a good summary review of the phenomena but their physical interpretation is less satisfactory. The article on acoustic properties by OBERST is a good account of the relevant basic physics. The article on non-linear deformation by MÜLLER is largely confined to his own work on the subject and takes little account of the many useful studies which have been made in other countries. The article on fracture by KERKHOF is much too theoretical and idealized; the author seems to be mainly interested in the fracture of glass and pays little attention to the many ways in which the fracture of plastics differs from that of glass.

To sum up, the most useful feature of this book, for English readers, is likely to be the large collection of references.

P. I. VINCENT

Notes

The ϕ-Factor in Free-radical Copolymerization

THE rate of the free-radical copolymerization of two monomers, A and B, is frequently discussed in terms of a cross-termination factor,

$$\phi = k_{tab}/k_{taa}^{\frac{1}{2}}k_{tbb}^{\frac{1}{2}}$$

where the termination rate constants are defined by $-\mathrm{d}[\mathrm{R}\cdot]/\mathrm{d}t = k_t[\mathrm{R}\cdot]^2$, and the subscripts refer to the type of monomer unit upon which the electron of unpaired spin is localized. This ϕ factor is almost always evaluated by the use of a kinetic equation, the denominator of which contains terms descriptive of the overall rate of termination

$$-\frac{\mathrm{d}([\mathrm{A}]+[\mathrm{B}])}{\mathrm{d}t} = \frac{(r_1[\mathrm{A}]^2 + 2[\mathrm{A}][\mathrm{B}] + r_2[\mathrm{B}]^2)\,\mathrm{R}_i^{\frac{1}{2}}}{(r_1^2\delta_a^2[\mathrm{A}]^2 + 2\phi r_1 r_2 \delta_a \delta_b [\mathrm{A}][\mathrm{B}] + r_2^2\delta_b^2[\mathrm{B}]^2)^{\frac{1}{2}}} \qquad (1)$$

r_1 and r_2 are the monomer reactivity ratios given by the propagation rate constant ratios k_{paa}/k_{pab} and k_{pbb}/k_{pba} respectively, δ_a and δ_b represent the ratios $k_{taa}^{\frac{1}{2}}/k_{paa}$ and $k_{tbb}^{\frac{1}{2}}/k_{pbb}$ respectively. Subscripts, ab, represent reaction of radical of type A with either monomer or radical type B.

One of the problems to be considered in any free-radical polymerization is whether or not the rate of the termination reaction is determined by diffusive processes. If this should apply in a copolymerization, the rate of diffusion of two reacting polymeric radicals, and hence the observed rate of termination, can be considered independent of the nature of the radical end group[1-3]. This fact has led to the widely held[4], but erroneous, conclusion that in such a system a value of ϕ equal to unity must necessarily be observed. A measured value of ϕ greater than unity is then held to be incompatible with a mechanism of diffusion control for the termination step.

In fact any process whatsoever, chemical or physical, which causes the rate of termination to differ from that calculated on the basis of a simple combination of the rates of homotermination (weighted in accordance with the probability of finding either monomer unit at the reactive chain end) will cause an experimenter using equation (1) to obtain a value of ϕ other than unity. In other words, ϕ appears in equation (1) as a simple variable measuring any 'unforeseen' increase ($\phi > 1$) or decrease ($\phi < 1$) in the rate of termination. The effect of co-monomer units on the rate of diffusion of a polymeric radical is just one process which might conceivably alter the observed rate of termination in a complex way, thereby causing ϕ to be calculated as some value other than unity. The fact that equation (1) is not directly applicable[1] to diffusion-controlled systems is immaterial to this argument, just so long as it is appreciated that the parameter evaluated as ϕ using equation (1) is no longer the ratio $k_{tab}/k_{taa}^{\frac{1}{2}}k_{tbb}^{\frac{1}{2}}$.

Two factors obviously affect polymer diffusivities, specific solvation

(through the second virial coefficient) and polymer chain flexibility. There is evidence from dilute solution properties[5] and from glass transition temperatures[6] that both of these factors may vary with polymer composition in a non-linear fashion. In the much-studied styrene–methyl methacrylate system, both the second virial coefficient and the chain flexibility pass through a maximum[5,6] as the copolymer composition is varied. If, as is likely for copolymers rich in methyl methacrylate[7], termination in such a system should be diffusion-controlled, and should depend on the second virial coefficient, an experimental value of ϕ greater than unity would be predicted on both counts. It must be emphasized that in this system quite different effects, such as transfer to the aromatic nucleus[8], may also cause equation (1) to yield large ϕ values.

Evaluation of ϕ using equation (1) cannot, then, be applied as a diagnostic test for determining the mechanism of the termination process. Indeed the possible extension of ϕ to cover thermodynamic or rheological phenomena is one more intriguing aspect of the kinetics of copolymerization.

A. M. NORTH

Department of Inorganic, Physical and Industrial Chemistry, University of Liverpool

(Received November 1962)

REFERENCES

[1] ATHERTON, J. N. and NORTH, A. M. *Trans. Faraday Soc.* 1962, **58,** 2049
[2] BEVINGTON, J. C. *Radical Polymerization.* Academic Press: London and New York, 1961
[3] ALLEN, P. E. M. and PATRICK, C. R. *Makromol. Chem.* 1961, **47,** 154
[4] WEALE, K. E. *Quart. Rev. chem. Soc., Lond.* 1962, **16,** 267
[5] STOCKMAYER, W. H., MOORE, L. D., FIXMAN, M. and EPSTEIN, B. N. *J. Polym. Sci.* 1955, **16,** 517
[6] BEEVERS, R. B. *Trans. Faraday Soc.* 1962, **58,** 1465
[7] NORTH, A. M. and REED, G. A. *Trans. Faraday Soc.* 1961, **57,** 859
[8] BURNETT, G. M. and LOAN, L. D. *Trans. Faraday Soc.* 1955, **51,** 214, 219 and 226

The Constitution of Polypropylenes and Ethylene–Propylene Copolymers, Prepared with Vanadyl-based Catalysts

IT HAS been shown earlier[1] that ethylene–propylene copolymers prepared with $VOCl_3$- or $VO(OR)_3$-containing catalysts not only contain odd-numbered methylene sequences as was expected, but also sequences of two units. We even found some indications for the presence of methylene sequences of four units.

In the present note we report some additional experiments on copolymers with much lower ethylene contents and on pure polypropylenes prepared with catalysts consisting of $VOCl_3$ or $VO(OR)_3$ and alkylaluminium sesquichloride.

The infra-red spectra of the ethylene–propylene copolymers containing 15 to 30 mole per cent of ethylene show little or no absorption above 13·70μ (*Figure 1*). This means that very few methylene sequences of four

(through the second virial coefficient) and polymer chain flexibility. There is evidence from dilute solution properties[5] and from glass transition temperatures[6] that both of these factors may vary with polymer composition in a non-linear fashion. In the much-studied styrene–methyl methacrylate system, both the second virial coefficient and the chain flexibility pass through a maximum[5,6] as the copolymer composition is varied. If, as is likely for copolymers rich in methyl methacrylate[7], termination in such a system should be diffusion-controlled, and should depend on the second virial coefficient, an experimental value of ϕ greater than unity would be predicted on both counts. It must be emphasized that in this system quite different effects, such as transfer to the aromatic nucleus[8], may also cause equation (1) to yield large ϕ values.

Evaluation of ϕ using equation (1) cannot, then, be applied as a diagnostic test for determining the mechanism of the termination process. Indeed the possible extension of ϕ to cover thermodynamic or rheological phenomena is one more intriguing aspect of the kinetics of copolymerization.

A. M. NORTH

Department of Inorganic, Physical and Industrial Chemistry, University of Liverpool

(Received November 1962)

REFERENCES

[1] ATHERTON, J. N. and NORTH, A. M. *Trans. Faraday Soc.* 1962, **58,** 2049
[2] BEVINGTON, J. C. *Radical Polymerization.* Academic Press: London and New York, 1961
[3] ALLEN, P. E. M. and PATRICK, C. R. *Makromol. Chem.* 1961, **47,** 154
[4] WEALE, K. E. *Quart. Rev. chem. Soc., Lond.* 1962, **16,** 267
[5] STOCKMAYER, W. H., MOORE, L. D., FIXMAN, M. and EPSTEIN, B. N. *J. Polym. Sci.* 1955, **16,** 517
[6] BEEVERS, R. B. *Trans. Faraday Soc.* 1962, **58,** 1465
[7] NORTH, A. M. and REED, G. A. *Trans. Faraday Soc.* 1961, **57,** 859
[8] BURNETT, G. M. and LOAN, L. D. *Trans. Faraday Soc.* 1955, **51,** 214, 219 and 226

The Constitution of Polypropylenes and Ethylene–Propylene Copolymers, Prepared with Vanadyl-based Catalysts

IT HAS been shown earlier[1] that ethylene–propylene copolymers prepared with $VOCl_3$- or $VO(OR)_3$-containing catalysts not only contain odd-numbered methylene sequences as was expected, but also sequences of two units. We even found some indications for the presence of methylene sequences of four units.

In the present note we report some additional experiments on copolymers with much lower ethylene contents and on pure polypropylenes prepared with catalysts consisting of $VOCl_3$ or $VO(OR)_3$ and alkylaluminium sesquichloride.

The infra-red spectra of the ethylene–propylene copolymers containing 15 to 30 mole per cent of ethylene show little or no absorption above 13·70μ (*Figure 1*). This means that very few methylene sequences of four

or more units are present. The absorption peaks at 13·30 and 13·60μ reveal the presence of sequences of two and three units respectively. Thus, these copolymers, unlike those previously described, contain nearly all of the ethylene in isolated monomer units.

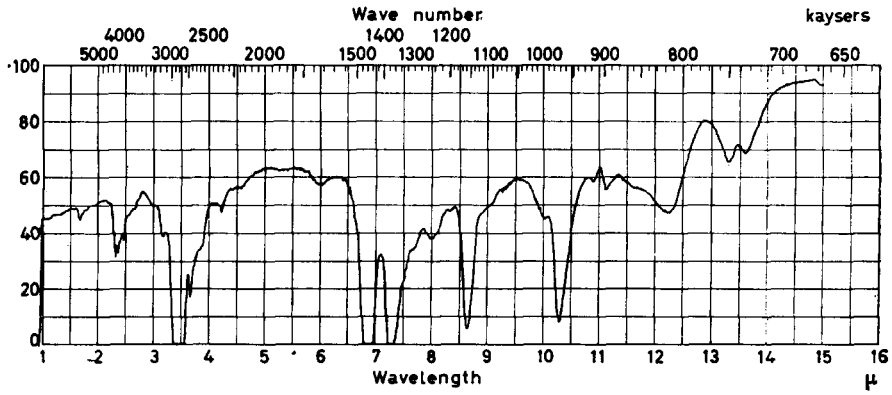

Figure 1—Infra-red spectrum of ethylene–propylene copolymer containing 85 mole per cent propylene

In ref. 1 it was stated that polypropylenes obtained with these vanadyl catalysts possessed the normal head-to-tail structure. More detailed examination, however, showed that the amorphous fractions isolated from these polypropylenes do show absorption at 13·3μ pointing to the presence of methylene sequences of two units, which can only mean that tail-to-tail arrangement of propylene units does occur [*Figure 2*(a)]. A very small absorption peak at 13·3μ was also found in the spectrum of the crystalline fractions [*Figure 2*(b)]. Care had been taken to prevent the catalyst components from liberating ethylene on reaction, so that no ethylene could have entered these polypropylenes from the catalyst. Polypropylenes prepared with catalysts based on VCl_3 show only the normal head-to-tail arrangement in both amorphous and crystalline fractions as do polymers prepared with $TiCl_3$-catalysts.

The amount of propylene units coupled tail-to-tail was estimated to range from about 5 to 15 per cent for the amorphous and from about 1 to 5 per cent for the crystalline fractions. The amount of propylene units in tail-to-tail arrangement was calculated from spectra of thin films by comparing the ratio of the absorbances at 13·30 and 8·65μ (methyl band) in the spectra of the polypropylenes with the ratio of the absorbances at 13·60 and 8·65μ in the spectrum of hydrogenated natural rubber. This implies the assumption that the absorbance per CH_2 group is the same at 13·30μ for $(CH_2)_2$ sequences as at 13·60μ for $(CH_2)_3$ sequences.

The differences in amount of tail-to-tail coupled units between crystalline and amorphous fractions are to be expected since every head-to-head and tail-to-tail configuration disturbs the regularity of the isotactic chain. In the polypropylenes every tail-to-tail configuration must necessarily be

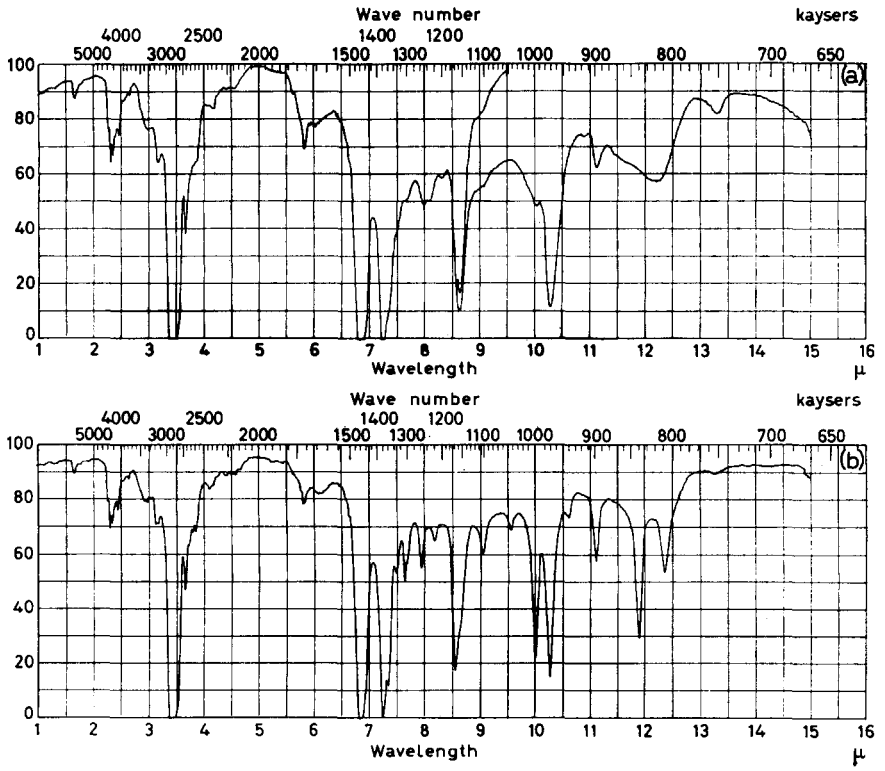

Figure 2—Infra-red spectrum of polypropylene prepared with vanadyl-based catalyst: (a) amorphous part, (b) crystalline part

accompanied by a head-to-head coupling. We should expect this to show up in an absorption peak at 8·8 to 9·0μ, characteristic of the structure

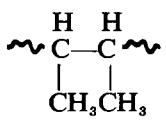

which is also found in hydrogenated poly-2,3-dimethylbutadiene*, used as a model compound (*Figure 3*) and in alternating copolymers of ethylene and butene-2[2]. In the polypropylenes examined and also in the copolymers we indeed find an absorption band near 9μ, although it is much less sharp than in the model compound.

All spectra containing the 13·3μ peak show a further small band at 10·9μ, which is also found in the spectrum of poly-2,3-dimethylbutadiene. The spectrum of the amorphous alternating copolymer of ethylene and butene-2, published by Natta[2], shows a band at about 10·8μ. The fact that the polypropylenes prepared with $VOCl_3$- or $VO(OR)_3$-containing catalysts

*The poly-2,3-dimethylbutadiene was prepared by emulsion polymerization.

show tail-to-tail arrangement means that tail-to-tail coupling of propylene units may also occur in the ethylene–propylene copolymers. However, because the content of $(CH_2)_2$ sequences in the copolymers is much higher than in the polypropylenes prepared with the same catalysts, a large part

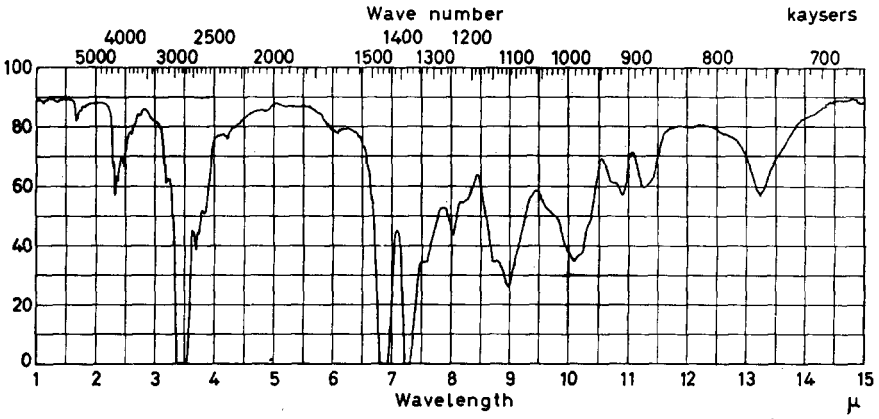

Figure 3—Infra-red spectrum of hydrogenated poly-2,3-dimethylbutadiene

of these sequences most likely stems from isolated ethylene units between two head-to-head oriented propylene units, their relative amount depending on the ratio of reaction rates of formation of the sequences

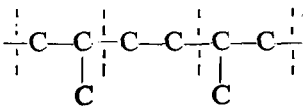

and

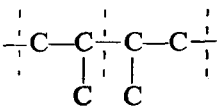

This possibility has been neglected by Veerkamp and Veermans[3] in their determination of the fraction of isolated ethylene units.

As a consequence, for a detailed study of the copolymerization of ethylene and propylene with these catalysts the reaction has to be considered as a terpolymerization of ethylene and propylene entering the chain either head-first or tail-first.

J. VAN SCHOOTEN
S. MOSTERT

Koninklijke/Shell-Laboratorium, Amsterdam
(Shell Internationale Research Maatschappij N.V.)

(Received January 1963)

REFERENCES

[1] VAN SCHOOTEN, J., DUCK, E. W. and BERKENBOSCH, R. *Polymer, Lond.* 1961, **2**, 357
[2] NATTA, G. *et al. Kolloidzschr.* 1962, **182**, No. 1–2, 50
[3] VEERKAMP, TH. A. and VEERMANS, A. *Makromol. Chem.* 1961, **50**, 147

Ethyl and n-*Butyl Lithium as Initiators of Anionic Polymerization*

IN THE course of an investigation on the mechanism of the polymerizations of isoprene and styrene initiated by alkyl lithium compounds, we have studied the kinetics of the polymerizations of these two monomers in toluene solution initiated by (*a*) *n*-butyl lithium and (*b*) ethyl lithium under comparable conditions of concentration and temperature. Both alkyl lithium solutions were prepared by carrying out the reaction between the appropriate alkyl bromide and metallic lithium in dry *n*-hexane under dry, oxygen-free nitrogen. The detailed procedure used for the preparation and analysis of these solutions was that described in an earlier communication[1]. The kinetic procedure was also identical to that employed previously in that the monomer concentration at any time was calculated from the observed volume contraction of a reaction mixture.

Figures 1 to *4* show that in both the styrene and isoprene polymerizations

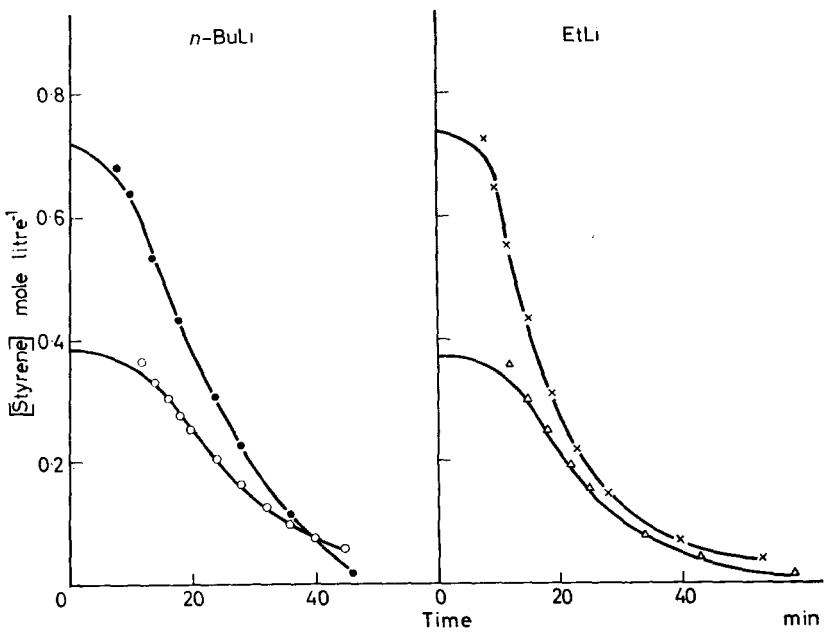

Figure 1—Influence of initial monomer concentration on polymerization of styrene at 30°C. $[n\text{-BuLi}]_0$ 0·053 M. $[EtLi]_0$ 0·044 M.

similar changes in the initial concentrations of monomer and initiator produce changes in the concentration/time curves within the experimental error irrespective of whether the initiator is ethyl or *n*-butyl lithium. Consequently we conclude that the mechanism of the polymerization of styrene or isoprene is unchanged by this change of initiator and that the scheme proposed by Worsfold and Bywater[2] for *n*-butyl lithium is applicable to the ethyl lithium initiated polymerization of styrene. Since

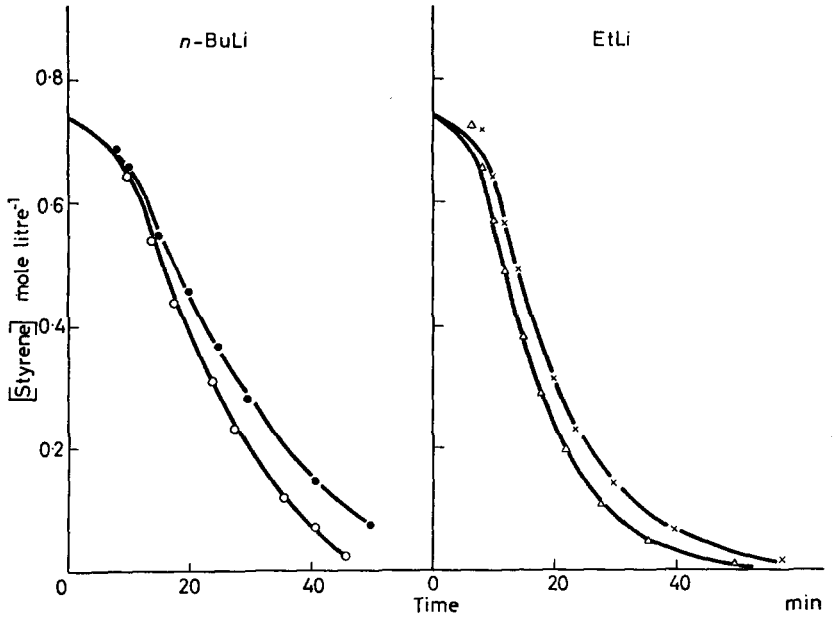

Figure 2—Influence of initial alkyl lithium concentration on polymerization of styrene at 30°C.

$[n\text{-BuLi}]_0$ ● 0·017 M ○ 0·044 M
$[EtLi]_0$ × 0·028 M △ 0·053 M

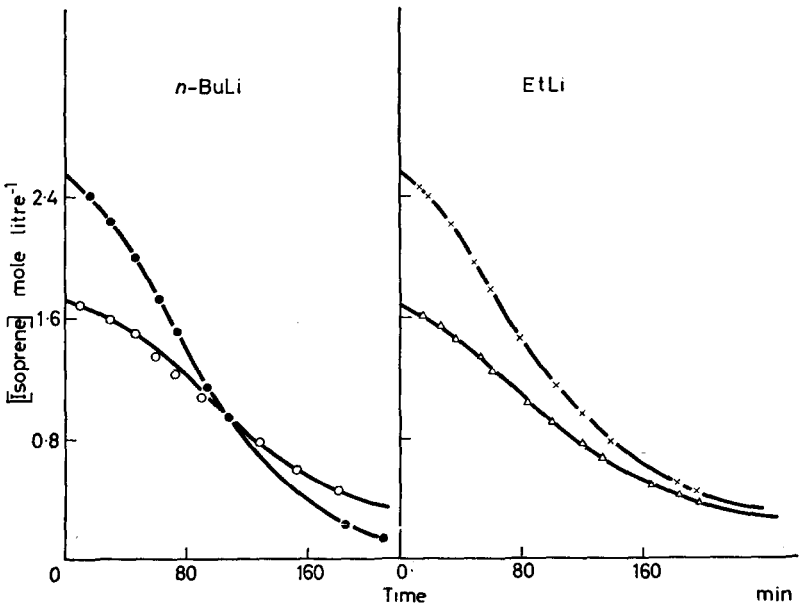

Figure 3—Influence of initial monomer concentration on polymerization of isoprene at 25°C.

$[n\text{-BuLi}]_0$ 0·050 M. $[EtLi]_0$ 0·090 M

our work with isoprene is incomplete, we can say nothing about the mechanism in this case. It is significant that the time scale of the experiments is little affected by the change of the alkyl group of the initiator so that the two constants whose influence on the kinetic behaviour of the

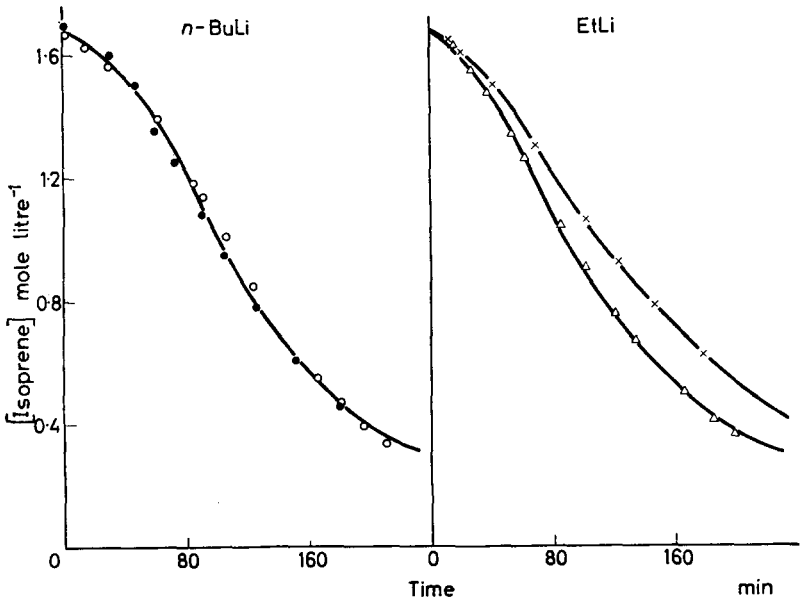

Figure 4—Influence of initial alkyl lithium concentration on polymerization of isoprene at 25°C.

$[n\text{-BuLi}]_0$	●	0·047 M	○	0·100 M
$[EtLi]_0$	×	0·045 M	△	0·090 M

system might be expected to be altered by such a change, namely the constants for the two reactions:

$$(RLi)_6 \rightleftharpoons 6RLi \quad K_1 \quad \text{association equilibrium}$$

and

$$RLi + M \longrightarrow RMLi \quad k_i \quad \text{initiation}$$

must be similar for ethyl and *n*-butyl lithium.

These results are not unexpected in view of the similar association[3-7] and similar chemical behaviour of the two compounds. On the other hand, Medvedev and co-workers[8,9] report that in the separate polymerizations of styrene and isoprene initiated by ethyl lithium in toluene, the rate of polymerization is directly proportional to the product of the concentrations of ethyl lithium and monomer at low concentrations of ethyl lithium while at high concentrations of this initiator, the rate becomes independent of the ethyl lithium concentration but remains first order with respect to monomer. Our results on the *n*-butyl lithium initiated polymerizations and those of other workers[1,2] do not show such simple kinetics.

We wish to thank Dr R. C. P. Cubbon for allowing us to use some of his results.

G. C. EAST
P. F. LYNCH
D. MARGERISON

Department of Inorganic, Physical and Industrial Chemistry, University of Liverpool

(*Received January 1963*)

REFERENCES

[1] CUBBON, R. C. P. and MARGERISON, D. *Proc. Roy. Soc. A*, 1962, **268**, 260
[2] WORSFOLD, D. J. and BYWATER, S. *Canad. J. Chem.* 1960, **38**, 1891
[3] HEIN, F. and SCHRAMM, H. *Z. phys. Chem.* 1930, **151**, 234
[4] BROWN, T. L. and ROGERS, M. T. *J. Amer. chem. Soc.* 1957, **79**, 1859
[5] BROWN, T. L., DICKERHOOF, D. W. and BAFUS, D. A. *J. Amer. chem. Soc.* 1962, **84**, 1371
[6] WITTIG, G., MEYER, F. J. and LANGE, G. *Ann. Phys., Lpz.* 1951, **571**, 167
[7] MARGERISON, D. and NEWPORT, J. P. To be published
[8] SPIRIN, YU. L., GANTMAKHER, A. R. and MEDVEDEV, S. S. *Vysokomol. Soedineniya*, 1959, **1**, 1258
[9] SPIRIN, YU. L., POLYAKOV, D. K., GANTMAKHER, A. R. and MEDVEDEV, S. S. *J. Polym. Sci.* 1961, **53**, 233

Contributions to Polymer

Papers accepted for future issues of POLYMER include the following:

Stress Relaxation of Vulcanized Rubbers I—Theoretical Study—S. BAXTER and H. A. VODDEN

Stress Relaxation of Vulcanized Rubbers II—Mathematical Analysis of Observations—L. A. EDELSTEIN, H. A. VODDEN and M. A. A. WILSON

Stress Relaxation of Vulcanized Rubbers III—Experimental Study—S. BAXTER and M. A. A. WILSON

A Kinetic Study of the Isothermal Spherulitic Crystallization of Polyhexamethylene Adipamide—J. V. MCLAREN

Crystallinity, Crystallite Size and Melting Point of Polypropylene—G. FARROW

The Influence of Particle Size and Distortions upon the X-ray Diffraction Patterns of Polymers—R. BONART, R. HOSEMANN and R. L. MCCULLOUGH

The Influence of Extrusion Conditions on the Crystallization of Polyethylene Terephthalate—R. P. SHELDON

Shear Modulus in Relation to Crystallinity in Polymethylene and Its Copolymers—J. B. JACKSON, P. J. FLORY, R. CHAING and M. J. RICHARDSON

Crystallization and Melting of Copolymers of Polymethylene—M. J. RICHARDSON, P. J. FLORY and J. B. JACKSON

A Study of X-ray Long Periods Produced by Annealing Polyethylene Crystals—F. J. BALTÁ CALLEJA, D. C. BASSETT and A. KELLER

The Constant Pressure Dynamic Osmometer—I. C. MCNEILL

The Crystallization of Polyethylene after Partial Melting—W. BANKS, M. GORDON and A. SHARPLES

The Diffusion and Clustering of Water Vapour in Polymers—J. A. BARRIE and B. PLATT

The Dielectric Behaviour of Oxidized High-pressure Polyethylene I—C. A. F. TUIJNMAN

Dipole Relaxation in the Crystalline Phase of Polymers II—C. A. F. TUIJNMAN

Crystallization of Gutta Percha and Synthetic trans-*1,4-Polyisoprenes*—W. COOPER and G. VAUGHAN

Solid State Polymerization of β-Propiolactone—G. DAVID, J. VAN DER PARREN, F. PROVOOST and A. LIGOTTI

Viscosity/Molecular Weight Relation in Bulk Polymers I—H. P. SCHREIBER, E. B. BAGLEY and D. C. WEST

Viscosity/Molecular Weight Relation in Bulk Polymers II—H. P. SCHREIBER

An Infra-red Study of the Deuteration of Cellulose and Cellulose Derivatives—R. JEFFRIES

The Glass Transition Temperature of Polymeric Sulphur—A. V. TOBOLSKY, W. MACKNIGHT, R. B. BEEVERS and V. D. GUPTA

Gamma-irradiation Polymerization of Isobutene and β-Propiolactone at Low Temperature—C. DAVID, F. PROVOOST and G. VERDUYN

Aminolysis of Polyethylene Terephthalate—H. ZAHN and H. PFEIFER

Molecular Motion in Polyethylene IV—D. W. MCCALL and D. C. DOUGLASS

A New Transition in Polystyrene, I, II, III—G. MORAGLIO, F. DANUSSO, V. BIANCHO, C. ROSSI, A. M. LIQUORI and F. QUADRIFOGLIO

The Radiation Chemistry of Some Polysiloxanes: An Electron Spin Resonance Study—M. G. ORMEROD and A. CHARLESBY

The Mechanical Degradation of Polymers—C. BOOTH

Dynamic Birefringence of Polymethylacrylate—B. E. READ

Polycarbonates from the 2,2,4,4-Tetramethylcyclobutane-1,3-diols, I, II—Miss M. GAWLAK, J. B. ROSE, A. TURNER JONES and R. P. PALMER

The Temperature Dependence of Extensional Creep in Polyethylene Terephthalate—I. M. WARD

CONTRIBUTIONS should be addressed to the Editors, *Polymer*, 4-5 Bell Yard, London, W.C.2.

Authors are solely responsible for the factual accuracy of their papers. All papers will be read by one or more referees, whose names will not normally be disclosed to authors. On acceptance for publication papers are subject to editorial amendment.

If any tables or illustrations have been published elsewhere, the editors must be informed so that they can obtain the necessary permission from the original publishers.

All communications should be expressed in clear and direct English, using the minimum number of words consistent with clarity. Papers in other languages can only be accepted in very exceptional circumstances.

A leaflet of instructions to contributors is available on application to the editorial office.

I.U.P.A.C. SYMPOSIUM

The International Symposium on Macromolecular Chemistry will be held in Paris from 1 to 5 July 1963 under the aegis of the International Union of Pure and Applied Chemistry. Further details are available from the Secrétariat du Symposium International de Chimie Macromoléculaire, 11 Rue Pierre Curie, Paris V^e^, France.

ERRATUM

RADIATION-INDUCED SOLID STATE POLYMERIZATION

The last line of the first text paragraph of the above article by P. G. GARRATT (*Polymer, Lond.* 1962, **3**, 323) should read: chains occlude the radical ends.

Stress Relaxation of Vulcanized Rubbers I — Theoretical Study

S. BAXTER and H. A. VODDEN

Consideration of the physical behaviour of polysulphide vulcanizates of natural rubber, when aged in air at elevated temperatures, has led to postulates of kinetic mechanisms which appear to explain the physical changes which occur. The basic postulates are that during thermal oxidation the rubber degrades by scissions at random points along the hydrocarbon polymer and by scissions of the polysulphide crosslinks. It is further postulated that scission of a crosslink is followed by a process of recombination leading to formation of new networks. Theoretical expressions have been derived for continuous relaxation of stress at constant elongation and for the variation of stress with time for a given elongation performed intermittently. It is shown that equations of this type lead to curves for continuous and intermittent stress relaxation similar to those obtained experimentally.

ON EXPOSURE to air or oxygen, vulcanized rubbers suffer degradation in physical properties. The rate of this degradation increases with rise of temperature and becomes a serious problem in many applications where reasonably high temperatures may be encountered. It is generally recognized that this degradation is caused by relatively small chemical changes arising from oxidation of the long chain network of which the material is composed. The accepted model for a vulcanized rubber is a three-dimensional network of long chain polymer molecules crosslinked at intervals to prevent mass flow in the material. Kinetic theory considerations enable the stress/strain characteristics of such a material to be predicted[1].

The stress in a vulcanizate, for a given strain, is proportional to the number of chains per unit volume, where a chain is defined as that portion of the polymer molecule between two crosslinks. Changes in the number of chains, and hence in the stress/strain characteristics, can be caused by scission of the network either at some point along a chain, or at a crosslink; formation of new crosslinks will also cause changes in the stress/strain behaviour. Measurements have been made on the changes in stress occurring during the oxidation of vulcanized rubbers under differing conditions and it has been found possible to postulate a mechanism to account for the principal observations. The work described in this paper deals with natural rubber, vulcanized with sulphur.

EXPERIMENTAL

Measurements of continuous stress relaxation in air, under conditions of constant elongation in an isothermal enclosure have been made using a modified form of the equipment described by Robinson and Vodden[2]. The modifications include the replacement of the resistance wire strain gauges by cantilever springs and differential transformer displacement gauges; the six rubber specimens are heated inside vertical holes bored in a block of aluminium, which is heated electrically as described previously by Vodden[3].

This aluminium block replaces the heat exchange tank of the earlier equipment. The differential transformer gauges are energized at approximately 2 000 c/s and the outputs are amplified, rectified and applied to a six-point electronic potentiometric recorder.

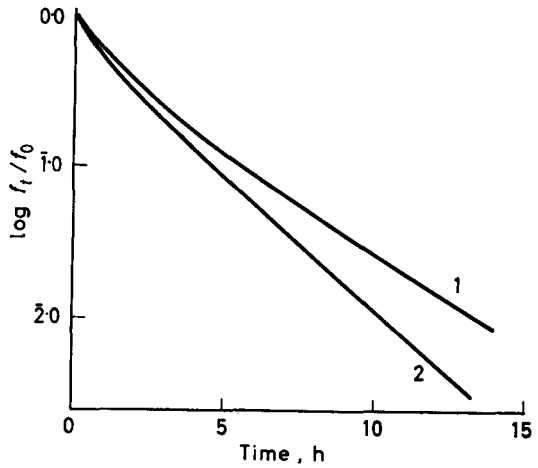

Figure 1—Continuous stress relaxation. 1 Diphenyl guanidine–sulphur stock. 2 Tetramethyl thiuram disulphide–sulphur stock

Figure 1 shows some typical stress relaxation curves for natural rubber stocks cured with diphenyl guanidine–sulphur and tetramethyl thiuram disulphide–sulphur respectively (extension 100 per cent: temperature 110°C).

From measurements of permanent set, made in the same equipment, calculations of the degree of new network formation in the rubber and of the modulus were made using a method similar to that of Andrews, Tobolsky and Hansen[4]. In *Figures 2* and *3* these are shown as functions of time.

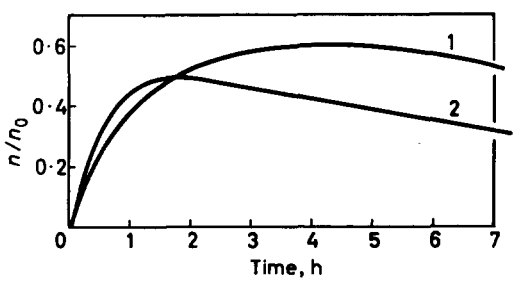

Figure 2—New network formation. n is number of new network chains, n_0 is the number of chains at time $t=0$. 1, 2 as for *Figure 1*

The effect of following one relaxation curve by another was also studied. In this experiment, an initial extension of 50 per cent was used and the stress was allowed to relax to less than 0·1 of the initial value. The relaxed sample was then extended by an extension equivalent to 125 per cent of its original length (i.e. 50 per cent of its new initial length). The two relaxation curves for a tetramethyl thiuram disulphide–sulphur cured natural rubber sample are shown in *Figure 4*

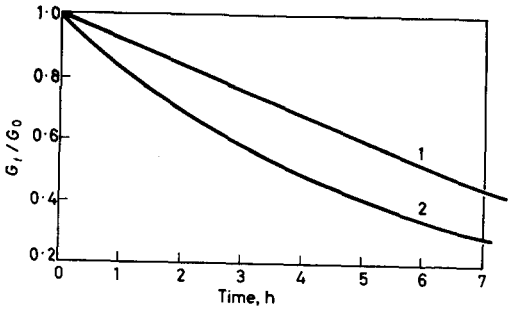

Figure 3—Variation of modulus. 1, 2 as for *Figure 1*

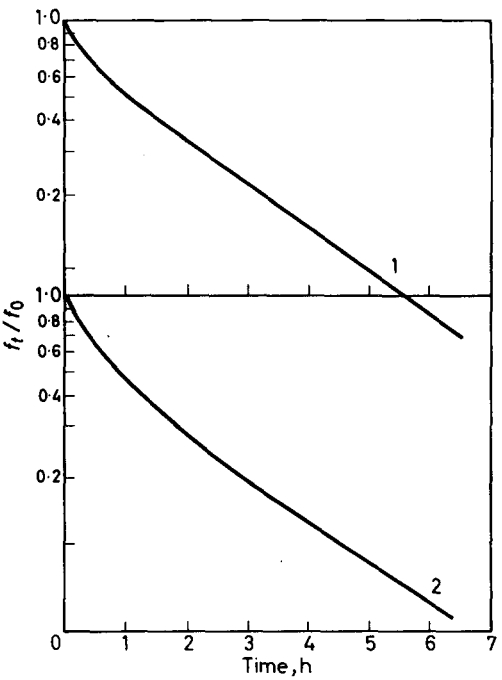

Figure 4—Successive stress relaxation curves. 1 Tetramethyl thiuram disulphide – sulphur stock extended 50 per cent. 2 Same sample extended 125 per cent

The rubber formulations used were as follows:

	Parts by weight	
	A	B
Pale crepe	100	100
Zinc oxide	3·0	3·0
Stearic acid	0·5	0·5
Sulphur	2·5	2·0
Diphenyl guanidine	0·5	—
Tetramethyl thiuram disulphide	—	0·375

Cure: A—60 minutes at 141·5°C; B—22·5 minutes at 126°C

These were moulded in a special mould to form elongated ring specimens of dimensions 4 mm × 1 mm suitable for fitting into the equipment.

Discussion of experimental results

In the stress relaxation curves (*Figure 1*) the logarithm of relative stress, f_t/f_0, is plotted against time. In both cases, pronounced curvature of the plot is obtained thus contradicting the concept of a simple exponential decay curve as required by Tobolsky, Prettyman and Dillon[5]. It is found, in fact, that the stress relaxation curves for sulphur vulcanizates of natural rubber can be fitted fairly well by expressions of the form

$$f_t/f_0 = A \exp(-K_1 t) + B \exp(-K_2 t)$$

This is in accord with the hypothesis, proposed by Berry[6], that relaxation of stress is caused by a first order oxidation of sulphur crosslinks, followed by thermal scission.

Examination of the new network formation arising from new crosslinking (*Figure 2*) shows that over a period of time when the stress at constant elongation is relaxing almost to zero, the number of new chains resulting from new crosslinking is of the same order as the number which have disappeared to allow relaxation of stress. Thus the modulus of the rubber changes only slowly when compared with the continuous stress relaxation and, in some cases, may even increase for a time. It is of interest to investigate the nature of the new crosslinks which arise during the oxidation of rubber. The marked similarity between the stress relaxation curves in *Figure 4* suggests that the crosslinks which break down to cause the second relaxation are of the same type as those giving the first curve. That is, the new crosslinks are also of sulphur. A further question then arises. From where do the new crosslinks derive their sulphur, as it is known that little, if any, free sulphur remains in a vulcanizate after curing? The suggestion here is that the new crosslinks arise from a reformation of those which have been broken during oxidation. The crosslinks in the rubber must be regarded as in a state of continuous break-down and reformation and on the evidence of stress relaxation and permanent set it appears that, in a matter of a few hours at 110°C, practically all of the original crosslinks will have been broken and reformed. Statistically, the reformed crosslinks will lead to chains in an unstrained state if the assumptions made in the kinetic theory of elasticity are valid.

On the basis of crosslink scission and reformation reactions, it might be expected that new network formation would tend to a constant equilibrium value. The experimental evidence (*Figures 2* and *3*) suggests that this is not so and both new network formation and modulus show evidence of ultimate decay with time. This behaviour can be explained if, in addition to scissions and recombinations of crosslinks, scissions of hydrocarbon chains also occur. It is known that, in unvulcanized natural rubber, degradation of molecular weight occurs due to oxidation thus implying scission of hydrocarbon chains. There seems no reason to suppose that this does not happen in vulcanized rubber. Measurements on the scission efficiencies of oxygen in vulcanized and unvulcanized systems by Tobolsky, Metz and Mesrobian[7], by Baxter, Potts and Vodden[8] and by Bevilacqua[9] suggest that the chain scission reaction is much less active than that of crosslink scission.

THEORETICAL

The proposed model for a sulphur vulcanizate consists of a number of long chain polymer molecules joined together at intervals by polysulphide crosslinks. During thermal oxidation of the rubber it is supposed that scission of hydrocarbon chains and crosslinks occurs and that free ends of crosslinks can combine with hydrocarbon chain segments.

Consider a system that has been vulcanized at random and then aged so that crosslink scissions and recombinations occur. If γ is the probability that any specific monomer unit will be joined to a crosslink which exists at time, t, then the probability of finding a chain of length x units, i.e. one in which $(x-1)$ units are left unvulcanized, at time, t, will be $\gamma(1-\gamma)^{x-1}$. The number of chains of length x units at time t will therefore be

$$N_x = N_t\gamma(1-\gamma)^{x-1}$$

where N_t is the total number of chains at time t.

If, at time t, there are X_t crosslinks in the system then

$$\gamma = \gamma_0 X_t / X_0$$

where $\gamma = \gamma_0$ and $X_t = X_0$ when $t = 0$. Therefore

$$N_x = N_t\gamma_0 (X_t/X_0)[(1-\gamma_0 (X_t/X_0)]^{x-1}$$

Ignoring the effects of chain ends,

$$N_t/N_0 = X_t/X_0$$

where N_0 is the total number of chains when $t = 0$. Therefore

$$N_x = N_0\gamma_0 (X_t/X_0)^2[1-\gamma_0 (X_t/X_0)]^{x-1}$$

Simultaneously with the crosslinking reaction, scission of hydrocarbon chains is assumed to take place at random. If p is the probability of a monomer scission up to time t then the probability of survival of a chain of length x will be $\gamma(1-\gamma)^{x-1}(1-p)^{x-1}$, since $(1-p)$ will be the probability of a monomer scission not occurring. The number of chains of length x existing at time t will therefore be

$$N_x = N_0\gamma_0 \left(\frac{X_t}{X_0}\right)^2 \left(1-\gamma_0 \frac{X_t}{X_0}\right)^{x-1} (1-p)^{x-1}$$

The total number of chains will then be

$$N_t = \sum_{x-1}^{\infty} N_0 \left(\frac{X_t}{X_0}\right)^2 \gamma_0 \left(1-\gamma_0 \frac{X_t}{X_0}\right)^{x-1} (1-p)^{x-1}$$

$$\simeq N_0\gamma_0 \left(\frac{X_t}{X_0}\right)^2 \Big/ \left(\gamma_0 \frac{X_t}{X_0} + p\right)$$

The kinetic theory of elasticity gives for the stress in a rubber specimen in simple elongation $f = N_t kT(\alpha - 1/\alpha^2)$ where α is the extension ratio.

For a given elongation, the relative stress will be

$$\frac{f_t}{f_0} = \frac{N_t}{N_0} \simeq \gamma_0 \left(\frac{X_t}{X_0}\right)^2 \Big/ \left(\gamma_0 \frac{X_t}{X_0} + p\right) \qquad (1)$$

In order to determine the time dependence of this function, it is necessary to postulate reaction mechanisms for chain scission, crosslink scission and crosslink recombination. If the stress is measured continuously at constant elongation, so that reformed crosslinks do not provide chains which contribute to the stress, then the recombination reaction can be ignored. To calculate the effects of new network formation and modulus changes, however, all these reactions should be taken into account.

Continuous relaxation

The simplest mechanism to postulate for chain scission is a first-order oxidation of monomer units resulting in scission of the hydrocarbon chain.

Thus $dZ/dt = -KZ$ where Z is the number of unreacted monomer units at time t, i.e.

$$Z = Z_0 \exp(-Kt)$$

The probability p is therefore given by

$$p = (Z_0 - Z)/Z_0 = 1 - \exp(-Kt) \tag{2}$$

For scission of sulphur crosslinks, following Berry[6] it will be assumed that the scission reaction occurs in two stages. The first, of rate constant K_1, leads to the formation of an oxygen complex and the second, of rate constant K_2, leads to scission. The scheme may be represented by

$$A + O_2 \xrightarrow{K_1} B$$

$$B \xrightarrow{K_2} \text{Scission}$$

i.e. $$-dA/dt = K_1 A$$

where A is the number of unreacted crosslinks.

$$-dB/dt = K_2 B - K_1 A$$

where B is the number of crosslink–oxygen complexes.

$$X_t = A + B$$

where X_t is the total number of crosslinks.

The solution to these equations is

$$\left(\frac{X_t}{X_0}\right)_{\text{cont.}} = \frac{A_0 K_2}{K_2 - K_1} \exp(-K_1 t) + \left(1 - \frac{A_0 K_2}{K_2 - K_1}\right) \exp(-K_2 t) \tag{3}$$

where X_0 is the total number of crosslinks when $t = 0$ and A_0 is the fraction of unreacted crosslinks when $t = 0$. The subscript $_{\text{cont.}}$ implies constant elongation conditons.

Thus, under conditions of constant elongation, the expression for stress relaxation can be obtained by substituting equations (2) and (3) in (1).

$$\left(\frac{f_t}{f_0}\right)_{\text{cont.}} = \gamma_0 \left(\frac{X_t}{X_0}\right)^2_{\text{cont.}} \Bigg/ \left[\gamma_0 \left(\frac{X_t}{X_0}\right)_{\text{cont.}} + 1 - \exp(-Kt)\right] \tag{4}$$

Intermittent relaxation

To determine the total number of crosslinks in the system at any time, the recombination reaction must also be considered. Since it seems likely

that recombination of a loose crosslink can occur in any segment of the polymer molecule, and since there are usually about one hundred or so segments for every crosslink, the simple assumption of a first-order reaction of ruptured crosslinks seems justifiable. The following kinetic scheme for crosslink reactions is therefore suggested.

$$A + O_2 \xrightarrow{K_1} B$$
$$B \xrightarrow{K_2} C$$
$$C \xrightarrow{K_3} A$$

where C is the number of ruptured crosslinks and K_3 the velocity constant for recombination, i.e.

$$dA/dt + K_1 A = K_3 C$$
$$dB/dt + K_2 B = K_1 A$$
$$dC/dt + K_3 C = K_2 B$$
$$A + B = X_t$$

These equations yield the following solutions:

$$(X_t/X_0)_{\text{int.}} = A_1 (1 + K_1/K_2) - (1/K_3)(\alpha + K_1) A_2 \exp(\alpha t) - (1/K_3)(\beta + K_1) A_3 \exp(\beta t) \quad (5)$$

where

$$A_1 = \frac{1 + C_0}{1 + K_1/K_2 + K_1/K_3}$$

$$A_2 = \left[K_3 C_0 - (K_1 + \beta) A_0 + \beta \frac{(1 + C_0)}{1 + K_1/K_2 + K_1/K_3}\right] \Big/ (\alpha - \beta)$$

$$A_3 = \left[K_3 C_0 - (K_1 + \alpha) A_0 + \alpha \frac{(1 + C_0)}{1 + K_1/K_2 + K_1/K_3}\right] \Big/ (\beta - \alpha)$$

$$2\alpha = -(K_1 + K_2 + K_3) - [(K_1 + K_2 + K_3)^2 - 4(K_1K_2 + K_2K_3 + K_3K_1)]^{1/2}$$

$$2\beta = -(K_1 + K_2 + K_3) + [(K_1 + K_2 + K_3)^2 - 4(K_1K_2 + K_2K_3 + K_3K_1)]^{1/2}$$

if $4(K_1K_2 + K_2K_3 + K_3K_1) > (K_1 + K_2 + K_3)^2$ the solution is

$$(X_t/X_0)_{\text{int.}} = A_1 (1 + K_1/K_2) - \{[(K_1 - \delta) A_2' + wA_3'] \cos wt\}/K_3 + [(K_1 - \delta) A_3' - wA_2'] \sin wt \exp(-\delta t) \quad (6)$$

where

$$A_2' = A_0 - (1 + C_0)/(1 + K_1/K_2 + K_1/K_3)$$
$$wA_3' = (\delta - K_1) A_0 + K_3 C_0 - \delta (1 + C_0)/(1 + K_1/K_2 + K_1/K_3)$$
$$2\delta = (K_1 + K_2 + K_3)$$
$$2w = [4(K_1K_2 + K_2K_3 + K_3K_1) - (K_1 + K_2 + K_3)^2]^{1/2}$$

where A_0 is the initial fraction of unreacted crosslinks, C_0 is the initial fraction of ruptured crosslinks, and X_0 is the initial total number of crosslinks.

The expression for variation of modulus with time can now be obtained by substituting equations (5) or (6) and (2) in (1). Thus,

$$\frac{G_t}{G_0} = \left(\frac{f_t}{f_0}\right)_{\text{int.}} = \gamma_0 \left(\frac{X_t}{X_0}\right)^2_{\text{int.}} \Big/ \left[\gamma_0 \left(\frac{X_t}{X_0}\right)_{\text{int.}} + 1 - \exp(-Kt)\right] \qquad (7)$$

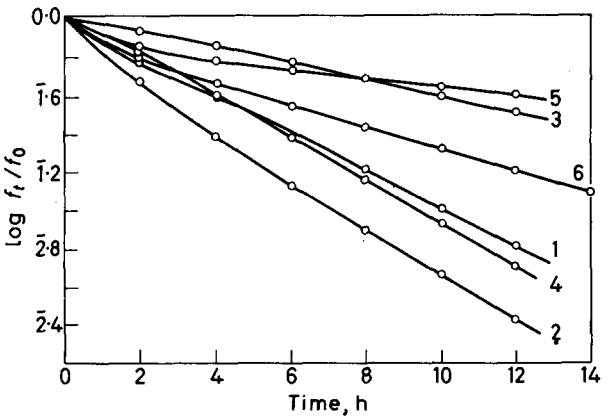

Figure 5—Continuous relaxation. $K_1=0{\cdot}1$, $K_2=1{\cdot}0$, $A_0=0{\cdot}7$, $\gamma_0=0{\cdot}01$. (1) $K=0{\cdot}0005$, (2) $K=0{\cdot}0015$. $K_1=0{\cdot}1$, $K_2=1{\cdot}0$, $A_0=1{\cdot}0$, $\gamma_0=0{\cdot}01$. (3) $K=0$, (4) $K=0{\cdot}0015$, $K_1=0{\cdot}05$, $K_2=1{\cdot}0$, $A_0=0{\cdot}7$, $\gamma_0=0{\cdot}01$. (5) $K=0$, (6) $K=0{\cdot}0005$

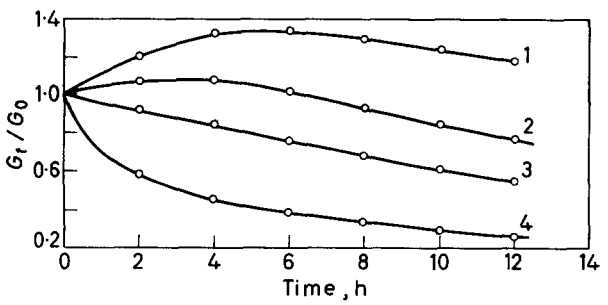

Figure 6—Intermittent relaxation. $K_1=0{\cdot}10$, $K_2=1{\cdot}0$, $A_0=0{\cdot}70$, $\gamma_0=0{\cdot}01$. (1) $K=0{\cdot}0005$, $K_3=0{\cdot}40$, $C_0=1{\cdot}0$. (2) $K=0{\cdot}0015$, $K_3=0{\cdot}40$, $C_0=1{\cdot}0$. (3) $K=0{\cdot}0015$, $K_3=0{\cdot}60$, $C_0=0{\cdot}5$. (4) $K=0{\cdot}0015$, $K_3=0{\cdot}20$, $C_0=0{\cdot}2$

Theoretical curves for stress relaxation and modulus variation are shown in *Figures 5* and *6* for different values of the constants. γ_0 which by definition is the ratio of crosslinked monomer units to total number of monomer units, is about 0·01 for the stocks used in these experiments. The points for the curves shown have been calculated using an electronic computer.

DISCUSSION

The theoretical curves of *Figures 5* and *6* show that the proposed mechanism for the oxidation of sulphur-vulcanized natural rubber can explain, in general terms, the forms of the continuous and intermittent stress relaxations. In order to progress further, it is necessary to apply the model mechanism to some real cases of stress relaxation or modulus variation and, by appropriate mathematical analyses, deduce the reaction-rate constants and initial states of the crosslinks. This has been done for continuous stress relaxation and the detailed method of analysis is described in subsequent papers by Edelstein, Vodden and Wilson[10] and Baxter and Wilson[11]. In certain cases it may be possible to extend this to include rubber stocks protected by antioxidants. Care must be exercised in the interpretation of very long time oxidation results, however, as it is known that some antioxidants are lost, by evaporation for example, during the course of the experiment. In such cases it is clear that deviations from theoretical prediction will occur and indeed this has been demonstrated[12]. Where the analysis is consistent with the proposed model, however, the results may be used to evaluate the behaviour of an antioxidant and the method provides a very powerful analytical tool for such an examination.

It is probable that the mechanism of degradation of vulcanized natural rubber is more complex than that postulated here. Within limits, modifications to the model mechanism can be made to allow more intricate chemical reactions. For example, if the scission of polymer chains follows an autocatalytic reaction, the equation for the probability of monomer scission, equation (2), should be altered as follows.

$$-\mathrm{d}Z/\mathrm{d}t = r_0 + K'(Z_0 - Z)$$

where r_0 is the initial rate and K' the autocatalytic reaction rate constant, i.e.

$$Z = Z_0 - r_0[\exp(K't) - 1]/K_1$$

and

$$p = r_0[\exp(K't) - 1]/K'Z_0$$

The relaxation equations should then be

$$\left(\frac{f_t}{f_0}\right)_{\text{cont.}} = \gamma_0 \left(\frac{X_t}{X_0}\right)^2_{\text{cont.}} \Bigg/ \left\{ \gamma_0 \left(\frac{X_t}{X_0}\right)_{\text{cont.}} + \frac{r_0}{K'Z_0}[\exp(K't) - 1] \right\} \qquad (9)$$

We are indebted to Mr J. Selvey for much of the experimental work and development of equipment.

Monsanto Chemicals Limited,
Ruabon, Wrexham,
Denbighshire

(*Received July 1962*)

REFERENCES

[1] TRELOAR, L. R. G. *The Physics of Rubber Elasticity*. Oxford University Press: London, 1949
[2] ROBINSON, H. W. H. and VODDEN, H. A. *Industr. Engng Chem. (Industr.)*, 1955, **47**, 1477
[3] VODDEN, H. A. *J. sci. Instrum.* 1960, **37**, 69

[4] ANDREWS, R. D., TOBOLSKY, A. V. and HANSEN, E. E. *J. appl. Phys.* 1946, **17,** 352
[5] TOBOLSKY, A. V., PRETTYMAN, J. B. and DILLON, J. H. *J. appl. Phys.* 1944, **15,** 380
[6] BERRY, J. P. *J. Polym. Sci.* 1956, **21,** 505
[7] TOBOLSKY, A. V., METZ, D. J. and MESROBIAN, R. B. *J. Amer. chem. Soc.* 1950, **72,** 1942
[8] BAXTER, S., POTTS, P. D. and VODDEN, H. A. *Industr. Engng Chem. (Industr.),* 1955, **47,** 1481
[9] BEVILACQUA, E. M. *Rubb. Age, N.Y.* 1956, **80,** 271
[10] EDELSTEIN, L. A., VODDEN, H. A. and WILSON, M. A. A. *Polymer, Lond.* 1963, **4,** 155
[11] BAXTER, S. and WILSON, M. A. A. *Polymer, Lond.* 1963, **4,** 163
[12] WILSON, M. A. A. Unpublished work

Stress Relaxation of Vulcanized Rubbers II — Mathematical Analysis of Observations

L. A. EDELSTEIN*, H. A. VODDEN and M. A. A. WILSON

The relaxation of stress of vulcanized rubber measured continuously at constant temperature and elongation can be described in terms of four physical constants associated with chain and crosslink scission. A method of evaluating these physical constants from experimental observations of continuous stress relaxation is described here. The method of analysis consists of fitting the logarithm of the stress data by a terminated series of Chebyshev polynomials; re-arranging to express the data as a Taylor series; equating the first four experimentally derived Taylor series coefficients with the theoretical expressions for these coefficients obtained from the postulated mechanism and hence obtaining sets of values for the constants. Chebyshev polynomial expressions of orders eight to four are fitted to the data successively and various sets of values of the physical constants obtained. Substitution of the sets of values of the constants in the theoretical expression for stress relaxation enables the stress to be calculated at various times and calculated values are compared with the observed values. The set of physical values selected as the solution is that which gives the best agreement between theoretical and observed values of stress.

BAXTER and Vodden[1] proposed a mechanism of degradation of polysulphide crosslinked vulcanizates which proceeded by a combination of random chain scission and crosslink scission. Crosslink scission was considered to proceed through the formation of an oxygen complex associated with the crosslink which subsequently split. When stress is measured continuously at constant elongation this mechanism leads to an expression of the form

$$\left(\frac{f_t}{f_0}\right)_{\text{cont.}} = \gamma_0 \left(\frac{X_t}{X_0}\right)^2_{\text{cont.}} \Bigg/ \left[\gamma_0 \left(\frac{X_t}{X_0}\right)_{\text{cont.}} + 1 - \exp(-Kt)\right] \qquad (1)$$

where

$$\left(\frac{X_t}{X_0}\right)_{\text{cont.}} = \frac{A_0 K_2}{K_2 - K_1} \exp(-K_1 t) + \left(1 - \frac{A_0 K_2}{K_2 - K_1}\right) \exp(-K_2 t) \qquad (2)$$

Here f_t denotes stress at time t, f_0 is the stress at time $t=0$, X_t is the number of crosslinks at time t, X_0 is the number of crosslinks at time $t=0$, γ_0 is the probability that any monomer unit is crosslinked at time $t=0$, K is the velocity constant for scission of monomer chains, K_1 is the velocity constant for oxygenated crosslink formation, K_2 is the velocity constant for thermal scission of oxygenated crosslinks, and A_0 is the fraction of unreacted crosslinks at time $t=0$. This paper describes a method of analysis which evaluates the physical constants K_0 ($K_0 = K/\gamma_0$), K_1, K_2 and A_0 from experimental observations of stress and time.

The method of analysis consists of fitting the logarithm of the stress data using the method of least squares by a terminated Chebyshev polynomial

*Now at Department of Physics, University College, London.

series, re-arranging to express the data as a Taylor series; equating the first four experimentally derived Taylor series coefficients with the theoretical expressions for these coefficients obtained from the postulated mechanism and so evaluating the physical constants K_0, K_1, K_2 and A_0. The mathematical basis of the analysis is described in Sections 1 and 2. Section 3 gives the results of the method of analysis applied to stress data obeying the postulated mechanism.

SECTION 1—FITTING THE EXPERIMENTAL CURVE AND DERIVING THE FIRST FOUR TAYLOR SERIES COEFFICIENTS

Let the experimental data be $f_0, f_{t_1}, f_{t_2} \ldots f_{t_n}$ where f_t is the stress at time t. Expansion of the logarithm of the data as an $(m-1)$th order Chebyshev polynomial leads to n equations:

$$\ln (f_{t_j}/f_0) = \sum_{i=0}^{m-1} A_i \overset{\star}{T}_i (x_j); \quad j = 1, 2 \ldots n \tag{3}$$

where A_i is the ith coefficient of the Chebyshev series, $\overset{\star}{T}_i$ is a Chebyshev polynomial of the first kind of degree i and x_j is $t_j/t_{\max.}$, i.e. t_j/t_n. Equations (3) are solved by the method of least squares giving the coefficients A_0, A_1, $A_2, \ldots A_{m-1}$. The logarithmic data may be expressed as a Taylor series

$$\ln f_t/f_0 = \delta_1 t + \delta_2 t^2 + \delta_3 t^3 + \ldots \delta_p t^p$$

$$(\delta_0 = \ln 1 = 0)$$

where $p \geqslant m-1$.

Using the Gauss hypergeometric form $\overset{\star}{T}_n (x) = (-1)^n F(n, -n;\ 1/2;\ x)$ we see that:

$$\delta_1 = -2 \sum_{L=0}^{\infty} (-1)^L A_L L^2 t_{\max.}^{-1}$$

$$\delta_2 = +\tfrac{2}{3} \sum_{L=0}^{\infty} (-1)^L A_L [L^2 (L^2-1)]\, t_{\max.}^{-2}$$

$$\delta_3 = -\tfrac{4}{45} \sum_{L=0}^{\infty} (-1)^L A_L [L^2 (L^2-1)(L^2-2^2)]\, t_{\max.}^{-3}$$

$$\delta_4 = +\tfrac{2}{315} \sum_{L=0}^{\infty} (-1)^L A_L [L^2 (L^2-1)(L^2-2^2)(L^2-3^2)]\, t_{\max.}^{-4} \tag{4}$$

The Taylor series for logarithmic data is next converted to a Taylor series for data

$$1 + \alpha_1 t + \alpha_2 t^2 + \ldots \alpha_p t^p = \exp [\delta_1 t + \delta_2 t^2 + \delta_3 t^3 + \ldots \delta_p t^p]$$

and hence

$$\alpha_1 = \delta_1$$

$$\alpha_2 = (1/2)\,\delta_1^2 + \delta_2$$

$$\alpha_3 = \delta_3 + (1/6)\,\delta_1^3 + \delta_2 \delta_1$$

$$\alpha_4 = \delta_4 + (1/2)\,\delta_2^2 + (1/24)\,\delta_1^4 + \delta_3 \delta_1 + (1/2)\delta_2 \delta_1^2 \tag{5}$$

Thus we have fitted the experimental curve and obtained the values of the first four Taylor series coefficients.

SECTION 2—EVALUATION OF K_0, K_1, K_2 AND A_0

Attempts to generate continuous stress relaxation curves similar to those obtained in practice[1] led to an estimated value of $K \sim 0{\cdot}001$. When K_t is small equation (1) may be written

$$\left(\frac{f_t}{f_0}\right)_{\text{cont.}} = \left(\frac{X_t}{X_0}\right)^2_{\text{cont.}} \Big/ \left[\left(\frac{X_t}{X_0}\right)_{\text{cont.}} + K_0 t\right] \tag{6}$$

where $K_0 = K/\gamma_0$. f_t/f_0 may be expressed as a Taylor series since examination of the analytic form shows that the series indicial exponent is zero

$$(f_t/f_0)_{\text{cont.}} = \sum_{l=0}^{\infty} \alpha_l t^l$$

Similarly

$$(X_t/X_0)_{\text{cont.}} = \sum_{l=0}^{\infty} \beta_l t^l$$

and hence

$$\left[\sum_{l=0}^{\infty} \beta_l t^l + K_0 t\right] \left[\sum_{j=0}^{\infty} \alpha_j t^j\right] = \left[\sum_{l=0}^{\infty} \beta_l t^l\right] \left[\sum_{j=0}^{\infty} \beta_j t^j\right] \tag{7}$$

It can be shown by equating powers of t that:

$$\begin{aligned}
K_0 &= (\beta_1 - \alpha_1) \\
K_0\alpha_1 &= (\beta_2 - \alpha_2) + \beta_1(\beta_1 - \alpha_1) \\
K_0\alpha_2 &= (\beta_3 - \alpha_3) + \beta_1(\beta_2 - \alpha_2) + \beta_2(\beta_1 - \alpha_1) \\
K_0\alpha_3 &= (\beta_4 - \alpha_4) + \beta_1(\beta_3 - \alpha_3) + \beta_2(\beta_2 - \alpha_2) + \beta_3(\beta_1 - \alpha_1)
\end{aligned} \tag{8}$$

By expansion of equation (2) it can also be shown that:

$$\begin{aligned}
\beta_1 &= -K_2(1 - A_0) \\
2!\beta_2 &= A_0K_2(K_2 - K_1) + K_2^2 - 2A_0K_2^2 \\
3!\beta_3 &= A_0K_2(K_2 - K_1)^2 - 3A_0K_2^2(K_2 - K_1) + 3A_0K_2^3 - K_2^3 \\
4!\beta_4 &= A_0K_2(K_2 - K_1)^3 - 4A_0K_2^2(K_2 - K_1)^2 + 6A_0K_2^3(K_2 - K_1) \\
&\qquad - 4A_0K_2^4 + K_2^4
\end{aligned} \tag{9}$$

The solution of equations (8) for K_0 can be reduced to the solution of a sixth order polynomial.

Let

$$\begin{aligned}
Q_2 &= 2!\beta_2 - \beta_1^2 = K_2A_0[(K_2 - K_1) - A_0K_2] \\
Q_3 &= 3!\beta_3 - \beta_1^3 = Q_2[(K_2 - K_1) + K_2(A_0 - 3)] \\
Q_4 &= 4!\beta_4 - \beta_1^4 = Q_2[(K_2 - K_1)^2 + A_0(K_2 - K_1)K_2 + A_0K_2^2 \\
&\qquad + 6K_2^2 - 4A_0K_2^2 - 4(K_2 - K_1)K_2]
\end{aligned}$$

We introduce the sixth order polynomial

$$N_6 = Q_2[(Q_4 + \beta_1^4) - (Q_2 + \beta_1^2)^2] - [(Q_3 + \beta_1^3) - (Q_2 + \beta_1^2)\beta_1]^2 \tag{10}$$

From equation (10) it may be shown that $N_6 = 0$. It can also be shown from equations (10) and (8) that:

$$Q_2 + \beta_1^2 = 2!(\alpha_2 - K_0^2)$$
$$Q_3 + \beta_1^3 = 3![\alpha_3 + K_0^2(\alpha_1 + 2K_0)]$$
$$Q_4 + \beta_1^4 = 4![\alpha_4 + K_0^2\{(\alpha_2 - K_0^2) - (\alpha_1 + 2K_0)^2\}]$$

An explicit form for N_6 is obtained

$$\begin{aligned} N_6 = 0 = {} & 44K_0^6 + 78\alpha_1 K_0^5 + (81\alpha_1^2 - 72\alpha_2)K_0^4 + (36\alpha_1^3 - 42\alpha_2\alpha_1 - 42\alpha_3)K_0^3 \\ & + (18\alpha_2^2 - 12\alpha_2\alpha_1^2 + 6\alpha_1^4 - 24\alpha_1\alpha_3 - 18\alpha_4)K_0^2 \\ & + (6\alpha_3\alpha_2 - 12\alpha_1\alpha_4)K_0 \\ & + (12\alpha_2\alpha_4 - 6\alpha_1^2\alpha_4 - 2\alpha_2^3 - 9\alpha_3^2 + 6\alpha_1\alpha_2\alpha_3) \end{aligned} \tag{11}$$

Thus if we know the values of α_1, α_2, α_3 and α_4 we can find six theoretically possible values of K_0.

The real part of the root K_0 is used to calculate K_1, K_2 and A_0.

In the analysis the logarithm of the experimental data is fitted successively by eighth to fourth order Chebyshev polynomials each of the fits resulting in six theoretically possible sets of values of the physical constants. This is done because it is not known in advance which order of polynomial will, when fitted to the data, produce the best solution. The best solution is considered to be that which, when the physical constants are substituted in equation (6), gives theoretical values of relative stress f_t/f_0 which show the best agreement with the observed values. It is apparent that thirty theoretically possible sets of values of the physical constants will be obtained in the analysis. In fact solutions which do not satisfy the following physical conditions are discarded. The conditions imposed are $K_0 > 0$, $K_1 > 0$, $K_2 > 0$ and $0 < A_0 < 1$. When the real part of the root K_0 is used to calculate K_1, K_2 and A_0, two constants Y and Z are first obtained and these correspond to K_1 and K_2 but it is not known which is which. On physical grounds it seems probable that $K_2 > K_1$ and this convention has been followed throughout. If, however, the analysis is followed through with $K_1 > K_2$ an alternative solution for each value of K_0 can be obtained, the two sets of physical constants being:

$$K_0,\ Y,\ Z,\ A_0 \qquad \text{where } Z > Y$$

and

$$K_0,\ Z,\ Y,\ A_0'$$

where

$$A_0' = 1 - Z(1 - A_0)/Y \tag{12}$$

If we regard K_0, Y, Z, A_0 as the normal solution it will be shown that when the normal solution does not satisfy the root restriction conditions neither does the alternative solution. Both solutions are obviously unacceptable if either K_0, Y or Z is < 0. The range of permissible values for A_0 is $0 < A_0 < 1$. If A_0 is > 1, it is apparent from equation (12) that A_0' is also > 1 whereas if $A < 0$ then A_0' is < 0. Thus if the normal solution is unacceptable so is the alternative solution.

Analysis of experimental observations by Baxter and Wilson[2] has shown

that usually only the normal solution is possible. A very few cases have been found in which both solutions are possible, but the alternative solution is not thought to be physically significant.

SECTION 3—RESULTS AND DISCUSSION

Stress relaxation data obeying equation (6) were analysed on the Ferranti Mercury computer by means of a programme written in 'Autocode'. *Table 1* shows calculated values of the first four Taylor series coefficients obtained by fitting Chebyshev polynomials of degree eight to four to the

Table 1

		$-\alpha_1$	$+\alpha_2$	$-\alpha_3$	$+\alpha_4$
Exact value		0·4	0·125	0·03516667	0·0085125
Order of Chebyshev	8	0·40228702	0·12987863	0·03971950	0·01098043
	7	0·39863643	0·12456434	0·03616365	0·00942590
	6	0·38819027	0·11205575	0·02909127	0·00673183
	5	0·36728667	0·09190462	0·01970353	0·00372652
	4	0·33690342	0·06899246	0·01124235	0·00157360

logarithmic data, *Table 2* shows the best solutions produced for each order of Chebyshev fit and *Table 3* shows the comparison of exact and calculated values of relative stress. Examination of *Tables 1*, *2* and *3* shows internal inconsistency since fitting the seventh order Chebyshev gives the best values of the Taylor series coefficients, whereas fitting the sixth order Chebyshev gives the best solutions and fitting the fifth order Chebyshev gives the best agreement between exact and calculated values of the relative stress, the sixth order fit giving the second best agreement. This discrepancy is due to the inherently unstable behaviour of the solution. The only practical criterion available when the correct solution is not known in advance is the best agreement of observed and calculated relative stress. Examination of *Tables 2* and *3* shows that a discrepancy of this sort does not introduce too serious an error in the values of the physical constants obtained.

Table 2

		$K_0 h^{-1}$	$K_1 h^{-1}$	$K_2 h^{-1}$	A_0
Exact value		0·1	0·1	1·0	0·7
Order of Chebyshev	8	0·1303	0·1009	1·1594	0·7654
	7	0·1257	0·0999	1·0995	0·7517
	6	0·1174	0·0991	0·9886	0·7261
	5	0·1355	0·0959	0·9189	0·7478
	4	0·1410	0·0993	0·0816	0·7598

Table 3

t hours	3·3	6·6	9·9	13·2	16·5	19·8
Exact f_t/f_0	0·358767	0·152370	0·065319	0·028264	0·012402	0·005521
Calculated f_t/f_0 Order 8	0·353209	0·143802	0·059636	0·025235	0·010903	0·004801
Calculated f_t/f_0 Order 7	0·354133	0·145528	0·060940	0·026009	0·011326	0·005024
Calculated f_t/f_0 Order 6	0·355515	0·147542	0·062487	0·026920	0·011815	0·005278
Calculated f_t/f_0 Order 5	0·357211	0·147162	0·062721	0·027390	0·011310	0·005568
Calculated f_t/f_0 Order 4	0·364414	0·146534	0·060908	0·025952	0·012230	0·005028

Unstable behaviour has been found at several stages in the development of the analysis. An example of this was that it was found that due to certain physical effects the first data point, f_0, of an experimental curve might be in error by less than five per cent. Although several hundred subsequent data points were accurate to less than one per cent, the error in f_0 resulted in a very large discrepancy between calculated and observed values of relative stress. Omission of the first data point reduced the discrepancy between observed and calculated values of relative stress of a rubber band at 12 hours from 72 per cent to 17 per cent as is seen in *Table 4*. The error arising from the unreliability of the first stress measurement was overcome by extrapolating to find the value of f_0.

The most difficult stage of the analysis is to obtain the Taylor series coefficients. Initially a power series fit of 20 natural data points was used but this resulted in an ill conditioned matrix since the diagonal terms in the matrix increased from 1 to 20^{20}. A Chebyshev polynomial was next

Table 4

	$K_0 h^{-1}$	$K_1 h^{-1}$	$K_2 h^{-1}$	A_0
Normal solution	0·372	0·100	3·517	0·949
Solution (first point omitted)	0·336	0·120	3·565	0·950
t hours	4	8	12	
Observed f_t/f_0 (normal solution)	0·16013	0·04277	0·01061	
Calculated f_t/f_0 (normal solution)	0·20060	0·05678	0·01838	
Observed f_t/f_0 (first point omitted)	0·16608	0·04440	0·01096	
Calculated f_t/f_0 (first point omitted)	0·19014	0·04650	0·01282	

fitted to the natural data, but poor values of the Taylor series coefficients were again obtained. Finally it was decided to fit the logarithm of the data with a Chebyshev polynomial expression by the method of least squares and the results of this method are seen in *Tables 1, 2* and *3*. The errors arising at various stages of the analysis led to the discrepancies

previously noted. Frequently the error causes the real roots to become complex and the imaginary part of the root has to be neglected, further increasing the error.

Whatever criticism may be made of the method, it has been shown to produce a reasonably satisfactory solution for exact data and it will be seen in a later paper[2] that the application of this method of analysis to experimental observations of continuous stress relaxation results in solutions which give good agreement between calculated and observed relative stress and furthermore the physical constants K_0, K_1, K_2 and A_0 appear to be physically significant.

Monsanto Chemicals Limited,
Ruabon, Wrexham,
Denbighshire

(*Received July 1962*)

REFERENCES

[1] BAXTER, S. and VODDEN, H. A. *Polymer, Lond.* 1963, **4**, 145
[2] BAXTER, S. and WILSON, M. A. A. *Polymer, Lond.* 1963, **4**, 163

Stress Relaxation of Vulcanized Rubbers III — Experimental Study

S. BAXTER and M. A. A. WILSON*

Three polysulphide crosslinked vulcanizates have been aged in air at elevated temperature and constant elongation and the consequent relaxation of stress measured continuously. The stocks were natural rubber vulcanized with sulphur and tetramethyl thiuram disulphide, sulphur and diphenyl guanidine and sulphur and N *cyclohexyl benzthiazyl sulphenamide. Analysis of the experimental observations by a method due to Edelstein, Vodden and Wilson has enabled the velocity constants associated with chain scission and crosslink scission to be calculated. Experiments carried out on two of the stocks at temperatures ranging from 100° to 115°C have shown that the velocity constants obey the Arrhenius equation and activation energies have been obtained for the reactions involved. It is postulated that crosslink scission proceeds through the formation of an oxygen complex at the crosslink. An experiment in which a rubber specimen was heated* in vacuo *prior to relaxation in air provided confirmatory evidence for this mechanism of degradation as the specimen behaved according to theoretical predictions. It is concluded that the postulated theory fits the experimental observations well and that these polysulphide stocks degrade by a combination of chain and crosslink scission.*

IN PART I of this series[1] a mechanism of degradation of the vulcanized rubber network was proposed in which random chain scission and crosslink scission are considered to occur simultaneously. At the same time broken crosslinks may recombine with main chains giving rise to a second network which does not contribute significantly to the stress when this is measured continuously. The simple assumptions were made that random chain scission takes place by a single stage reaction, and that crosslink scission proceeds by two single-stage reactions, the first leading to the formation of an oxygen complex and the second to scission. When relaxation is measured continuously, the relationship between stress and time, at constant temperature and elongation, is of the form

$$\left(\frac{f_t}{f_0}\right)_{\text{cont.}} = \gamma_0 \left(\frac{X_t}{X_0}\right)^2_{\text{cont.}} \Bigg/ \left[\gamma_0 \left(\frac{X_t}{X_0}\right)_{\text{cont.}} + 1 - \exp(-Kt)\right] \qquad (1)$$

where

$$\left(\frac{X_t}{X_0}\right)_{\text{cont.}} = \frac{A_0 K_2}{K_2 - K_1} \exp(-K_1 t) + \left[1 - \frac{A_0 K_2}{K_2 - K_1}\right] \exp(-K_2 t) \qquad (2)$$

and f_t is the stress at time t, f_0 is the stress at time $t=0$, X_t is the number of crosslinks at time t, X_0 is the number of crosslinks at time $t=0$, γ_0 is the probability that any monomer unit is crosslinked at time $t=0$, K is the velocity constant for scission of monomer chains, K_1 is the velocity constant for oxygen complex crosslink formation, K_2 is the velocity constant for thermal scission of crosslinks, and A_0 is the fraction of unreacted crosslinks at time $t=0$.

*Now at Monsanto Chemicals Limited, Ruabon.

When Kt is small equation (1) may be written

$$\left(\frac{f_t}{f_0}\right)_{\text{cont.}} = \left(\frac{X_t}{X_0}\right)^2_{\text{cont.}} \Big/ \left[\left(\frac{X_t}{X_0}\right)_{\text{cont.}} + K_0 t\right] \tag{3}$$

where $K_0 = K/\gamma_0$.

In part II of this series of papers[2] a method of analysis was described which enables K_0, K_1, K_2 and A_0 to be calculated from a series of observations of stress and time. Several sets of values of these constants are obtained in any one analysis, these sets are substituted in equation (3) and the relative stress f_t/f_0 calculated at various times and compared with the experimental observations at the same times. The set of values of K_0, K_1, K_2 and A_0 which gives closest agreement between calculated and observed relative stress, f_t/f_0, is selected as best.

This paper describes work in which experimental observations on several vulcanized rubber stocks are analysed in order to determine if the theory provides a satisfactory description of the observations.

EXPERIMENTAL DETAILS

Equipment and preparation of rubber samples

Continuous measurements of stress relaxation were made in the equipment described[1]. The rubber bands were allowed to remain unstrained in the equipment for a period of ten minutes to attain thermal equilibrium before the start of the experiment. Relaxation was carried out in air at 110°C with the bands linearly extended by 75 per cent unless otherwise stated.

The samples were in the form of moulded bands 1 mm thick, 4 mm wide and of 3 in. overall length. These bands fitted over pulleys of $\frac{3}{8}$ in. diameter. The bands were prepared by conventional methods; the vulcanizing ingredients and antioxidants, when present, were incorporated by milling and the bands cured in a steam heated press.

The experiments described in this paper have, for each vulcanizing system, been carried out with bands made from the same rubber mix. The stocks were of the following composition:

	A and B	C	D
Pale crepe	100	100	100
Zinc oxide	3·0	3·0	3·0
Stearic acid	0·5	0·5	0·5
Sulphur	2·5	2·0	2·5
Diphenyl guanidine	0·5	—	—
Tetramethyl thiuram disulphide	—	0·4	—
N cyclohexyl benzthiazyl sulphenamide	—	—	0·5

The proportions of the ingredients are given in parts by weight per hundred parts of rubber. The stocks were cured as follows:

A cured for 20 minutes at 153°C
B cured for 30 minutes at 153°C
C cured for 20 minutes at 126°C
D cured for 30 minutes at 142°C.

RESULTS

Three natural rubber gum stocks produced by vulcanization with sulphur and diphenyl guanidine, sulphur and *N* cyclohexyl benzthiazyl sulphenamide and sulphur and tetramethyl thiuram disulphide were studied. The stress of each of these stocks was measured continuously at 75 per cent elongation in air at 110°C over two to three decades of relaxation and the experimental observations analysed. The best sets of values of the constants K_0, K_1, K_2 and A_0 for each stock are quoted in *Table 1*. Substitution of the quoted values of the physical constants in equation (3) gives rise to calculated values of relative stress, f_t/f_0, at various times which are compared in *Table 2* with the directly observed values of relative stress at these times.

Table 1

Vulcanizing system	$K_0\,h^{-1}$	$K_1\,h^{-1}$	$K_2\,h^{-1}$	A_0
Diphenyl guanidine–sulphur (A)	0·497	0·100	3·662	0·976
N cyclohexyl benzthiazyl sulphenamide–sulphur	0·095	0·064	0·894	0·796
Tetramethyl thiuram disulphide–sulphur	0·089	0·164	1·059	0·477

Table 2

Diphenyl guanidine–sulphur stock (A)						
Calculated f_t/f_0	0·37221	0·17048	0·04616	0·01469	0·00509	
Observed f_t/f_0	0·36735	0·17177	0·04859	0·01515	0·00582	
t hours	2	4	8	12	16	
N *cyclohexyl benzthiazyl sulphenamide–sulphur stock*						
Calculated f_t/f_0	0·566090	0·355139	0·227308	0·146502	0·094990	0·061977
Observed f_t/f_0	0·565881	0·359501	0·235746	0·151030	0·091768	0·053361
t hours	2·5	5·0	7·5	10·0	12·5	15·0
Tetramethyl thiuram disulphide–sulphur stock						
Calculated f_t/f_0	0·298124	0·114023	0·046140	0·018856	0·007777	0·003246
Observed f_t/f_0	0·275668	0·113156	0·045363	0·018339	0·007416	0·003050
t hours	2·2 ⊙	4·4 ⊙	6·6 ⊙	8·8 ⊙	11·1 ⊙	13·3 ⊙

It is seen from *Table 2* that good agreement has been obtained between calculated and observed values of relative stress.

The reproducibility of the physical constants obtained on analysis is indicated by the results given in *Table 3* for a duplicate experiment on tetramethyl thiuram disulphide–sulphur accelerated stocks.

Table 3

$K_0\,h^{-1}$	$K_1\,h^{-1}$	$K_2\,h^{-1}$	A_0
0·100	0·165	1·139	0·505

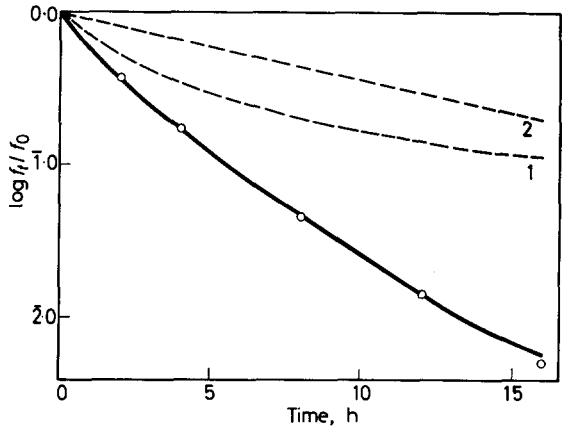

Figure 1—Diphenyl guanidine–sulphur stock A. o—calculated f_t/f_0; 1—chain scission only; 2—crosslink scission only

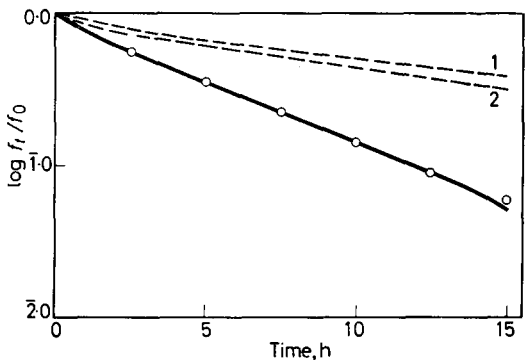

Figure 2—*N* cyclohexyl benzthiazyl sulphenamide–sulphur stock. o—calculated f_t/f_0; 1—chain scission only; 2—crosslink scission only

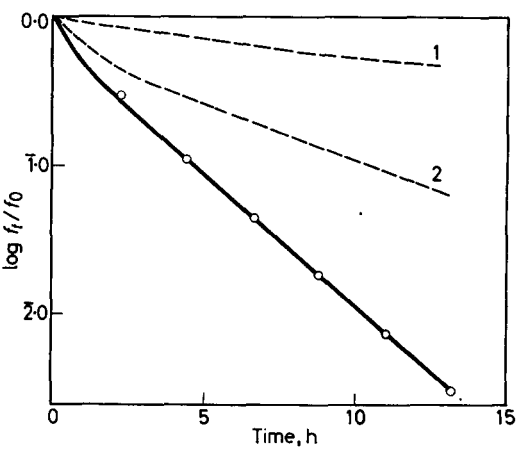

Figure 3—Tetramethyl thiuram disulphide–sulphur stock. o—calculated f_t/f_0; 1—chain scission only; 2—crosslink scission only

The sets of physical constants in *Table 1* indicate that, if the theoretical treatment is valid, both chain scission and crosslink scission occur during oxidative degradation of the three stocks. *Figures 1, 2* and *3* illustrate the relative importance of the two modes of degradation. If no crosslink scission occurs, the expression relating stress and time can be reduced to

$$(f_t/f_0)_{\text{cont.}} = \gamma_0/[\gamma_0 + 1 - \exp(-Kt)] \tag{4}$$

which when Kt is small may be used in the approximate form

$$(f_t/f_0)_{\text{cont.}} = 1/(1 + K_0 t) \tag{5}$$

and the broken line 1 in *Figures 1, 2* and *3* shows the relaxation of stress which, according to our analysis, would occur if crosslink scission could be entirely suppressed. Similarly, if chain scission does not take place the stress/time relation can be reduced to

$$(f_t/f_0)_{\text{cont.}} = (X_t/X_0)_{\text{cont.}}$$

and the broken line 2 in *Figures 1, 2* and *3* shows the relaxation of stress which would take place if chain scission could be suppressed.

It is apparent that, if the theoretical treatment is valid, both mechanisms are of importance during the degradation of these stocks.

It has been demonstrated that quantitative agreement can be obtained between the postulated theory and experimental observations. Further experiments were carried out to endeavour to establish the real significance of the physical constants obtained. Continuous stress relaxation experiments were carried out at various temperatures on tetramethyl thiuram disulphide–sulphur and diphenyl guanidine–sulphur stocks. The results are given in *Tables 4* and *5*.

Table 4—Tetramethyl thiuram disulphide–sulphur stock

Temperature °C	$K_0\,h^{-1}$	$K_1\,h^{-1}$	$K_2\,h^{-1}$	A_0
115	0·210	0·319	2·295	0·537
110	0·089	0·164	1·059	0·477
105	0·042	0·089	0·538	0·425
100	0·035	0·055	0·390	0·529

Table 5—Diphenyl guanidine–sulphur stock B

Temperature °C	$K_0\,h^{-1}$	$K_1\,h^{-1}$	$K_2\,h^{-1}$	A_0
115	1·021	0·267	7·276	0·966
110	0·705	0·147	5·129	0·975
105	0·508	0·107	3·690	0·975
100	0·344	0·055	2·612	0·982

Good agreement between calculated and observed values of relative stress has been obtained in all experiments. *Figures 4* and *5* show the plot of the logarithm of velocity constant versus reciprocal absolute temperature.

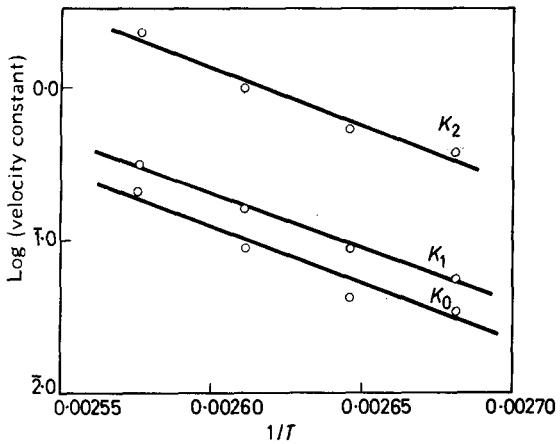

Figure 4—Tetramethyl thiuram disulphide – sulphur stock

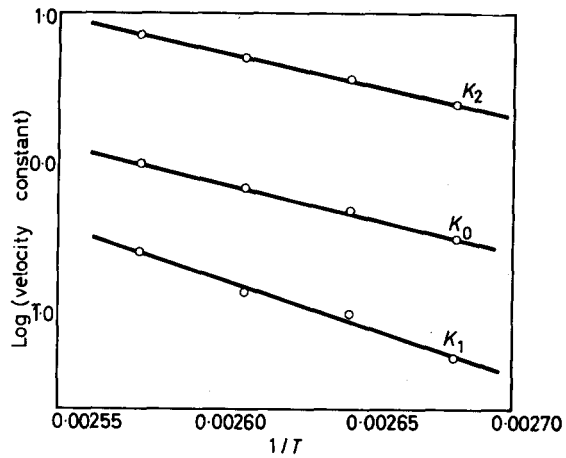

Figure 5—Diphenyl guanidine–sulphur stock

Reasonably straight lines are obtained and activation energies for the three postulated reactions have been calculated. For the tetramethyl thiuram disulphide–sulphur stock the energy of activation of the chain scission reaction is 32·6 kcal/mole (γ_0 is assumed to be constant for the four samples from the same masterbatch and is estimated as 0·01), that of the formation of the oxygen complex 33 kcal/mole, and that of the scission of the complex crosslink 33·5 kcal/mole. For the diphenyl guanidine–sulphur stock the activation energies for these reactions are 18·8 kcal/mole, 27 kcal/mole and 18·5 kcal/mole respectively. γ_0 is estimated as 0·009 for this stock.

A_0, the fraction of unreacted crosslinks at time $t=0$ would be expected to remain constant for each stock in the experiments at varying temperature, and is found to do so within experimental error. These experiments constitute a fairly severe test of the real significance of the constants K_0, K_1 and K_2 since, if the fit obtained between theory and experiment were

fortuitous, it seems improbable that the constants would obey the Arrhenius equation.

It has not so far been demonstrated that oxygen plays the part ascribed to it in crosslink scission. A further experiment was therefore carried out to investigate the real significance of the constant A_0. A sample of the tetramethyl thiuram disulphide accelerated stock was heated unstrained at 110°C for two hours *in vacuo* (10^{-6} mm of mercury), cooled *in vacuo*, and a stress relaxation experiment carried out at 110°C in air. According to theory, heat treatment *in vacuo* should cause thermal scission of the oxidized crosslinks. The simplest assumption would be that any crosslink recombination which takes place *in vacuo* would be in the unoxidized form. It would therefore be expected that the fraction of unoxidized crosslinks would increase. Subsequent relaxation at 110°C would be expected to yield, on analysis, a higher value of A_0 and unchanged values of K_1 and K_2. Some change would be expected in K_0 since γ_0 will be modified somewhat depending upon the extent of crosslink recombination. *Table 6* shows the results of analysis of the heat treated sample compared with untreated.

Table 6

Specimen	$K_0\,h^{-1}$	$K_1\,h^{-1}$	$K_2\,h^{-1}$	A_0
Tetramethyl thiuram disulphide–sulphur	0·089	0·164	1·059	0·477
Tetramethyl thiuram disulphide–sulphur heat treated *in vacuo*	0·217	0·163	0·862	0·800

Good agreement between calculated and observed relative stress was obtained. It is seen that the vacuum heated stock has behaved in accordance with theoretical predictions. A_0 has increased significantly, and K_1 and K_2

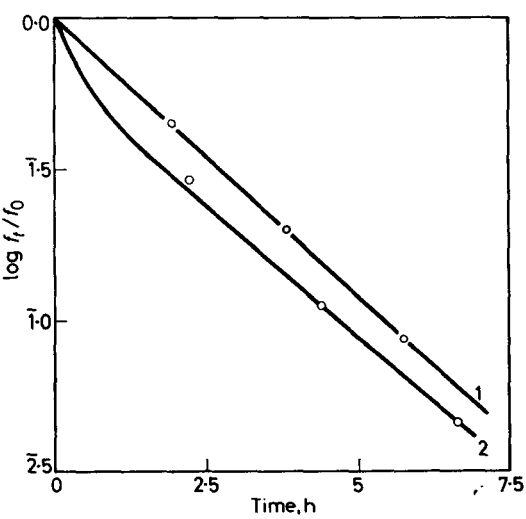

Figure 6—1 Tetramethyl thiuram disulphide–sulphur stock heat treated. ○—calculated log f_t/f_0; 2—Tetramethyl thiuram disulphide–sulphur stock; ○—calculated log f_t/f_0

are unchanged within experimental error. K_0, which is the constant determined with the poorest accuracy in the analysis, has increased rather more than would have been expected. *Figure 6* shows the relaxation curves for the treated and untreated bands.

DISCUSSION

In this paper an attempt has been made to determine if the physical mechanism for oxidative degradation of vulcanized rubber postulated by Baxter and Vodden[1] does fit experimental observations of stress relaxation. A good fit of theory to experiment has been obtained for natural rubber vulcanized with tetramethyl thiuram disulphide–sulphur, diphenyl guanidine–sulphur and *N* cyclohexyl benzthiazyl sulphenamide–sulphur. All of these stocks are considered to contain polysulphide crosslinks. Analysis of the continuous relaxation experiments yields velocity constants K_0, K_1 and K_2 for the postulated reactions of chain scission, formation of oxygen complex at the crosslink and decomposition of that complex. The significance of K_0, K_1 and K_2 has been confirmed by analysis of continuous relaxation at temperatures varying from 100° to 115°C for two of these vulcanizates. It is shown that the Arrhenius equation is obeyed and that the fourth constant A_0 remains constant within experimental error. Heat treatment *in vacuo* prior to relaxation at 110°C has provided confirmatory evidence of the significance of A_0 as this value was increased markedly by the heat treatment whereas K_1 and K_2 were unchanged as required by theory.

The mechanism of degradation of sulphur vulcanizates of natural rubber has been the subject of much controversy. Mercurio and Tobolsky[3] consider that both sulphur and sulphurless vulcanizates of natural rubber degrade predominantly by random chain scission by a single stage reaction and the dependence of stress upon time is given by

$$(f_t/f_0)_{\text{cont.}} = \exp(-Kt)$$

where K is the velocity constant for chain scission. The curvature frequently encountered in plots of the logarithm of relative stress against time (see *Figures 1, 2* and *3*) shows that departure from the exponential relation occurs. A more rigorous treatment which takes account of the distribution of chain lengths such as that of Berry and Watson[4] would lead to an expression

$$(f_t/f_0)_{\text{cont.}} = \gamma_0/[\gamma_0 + 1 - \exp(-Kt)] \qquad (4)$$

for random chain scission by a single stage reaction. This relation would show curvature of the type most commonly observed in plots of the logarithm of relative stress versus time. Bevilacqua[5] also considers degradation to proceed by random chain scission. In the type of experiment carried out by Bevilacqua in which the swelling characteristics of the degraded rubber are examined by a method due to Horikx[6] the crosslinks of the original network and the crosslinks of the second network will be measured without distinction. Where second network formation takes place to a marked extent chain scission will be the predominant measurable change in the system.

Dunn, Scanlan and Watson[7] on the other hand consider that vulcanizates containing carbon–carbon links, such as peroxide or radiation cured stocks, or vulcanizates containing mono- or di-sulphide links degrade by random chain scission, whereas vulcanizates containing polysulphide links degrade by another mechanism probably involving the crosslink. Earlier Berry and Watson[4] proposed that degradation of polysulphide crosslinked stocks proceeded by crosslink scission. Berry[8] advanced the hypothesis that crosslink scission proceeded by two single-stage reactions, the first leading to the formation of an oxygen complex at the crosslink, the second to scission of the complex link. The general theory of degradation postulated here is a combination of random chain scission by a single stage reaction with crosslink scission by two single-stage reactions according to the postulates of Berry[8]. The analysis applied to the experimental observations of stress and time has, however, a certain versatility, and is capable of producing solutions corresponding to several mechanisms, namely predominant random chain scission by a single-stage reaction, predominant crosslink scission by either a single stage or two single-stage reactions, or a combination of random chain scission with crosslink scission by either a single stage or two single-stage reactions. All solutions obtained so far have corresponded to a combination of random chain scission with crosslink scission proceeding by two single-stage reactions. It is concluded that the degradation of the polysulphide stocks examined proceeds by both chain and crosslink scission and the relative importance of the two mechanisms is indicated in *Figures 1, 2* and *3*.

The results of analysis of the continuous stress relaxation curves are, however, capable of alternative interpretations. If the scheme of random chain scission combined with crosslink scission is adhered to an identical stress relaxation curve would be produced if the velocity constants K_1 and K_2 were interchanged, i.e. if the velocity constant for the rate of formation of the oxygen complex is greater than that for the decomposition of the complex. If this were so, the value of the initial fraction of oxidized crosslinks A'_0 would be given by the relation

$$A'_0 = 1 - K_2(1 - A_0)/K_1 \tag{6}$$

which leads to negative values of A'_0 for all analyses quoted with the exception of the diphenyl guanidine–sulphur stock and requires no further consideration.

It is also possible that the mechanism of degradation of vulcanized natural rubber is more complex than is postulated here.

Dunn, Scanlan and Watson[7] and Dunn[9] find that in gum stocks based on very pure rubber degradation of vulcanizates containing carbon–carbon or mono- or di-sulphide crosslinks proceeds by autocatalytic chain scission. A combination of autocatalytic chain scission with crosslink scission by two single-stage reactions would lead to the following relation between stress and time

$$\left(\frac{f_t}{f_0}\right)_{\text{cont.}} = \gamma_0 \left(\frac{X_t}{X_0}\right)^2_{\text{cont.}} \Big/ \left[\gamma_0 \left(\frac{X_t}{X_0}\right)_{\text{cont.}} + \frac{r_0}{K'Z_0}\{\exp(K't) - 1\}\right] \tag{7}$$

where r_0 is the initial rate of reaction, K' is the velocity constant for the reaction, and Z_0 is the total number of monomer units present at $t=0$.

When $K't$ is small equation (7) can be reduced to

$$\left(\frac{f_t}{f_0}\right)_{\text{cont.}} = \left(\frac{X_t}{X_0}\right)^2_{\text{cont.}} \Big/ \left[\left(\frac{X_t}{X_0}\right)_{\text{cont.}} + \frac{r_0 t}{Z_0 \gamma_0}\right] \tag{8}$$

which would be indistinguishable mathematically from equation (3) but the interpretation of K_0 is different, $K_0 = r_0/Z_0\gamma_0$. Equation (7) would correspond to the simplest case of autocatalytic chain scission, not to the mechanism postulated by Dunn, Scanlan and Watson[7]. It seems rather unlikely, however, that chain scission in the conventionally prepared stocks used in this work would proceed by an autocatalytic mechanism since the oxygen absorption of such stocks is linear with time[10].

It has also been suggested that polysulphide stocks may degrade by directed chain scission, i.e. scission of the chain adjacent to the crosslink rather than scission of the crosslink itself[11]. Degradation by a combination of random chain scission and directed chain scission proceeding by two single-stage reactions would be mathematically indistinguishable from the mechanism postulated here. Directed chain scission, or any other mechanism in which scission is considered to take place only in the chains, leads to considerable difficulty when the formation of the second network is considered. In the mechanism proposed here, the crosslinks in the rubber are regarded as being in a state of continuous breakdown and reformation, the new crosslinks are considered to be identical with the original crosslinks and the second network to degrade in the same manner as the first. A theoretical expression for intermittent modulus has been derived

$$\frac{G_t}{G_0} = \left(\frac{f_t}{f_0}\right)_{\text{int.}} = \gamma_0 \left(\frac{X_t}{X_0}\right)^2_{\text{int.}} \Big/ \left[\gamma_0 \left(\frac{X_t}{X_0}\right)_{\text{int.}} + 1 - \exp(-Kt)\right] \tag{9}$$

and it has been shown that insertion of suitable values of the physical constants K, K_1, K_2, K_3, A_0 and C_0 (where K_3 is the velocity constant for recombination of crosslinks and C_0 the fraction of ruptured crosslinks at time $t=0$) leads to curves for intermittent modulus of the same forms as encountered in practice[1]. The theory can thus account qualitatively for the phenomena associated with second network formation. If, however, the crosslink is considered to remain intact during oxidative degradation, how is a second network formed? It has commonly been suggested that the second network is built by continued vulcanization[12] but Dunn, Scanlan and Watson[7] have shown that second network formation takes place to an appreciable extent in stocks which have been extracted with acetone before subjection to oxidative degradation. It seems unlikely that sufficient free sulphur or accelerator residues remain in the stock to account for the new crosslinking observed by intermittent modulus measurements. If the crosslink is not broken during degradation it would appear second network formation must take place either through some reaction not associated with the original crosslink such as continued vulcanization or crosslinking, or by chain recombination. The crosslinks produced by the two latter reactions will not be sulphur crosslinks. Baxter and Vodden[1] described an

experiment in which the stress of a tetramethyl thiuram disulphide–sulphur vulcanizate was allowed to relax to a tenth of its original value whereupon a further linear extension was applied to the sample and the subsequent relaxation curve examined. The overall slopes of the $\ln(f_t/f_0)$ curves were very similar. The first relaxation curve is that of the original network system; the second that of the second network system with a contribution from what remains of the original network system. By extrapolation of the first relaxation curve, an approximate estimate can be made of the contribution of the original network system to the stress at the second extension, and a corrected relaxation curve due to the second network system may be obtained. The overall slope of this curve is slightly faster than that of the original network system.

This result is what would be expected from the mechanism postulated here since γ_0 has decreased (*Figure 2*, Baxter and Vodden[1]) and K_0 increased. Whatever mechanism of degradation is postulated, it has been observed that the overall rate of degradation of vulcanizates containing carbon–carbon crosslinks is very much slower than that of polysulphide crosslinked vulcanizates[13]; if the second network links were carbon–carbon links, the second network would be expected to relax very much more slowly than the original which is contrary to experimental observation.

It appears most probable that the new crosslinks are formed from the original crosslinks by scission followed by recombination.

Monsanto Chemicals Limited,
Fulmer

(*Received July 1962*)

REFERENCES

[1] BAXTER, S. and VODDEN, H. A. *Polymer, Lond.* 1963, **4,** 145
[2] EDELSTEIN, L. A., VODDEN, H. A. and WILSON, M. A. A. *Polymer, Lond.* 1963, **4,** 155
[3] MERCURIO, A. and TOBOLSKY, A. V. *J. Polym. Sci.* 1959, **36,** 467
[4] BERRY, J. P. and WATSON, W. F. *J. Polym. Sci.* 1955, **18,** 201
[5] BEVILACQUA, E. M. *J. Amer. chem. Soc.* 1958, **80,** 5364
[6] HORIKX, M. M. *J. Polym. Sci.* 1956, **19,** 445
[7] DUNN, J. R., SCANLAN, J. and WATSON, W. F. *Trans. Faraday Soc.* 1959, **55,** 667
[8] BERRY, J .P. *J. Polym. Sci.* 1956, **21,** 505
[9] DUNN, J. R. *Kautsch. u. Gummi,* 1961, **14,** W.T. 114
[10] BAXTER, S., POTTS, P. D. and VODDEN, H. A. *Industr. Engng Chem. (Industr.),* 1955, **47,** 1481
[11] DUNN, J. R. and SCANLAN, J. *Trans. Faraday Soc.* 1961, **57,** 160
[12] TOBOLSKY, A. V. and MERCURIO, A. *J. appl. Polym. Sci.* 1959, **2,** 186
[13] WILSON, M. A. A. Unpublished work

A Kinetic Study of the Isothermal Spherulitic Crystallization of Polyhexamethylene Adipamide

J. V. McLaren

The kinetics of the isothermal spherulitic crystallization of polyhexamethylene adipamide have been studied in the temperature range 241° to 252°C. The effects of film thickness, moisture, previous thermal history and molecular weight on the rates of isothermal crystallization have been studied. Equilibrium melting temperatures (T_m) have been determined from the kinetic data and these have been found to be consistent with the theory of Flory concerning the molecular weight dependence of T_m. Comparison between induction times of crystallization and the rate parameters has been made. The results of this work are consistent with spherulitic growth proceeding by a three-dimensional nucleation process and a considerable degree of order in the molten polymer.

THE crystallization kinetics of polyhexamethylene adipamide have been studied by a number of workers using a variety of techniques[1–4]. Whilst the general nature of the isothermal crystallization has been established there are factors relevant to such crystallization that have not been fully investigated. For example, it is known that the previous thermal history of the polyhexamethylene adipamide can affect the subsequent crystallization[1]. However, a lot more detailed quantitative data are required before any definite conclusions regarding the effects of previous heat treatment on the crystallization can be made. The study of all factors affecting the crystallization kinetics of polyhexamethylene adipamide must be made before any reliable mechanism of crystallization for this polymer can emerge. In addition the kinetic data must be compatible with the results of morphological studies.

The present investigation deals with the effects of moisture, sample thickness, crystallization temperature, polymer molecular weight and previous thermal history on the isothermal crystallization kinetics of polyhexamethylene adipamide. In all experiments spherulitic growth has been studied. Such measurements have been shown to give a true measure of the overall rate of crystallization[5].

EXPERIMENTAL

Materials

The polyhexamethylene adipamide polymers had number average molecular weights in the range 2 500 to 20 000. The molecular weight values were obtained from relative viscosities of 8·4 per cent solutions of the polymer (w/w) per cent formic acid. They contained no titanium dioxide.

Apparatus

The apparatus consisted of a Köfler hot-stage mounted on a polarizing microscope (Cooke, Troughton and Simms). The microscope was fitted with

an attachment which enabled a Schachman 35 mm time lapse camera to be fitted to the eyepiece. The camera in turn was connected to a Schachman Intervalometer (type T.V.1) which enabled exposures to be made at predetermined time intervals. The maximum exposure rate was four frames per second. Photographs were taken on Kodak Panatomic X film using an exposure time of 0·1 sec. Illumination of the sample on the Köfler hot-stage was by means of a 250 W mercury lamp. The negatives were enlarged for actual measurement of spherulite size by using an Ediswan microfilm reader. Magnifications of up to 600× were used. The system was calibrated using films containing spherulites of known dimensions and an eyepiece graticule of known line separation. For melting prior to crystallization a Gallenkamp hot-stage was used. This was situated close to the Köfler hot-stage.

Methods

Sections of dry polymer chip were mounted in degassed silicone oil (MS550) between ½ in. diameter No. 1 microscope cover slips. The samples were melted for a given time at the appropriate melt temperature on the Gallenkamp hot-stage. The melting temperature was controlled to ±1°C. After the requisite time of melting, the sample was rapidly transferred to the Köfler hot-stage, which had been set at the required crystallization temperature. The Köfler hot-stage was controlled to ±0·5°C at all crystallization temperatures. Zero time for a given run was taken as the time the sample touched the Köfler hot-stage. The sample film was focused in the plane of the camera film and exposures were taken at various time intervals with the aid of the Intervalometer. The time was recorded with a stopwatch reading to 0·1 sec.

The microscope cover slips were cleaned prior to use by immersion in chromic acid for 48 hours, followed by repeated rinsing in distilled water. They were stored under a 50/50 (v/v) mixture of petroleum ether and ethanol. This 50/50 mixture had been thoroughly filtered through a fine sintered glass filter.

The samples of polymer were dried by heating the sliced chip at 75°C for 24 hours under a vacuum of 0·05 mm of mercury and stored in a desiccator over phosphorus pentoxide prior to use.

Final film thickness was measured with a screw micrometer for thicknesses greater than 30μ. For the thinner films, 25μ thick cross sections were initially microtomed, which when measured subsequent to the crystallization were found to be less than 10μ thick. This was deduced by removing the top cover slip and focusing the microscope on the bottom cover slip and the top of the film in turn.

RESULTS AND DISCUSSION

General characteristics of the crystallization kinetics

The isothermal crystallization of polymeric materials can be described by the equations due to Avrami[6–9]. The important relationship is

$$\theta = \exp(-Kt^n) \tag{1}$$

where θ is the volume fraction of unchanged amorphorus phase at time

t, K is the overall rate constant and n is an integer, the value of which depends on the nature of the growth and nucleation. Morgan[10] and others have interpreted the values of n as follows:

(*a*) For $n=2$ fibrillar growth from sporadic nuclei is postulated.

(*b*) For $n=3$ fibrillar spherulitic growth from predetermined nuclei.

(*c*) For $n=4$ fibrillar spherulitic growth from sporadic nuclei.

In this context, sporadic nucleation refers to the appearance of spherulites randomly in time and space. Predetermined nucleation refers to the non-random appearance of spherulites as evidenced by the very small size distribution in a given sample at any given time. Mandelkern[11] has pointed out that if heterogeneous material is present, the nucleation process can be affected. In the present work, all the materials were kept under conditions that minimized the chances of dust and the like being incorporated in the molten samples.

The relationships between the overall rate constant K and the microscopically measured quantities are[10]:

$$K=\tfrac{1}{3}\pi G^3 k_n \tag{2}$$

where G is the rate of radial growth of the spherulites (μ/min) and k_n is the rate of increase of nuclei per unit volume per unit time (No. cm^{-3} min^{-1}), and

$$K=\tfrac{4}{3}\pi G^3 N \tag{3}$$

where N is the number of nuclei per unit volume.

Thus equation (2) holds for conditions of sporadic nucleation and equation (3) relates to predetermined nucleation.

The crystallization was characterized by an initial induction period in which no spherulites were evident. Following this, small birefringent sheaf-like arrangements were observed which grow into larger spherulites. In all experiments the number of spherulites increased with time, indicating sporadic nucleation. The radial growth rates of the spherulites were always constant, and the growth linear. Assuming that each nucleus results in a single spherulite, nucleation rates were essentially linear. *Figures 1* and *2* show typical results from which G and k_n were derived. At most temperatures there was an initial slow rate of nucleation, but after a relatively short time the more rapid and characteristic nucleation rate was observed. Similar nucleation behaviour has been reported for polydecamethylene sebacate[5].

The accuracy of the determinations of G and k_n can be assessed by reference to *Figures 1* and *2*. In *Figure 1* different symbols on a given isothermal denote different spherulites in the same field of observation. Clearly the different spherulites grew at the same rate, indicating that a uniform temperature existed. Repeat runs at a given temperature gave satisfactory reproducibility. Repeat determinations of k_n gave reasonable reproducibility. *Figure 2* illustrates this point, different symbols denote separate determinations at a given temperature. An error of ± 5 per cent is to be expected from the statistics of the nucleation process[12]. Measurements of nucleation and growth rates were limited to the times taken for overlapping and mutual interference of the spherulites to occur.

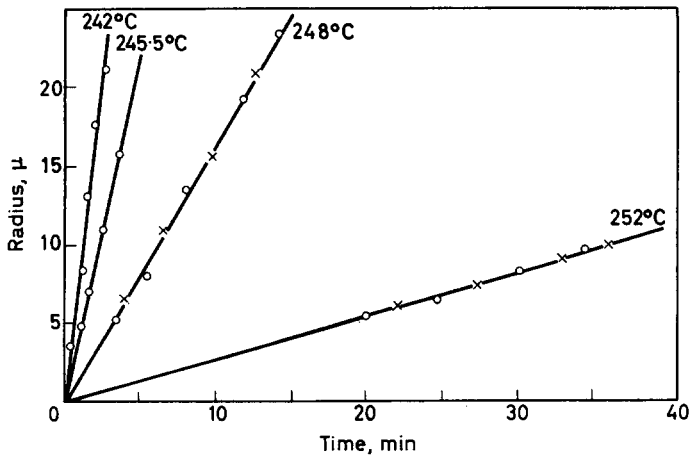

Figure 1—Radial growth rates of spherulites at various temperatures for a polymer of $M_n = 14\,600$ melted at 300°C for 30 minutes

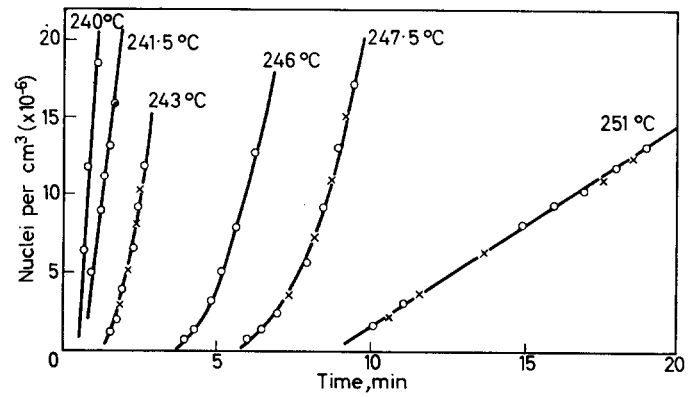

Figure 2—Nucleation rates at various temperatures for a polymer of $M_n = 14\,600$ melted at 300°C for 30 minutes

Table 1 shows some kinetic data for a sample of polymer of $M_n = 12\,900$. Magill[4], using the light depolarization technique, has obtained results for a sample of polyhexamethylene adipamide having similar characteristics. He used similar melting conditions to those employed in the present study, but in the temperature range 240° to 251°C. The nucleation was found to be predetermined. However, subsequent detailed investigation[13] has shown that for crystallization temperatures above about 245°C nucleation is sporadic, and that the rate constants agree very well with those presented in *Table 1*. The results of Morgan *et al.*[1] tend to be lower than those reported here, and this may be due to the different technique used. The data of Lindegren[3] for spherulitic growth rates are higher than those of *Table 1* but molecular weight effects account for this. The importance of molecular weight as regards crystallization will be discussed later.

Table 1. Kinetic data for a sample of polyhexamethylene adipamide of $M_n = 12\,900$ melted at 300°C for 30 minutes prior to crystallization

Crystallization temp. (°C)	G (μ/*min*)	k_n (*No.* cm^{-3} min^{-1})	K (min^{-4})
246·0	6·40	$1{\cdot}16 \times 10^{6}$	$3{\cdot}04 \times 10^{-4}$
248·0	3·38	$0{\cdot}88 \times 10^{6}$	$3{\cdot}4 \times 10^{-5}$
253·0	0·65	$0{\cdot}12 \times 10^{6}$	$3{\cdot}38 \times 10^{-8}$

Some experiments were carried out to assess the effect of moisture on the crystallization kinetics. It was found that the undried polymer crystallized at a faster rate. At 248°C the value of K for the undried polymer of $M_n = 12\,900$ was $1{\cdot}96 \times 10^{-4}$ when identical conditions to those quoted in *Table 1* were used. Since the amount of moisture varied from sample to sample, all polymers were vacuum dried prior to use. The amount of moisture removed was usually 1 to 2 per cent w/w. The increase in rate of crystallization brought about by water suggests that polymer chain mobility is enhanced due to a plasticizing action of the water.

Influence of film thickness on the kinetics

Table 2 shows some data obtained for a polymer of $M_n = 8\,700$. The film thicknesses quoted are only accurate to about $\pm 3\mu$ yet a clear trend to more rapid crystallization in thinner films can be seen. Flory and McIntyre[5], working with polydecamethylene sebacate, state that the kinetics were unchanged by a fourfold change in film thickness. They did not state, however, whether any very thin films (5 to 10μ) had been used. This present work suggests that only above about 50μ will the rate of crystallization be unaffected by film thickness. Buchdahl and co-workers[14] found that for branced polyethylene induction times of crystallization (τ) decreased as the surface to volume ratio of the sample increased. Column three in *Table 2* shows values of surface to volume ratio assuming a disc-shaped polymer sample of the quoted thickness. The results are in accord with the findings of Buchdahl.

Table 2. Effect of film thickness on the kinetic constants for a polymer of $M_n = 8\,700$ crystallized at 250°C after melting at 300°C for 30 minutes

Film thickness (μ)	τ (*min*)	$\frac{A}{V}$ ($\times 10^2$)	G (μ/*min*)	k_n (*No.* cm^{-3} min^{-1})	K (min^{-4})
150	8·4	1·91	1·5	$1{\cdot}65 \times 10^{6}$	$5{\cdot}6 \times 10^{-6}$
60	5·2	3·91	1·7	$1{\cdot}18 \times 10^{6}$	$5{\cdot}8 \times 10^{-6}$
30	3·2	7·24	2·1	$1{\cdot}95 \times 10^{6}$	$1{\cdot}95 \times 10^{-5}$
10	3·4	20·6	8·7	$21{\cdot}4 \times 10^{6}$	$1{\cdot}4 \times 10^{-2}$

The greater rate of crystallization in the thin films may be due *inter alia* to three factors: first, surface nucleation; secondly, more efficient dissipation of the heat of crystallization; and thirdly, the near two-dimensional growth may differ from the three-dimensional growth possible in the thick films. *Table 2* shows that k_n increases markedly at low film thickness, suggesting that surface nucleation is a contributing factor. At the same time, G is

shown to be increased at lower film thicknesses. The linear radial growth rates of spherulites is generally accepted as evidence for growth by secondary nucleation. It may be that in thin films both primary and secondary nucleation is enhanced. The present study does not attempt to estimate the effects of heat dissipation and possible two-dimensional growth of the spherulites. In all other experiments in this work, sample thicknesses were in the range 100 to 150μ.

The influence of melting conditions on the kinetics

(*1*) *Temperature of melting*—It was known that for polyhexamethylene adipamide the induction time of crystallization was dependent on the temperature of melting[15]. Determination of the kinetic constants using various melt temperatures not only gives more precise information but serves to correlate induction times with other rate parameters. *Tables 3* and *4* show some typical data. G is the parameter most affected by melt

Table 3. Dependence of kinetic constants on melt temperature for a polymer of $M_n = 14\,600$ melted for 30 minutes

T_c (°C)	Melt temperature (°C)								
	280			300			315		
	G	k_n	K	G	k_n	K	G	k_n	K
241·5	17·0	48·5	$2{\cdot}49\times10^{-1}$	12·26	14·4	$2{\cdot}66\times10^{-2}$	16·8	45·0	$2{\cdot}24\times10^{-1}$
242	15·75	39·2	$1{\cdot}5\times10^{-1}$	11·5	13·0	$2{\cdot}07\times10^{-2}$	14·5	31·7	$9{\cdot}6\times10^{-2}$
243	13·8	22·5	$6{\cdot}19\times10^{-2}$	10·5	10·5	$1{\cdot}27\times10^{-2}$	10·1	10·5	$1{\cdot}13\times10^{-2}$
245	10·85	5·73	$8{\cdot}11\times10^{-3}$	7·7	6·2	$2{\cdot}36\times10^{-3}$	6·8	6·7	$2{\cdot}1\times10^{-3}$
247·5	6·3	2·85	$7{\cdot}46\times10^{-4}$	4·1	3·15	$5{\cdot}38\times10^{-4}$	3·95	3·25	$2{\cdot}1\times10^{-4}$
248	5·74	2·26	$4{\cdot}3\times10^{-4}$	3·5	2·80	$1{\cdot}26\times10^{-4}$	3·4	2·89	$1{\cdot}3\times10^{-4}$
251				0·46	0·18	$1{\cdot}63\times10^{-7}$			
252	0·88	0·33	$2{\cdot}24\times10^{-7}$	0·33			0·38	0·09	$4{\cdot}9\times10^{-8}$

T_c denotes crystallization temperature. G is in μ/min. k_n is the number of nuclei cm^3 per min$\times10^{-6}$ and K is in min^{-4}.

Table 4. Variation of total numbers of spherulites with melt temperature for a polymer of $M_n = 14\,600$ melted for 30 minutes

Crystallization temp. (°C)	*Duration of crystallization* (*min*)	*No. of spherulites/cm³ for given melt temperature*	
		280°C	*315°C*
241	1·5	$13{\cdot}2\times10^6$	$15{\cdot}6\times10^6$
245	4·5	$10{\cdot}9\times10^6$	$4{\cdot}1\times10^6$
248	6·0	$3{\cdot}2\times10^6$	$0{\cdot}5\times10^6$
252	30·0	$3{\cdot}1\times10^6$	1×10^6

temperature. Although k_n does not alter markedly, the total number of spherulites present at a given time from the commencement of crystallization is greater the lower the melt temperature.

Burnett and McDevitt[2] found that G did not vary with melt temperature. However, they only melted their samples for 30 seconds, and so any effects encountered in the present work would go undetected. Hartley, Lord and Morgan[1], using the density balance technique, found that the overall rate constant (K) increased as the melt temperature decreased. Their rate studies using optical techniques, though not comprehensive, suggest that G increases as the temperature of melting decreases. An important difference between the work of Hartley, Lord and Morgan and the present study is

that they found sporadic nucleation only at crystallization temperatures above about 250°C. No correlation as regards k_n is thus possible. However, the data of *Table 4* are consistent with Morgan and co-workers' values for the number of nuclei present at 247°C after melting at 295°C and 285°C.

(2) *The effect of time at the melt temperature*—Any process associated with the melting of crystalline regions might be expected to be dependent on the time of holding at the melt temperature. Induction times of crystallization for polyhexamethylene adipamide are dependent on the time of melting[15]. *Table 5* shows typical results. Once again G is found to be the

Table 5. Effect of holding time at 300°C on the crystallization kinetics at 247·5°C for a polymer of $M_n = 8\,700$

Time of melting (min)	G (μ/*min*)	k_n (*No. cm*$^{-3}$ *min*$^{-1}$)	K (*min*$^{-4}$)
5	8·7	$1{\cdot}20\times10^{6}$	$8{\cdot}04\times10^{-4}$
10	8·0	$1{\cdot}23\times10^{6}$	$6{\cdot}3\times10^{-4}$
15	7·7	—	—
20	6·5	$0{\cdot}93\times10^{6}$	$2{\cdot}54\times10^{-4}$
30	5·7	$1{\cdot}65\times10^{6}$	$3{\cdot}14\times10^{-4}$

most sensitive parameter. Since the overall rate constant (K) depends on G^3 the rate of crystallization is dependent on time of melting.

Up to a holding time of 30 minutes G varies linearly and inversely with time of melting.

The effect of melt history on the kinetics suggests that spherulite growth is not by successive additions of single chain segments to the crystalline phase, but that some larger units add on to the spherulite surface. These units would themselves be partly ordered and their numbers and degree of order would be dependent on the melting conditions. The relative insensitivity of k_n to melting conditions suggests that the units governing G are different from those from which primary nuclei form.

It has been reported[16,17] that for isotactic polypropylene melt temperature has little or no effect on the rate of crystallization. On the other hand, polyethylene terephthalate behaves like polyhexamethylene adipamide in this respect[18]. The reasons for such differences are not clear. The degree of order remaining in the molten polymers after fusion will be an important factor. Possibly some polymers have greater order in the melt than others. Certainly polyhexamethylene adipamide would be expected to retain some measure of order by virtue of its marked tendency for hydrogen bonding[19,20].

Molecular weight dependence of the kinetics

Figure 3 shows some results for samples of polyhexamethylene adipamide having M_n values in the range 2 500 to 15 000. Experiments were carried out with samples having greater molecular weights, but it was not possible to obtain any satisfactory results. The films were of poor quality in that they were discontinuous, and a considerable amount of fine granular birefringent material always appeared. It is thought that the very high melt viscosities of these higher molecular weight polymers modify the flow

properties of the films and cause strain. This strain could induce crystallization.

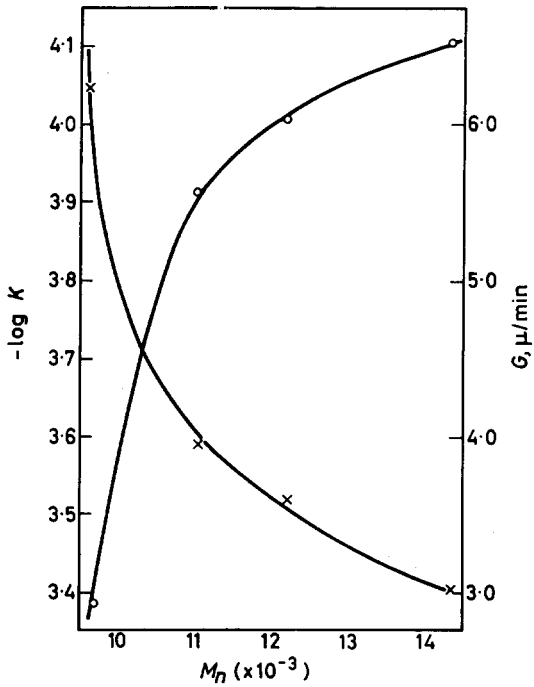

Figure 3—Molecular weight dependence of the kinetic parameters. ○ log K, × G. Polymer of $M_n = 14\,600$ melted at 300°C for 30 minutes

Figure 3 clearly shows that the rate of crystallization at any given temperature decreases with increasing molecular weight. The results suggest that there is a levelling off of both K and G at higher molecular weights although this could not be definitely confirmed for the reasons cited above. It is worth noting that the induction times of crystallization (τ) level off at higher molecular weights[15]. It was found that k_n varied little with molecular weight and once again the change in G is controlling the variation in the rate of crystallization.

Since the equilibrium melting temperature of polyhexamethylene adipamide increases with increased molecular weight, the effect shown in *Figure 3* is a minimum one. If crystallization is compared at corresponding degrees of supercooling, and with melt temperatures at corresponding intervals above the melting point, then the differences in the rate of crystallization will be more pronounced. Hartley, Lord and Morgan[1], using a density balance, showed that K increased as the molecular weight decreased for polyhexamethylene adipamide. Lindegren[3] states that for this polymer, varying the number average molecular weight from 11 600 to 26 300 caused a decrease of about 30 per cent in the value of G. Molecular weight also influences the overall rate of crystallization of isotactic polypropylene[17], and polyethylene terephthalate[21] in the same manner.

The present study emphasizes that the radial growth rate (G) is the parameter affected most by the molecular weight. It is suggested that in the supercooled polymers, mobility is decreased as the molecular weight

increases, and hence the units that build up the spherulite reach the growing spherulite surface at a slower rate. The molecular weight may affect the structure of spherulites[22], and hence a correlation between kinetics and morphology might possibly emerge. Much more detailed information on a wide variety of crystallizing polymers is needed so that the effects of molecular weight and crosslinking may be understood and perhaps related to the structures produced.

Relationship between induction times of crystallization and other kinetic parameters

A feature of the crystallization of polymers is an initial period of time in which no apparent crystallization takes place. This induction time (τ) has been detected by various methods and in fact the magnitude of τ depends on the sensitivity of the detecting device. In the present investigation, τ was determined by two methods, namely a static method and a dynamic method. The former consisted of crystallizing a number of films of polyhexamethylene adipamide at a given temperature for various lengths of time, arresting the crystallization by quenching at $-30°C$ in acetone, and then studying the quenched films under the polarizing microscope. The dynamic method utilizes the plot of number of spherulites versus time (see *Figure 2*). Extrapolation to the time for zero number gives a value of τ. The values of τ obtained by this latter method were always greater by a factor of 1·5 to 2·0. This was due to inaccuracies of extrapolation and a poorer resolving power of the optical system used with the hot-stage. Both sets of results obeyed the empirical relationship

$$\tau = A\,[1/\Delta T]^n \qquad (4)$$

where A and n are constants and ΔT is the degree of supercooling. The value of T_m, the equilibrium melting temperature, for a polymer of $M_n = 14\,600$ was obtained from kinetic data as shown in a subsequent section. The static and dynamic methods gave values for n of 8·25 and 8·34 respectively. These compare with values of $n = 6$ to 7 for 66 nylon obtained by Allen[23]. Magill[24] has found a value of 7 for 6 nylon from measurements of induction times. A value of 9 has been obtained for other polymers[25].

Comparison between $1/\tau$ and the other kinetic parameters is made in *Table 6*. The method adopted has been to assign a value of unity to all the parameters at 251°C and determine the ratios (R) at other temperatures with respect to 251°C. The subscripts on R relate to the appropriate parameter. *Table 6* was compiled from the data in *Table 3*.

Table 6. Relationship between $1/\tau$ and the kinetic parameters for a polymer of $M_n = 14\,600$ melted at 300°C for 30 minutes

T_c (°C)	$\frac{1}{\tau}$ (min^{-1})	R_τ	R_G	R_{K_n}	R_K
241·5	2·44	39·1	26·6	80·2	$1{\cdot}5 \times 10^5$
243·0	1·33	21·3	22·9	58·5	$8{\cdot}0 \times 10^4$
245·0	0·25	3·9	16·7	34·4	$1{\cdot}4 \times 10^4$
247·5	0·154	2·5	8·9	20·8	$3{\cdot}3 \times 10^3$
248·0	0·140	2·2	7·6	10·6	$7{\cdot}6 \times 10^2$
251·0	0·063	1·0	1·0	1·0	1·0

Similar results were obtained for a polymer having $M_n = 8\,700$ and also when other melt temperatures were used. It is clearly necessary to be careful when using induction time as a kinetic parameter. For polyhexamethylene adipamide $1/\tau$ is affected by temperature qualitatively in the same manner as G, k_n and K.

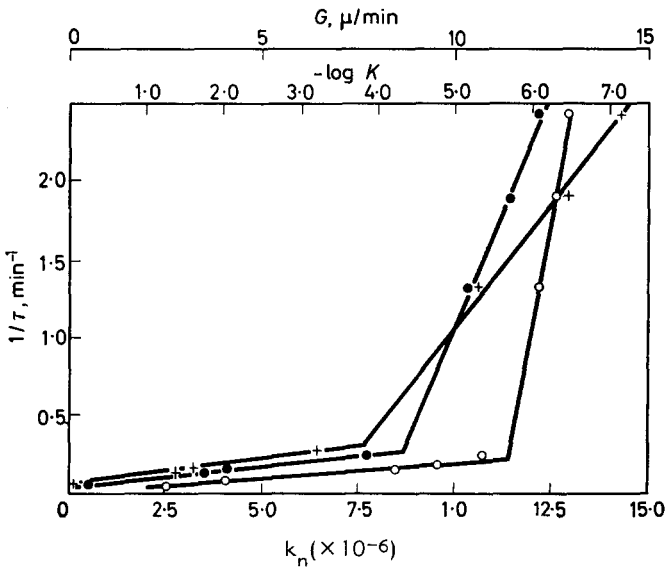

Figure 4—Relationships between induction times of crystallization (τ) and the kinetic parameters. ○ log K, × G, ● k_N. Polymer of $M_n = 14\,600$ melted at 300°C for 30 minutes

Empirical relationships may be obtained between $1/\tau$ and the kinetic parameters as is shown from *Figure 4*. A most notable feature is the discontinuities in the curves at 246°C which are probably caused by predetermined (i.e. simultaneous) nucleation playing a dominant role in the crystallization at crystallization temperatures below 246°C.

The empirical equations relating $1/\tau$ to the crystallization rate parameters are as follows:

$$1/\tau = 0{\cdot}28 + m_1 (G - 8{\cdot}8) \tag{5}$$

m_1 is 0·63 at temperatures above 246°C and 0·043 below 246°C.

$$1/\tau = 0{\cdot}25 + m_2 (k_n - 7{\cdot}0) \tag{6}$$

m_2 is 0·29 above 246°C and 0·022 below 246°C.

$$1/\tau = 0{\cdot}25 + m_3 (\log K + 2{\cdot}4) \tag{7}$$

m_3 is 2·68 above 246°C and 0·03 below 246°C. τ is in minutes, G in μ/min and k_n is No. cm^{-3} min^{-1} × 10^6. It must be emphasized that these equations are only valid over the fairly narrow temperature range studied.

Other workers[14] have shown that for branched polyethylene τ bears no relation to the subsequent growth of crystallization. This is not so for polyhexamethylene adipamide although $1/\tau$ cannot be equated quantitatively

with the subsequent rate of crystallization, τ is probably associated with the initial attainment of steady state nucleation and slow initial growth rates of these nuclei. The discontinuities in the plots in *Figure 4* are not inconsistent with the work of Magill[4,13]. He found that below about 245°C growth was from predetermined nuclei. The breaks in *Figure 4* occur at about 246°C. Although in the present work the number of spherulites always increased with time, the crystallization could still have been from both predetermined and sporadically formed nuclei. As long as there is an appreciable contribution from sporadic nucleation, then the overall effect is as though crystallization is from sporadically formed nuclei. Below about 246°C the predetermined nucleation becomes dominant.

Influence of supercooling on the crystallization kinetics and determination of equilibrium melting temperatures

The degree of supercooling affects the crystallization of both monomeric[26] and polymeric[11] systems. Determination of the degree of supercooling requires a knowledge of the melting temperature of the material. With polymeric systems, accurate values of the equilibrium melting temperature (T_m) are difficult to obtain, since T_m is a function of the rate of heating of the sample. Frank (see ref. 11) has proposed a method for determining the melting point of a polymer from kinetic measurements which is based on the principle of supercooling. Two relationships proposed by Frank are:

$$\log(\text{rate}) = k_1' + k_1/(T_m - T) \tag{8}$$

$$\log(\text{rate}) = k_2' + k_2/(T_m - T)^2 \tag{9}$$

where T is the crystallization temperature, T_m the equilibrium melting temperature and k_1, k_1', k_2 and k_2' are constants. Equations (8) and (9) relate to two-dimensional and three-dimensional nucleation respectively. The temperature coefficient of the crystallization is defined as

$$u = \mathrm{d}\log(\text{rate})/\mathrm{d}T$$

Thus from equations (8) and (9) we have:

$$u = -k_1(T_m - T)^{-2} \tag{10}$$

$$u = -k_2(T_m - T)^{-3} \tag{11}$$

Equations (10) and (11) can be tested by plotting $u^{-\frac{1}{2}}$ and $u^{-\frac{1}{3}}$ against T. A straight line should be obtained if either equation (10) or (11) is obeyed. This should extrapolate to zero rate at $T = T_m$.

Figure 5 shows results for two samples of polyhexamethylene adipamide having M_n values of 8 700 and 14 600. It was found that equation (11) relating to three-dimensional nucleation gave the best fit to the experimental data. The values of T_m obtained in this way are shown in *Table 7*. It is seen that melt temperature affects T_m slightly.

Flory[27] has derived the following expression relating T_m to molecular weight

$$1/T_m - 1/T_m^0 = 2R/\Delta H_u X_n \tag{12}$$

where T_m is the equilibrium melting temperature for a polymer of number average degree of polymerization X_n, T_m^0 is the limiting value of T_m for

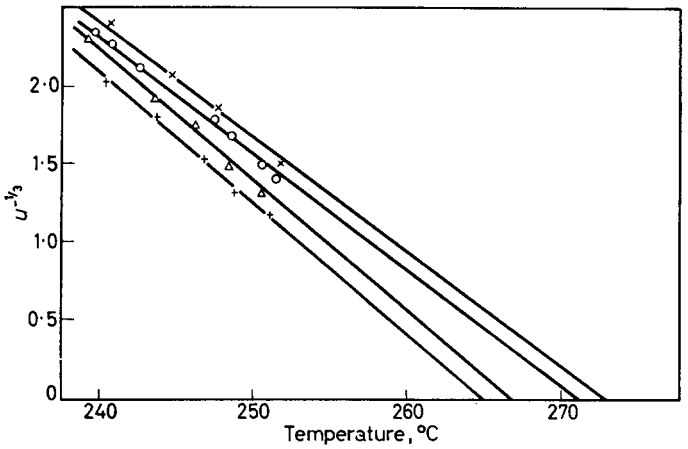

Figure 5—Plots of $u^{-\frac{1}{3}}$ versus temperature used for determination of equilibrium melting temperatures. ○ Polymer of $M_n = 14\,600$ melted at 315°C for 30 minutes. × Polymer of $M_n = 14\,600$ melted at 280°C for 30 minutes. + Polymer of $M_n = 8\,700$ melted at 315°C for 30 minutes. △ Polymer of $M_n = 8\,700$ melted at 280°C for 30 minutes

values of X_n greater than about 100, R is the gas constant and ΔH_u is the latent heat of fusion per mole of repeating unit. From the molecular weight distribution studies of Howard[28], it may be concluded that equation (12) is applicable to polyhexamethylene adipamide. If T_m^0 is taken as 272·5°C (*Table 7*), T_m can be calculated for other values of X_n. This has been done for $X_n = 39$, i.e. $M_n = 8\,700$, and the calculated value of T_m shown in *Table 7* agrees very well with the measured value using equation (11). Although such close agreement may be partly fortuitous, it does give confidence in treating the kinetic data in this way.

Table 7. Equilibrium melting temperatures obtained from kinetic data. Time of melting 30 minutes

	$M_n = 8\,700$		$M_n = 14\,600$
Melting temp. (°C)	T_m°C	$T_{m\,(calc.)}$°C	T_m^0 (°C)
280	267	266·0	272·5
315	265	265·2	271·5

ΔH_u taken as 4 972 cal/mole repeat unit, i.e. per 226 g (ref. 29).

Mandelkern[11] has shown that for growth by three-dimensional nucleation, the following relationships exist between the kinetic parameters and the degree of supercooling.

$$\log X = \text{constant} - C T_m^2 / T (T_m - T) \qquad (13)$$

where X is one of G, k_n or K and C is a constant for a given polymer. The other symbols have their usual meanings.

Figure 6 gives some results for a polymer of $M_n = 14\,600$ where the data have been plotted according to equation (13). Similar plots were obtained using k_n and K. Also in *Figure 6* are the same data plotted according to a relationship applicable to two-dimensional nucleation, i.e. $\log G$ versus $T_m/T(T_m - T)$. Satisfactory straight lines are obtained using both relationships when $(T_m - T)$ is relatively small. The data for two-dimensional nucleation in *Figure 6* do show consistent deviation from linearity at larger values of $(T_m - T)$, i.e. at lower crystallization temperatures. This is not surprising, since the theory is only applicable to low values of the supercooling (ΔT). Mandelkern[11] has shown that for polydecamethylene sebacate the kinetic data obey the relationships for both two- and three-dimensional

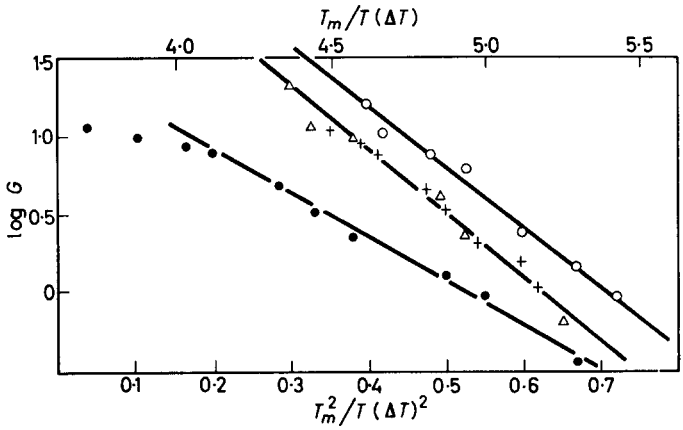

Figure 6—Dependence of radial growth rate on extent of supercooling. Polymer of $M_n = 14\,600$. ○ Melted for 30 minutes at 280°C. + Melted for 30 minutes at 300°C. △ Melted for 30 minutes at 315°C. ● Melted for 30 minutes at 315°C plotted according to equation for two-dimensional nucleation

nucleation and he suggested that three-dimensional nucleation was the more physically tenable situation. The present study would seem to support this. In this study, the range of ΔT used was 20° to 32°C. The values of ΔT are thus comparatively large compared with studies on other polymers[5,11].

The values of the functions $T_m^2/T(\Delta T)^2$ are very sensitive to the value assigned to T_m and the fact that fairly good agreement with theory was obtained using the values of T_m derived from kinetic data gives added support for this method of obtaining T_m. Using other values of T_m in equation (13) gave inferior plots. Burnett and McDevitt[2] had to assume a value of 280°C for T_m for polyhexamethylene adipamide in order to correlate their experimental data with theory. This would seem somewhat high on the basis of the present results. The melting point of the sample of $M_n = 14\,600$ as obtained from optical measurements using fairly slow heating rates (~ 1°C/minute) was 264°C. Of course the exact history of the samples during manufacture can affect subsequent behaviour, and hence comparisons are difficult.

The slightly lower values of T_m obtained using a higher melt temperature (*Table 7*) can be explained in terms of the melting point being lowered by the more complete melting at the higher melt temperature. The influence of the time of melting on the kinetics (*Table 5*) may also be explained on the basis of more complete melting. Moreover, the insensitivity of the rate of crystallization to change in molecular weight above an M_n value of about 14 000 can partly be accounted for by a constancy of supercooling which arises from the melting point being independent of molecular weight at higher molecular weights. Many more observations are required to establish this supercooling concept, although Price[30] has shown that for polyethylene crosslinked with high energy electrons, the isothermal growth rates of the spherulites depended only on the degree of supercooling despite the melting points of samples crosslinked to different extents varying from 133° to 113°C.

The main point to be borne in mind is that the process of fusion should not be equated to true melting for a crystalline polymer. There will probably be remnants of order in the molten polymer to a degree dependent on the melt history of the material. It is this residual ordered material which affects the subsequent crystallization. More information on the structures present in molten polyhexamethylene adipamide are needed to substantiate this idea.

Since this work was completed, Rabesiaka and Kovacs[31] have suggested that melted polyethylene is not in true thermodynamic equilibrium and that some quasi-indestructible clusters of polymer can remain even after melting for prolonged periods. These clusters are thought to act as heterogeneous nuclei for subsequent crystallization.

The author is indebted to Mr H. J. Palmer for his continual helpful discussion. Thanks are due to Dr J. H. Magill for private information, and to British Nylon Spinners Limited, for permission to publish.

Research Department,
British Nylon Spinners Ltd,
Pontypool, Mon.

Present address:
Loughborough College of Technology,
Loughborough, Leics.

(*Received July 1962*)

REFERENCES

[1] HARTLEY, F. D., LORD, F. W. and MORGAN, L. B. *Ric. Sci.* (Suppl. A), 1955, **25,** 577
[2] BURNETT, B. R. and MCDEVITT, W. F. *J. appl. Phys.* 1961, **28,** 1107
[3] LINDEGREN, C. R. *J. Polym. Sci.* 1961, **50,** 181
[4] MAGILL, J. H. *Polymer, Lond.* 1961, **2,** 221
[5] FLORY, P. J. and MCINTYRE, A. D. *J. Polym. Sci.* 1955, **18,** 592
[6] AVRAMI, M. *J. chem. Phys.* 1939, **7,** 1103
[7] AVRAMI, M. *J. chem. Phys.* 1940, **8,** 212
[8] AVRAMI, M. *J. chem. Phys.* 1941, **9,** 177
[9] MORGAN, L. B. *Chem. & Ind.* **1951,** 796
[10] MORGAN, L. B. *Phil. Trans. A,* 1954, **247,** 13

[11] MANDELKERN, L. *Growth and Perfection in Crystals,* p 467. Edited by DOREMUS, R., ROBERTS, B. W. and TURNBULL, D. Wiley: New York, 1958
[12] MCINTYRE, A. D. *Thesis,* Cornell University, 1956, *Univ. Microfilm No. 16,* 256
[13] MAGILL, J. H. Private communication
[14] BUCHDAHL, R., MILLER, R. L. and NEWMAN, S. *J. Polym. Sci.* 1959, **36,** 215
[15] MCLAREN, J. V. Unpublished work
[16] MARKER, L., HAY, P. M., TILLEY, G. P., EARLY, R. M. and SWEETING, O. J. *J. Polym. Sci.* 1959, **38,** 33
[17] GRIFFITH, J. H. and RANBY, B. G. *J. Polym. Sci.* 1959, **38,** 107
[18] HARTLEY, F. D., LORD, F. W. and MORGAN, L. B. *Phil. Trans. A,* 1954, **247,** 23
[19] CANNON, C. G. *Spectrochim. Acta,* 1960, **16,** 302
[20] TRIFAN, D. S. and TERENZI, J. F. *J. Polym. Sci.* 1958, **28,** 443
[21] KELLER, A., LESTER, G. R. and MORGAN, L. B. *Phil. Trans. A,* 1954, **247,** 1
[22] REDDING, F. P. and WALTER, E. R. *J. Polym. Sci.* 1959, **38,** 141
[23] ALLEN, P. W. *Trans. Faraday Soc.* 1952, **48,** 1178
[24] MAGILL, J. H. *Polymer, Lond.* 1962, **3,** 43
[25] MANDELKERN, L., QUINN, F. A. and FLORY, P. J. *J. appl. Phys.* 1954, **25,** 830
[26] TURNBULL, D. and FISHER, J. C. *J. chem. Phys.* 1949, **17,** 71
[27] FLORY, P. J. *J. chem. Phys.* 1949, **17,** 17
[28] HOWARD, G. J. *J. Polym. Sci.* 1959, **37,** 310
[29] ALLEN, P. W. *Research, Lond.* 1952, **5,** 492
[30] PRICE, F. P. *J. phys. Chem.* 1960, **64,** 169
[31] RABESIAKA, J. and KOVACS, A. J. *J. appl. Phys.* 1961, **32,** 2314

Crystallinity, 'Crystallite Size' and Melting Point of Polypropylene

G. FARROW*

Samples of polypropylene polymer, containing no additives and sealed into evacuated glass tubes, have been annealed for long periods at a temperature (160°C) close to the melting point. The melting points of the specimens increase with annealing time and evidence suggests that this is principally due to an increase in 'crystallite size' rather than crystallinity. The results tend to support a previous suggestion that the atactic content of this type of polypropylene is of the order of 15 per cent. The results also suggest that if polypropylene polymer could be made with little or no atactic content, then its melting point after suitable annealing would be about 200°C.

IN A previous publication[1] a method was suggested for estimating the atactic content of polypropylene polymer which depends on heat crystallizing the polymer to its maximum attainable degree of crystallinity. Only relatively short crystallization times were used in these initial experiments. Polymer specimens have now been annealed, for long periods, at a temperature close to the melting point as has been done with linear polyethylenes[2]. The results together with some other aspects are discussed in this paper.

EXPERIMENTAL

Preparation of samples

Five 2 g samples of polypropylene polymer containing no additives were placed in separate lengths of Pyrex tubing, evacuated and sealed. They were then placed in a silicone oil bath maintained at 160°C (±2°C), a sample being withdrawn after 10 days, 20 days, 40 days and 70 days. The 70 day period was intended to be 80 days but the thermostat on the temperature bath failed after this length of time. In fact two samples were held in the bath for 70 days. One sample, evacuated and sealed in the Pyrex tubing, was heated at 300°C for a half hour to completely melt the original crystallites and destroy any residual nuclei, apart from those existing under equilibrium conditions, and then plunged immediately into the bath held at 160°C. The other sample was not heated prior to being placed in the annealing bath.

X-ray measurement

The crystallinity and 'crystallite sizes' of the specimens were measured by X-ray diffraction techniques[1,3].

The X-ray method for the measurement of crystallinity has been described in detail elsewhere[1]. It consists, in principle, of a comparison between the integrated intensity of the crystalline reflections and those of the non-crystalline background, considerable refinements of X-ray technique being necessary to make this comparison quantitatively valid.

*Now at Fiber Industries Inc., Box 834, Shelby, N.C., U.S.A.

The X-ray method of measuring crystallite size is based on the line-broadening of X-ray diffraction intensities by crystallites of less than 1 000 Å. Sizes greater than 1 000 Å cause no appreciable broadening of X-ray intensities. The method requires very careful experimental techniques[4]. Furthermore, it is arguable to what extent changes in the line-broadening may be interpreted as true changes in crystallite size for other effects can give rise to this phenomenon[4]. The view adopted here is that a decrease in the 'line-width' of an X-ray diffraction arc represents an increase in molecular perfection and it is in this context that the 'crystallite sizes' must be considered.

In order to correct for line-broadening due to instrumental conditions alone it is customary also to record the X-ray diffraction pattern from a sample which is wholly crystalline and has crystallites greater than 1 000 Å. In our experimental work an annealed sample of sebacic acid was used for this purpose. When, however, the line-widths of the reference and sample under test are not very different then large errors are introduced into the calculation of 'crystallite sizes' by these methods; such a situation arises here as will be seen from experimental results.

Only the X-ray intensities from crystal planes parallel to the *c* axis (110 and 040) of the unit cell were used in this investigation[5,6]. The reflections were recorded on film which after standard processing was scanned by a recording microdensitometer. The line-width in question was obtained by measuring the area underneath the appropriate peak on the trace and dividing by the height of the peak. Each measurement of 'crystallite size' quoted is a mean value of the 110 and 040 planes. Full practical details are given in a forthcoming publication[3].

Other measurements

The melting points of the samples were measured by the use of a hot-stage microscope and polarized light whilst raising the temperature of the stage by 2°C/min. The melting point was recorded when the mass of spherulites disappeared from the field of view using a low-powered objective. Densities of the specimens were also measured using a density gradient column maintained at 30°C.

RESULTS

The results are plotted in graphical form. *Figure 1* represents the change in crystallinity and 'crystallite size' with increasing annealing time in days, a day being defined as a period of 24 hours. *Figure 2* is a plot of the change in crystallinity with increasing temperature for a sample of polymer annealed previously for two hours in a vacuum oven at 145°C and also included is the apparent change in 'crystallite size' with increasing temperature. *Figure 3* contains a plot of melting point and density against annealing time and *Figure 4* the percentage crystallinity against change in density*. The annealing temperature in *Figures 1* and *3* was 160°C. This temperature was also used for the 'long term annealing' results presented in *Figure 4*.

The 'crystallite size' measurements (*Figure 1*) in general are quite large.

*The crystalline density was taken from a paper by Natta *et al.*[5] on the crystal structure of polypropylene.

This introduces large errors into their calculation, as mentioned previously. In this situation there is little difference between the line-widths of the samples under test and the reference sample. There is, however, an unmistakable trend in the results for the longer the annealing time of the polymer the greater is the final 'crystallite size'.

The highest melting point recorded (189°C) was re-checked using another specimen, but besides increasing the temperature of the sample by 2°C per minute it was held for an additional period of ten minutes at 175°C and then again for a further ten minutes at 180°C. The rate of heating was resumed at 2°C per minute and the sample subsequently melted at 187°C. One of the two samples left in the silicone oil bath for 70 days, previously heated at 300°C before being plunged into the bath, took approximately 30 days from the date of entering before it showed signs of heat crystallizing. Different specimens of this sample had different melting points when examined under the hot stage microscope. They ranged from 163°C to 170°C, the outer surface of the crystallized 'rod' having the lowest melting point. This anomalous behaviour was not observed in any of the other samples. Furthermore, the 'crystallite sizes' were relatively 'low' in the specimens taken from this polymer. No further measurements were performed on this sample.

All the samples, including the original, showed spherulitic clusters under the polarizing microscope but it was found that the longer the annealing time the greater was the size of the spherulites.

The intrinsic viscosity of the original material was 2·20 and that of the specimen annealed for 70 days without prior heat treatment was 2·13. It was therefore presumed that in all specimens the thermal degradation at 160°C was exceedingly slow. Low-angle X-ray diffraction patterns of some of the specimens were not informative. This may have been due to the poor resolution of the low angle camera which is only of the order of 250 Å. Further measurements are being carried out.

DISCUSSION

It was considered previously that the maximum attainable degree of crystallinity of this polypropylene polymer, as measured by X-ray diffraction, was between 65 and 70 per cent. These results confirm this (*Figure 1*). Consequently the value given for the atactic content, 15 to 20 per cent is still a reasonable suggestion[1]. It is an interesting fact that a high degree of crystallinity is attained relatively quickly (*Figure 1*), the annealing process tends to increase the 'crystallite size' rather than to increase the degree of crystallinity to any great extent. This probably comes about by a partial melting and recrystallization process, preferably in the smaller crystallites, as would be expected from thermodynamic considerations. This is confirmed by an examination of high temperature X-ray diffraction photographs of an annealed sample of polymer as illustrated in *Figure 2*. For example, at 130°C the crystallinity had dropped to 48 per cent but the X-ray diffraction lines had narrowed and were as sharp as those of the sample annealed for 70 days without preheating at 160°C (*Figure 2*). That is, the size of the unmelted crystallites was extremely large, so large that the X-ray technique breaks down at these levels (see above).

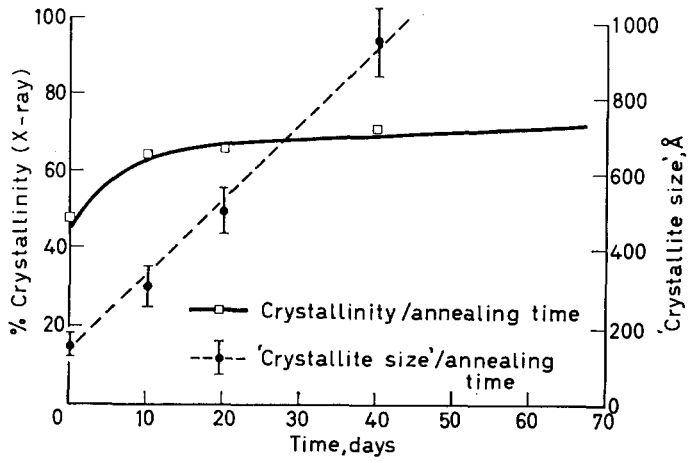

Figure 1—Crystallinity (X-ray) versus annealing time in days and 'crystallite size' (Å) against annealing time for specimens of poplypropylene polymer. Annealing temperature 160°C

The steady increase in the melting points of these samples (*Figure 3*) is, therefore, more related to increase in crystallite size and perfection rather than to increase in crystallinity. There is also a corresponding increase in the density of samples as is seen from *Figure 3* but there is a breakdown in the correlation between density and X-ray crystallinity, under these conditions (*Figure 4*), found previously for unoriented specimens[1].

The density data suggest a higher crystallinity than that found by X-ray methods, in fact a maximum attainable degree of crystallinity of 89 per cent taking a density value of 0·870 g/cm³ for the non-crystalline material

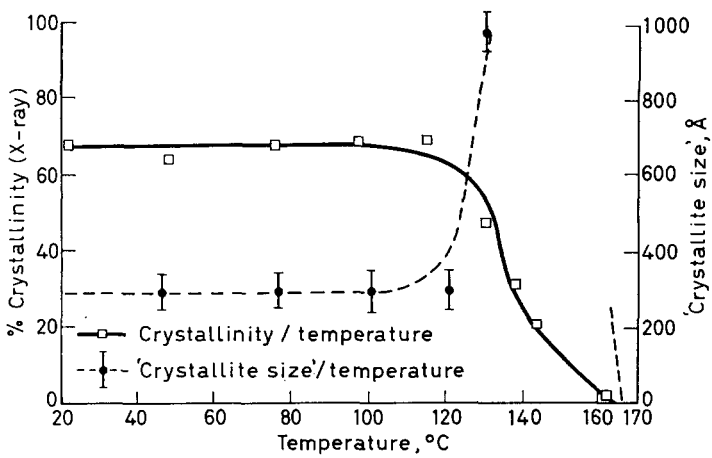

Figure 2—Crystallinity (X-ray) versus increasing temperature and 'crystallite size' (Å) versus temperature for a specimen of polypropylene previously annealed two hours at 145°C

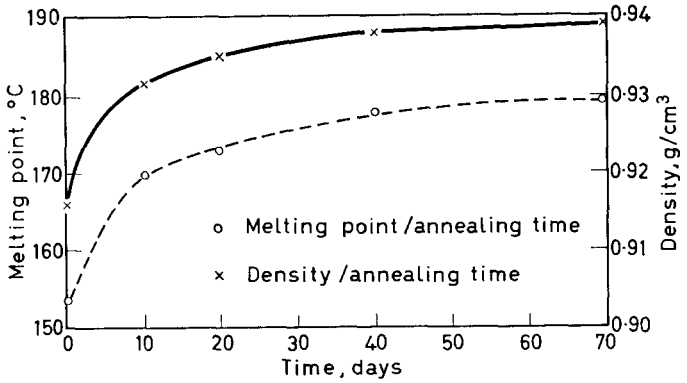

Figure 3—Change in melting point, and density, with increasing annealing time for polypropylene samples. Annealing temperature 160°C

and one of 0·936 g/cm³ for the crystallites. Using this value it suggests that if a value of about 15 per cent is accepted for the atactic content then the sample contains no other non-crystalline material and that the atactic material exists as defects in the crystal lattice, i.e. in or between the very large crystallites. The fact that the X-ray measure of crystallinity gives an apparently lower value than that obtained by density methods when very large crystallites are present could be due to lattice distortion. This could give rise to diffuse X-ray scattering (interpreted as from non-crystalline material) without any serious change in the observed density. On the other hand, the diffuse background scattering on the X-ray photographs of the samples containing large crystallites still retains (as far as one can measure) the same shape as the 'background' used for the measurement of crystallinity, by the X-ray technique, in samples of lower crystallinity. It is, therefore, possible that the difference between the two methods arises due to a 'compression' of the non-crystalline regions in the annealed polymer

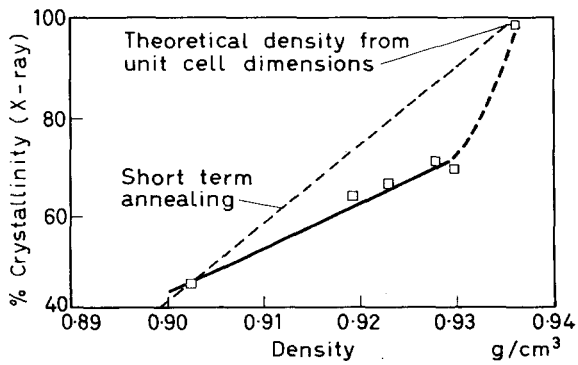

Figure 4—Crystallinity (X-ray) against density for samples of polypropylene polymer for long term annealing

by the very large 'crystallites'. That is, the non-crystalline regions together with the atactic segments are now considered as trapped within the large 'crystallites' themselves producing an increase in density with no similar increase in crystallinity. These suggested explanations are compatible with the concept of the paracrystalline state postulated by Hosemann[7] and others[8] for synthetic polymers.

If the fact is accepted that this polymer contains atactic material, material that cannot crystallize, then it suggests that the melting point of an annealed polymer containing less atactic material would be greater than 189°C which is the maximum observed in this study. Excluding stereoblock effects, molecular entanglements, etc., it is of interest to calculate what this would be for a polymer containing no atactic material.

If it is considered that the polymer is made up of A units (the isotactic segments) which crystallize and B units which do not (the atactic segments) and that the units occur in random sequence along the chain it then seems permissible to apply Flory's equation[9] for the depression of melting point of a pure polymer by another constituent, thus

$$(1/T_m)-(1/T_M^0)=-(R/\Delta H_u)\ln N_A \qquad (1)$$

where T_M^0 is the melting point of the pure polymer, T_m the melting point of the 'copolymer', R the gas constant, ΔH_u the heat of fusion of a monomeric unit (2 400 cal[10]) and N_A the mole fraction of A units in the random copolymer. Assuming a value of 15 per cent for the atactic content (i.e. $N_A=0{\cdot}85$) and that $T_m=189°C$, on substitution in equation (1) a value of 219°C is obtained for T_M^0. It has been pointed out by Flory that if the A and B units tend to occur in separate sequences, which is likely in this case, then the melting point depression will be less than that given in equation (1). That is, the value of 219°C is probably too high, also on one further account, for it is improbable that even if a polymer contained isotactic sequences only it would crystallize completely. After long term annealing we might expect to achieve a crystallinity of about 90 per cent the other 10 per cent being lost in entanglements, lattice distortion, etc. This sort of crystallinity level has been achieved in straight chain polymers such as unbranched polyethylene[1,2,11]. It is possible, therefore, to modify the value of 219°C by again applying equation (1) assuming now that the B units are isotactic segments which do not crystallize and that the A units are the ones that do. Setting $T_M^0=219°C$ and $N_A=0{\cdot}90$ a value of approximately 200°C is obtained for the melting point of an annealed sample of polypropylene containing only isotactic sequences. This is probably a more practical value than that of 219°C.

CONCLUSIONS

The long term annealing of polypropylene polymer samples at temperatures close to the melting point increases the melting point and evidence suggests that this is principally due to an increase in 'crystallite size' rather than crystallinity. The results lend support to the value of about 15 per cent, suggested previously, for the atactic content of the polymer now in use, as measured by X-ray diffraction methods. Furthermore they suggest that if

isotactic polypropylene polymer could be made with little or no atactic content then its melting point, after suitable annealing of the polymer, would be about 200°C.

The author would like to thank Dr G. W. Taylor for the intrinsic viscosity measurements.

Research Department,
I.C.I. Ltd, Fibres Division,
Hookstone Road, Harrogate, Yorkshire

(*Received July 1962*)

REFERENCES

[1] FARROW, G. *Polymer, Lond.* 1961, **2,** 409
[2] MANDELKERN, L., POSNER, A. S., DIORIO, A. F. and ROBERTS, D. E. *J. appl. Phys.* 1961, **32,** 1509
[3] BAGLEY, J. and FARROW, G. To be published
[4] KLUG, H. P. and ALEXANDER, L. E. *X-ray Diffraction Procedures,* Chaper 9. Wiley: New York, 1954
[5] NATTA, G., CORRADINI, P. and CESARI, M. *R.C. Accad. Lincei,* 1956, **21,** 365
[6] NATTA, G. and CORRADINI, P. *Nuovo Cim.* 1960, **15,** 41
[7] HOSEMANN, R. *Z. Phys.* 1950, **128,** 1 and 465
[8] STUART, H. A. *Die Physik der Hochpolymeren.* Springer: Berlin–Göttingen–Heidelberg, 1955
[9] FLORY, P. J. *Principles of Polymer Chemistry,* Chapter 13. Cornell University Press
[10] DANUSSO, F., MORAGLIO, G. and FLORES, E. *R.C. Accad Lincei,* In press
[11] HERMANS, P. H. and WEIDINGER, A. *Makromol. Chem.* 1961, **44,** 24

*The Influence of Particle Size and Distortions upon the X-ray Diffraction Patterns of Polymers**

R. BONART†, R. HOSEMANN‡ and R. L. MCCULLOUGH§

The theory of the paracrystal is used in the development of a general method whereby the effects upon the diffraction patterns of the short-range displacement-type distortions, the long-range liquid-like distortions, and particle size may be separated and analysed. The application of this method for a given profile requires that at least two orders of reflections be observed or that the crystallite size be reasonably large.

THE X-RAY diffraction patterns of most high molecular weight compounds usually consist of a few broadened 'crystal-like' reflections superimposed upon a diffuse background. This apparent composite nature of the X-ray diffraction pattern is ordinarily explained in terms of the 'fringe-micelle' model.

Methods based upon this 'fringe-micelle' model have been developed which assume that the intensity of the 'crystalline peaks' and the 'amorphous' (or diffuse) background can be correlated with the relative fractions of crystalline and amorphous material in the sample (e.g. Krimm and Tobolsky[1]). The application of this approach to the determination of crystallinity can lead to systematic errors in the interpretation of the diffraction patterns of polymers, since even a single crystal can give rise to a diffuse scattering and suffer a loss in intensity of the diffraction peaks due to thermal vibrations and various imperfections which affect the short-range order of the system (see *Proc. Roy. Soc. A*, 1941, **179,** No. 976, 1–101).

Attempts have also been made to relate the average dimension of the 'crystallites' of the 'fringe-micelle' model with the breadth of the 'crystal-like' reflections. Methods of separating displacement distortions and size effects on the broadening of X-ray profiles by means of a Fourier analysis[2–6] have recently been applied to highly oriented 'Marlex–50' filaments[7]. These methods were originally developed for application to powder diffraction line profiles of cold worked metals and are subject to several limitations[8–11]; in particular, these methods only consider 'short range' disturbances.

**Contribution No. 122* from Chemstrand Research Center, Inc. Durham, North Carolina.

†Fritz Haber Institut der Max Planck Gesellschaft, Berlin-Dahlem, Germany. (Present address: Bayer-Werke, Leverkusen, Germany.)

‡Visiting Lecturer at the Chemstrand Research Center from the Fritz Haber Institut der Max Planck Gesellschaft, Berlin-Dahlem, Germany.

§Chemstrand Research Center, Durham, North Carolina. U.S.A.

Because of the contiguous nature of the molecular chains of a polymer, it is reasonable to expect entirely different disturbances of a 'liquid-statistical' nature (which affect the long range order of the system) to occur in place of, or in addition to, the short range disturbances.

The model of the paracrystal affords a general basis for the interpretation of diffraction patterns, since this model takes into account the effect upon the diffraction pattern of both the short range and long range distortions, as well as the dimensions of distorted 'crystallites'. Moreover, this model does not require, nor does it preclude, the existence of a crystalline and an amorphous phase to account for the apparent composite nature of the X-ray diffraction patterns of polymers.

The concept of the paracrystal was presented by Hosemann[12,13] in 1950 as a feasible model for the condensed state of matter. Subsequent papers[14,15] discussed the geometric properties of paracrystalline organization. The diffraction effects produced by paracrystalline structures were analysed by Hosemann[16], by Hosemann and Bagchi[17,18] and by Bonart[19]. It seems worthwhile at this time to summarize some of the pertinent aspects of these papers and in so doing outline a method by which the effects of the short range and long range disturbances, as well as the effect of particle size, upon the diffraction patterns of high molecular weight compounds may be separated and analysed.

THEORETICAL BASIS

In a 'crystalline' region of the polymer, the periodic cell edges of the ideal lattice are replaced by statistically determined vectors which can vary both in magnitude and direction from cell to cell. These liquid-like disturbances of the lattice components are then characterized by probability functions, H. Thus the probability that a given point in a paracrystalline lattice cell (i, j, k) can be encountered in a volume element dv_x at the vector $\mathbf{x}$ from the origin is given by

$$H_{i,j,k}(\mathbf{x})\, dv_x$$

These long range disturbances are referred to as distortions of the second kind; the arrangement produced by the effect of these disturbances is called a paracrystalline lattice. The probability function, $H_{i,j,k}$, for the paracrystalline lattice may be calculated by multi-convolution products.

The paracrystalline lattice can be further perturbed, as was the ideal crystal lattice, by distortions of the first kind which affect the 'short range' order of the system. Distortions of the first kind may include, *inter alia*: (*a*) thermal vibrations, (*b*) frozen displacements or strains, (*c*) Frenkel defects, (*d*) vacancies, (*e*) dislocations, (*f*) substituted mixed crystals, and (*g*) internal distortions of the atoms.

These distortions of the first kind may be further distinguished as displacement defects or physical defects. The displacement defects are characterized by displacements of structure points away from predetermined 'equilibrium' lattice sites; a physical defect implies that an occupant of a lattice site does not have equivalent physical properties to the occupants

of the adjoining equivalent lattice sites. These two types of distortions may occur separately or concomitantly.

For simplicity the distortions of the first and second kind may be taken to be mutually and internally statistically independent. Thus, for distortions of the second kind,

$$H_{i,j,k} = \underbrace{H_{100} \widehat{H_{100}} \cdots \widehat{H_{100}}}_{i \text{ times}} \underbrace{H_{010} \widehat{H_{010}} \cdots \widehat{H_{010}}}_{j \text{ times}} \underbrace{H_{001} \widehat{H_{001}} \cdots \widehat{H_{001}}}_{k \text{ times}} *$$

It follows then that the paracrystalline lattice is characterized along a given crystallographic direction (say the 100) by a single probability function, e.g. H_{100}. We will use the abbreviation H_1 for this cell-edge probability function. a is the mean value of this cell edge.

Similarly, the displacement distortions of the first kind may be characterized, along a given crystallographic direction, by the probability function, H_r.

Applying these concepts to diffraction theory, Hosemann *et al.*[16–19] arrived at the following relationship for the Intensity profile, $I(b)$:

$$I(b) = \underbrace{\underbrace{N\{\overline{[f^2(b)]} - \bar{f}^2(b)\}}_{I_{d_1}} + \underbrace{N\bar{f}^2(b)[1 - D^2(b)]}_{I_{d_2}} + \underbrace{N\bar{f}^2(b)\,D^2(b)\,Z_d(b)}_{I_{d_3}}}_{\substack{\text{(Diffuse or 'Amorphous-like')} \\ I_d}} + \underbrace{(1/v)\,\bar{f}^2(b)\,D^2(b)\,\widehat{[Z_s(b)\,S^2(b)]}}_{\substack{\text{('Crystal-like')} \\ I_s}}$$

where b is a distance in Fourier (or reciprocal) space along the prescribed profile direction, N is the total number of scattering units along the given direction in physical space, $f(b)$ is the well known structure amplitude for the structure elements, v is the mean volume of a paracrystalline lattice cell, $S^2(b)$ is the shape factor, $D^2(b)$ is the distortion factor for displacement distortions of the first kind, $Z_d(b)$ is the component of the paracrystalline lattice factor which gives rise to the diffuse scattering from the liquid-statistical arrangement, and $Z_s(b)$ is the component of the paracrystalline lattice factor which gives the 'crystal-like' peaks.

The distortion factor, $D^2(b)$, is the square of the real value of the distortion amplitude, $D(b)$. The magnitude of the distortion amplitude is

*The symbol $\widehat{\ }$ represents the convolution product. In general, the convolution product is defined as

$$\widehat{g_1 g_2} = \int g_1(y)\, g_2(x-y)\, dv_y$$

the Fourier transform of the distribution function $H_r(x)$ for the displacement distortions of the first kind

$$D(b)=\int H_r(x)\exp(-2\pi ixb)\,dx$$
$$0\leqslant D^2(b)\leqslant 1$$

For the special case of thermal vibrations, $D^2(b)$ corresponds to the Debye factor.

The shape factor, $S^2(b)$, is the square of the real value of the shape amplitude, $S(b)$; the shape amplitude, in turn, is the Fourier transform of the shape function $s(x)$

$$S(b)=\int s(x)\exp(-2\pi ixb)\,dx$$

$$s(x)\begin{cases}=1; & |x|\leqslant L/2\\ =0; & |x|>L/2\end{cases}$$

where L is the dimension of the 'crystalline' region in the given crystallographic direction.

The sum of the two components $Z_s(b)$ and $Z_d(b)$ is the paracrystalline lattice factor $Z(b)$

$$Z(b)=Z_s(b)+Z_d(b)$$

where

$$Z(b)=R_e\frac{1+F(b)}{1-F(b)}=\frac{1-|F(b)|^2}{[1-|F(b)|]^2+4|F(b)|\sin^2\pi ab}$$

$$Z_s(b)=\frac{4|F(b)|}{1-|F(b)|^2}\cdot\frac{[1-|F(b)|]^2\cos^2\pi ab}{[1-|F(b)|]^2+4|F(b)|\sin^2\pi ab}$$

$$Z_d(b)=\frac{1-|F(b)|}{1+|F(b)|}$$

$|F(b)|$, the positive real value of $F(b)$, is the Fourier transform of the probability function for the distortions of the second kind, i.e.

$$|F(b)|=\int H_1(x)\exp(-2\pi ixb)\,dx$$

The general intensity profile equation predicts that the diffracted intensity will consist of relatively sharp 'crystal-like' reflections (as given by I_s) superimposed upon a diffuse background (as given by I_d). The diffuse background is made up of three components, I_{d_1}, I_{d_2}, I_{d_3}, which have as their respective origins: physical defects, displacement defects of the first kind, and distortions of the second kind.

For simplicity, we will henceforth assume that the scattering sources are physically identical, i.e. $\overline{[f^2(b)]}=\bar{f}^2(b)$, so that the term I_{d_1} vanishes. This simplification directs attention to the geometrical disturbances of the structure.

It can be shown that for a finite ideal crystal

$$D^2(b)=1$$
$$Z_d(b)=0$$

and $Z_s(b)$ degenerates into the well known 'peak function' of the reciprocal

lattice. Hence, the general intensity profile equation can be reduced to the well known relationship

$$I(b) = (1/v^2)\,\overline{f}^2(b) \sum_h S^2(b - b_h)$$

where b_h is the distance to the point h of the reciprocal lattice.

The character of the diffraction profile for non-ideal 'crystals' can best be illustrated by means of examples.

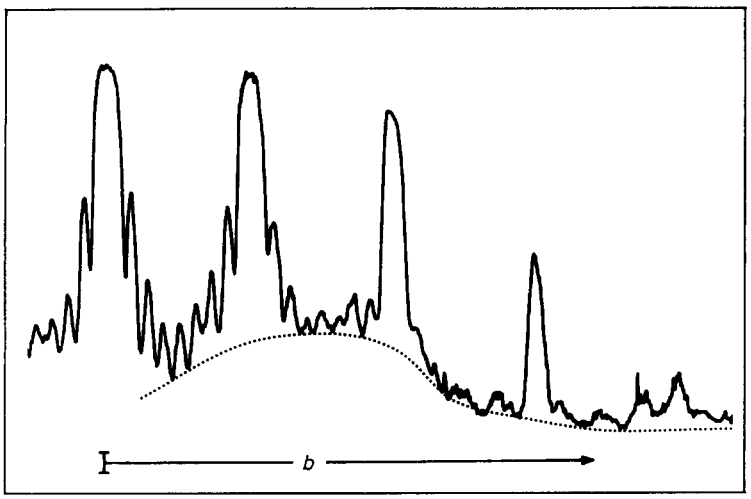

Figure 1—The effect of distortions of the first kind ($g_r = 9{\cdot}2\%$) on the intensity profile (model g)

Figure 1 shows a microdensitometer tracing of an optical diffraction pattern from a one-dimensional point structure with displacement defects of the first kind (see model g, *Figure 3*). From this figure, it can be seen that a distortion of the first kind acts in such a way that the integral intensity of the 'crystal-like' reflections decreases with increasing scattering angle. The reflection widths, on the contrary, do not change with increasing scattering angle*.

As a further consequence of distortions of the first kind, a diffuse scattering appears for which the intensity increases at first with the scattering angle, and then decreases, with the 'atom' form factor, for larger scattering angles.

Figure 2 shows the tracing of a diffraction pattern from a one-dimensional paracrystalline lattice (see model c, *Figure 3*). In this scattering pattern of a paracrystal, the characteristics of crystal interference and liquid interference are superimposed. As in a crystal pattern, individual reflections also appear in the pattern of a paracrystal. The widths of these reflections,

*If there are correlations between the thermal vibrations of the single atoms in a real crystal, giving rise to an elastic wave, then broadening may occur in the form of very diffuse so-called 'extra Laue spots'[20–22]. If, on the other hand, there is no correlation between the single oscillations, absolutely no broadening will occur[23–25].

The existence of correlations for the distortions of the first kind, in general, as well as distortions of the second kind, may be taken into account by the introduction of a term in the intensity expression containing a correlation factor[26].

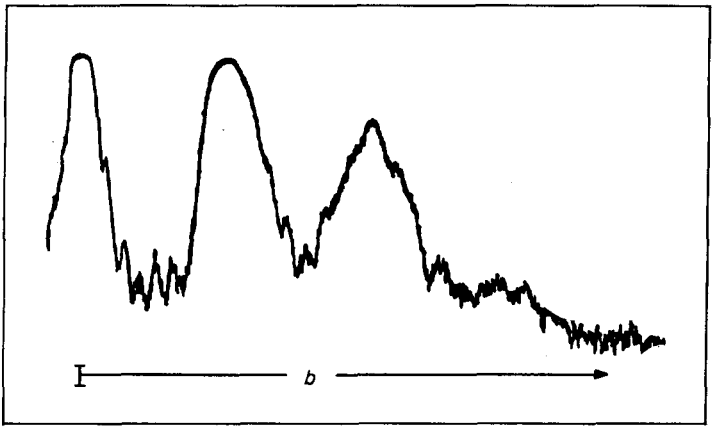

Figure 2—The effect of distortions of the second kind ($g_1 = 15\%$) on the intensity profile (model c)

however, are not only determined by the basic particle size, but are also dependent upon the degree of distortions of the second kind. Notice that the reflection widths increase with increasing scattering angle, similar to the widths of the interference ring in a liquid pattern.

These two figures indicate that an investigation of the increase of the 'crystal-like' reflection widths as a function of the scattering angle (or b) should give information concerning the extent of the paracrystalline distortions and the particle size. From this information, the contribution of the paracrystalline distortions to the diffuse scattering may be determined; hence, the extent to which the displacement defects of the first kind contribute to the diffuse scattering may be indirectly obtained.

In the following section an analysis of the intensity function is performed which quantitatively relates the extent of paracrystalline distortions and particle size to the integral width of the 'crystal-like' reflections and the amount of diffuse scattering to the extent of the displacement distortions of the first kind.

ANALYSIS OF THE INTENSITY PROFILE FUNCTION

Width analysis

The observed integral breadth is related to the width of the shape factor and the width of the paracrystalline factor, Z_s, by the equation

$$\delta B^2(h) = \delta\beta^2(h) + \delta S^2 \tag{1}$$

where $\delta B(h)$ is the observed integral line breadth (in the units of reciprocal space) of the crystal-like reflection of order h, which has been suitably corrected for 'instrument broadening'[27]; $\delta\beta(h)$ is the integral width of Z_s around $b = h/a$; and δS is the integral width of the shape factor.

From the definition of the integral width and the properties of the shape factor,

$$\delta S^2 = \frac{\int S^2(b)\,db}{S^2(0)} = \frac{\int s^2(x)\,dx}{[\int s(x)\,dx]^2} = \frac{1}{L} \tag{2}$$

Similarly,

$$\delta\beta(h) = \frac{\int Z_s(b)\,\mathrm{d}b}{Z_s(b=h/a)}$$

It can be shown that the integral of $Z_s(b)$ over a 'lattice' cell in Fourier space is

$$\int_h Z_s(b)\,\mathrm{d}b = (1/a)\,(2\,|\,F(h)\,|\,)/(1+|\,F(h)\,|\,)$$

where $|\,F(h)\,|$ is the positive real value of $F(b)$ at the reciprocal lattice point $b=h/a$.

Furthermore, the maximum value of $Z_s(b)$ at $b=h/a$ is given by

$$Z_s(b=h/a) = 4\,|\,F(h)\,|\,/(1-|\,F(h)\,|^2)$$

Hence

$$\delta\beta(h) = (1/2a)\,[1-|\,F(h)\,|\,] \tag{3}$$

If we take the distribution function, $H_1(x)$, to be of the form of a gaussian distribution, i.e.

$$H_1(x) = [1/\Delta_1(2\pi)^{1/2}]\exp[-(1/2)(x/\Delta_1)^2]$$

then

$$|\,F(h)\,| = \exp(-2\pi^2\Delta^2h^2/a^2) = \exp(-2\pi^2g^2h^2) \tag{4}$$

where

$$g_1 = \Delta_1/a$$

We will use this parameter, g_1, as an index of the extent of the paracrystalline distortions. This parameter gives the fluctuations of the paracrystalline distortions relative to the average separation distance of adjacent structure points.

Substitution of equations (2), (3) and (4) into equation (1) with subsequent rearrangement gives

$$g_1 = \frac{0{\cdot}34}{h}\left[-\log\left[1-2a\left\{\delta B^2(h)-(1/L)^2\right\}^{1/2}\right]\right]^{1/2} \tag{5}$$

By measuring $\delta B(h)$ for at least two orders of reflections, one can adjust the value of L so that g_1 becomes a constant for the observed reflections.

Notice that if the dimensions of the crystallite are large or if the distortions are large so that

$$\delta\beta^2(h) \gg (1/L)^2$$

then

$$g_1 = \frac{0{\cdot}34}{h}\left[-\log\left[1-2a\delta B(h)\right]\right]^{1/2} \tag{6}$$

For this condition, a single reflection will give the relative fluctuation of the distortions of the second kind.

Diffuse background analysis

It will be convenient, for the purpose of this analysis, to construct a new observable, $A(h)$, by taking the area under the 'crystal-like' portion of the reflection of order h and dividing it by the height of the diffuse background at $b=h/a$.

Thus
$$A(h) = \frac{\int_h I_s(b)\,db}{I_d(b=h/a)} \tag{7}$$

If we assume that $D^2(b)$ and $\bar{f}^2$ are slowly varying functions as compared to $Z_s(b)$, i.e. in the neighbourhood of $|b| = h/a$,

$$D^2(b) \simeq D^2(h)$$

$$\bar{f}^2(b) \simeq \bar{f}^2(h)$$

then the integral of $I_s(b)$ over a direction of the unit cell in reciprocal space is given by

$$\int_h I_s(b)\,db = (1/a)\,\bar{f}^2(b)\,D^2(h)\int_h \widehat{Z_s(b)\,S^2}(b)\,db \tag{8}$$

Now

$$\int \widehat{Z_s(b)\,S^2}(b)\,db = \int Z_s(b)\,db \int S^2(b)\,db$$

Thus
$$\int I_s(b)\,db = (N/a)\,\bar{f}^2 D^2(h)\,(2\,|F(h)|\,/1+|F(h)|) \tag{9}$$

since
$$N = L/a$$

Hence
$$A(h) = \frac{1}{a}\left[\frac{2D^2(h)\,|F(h)|}{1+|F(h)|-2D^2(h)\,|F(h)|}\right] \tag{10}$$

therefore
$$D^2(h) = \left[\frac{aA(h)}{1+aA(h)}\right]\left[\frac{1+|F(h)|}{2\,|F(h)|}\right] \tag{11}$$

Notice that for the special case of negligibly small distortions of the second kind; $g_1 \simeq 0$, hence

$$D^2(h) \simeq \frac{aA(h)}{1+aA(h)}$$

If we also take H_r to be of the form of a gaussian distribution, then

$$H_r(x) = [1/\Delta_r(2\pi)^{1/2}]\exp[-(1/2)(x/\Delta_r)^2]$$

hence
$$D^2(h) = \exp(-4\pi^2 h^2 g_r^2) \tag{12}$$

where
$$g_r = \Delta_r/a$$

This parameter, g_r, will serve as an index of the extent of the displacement distortions of the first kind. This parameter gives the fluctuations of the displacement distortions of the first kind relative to the average separation distance of adjacent structure points.

Substitution of equations (4) and (12) into equation (11) gives, after rearrangement

$$g_r = \frac{0{\cdot}24}{h}\left[\log\left[\frac{1+aA(h)}{aA(h)}\right] + \log\left[\frac{2\exp(-2\pi^2 g_1^2 h^2)}{1+\exp(-2\pi^2 g_1^2 h^2)}\right]\right] \tag{13}$$

Thus, by measuring the integral widths of two or more orders of the 'crystal-like' reflections and the height of the diffuse background for these

reflections, one can determine the relative fluctuations for the distortions of the first and second kinds as well as an average dimension of the crystallite (or paracrystallite).

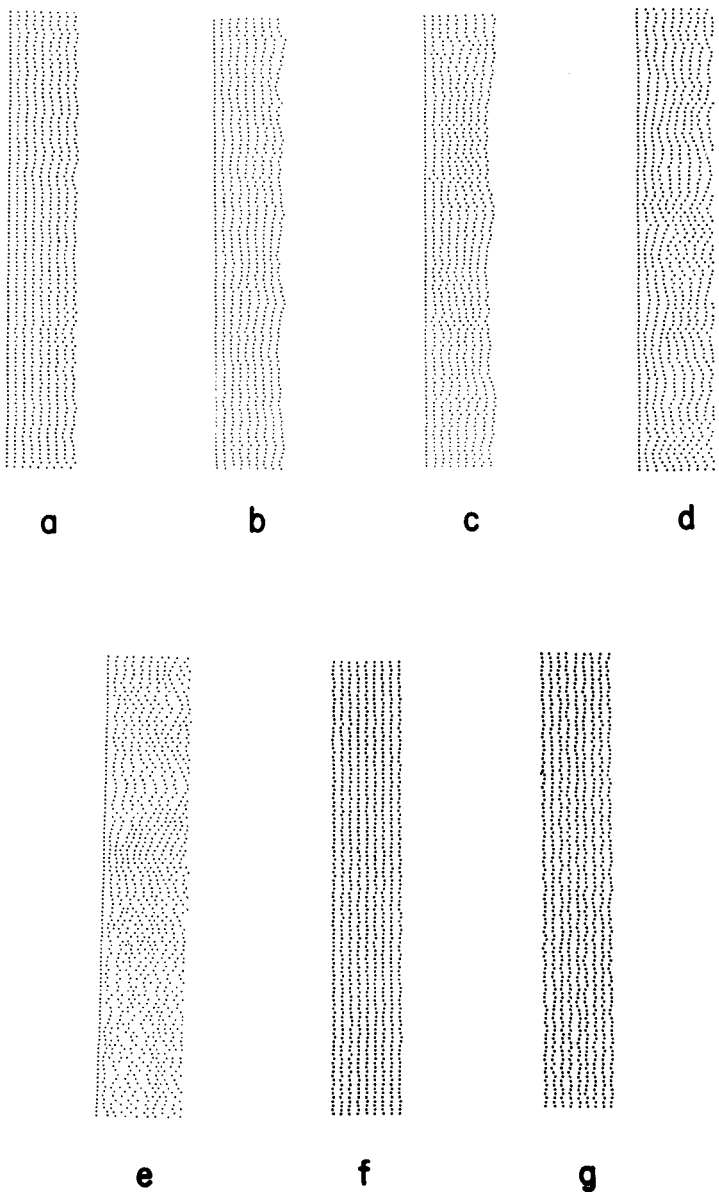

Figure 3—Models of one-dimensional paracrystalline lattices with distortions of the first (g_r) and second (g_1) kinds (for details see *Table 1*)

APPLICATION TO ONE-DIMENSIONAL OPTICAL DIFFRACTION PATTERNS

It is of interest to compare the results obtained by the application of this analysis with the parameters from known structures. For the present purpose, optical diffraction patterns from one-dimensional models will be sufficient to illustrate this approach.

Model structures were constructed in such a manner as to give arrangements having distortions of the first and second kinds[28]. Nine point-atoms were taken for each one-dimensional structure and a collection of about a hundred such one-dimensional structures was taken for each model.

The optical diffraction patterns for these models were obtained by Bonart[29]. Bonart used a Fraunhofer diffraction arrangement with a long, uniformly illuminated slit normal to the direction of the one-dimensional structures. By the use of this arrangement and the large number of lattice rows in one collection, the diagrams were made practically free from ghosts, even though each lattice row was made up of only nine point-atoms*.

For the reasonably small angles encountered in Fraunhofer diffraction, db is simply an element of distance along the film.

Seven models, which were investigated by Bonart, are shown in *Figure 3*. The optical Fraunhofer diffraction patterns of these models are shown in *Figure 4*. The line profiles of the diffraction patterns for models g and c were given in *Figures 1* and *2* respectively.

The size parameter, L, may be measured directly from the models; the fluctuation parameters g_1 and g_r, however, must be extracted[19, 26] from the 'distance statistics' for each model. The distance statistics, in turn, may be obtained either by (*i*) counting the number of pairs of points having a given spacing x; or by (*ii*) producing the auto-correlation function of the structure in a 'folding machine'[30].

Table 1 compares the values of the parameters calculated from the models

Table 1. (After Hosemann[26]). The parameters of 'particle size', L, and distortions of the first, g_r, and second, g_1, kinds calculated from models of one-dimensional structures and compared with the values determined from the observed diffraction patterns

Model	*From models*			*From diffraction*		
	g_r %	g_1 %	L *mm*	g_r %	g_1 %	L *mm*
a	3·2	4·1	2·3	2·8	4·5	2·3
b	—	9·2	2·3	—	8·2	3·1
c	—	13·7	2·3	—	15·0	2·4
d	3·0	16·2	2·3	—	(18)	—
e	—	~25·0	2·3	—	~30·0	—
f	6·4	0	2·3	6·5	0	2·3
g	9·0	0	2·3	9·2	0	2·3

*If the number of rows goes *ad infinitum*, the observed Fraunhofer diffraction would give a continuous intensity distribution. For a finite number of rows statistical fluctuations appear, which are called 'ghosts' (*see* Hosemann and Bagchi[28]) and in practice can sometimes be neglected in *Figure 4* within experimental error.

and the values calculated from the diffraction patterns. The agreement is satisfactory.

A difficulty was encountered in the analysis of the distance statistics for models b, c and e, because of apparent accidental correlations between the individual statistics (see *Figure 3*). Only g_1 and L could be obtained from models b and c; only L could be obtained from model e.

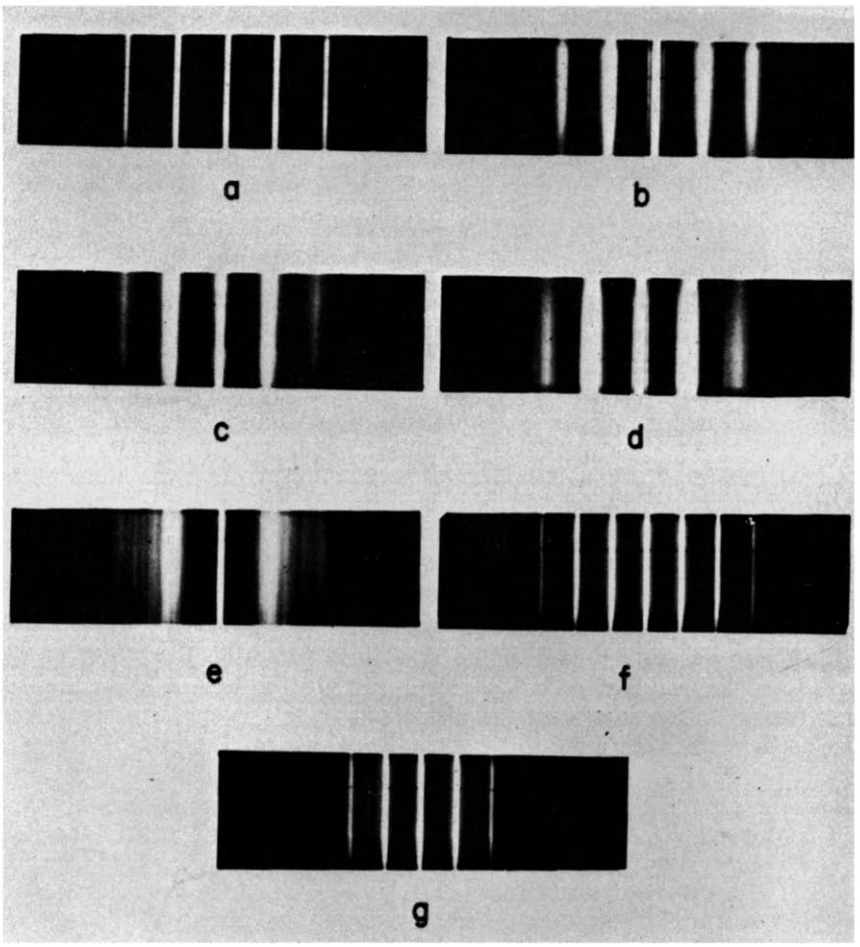

Figure 4—Optical diffraction patterns of the models shown in *Figure 3*

The parameters g_1, g_r, and L could not be uniquely determined from diffraction patterns d and e. However, by assuming that all distortions were of the second kind, an estimate for g_1 was obtained from d.

It is interesting to note that for relative fluctuations of the second kind as low as about ten per cent, the diffraction patterns are beginning to take on the diffuse appearance of so-called 'amorphous' scattering.

DISCUSSION

The application of the above methods to polymer systems requires that at least two orders of reflections be observed. Unfortunately, however, the X-ray patterns of high polymers often show so few reflections, that no two reflections can be found, of which one is a higher order of the other. This difficulty could possibly be surmounted by improving the quality of the diffraction patterns from polymers by using special cameras[31], monochromatized X-rays, and long exposure times.

Another difficulty will be encountered if an amorphous phase is present. The presence of an amorphous phase will contribute to the diffuse background and, hence, will give larger values for the apparent gs. However, it is of interest to note that the presence of a diffuse background does not necessarily mean that an amorphous phase is present. Hence, as a first approach to the analysis of line profiles, one could assume that no amorphous material is present. If the results obtained are unreasonable, or if third and fourth order reflections are present whose analyses are inconsistent with this assumption, then appropriate modifications can be made.

The realization that distortions of the second kind can contribute to the intensity of the diffuse background is of great consequence to the study of high polymers, for in view of the degrees of distortions anticipated in high polymers, this diffuse scattering may be so substantial that it cannot be ignored[32]. This means that the ordinary methods used to determine the crystallinity of high polymers, in which the diffuse scattering is attributed to the amorphous part of the substance, can yield, at best, a lower limit to the degree of crystallinity. Recently, Ruland[33] has suggested a method which is appropriate if the lattice disturbances are primarily distortions of the first kind. When distortions of the second kind become significant, Ruland's method must be refined[26].

Furthermore, an estimate of the crystallite size from the width of the broadened 'crystal-like' reflections again can give, at best, a lower limit to the true crystallite size, since the distortions of the second kind as well as the particle size contribute to the breadth of these reflections.

Basic Research Department,
Chemstrand Research Center,
Durham, North Carolina, U.S.A.

(*Received June 1962*)

REFERENCES

[1] KRIMM, S. and TOBOLSKY, A. V. *J. Polym. Sci.* 1951, **7**, 57
[2] STOKES, A. R. and WILSON, A. J. C. *Proc. Camb. phil. Soc.* 1942, **38**, 313
[3] STOKES, A. R. and WILSON, A. J. C. *Proc. phys. Soc., Lond.* 1949, **56**, 174
[4] BERTAUT, M. F. *C.R. Acad. Sci., Paris,* 1949, **228**, 492
[5] WARREN, B. E. and AVERBACH, B. L. *J. appl. Phys.* 1950, **21**, 595
[6] WARREN, B. E. *Acta cryst., Camb.* 1955, **8**, 483
[7] KATAYAMA, K. *J. phys. Soc., Japan,* 1961, **16**, 462
[8] BIENENSTCOK, A. *J. appl. Phys.* 1961, **32**, 187
[9] WARREN, B. E. *Progr. Metal Phys.* 1959, **8**, 147
[10] HAUCK, V. and HUMMEL, C. *Z. Metallk.* 1956, **47**, 254
[11] DOI, K. *Acta cryst., Camb.* 1961, **14**, 830

[12] HOSEMANN, R. *Z. Phys.* 1950, **128,** 1
[13] HOSEMANN, R. *Z. Phys.* 1950, **128,** 465
[14] HOSEMANN, R. *Naturwissenchaften,* 1954, **41,** 440
[15] HOSEMANN, R. and SCHOKNECHT, G. *Kolloidzschr.* 1957, **152,** 45
[16] HOSEMANN, R. *Acta cryst., Camb.* 1951, **4,** 520
[17] HOSEMANN, R. and BAGCHI, S. N. *Acta cryst., Camb.* 1952, **5,** 612
[18] HOSEMANN, R. and BAGCHI, S. N. *Phys. Rev.* 1953, **94,** 71
[19] BONART, R. *Z. Kristallogr.* 1957, **109,** 296
[20] VON LAUE, M. *Ann. Phys., Lpz.* 1926, **81,** 877
[21] VON LAUE, M. *Z. Kristallogr.* 1926, **64,** 115
[22] LAVAL, J. *Bull. Soc. franç. Minér.* 1941, **64,** 1
[23] DEBYE, P. P. *Verh. dtsch. phys. Ges.* 1913, **15,** 678 and 857
[24] WALLER, I. *Z. Phys.* 1923, **17,** 398
[25] WALLER, I. *Ann. Phys., Lpz.* 1926, **79,** 261
[26] HOSEMANN, R. and BAGCHI, S. N. *Direct Analysis of Diffraction by Matter.* North Holland Publishing Co.: Amsterdam, 1962
[27] STOKES, A. B. *Proc. phys. Soc., Lond.* 1948, **61,** 382
[28] KLEIN, A. M. *Diplom-Arbeit.* Freie Universität Berlin, 1960
[29] BONART, R. *Z. Kristallogr.* 1957, **109,** 309
[30] HOSEMANN, R. and SCHOKNESCHT, G. *Kolloidzschr.* 1957, **152,** 45
[31] HOFMANN, E. and JAGODZINSKI, H. *Z. Metallk.* 1955, **46,** 601
[32] BONART, R., HOSEMANN, R., MOTZKUS, F. and RUCK, H. *Norelco Reports,* 1960, **7,** 31
[33] RULAND, W. *Acta cryst., Camb.* 1961, **14,** 1180

The Influence of Extrusion Conditions on the Crystallization of Polyethylene Terephthalate Film

R. P. SHELDON

The influence of extrusion conditions on the benzene-induced and heat or 'thermal' crystallization of polyethylene terephthalate has been studied. Samples of film with extrusion rate/melt temperature properties of 70/270, 155/270, 75/280, 160/280, 75/290 and 160/290 lb per hour per °C were either treated with benzene at 25°C or heated in air at 110°C. It was found that in the former case there was no apparent influence of extrusion conditions on the rate of crystallization whereas with the latter, where an Avrami type of behaviour is observed, there is a significant dependence on both extrusion parameters although extrusion rate has no appreciable effect at 290°C. In neither study did there appear to be any influence on the apparent equilibrium density of the polymer, this being higher (1·393 g/cm³) for the benzene-induced crystallization case than for the heat treated (1·374 g/cm³).

POLYETHYLENE terephthalate(PET), may be obtained as a transparent non-crystalline film or fibre by rapid cooling of the molten polymer following extrusion from a suitable die. That the material is in a metastable state is clearly revealed by its ability to crystallize under a number of environmental conditions. For example, if the film is stretched under optimum temperature conditions a substantial degree of crystallinity may be developed. This behaviour has attractive commercial potential in that not only is there a useful increase in strength but the original clarity of the film is retained. Another way in which the process may be carried out is to heat the polymer at some temperature between its glass temperature and melting point. However, in this case opacity is seen to result, this being attributed to the growth of spherulites. Aspects of this behaviour with PET have been studied by a number of workers[1–3]. A third method, and one which again is accompanied by opacity, is to treat the film with various organic liquids[1,4] the phenomenon being confirmed by X-ray diffraction as well as by density studies[5]. Investigations into the kinetics of the latter process have indicated that the rate of crystallization increases with temperature, has an inverse dependence on sample thickness and is also influenced by the nature of the liquid[6]. At the same time it appears that the equilibrium crystallinity is unaffected by the temperature at which the process is carried out, a conclusion which is not immediately obvious in the results of the heat crystallization studies. These and other considerations have led to the suggestion that whereas the 'thermal' process involves gross macromolecular diffusion throughout a particular sample the liquid-induced mechanism is one of diffusion of imbibed liquid into the molecular matrix leading to localized crystallization on a progressive front.

As mentioned above, the film is obtained by extrusion of polymer at

some temperature above the melting point. It is conceivable therefore that the rate of extrusion and the melt temperature may exert an influence on the crystallization kinetics of the shock-cooled material. The former may be of importance through some molecular orientation mechanism, or by an effect on melt dwell time, whereas the latter could possibly have a moderating influence on orientation from a melt-viscosity viewpoint and also like that of melt dwell time it could have an action resulting from polymer degradation and nuclei destruction. The latter aspect has been the subject of a thorough investigation of the thermal process by Morgan *et al.*[3]. It was concluded from these studies that the melt can contain, even at temperatures above the observed melting point, thermodynamically stable minute crystals of polymer and that these, quite apart from any foreign body source of nucleation, will exert a subsequent influence on the crystallization process. In particular, other factors being equal, it appears that the higher the temperature of the melt the less rapid is the process at a given temperature. It was also noted that although the molecular weight may be important there was no definite correlation of rate with intrinsic viscosity at higher values of the latter. This was attributed to a secondary chemical effect occurring during the polymerization stage.

The present paper describes an investigation into the importance of melt temperature and extrusion rate on the rate of the benzene-induced crystallization of PET, benzene causing disappearance of the amorphous phase at a rate convenient for kinetic study. At the same time a thermal crystallization in air has been followed so that comparison may be made between the two processes.

EXPERIMENTAL

Materials

Samples of six films made from the same original batch of PET were used. Their melt temperatures, extrusion rates and other relevant properties including those measured by methods which are to be described presently are given in *Table 1*.

Table 1. Properties of PET films

Extrusion rate/melt temp. (lb/min/°C) (Code No.)	*Melt dwell-time (min)*	*Film thickness (cm)*	*Bire-fringence*	*Intrinsic viscosity*	*Density (g/cm^3)*
70/270	5·7	0·019	−0·0006	0·49	1·338
155/270	2·6	0·019	+0·0004	0·51	1·338
75/280	5·2	0·021	−0·0006	0·49	1·338
160/280	2·5	0·021	+0·0005	0·50	1·338
75/290	5·2	0·022	−0·0004	0·53	1·338
160/290	2·5	0·022	+0·0003	0·54	1·338

The benzene used as immersion liquid was of A.R. quality and was dried and fractionally distilled before use as were also the carbon tetrachloride

and ethyl alcohol for the density measurements, and the *o*-chlorophenol used in the viscosity determinations.

Procedure

Film thickness—This was measured by means of a micrometer.

Birefringence—All evaluations were made from results obtained with the aid of a polarizing microscope using a retardation technique.

Intrinsic viscosity—The flow times of solutions of the different samples in *o*-chlorophenol were determined using an Ubbelohde suspended-level type viscometer. Each original solution was allowed to stand three days before measurements were made and repeat measurements were made after five days in order to ascertain that there had been no change in viscosity on more prolonged standing. The flow times were obtained with the viscometer immersed in a thermostatically controlled bath maintained at 25° ±0·01°C, in each case at four concentrations so that linear extrapolation of the results could be made in the usual way for the evaluation of the corresponding intrinsic viscosities.

Density—This was determined by a method previously described[4], being essentially a flotation technique in which a polymer sample is introduced into a 10 ml volume of carbon tetrachloride followed by addition of ethyl alcohol from a microburette until the sample is on the point of sinking. Density results which are reproducible to ±0·001 g/cm³ were interpolated from a calibration curve of various mixtures of the flotation liquids and their densities. For the liquid-treated samples allowance was made for the residual benzene to convert the apparent density to a corrected value.

Benzene-induced crystallization—Samples of the six films indicated in *Table 1* were cut into small pieces of approximately 1 cm² in surface area. These were then immersed in benzene at 25° ±0·01°C after weighing on a balance capable of reading to 0·01 mg. After predetermined intervals of time the samples were removed, surface dried and transferred to an evacuated desiccator where they remained for at least 48 hours before being reweighed in preparation for the density studies.

Thermal crystallization—Samples of the six films were cut into pieces of approximately 0·1 cm² in area and introduced to ignition tubes immersed in silicone oil which was maintained at a temperature of 110° ±0·5°C in an oven. The samples were removed after given periods of time as before in preparation for density determinations.

RESULTS

Attention has already been drawn to the relevant properties of the polymer films including intrinsic viscosity, density and birefringence with reference to the extrusion direction, which are shown in *Table 1*. The results of the benzene-induced crystallization are shown in graphical form in *Figure 1* and are expressed in terms of density change as a function of time. It

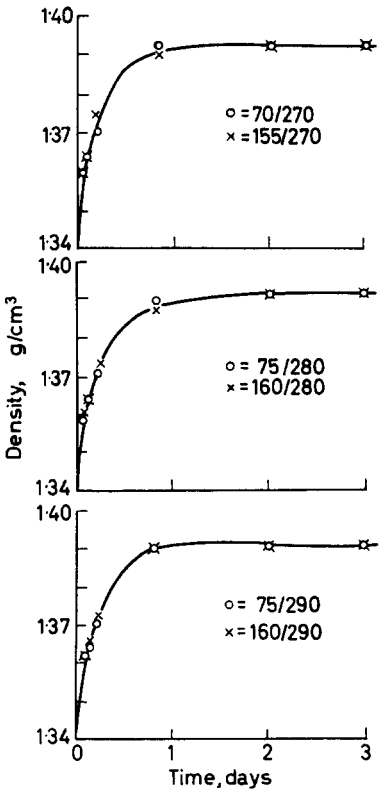

Figure 1—Rate of increase of density with time (benzene-crystallized)

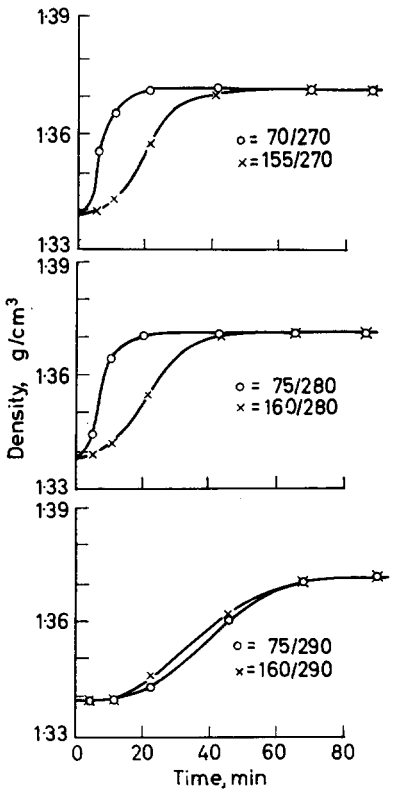

Figure 2—Rate of increase of density with time (thermal-crystallized)

should be remembered that density and the degree of crystallinity are directly related. The corresponding results for the thermal crystallization are similarly expressed in *Figure 2*.

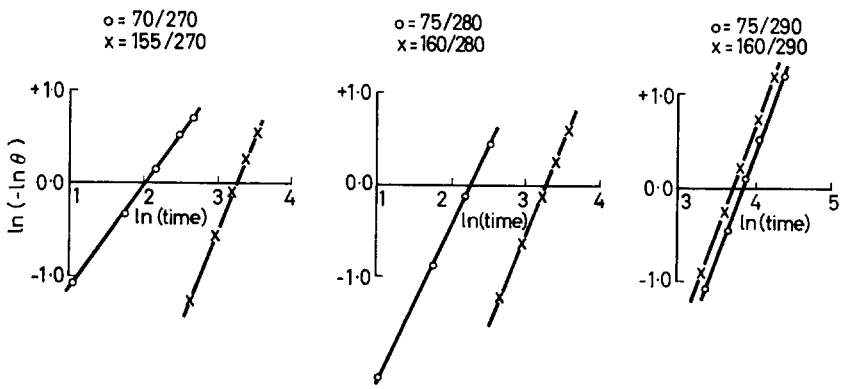

Figure 3—Plots in $\ln(-\ln\theta)$ versus ln(time) for thermal-crystallized samples

Further analysis of the latter results has been carried out on the basis of the theoretical treatments of Avrami[7]. It has been shown that the overall crystallization process in general may be represented by an equation of the form $\theta = \exp(-Kt^n)$ where θ is the fraction remaining at time t of the original amorphous material $[=(d_\infty - d_t)/(d_\infty - d_0)]$ where d_∞ is the final value of the density, d_0 the value of the original polymer and d_t the value at time t. K and n are constants, n taking values which depend upon the nature of the nucleation and growth processes (e.g. a value

Table 2. Avrami equation indices of thermal crystallized samples of PET

PET sample	70/270	155/270	75/280	160/280	75/290	160/290
Avrami eqn index (n)	1·2	2·0	1·7	2·0	2·2	2·2

of unity may be ascribed to predetermined nucleation followed by either fibrillar or laminar-spherulitic growth whilst a value of two differs only in that the nature of the nucleation is sporadic. *Figure 3* shows plots of $\ln(-\ln\theta)$ versus $\ln t$ for the various samples, and the corresponding values of n, which may be obtained from the slopes, are listed in *Table 2*.

DISCUSSION

Figure 1 shows that for the benzene-induced crystallization there is no apparent dependence of rate on the extrusion variables. The significance of this will be discussed later. In the case of the heat-crystallized samples it is seen that there is a marked influence of these variables on the rate.

That this difference of behaviour of the samples is probably not due to molecular orientation is suggested on a number of counts. In the first place the birefringence values are very small and hence the corresponding differences in birefringence are also small. It should be remembered, however, that we are dealing with amorphous polymer and thus the value of birefringence will be less dependent on order than it would presumably be for crystalline polymer. Secondly, the density of each sample of polymer is initially the same which would probably not be true where there are large differences in molecular orientation. Again, if we assume that liquid-induced crystallization is a diffusion-controlled process then it is reasonable to assume that molecular orientation would influence the rate of diffusion and hence the rate of liquid-induced crystallization. *Figure 1* gives no indication of such behaviour and thus supports the suggestion of low orientation.

However, there is some small indication of a difference in initial film structure in that the birefringence results suggest that the 'fast' direction of the film is in the direction of extrusion for the films with the higher extrusion rate whereas it is the 'slow' direction for the films of lower extrusion rates. That the latter phenomenon occurs at all might be attributed to some shearing action of the die, the tendency being overcome and exceeded following extrusion at higher flow rates. Some possible implications of this are discussed later.

It has previously been suggested that the liquid-induced crystallization process is quite different from that of the thermal[6]. That this is so is of course confirmed by *Figure 2*. Here we have typical Avrami-type curves similar to those obtained by previous workers[1-2] with the characteristic sigmoidal shapes. Furthermore, the equilibrium density values are of the same order as those found by previous workers in a similar temperature range[2,3]. This is surprising in some ways and bearing in mind that the equilibrium values of the present investigation are themselves virtually the same it would suggest that the equilibrium degree of crystallinity at a given temperature is insensitive to possibly a fairly wide variation in polymer processing conditions.

Returning to a consideration of the factors influencing the rate of the thermal crystallization it is suggested that in the present investigations molecular weight has little bearing on the observed differences. In the first place the films were prepared from the same original batch of polymer and although the intrinsic viscosity values differ slightly this may be disregarded on account of experimental error and by lack of correlation with the rate variations.

The rates associated with the higher melt temperature samples of 290°C are significantly less than those at 270°C and 280°C. The same behaviour was found by Morgan *et al.*[3] with samples prepared from melt temperatures of 294°C, 275°C and 268°C. The Avrami index n has values of approximately two with the 290°C samples and is therefore similar to that found by the previous workers at the same crystallization temperature with their 294°C sample. It would appear therefore that predetermined nuclei have been avoided, presumably due to the breakdown effect of the high temperature, and thus the process is one of sporadic nucleation and, following the suggestion of the previous workers, one of fibrillar growth.

At the lower melt temperatures it will be observed that the rates are higher and at a given temperature the rate is again higher for samples obtained at the lower extrusion rates. This is contrary to what was originally expected as it was thought probable that even in the absence of orientation the shorter residence in the melt of the higher extrusion rate films would allow the retention of nuclei which should enhance the rate of any subsequent crystallization process. The Avrami treatment is, however, in agreement with the form of the curves in that it would appear that the latter films are more associated with sporadic nucleation than are the films at the low extrusion rates. In an attempt to explain the results it is suggested that under conditions of higher extrusion rates there is a tendency to degrade crystallites or other sources of nucleation, shearing stresses at the point of extrusion perhaps being greater than indicated from the birefringence results owing to relaxation immediately following extrusion. If this is true it would appear that the time of residence in the melt is of secondary importance. In this context it may be relevant to mention a reference to the destruction of crystallinity by stretching in the solid state of non-oriented PET[8].

In conclusion we can say that the process of liquid-induced crystallization is independent of extrusion variables as have been described. In other

words, the absence or presence of nuclei has no apparent bearing either on the rate or the equilibrium aspects of the process. On the other hand it has been once again demonstrated that the fabrication history of a polymer does have an influence, if not on the equilibrium condition, then on the rate at which this is achieved.

The author wishes to thank I.C.I. Ltd, Plastics Division for their generous gift of polyethylene terephthalate film used in these studies and Mr R. A. Hudson for his encouragement and advice.

Polymer Research Laboratories,
Department of Chemical Technology,
Institute of Technology, Bradford, Yorkshire

(*Received August 1962*)

REFERENCES

[1] KOLB, H. J. and IZARD, E. F. *J. appl. Phys.* 1949, **20,** 571
[2] COBBS, W. H., Jr and BURTON, R. L. *J. Polym. Sci.* 1953, **10,** 275
[3] KELLER, A., LESTER, G. R. and MORGAN, L. B. *Phil. Trans.* 1954, **247,** 1
MORGAN, L. B. *Phil. Trans.* 1954, **247,** 13
HARTLEY, F. D., LORD, F. W. and MORGAN, L. B. *Phil. Trans.* 1954, **247,** 23
[4] MOORE, W. R. and SHELDON, R. P. *Polymer, Lond.* 1961, **2,** 315
[5] BLAKEY, P. B. and SHELDON, R. P. *Nature, Lond.* 1962, **195,** 172
[6] SHELDON, R. P. *Polymer, Lond.* 1962, **3,** 27
[7] AVRAMI, M. *J. chem. Phys.* 1939, **7,** 1103; 1940, **8,** 212
[8] KOZLOV, P. V., KABANOV, V. A. and FROIOVA, A. A. *Dokl. Akad. Nauk S.S.S.R.* 1959, **125,** 118

Crystallization and Melting of Copolymers of Polymethylene

M. J. RICHARDSON*, P. J. FLORY and J. B. JACKSON

Copolymers of —CH_2— *with from 1·8 to 7·7 mole per cent* —CH·R—, *where* R = *n*-C_3H_7, C_2H_5 *or* CH_3, *have been prepared by copolymerizing diazomethane with the appropriate diazoalkane. That the co-units are distributed approximately at random was assured by analysis of the composition of the unreacted monomers, and by analysis of fractions separated from one of the copolymers by column fractionation. The copolymers were crystallized by stepwise cooling in small intervals over the crystallization range, each temperature being maintained for a period of two days. Melting was followed dilatometrically by raising the temperature in increments according to a similar schedule. Degrees of crystallinity calculated from the specific volume at each temperature are compared with the equilibrium theory of crystallization of copolymers. The comparison involves a single arbitrary parameter, from which we calculate an interfacial free energy of 170 ergs* cm^{-2} *(4 600 cal* $mole^{-1}$ *of emerging chains) for the 001 face. The range over which melting is most marked shifts to lower temperatures with increase in the proportion of co-unit as expected, and in a manner accountable by the theory. For a given copolymer, however, the melting is restricted to a narrower temperature range than that predicted. At temperatures far below the melting point* T_m, *the extent of crystallization fails to rise to the level predicted by theory, owing presumably to restraints imposed by involvement of the longer methylene sequences of the copolymer molecules in crystals formed at higher temperatures. As the melting point is approached, the degree of crystallinity falls to zero more rapidly than the equilibrium theory prescribes. This general observation is attributed to the kinetic difficulty of bringing together the comparatively sparse long methylene sequences required for crystallites which are stable near* T_m. *Copolymers in which* R = CH_3 *melt, and crystallize, at higher temperatures than those for which* R = C_2H_5 *and n-*C_3H_7. *This fact, in conjunction with the melting point/composition relationship for low proportions of the co-unit, indicates the formation of a crystalline*

$$\begin{array}{c} CH_3 \\ | \end{array}$$

phase which is a solid solution of —CH— *dispersed among* —CH_2— *units. In copolymers of the larger co-units formation of a pure phase is indicated under the experimental conditions here employed.*

THE process of crystallization of long macromolecular chains, expressed in the most elementary terms, consists of the transfer of sequences of consecutive chain units from the amorphous to the crystalline phase. Coherence of the crystallites thus formed demands that neighbouring sequences therein be of nearly equal length. We designate this sequence length by ζ, expressed as the number of repeating units. The magnitude of ζ, and its variation among different crystallites, depends in general on the structural regularity of the macromolecular chains and also upon the conditions attending crystallization[1]. The stability of a crystallite should increase asymptotically with its length. This follows directly from the positive interfacial free energy σ_e associated with each chain which protrudes from the end face of a crystallite.

*Present address: National Physical Laboratory, Teddington.

In the case of a homopolymer consisting of very long chains of stereoregular repeating units, ζ is limited by kinetic factors operative in the process of crystallization. Under favourable conditions (i.e. low supercooling) ζ may approach 10^3 for linear polymethylene[2,3]. In copolymers, on the other hand, ζ is reduced owing to the presence of co-units B which in general are excluded from the crystal lattice occupied by sequences of the principal chain units A[1,4]. Rejection of the co-unit B by the crystal lattice of A enforces the requirement that crystallites of length ζ be formed from sequences of A units of length $j \geqslant \zeta$. The lengths of the crystallites formed from a copolymer are therefore intimately related to the statistical distribution of sequences of various lengths within the copolymer chains, and the availability of appropriate sequences at the site of crystallization[4].

If crystallization of a copolymer is brought about by gradual cooling from the melt over a very long period of time, the first crystallites which appear must be comparatively large in the dimension ζ inasmuch as shorter crystallites would be unstable under conditions of small undercooling. The longer A sequences will consequently be removed preferentially from the melt at the outset. Such sequences are present in only limited amounts, hence the degree of crystallinity attainable with small undercooling is necessarily very low. With further cooling, progressively shorter sequences become eligible for the formation of shorter crystallites. Melting of the semi-crystalline copolymer occurs over a broad range of temperature for reasons which follow directly from the foregoing description of the crystallization process; shorter crystallites melt first, and those of greatest length persist (at equilibrium) up to the melting point T_m of the copolymer.

The melting point of a crystallite does not, however, depend solely on its length, as frequently is incorrectly assumed. Quite obviously, and as the theory of phase equilibrium in copolymers clearly shows[1,4] the temperature at which a crystallite melts depends not only on its dimensions but also on the chemical potential of A sequences of the required length in the adjoining melt phase. Thus, as is well established by theory, the *equilibrium* melting point T_m of a copolymer must depend on the melting point T_m^0 of the homopolymer, on the heat of fusion ΔH_u per A unit *and* on the copolymer composition according to the relationship

$$1/T_m - 1/T_m^0 = -(R/\Delta H_u) \ln p \qquad (1)$$

where p is the sequence perpetuation probability, which for a *random copolymer* may be identified with the mole fraction of the crystallizing unit (CH_2 in the present case). The difference between T_m for the copolymer and the melting point T_m^0 for the homopolymer depends on the sequence perpetuation probability p in the manner prescribed by this equation. It is noteworthy that the final disappearance of crystallinity is predicted according to theory to be discontinuous; i.e. a melting point should exist notwithstanding the broad range of temperature over which pre-melting occurs[4]. Despite the survival of only those crystallites having substantially infinite length at the theoretical melting point, this melting point T_m occurs at a temperature lower than T_m^0. The fallacy of assigning a melting point to crystallites of specified length, without regard for the composition of the copolymeric liquid phase with which it is in equilibrium, is obvious.

For the development of the theory from which these conclusions are derived, the reader is referred to ref. 4. Inasmuch as this theory is premised on statistical thermodynamics, states of equilibrium are implicitly assumed. No account is taken of kinetic limitations set by the necessarily finite rate of transport of an acceptable sequence to the site of the crystallite. With the further assumption that each sequence of A units participates in at most one crystallite, the following expression for the weight fraction of crystalline phase has been deduced[4]

$$w^c = (1-p)^2 p^{\zeta\star} \{p(1-p)^{-2} - e^{-\theta}(1-e^{-\theta})^{-2} + \zeta\star [(1-p)^{-1} - (1-e^{-\theta})^{-1}]\} \tag{2}$$

where θ is a function of the temperature given by

$$\theta = (\Delta H_u / R)(1/T - 1/T_m^0)$$

and $\zeta\star$ is the minimum sequence length which is susceptible to crystallization for the given value of p and the temperature as specified by θ. It is given by

$$\zeta\star = -\{\ln D + 2\ln[(1-p)(1-e^{-\theta})^{-1}]\}(\theta + \ln p)^{-1} \tag{3}$$

The quantity D is formally related to the interfacial free energy σ_e associated with each terminus of a crystalline sequence according to

$$\ln D = -2\sigma_e / kT \tag{4}$$

In consequence of the connection of one A sequence to another via intervening sequences of B units, crystallization of an A sequence, or a portion thereof, restricts diffusional displacements of other sequences of A units in the same chain molecule. The gathering together of a group of A sequences, each being of the length required ($\geqslant \zeta$) for formation of a crystallite of specified dimension (ζ) will thus be impeded by those crystallites formed previously. The impact of this circumstance is not readily amenable to theoretical treatment. Its severity should obviously diminish with decrease in crystallinity; in the limit of very low degrees of crystallinity its effect must vanish.

In this paper we report an experimental investigation of the dependence of the degree of crystallinity in copolymers on temperature and on the proportion of randomly distributed co-units. Copolymers of a preponderance of methylene —CH_2— units with small proportions of co-units of the

type —CH— have been chosen for this purpose. The principal experiments were performed on copolymers in which R = n-C_3H_7; others are reported on copolymers in which R = CH_3 and C_2H_5. These various copolymers were prepared by polymerization of mixtures of diazomethane and the corresponding higher diazoalkane. Special measures were adopted to assure the random distribution of co-units, as required to justify characterization of the copolymer sequence distribution by the single parameter p introduced above. Crystallization was allowed to occur while the temperature of the initially molten copolymer was reduced gradually by small increments over periods of many days. This procedure was adopted in order to provide optimum opportunity for approach to equilibrium. The results are compared with the relationships adduced from the statistical thermodynamic

theory outlined above. The premises of this theory are thus put to test and information bearing on the morphology of semicrystalline copolymers is presented.

EXPERIMENTAL

Preparation of the diazoalkanes and their copolymerization

Diazoalkanes were prepared from the corresponding nitrosoureas[5]. In a typical preparation the finely powdered nitrosourea (0·6 mole) was slowly added to a mixture of 50 per cent aqueous potassium hydroxide solution (180 ml) and ether (600 ml). When the reaction reached completion the ethereal layer was decanted off and dried over potassum hydroxide pellets. As first prepared the homologous diazoalkanes above diazoethane contained finely divided inorganic salts which settled very slowly. They were clarified by centrifuging. Concentrations of the diazoalkanes were determined by treating 5 ml of the ethereal solution with a weighed excess of propionic acid and back titrating the excess acid with 0·1 N sodium hydroxide solution. Diazomethane solutions used were of the order of 0·6 molar and the higher homologues 0·25 molar. Isolation of the pure diazoalkanes was not attempted.

Diazomethane was copolymerized with the higher diazoalkane at 0°C using trimethyl borate as a catalyst exactly as described by Buckley and Ray[6]. The product precipitated as formed. The reaction was terminated after about 24 hours by the addition of excess propionic acid. Total residual unreacted diazoalkanes were determined by back-titrating the excess acid as above. The copolymer was washed repeatedly with ether, then dried *in vacuo* at 150°C for 4 h and weighed. Sheets 1/16 in. thick were prepared by compression moulding; the copolymers ranged from hard, white, horny materials to soft, transparent rubbers.

Data pertaining to the various preparations are summarized in *Table 1*.

Table 1. Copolymerization of diazomethane with various higher diazoalkanes in ethereal solution, catalysed by 0·02 mole trimethyl borate/mole diazoalkanes at 0°C

Copolymer No.	*Mole % $RCHN_2$ in initial mixture*	R	*% Conversion*	*% Yield (based on conversion)*	*Copolymer composition CHR/100 chain C atoms*
1	3·7	*n*-C_3H_7	71	34	1·8 ± 0·4
2	4·9	*n*-C_3H_7	72	40	2·0 ± 0·4
3	13·1	*n*-C_3H_7	79	37	4·2 ± 0·2
4	13·9	*n*-C_3H_7	60	18	4·6 ± 0·2
5	15·2	*n*-C_3H_7	85	35	6·4 ± 0·1
6	15·1	*n*-C_3H_7	64	53	6·8 ± 0·1
7	17·0	*n*-C_3H_7	69	48	7·7 ± 0·2
8	14·0	C_2H_5	67	55	7·3 ± 0·2
9	2·2	CH_3	73	56	1·2 ± 0·4
10	3·3	CH_3	63	73	2·1 ± 0·2
11	3·9	CH_3	70	69	3·7 ± 0·1
12	5·6	CH_3	83	87	4·5 ± 0·1
13	7·7	CH_3	80	69	5·9 ± 0·3
14	8·7	CH_3	85	58	6·1 ± 0·4

Yields given in the fifth column have been computed from the weight of copolymer isolated and the extent of reaction of the monomers given in column four. For the purpose of this calculation, the two monomers have been assumed to react in proportion to the monomer composition; the actual difference in composition between copolymer and initial reaction mixture has been ignored. Departures from these assumptions are unimportant for the purpose. It is apparent from the yields that extensive decomposition accompanies copolymerization.

Determination of the monomer composition ratio during copolymerization

To the extent that the monomer ratio changes during the course of a copolymerization, a corresponding change in the *average* composition ratio for species formed at different stages of the process may be expected. Thus, constancy of the monomer ratio may be regarded as a condition which must be fulfilled if the co-units are to be distributed equitably over all copolymer species in the final product. Fulfilment of this condition is not sufficient, however, to assure a random distribution of the co-units, as required by the theory with which present results are to be compared. It is possible for concurrent processes to yield copolymer molecules differing in composition. Constancy of the monomer composition, within tolerable limits, is nevertheless a requisite meriting examination.

To this end, the copolymerizing mixture in several of the preparations was sampled throughout the reaction. Each sample was immediately added to excess propionic acid to give a mixture, dissolved in ether, of the methyl and higher propionate ester together with excess propionic acid, and about 0·5 per cent of unidentified products. The mixtures were separated by gas–liquid chromatography on a 9 ft column (15 per cent 'Ucon' on 50–HB–660* substrate) operated at a temperature of 64°C and using helium as the carrier gas at a flow rate of 68 cm^3/min. Results for three polymerizations are presented in *Table 2*. Although the analyses are not

Table 2. Unreacted monomer ratio versus conversion

% *Conversion*	*Methyl : ethyl*	% *Conversion*	*Methyl*:n-*butyl*	% *Conversion*	*Methyl*:n-*butyl*
0	15·3 : 1	0	6·6 : 1	0	6·2 : 1
11	15·5 : 1	12	4·7 : 1	11	5·0 : 1
23	20·3 : 1	26	5·3 : 1	25	6·5 : 1
43	18·5 : 1	79	5·3 : 1	44	2·8 : 1
69	19·5 : 1	—	—	60	8·2 : 1

as precise as might have been desired, they suffice to show that the composition ratios of the unreacted diazoalkane mixtures changed by no more than about 20 per cent over the range of conversion used. Corresponding compositional variations among copolymer species are tolerable for present purposes.

The copolymer composition

The *n*-propyl substituents in the copolymer were determined spectroscopically by observing the relative absorbances at 150°C of the infra-red

*Union Carbide Co.

bands at 1 370 cm^{-1} (methylene) and 1 378^{-1} (methyl) and comparing these with values for the *n*-paraffin hydrocarbons $C_{20}H_{42}$, $C_{28}H_{58}$, and $C_{32}H_{66}$[7]. A Perkin–Elmer model 13 double-beam spectrometer was used. Methyl and ethyl substituents were estimated similarly, except that a correction was applied to compensate for the increased absorbance for a methyl group occurring as a substituent on the main chain rather than as the terminal member of a higher alkyl substituent[8]. Following Reding and Lovell[8], methyl unit absorbances for copolymers with methyl and ethyl substituted co-units ($R=CH_3$ and $R=C_2H_5$) were divided by 1·55 and 1·25 respectively. The methyl content (4·3 CH_3/100 chain C atoms) of an ethylene–propylene copolymer determined in this way was in excellent agreement with the value (4·5 CH_3/100 chain C atoms) obtained using methyl-branched hydrocarbons as calibration standards. This measurement was made by G. A. Tirpak, W. R. Grace and Co., Polymer Chemicals Division. In all cases the copolymers in which $R=n\text{-}C_3H_7$ invariably contained a lower ratio of co-unit than the monomer ratio in the reaction mixture. It proved, in fact, impossible to prepare a copolymer containing more than 8 per cent *n*-propyl substituents, even using much larger monomer ratios.

The distribution of co-units

If, in spite of the approximate constancy of the monomer ratio during copolymerization (*Table 2*), molecules differing materially in composition are formed, these should be amenable to separation by fractional solution. Accordingly, the copolymer containing 6·8 per cent *n*-propyl substituents was fractionated by column elution. The copolymer was deposited on an inert base ('Celite 545') and eluted at 82°C with *n*-butyl cellosolve–xylene mixtures[9]. The results are given in *Table 3*. Viscosities were determined at 135°C in 0·1 per cent decalin solution using an Ubbelohde viscometer.

Table 3

Fraction	*Wt %*	η_{sp}/c $dl\ g^{-1}$	*Composition* $n\text{-}C_3H_7$/100 *chain C atoms*
1	1·9	2·37	6·7
2	3·5	4·81	7·8
3	6·3	10·55	7·3
4	10·8	11·57	7·5
5, 6, 7*	21·8		
8	5·5	12·92	6·7
9, 10, 11*	29·0		
12	5·8	32·19	6·0
13	16·2	20·59	5·8
Unfractionated		20·37	6·8

*These fractions were not characterized.

As is apparent from the tabulated results, separation of the higher fractions was inefficient. Difficulties arising from a tendency of the column to become clogged may have been a contributing factor. The lower reduced viscosity of the last fraction compared to its predecessor, in conjunction with its slightly lower substituent percentage, suggests that composition

may have dominated chain length in controlling solubility in this range. In any case, the variation or composition among the fractions is small. The complete solubility of the copolymer in *n*-butyl cellosolve–xylene mixtures at 82° assures against the presence of measurable quantities of the homopolymer, polymethylene, inasmuch as the homopolymer does not dissolve in pure solvent (xylene) below 100°C.

These results, in conjunction with those of *Table 2*, justify treatment of the products of polymerization as random copolymers.

Crystallization and melting procedures

Conventional dilatometers of the type described by Bekkedahl[10] were used to observe the changes in volume associated with crystallization and melting. To avoid clogging of the 1 mm precision bore capillary tube by molten copolymer, the lower end of the capillary was shaped into a U which was joined to the bottom of the dilatometer bulb. Copolymer strips cut from sheets moulded in a hot plate press were packed into the unsealed bulb, a hollow glass spacer was placed on top of the copolymer, and the bulb was sealed off just above the top of the spacer. The internal volume of the dilatometer varied from 3·5 to 4·5 ml and the weight of copolymer from 1 to 2 g. Before filling with mercury[11] the dilatometer was evacuated for several hours at 150°C to remove air from the copolymer. Although this temperature is above the melting point, no appreciable viscous flow was observed, owing no doubt to the very high molecular weights of these samples. This behaviour is in contrast with that of Marlex–50 which flows readily at this temperature.

The weights of sample and mercury enclosed in the dilatometer having been determined, displacements in capillary level could be converted to changes in specific volume of the sample. The volume within the dilatometer was not measured; hence, the absolute specific volume of the copolymer had to be established independently (cf. seq.).

All samples were crystallized according to a standard procedure. The sample, sealed in a dilatometer as described above, was completely melted by holding it at about 160°C for an hour. It was then brought to the vicinity of the anticipated melting point T_m of the copolymer. It was subsequently cooled in 1° steps, each temperature being maintained for 30 minutes until the onset of crystallization was observed. The sample was then allowed to crystallize at this temperature for two days. The temperature was subsequently reduced in 5° increments, the sample being held at each temperature for periods of two days. When the temperature was about 40° below T_m, the steps were increased to 10°. This procedure was adopted for the express purpose of affording favourable opportunity for incorporation of long sequences of CH_2 units in crystallites of comparable lengths before lowering the temperature to a point where much shorter crystallites are stable and hence become eligible for formation from the molten phase.

The course of melting of the copolymer was recorded by observing the change of volume as the temperature was gradually raised incrementally at intervals of one day. The temperature was increased by 5° to 10° each day up to about 15° below the apparent melting point; thereafter the

increment was decreased to 1° per day. Pre-melting and subsequent recrystallization, characteristic of poorly crystallized specimens, was largely suppressed by adoption of the crystallization procedure and melting schedules described. After each copolymer had melted, it was heated stepwise to about 150°C, and then cooled in a similar fashion to a temperature at least 10° below T_m, but short of the temperature at which crystallization set in. In this way the liquidus was accurately determined and the final stages of melting could be more clearly delineated (see *Figure 2*).

Before carrying out the fairly lengthy dilatometric cycle described above, the approximate melting point of the sample was located using a hot-stage polarizing microscope. This method gave reproducible results. The melting points thus determined, when plotted against the percentage composition, displayed greater scatter than the dilatometric results. The dependence of T_m on copolymer composition was similar, however.

Copolymer 4 (4·6 per cent *n*-propyl substituent) was slowly recrystallized from a 4 per cent solution in benzene. After drying the product, its melting point, determined microscopically, was compared with that of a sample crystallized from the melt according to the procedure set forth above. No difference could be detected. Evidently crystallization of the copolymer from solution does not yield a crystalline morphology of reduced stability, as has been observed for homopolymers[12].

Absolute specific volumes in the liquid state

The absolute specific volumes of liquid polyethylenes have been shown[13] to be independent of the presence and type of branching. Hence, the relationship of the specific volume of polymethylene to temperature should suffice as a reference line for determining absolute specific volumes of all of the various copolymers in the liquid state. Inspection of the literature suggested the desirability of re-examination of this relationship. A special dilatometer was therefore constructed and calibrated for the determination of absolute specific volumes. It was similar in design to that described above, except that it was fitted with a ground glass 14/20 standard taper stopper for filling and closing. This arrangement permitted its repeated use for successive samples. The dilatometer was calibrated with mercury from 50° to 180°C. Results for Marlex–50 and Super Dylan (melt index 3·4) were accurately fitted over the temperature range 140° to 180°C by the linear relationship

$$\bar{v}_l = 1{\cdot}152 + 8{\cdot}8 \times 10^{-4} t \qquad (5)$$

where $\bar{v}_l$ is the specific volume of the liquid polymer at the temperature t expressed in °C. This relationship accords with that of Gubler and Kovacs[13]. The specific volume at 0°C is identical with the value given by Nielsen[14] and by Bueche[15]. These workers reported a somewhat lower value for the expansion coefficient; our result for the expansion coefficient agrees with that of Quinn and Mandelkern[16].

The specific volume of a copolymer (not included in *Table 1*) containing 7·6 mole per cent of *n*-propyl substituent, and determined at 55°C, agreed within 0·5 per cent with equation (5). In view of this result and the observations cited above[13], the use of equation (5) for calculating the liquid

specific volumes of all polymers and copolymers included in this investigation was considered justified. Through its use, results with sealed dilatometers could be converted, when desired, to absolute specific volumes.

Calculation of degrees of crystallinity

Degrees of crystallinity were deduced from measured specific volumes on the assumption of additivity of volumes of the two phases[17], each being assigned its characteristic specific volume for the specified temperature. On this basis, the weight fraction of crystalline phase is given by

$$w^c = (\bar{v}_l - \bar{v})/(\bar{v}_l - \bar{v}_c) \tag{6}$$

where $\bar{v}$ is the measured specific volume of the copolymer; $\bar{v}_l$ is the liquid phase specific volume given as a function of temperature by equation (5); and $\bar{v}_c$ is the specific volume of the crystalline phase, given reliably and with excellent precision by

$$\bar{v}_c = 0{\cdot}993 + 3{\cdot}0 \times 10^{-4} t\,(^\circ\mathrm{C}) \tag{7}$$

This relationship is based on the crystal unit cell dimensions as determined by Cole and Holmes[18] and by Swan[19] from X-ray diffraction measurements over the temperature range from below 0°C to the proximity of the melting point. Their results are well represented by equation (7) for temperatures up to 110°C. The quartic expression proposed by Swan[19] offers no perceptible advantage over the linear equation (7) below 110°C. The accelerated increase in the *a* spacing at higher temperatures, as indicated by Swan's results, occasions inclusion of higher powers of *t*. This range is, however, of little interest here. It is noteworthy also that Bunn's[20] early value of the crystal specific volume of polyethylene at 25°C, namely 1·000 $cm^3\ g^{-1}$, stands in good agreement with more recent work as attested by virtual coincidence with the value calculated from equation (7).

RESULTS AND DISCUSSION

The melting of copolymers, previously crystallized according to the cooling schedule detailed above, is portrayed in *Figure 1*. For simplicity, points are omitted from the curves. As described in the experimental section, the temperature at each point was maintained for one day before proceeding to the next higher temperature. The sigmoidal character of the melting curves is evident. They resemble the curves similarly determined by Mandelkern, Tryon and Quinn[21] for a series of polybutadienes containing varying percentages of the 1,4-*trans* unit, which were appropriately treated as copolymers comprising isomeric units. As in the present experiments, melting takes place over a range of temperature which increases with the proportion of the co-unit. Mergence with the liquidus appears to be gradual and asymptotic.

Figure 2 presents an enlargement of the portion of one of the curves in the vicinity of the melting point. There is no evidence of a discontinuity. This is in accord with theory which, although it predicts a discontinuity, assigns it a magnitude beyond reach of experimental detection. The *theoretical* copolymer melting point T_m refers to this experimentally

inaccessible discontinuity. As a practical measure, we take the temperature at which measurable departure from the liquidus vanishes to be the *experimental* T_m.

Melting points assigned in this necessarily arbitrary manner are presented in *Figure 3* where they are compared with the theoretical melting point relationship. The dashed line representing this relationship has been calculated according to equation (1), taking $\Delta H_u = 970$ cal/mole CH_2 and $T_m^0 = 411{\cdot}7°K$, or $138{\cdot}5°C$[16,17]. The experimental melting points fall considerably below the calculated curves. This observation accords with

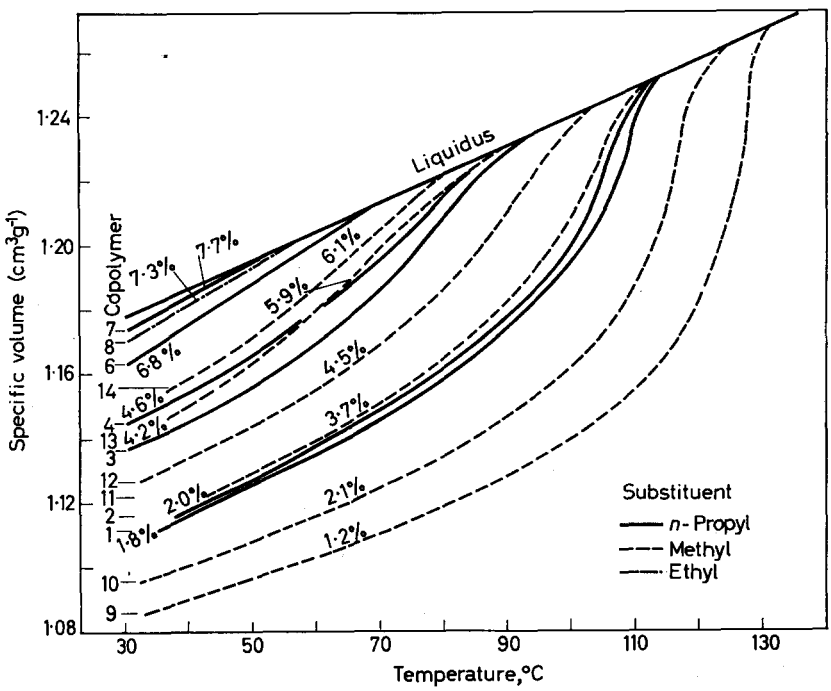

Figure 1—Melting curves for the copolymer series described in *Table 1*

previous results[22,23] on the apparent melting points of various copolymers. It finds partial explanation in the theoretically predicted decrease in the equilibrium degree of crystallinity to a level too low to be detected some number of degrees below the melting point. The difficulty of gathering together the very small proportion of long sequences required for the formation of those crystallites which would, if present, survive up to temperatures approaching the theoretical T_m may be a further factor contributing to the discrepancy.

The melting points for the methyl substituted copolymers are consistently higher than those for the *n*-propyl substituted series; the ethyl substituted copolymer falls on the line for the latter series. The fact that the points for the methyl series do not extrapolate to T_m^0 in the limit of vanishing co-unit concentration indicates that very small quantities of this co-unit have little

effect on T_m. This feature of the phase diagram is at once suggestive of the formation of a solid solution, i.e. of formation of a solid phase which, *at equilibrium*, accommodates the $-\overset{CH_3}{\overset{|}{C}}H-$ co-unit. The steady decrease of

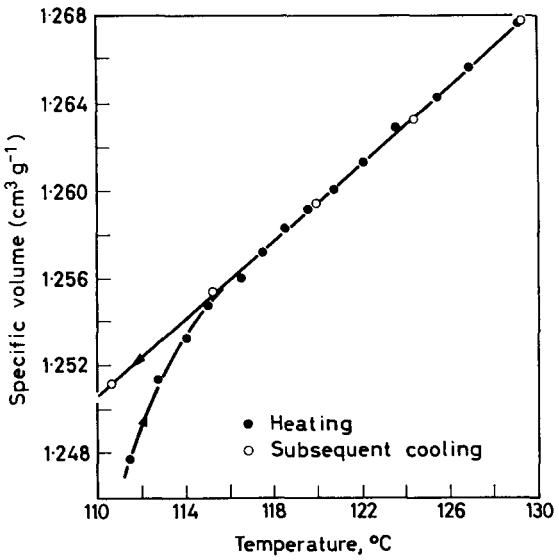

Figure 2—Melting curve and subsequent cooling curve for copolymer 1 in the vicinity of its melting point

T_m with co-unit concentration in the *n*-propyl series, on the other hand, indicates separation of a pure phase. These deductions follow from primary principles of phase equilibria of the utmost generality.

Walter and Reding[24] called attention to increases in unit cell dimensions brought about by branches in polyethylene, and suggested therefore that the lattice may be expanded by incorporation of branched units. Eichorn[25] observed a regular increase in the 110 spacing with the proportion of co-unit in copolymers of propylene with ethylene. Cole and Holmes[18], and more recently Swan[26], have identified the *a* axis spacing as the dimension predominantly affected. These investigators reported similar increases for co-units bearing ethyl, *n*-propyl, *n*-butyl and *n*-amyl substituents. Cole and Holmes[18] found the effect of butyl to differ imperceptibly from that of methyl.

In this latter respect, the results of X-ray diffraction appear to be at variance with our results, according to which only the methyl group enters the crystal lattice to an appreciable degree. It is important to note, however, that the X-ray diffraction measurements were carried out on samples in which the degree of undercooling was sufficient to sanction existence of imperfect crystalline regions, including 'impure' crystallites which accommodate the branched co-units either as defects or in interstitial positions. At higher temperatures, such crystallites would be unstable relative to the melt, and hence should vanish in the vicinity of T_m. If crystallization of

the samples used for X-ray diffraction had been conducted under conditions permitting a higher degree of discrimination in the selection of sequences for crystallization, the extent of incorporation of co-units in the crystal lattice might have been materially reduced. Irrespective of the validity of

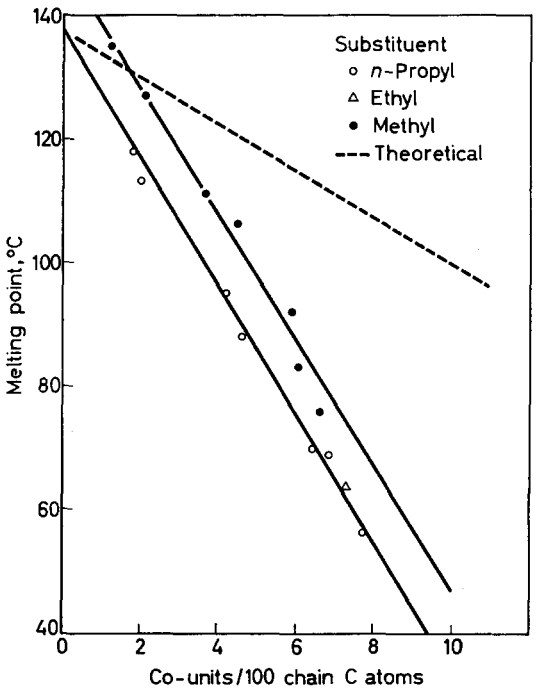

Figure 3—Melting points of the copolymer series as a function of composition. The theoretical values have been calculated from equation (1)

this latter conjecture, the system may differ markedly in its tolerance of co-units in the crystal lattice under the conditions prevailing in the two sets of experiments; in ours the degree of crystallinity is vanishingly small at T_m, whereas the X-ray diffraction studies were conducted at temperatures much farther removed from the melting point and at comparatively high degrees of crystallinity.

A further factor of possible importance in this connection is the decrease in average crystal size[25] with the proportion of co-units. The sizes of the crystallites may of course vary over a wide range for the large undercooling prevailing at room temperature. Not only is the longitudinal (chain axis) dimension reduced by the frequent incidence of co-units; transverse dimensions must be reduced also, as we have pointed out elsewhere[27]. This follows as a consequence of the impedance of lamellar development in copolymers, wherein 'folding' is largely precluded by the infrequent occurrence of two or more acceptable sequences of units in succession along a given chain. Reduction of crystal size introduces a source of error in the X-ray diffraction spacing. Moreover, if the crystallite is sufficiently small, its dimensions may be altered by local stresses of the matrix in which it

is embedded. It is apparent that interpretation of small changes in the X-ray diffraction spacings for copolymers is by no means as unambiguous as might at first sight seem to be the case.

Degrees of crystallinity calculated from the specific volumes using equation (6) are shown in *Figures 4* and *5* for copolymers having R = *n*-propyl and R = methyl, respectively. Results for the ethyl substituted copolymer are included also in *Figure 4*. The dashed lines in this figure

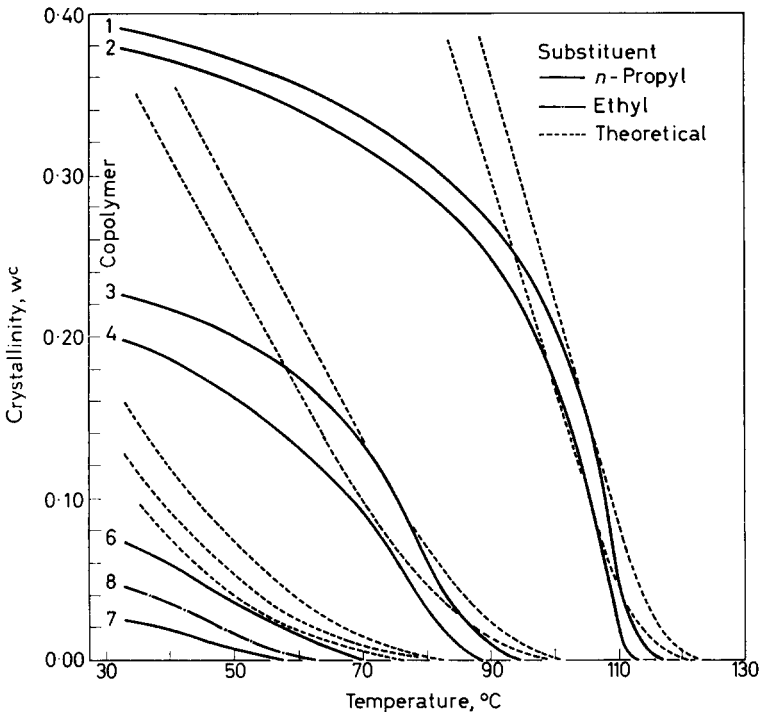

Figure 4—The degree of crystallinity [calculated from the specific volume data using equation (6)] as a function of temperature for the copolymers with *n*-propyl and ethyl substituents. The theoretical curves have been calculated via the equations set forth in the introduction taking $\ln D = -11{\cdot}5$

have been calculated according to the theoretical equations (2) and (3) using a single set of values of the parameters T_m^0, ΔH_u and $\ln D$ for all copolymers. The remaining parameter p is identified with the mole fraction of CH_2 units in each copolymer, in accordance with the assumption of random distribution of co-units. The independently established values of T_m^0 and ΔH_u given above were used in these calculations. For $\ln D$ we have arbitrarily selected the value $-11{\cdot}5$ in order to achieve the best fit with the experimental curves in the temperature ranges where the degrees of crystallinity undergo most rapid changes. The entire set of theoretical curves therefore rests on the choice of this one independent parameter. The shift

of the curves with $1-p$ in *Figure 4* is fairly well represented except for the highest percentage of co-units. To this extent, the theory finds substantial support.

The observed degrees of crystallinity for a given copolymer depart from the theoretical curve at both low and high degrees of crystallinity. The onset of crystallization is displaced to lower temperatures than those predicted by the theoretical curves. As we have suggested above, this departure from the equilibrium theory is attributable to the kinetic difficulty of gathering together those rarely occurring long sequences which are required for formation of stable crystallites at small undercoolings. At higher degrees of crystallization, the experimental line again falls well below theoretical

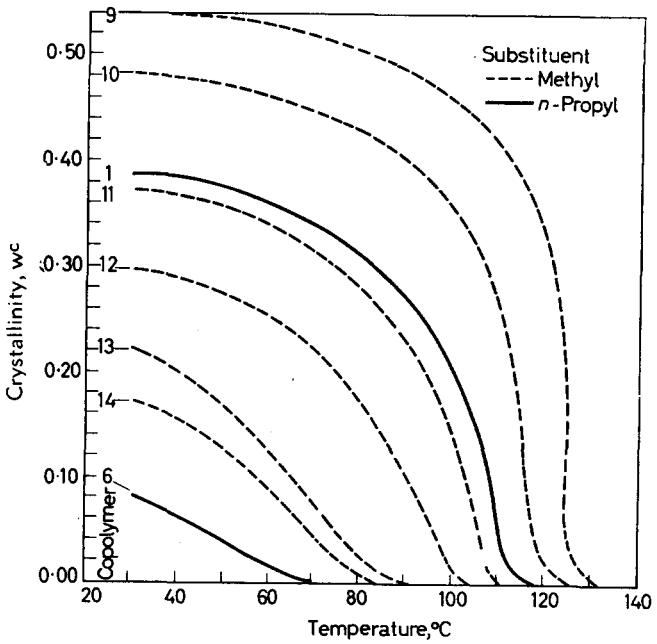

Figure 5—The degree of crystallinity [calculated from the specific volume data using equation (6)] as a function of temperature for the copolymer with methyl substituents. The data for two *n*-propyl substituted copolymers are included for comparison

predictions. Restrictions imposed by crystalline regions previously generated at higher temperatures in the cooling cycle are suggested as responsible for this discrepancy. The interconnections resulting from prior crystallization greatly limit the diffusion of the remaining amorphous sequences. Hence, their collection in a given locality, and their further re-arrangement as required for crystallization, is severely impeded.

In this respect the crystallization of a copolymer (by slow cooling) differs strikingly from the crystallization of a homopolymer. High degrees of crystallinity may be attained in the latter at comparatively low under-

coolings. At an intermediary stage in the transformation, the semi-crystalline (spherulitic) and amorphous regions are sharply differentiated. In the crystallization of copolymers, on the other hand, the more eligible long sequences tend to be selectively crystallized *throughout the sample.* At small undercoolings, transformation proceeds only to a limited degree but all macroscopic elements of the volume participate in the transformation. Each such element is susceptible to further crystallization with lowering of the temperature. Hence, in contrast to the essentially discontinuous transformation of a given region in a homopolymer, crystallization of a copolymer proceeds more gradually, and from a macroscopic standpoint more uniformly. It is thus that processes of re-alignment of chains required for achieving higher degrees of crystallinity are especially susceptible to impedance by previous crystallization in a copolymer.

Our empirical value of $\ln D$ leads to a surprisingly large interfacial free energy σ_e [see equation (4)]. Thus, we find $\sigma_e \simeq 4\,600$ cal mole^{-1} of chains emerging from the 110 surface, cr $\sigma_e \simeq 170$ ergs cm^{-2}. This interfacial free energy should not, of course, be compared to values for non-polymeric crystals; it includes contributions to the free energy associated with dissipation of crystalline order throughout the depth of the interfacial layer. As emphasized in a recent paper[27], the order characteristic of the crystal must be propagated by the emerging chain some distance into the amorphous regions. The situation is further complicated in the case of copolymers owing to the infrequency with which the flux of chains in this region can be diminished by re-entry of a chain trajectory into the crystallite, in consequence of the improbability of occurrence of a second acceptable sequence in close proximity along the same chain. For these reasons, the lamellar morphology believed to prevail in homopolymers where lateral growth of crystallites is unimpeded, probably is suppressed in copolymers.

Mandelkern and co-workers[2] have estimated σ_e for linear polyethylene from the change in the low angle X-ray spacing with temperature of crystallization. Their result, 95 ergs cm^{-2}, is predicated on a melting point $T_m^0 = 137{\cdot}5$°C for the homopolymer. The latter value is unquestionably low. Choice of a value in the more probable range 140° to 145°C would increase their σ_e, bringing it into proximity with our result derived in an entirely independent manner from observations on copolymers. Cormia, Price and Turnbull[28] have recently estimated σ_e for linear polyethylene from observation of the supercooling required for homogeneous nucleation in small droplets of the molten polymer. The probable difference in morphology cited above between copolymers and the homopolymer notwithstanding, their result, 168 ergs cm^{-2}, is remarkably close to our value. The agreement between the results of these quite unrelated methods affords strong support for a large interfacial free energy for the 001 crystal boundary.

The experimental work reported in this paper was carried out at the Mellon Institute, Pittsburgh, Pa. Support of the National Science Foundation under grant NSF–G15051 is gratefully acknowledged.

Department of Chemistry,
Stanford University,
Stanford, Calif., U.S.A.

(Received August 1962)

REFERENCES

[1] FLORY, P. J. *J. chem. Phys.* 1949, **17,** 223
[2] MANDELKERN, L., POSNER, A. S., DIORIO, A. F. and ROBERTS, D. E. *J. appl. Phys.* 1961, **32,** 1509
[3] POLLACK, S. S., ROBINSON, W. H., CHIANG, R. and FLORY, P. J. *J. appl. Phys.* 1962, **33,** 237
[4] FLORY, P. J. *Trans. Faraday Soc.* 1955, **51,** 848
[5] *Organic Syntheses,* Coll. Vol. II, 165 (1943)
[6] BUCKLEY, G. D. and RAY, N. H. *J. chem. Soc.* **1952,** 3701
[7] SLOWINSKI, E. J., WALTER, H. and MILLER, R. L. *J. Polym. Sci.* 1956, **19,** 353
[8] REDING, F. P. and LOVELL, C. M. *J. Polym. Sci.* 1956, **21,** 157
[9] HENRY, P. M. *J. Polym. Sci.* 1959, **36,** 3
[10] BEKKEDAHL, N. *J. Res. Nat. Bur. Stand.* 1949, **43,** 145
[11] MARKER, L., EARLY, R. and AGGARWAL, S. L. *J. Polym. Sci.* 1959, **38,** 369
[12] CHIANG, R., JACKSON, J. B. and FLORY, P. J. Unpublished
[13] GUBLER, M. G. and KOVACS, A. J. *J. Polym. Sci.* 1959, **34,** 551
[14] NIELSEN, L. E. *J. appl. Phys.* 1954, **25,** 1209
[15] BUECHE, F. *J. Polym. Sci.* 1956, **22,** 113
[16] QUINN, F. A. Jr, and MANDELKERN, L. *J. Amer. chem. Soc.* 1958, **80,** 3178
[17] CHIANG, R. and FLORY, P. J. *J. Amer. chem. Soc.* 1961, **83,** 2857
[18] COLE, E. A. and HOLMES, D. R. *J. Polym. Sci.* 1960, **46,** 245
[19] SWAN, P. R. *J. Polym. Sci.* 1962, **56,** 403
[20] BUNN, C. W. *Trans. Faraday Soc.* 1939, **35,** 482
[21] MANDELKERN, L., TRYON, M. and QUINN, F. A. Jr. *J. Polym. Sci.* 1956, **19,** 77
MANDELKERN, L. *Rubber Chem. Technol.* 1959, **32,** 1392
[22] EVANS, R. D., MIGHTON, H. R. and FLORY, P. J. *J. Amer. chem. Soc.* 1950, **72,** 2018
[23] MANDELKERN, L. *Chem. Rev.* 1956, **56,** 903
[24] WALTER, E. R. and REDING, F. P. *J. Polym. Sci.* 1956, **21,** 561
[25] EICHORN, R. M. *J. Polym. Sci.* 1958, **31,** 197
[26] SWAN, P. R. *J. Polym. Sci.* 1962, **56,** 409
[27] FLORY, P. J. *J. Amer. chem. Soc.* 1962, **84,** 2857
[28] CORMIA, R. L., PRICE, F. P. and TURNBULL, D. *J. chem. Phys.* 1962, **37,** 1333

Shear Modulus in Relation to Crystallinity in Polymethylene and Its Copolymers

J. B. JACKSON, P. J. FLORY, R. CHAING* and M. J. RICHARDSON†

Shear moduli of the copolymers of —CH_2— with small proportions of —CHR— described in the preceding paper have been measured over their melting ranges using a low frequency torsion method. The observed moduli exceed by an order of magnitude the values calculated from the theory of rubber elasticity on the assumption that crystallites function as crosslinkages. Dynamic mechanical loss maxima are reported at temperatures which correlate qualitatively with the melting range.

THE results of elastic modulus measurements on the series of copolymers

of methylene —CH_2— units with —CH— co-units, where R = n-C_3H_7 and CH_3, preparation of which was described in the previous paper[1], are presented in this communication. The shear modulus, determined by a low frequency torsion method, has been investigated as a function of the proportion of co-unit over a range of temperatures below the melting point. Samples were crystallized by gradual stepwise cooling in accordance with the procedure applied in the preceding paper dealing with the degree of crystallinity and its dependence on temperature. Hence, results of that paper in conjunction with those presented here permit comparison of the modulus of elasticity with the degree of crystallinity.

Partial crystallization may be considered to confer a network structure on a system of macromolecular chains, with the crystallites performing the function of chemical crosslinkages in conventional networks. The elastic properties of partially crystalline polymers and copolymers have often been interpreted, qualitatively, from this point of view. Inasmuch as the modulus of elasticity of the crystalline regions[2] so greatly exceeds that of the amorphous phase, it is a usually satisfactory approximation to attribute the observed elastic compliance entirely to the latter phase. The stress response of the semi-crystalline polymer is accordingly ascribed to orientation of chains within the amorphous region.

Pursuant to quantitative elaboration of this point of view, the macromolecule may be considered to be subdivided into successions of crystalline and amorphous sequences of units. An amorphous sequence bounded at either end by crystalline sequences which occupy separate and independent crystallites contributes an elastic element to the network comprising macromolecules joined together by crystallites. Deformation of the sample alters the distribution of amorphous chain configurations, much as in a network formed from chemical crosslinkages. On this basis, the modulus of elasticity should depend directly on the number of amorphous chain sequences, or

*Present address: Basic Research Department Chemstrand Research Center, Inc., Durham, North Carolina.
†Present address: National Physical Laboratory, Teddington.

elastic elements[3]. Each crystallite joins a large number of chains in a given locality; its functionality is much greater than that of a chemical cross-linkage. According to theory, however, the elastic equation of state should depend only on the number of chains and not on the functionality of its junctions. Partial justification is thus provided for disregard of the peculiar character of the junctions in semi-crystalline polymers. Hence the number of elastic elements in the amorphous phase can be equated to the number of crystalline sequences, assuming of course that the copolymer molecules are of sufficient length to reduce the number of terminal chains to a negligible level. The present investigation was undertaken for the purpose of exploring the validity of the viewpoint outlined above.

Amorphous sequences which loop back to the same crystallite from which they emerge obviously contribute nothing to the elastic stress (except possibly through entanglements[3]). In copolymers, however, the incidence of back looping of this nature should be rare for reasons cited in the preceding paper, and the problem differs considerably from that in homopolymers where extensive looping may occur under certain conditions[4]. Crystallization in copolymers involves deposition of the longer preferred sequences of crystallizing unit, type A. (It is here assumed that the B units are of such a nature as to be excluded from the lattice characteristic of A.) Qualitatively, after deposition of a preferred sequence of A units, the formation of a loop or fold requires the presence of a second uninterrupted run of units of the same length immediately following the loop. The probability of two such sequences being found in close proximity in a single chain is low. More likely, the required sequence will be found in a neighbouring chain. When such a number of A units does occur farther down the same chain it will most probably participate in another crystallite. Hence, repetitive participation in the same chain in a given crystallite can rarely occur in a copolymer. A detailed discussion of this subject has been given elsewhere[4].

The number ν^c of crystalline sequences may be calculated according to theory[5] previously developed along the lines described in the preceding paper[1]. The relevant equations are:

$$\nu^c/N_A=(1-p)^2p^{\xi\star}[(1-p)^{-1}-(1-e^{-\theta})^{-1}] \tag{1}$$

and

$$\xi\star=-\{\ln D+2\ln[(1-p)(1-e^{-\theta})^{-1}]\}(\theta+\ln p)^{-1} \tag{2}$$

where N_A is the number of A units in the random copolymer; other quantities are defined in the preceding paper[1]. According to the theory of rubber elasticity the shear modulus (real part) is[6]

$$G=(\nu/V)(\langle r^2\rangle_i/\langle r^2\rangle_0)\,kT \tag{3}$$

where ν/V is the number of network chains in the volume V, $\langle r^2\rangle_i$ is the mean-square chain displacement length in the absence of strain imposed by an external stress, and $\langle r^2\rangle_0$ is the value of the same quantity for the free chains unconstrained by the network junctions, which in this case consist of crystallites. The ratio $\langle r^2\rangle_i/\langle r^2\rangle_0$ evades evaluation for the systems here considered; we are obliged therefore to adopt the approximation $\langle r^2\rangle_i=\langle r^2\rangle_0$, which may in fact introduce appreciable error. With

the further identification of the number ν of amorphous chains with the number ν^c of crystalline sequences, on the basis set forth above, we have

$$G = kT(\nu^c/N_A)/V_u \tag{4}$$

where V_u is the volume occupied by an A unit.

The assumption underlying equation (1), according to which each sequence of A units (—CH_2—) enters into at most a single crystallite, assumes dominant importance with reference to the present application of theory. Other limitations on the application of the statistical thermodynamic (equilibrium) theory are discussed in the previous paper. Reiterating briefly, these deviations appear to arise from kinetic limitations on attainment of the state of equilibrium envisioned by the theory. At temperatures approaching T_m only long A sequences are eligible for stable crystallite formation. Hence the difficulty of assembling a sufficiency of such long sequences at a given locality suppresses the degree of crystallinity below theoretical prediction. At large undercoolings diffusional displacements of residual amorphous sequences are severely restricted by prior crystallization of other sequences in the same molecule. Within the range of intermediate degrees of crystallinity where approximate agreement between theory and experiment is achieved through arbitrary choice of the parameter D, the theory may for purposes of this paper be regarded as a device for relating the number of elastic elements (amorphous sequences) to the degree of crystallinity.

A further consideration, implicit in the interpretation set forth above, is the assumed invariance with strain of the network structure joined by crystalline crosslinkages. Any increase or decrease in the degree of crystallinity with strain must be reflected in the elastic properties. Thus, it is essential to bear in mind that changes of degree of crystallinity with strain may contribute to the elastic compliance.

Previous studies[7–9] of mechanical properties of polymethylene have dealt in detail with the temperature dependence of the elastic modulus as a means of elucidating the second and higher order transitions. The few data for 'branched' polymethylenes[8,9] relate principally to methyl substituents and these are atypical, as discussed in the preceding paper, owing to the ability of the polymethylene lattice to accommodate them. In this investigation we have attempted to cover more systematically a range of concentration of co-units where the copolymer is still both partially crystalline and the distribution of co-units random.

EXPERIMENTAL

Samples used in this investigation are listed in *Table 1*. Two linear polymethylenes* were included for examination, the first being an unfractionated Marlex–50 sample (mol. wt = 80 000). and the second a fraction from a Marlex–50 sample (mol. wt = 490 000). Compositions of the copolymers selected for investigation of the modulus/temperature relationship are taken from the preceding paper[1]. Degrees of crystallinity given in the last column of *Table 1* have been calculated from the specific volume at 30°C.

*Further data on these two samples have been given in ref. 10. They correspond to the unfractionated Marlex–50 and the last Marlex–50 fraction, respectively, of ref. 10, Table 1.

Table 1. Polymer and copolymer samples

Sample	*Co-unit substituent* R	*Copolymer* composition* CH · R/100 *chain* C *atoms*	% *Crystallinity at 30°C*
Linear polymethylene, whole Marlex	None		83·3
Linear polymethylene, Marlex fraction	None		76·8
Copolymer 1	n-C_3H_7	1·8	41·0
Copolymer 3	n-C_3H_7	4·2	23·4
Copolymer 5	n-C_3H_7	6·4	10·0
Copolymer 9	CH_3	1·2	55·4
Copolymer 10	CH_3	2·1	50·0
Copolymer 12	CH_3	4·5	30·9
Copolymer 14	CH_3	6·1	17·1

*cf. ref. 1, Table 1.

The required test specimens for modulus measurements were pressed in a small metal mould forming thin rectangular strips approximately 0·05 in. × 0·25 in. × 2 in., the thickness being determined by the amount of copolymer. The mould was filled and placed in a large glass tube which was evacuated and heated in an oil bath to about 160°C. After several hours of continued evacuation, the tube was sealed off the vacuum line and transferred to a thermostat bath. The determination of the initial holding temperature, i.e. the highest practicable crystallization temperature for the particular sample, and the subsequent cooling cycle have been described in the preceding paper[1]. After removal from the mould the dimensions of the sample were carefully measured before suspending it from the torsion pendulum.

Shear moduli were determined using the torsion pendulum described by Nielsen[11]. The sample was enclosed in a glass envelope continually flushed with a slow stream of dry nitrogen, and mounted in a thermostat bath controlled at the desired temperature ±0·1°C. Measurements were carried out from room temperature to the melting point of each sample. It was deemed unnecessary to extend the determinations to lower temperatures, inasmuch as the degrees of crystallinity show little change with temperature with further cooling.

The dynamic shear modulus G was calculated from the period T of the torsion pendulum, its moment of inertia I, and the sample dimensions, according to the relationship

$$G = 64\pi^2 Il/cd^3\mu T^2 \tag{5}$$

where l, c and d are the length, breadth and thickness respectively, of the sample, and μ is a shape factor. Following the procedure set forth by Nielsen[11], we have used the values of μ computed by St Venant[12] as a function of c/d.

A slow stepwise heating schedule was followed to obtain the modulus as a function of temperature, each successive temperature being maintained for 24 hours. Up to 40° below the melting point, the temperature was raised in increments of 10°; 5° steps were adopted over the next 30°;

thereafter the temperature was increased in 1° increments, and measurements continued until the sample ruptured. In a few cases reversibility was tested by decreasing the temperature in similar steps. In these instances the operation was reversed a few degrees below the melting point to prevent breakage of the strip due to the low crystallinity remaining just below the melting point. Moduli observed as the temperature was decreased agreed closely with those found with ascending temperature.

The characteristic frequencies covered in a typical experiment from room temperature to the melting point were usually in the range 0·25 to 0·01 c/s, this being the natural frequency span for the instrument with the samples investigated.

RESULTS

The principal experimental data are summarized by the upper set of curves in *Figure 1*. Individual points have been omitted from most of the curves in the interest of clarity. As previously noted, the curves are well reproduced upon lowering the temperatures in incremental stages.

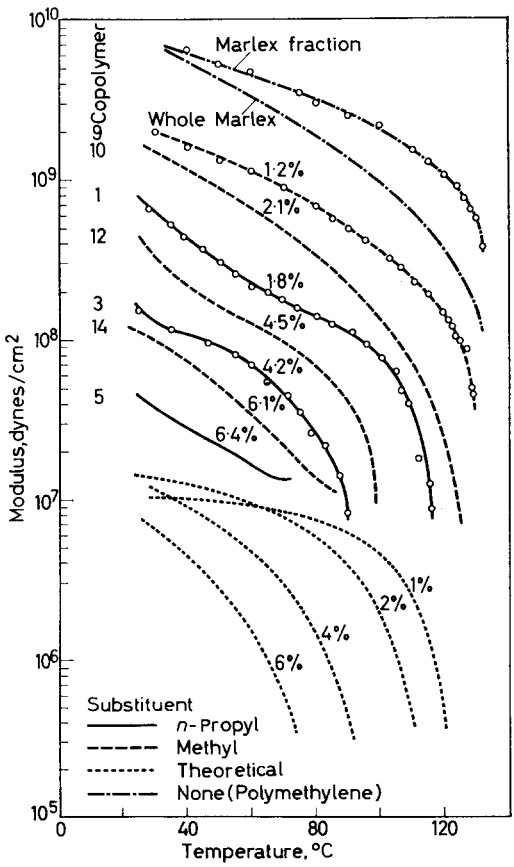

Figure 1—Shear moduli as functions of temperature for the homopolymers and copolymers listed in *Table 1*. Experimental points are omitted from most of the curves in the interest of clarity. The theoretical curves have been calculated via the equations set forth in the introduction

Polymethylene

The two curves at the top of *Figure 1* represent the fractionated and unfractionated homopolymers, respectively. As expected the fraction displays a higher modulus throughout the range of these measurements. The polydispersity of the unfractionated polymer is known to be great. Constituents of quite low molecular weight are included in substantial amount; hence, the number average molecular weight is much lower than that of the fraction. The melting range of the whole polymer is consequently broader than that of the fraction[10]. At temperatures approaching the melting point the degree of crystallinity is reduced by the presence of low molecular weight constituents. However, as the temperature is lowered, the same constituents, being less restricted by attachments to crystalline regions, are capable of raising the degree of crystallinity above that for the fraction[10,13], as is recorded in the last column of *Table 1*. This enhanced degree of crystallinity is not reflected correspondingly in the modulus, which does, however, approach that of the fraction at the lowest temperature of measurement. Low molecular weight constituents evidently are comparatively less effective than longer chains in contributing to the elastic modulus through crystallization. This is in accordance with expectation.

Copolymers

The copolymer curves in *Figure 1* are remarkably similar in shape to those for the homopolymers considered above. They are displaced downward, i.e. their moduli are lower, and the accelerated decrease in the modulus sets in at lower temperatures in accordance with their lower melting ranges[1]. At higher concentrations of co-unit the degrees of crystallinity are sufficiently suppressed to render the copolymers rubber-like even at room temperature. Such copolymers do not therefore exhibit the precipitous drop of modulus with temperature which is characteristic of the homopolymer and of copolymer containing smaller proportions of the co-unit. In all cases the observed shear moduli are much greater than those calculated from equations (1) and (2), as shown by the lower set of curves in *Figure 1* (cf. seq.).

The elastic moduli of copolymers bearing methyl substituents are higher than those for the *n*-propyl substituted copolymers. This is in accordance with the results presented in the previous paper which leads to the conclusion that the methyl substituent group, unlike the *n*-propyl homologue, may be incorporated in the crystal lattice even under equilibrium conditions. The higher moduli of the former copolymers are consistent with their higher degrees of crystallinity resulting from the tolerance of the crystal lattice for the methyl substituent.

Dynamic damping

In the course of carrying out the dynamic modulus determinations, the damping was also recorded. Although not germane to the primary objectives of this investigation, the data are nevertheless of interest. The main feature is the presence of a maximum in the damping, expressed as the logarithmic decrement, which occurs within the temperature range of melting (compare

Figures 4 and 5 of ref. 1). Maxima were not observed for copolymers containing larger percentages of the $-\overset{C_3H_7}{\overset{|}{C}}H-$ unit. In these cases the maxima are presumed to have been displaced below the temperature range of the measurements. Curves for these copolymers are therefore omitted from *Figure 2*. Loss maxima in the interval from −20° to 70°C have been cited previously[8] as being characteristic of branched polyethylenes and of copolymers of $-CH_2-$ with $-\overset{R}{\overset{|}{C}}H-$ where R is alkyl.

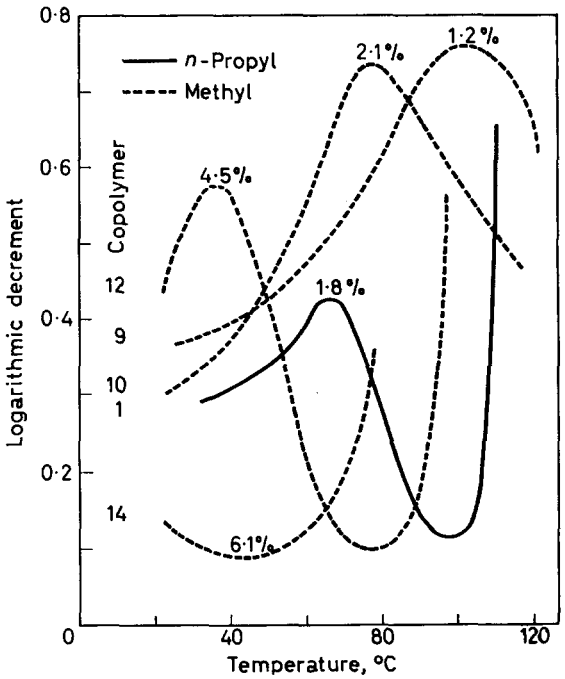

Figure 2—Variation of logarithmic decrement with temperature for several copolymers

The positions of the maxima in *Figure 2*, far from being characteristic of the substituent group, depend markedly on composition. They correlate qualitatively with the melting ranges of the respective copolymers. Both methyl and propyl substituted co-units conform to this correlation. The former melt higher at the same composition as previously noted; the maxima in their damping curves are similarly displaced. These observations suggest crystallization and melting, induced by the deformation cycle, as the mechanism responsible for the mechanical losses in the temperature range here considered. Within the neighbourhood of a given crystalline region the balance between crystallization and melting processes will depend in general on the strain. Inasmuch as these processes are time dependent they must contribute in some degree to the mechanical losses. A mechanism of this nature is unrelated to a glass-type transition. The possibility of error

arising from attribution of all loss peaks observed in semi-crystalline polymers and especially in copolymers to glass transitions is implicit in these considerations.

DISCUSSION

The theoretical curves appearing in the lower portion of *Figure 1* have been calculated taking $\ln D = -11{\cdot}5$ as found from analysis of the degrees of crystallinity presented in the previous paper[1]. These curves are fairly insensitive to the precise value of this parameter; e.g. choice of a much different value $-8{\cdot}0$ raises the calculated modulus only about ten per cent in the higher range of each curve. This calculation of the modulus takes no account of possible effects of the crystalline regions other than their function in joining elastic chains to one another. The crystallites may be expected to act as rigid inclusions in an elastic medium, their elastic compliance being negligible compared with that of the surrounding amorphous matrix. This secondary effect of the crystallites must depend not only on their volume fraction but also on the geometric shapes of the crystalline lattice and their dispersion in the surrounding medium. Estimates made on the assumption that they are uniformly dispersed, and with neglect of their probable asymmetry of shape suggest that observed moduli may be altered by factors of three or four at the higher degrees of crystallinity ranging up to 40 per cent at 30°C for samples having about two per cent of co-unit; the correction factor is much less severe at lower degrees of crystallinity. Even with allowance for this further contribution of the crystallites to the shear modulus, the residual discrepancy between theory and experiment approximates one order of magnitude.

Newman[14] has reported an attempt to correlate the shear modulus of isotopic polypropylene determined using a torsion pendulum with that calculated via the above theory. Similar results were obtained in that calculated values were one or two orders of magnitude below experimentally determined moduli. Also mentioned in this paper[14] is a private communication from Neilsen who observed similar behaviour for ethylene copolymers.

In quest of the basis for the discrepancy the following factors have been considered: (*1*) departure of the dynamic shear modulus from its value (under static equilibrium) to which the theoretical equations refer, (*2*) propagation of crystalline order into amorphous regions surrounding the crystallites, with consequent restrictions on configurational rearrangements of chains, (*3*) interactions between crystallites, either through mechanical interlocking at higher degrees of crystallinity or through regions of mesomorphic order persisting between neighbouring crystallites. Only the first of these should prevail at low degrees of crystallinity and it is highly improbable that it alone would account for the magnitude of the discrepancy observed.

The results of this investigation cast doubt on the adequacy of the basic premises underlying the treatment of the elastic properties of semi-crystalline polymers by analogy with ordinary networks consisting of polymer chains *in random configurations* joined one to another by *chemical bonds* which do not otherwise perturb the statistical array.

Selective crystallization of the more eligible sequences may impose severe departures from a state of randomness in the configurations of the amorphous chains in the state of null macroscopic strain. If many of the chains are highly distended on this account, the elastic response of the system to deformation will be increased. Secondly, the crystallites in the 'networks' here considered introduce interfaces which are impenetrable to the elastic elements of the structure (i.e. to the amorphous chains), and which have no counterpart in ordinary networks. The effect of the presence of such interfaces on the statistical properties of the network as they relate to its elasticity are difficult to assess, but it is well known that they markedly limit the configurations otherwise possible. Hence an increase in the modulus on this account is also to be expected.

Support of the Air Force Office of Scientific Research under grant AF-AFOSR 62-131 is gratefully acknowledged.

Department of Chemistry,
Stanford University,
Stanford, Calif., U.S.A.

(*Received August 1962*)

REFERENCES

[1] RICHARDSON, M. J., FLORY, P. J. and JACKSON, J. B. *Polymer, Lond.* 1963, **4,** 221
[2] TRELOAR, L. R. G. *Polymer, Lond.* 1960, **1,** 95
[3] FLORY, P. J. *Principles of Polymer Chemistry,* p 470. Cornell University Press: Ithaca, N.Y., 1953
[4] FLORY, P. J. *J. Amer. chem. Soc.* 1962, **84,** 2857
[5] FLORY, P. J. *Trans. Faraday Soc.* 1955, **51,** 848
[6] FLORY, P. J. *Trans. Faraday Soc.* 1961, **57,** 829
FLORY, P. J. *J. Amer. chem. Soc.* 1956, **78,** 5222
[7] OAKES, W. G. and ROBINSON, D. W. *J. Polym. Sci.* 1954, **14,** 505
HELLWEGE, K. H., KAISER, R. and KUPHAL, K. *Kolloidzschr.* 1956, **147,** 155
DEELEY, C. W., KLINE, D. E., SAUER, J. A. and WOODWARD, A. E. *J. Polym. Sci.* 1958, **28,** 109
BUCHDAHL, R., MILLER, R. L. and NEWMAN, S. *J. Polym. Sci.* 1959, **36,** 215
SCHMIEDER, K. and WOLF, K. *Kolloidzschr.* 1952, **127,** 65
[8] WILLBOURN, A. H. *Trans. Faraday Soc.* 1958, **54,** 717
[9] KLINE, D. E., SAUER, J. A. and WOODWARD, A. E. *J. Polym. Sci.* 1956, **22,** 455
[10] CHAING, R. and FLORY, P. J. *J. Amer. chem. Soc.* 1961, **83,** 2857
[11] NIELSEN, L. E. *Rev. sci. Instrum.* 1951, **22,** 690
NIELSEN, L. E. *J. appl. Phys.* 1954, **25,** 1209
[12] ST VENANT. 'De la Torsion des Prismes'. Extract from Chapter IX Tome **XIV,** *Mém. Acad. Sci., Paris,* 1855
[13] TUNG, L. H. and BUCKSER, S. *J. phys. Chem.* 1958, **62,** 1530
[14] NEWMAN, S. *J. Polym. Sci.* 1960, **47,** 111

The Constant Pressure Dynamic Osmometer

I. C. McNeill

The trend in osmometer design has been towards large membrane areas and small capillaries. It is suggested that this results in serious deficiencies and that a more satisfactory design is one in which the membrane area is very small and the pressure-measuring tubes are wide. Such an instrument approaches osmotic equilibrium so slowly that over short periods of time the observed head is almost constant, and thus the net rate of transfer of solvent across the membrance is constant. The design and operation are described of an osmometer in which osmotic pressures of polymer solutions are calculated from measurements of the rate of solvent diffusion at a constant hydrostatic pressure. Results are given for six polymethyl methacrylate and three polystyrene samples which compare favourably with results for the same polymers obtained using other osmometers. The osmometer described is much less subject to polymer diffusion; it is very simple, robust, easy to use, and results are obtained rapidly. The advantages and disadvantages of the osmometer, compared with conventional osmometers, are discussed.

ALTHOUGH it is possible to measure the equilibrium pressure difference in the capillaries of an osmometer to $\pm 0{\cdot}005$ cm of solvent, or better, it has become abundantly clear in recent years[1–8] that the true accuracy in determining the osmotic pressures of polymer solutions is very much poorer than this: because of practical difficulties, equilibrium pressures have been found to be reproducible to only 0·1 to 0·2 cm of solvent using the same solution, the same osmometer, and the most careful technique[3]. Furthermore, the equilibrium pressure may differ very considerably from the true osmotic pressure of the solution for polymers of number-average molecular weight 100 000 or less, particularly for polydisperse materials, depending on the choice of membrane material. The latter discrepancy, rather than the reproducibility (which is adequate for many purposes), has been the major disadvantage of the osmotic method for determining the molecular weights of polymers.

It is arguable that most of the practical difficulties encountered in osmometry, and particularly the low accuracy of the method for molecular weights below 100 000, are due not only to the limitations of available membrane materials, but also to deficiencies in osmometer design which arise from the premise that the ideal osmometer is one in which osmotic equilibrium is established as rapidly as possible. In support of this contention, it is necessary to consider briefly the main sources of error in osmotic measurements. These are,

(1) *Use of fine capillaries* ($< 0{\cdot}1$ cm diameter)

Traces of grease or dust particles can obstruct free movement of the

solution. Slight differences in bore can cause significant differences in capillary rise.

(2) *Mechanical leaks*

In any osmometer leakage might occur between the membrane, the gasket holding it in place and the cell. Instruments with fine capillaries, however, must have additional tubes for filling and removing solution and solvent. The seals between these tubes and the cell are potential sites for leakage. The greater the size of the membrane, the greater the possibility of a leak due to some mechanical imperfection in the membrane.

(3) *Variation in asymmetry pressure*

With solvent only in the osmometer, the observed difference in level in the capillaries at equilibrium should be zero. In practice pressures of $+0{\cdot}1$ cm to $-0{\cdot}1$ cm are usually observed. Duplicate determinations of asymmetry pressure can differ by up to $0{\cdot}1$ cm.

(4) *Membrane movement*

If the pressure on the membrane changes by several centimetres in the course of a determination, the membrane may shift its position slightly, causing a disturbance of the levels. Osmometers are always designed to minimize this effect, but it is impossible to support the membrane over its entire area.

(5) *Bubble formation*

If an air bubble becomes trapped inside the osmometer cell during filling, highly erratic results may be obtained. In some osmometers it is not possible to see into the cell at all; in others one cannot see very clearly, so that it is not always possible to detect the presence of a bubble visually. The greater the number of points of entry into the cell, the greater the number of potential sites for a bubble to be trapped.

(6) *Polymer diffsion*

Osmometer membranes are not ideally semipermeable and if a polymer contains even a small proportion of material able to diffuse through the membrane serious errors result. Diffusion will be greater the larger the membrane area and the longer the time of measurement.

These difficulties in osmotic measurements have been discussed in greater detail by several authors[3,7].

The trend in osmometer design has been towards the largest convenient membrane area and the smallest practicable capillary bore, with the object of reducing the time of measurements. Large area and small bore are, however, precisely the factors leading to the difficulties (1), (4) and (6) and leading indirectly, from the design of the osmometer, to (2) and (5) also. It is logical to argue, therefore, that an osmometer with a very small membrane area and wide 'capillaries' would give results less subject to error from the causes listed. To operate an instrument of this type by the static equilibrium method[3] would clearly be impracticable since

it would take weeks or months to attain equilibrium. Dynamic measurements[3,7,9] of the type commonly carried out with the Fuoss–Mead[9] or Pinner–Stabin[10] instruments would also be inconveniently slow. The osmometer proposed has, however, one unique feature: over short periods of time (1 to 2 hours) the hydrostatic pressure is almost constant and thus the net transfer of solvent across the membrane occurs at an effectively constant rate. If the rate of diffusion can be measured with sufficient accuracy, the osmotic pressure of the solution can be calculated. The design, construction and use of a simple instrument based on this principle are described subsequently.

MEASUREMENTS OF SOLVENT DIFFUSION

Previous determinations of osmotic pressures from rates of solvent diffusion have been based upon extrapolation to zero rate of data obtained at various hydrostatic heads[3,11–14]. The osmotic pressure is then equal to the hydrostatic pressure.

An alternative approach consists of comparing the rates of diffusion (measured by the small decrease in hydrostatic head with time) at the same hydrostatic head when the osmometer is filled in turn with pure solvent and with the polymer solution. If these rates are R_0 and R cm/h, respectively, and the head is H cm, then

$$R_0 = kH$$

and

$$R = k(H - \pi)$$

where k is a constant depending upon tube bore, membrane area and membrane permeability, and π cm is the osmotic pressure of the solution. π may therefore be calculated readily from R_0 and R.

EXPERIMENTAL

Design of the constant pressure dynamic osmometer

The membrane is of small area and it is convenient to mount it horizontally. Since wide measuring tubes are employed, one of these also serves for filling and emptying the osmometer. An instrument of the utmost simplicity is therefore possible (*Figure 1*). The glass cell of the osmometer is constructed from a standard Quickfit flat flange (FG 15) drawn down near the flange and joined to a length of 2·5 mm precision bore tubing*, which in turn is joined to a filling cup of wider bore. A reference tube of 2·5 mm precision bore is provided to enable the correction for capillary rise to be made. The membrane, which has an outer diameter of 35 mm and a working diameter of 15 mm, is held in place across the flange by means of a Teflon gasket and two circular brass plates secured by bolts. Solvent is contained in the outer cylindrical jacket which is provided with a glass lid. The osmometer cell requires 4 to 5 ml of solution and a minimum of 20 ml of solvent is required in the outer jacket.

The osmometer was rigidly supported in a thermostat at 25° ±0·005°C.

*In more recent work 2·0 mm precision bore tubing has been found preferable.

A cathetometer (Precision Tool and Instrument Co. Ltd) with 50 cm column and lenses giving a focal length of approximately 15 cm was used. Both thermostat and cathetometer were placed on the same rigid, vibration-free bench. With suitable illumination giving very sharp images of the menisci, it was possible to read the position of each level to the nearest 0·001 cm without any difficulty.

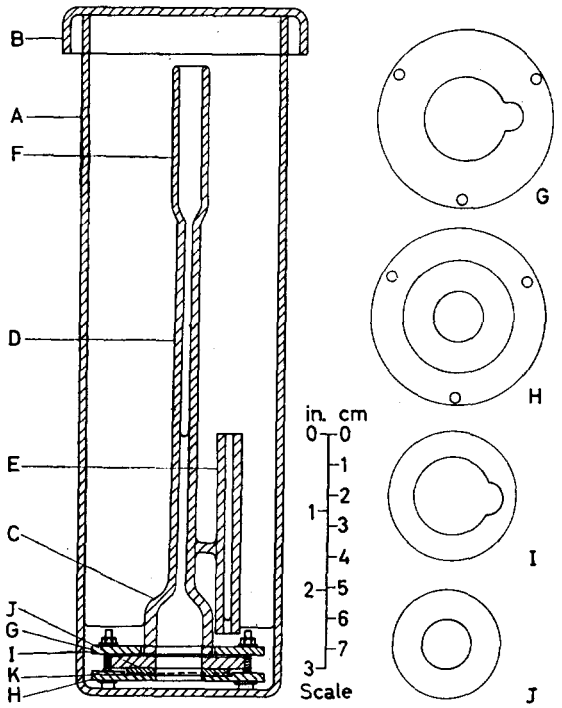

Figure 1—The constant pressure dynamic osmometer. (Key: A outer jacket of osmometer; B glass lid; C osmometer cell, based on 'Quickfit' flat flange FG 15; D measuring tube, 2·5 mm precision bore tubing; E reference tube, 2·5 mm precision bore tubing; F filling cup; G upper securing plate, brass; H lower securing plate, brass, with rebate for membrane; I polythene washer; J Teflon gasket; K membrane)

Polymer samples

Six samples of polymethyl methacrylate were prepared by polymerization in a high vacuum of carefully purified monomer (I.C.I. Ltd) at 60° (80° for sample D3) in 50 per cent, dried, AR grade benzene solution, using azobisisobutyronitrile as initiator. Polymerizations were carried to ten per cent conversion, after which the polymers were isolated by precipitation with methanol. The polymers were purified by reprecipitation from AR benzene solution with methanol. They were dried under vacuum and finely powdered.

Three pure, unfractionated polystyrenes of known molecular weight were kindly supplied by Dr N. Grassie. The molecular weights of these polymers had been determined in benzene solution using a modified Fuoss–Mead osmometer with gel cellophane membrane, by the static equilibrium method.

Membrane conditioning

'PECEL' 600 grade cellophane membranes (35 mm diameter) supplied by Polymer Consultants Ltd, were used in the constant pressure dynamic

osmometer and in the Pinner–Stabin osmometer. The membranes, initially packed in aqueous acetone, were conditioned by soaking for 12 h in each of the following baths, prior to storage in benzene: 100 per cent acetone, 33 per cent benzene–acetone, 66 per cent benzene–acetone, and 100 per cent benzene. The solvent permeability constant[3,8] for these membranes was of the order of 2×10^{-4} h^{-1}. Subsequent experiments have shown that Sylvania 300 grade cellophane membranes, conditioned in the same way, have higher solvent permeability without being less retentive to polymer.

Molecular weights using the Pinner–Stabin osmometer

The molecular weights of the six polymethyl methacrylate samples were determined in AR benzene solution using a Pinner–Stabin osmometer supplied by Polymer Consultants Ltd. Pinner's technique was used[15]. The results of these measurements are shown in *Figure 4* and in *Table 1*.

Table 1. Results of molecular weight determinations for polymethyl methacrylate samples

Polymer	*Molecular weight by*	
	Pinner–Stabin osmometer	*constant pressure dynamic osmometer*
D 7	486 000	460 000
D 6	316 000	316 000
D 4	224 000	230 000
D 2	131 000	126 000
D 1	116 000	97 000
D 3	33 000*	28 000

*Result after correction for solute diffusion.

The data for sample D3 have been corrected for solute diffusion by a linear extrapolation to the time of filling the osmometer of the plot of head versus time after a constant decay rate had been established. This method of correction has been demonstrated to be unreliable when 'fast' membranes are used[8,16], but has been employed by recent workers[17] using slower membranes. The results to be discussed below suggest that in the present work, with slow membranes, the correction is inadequate.

Preparation of polymer solutions

A stock solution of polymer, containing 1·3 to 1·5 g/100g solution, was first prepared in 50 ml AR benzene; dilutions of this solution were made by weighing a suitable quantity, making the volume up to about 15 ml with benzene, and reweighing.

Filling the osmometer

Solutions and solvent were preheated to 25° before use in the osmometer. The solvent in the outer jacket was changed first; the osmometer cell was then filled by using a hypodermic syringe, the 8 in. long plain-ended needle of which was inserted through the filling cup and measuring tube. It was emptied by a similar method. After two rinses with 3 ml portions of the solution to be used, each portion being left in the osmometer for two

minutes, the cell was filled to the desired level, which could be adjusted readily by adding or withdrawing liquid with the syringe. None of these operations requires the osmometer to be moved from its normal position in the outer jacket.

The trapping of air bubbles in an osmometer is a problem which arises from time to time with most types. It will be noted that the design of this instrument makes it impossible for a bubble to become trapped inside the cell: any bubble present must rise up the measuring tube and thereby escape. It is possible for bubbles to be trapped underneath the osmometer when the solvent in the outer jacket is changed. These are immediately obvious to the eye and are readily displaced.

The hydrostatic pressure at which the osmometer is used can be varied as desired. Selection of a constant value for all experiments is advantageous, however, since it removes a variable factor. In all the measurements subsequently described a hydrostatic pressure of $6 \pm 0{\cdot}2$ cm was employed. The time allowed for thermal equilibrium, and equilibrium between the membrane and the solution, to be established, was also kept strictly standardized. Readings were commenced 50 minutes after filling the osmometer.

Measurement of rate of solvent diffusion

Initial readings were made of the liquid levels first in the reference tube and then in the measuring tube. Readings of the level in the measuring tube were then made at regular time intervals chosen such that the fall between readings was appreciable. Since only the fine adjustment of the

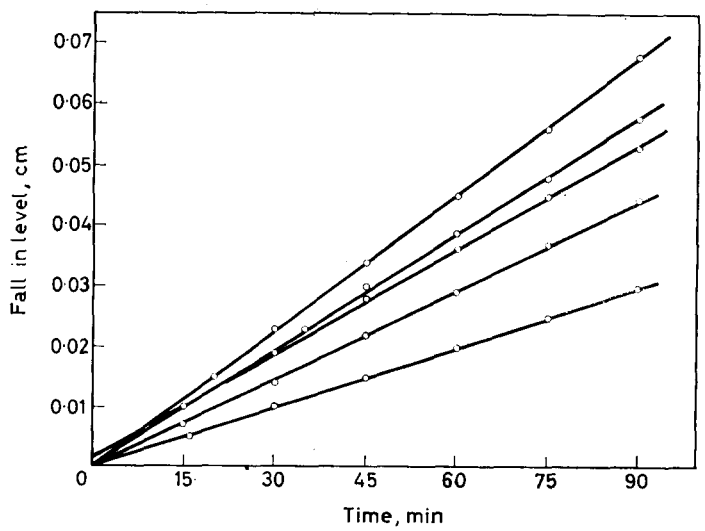

Figure 2—Typical rate plots obtained with the constant pressure dynamic osmometer. Polymethyl methacrylate sample D1. The plot with greatest slope is for solvent and the remaining plots are for the polymer solutions, the most concentrated solution giving the plot of least slope

cathetometer was touched during these readings, each one could be made with confidence to the nearest 0·001 cm. It is of course essential that the osmometer, thermostat and cathetometer should not be subjected to movement of any kind or vibration during the series of readings. A simple source of error which might be overlooked is to rest the elbows on the bench while reading the cathetometer. After at least six readings of the level in the measuring tube the level in the reference tube, which undergoes very little change, was again noted. The fall in level in the measuring tube (or, less commonly, when the osmotic pressure is greater than the hydrostatic pressure, the rise in level) with time was plotted. In all cases the plots obtained were linear with very little scatter, and the slopes, giving the rates of diffusion in cm/h, could be determined unambiguously (*Figure 2*). The total fall in any one such determination was 0·03 to 0·10 cm and the mean hydrostatic pressure during the fall was obtained by taking the mean of the two readings of the reference tube and subtracting this value from the reading of the measuring tube half way through the experiment.

Determination of molecular weights

The osmometer was first conditioned to the polymer being used by filling it with a portion of the most concentrated solution and allowing it to stand overnight. On the following morning the osmometer was emptied and (after two rinses as described above) refilled with solution of the same concentration. The hydrostatic pressure was adjusted to $6 \pm 0{\cdot}2$ cm and the rate of diffusion was determined (after allowing 50 minutes for equilibration) as described previously. This procedure was repeated for the remaining solutions, in order of decreasing concentration, and finally for solvent. It was important that the rate with solvent was determined immediately after the polymer solutions and that the osmometer received only the same amount of rinsing as when it was filled with solution. All the solutions and the solvent should be examined on the same day.

These measurements yielded a series of linear plots (*Figure 2*), the greatest slope being obtained with the solvent and the smallest slope with the most concentrated polymer solution. These slopes give the rates of diffusion, R, in cm/h. Using the relations

$$R_0 = kH_0 \quad \text{and} \quad R = k(H - \pi)$$

where H_0 and H cm are the mean hydrostatic pressures during the experiments, π was calculated for each solution. The value of R_0 (rate with solvent in the osmometer) determined directly should be regarded as only approximate. Experimental values tend to be too high. For this reason the direct determination of R_0 may be omitted if desired. A true R_0 value was obtained by plotting values of R, corrected to a constant value of H (using an approximate value of R_0 to give a value of k for this purpose) against solution concentration and extrapolating the curve to zero concentration (*Figure 3*). It is important to emphasize that these plots are curves for the polymers examined. High experimental R_0 values and high R values for very dilute solutions can sometimes give a misleading impression that the plot is linear, resulting in an erroneous extrapolation.

Molecular weights were obtained from the π/c against c plots in the usual way[15].

Results for the polymethyl methacrylate samples are compared in

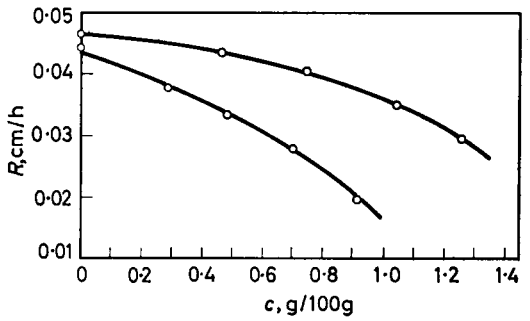

Figure 3—R versus c plots for two methyl methacrylate polymers: D1 (lower curve) and D7 (upper curve)

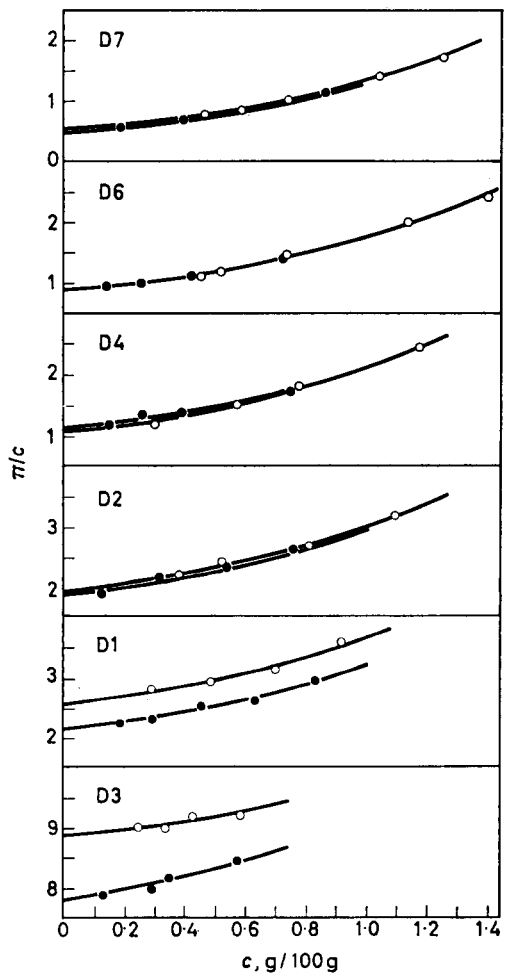

Figure 4—π/c versus c plots for a series of polymethyl methacrylate samples. π is expressed in cm solvent and c in g/100 g solution. ● Data obtained with Pinner–Stabin osmometer; ○ Data obtained with the constant pressure dynamic osmometer

Table 1 with the corresponding values obtained with the Pinner–Stabin osmometer. The π/c against c plots obtained with the two osmometers for the same polymers are shown in *Figure 4*.

The molecular weights of the polystyrene samples are compared in *Table 2* with the corresponding results obtained with a Fuoss–Mead osmometer. The π/c against c plots determined for these polymers using the constant pressure dynamic osmometer are given in *Figure 5*.

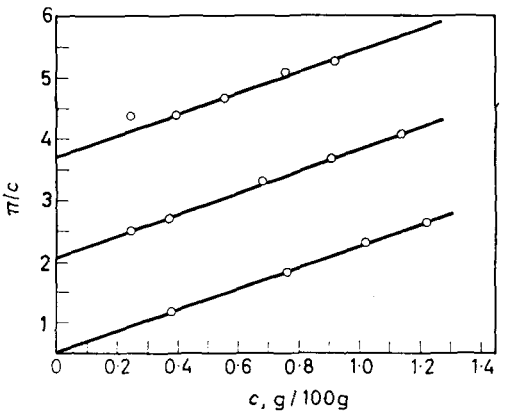

Figure 5—π/c versus c plots for three polystyrene samples. π is expressed in cm solvent and c in g/100 g solution. Data obtained with the constant pressure dynamic osmometer

Table 2. Results of molecular weight determinations for polystyrene samples

Polymer	*Molecular weight by* *Fuoss–Mead osmometer*	*constant pressure dynamic osmometer*
A	421 000	460 000
B	130 000	120 000
C	99 000	68 000

DISCUSSION

Adsorption and membrane permeability

It has been found in these investigations that with the same membrane in the osmometer, the value of R_0 does not remain constant over a period of weeks. This is attributed to polymer adsorption effects and is illustrated most clearly when a new membrane is used. Changes in permeability of the order of 10 to 20 per cent may then be observed after the osmometer has first been filled with a polymer solution. Similar effects have been reported by Vaughan[18]. The behaviour normally observed in the course of a series of molecular weight measurements is that the membrane permeability tends to decrease slowly over a long period. Low molecular weight polymers produce a more rapid decrease in membrane permeability than those of higher molecular weight. If the osmometer is subsequently rinsed repeatedly and left standing with solvent this effect can be reversed, but desorption has been found to occur less readily than adsorption. It is for these reasons that in these molecular weight determinations the

osmometer was always conditioned to the polymer to be used by allowing it to stand overnight in contact with the solution of the highest concentration to achieve 'adsorption equilibrium'. It appears to be necessary to carry out this conditioning with a stock solution of concentration 1·3 to 1·5 g/100g solution; with lower concentrations some experiments suggest that the desired effect is not achieved overnight. The fact that this equilibration is a slow process is emphasized by observations of Alvang and Samuelson[19]. Since the π/c against c plots have exactly the same slopes as those obtained for the same polymers with a Pinner–Stabin osmometer, by the static equilibrium method, this is taken as proof that there is no significant change in membrane permeability in the course of each individual molecular weight determination. Changes in permeability of the membrane can occur, however, when solvent or very dilute polymer solution are examined in the osmometer: some desorption appears to occur and rates are then too high. It is for this reason that experimentally determined R_0 values and R values for solutions with $c < 0{\cdot}4$ g/100g may be unreliable. The recommended method of evaluating R_0 is by extrapolation of the R versus c plot as described above. The effect of an erroneous value of R_0 (and hence k) is that the π/c versus c plot obtained shows very bad curvature or an anomalous slope.

Sensitivity and accuracy of the osmometer

The osmometer has in theory a considerably poorer sensitivity than conventional instruments operated by the static equilibrium method, because of limitations in the measurement of very small changes in liquid levels. It is not advisable to use solutions with concentrations lower than 0·4 g/100g solution. Above this value, however, the results of *Figure 4* show that the scatter of points is not significantly worse than for data obtained by use of the Pinner–Stabin osmometer. The great speed with which measurements can be carried out makes it feasible to duplicate determinations if desired.

An inspection of *Tables 1* and *2* shows that for molecular weights above 150 000 the constant pressure dynamic osmometer gives results in excellent agreement with those obtained by the Pinner–Stabin and Fuoss–Mead instruments. Below this value, however, there are differences in the results, and the lower the molecular weight of the polymer, the bigger is the discrepancy. It is significant that in this region of molecular weight the constant pressure dynamic osmometer consistently gives lower results. This is a very strong indication that this osmometer is less subject to errors due to diffusion of low molecular weight polymer through the membrane. This is an advantage at which the design of the osmometer aimed. It is explained by the following considerations. If the total amount of polymer diffused during the period of measurement is assumed to be proportional to the available membrane area and to the time, then the relative amounts diffused for the three types of osmometer would be expected to be, as a rough approximation, as given in *Table 3*. Clearly the constant pressure dynamic osmometer ought to be considerably less affected by diffusion of solute: this is in keeping with the results obtained.

Proof of the absence of significant amounts of diffusion with this

Table 3. Comparison of amounts of polymer diffused through membrane during measurements with three types of osmometer

Osmometer	*Membrane area* (cm^2)	*Time taken per measurement* (*h*)	*Relative amount diffused*
Fuoss–Mead	80	4	89
Pinner–Stabin	9·0	24	60
Constant pressure dynamic	1·8	2	1

osmometer is provided by the linearity of the rate plots obtained. Diffusion of polymer would cause these plots to show upward curvature; this has not been observed with the present group of polymer samples.

CONCLUSIONS

The osmometer described in this paper has some advantages over previous types of osmometer. In particular, by virtue of its extremely small membrane area and short measurement time, it is less subject to errors due to diffusion of polymer through the membrane. It is of low cost, easily constructed, robust, and extremely easy to manipulate. The amounts of solution and solvent required are small. The entire cell volume is clearly visible at all times. The osmometer yields results very quickly: eight to twelve hours are required for a complete molecular weight determination. It appears to be free from many of the difficulties associated with other types of osmometer.

These advantages are achieved at the expense of some loss in sensitivity. It is not feasible, therefore, to work at very low solution concentrations. Since conventional osmometers do not attain anything near their theoretical sensitivity in practice, this reduced sensitivity is less important than it appears at first sight. The method of use of the osmometer is based on the assumption that the membrane permeability remains constant throughout investigation of a series of solutions of a given polymer on the same day. Provided overnight conditioning, rinsing procedure, equilibration time, etc., are strictly standardized, this assumption has been found valid for the polymers studied, in the concentration range 0·4 to 1·5 g/100g solution; it may not be valid outside this range, and for other polymer–solvent systems it would be desirable to establish that the assumption is sound. The most serious disadvantage of the osmometer is the difficulty in measuring true R_0 values directly: this makes it necessary to rely on an extrapolation, curved in the present cases, with the inevitable uncertainty that this involves. It is believed, however, that the disadvantages the osmometer possesses are outweighed by its speed in use, its simplicity, and the freedom from the many troubles associated with conventional osmometers, and that it offers a promising alternative approach to osmotic pressure measurements.

Chemistry Department,
The University,
Glasgow, W.2, Scotland

(*Received August 1962*)

REFERENCES

[1] FRANK, H. P. and MARK, H. F. *J. Polym. Sci.* 1953, **10,** 129
[2] FRANK, H. P. and MARK, H. F. *J. Polym. Sci.* 1955, **17,** 1
[3] BONNER, R. U., DIMBAT, M. and STROSS, F. H. *Number-Average Molecular Weights.* Interscience: New York, 1958
[4] CLEVERDON, D., LAKER, D. and SMITH, P. G. *J. Polym. Sci.* 1953, **11,** 225
[5] BROATCH, W. N. and GREENWOOD, C. T. *J. Polym. Sci.* 1954, **14,** 593
[6] DONNET, J. B. and ROTH, R. *Bull. Soc. chim. Fr.* **1954,** 1255
[7] ALLEN, P. W., Ed. *Techniques of Polymer Characterization.* Butterworths: London, 1959
[8] PHILIPP, A. J. and BJORK, C. F. *J. Polym. Sci.* 1951, **6,** 383
[9] FUOSS, R. M. and MEAD, D. J. *J. phys. Chem.* 1943, **47,** 59
[10] PINNER, S. H. and STABIN, J. V. *J. Polym. Sci.* 1952, **9,** 575
[11] GEE, G. *Trans. Faraday Soc.* 1940, **36,** 1162
[12] MONTONNA, R. E. and JILK, L. T. *J. phys. Chem.* 1941, **45,** 1374
[13] CLAESSON, S. and JACOBSSON, G. *Acta chem. scand.* 1954, **8,** 1835
[14] JACOBSSON, G. *Acta chem. scand.* 1954, **8,** 1843
[15] PINNER, S. H. *A Practical Course in Polymer Chemistry.* Pergamon: Oxford, 1961
[16] STAVERMAN, A. J., PALS, D. T. F. and KRUISSINK, CH. A. *J. Polym. Sci.* 1957, **23,** 57
[17] FOX, T. G, KINSINGER, J. B., MASON, H. F. and SCHUELE, E. M. *Polymer, Lond.* 1962, **3,** 71
[18] VAUGHAN, M. F. *J. Polym. Sci.* 1958, **33,** 417
[19] ALVANG, F. and SAMUELSON, O. *J. Polym. Sci.* 1957, **24,** 353

The Dielectric Behaviour of Oxidized High-pressure Polyethylene I

C. A. F. TUIJNMAN

Dielectric measurements on oxidized high-pressure polyethylene and mixtures of model substances in high-pressure polyethylene can be explained by assuming that the low-frequency (α) dispersion is due to chain movement in the crystallites and that the high-frequency (γ) dispersion is related to movements in the amorphous phase.

IN THE last few years a number of dielectric investigations have been carried out on oxidized polyethylenes. Reddish and Barrie[1] examined a linear polyethylene (Marlex–50), paying special attention to the low-frequency losses (main maximum or α-peak). From the calculation of the effective dipole moment they concluded, in agreement with Michailov[2], that the existence of the α-peak is related to the movement of the carbonyl groups in the crystalline phase of the polymer.

High-pressure polyethylene has been examined extensively in particular by Michailov and co-workers[2,3]. The effect of mechanical and thermal treatments on the frequency and temperature location of the loss peaks was examined. The same authors calculated the concentration of carbonyl groups in the low- and high-frequency loss peaks.

German investigators, including Becker and Wolf[4], ascribed the existence of the α-peak to movements of chains in the amorphous phase between the crystallites and/or crystallite blocks, and not to a molecular movement in the crystallites.

In the light of this controversy attention in the present study is paid chiefly to the collection of further information on the background of the existence of the main maximum.

APPARATUS

The dielectric measurements were performed in the frequency range 10^2 to 3×10^8 c/s; except at higher frequencies, the temperature interval was from $-100°$ to $+80°$C. Between 10^2 and 2×10^5 c/s use was made of a Schering bridge (Rohde-Schwarz, München, Germany).

The measurements in the range 10^5 to 10^8 c/s were carried out by means of capacity variation in a tuned circuit[5] (Marconi Instruments Ltd, St Albans, England). At frequencies exceeding 8×10^7 c/s we used a re-entrant resonant cavity made in this laboratory[6].

EXPERIMENTAL RESULTS

Oxidized high-pressure polyethylene

The oxidation of the polyethylene was effected in two different ways:

(*i*) by ageing in an air-conditioning cabinet, and

(*ii*) by milling for three hours at 160°C.

Polyethylenes oxidized by these methods yield different tan δ/log f curves (f denotes frequency) at room temperature (see *Figure 1*).

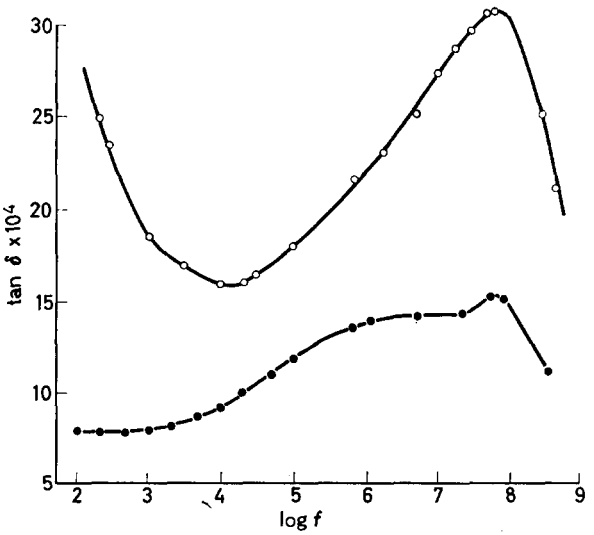

Figure 1—Dielectric loss/frequency curves of oxidized high-pressure polyethylene: ● Artificially aged at 25°C by means of ultra-violet light; ○ Artificially aged at 160°C by milling for three hours

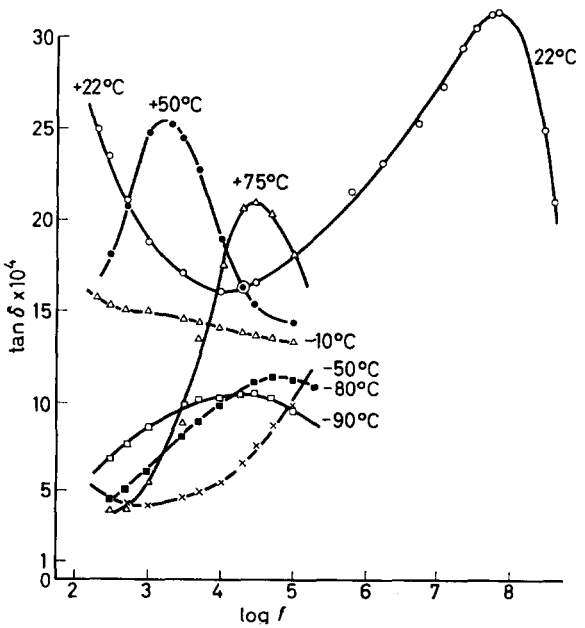

Figure 2—Dielectric loss/frequency curves of oxidized high-pressure polyethylene at different temperatures

The low, medium and high frequency peaks are referred to as the α-, β- and γ-transitions. In the curves for 'mildly' oxidized polyethylene the α-peak can hardly be observed. The results set forth below were obtained with material aged on a mill. The oxygen content proved to have no important effect on the frequency pertaining to the maximum in the α-peak. *Figure 2* shows the dielectric loss as function of the frequency at various temperatures.

Interest here centres on the area under the peaks and the frequencies pertaining to the various maximum peak values at different temperatures.

To separate the peaks use was made of the empirical relation of Fuoss and Kirkwood[7]

$$\varepsilon''_m / \varepsilon'' = \cosh a \ln (\omega_m / \omega) \tag{1}$$

where $\omega = 2\pi f$ and ω_m denotes the value of ω for which ε'' is a maximum: $\varepsilon'' = \varepsilon''_m$. The parameter a is a measure of the width of the dispersion peak: $0 \leqslant a \leqslant 1$.

The procedure used was as follows. For ε'' values not too far from the maximum of a given peak $\cosh^{-1}(\varepsilon''_m/\varepsilon'')$ was plotted versus the logarithm of the frequency. a was calculated from the slope of the straight line thus found. Furthermore, using (1), the values of ε'' in the neighbourhood of the maximum of an adjoining peak were calculated. The experimental values in the neighbourhood of this maximum were diminished by these ε'' values, after which the a value of the neighbouring peak was determined graphically. Then the disturbing effect of this peak on the former one was brought into account. Especially in those cases where the interfering effect of other peaks is small, relation (1) is adequately satisfied.

Independently of the shape of the distribution function, the surface A under a dispersion peak is given by the relation

$$A \equiv \int_{-\infty}^{+\infty} \varepsilon'' \mathrm{d} \ln \omega = \tfrac{1}{2}\pi (\varepsilon_s - \varepsilon_\infty) \tag{2}$$

The difference between the static dielectric constant ε_s and the dielectric constant for infinitely high frequency ε_∞ is proportional to $n\mu^2/T$ where n denotes the number of dipoles per cm³ active in the relaxation process, T being the absolute temperature and μ the effective dipole moment of the dipoles considered. In the diluted dipole system with which we are

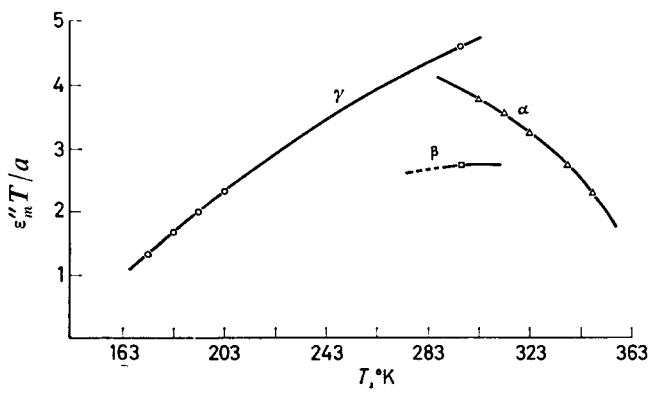

Figure 3—$(\varepsilon''_m T/a)$ versus temperature curves for oxidized high-pressure polyethylene

concerned here, the short range dipole–dipole interaction can be neglected and the effective moment equals the dipole moment of the polar group in the solid phase. Substitution of (1) in (2) and integration gives

$$A = (\pi \varepsilon''_m / a) \tag{3}$$

Consequently, quantity (ε''_m / a) is a measure of surface under the ε'' versus log ω curve and is directly related to the number of dipoles per cm^3.

In *Figure 3* this quantity has been plotted versus the temperature for the three peaks. The value of $\varepsilon''_m T / a$ for the γ-peak, and probably also for the β-peak, increases with rising temperature. The α-peak however, decreases as the temperature goes up and disappears altogether at the melting point of this polyethylene.

The temperature and frequency locations of the various maxima are indicated in *Figure 4*, both for normally compressed and heat-treated plates.

Such a heat-treatment, in which the material, while being cooled down from the molten state is kept a few degrees below the melting point for a period of 48 hours and subsequently slowly cooled down further, causes a widening of the loss spectrum. The maximum of the α-peak at a given temperature is now found at a lower frequency, while at a given frequency the maximum is found at a higher temperature. For the β- and γ-peaks the opposite holds true. The slopes of the curves in *Figure 4*, which are a measure of the activation energies of the relaxation processes, are indicated in the figure. The relation between log f_m and $1/T$ for the γ maxima is not quite linear.

High-pressure polyethylene mixed with model substances

As is well known, the tan δ versus temperature (tan δ versus frequency) curve obtained in mechanical loss measurements on high-pressure polyethylene also shows three maxima. In studying comparable dielectrical and mechanical loss peaks it is mostly assumed that identical chain elements take part in the movements. Willbourn[8] ascribes the existence of the mechanical β-peak to movements of the chain parts containing the branching points. Measured dielectrically therefore this peak would be due mainly to movements of dipoles on tertiary C atoms (OH groups). Such a structure exists in bis-heptadecyl-*n*-butyl carbinol. The view that the mechanical γ-peak is related to movements of short linear chain parts of the polyolefin chain in the amorphous part of the material is quite generally accepted. So it is instructive to compare the results mentioned above with those obtained on a mixture of high-pressure polyethylene with ketones and a tertiary alcohol.

Furthermore, the content of polar groups calculated from the surface of the dispersion peaks can be directly checked by means of calibration substances. The following admixtures were used: stearone ($C_{17}H_{35}(CO)C_{17}H_{35}$), nonapentacontanone ($C_{29}H_{59}COC_{29}H_{59}$) and bis-heptadecyl-*n*-butyl carbinol

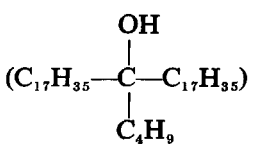

These substances were prepared synthetically by Mr Bos of this laboratory. The model substances, together with the polyethylene, were dissolved in xylene at 120°C, after which the whole system was cooled down to about 40°C at which temperature the solvent was removed by evaporation *in vacuo*. This procedure gave identical results as compounding on the mill.

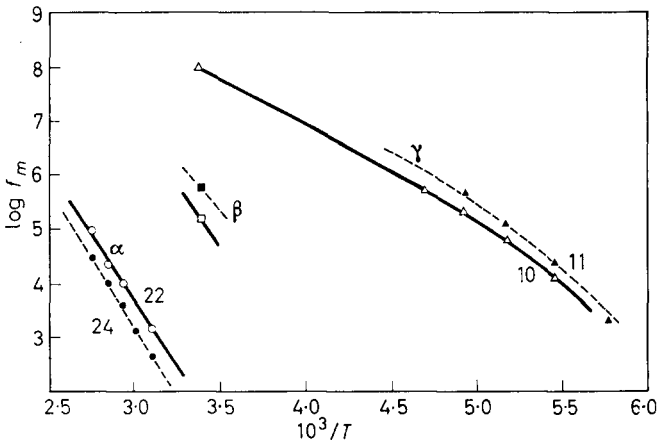

Figure 4—Log $f_{max.}$ versus $(1/T)$ curves of α, β and γ dispersion peaks for oxidized high-pressure polyethylene: ——— normal; – – – – after heat treatment

Figure 5—Dielectric loss/frequency curves at 23°C of mixtures of high-pressure polyethylene and model substances: I Stearone $(C_{17}H_{35})_2CO$; II High-pressure polyethylene + 3% $(C_{17}H_{35})_2CO$; III High-pressure polyethylene + 3% $(C_{17}H_{35})_2CO$ + 3% $(C_{17}H_{35})_2C<^{C_4H_9}_{OH}$; IV High-pressure polyethylene + 1·5% $(C_{29}H_{59})_2CO$

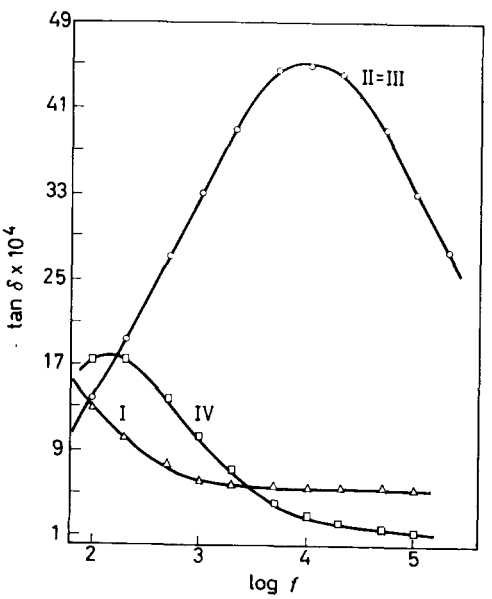

Figure 5

Figure 5 shows the tan δ versus log f curve at room temperature for: I. Stearone; II. Stearone mixed with high-pressure polyethylene; III.

Stearone + tertiary alcohol mixed with high-pressure polyethylene; and IV. Nonapentacontanone mixed with high-pressure polyethylene.

The mixtures show a picture differing from that of stearone alone. It is noteworthy that the admixed tertiary alcohol cannot be traced in the frequency range examined (no β-peak).

Figure 6 shows $\varepsilon''_m T/a$ as function of the absolute temperature T for the two ketone mixtures. Here, too, the quantity is not constant and varies in the same way as in oxidized polyethylene. Compared with the α-peaks the γ-peaks are small. For the short ketone a maximum in $(\varepsilon''_m T/a)_\alpha$ is found. *Figure 7* shows the frequency location of the maximum losses as function

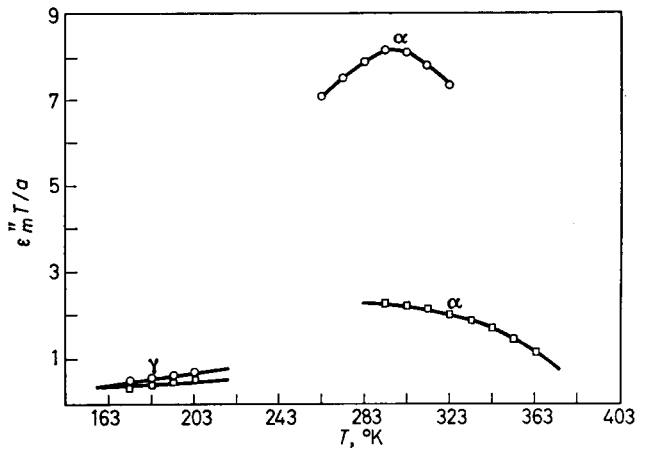

Figure 6—$(\varepsilon''_m T/a)$ versus temperature curves of α and γ dispersion peaks for mixtures of high-pressure polyethylene and normal ketones: ○ High-pressure polyethylene + 3% $(C_{17}H_{35})_2CO$; □ High-pressure polyethylene + 1·5% $(C_{29}H_{59})_2CO$

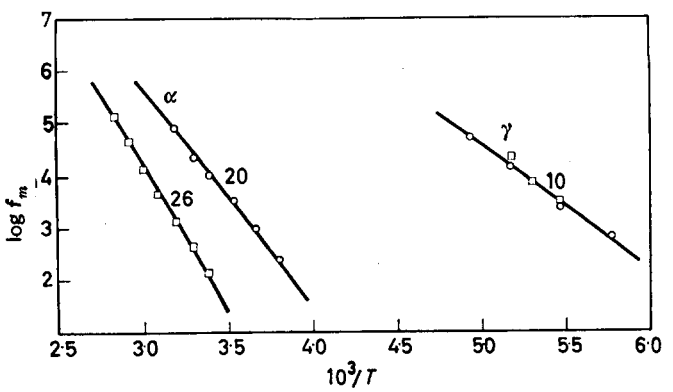

Figure 7—Log $f_{max.}$ versus $(1/T)$ curves of α and γ dispersion peaks for mixtures of high-pressure polyethylene and normal ketones: ○ High-pressure polyethylene + 3% $(C_{17}H_{35})_2CO$; □ High-pressure polyethylene + 1·5% $(C_{29}H_{59})_2CO$

of $1/T$. The activation energies of the α-peaks for the C_{35} and C_{59} mixtures amount to 20 kcal/mol and 26 kcal/mol respectively.

DISCUSSION

The experimental results can be explained by assuming that the γ-dispersion has an amorphous character and that the contributions to the α-dispersion are related to the movement of chains in the crystallites, more specifically to an internal rotary movement around the longitudinal axis of the chain. It is reasonable to assume that during cooling of the melt after previous oxidation, a portion of the carbonyl groups will be taken up in the crystalline phase.

Diffusion of oxygen will take place preferentially in the amorphous phase. From *Figure 1* it follows that the chains contributing to the α-dispersion will be less liable to oxidation at room temperature than the chains contributing to the β- and γ-peaks. In *Figure 2* it can be seen that during melting of the crystallites the α-peak decreases and disappears at the melting point. The curve resembles the crystallinity/temperature curve.

X-ray investigations carried out by Dr Vonk[9] in this laboratory have shown that cooling of high-pressure polyethylene at sub-normal rate reduces the size of the crystalline unit cell ($\Delta ab \approx 0{\cdot}5$ per cent) and slightly increases the length of the crystallite in the direction of the chain axis. This may account for the shifting of the peak towards lower frequencies after the heat treatment.

The calculated result (see below) shows that the number of carbonyl groups contributing to the α and γ dispersions is nearly equal to the total number of carbonyl groups found in the material by other analytical methods. For systems of the type considered here, in which short-range interaction between the dipoles is small, the various theoretical relations for calculating the dipole concentration from $\varepsilon_s - \varepsilon_\infty$ lead to practically identical results. The calculation was carried out by means of Harris and Alder's formula[10] (H.A.).

The values found with the Onsager–Fröhlich's relation

$$\varepsilon_s - \varepsilon_\infty = \left(\frac{3\varepsilon_s}{2\varepsilon_s + \varepsilon_\infty}\right)\left(\frac{\varepsilon_\infty + 2}{3}\right)^2 \frac{4\pi n}{3kT}\mu_v^2$$

are about seven per cent higher (μ_v denotes vacuum moment and n the number of dipoles per cm^3) [H. FRÖHLICH. *Theory of Dielectrics.* Clarendon Press: Oxford, 1949].

With n dipoles per cm^3, with dipole moment μ, contributing to $\varepsilon_s - \varepsilon_\infty$, the H.A. formula reads

$$\varepsilon_s - \varepsilon_\infty = 4\pi n\left(\frac{3\varepsilon_s}{2\varepsilon_s + 1}\right)\left(\frac{\mu^2}{3kT}\right)\left(\frac{\varepsilon_\infty + 2}{3}\right) \tag{4}$$

For the three types of relaxation α, β and γ equation (4) can be written as follows

$$\varepsilon_s - \varepsilon_\infty = \frac{4\pi}{3kT}\left(\frac{3\varepsilon_s}{2\varepsilon_s + 1}\right)[(n\mu^2)_\alpha + (n\mu^2)_\beta + (n\mu^2)_\gamma]\left(\frac{\varepsilon_\infty + 2}{3}\right) \tag{5}$$

Furthermore

$$\varepsilon_s - \varepsilon_\infty = (2/\pi)(A_\alpha + A_\beta + A_\gamma) \tag{6}$$

The quantities $(n\mu^2)_{\alpha,\beta}$ and $_\gamma$ in (5) are calculated by means of the following relation

$$\left(\frac{2A}{\pi}\right)_{\alpha,\beta,\gamma} = \frac{4\pi}{3kT}\left(\frac{3\varepsilon_s}{2\varepsilon_s+1}\right)\left(\frac{\varepsilon_\infty+2}{3}\right)(n\mu^2)_{\alpha,\beta,\gamma} \tag{7}$$

where the surface A of the relative loss peak is related, according to (3), with ε_m''/a and the dipole moment μ in the solid substance can be related with the vacuum moment μ_v by means of the Onsager equation

$$\mu = \mu_v\left(\frac{\varepsilon_\infty+2}{3}\right)\left(\frac{2\varepsilon_s+1}{2\varepsilon_s+\varepsilon_\infty}\right) \tag{8}$$

The dielectric constant of the oxidized high-pressure polyethylene at 3×10^8 c/s was found to be 2·23; the value derived from the refractive index was 2·334.

This value was used for ε_∞. Subsequently, the static dielectric constant was calculated with the aid of (6). The difference $\varepsilon_s - \varepsilon_\infty$ amounted to at most five per cent of the value for ε_∞.

The dipole moments μ_α and μ_γ were calculated by means of (8) from the vacuum moment of methylethylketone, μ_β is calculated from the moment of *n*-butylalcohol.

Comparing curves I and II in *Figure 5*, we may conclude that small amounts of stearone are miscible in polyethylene. According to *Figure 6* the value of $\varepsilon_m''T/a$ corresponding to the low frequency peaks of the two

Table 1. Oxygen content of samples investigated

Specimen	*Infra-red*	*Dielectric*				*Added*	
	No. of carbonyl groups $\times 10^{-19}$ *per cm³*	*No. of carbonyl groups* $\times 10^{-19}$ *per cm³*			*No. of hydroxyl groups* $\times 10^{-19}$ *per cm³*	*No. of carbonyl groups* $\times 10^{-19}$ *per cm³*	*No. of hydroxyl groups* $\times 10^{-19}$ *per cm³*
		α	γ	$\alpha+\gamma$	β		
PO 43 High-pressure polyethylene ageing time 3 h	3·99	1·38	1·51	2·89	2·64	—	—
PO 90 High-pressure polyethylene ageing time 3 h	2·19	0·91	0·50	1·41	1·52	—	—
PO 425 A High-pressure polyethylene $+(C_{17}H_{35})_2CO$	2·22	3·11	—	—	—	3·33	—
PO 425 A High-pressure polyethylene $+(C_{17}H_{35})_2CO$ $+(C_{17}H_{35})_2C<^{C_4H_9}_{OH}$	1·98	2·76	<0·40	—	0	3·36	3·00
PO 425 A High-pressure polyethylene $+(C_{29}H_{59})$ CO	0·83	0·79	<0·20	—	—	0·88	—

ketone mixtures decreases with increasing temperature. This tendency is analogous to that of the α-peak in oxidized polyethylene. Below room temperature, however, the stearone mixture shows different behaviour. We also noted slight high-frequency losses in the two mixtures; plotted as a function of the temperature these losses varied in the same way as the γ-dispersion in oxidized polyethylene. Curves II and III in *Figure 5* are identical, the effect of the bisheptadecyl-*n*-butyl carbinol will probably become noticeable at frequencies higher than those applied here. This suggests that the hydroxyl groups on tertiary carbon atoms, which contribute to the β-peak in oxidized polyethylene, are less mobile and are enclosed, for example, between crystalline particles.

The mixing experiments may be used to check the procedure of calculating the dipole concentration. It appears that the content of carbonyl groups in the ketone mixtures calculated by means of the dielectric theory is in reasonable agreement with the amount admixed.

The values found by infra-red analysis are slightly low; the infra-red values for oxidized polyethylene, however, are higher than the corresponding dielectric values, as can be seen in *Table 1*.

Sillars[11] and Pelmore[12] carried out dielectric measurements on esters of different length dissolved in paraffin. The frequencies pertaining to the maxima found by these authors have been plotted versus the number of carbon atoms in the chain (*Figure 8*).

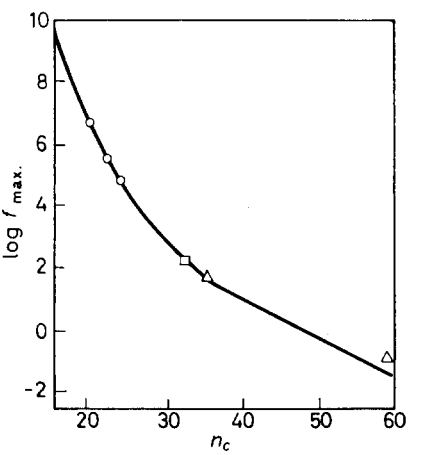

Figure 8—Frequency of maximum loss $f_{max.}$ as a function of chain length: n_C. ○ SILLARS, R. W. *Proc. Roy. Soc. A*, 1938, **169**, 66; Esters in paraffins: □ PELMORE, D. R. *Proc. Roy. Soc. A*, 1939, **172**, 502; Ketones in high-pressure polyethylene: △ Author

These values can be readily extrapolated towards our results found for the ketones in polyethylene. Assuming internal rotation taking place in the crystallite, the curve can be calculated theoretically. This will be done in paper II of this series.

The author is indebted to Dr Th. A. Veerkamp who kindly supplied the infra-red data and to Dr C. van Heerden with whom he had several helpful discussions. Thanks are also due to Mr P. L. C. Jetten for carrying out the measurements.

Centraal Laboratorium,
Staatsmijnen in Limburg,
Geleen, The Netherlands

(*Received August 1962*)

REFERENCES

[1] REDDISH, W. and BARRIE, J. T. *I.U.P.A.C. Symposium über Makromoleküle, Wiesbaden, 1959.* Kurzmitteilung I A 3
[2] MICHAILOV, G. P., LOBANOV, A. M. and SAZKIN, B. I. *Zh. tekh. Fiz., Mosk.* 1954, **24,** 1553
[3] MICHAILOV, G. P. *Zh. tekh. Fiz., Mosk.* 1957, **27(3),** 2052
[4] BECKER, G. W. *Kolloidzschr.* 1961, **175,** 99
WOLF, K. A. *Z. Elektrochem.* 1961, **65,** 615
[5] HARTSHORN, L. and WARD, W. H. *J. Instn elect. Engrs,* 1936, **79,** 597
[6] PARRY, J. V. L. *Proc. Instn elect. Engrs,* 1951, **98,** 303
[7] FUOSS, R. M. and KIRKWOOD, J. G. *J. Amer. chem. Soc.* 1941, **63,** 385
[8] WILLBOURN, A. H. *Trans. Faraday Soc.* 1958, **54,** 717
[9] VONK, C. Private communication
[10] HARRIS, F. E. and ALDER, B. J. *J. chem. Phys.* 1953, **21,** 1031
[11] SILLARS, R. W. *Proc. Roy. Soc. A,* 1938, **169,** 66
[12] PELMORE, D. R. *Proc. Roy. Soc. A,* 1939, **172,** 502

A Study of X-ray Long Periods Produced by Annealing Polyethylene Crystals

F. J. BALTÁ CALLEJÁ*, D. C. BASSETT† and A. KELLER

Several new effects found by annealing polyethylene crystals in air are reported. The onset of the increase of spacing is at lower temperatures for crystals of lower fold length. In addition crystals with lamellae thicker than 120 Å show a decrease of the long spacing when annealed between 95°C and 125°C. This does not affect the fold length but involves an increased molecular tilt within the crystal lamellae. An explanation in terms of the rearrangement of fold packing is given in agreement with other recent findings. The increase of fold length occurring at higher temperatures is accompanied by a molecular reorientation (rotation of crystal axes around b_s) in these specimens. For lamellae thinner than 120 Å the increase of fold length is the first noticeable effect; it occurs with increasing rate the lower the initial fold length. Near the melting point a molecular reorientation by rotation around a_s takes place. To account for the behaviour of the different samples both thermodynamic and kinetic arguments are put forward. The dominant part played by the latter is demonstrated, and the possible role played by defects in the packing of chain-folded molecular ribbons is emphasized.

IT is now established that the discrete low-angle X-ray diffraction maxima exhibited by solution-crystallized high polymers derive from the packing of chain-folded lamellae where the long spacings have been identified with the thickness of the lamellae and this in turn with the length of the fold. The exact identity of the fold length and layer thickness will be scrutinized further below; for the immediate purpose it should suffice that the low-angle reflections provide a measure of fold length. In a given solvent–polymer system these spacings are uniquely determined by the temperature at which the crystals are grown, higher crystallization temperatures giving higher spacings. However, when the crystals already formed are annealed subsequently, these spacings may increase. Bassett and Keller[1] first found the increase to be associated with a rearrangement of the molecular orientation within the polyethylene crystals studied, corresponding to a rotation of the unit cell around the b_s crystallographic axis. In Statton and Geil's experiments[2], the long spacings increased with unaltered orientation of the molecules, the increase being associated with a corresponding lamellar thickening. They concluded that the molecules must refold to a longer fold length, a conclusion substantiated by the subsequent work of Hirai *et al.*[3], Statton[4], Fischer[5], and Fischer and Schmidt[6]. The phenomenon of refolding is of great intrinsic interest for the understanding of molecular motion within the solid state, and is relevant to all annealing phenomena in general. Secondly, it is of interest for comparison with the predictions of the theories of chain folding. Such theories are basically of two types, the kinetic and the equilibrium. A kinetic theory[7–9] supposes that a chain-folded crystal corresponds to the state which allows quickest nucleation and growth sequence and thus need not be in a state of lowest free energy. In contrast, an equilibrium theory[10] supposes that there is an optimum crystal dimension

*Present address: Instituto de Fisica 'Alonso de Sta Cruz', C.S.I.C., Serrano 119, Madrid 6, Spain.
†Present address: Bell Telephone Laboratories, Inc., Murray Hill, New Jersey, U.S.A.

when the free energy is minimized. Several attempts have been made to discriminate between these two types of theory by looking for reversibility in the change of long period with suitable annealing, the argument being that such a reversibility would be expected only if the long period were an equilibrium property.

With the exception of the work by Ranby and Brumberger[11], the increase of the long spacing on heating was found to be irreversible (refs. 3, 6, and our own experiments reported here). The experimental conditions of Ranby and Brumberger[11] are not straightforward. First, their annealing at lower temperature, which they claim to result in a decrease of the long spacing, was carried out in a liquid which is a better solvent than the one from which the crystals grew. Hence dissolution and subsequent recrystallization at the lower temperatures remains a possibility. Secondly, they used substantial pressure in compressing their sediments, which is itself sufficient to produce a decrease of the spacing, for reasons which may well be similar to those to be discussed below. Thus on present evidence the decrease of long spacing on cooling cannot be considered proved. However, a decrease of long periods has recently been reported by Zachmann and Schmidt[12], working with bulk polyethylene terephthalate, not on cooling but when heated—an effect which these authors cannot explain. The morphology of the latter system is not exactly known.

A decrease of the long spacing on heating has also been found by us in solution-crystallized polyethylene single crystals and this effect is attributed not to a decrease in the fold period, but to a decrease in thickness of crystal lamellae caused by a change in molecular orientation in their interior. Some experiments on the dependence of subsequent annealing behaviour on initial fold period will also be described.

EXPERIMENTAL RESULTS

Materials and techniques

Low pressure polyethylene Marlex–50 was crystallized from dilute ($< 0{\cdot}1$ per cent) xylene solutions at various temperatures. After precipitation the crystals were filtered from suspension either at room temperature or at the crystallization temperature[13] to form oriented crystal mats in which the lamellae of the individual crystals lie essentially in the plane of the specimens. X-ray photographs taken with the beam parallel to the mat show fibre orientation with low-angle maxima on the meridian[14].

At first the X-ray patterns were recorded by a Kratky type low-angle camera and later with a focusing Franks camera[15]. The latter has the double advantage of pinhole collimation and short exposure time. With polyethylene specimens it took about 30 minutes exposure to obtain two orders of reflections, the first-order reflection being detected after five minutes. This was advantageous for examination at the annealing temperature of specimens which might alter during longer exposure times. Also the short specimen–plate distance (4 to 5 cm) still coupled with high resolution (better than 600 Å) facilitated simultaneous recording of wide- and low-angle reflections, both with undistorted azimuthal intensity distribution.

1 mm square specimens were annealed in air on a bar controlled within $\pm 2°C$; the quoted temperatures are the maximum ones. Some X-ray photographs showing both low- and wide-angle patterns were taken of hot specimens, but as this was found not to have any effect on spacing values, most specimens were examined after cooling. This point was checked by comparing identical specimens one of which was cooled between successive anneals and the other was not. No difference in long period values was found. A rapid heating rate was used; the cold specimen reached the desired temperature within a few seconds.

Decrease of long spacing

Observations showing a decrease of long spacing were mostly made on crystals grown at 90°C, having a long period of 145 to 165 Å. As grown these crystals are monolayer truncated lozenges of {(312)(110); (*h*0*l*)(100)} type, i.e. which have fold surfaces of $\{312\}_s$ type in the {110} sectors, forming either a hollow pyramid or a particular related habit (Bassett, Frank and Keller[16]). If this fold surface is preserved in the layers when they lie flat after sedimentation, it would imply a fold length some 15 per cent greater than the layer thickness, in the range of 160 to 180 Å. This is in agreement with the observed splitting of the 200 X-ray wide-angle arc whose maxima are found at 25° to 30° from the equator[1,17], implying that the molecules are tilted through a substantial angle (in fact through 25° to 30°) with respect to the plane of sedimentation. Thus for a given fold length the long period will be a function of the molecular tilt as revealed by the split of the 200 reflections. We find that the smallest long periods are associated with the largest tilts (*Table 1*) and, as we shall show, give the smallest decrease of long period when annealed. Conversely, a change in fold period can be safely inferred from a change in long spacing only if the latter lies beyond any effect attributable to a molecular reorientation within the azimuthal spread of the arcs in the diffraction pattern. This spread is necessarily large, because of the inherent disorientation within the sedimented specimen. For this reason the much smaller splits of the 020 and 110 arcs (the latter consisting of two components) expected from the above crystal habit cannot be clearly resolved, though maximum values may be assigned[16].

In contrast to the usual monotonic increase of long period on annealing polyethylene single crystal specimens[2,3,6], these 90°C specimens show a decrease of up to 15 Å to a constant value which does not increase again until beyond 122°C. After 30 minutes at 127°C, the spacing is approximately the same as the original one. The decrease of spacing correlates with the sharpening of the low-angle maxima which subsequently broaden only with the eventual increase of spacing. Simultaneously with the decrease of spacing, the 200 reflection moves noticeably further from the equator to a value of approximately 32°.

The spacing decrease is complete after 15 hours annealing at 97°C, thereafter subsequent treatment, e.g. 15 hours at 117°C, or 30 minutes at 122°C has not changed it. The decrease itself is apparently continuous, 30 minutes annealing at 95°C giving an intermediate value of the spacing decrease. These and other details are given in *Table 1* and *Figure 1*.

The decrease of spacing can be accounted for by the increased molecular tilt. For suppose initially the fold surface in the (110) sector of a crystal is $(hkl)_s$ and finally $(hkl')_s$ both fold surfaces being horizontal, i.e. in the

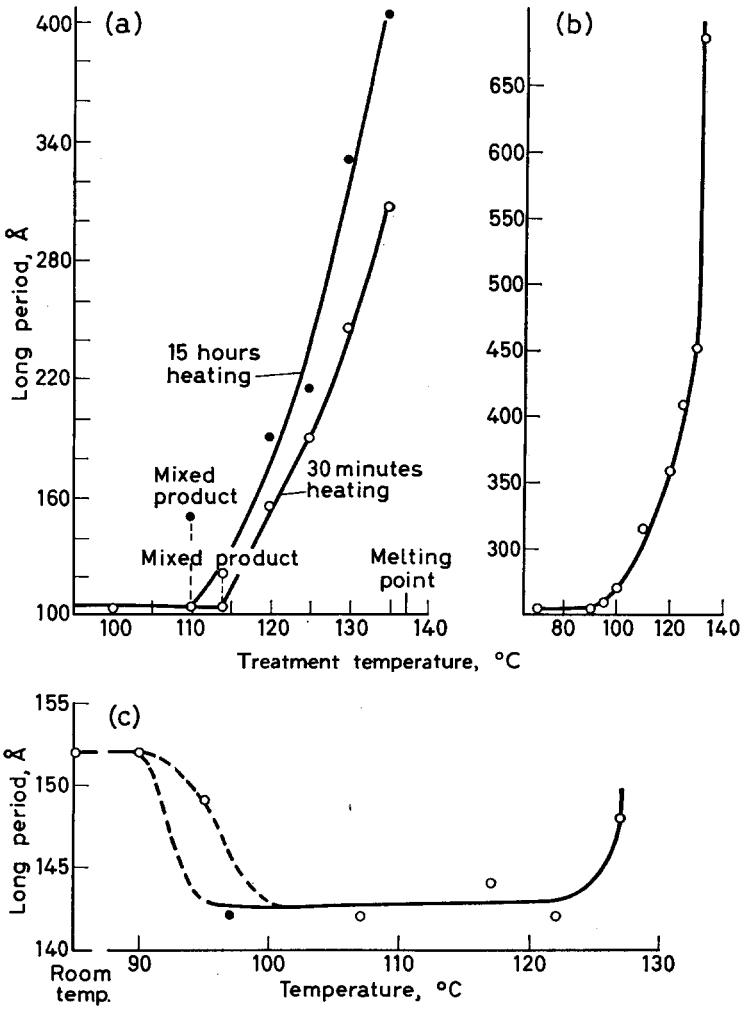

Figure 1—X-ray long period/annealing temperature curves for polyethylene: (a) for sedimented single crystals of initial fold length 104 Å, with annealing times of 30 minutes and 15 hours. (Reprinted with permission from Statton and Geil; *J. appl. Polym. Sci.* 1960, **3**, 357); (b) for unstretched melt-crystallized bulk, quenched to 0°C with annealing times of 24 hours. (Reprinted with permission, from Fischer and Schmidt, *Angew. Chem.* 1962, **74**, 551); (c) for a sedimented aggregate of crystals grown at 90°C. Full lines indicate where the same specimen was annealed successively at different temperatures. Annealing times: 30 minutes (open circles), 15 hours (full circles)

Table 1. A comparison of the X-ray long period d and the rotation θ of the 200 reflection maximum from the equator for various specimens both at room temperature and after 30 minutes annealing at 117°C

Specimen	*Crystallization temp.* °C	$d_{orig.}$ Å	$\theta°_{orig.}$	d_{117} Å	$\theta°_{117}$
6	90	152	27	144	32
9	90	160	27	153	32
13	90	148	32	147	31
39	90	162	26	147	31
41	85	128	23	123	28

specimen plane. Then the tipping of the 200 reflections away from the equator, ϕ, is given by

$$\sin\phi = \sin\theta \cdot \cos\chi \tag{1}$$

for the $(hkl)_s$ surface, where θ is the angle $(hkl)_s \wedge (001)_s$, i.e. the molecular inclination in the layer and χ is the angle $(hk0)_s \wedge (100)_s$. In particular, let us set $h:k=3:1$ and let the (200) tilt change from 27° to 32° (as observed), then the molecular inclination in the layer changes from 30° to 36°. This involves a six per cent decrease in layer thickness (i.e. long period) which is in good agreement with experiment.

Annealing beyond 127°C causes both the low-angle spacing to increase very rapidly and the reflection to broaden so that it cannot readily be resolved, though maxima of about 400 Å have been detected. This is also the region of the pronounced molecular reorientation effects reported previously[1] and to be referred to again later. Complete randomization resulting from visible melting and recrystallization occurs by 130°C; up to this point the low-angle scattering remains meridional. This early 'melting' of the crystals several degrees below the conventional melting point may be attributed to the presence of the chain folds. The finding of Fischer and Schmidt[6] that at 130°C, and for a similar heating rate to ours, the birefringence drops within a few minutes to a low value which it keeps for at least 30 minutes, is support for these observations. The spacing decrease on heating is not restricted to crystals grown at 90°C. We examined one specimen formed at 85°C of long period 128 Å. This also shows similar behaviour, the spacing decreasing to 123 Å and then remaining constant to beyond 122°C; there may be also a slight increase in 200 splitting. In summary: the annealing of polyethylene crystals grown at higher temperatures proceeds in a different way both from thinner crystals and from the unoriented quenched bulk[2,6]. The comparative annealing temperature/time curves are shown in *Figure 1.*

Dependence of annealing behaviour on fold period

Statton and Geil[2] found that in their crystals which were of 104 Å step height the long period began to increase suddenly at 110°C. According to our results, crystals of 145 to 165 Å initial fold period behave differently from those of Statton and Geil implying that the annealing behaviour is a function of the initial fold length. We examined two further specimens with different initial long periods, namely 114 Å and 98 Å, first to compare

the temperatures where the increase of spacing starts, and secondly to compare the course of the increase of spacing in the two specimens subjected to identical treatments.

Again we found that the temperature of 110°C is not unique. The 98 Å specimen had increased its spacing to 105 Å after 30 minutes at 102°C whereas the 114 Å specimen showed no change after 30 minutes at 112°C but had increased to 128 Å after 30 minutes at 117°C.

For the comparative annealing experiment both specimens were placed side by side on the hot bar and annealed for 30 minutes at 117°C, 122°C and 127°C respectively. As *Figure 2* shows, the 98 Å specimen exhibited a much greater increase in long spacing and the two spacing/temperature curves cross.

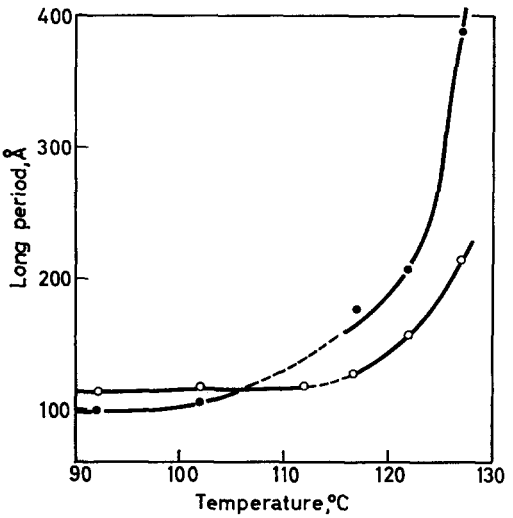

Figure 2—Comparative X-ray long period/annealing temperature curves for two polyethylene single crystal samples of initial long periods 114 and 98 Å respectively. Full lines indicate where the same specimen was annealed successively at different temperatures. Annealing time: 30 minutes

Molecular reorientation coupled with increase of fold length

Molecular reorientation[1] which is associated with a pronounced increase of the long period up to 300 Å or more can occur in the course of annealing, the corresponding reflection often becoming unresolvable owing to the continuous central scatter. These effects occur in the upper range of annealing temperatures between 125°C and the melting point. The exact temperature values depend on the specimen and on the heating rate. They fall in two classes:

(*a*) In crystals with initial long spacings above 120 Å, i.e. those which form above 80°C the unit cell rotates through a discrete angle around b_s which stays in the plane of the mat. This is revealed by pronounced splitting of the 200 reflections with the 020 arcs staying at and even further contracting to the equator. This 200 splitting is much larger than that which is observed at lower temperatures associated with the decrease of long spacing and can even result in the 200 arc becoming meridional. Earlier this trend has also been followed on individual single crystal layers

by means of electron diffraction[1] when the associated morphological effects were also described.

(*b*) In crystals with initial fold length less than 120 Å the unit cell rotates around the a_s axis, this axis remaining in the plane of the crystal mat. So far this change was observed to be discontinuous. Within a temperature interval of 1° the 020 reflection moves apparently discontinuously from the equator to the meridian.

DISCUSSION

Annealing was found to produce two effects; an increase of fold length and a change of orientation of the straight segments of the folded molecules with respect to the plane of the lamellae. Depending on specimen and condition of heating these effects can occur separately and successively or simultaneously. They both affect the long spacings recorded, which accordingly can be taken as a measure of the fold length only if the effect of molecular reorientation is accounted for.

One kind of molecular reorientation consists of an increase in the molecular tilt which occurs a little above the temperature of crystallization (95° to 120°C) in crystals having initial fold length greater than 120 Å. It takes place without change in the fold length and results in a decrease of the long period. This effect can best be discussed in connection with single crystal growth with which we believe it is closely associated.

Studies on the morphology of single crystals have revealed that the folds arrange themselves in a staggered configuration where the fold surfaces and thus the lamellar planes are inclined to the straight segment direction. The regularity of the staggering results in well-defined pyramidal and related habits[17]. On the other hand recent formulation of the kinetic theory of polymer crystal growth visualizes crystals forming with a fluctuating fold length, i.e. with an irregular fold surface[9]. Such a surface could, however, rearrange subsequently to a more regular geometry leading to uniform fold length with the folds staggering regularly as required for the most efficient packing. Indeed, strong indications of the existence of such rearrangements have been found experimentally[16]. While the rearrangement must occur at the crystallization temperature to account for the regular geometries observed, annealing at higher temperatures might be expected to result in still greater degree of perfection. There is recent calorimetric evidence that such changes do occur once the annealing temperature exceeds the crystallization temperature even before an increase of the fold length becomes noticeable (Karasz; private communication).

With the crystals grown at 80° to 90°C we observe three effects: decrease of long spacing, increase of molecular tilt and sharpening of the low angle reflection. The last is evidence in itself for increasing order. The first two effects are clearly linked, the increase of tilt resulting in lower spacing. An explanation for the latter would be that greater staggering is produced by annealing to a more ordered state of packing involving a larger inclination of the molecules to the lamellar surfaces. The possibility that larger staggering may be favoured by the higher temperatures is indicated by the observation that crystals grown at 90°C have a more oblique structure,

$\{312\}_s$ fold surfaces, than the ones grown at lower temperatures (76°C) which have $\{314\}_s$ fold surfaces[16]. Also with *n*-paraffins, the staggering can be increased with annealing[18] against all previous expectations according to which form of higher symmetry would be favoured at higher temperatures. Bassett, Frank and Keller[16] also find indications of $\{311\}_s$ fold surfaces possibly forming from $\{312\}_s$ when 90°C grown truncated lozenges are annealed in xylene suspension. However, in the present case the increase in obliquity is small and if we start from $\{312\}_s$ fold surfaces this increase could only lead to fractional l indices provided there is no major change in the h and k indices. This would be an irregular surface if the sub-cell is preserved after the transition and it is not clear why this should correspond to a more stable final state towards which the system would tend, nor why this should be a more ordered packing.

A more likely alternative is the elimination of defects in the overall envelope of the layer. Thus we suppose that after growth plus rearrangement, the final fold surface consists of domains of one staggered structure diluted with non-staggered regions to give a smaller overall stagger. It is unlikely that the unstaggered regions have their optimum fold packing, and annealing may allow them to move towards this. One would expect any change of staggering to occur in a similar direction to that already existing, when the inclination of the molecules within the layer envelope would increase, the fold packing would be more regular and the long period would decrease, provided the regions of uniform stagger are of dimensions of the order of the layer thickness.

Summing up, we consider the phenomena under discussion as a result of changes in fold packing due either to a change to a structure of increasing stagger or, more probably, to the elimination of defects in the overall envelope of a folded layer.

The second type of molecular reorientation near the melting point, where the fold length also increases considerably, is of greater magnitude and is not obviously associated with fold staggering or with crystal growth. It resembles the reorientation effects associated with the relaxation of drawn fibres. The rotation around the b_s axis to the final state with the 200 reflection meridional is reminiscent of both relaxation effects and spherulite growth as has been pointed out previously[1]. The rotation around the a_s axis observed with crystals of lower fold length has no counterpart in the bulk polymer according to our present knowledge.

The first type of molecular reorientation with unaltered fold length is not observed in crystals formed below about 80°C (long spacing < 120 Å). Here the first noticeable change is the increase of the long period unequivocally identified with the increase in the fold length[2]. This is preceded by an intermediate state of partial melting[5,6], after which the system recrystallizes with an increased fold length. (We have confirmed this intermediate partial melting when annealing 150 Å layers just below their melting point after having annealed previously at 120°C. The sharp wide-angle pattern disappears and does not reappear until after about 30 minutes). If the specimen is kept at the annealing temperature the fold length

increases with time apparently indefinitely. Fischer and Schmidt[6] express this time dependence by the relation

$$P = K \log (t/t_0) + P_0 \tag{2}$$

involving P_0 the long period at time t_0, P the long period at time t and a constant K which is an increasing function of temperature. As it stands this relationship would, at a given temperature, imply that all specimens with the same long period would show identical rates of increase of long period. The cross-over of the curves in our *Figure 2*, however, implies that K is also a decreasing function of long period though we have not checked that the time/long period relationship of the type in equation (2) actually holds for the specimens in question.

Figures 1 and *2* show that the increase of fold length for single-crystal specimens occurs at successively higher temperatures the greater the initial value. Insofar as the observed 'partial melting' is related to true thermodynamic melting, this is in qualitative agreement with expectation and it is of interest to use our data for comparison with theory.

For a quantitative assessment we invoke the melting point fold length relation

$$T'_m = T_m \left(1 - \frac{2\sigma_e}{\Delta h l}\right) \tag{3}$$

which Hoffman and Weeks[19] derived by considering the basal surfaces only and by replacing Δf (free energy difference between the bulk phases) with $\Delta f \cdot T_m / T'_m$. Here T_m is the melting point for infinite fold length, T'_m that of fold length l, Δh is the heat of fusion per unit volume and σ_e the free energy per unit area of the basal surface. The latest estimate[20] for T_m is 141 °C, Δh is $2{\cdot}8 \times 10^9$ erg/cm^3, σ_e is somewhat controversial ranging from 30 to 140 erg/cm^2 as quoted by various crystallization theories where it appears as a parameter. An *a priori* geometric argument (Frank, unpublished) gives 100 erg/cm^2 as a lower limit (see review by Keller[21]). In *Table 2* we compare the predicted melting point $(T'_m)_{\text{calc.}}$ with the observed

Table 2. Comparison of melting points ($(T_m')_{\text{calc.}}$) calculated for three different fold lengths, for different values of σ_e with the observed lowest transformation temperature ($(T_m')_{\text{obs.}}$)

Sample No:	*Fold length Å*	$(T_m')_{\text{obs.}}$ °C	$(T_m')_{\text{calc.}}$ °C σ_e erg/cm^2				
			30	50	80	110	140
1	170	122–127	134	132	127	122	117
2	114	112–117	133	128	120	112	105
3	98	<102	132	126	117	108	99

transformation temperature $(T'_m)_{\text{obs.}}$ for our three samples for different values of σ_e. While reasonable agreement is obtained it is not possible to fit all values for σ_e constant. For samples 1 and 2 σ_e at about 100 erg/cm^2 gives the best fit while for sample 3 it is about 140 erg/cm^2. σ_e may vary slightly with temperature but particularly so with the nature of the fold

surface. After flattening, fold surfaces as distinct as (001), and (312), occur between which some variation of σ_e seems reasonable. Larger σ_e values are expected from less regular fold packings which in fact are found in samples with lower fold lengths, this being in the right direction for a successful fit for sample 3. However, an increase in σ_e by as much as 40 per cent (due to packing considerations alone) may be questionable, which might indicate that sample 3 transforms at somewhat lower temperatures than required by this approach.

This last point is brought out much more strongly by the behaviour of the quenched bulk [*Figure 1*(b)] with a lowest transformation limit at 90°C. This would require σ_e to be about 800 erg/cm^2. It would be smaller than this if the crystallite length (fold length?) were only a portion of the long period[6]. Even so the σ_e values obtainable by this approach are unreasonably large. Discrepancies like these point to the role played by other, essentially kinetic, factors in influencing the increase of fold length which on the other hand would be sensitively affected by defects. A likely example for this will now be quoted.

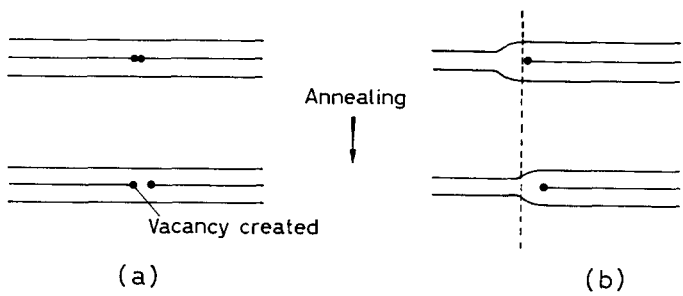

Figure 3—Schematic representation of the advantage an interstitial folded ribbon confers on a crystal in increasing its fold period. In (b) the interstitial ribbon may increase its fold length and contract laterally without creating vacancies in the crystal. This is not possible for the more regular ribbon-packing shown in (a)

During the refolding process, a molecule must, as it were, pull in its end and in so doing leave a row of lattice vacancies. This, as pointed out to us by F. C. Frank, requires considerable energy and would probably be helped if the folded ribbon in question were interstitial so that the vacant segment portion could be filled by contraction of the adjacent ribbons (*Figure 3*). In c_s projection, this process would appear as the climb of an edge of dislocation. Such a mechanism would clearly be a function of crystal perfection and thus of crystal growth. Hence, crystals of longer fold length, being grown more slowly, could well contain fewer interstitial ribbons and other suitable defects. This would delay the sliding-chain diffusion processes required for increase of fold lengths to progressively higher temperatures than thermodynamic considerations would suggest.

Figure 2 shows an effect which seems clearly attributable to such factors. After identical anneals, a 98 Å sample eventually changes to a higher fold length than a 114 Å sample. This would not be so if the transformation

were purely a melting phenomenon. However, the 98 Å sample is expected to contain more defects than the 114 Å and therefore has an ingrown facility for more rapid changes of fold length.

The quenched bulk, regarded as a highly defective chain-folded system, would also be able to increase fold length easily and it may well be that the higher transition temperatures shown by the single-crystal specimens represent the varying extents of delayed transformation produced by increasing crystal perfection.

We wish to thank Professor F. C. Frank, F.R.S., for his continued interest and advice throughout the work and Dr T. Kawai for valuable suggestions.

One of us (F.J.B.) wishes to acknowledge the tenure of a Ramsay Memorial Fellowship and of a Fellowship from the C.S.I.C. (Spain) during part of this work.

H. H. Wills Physics Laboratory,
University of Bristol

(*Received August 1962*)

REFERENCES

[1] BASSETT, D. C. and KELLER, A. *J. Polym. Sci.* 1959, **40,** 565
[2] STATTON, W. O. and GEIL, P. H. *J. appl. Polym. Sci.* 1960, **3,** 357
[3] HIRAI, N., YAMASHITA, Y., MITSUHATA, T. and TAMURA, Y. *Rep. Res. Lab. Surface Sci., Fac. Sci. Okayama Univ.* 1961, **2,** 1
[4] STATTON, W. O. *J. appl. Phys.* 1961, **32,** 2332
[5] FISCHER, E. W. *Ann. N.Y. Acad. Sci.* 1961, **89,** 620
[6] FISCHER, E. W. and SCHMIDT, G. F. *Angew. Chem.* 1962, **74,** 551
[7] LAURITZEN, J. I. and HOFFMAN, J. D. *J. Res. Nat. Bur. Stand. A,* 1960, **64,** 73
[8] PRICE, F. P. *J. Polym. Sci.* 1960, **42,** 49
[9] FRANK, F. C. and TOSI, M. P. *Proc. Roy. Soc. A,* 1961, **263,** 323
[10] PETERLIN, A. and FISCHER, E. W. *Z. Phys.* 1960, **159,** 272
[11] RANBY, B. G. and BRUMBERGER, H. *Polymer, Lond.* 1960, **1,** 399
[12] ZACHMANN, H. G. and SCHMIDT, G. F. *Makromol. Chem.* 1962, **52,** 23
[13] BASSETT, D. C. and KELLER, A. *Phil. Mag.* 1962, **7,** 1553
[14] KELLER, A. and O'CONNOR, A. *Nature, Lond.* 1957, **180,** 1289
[15] FRANKS, A. *Brit. J. appl. Phys.* 1958, **9,** 349
[16] BASSETT, D. C., FRANK, F. C. and KELLER, A. *Phil. Mag.* In press
[17] BASSETT, D. C. and KELLER, A. *Phil. Mag.* 1961, **6,** 345
[18] KELLER, A. *Phil. Mag.* 1961, **6,** 329
[19] HOFFMAN, J. D. and WEEKS, J. J. *J. Res. Nat. Bur. Stand. A,* 1962, **66,** 13
[20] BROADHURST, M. G. *J. chem. Phys.* 1962, **36,** 2578
[21] KELLER, A. *Polymer, Lond.* 1962, **3,** 393

Correction

Solution and Diffusion in Silicone Rubber I—A Comparison with Natural Rubber

BARRER, BARRIE and RAMAN, *Polymer, Lond.* 1962, **3**, 595

REPLACE *Table 7* by the following *Table*, containing corrected values of D_0:

Substance	*Rubber A*		*Rubber B*		*Rubber C*	
	E_D	$D_0 \times 10^3$	E_D	$D_0 \times 10^3$	E_D	$D_0 \times 10^3$
n-C_4H_{10}	4 200	6·01	3 800	3·57	4 300	9·06
iso-C_4H_{10}	4 000	3·95	4 500	7·98	4 400	8·73
n-C_5H_{12}	4 300	5·74	3 900	3·12	3 700	3·10
neo-C_5H_{12}	4 200	3·05	4 000	2·24	4 500	7·16

Figure 2 is then replaced as below:

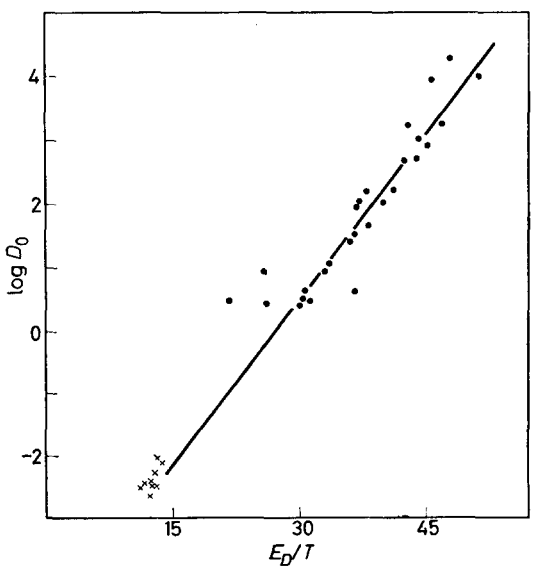

Figure 2—Log D_0 versus E_D/T. ●—natural rubber; ×—silicone rubber

It is now seen that the points for silicone rubber in the plot of log D_0 versus E_D/T lie on the same curve as those for the natural rubbers of ref. 5. A linear plot is expected according to the zone theory.

Notes

Viscosity and Swelling Behaviour of Lightly Crosslinked Microgels

MICROGELS[1] are unique materials and present an ideal opportunity for the study of the solution properties of polymers. Incorporating an adequate amount of crosslinking agent in a latex produces a molecule which retains its spherical structure on isolation and dissolution in a suitable solvent. Thus, the question of a suitable model for the solute is obviated. Since viscosity is an absolute method for size determination of spheres, a correlation of solvent–polymer interactions with swelling behaviour can readily be made utilizing viscosity measurements of these microgel particles in various solvents.

EXPERIMENTAL

The various microgels used in this study were prepared by emulsion copolymerization of styrene and divinylbenzene (DVB). A typical recipe is:

20·0 cm^3	20 per cent Dupanol ME solution
9·6 cm^3	5 per cent $K_2S_2O_8$ solution
9·6 cm^3	5 per cent $NaHCO_3$ solution
79·9 g	Styrene
0·6 g	78·6 per cent active DVB
205·0 cm^3	water

The monomers used were Dow Chemical Co. materials. The resultant latex was freeze-coagulated, filtered and washed free of emulsifier with water and methanol. Drying at a temperature less than 50°C in a vacuum oven produced a white fluffy powder which could readily be dispersed in a suitable solvent. Latexes containing various DVB contents and of various particle diameters were prepared in a similar fashion. Electron micrographs of all dried latexes were obtained to determine original diameters.

Viscosity measurements were made at 25° ±0·1°C using modified 5 cm^3 Ostwald viscometers. Flow times ranged from 100 to 1 000 seconds, generally being about 200 seconds.

THEORY

The introduction of a colloidal material into a solvent causes an increase in the viscosity. The extent of the increase varies widely with the nature of the particles. Einstein[2] calculated the change in the viscosity of a system

containing hard spheres. His result, valid only for very dilute systems, is usually written

$$\lim_{\phi_2 \to 0} \frac{\eta_{sp}}{\phi_2} = 2{\cdot}5$$

where ϕ_2 is the volume fraction of solute.

If the hydrodynamic behaviour of microgel particles in dilute solution follows Einstein's theory, it should be possible to correlate the viscosity data for all of the solvent–microgel systems by a single curve which is independent of initial particle size, dispersing media and DVB content of microgel. The only dependency should be on the fraction of the volume occupied by the solute. Such a correlation should also be independent of the value of the constant of the Einstein equation.

RESULTS

Since one of the problems is to determine the swollen particle diameters, it is not possible *a priori* to calculate the volume fraction occupied by the microgel. In order to surmount this difficulty, it was assumed that solutions having the same specific viscosity contained the same volume fraction of

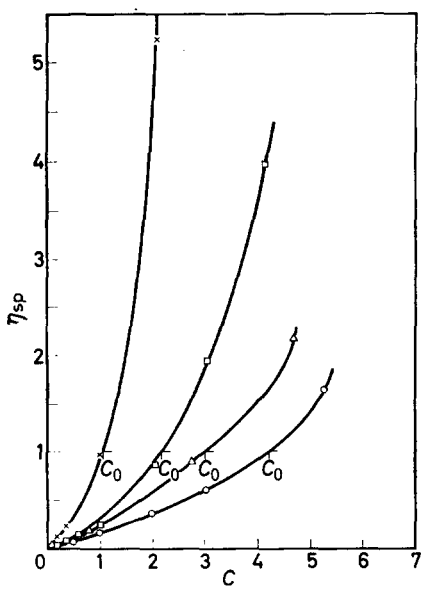

Figure 1—Viscosity behaviour of microgels. ○ 46B in methylethylketone; △ 46B in perchlorethylene; × 50A in chloroform; □ 50C in chloroform

microgel. A specific viscosity of 1·0 was chosen as the reference point. The concentration of microgel which gave a specific viscosity of 1·0 was found by examination of the η_{sp} versus C plots and was given the designation C_0 (*Figure 1*). The microgel particles have a different C_0 in each of the solvents used. Dividing the weight concentration by the pertinent C_0 reduces all of the data to the same arbitrary volume concentration scale.

A plot of $\eta_{sp}/(C/C_0)$ versus C/C_0 is shown in *Figure 2*. At low concentrations the data fit a single curve as predicted by the Einstein equation.

At higher concentrations the viscosity characteristics of the solutions are non-Newtonian. Since no effort was made to correct the measured viscosities to zero shear rates, it is not surprising that the data exhibit some scatter at higher concentrations of microgel. This good correlation of the viscosities

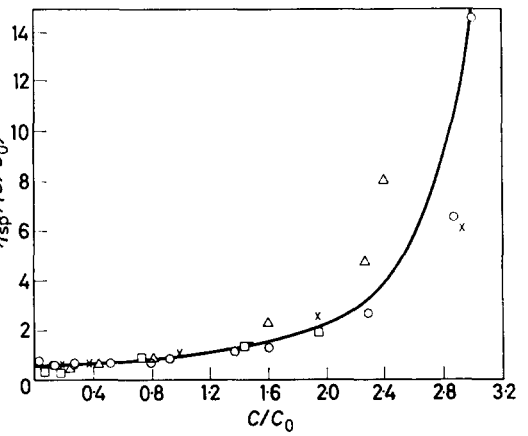

Figure 2—Master plot of microgel viscosity behaviour. ▲ 50A in ethylbenzene; △ 50B in chloroform; × 50A in chloroform; ○ 50C in perchlorethylene; ● 46B in MEK; □ 50C in chloroform

of such disperse systems seems to show that the dilute microgel solutions can be described by the Einstein law. This being so allows the calculation of volume swelling, or swelling factor, of the microgel spheres from the intrinsic viscosities by assuming an Einstein constant of 2·5 and a dry density of 1·0 for the microgel. The intrinsic viscosities and calculated swelling factors are listed in *Table 1*.

Table 1. Composition and solution properties of microgels

Sample	*DVB content per cent*	*Initial diameter Å*	*Solvent*	$[\eta]$ $dl\ g^{-1}$	*Swelling factors*	
					Viscosity	*Light scattering*
50A	0·1	738	Toluene	0·69	27·6	13·2
			Chloroform	0·59	23·6	—
			Ethylbenzene	0·37	14·8	—
50B	0·3	740	Chloroform	0·50	20·0	—
			Toluene	0·32	12·8	—
			Ethylbenzene	0·31	12·4	—
17D	0·3	1306	Toluene	—	—	13·5
17E	0·3	1294	Toluene	—	—	14·5
17G	0·3	743	Toluene	—	—	13·9
			Toluene	—	—	12·7
			Toluene	—	—	12·7
			Butanone	—	—	9·91
			Butanone	—	—	9·17
50C	0·5	743	Chloroform	0·30	12·0	13·4
			Perchlorethylene	—	—	9·32
			Toluene	0·21	8·4	7·95
			Toluene	—	—	8·40
			Ethylbenzene	0·18	7·2	8·42
			Butanone	—	—	7·56
46B	0·5	746	Chloroform	0·32	12·8	18·8
			Toluene	0·28	11·2	14·1
			para-Xylene	0·28	11·2	—
			Perchloroethylene	0·24	9·6	—
			Ethylbenzene	0·24	9·6	—
			Butanone	0·16	6·4	—
50D	1·0	740	Toluene	0·20	8·0	—
			Chloroform	0·18	7·2	—
			Ethylbenzene	0·15	6·0	—
50E	3·0	740	Toluene	0·20	8·0	—
			Chloroform	0·18	7·2	—
			Ethylbenzene	0·08	3·2	—

DISCUSSION

Examination of *Table 1* shows that the swelling factor increases with decreasing crosslinking, just as one would expect. The agreement between the diameters calculated from viscosity measurements and those obtained by light scattering is good at higher DVB contents. At low DVB content (0·1 per cent) the two methods do not agree. Light scattering data obtained on these particles do not show an increase in swelling at low DVB content. Shashoua and Beaman[1] reported that styrene–DVB microgels at 0·25 per cent DVB and less exhibited two components when they were ultracentrifuged. The suggestion is that these lightly crosslinked polymers are a mixture of highly branched and essentially linear molecules. It is felt that the present results are in line with those of the earlier investigators and that the probable branched nature of the low DVB materials renders them susceptible to analysis using a sphere model in viscosity studies beyond the point where light scattering supports this viewpoint.

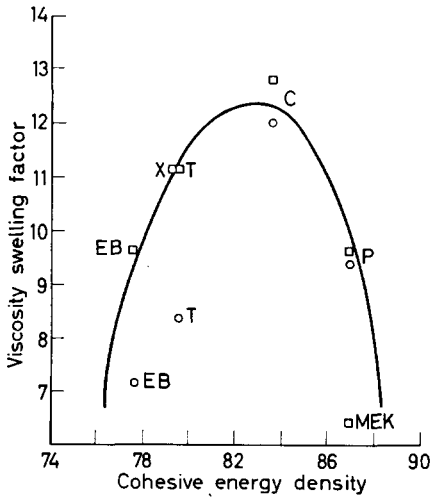

Figure 3—Relationship between swelling factor and solvent. P denotes perchlorethylene; C, chloroform; T, toluene; X, *p*-xylene; EB, ethylbenzene; ○ 50C; □ 46B

Finally, a plot of the swelling factor against the solvent cohesive energy density is presented in *Figure 3*. This plot has the same qualitative features as a plot of intrinsic viscosity versus cohesive energy density for linear polymers. Thus, the swelling of microgel and the extension of linear polymers have their origin in similar thermodynamic solvent–solute interactions.

The author wishes to express his appreciation to Dr W. A. Pavelich for the light scattering data and his many helpful discussions of the problem. Also, to the Dow Chemical Co. for sponsoring and releasing this work for publication.

C. L. SIEGLAFF

Diamond Alkali Company Research Center,
P.O. Box 348, Painesville, Ohio

(Received January 1963)

REFERENCES

[1] SHASHOUA, V. E. and BEAMAN, R. G. *J. Polym. Sci.* 1958, **33**, 101–117
[2] EINSTEIN, A. *Ann. Phys., Lpz.* 1906, **19**, 289; 1911, **34**, 591

The Effect of Zinc Oxide on the Cobalt-60 Gamma Initiated Polymerization of Vinyl Monomers at Low Temperatures

A NUMBER of papers have been published in which the effect of various solid additives on the radiation initiated polymerization of isobutene at solid carbon dioxide temperatures has been discussed[1-4], and it has been shown that many inorganic materials can cause striking increases in the *G* value observed for monomer consumption. It has been generally accepted that the additives are able to capture electrons produced by ionization of the isobutene and the lifetime of the positive ions in the liquid phase is thus increased, so that cationically propagated chains are able to grow to a greater extent than would otherwise be possible. It would appear on the basis of such a mechanism that the effect should not be confined to isobutene, and similar rate increases would be expected in any monomer capable of undergoing a cationic propagation process. We have accordingly studied the effect of zinc oxide on the polymerization of styrene, α-methyl styrene and cyclohexene, which are known to polymerize by a cationic mechanism: methyl methacrylate and isoprene were also investigated although it is not certain that a cationic polymerization can occur with these two monomers. All the experiments were carried out at as low a temperature as possible without freezing the monomers and conversions were followed either by dilatometry or by a simple gravimetric technique.

Purification of the monomers was rigorous, and each purified monomer was outgassed and dried *in vacuo* over a suitable drying agent (see *Table 1*).

Table 1

Monomer	*Drying agent*	*Wt fraction zinc oxide*	*Temperature of irradiation (°C)*	*Radiation intensity (rad/h)*	*Method of rate measurement*	*Rate of polymerization (%/h)*
Isoprene	Sodium	0	−78·5	$6·9\times10^4$	Gravimetric	0·005
		0·25	−78·5	$6·9\times10^4$	Gravimetric	0·013
Methyl methacrylate	Barium oxide	0	−40·5	$3·1\times10^3$	Gravimetric	0·388
		0	−40·5	$3·1\times10^3$	Dilatometer	0·444
		0·30	−40·5	$3·1\times10^3$	Gravimetric	0·317
		0·45	−40·5	$3·1\times10^3$	Dilatometer	0·432
Cyclohexene	Barium oxide	0	−78·5	$2·0\times10^4$	Dilatometer	*Nil*
		0·50	−78·5	$2·0\times10^4$	Dilatometer	*Nil*
Styrene	Calcium hydride	0	−25·0	$3·1\times10^3$	Dilatometer	<0·005
		0·50	−25·0	$3·1\times10^3$	Dilatometer	<0·005
α-Methyl styrene	Silica gel	0	−18·0	$3·1\times10^3$	Dilatometer	<0·005
		0·50	−18·0	$3·1\times10^3$	Dilatometer	<0·005

It was then distilled on the vacuum line into a vessel containing zinc oxide made and outgassed as described in ref. 4. The results obtained are summarized in *Table 1*. The radiation intensities used were chosen so that if zinc oxide gave rate increases comparable with those produced in isobutene conversions of about 60 per cent per hour would be obtained. In fact, the additive produced very little change in polymerization rate of any of the monomers studied, and although the rates are generally too low for accurate measurement, it is clear that nothing like the increase in

rate by a factor of 10^3 to 10^4 which we have obtained with isobutene is involved.

It has also been shown in this laboratory[5] that zinc oxide has little effect on the rate of polymerization of butyl vinyl ether at $-78°C$, and it would therefore appear that the very large effect of additives on the polymerization rate of isobutene is not a general phenomenon but is confined to this monomer. The reason for this specificity is not as yet clear, but it would seem that the mechanism of the additive effect in isobutene must be rather more complex than has been previously envisaged.

F. L. DALTON
K. HAYAKAWA

Wantage Research Laboratory (A.E.R.E.),
Radiation Branch,
Isotope Research Division,
Wantage, Berks.

(Received February 1963)

REFERENCES

[1] WORRALL, R. and CHARLESBY, A. *Internat. J. appl. Radiation and Isotopes,* 1958, **6,** 8
[2] DAVISON, W. H. T., PINNER, S. H. and WORRALL, R. *Proc. Roy. Soc. A,* 1959, **252,** 187
[3] WORRALL, R. and PINNER, S. H. *J. Polym. Sci.* 1959, **34,** 229
[4] DALTON, F. L., GLAWITSCH, G. and ROBERTS, R. *Polymer, Lond.* 1961, **2,** 419
[5] BALLANTINE, D. S. Unpublished results

Contributions to Polymer

Papers accepted for future issues of POLYMER include the following:

The Crystallization of Polyethylene after Partial Melting—W. BANKS, M. GORDON and A. SHARPLES

The Diffusion and Clustering of Water Vapour in Polymers—J. A. BARRIE and B. PLATT

Dipole Relaxation in the Crystalline Phase of Polymers II—C. A. F. TUIJNMAN

Crystallization of Gutta Percha and Synthetic trans-1,4-Polyisoprenes—W. COOPER and G. VAUGHAN

Solid State Polymerization of β-Propiolactone—G. DAVID, J. VAN DER PARREN, F. PROVOOST and A. LIGOTTI

Viscosity/Molecular Weight Relation in Bulk Polymers I—H. P. SCHREIBER, E. B. BAGLEY and D. C. WEST

Viscosity/Molecular Weight Relation in Bulk Polymers II—Onset of non-Newtonian Flow—H. P. SCHREIBER

An Infra-red Study of the Deuteration of Cellulose and Cellulose Derivatives—R. JEFFRIES

The Glass Transition Temperature of Polymeric Sulphur—A. V. TOBOLSKY, W. MACKNIGHT, R. B. BEEVERS and V. D. GUPTA

Gamma-irradiation Polymerization of Isobutene and β-Propiolactone at Low Temperature—C. DAVID, F. PROVOOST and G. VERDUYN

Aminolysis of Polyethylene Terephthalate—H. ZAHN and H. PFEIFER

Molecular Motion in Polyethylene IV—D. W. MCCALL and D. C. DOUGLASS

A New Transition in Polystyrene, I, II, III—G. MORAGLIO, F. DANUSSO, V. BIANCHO, C. ROSSI, A. M. LIQUORI and F. QUADRIFOGLIO

Free Radical Reactions in Irradiated Polyethylene—M. G. ORMEROD

The Radiation Chemistry of Some Polysiloxanes: An Electron Spin Resonance Study—M. G. ORMEROD and A. CHARLESBY

The Mechanical Degradation of Polymers—C. BOOTH

Dynamic Birefringence of Polymethylacrylate—B. E. READ

Solution and Bulk Properties of Branched Vinyl Acetates, I, II, III—L. M. HOBBS, V. C. LONG, G. C. BERRY and R. G. CRAIG

Polycarbonates from the 2,2,4,4-Tetramethylcyclobutane-1,3-diols I—Preparation and Structure—Miss M. GAWLAK and J. B. ROSE

Polycarbonates from the 2,2,4,4-Tetramethylcyclobutane-1,3-diols II—Crystal Structure and Melting Behaviour—A. TURNER JONES and R. P. PALMER

The Temperature Dependence of Extensional Creep in Polyethylene Terephthalate—I. M. WARD

The Radiation Chemistry of Polymethacrylic Acid, Polyacrylic Acid and Their Esters; An Electron Spin Resonance Study—M. G. ORMEROD and A. CHARLESBY

Crystallinity and Disorder Parameters in Nylon 6 and Nylon 7—W. RULAND

Mechanism of the Ductile–Brittle Transition in Linear Polyethylene—S. STRELLA and S. NEWMAN

A Thermodynamic Description of the Defect Solid State of Linear High Polymers—B. WUNDERLICH

*Graft Copolymerization Initiated by Poly-*p*-lithiostyrene*—M. B. HUGLIN

Structure and Properties of Crazes in Polycarbonate and Other Glassy Polymers—R. P. KAMBOUR

The Crystallization of Polymethylene Copolymers: Morphology—J. B. JACKSON and P. J. FLORY

Description and Calibration of an Elasto-osmometer—H. J. M. A. MIERAS and W. PRINS

Resonance-induced Polymerizations—R. J. ORR

CONTRIBUTIONS should be addressed to the Editors, *Polymer*, 4-5 Bell Yard, London, W.C.2.

Authors are solely responsible for the factual accuracy of their papers. All papers will be read by one or more referees, whose names will not normally be disclosed to authors. On acceptance for publication papers are subject to editorial amendment.

If any tables or illustrations have been published elsewhere, the editors must be informed so that they can obtain the necessary permission from the original publishers.

All communications should be expressed in clear and direct English, using the minimum number of words consistent with clarity. Papers in other languages can only be accepted in very exceptional circumstances.

A leaflet of instructions to contributors is available on application to the editorial office.

The Crystallization of Polyethylene after Partial Melting

W. BANKS, M. GORDON* and A. SHARPLES

The crystallization of polyethylene has been shown to be independent of the previous temperature of melting, even when the melting point is exceeded by as little as 0·3°C. The persistence of nuclei which are progressively removed as the temperature is raised above the melting point is thus excluded. Partial melting at temperatures below *the melting point, however, does leave seeds which can act as centres for further growth on subsequent cooling, and this seeded crystallization appears to involve sub-units of structure within the outlines of the original spherulites. A detailed account is given of this new type of crystallization, and possible mechanisms for the process are considered.*

THE growth of the solid phase in a crystallizing polymer arises from nuclei which form in the super-cooled melt, and is generally considered to develop in three dimensions to give spherulitic structures[1]. Previous workers have observed that the temperature to which the molten polymer is raised prior to crysallization may be an important factor in determining subsequent behaviour[1-3] and this has led to the hypothesis that, on melting, remnants of the previous structure may act as nuclei, or seeds, unless temperatures well above the melting point are used to destroy them. This hypothesis is considered here in relation to polyethylene.

In addition, a new type of crystallization process is reported, which occurs when a solid sample of polymer is partially melted at temperatures below the melting point, and subsequently crystallized in the presence of the unmelted material.

EXPERIMENTAL

Materials

The polyethylene samples used were identical with those reported in an earlier publication[4]; the important characteristics are summarized here in *Table 1*. Degrees of polymerization, $\overline{P}_v$, were determined viscometrically, and the melting point, T_m, was found from the volume/temperature relationship, for samples which had been crystallized for up to 30 000

Table 1. Characteristic parameters of polyethylene samples

Sample	$\overline{P}_v$	T_m°C	*Comments*
3	670	135·9	Fraction from Phillips Polyethylene A
5908	350	135·5	Fraction from Phillips Polyethylene B
5907	1 800	136·1	Fraction from Phillips Polyethylene B
5905	7 300	136·6	Fraction from Phillips Polyethylene B
5902	14 800	136·8	Fraction from Phillips Polyethylene B
5901	18 500	136·8	Fraction from Phillips Polyethylene B

*Present address: Chemistry Department, Imperial College, South Kensington, London.

minutes at temperatures such that the half-lives of the primary crystallization were *ca.* 30 min. The poly(ethylene oxide) sample was supplied by Polymer Consultants Ltd.

Dilatometry

The techniques used in the present investigation have been described in a previous paper[4]. The samples were moulded to suitable shapes for insertion into the dilatometers at temperatures just sufficient to enable flow to occur. The melt temperature varied from sample to sample but never exceeded 180°C, and this was the only prior heat treatment to which the samples were subjected. Values for the fraction of crystalline material, χ, were determined from density measurements[4].

Microscopy

Readily observable spherulites are not normally found in polyethylene unless the sample is subjected to drastic pretreatment[6]. Consequently, the histories of the samples used in the present study are given in the next section and considered in relation to the results obtained. Sample thicknesses of approximately 10μ were used throughout, and crystallization temperatures were controlled by a thermostatted hot-stage to $\pm 0{\cdot}05$°C. Visual observations were taken using a 10× eyepiece, and a 6 mm objective; photographs were made using the 6 mm objective alone.

RESULTS

Dilatometry

It has previously been shown[4] that the primary crystallization of polyethylene conforms to the Avrami equation

$$W_L/W_0 = \exp(-zt^n) \tag{1}$$

where W_L/W_0 is the weight fraction of the liquid phase remaining after time t and z is constant for a given temperature. Current theory[5] requires that n be an integer with a value of 1, 2, 3 or 4, but in practice fractional values have been observed[4] for polyethylene. The process can be followed dilatometrically and the fraction of unconverted material found from the equation

$$W_L/W_0 = (h_t - h_\infty)/(h_0 - h_\infty) \tag{2}$$

where h_t is the dilatometric height at time t and ∞ indicates the end of the primary stage. In some polymers, including polyethylene, the primary crystallization is followed by a secondary process which has a different time dependence, and this complicates the analysis of the data. However, a method has been proposed for separating the two processes, and the results given here for the Avrami parameters, n and z, are obtained using this approach[4].

(a) *Effect of melt temperature on subsequent crystallization*—In *Figure 1* the crystallization of a polyethylene fraction, 5901 ($T_m = 136{\cdot}8$°C), is given as typical of the behaviour of all the samples studied. Premelting the sample for 15 minutes at 210°C or 137·1°C leads to identical results;

when the sample is heated at 0·9°C *below* its melting point, however, a considerable difference in behaviour is observed, and the half-life of the process decreases from 100 min to 17·5. It is evident that all memory of previous crystallizations is effectively removed at the melting point, and that no further change occurs even when the melt temperature is increased by 70°C. (At much higher temperatures changes are observed but these are more consistent with degradation.) Consequently, the persistence above the melting point of nuclei whose concentration is reduced only by prolonged heating can be excluded as a possibility in the case of polyethylene.

(b) *Crystallization from seeds formed by partial melting*—The work of Hoffman, Weeks and Murphey[2] using poly(chlorotrifluorethylene) suggests that on partial melting the growth from primary nuclei is reversed until some at least of the original sporadically formed nuclei remain. These are then assumed to be capable of acting as seeds when the polymer is

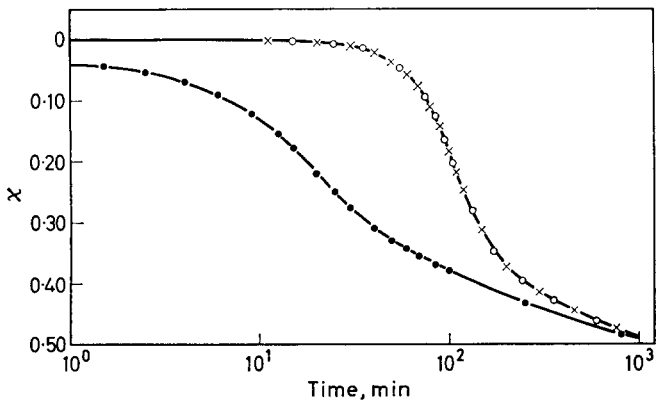

Figure 1—Crystallization of polyethylene fraction 5901 (T_m=136·8°C) at 127·50°C. × preheated at 210°C; ○ preheated at 137·1°C; ● preheated at 135·90°C

again crystallized at a lower temperature. The nucleation process thus changes from being sporadic to being predetermined, and the Avrami exponent, n (equation 1), is expected to decrease by one unit[1,5]. The results in *Figure 1* show that partial melting in polyethylene does lead to an increase in rate during subsequent crystallization, as would be expected from the above hypothesis, and so a more detailed analysis of the data is made below to test whether the proposed mechanism is operative in the present case.

The seeded process indicated in *Figure 1* was carried out on several polyethylene fractions by first crystallizing to well into the secondary stage, and then raising the temperature to various values below the melting point, to leave differing amounts of seed crystallinity, χ_s, at equilibrium. The temperature was then lowered to enable the seeded crystallization process to occur.

(i) *Time dependence of seeded crystallization.* In all cases it was found that the results conform to an Avrami-type equation of the form

$$(h_t - h_\infty)/(h_s - h_\infty) = \exp(-z_s t^n) \tag{3}$$

where h_s is the dilatometric height at the start of the process when the seed crystallinity is equal to χ_s, and z_s is a constant for given values of crystallization temperature and χ_s. The results for fraction 5907 at a fixed

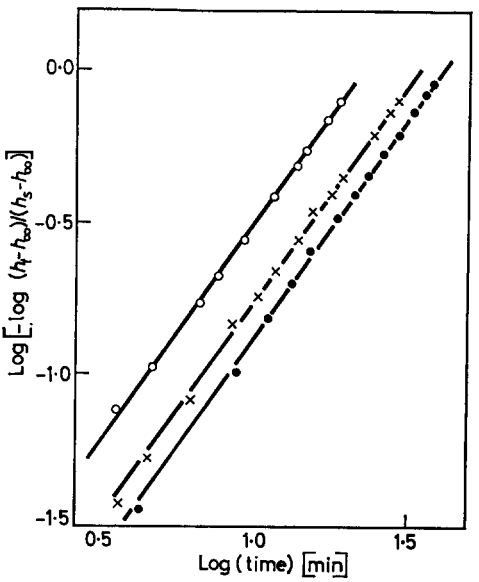

Figure 2—Polyethylene fraction 5907 crystallized at 130·00°C after partial melting at various temperatures below the melting point to leave different amounts of seed crystallinity. Plot of log $\left(-\log \frac{h_t - h_\infty}{h_s - h_\infty}\right)$ versus log t for $\chi_s = 0{\cdot}1108$ ●; $\chi_s = 0{\cdot}1806$ ×; $\chi_s = 0{\cdot}3315$ ○

temperature of crystallization but for different values of χ_s are given in *Figure 2*, and it can be seen that they are in excellent agreement with equation (3). An important feature is that χ_∞, the crystallinity at the end of the Avrami or primary crystallization[4], as characterized by h_∞ in equation (3), is the same for the seeded crystallization as for the unseeded process (see *Table 2*).

(ii) *The value of the exponent, n.* The Avrami exponent, n (from equation 3), decreases as the amount of seed crystallinity is increased, until eventually a constant value is attained. This is illustrated in *Figure 3*, and results for the limiting value are given in *Table 2*. These vary from sample to sample over the range 1·25 to 1·58 and, as for the unseeded crystallization[4], are significantly different from any of the integral values required by existing theory[1,4,5]. The point of immediate interest, however, is that n decreases by considerably more than one unit on seeding, which is more than would be expected if the Hoffman, Weeks and Murphey mechanism were operative[2]. Consequently, their picture does not apply in the present

case and, in particular, melting and seeded crystallization cannot be considered as reversible processes, involving contraction and expansion of the original units of growth.

Table 2. Representative figures for seeded and unseeded crystallization parameters

Sample	Unseeded				Seeded			
	Temp. °C	χ_∞	n	B	Temp. °C	χ_∞	n (at limit)	B
5901	127·50	0·34	2·97	200	127·50	0·35	1·35	200
	125·36	0·34	3·12		129·10	0·35	1·36	
5902	128·40	0·38	3·03	150	128·14	0·36	1·25	140
	125·73	0·36	3·54		127·82	0·36	1·29	
5905	128·49	0·45	3·48	100	128·70	0·41	1·58	—
5907	130·00	0·56	3·87	85	130·00	0·57	1·42	70
	128·26	0·55	3·47		130·50	0·57	1·40	

(iii) *The seeded rate constant, z_s.* It has already been noted above that the seeded crystallization is more rapid than the unseeded process; in fact it was found that the seeded rate constant, z_s, increases in direct proportion to the amount of seed crystallinity present, and in *Figure 4* results given

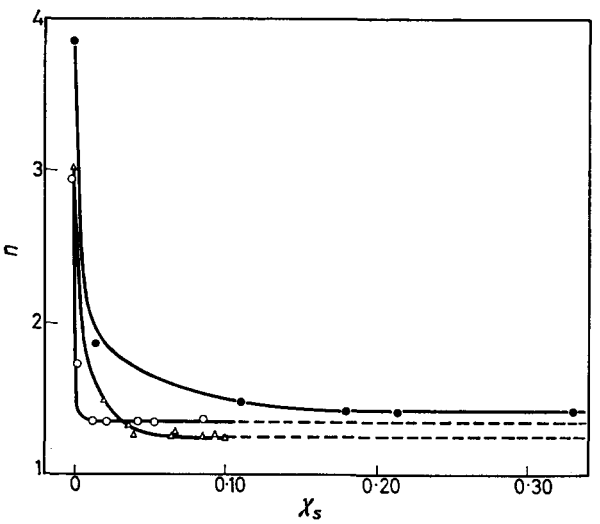

Figure 3—Avrami exponent n plotted as a function of seed crystallinity χ_s. ○ fraction 5901 crystallized at 127·50°C; △ fraction 5902 crystallized at 128·14°C; ● fraction 5907 crystallized at 130·00°C

for three samples can be seen to establish this point. The plots appear to pass through the origin, and this at first sight might seem to lead to the unacceptable conclusion that the unseeded rate constant, z, is zero. In fact, for the cases quoted, the unseeded rate constant, z, is in the region of 10^{-8}, and this is indistinguishable from zero on the scale used in *Figure 4*. A

comparison of this figure with z_s does not of course give a quantitative comparison of overall rate, as this depends also on the exponent, n (equation 1), which differs considerably for the seeded and unseeded cases.

(iv) *Temperature dependence of seeded rate constant.* It has previously been established[4] that the unseeded rate constant is related to temperature of crystallization, T_c, and melting point, T_m, by the equation

$$\log z = A - nB/\Delta T^2 \tag{4}$$

where $\Delta T = T_m - T_c$. For the limited range of temperatures over which it is possible to make measurements (i.e. *ca.* 2°C), an identical relation

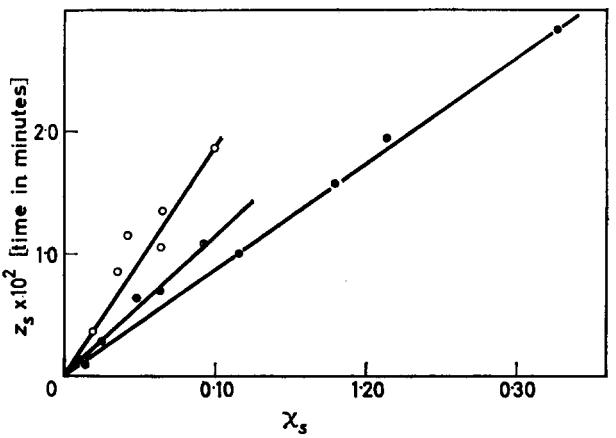

Figure 4—Seeded rate constant z_s plotted as a function of seed crystallinity χ_s; ○ fraction 5902 crystallized at 128·14°C; △ fraction 5905 crystallized at 128·70°C; ● fraction 5907 crystallized at 130·00°C

was found to hold for z_s (at a fixed value of χ_s) using the same values of T_m as for the unseeded experiments. Also, the parameter, B, which is characteristic of the nature of the growing surface[5], has, within experimental error, the same value for the two types of crystallization, even though it varies considerably from one sample to another (*Table 2*).

(v) *Secondary crystallization.* During the secondary stage, which accounts for the production of a significant fraction of crystalline material in polyethylene, the crystallinity increases with time according to the equation[4]

$$\chi = C + D \log t \tag{5}$$

where D is a constant which is very little affected by changes in temperature and molecular weight and t has its origin at the beginning of the secondary process. In a previous study[4] of the unseeded crystallization of polyethylene, D was found to have a value of $0{\cdot}09 \pm 0{\cdot}01$ for a wide

range of samples and crystallization temperatures. In the present study of the seeded process, a similar secondary crystallization was found to occur after the completion of the primary, or Avrami, stage with an identical value of D. A typical set of results is given in *Figure 5* and it can be seen that the secondary crystallization is the same for seeded and unseeded runs.

Microsopy

Comparative observations on the same sample by the two techniques of dilatometry and microscopy could be considerably informative with regard to the phenomena reported in the previous section, but unfortunately they are restricted by the fact that, in general, polyethylene does not produce microscopically resolvable growth units during its normal crystallization[6]. Spherulites of observable dimensions ($>10^{-3}$ cm diameter) can be obtained, but it is considered that the methods used to produce them result in a stage which is not characteristic of the original material. It is possible that the unresolvable structures normally obtained may consist

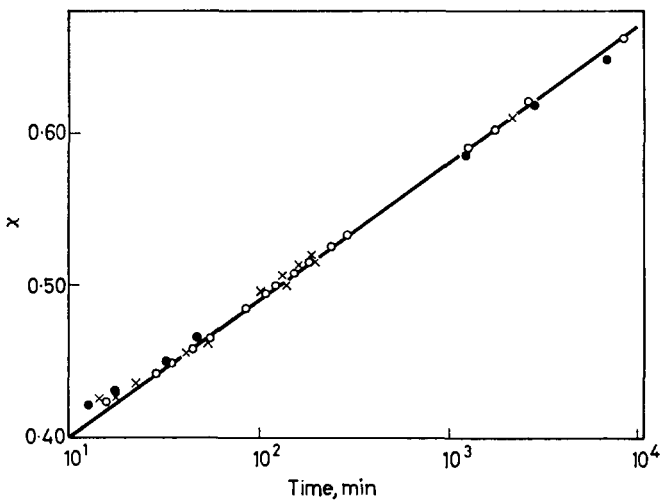

Figure 5—Post-Avrami stage kinetics for fraction 5905 crystallized at 128·70°C; ○ $\chi_s = 0{\cdot}0125$; × $\chi_s = 0{\cdot}0644$; ● $\chi_s = 0{\cdot}0934$. The straight line represents the data for the unseeded experiment

of very small spherulites, or at least of units of structure which represent the first stage in the growth of a spherulite, with dimensions in the range 10^{-5} to 10^{-4} cm, and if this is so the observations recorded below on larger spherulites may be applicable to the normal structures, such as are formed during the dilatometric experiments. However, this point has not yet been conclusively established.

First, in a sample which has not been specially treated, and hence where

observations on resolvable spherulites are not possible, the overall appearance of the birefringent structure undergoes the changes recorded in *Table 3*, on partial melting and seeded crystallization. The point at which birefringence disappears completely, as judged visually, depends considerably on the sample, and on the time and temperature of crystallization, and may sometimes be as much as 4°C below the dilatometrically determined melting point. This presumably reflects the differences also to be found in the melting distribution curves, or volume/temperature relationships. Consequently the values of χ_s determined dilatometrically (*Table 3*) were

Table 3. Polyethylene fraction 5907 ($T_m = 136{\cdot}1$°C). Microscopic appearance on partial melting and seeded crystallization (Crystallized initially at 128·0°C for 270 min)

Seed crystallinity χ_s	*Temp. of partial melting* °C	*Intensity of birefringence*	*Time for first sign of b.r. to appear during subsequent crystallization at 128·0°C*
0·60	134·0	Starts to decrease	—
0·04	135·8	Completely disappears	2 min
0·01	136·0	Completely disappears	5 min
0	136·1	Completely disappears	12 min
0	136·2	Completely disappears	12 min
0	150	Completely disappears	12 min

measured for a sample of fraction 5907 crystallized under the same conditions as were used in the microscopy experiments. The time for the first sign of birefringence to reappear on crystallizing after partial melting is taken as an inverse measure of the rate, and this can be seen to regain its value for the unseeded process at the same temperature as that at which all crystallinity is lost, i.e. at the dilatometric melting point. Thus it is confirmed that all memory of previous structure is removed at the melting point.

Next a sample of fraction 5908 was studied, after it had been subjected to a prior heat treatment which converted it to a form where large spherulites ($>10^{-2}$ cm) could be observed. The treatment involved four hours heating at 300°C *in vacuo* between glass slides, and resulted in a film whose melting point determined microscopically, was found to be 131·2°C. The effect of this treatment is not established with certainty, but it is possible that physical aggregation of nuclei occurs, thereby effectively reducing their number, and so increasing the size of the bodies grown from them[6]. In the present case, the reduced melting point indicates that degradation had also occurred.

A typical photograph of the spherulites produced in this sample is given in *Figure 6*. On partial melting to the point where no birefringence is left,

and crystallizing by lowering the temperature, the birefringence reappears *uniformly* within the outlines of the original spherulites, and has the granular appearance typified in *Figure 7*. This confirms the conclusion reached

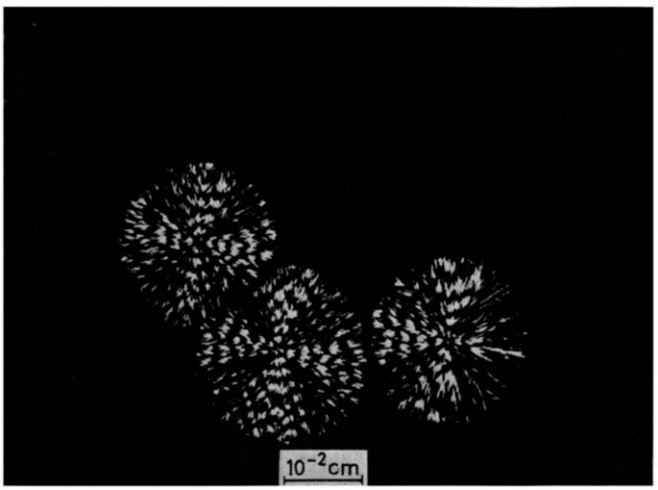

Figure 6—A spherulitic sample of fraction 5908, produced by an arbitrary heat treatment. Spherulites grown from the melt at 118·4°C for 8 minutes

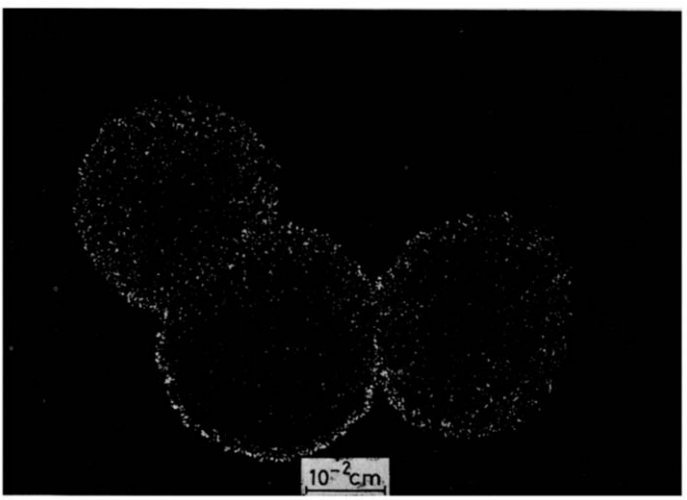

Figure 7—Granular structure produced within spherulite outlines shown in *Figure 6*, by partial melting at 127·6°C followed by seeded crystallization at 118·4°C for 1 min

above, that partial melting and seeded crystallization do not involve the contraction and expansion of the spherulites along their original lines of growth. Instead it is evident that partial melting leaves seeds within the

original spherulites, which then initiate the growth of sub-units of structure during the subsequent seeded crystallization. Unfortunately, it is not possible to relate the formation of this granular structure to the quantitative amount of seeded crystallinity remaining as a result of partial melting, owing to the unrepresentative nature of the large spherulites, as noted above. It can be said, however, that the granular structure typified by *Figure 7* can be obtained in a wide variety of spherulitic polymers (polyesters, polyamides, polypropylene and polyethylene oxide[7]), if suitable temperatures of partial melting are chosen. In addition, there are indications

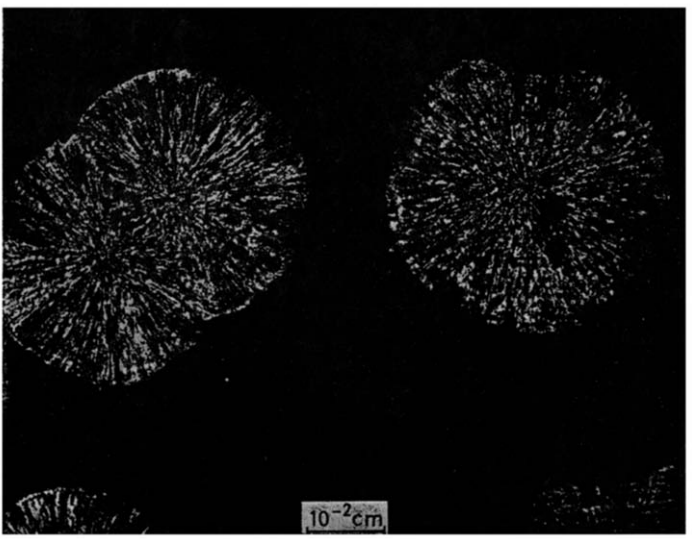

Figure 8—Spherulites in poly(ethylene oxide) obtained by completely melting at 80°C, and then crystallizing at 56·8°C for 20 min

in the literature that this type of structure has been obtained by previous workers[8,9].

If the granular appearance in *Figure 7* arises from a large number of sub-units of structures formed within the original spherulite outline, and if progressive increase of temperature of partial melting reduces the number of seeds from which these structures are formed (as is implied by the correlation given in *Figure 4*), then careful control of conditions should reduce the number of seeds to an extent where subsequent growth is microscopically resolvable. This was found to be possible with the above sample of polyethylene fraction 5908, but the effect is easier to control and demonstrate in poly(ethylene oxide), whose temperature coefficient is more favourable. In *Figure 9*, the seeded growth within the original outlines of poly(ethylene oxide) spherulites (*Figure 8*) can be seen to stem from easily resolvable centres, and to take the form of small spherulites similar in appearance to those arising during the unseeded process (*Figure 8*). In

addition, measurements made on these seeded spherulites showed that the radial growth rates are the same for the two cases.

Finally, if a polyethylene spherulite is partially melted and allowed to crystallize from seeds (*Figure 7*), subsequent growth, after the original

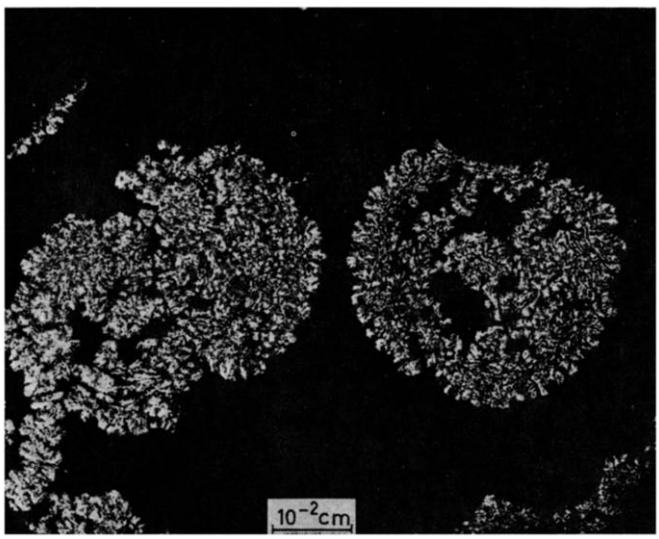

Figure 9—Resolvable structures formed within outlines of spherulites shown in *Figure 8* by partial melting at 65·7°C followed by seeded crystallization at 56·8°C

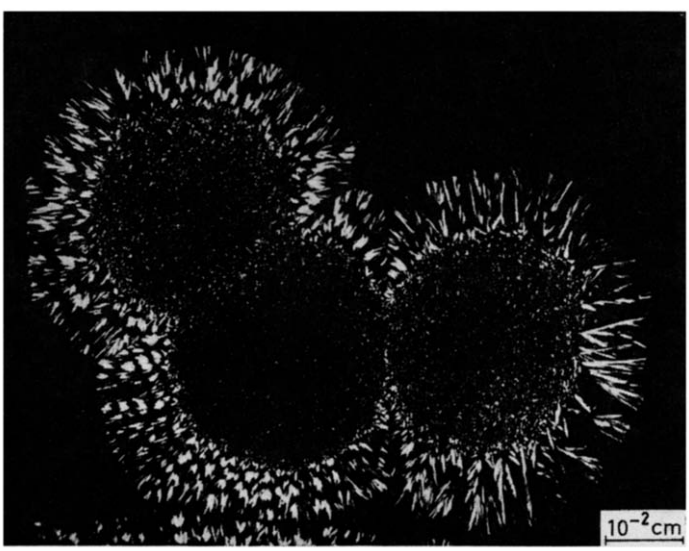

Figure 10—Same field as shown in *Figure 7*, but after a further 5 min growth at 118·4°C

spherulite outline is filled in to give a granular structure, continues in a way which is identical to the unseeded growth. This is demonstrated in *Figure 10*.

DISCUSSION

The dilatometric and microscopic experiments on polyethylene show that all memory of previous crystallizations is effectively removed at the melting point, and that subsequent kinetic behaviour is reproducible even when the sample is heated further to as much as 70°C above this temperature. Thus the persistence of nuclei in the melt, either as aggregates of polymer molecules[1], or in cracks in impurities[3], is excluded in the present case. Similar results on poly(decamethylene terephthalate[10,11]) indicate that the situation is not unique. This does not exclude the possibility that the unseeded crystallization is nucleated by heterogeneities (in fact the indications are that this is so[6,11]) but it does mean that, if heterogeneous nuclei are present, they are not *progressively* decreased in number when the temperature is raised, and then reformed on subsequent crystallization, as is required by the above hypotheses[1,3].

When the sample is partially melted at temperatures below the melting point, seeds do remain which can act as nuclei for further growth on subsequent cooling. The possibility that the observed effects may be explained in terms of simple contraction and expansion of the original spherulites, however, as suggested by Hoffman, Weeks and Murphey for poly(chorotrifluorethylene)[2], is ruled out first by the fact that the Avrami exponent n decreases in the present case by considerably more than the predicted value of one unit (*Table 2*); and secondly by the microscopic appearance of seeded spherulites (*Figures 7* and *9*). Previous workers[12,13] have found that the intensity of scattered light follows different paths during melting and cooling, thus confirming the contention that melting is not a simple reversal of the unseeded crystallization process.

The values of n obtained for seeded crystallization are quite low (1·25 to 1·58), and in all cases they are significantly different from the integers required by theory[5]. Fractional and constant values of n (2·0 to 4·0) have similarly been found[4] for the unseeded process but no satisfactory explanation has so far been advanced to account for the effect. There is an indication[4], however, that low values of n occur when the final size of the growth unit is small so that it is reasonable to deduce that the growth units formed during seeded crystallization are very much smaller than those produced in the unseeded process. This is of course confirmed by the microscopic observations which show that sub-units of structure are formed from a large number of seeds left within the outlines of the original spherulites (*Figure 9*). It has previously been suggested[14] that low values of n may occur when the structure is a granular one consisting of many small growth units, on the assumption that the number of dimensions in which growth can occur is similarly reduced during the early stages in their formation. However, if this explanation is applicable here, it requires modification to account for the fact that the values of n observed are both fractional and constant throughout a given crystallization run.

In untreated polyethylene even the unseeded crystallization gives rise to very small growth units which are in fact microscopically unresolvable ($<10^{-4}$ cm). As the seeded growth must involve sub-units which are even smaller, one possibility which immediately suggests itself is that these sub-units are the microcrystallites of size approximately 10^{-6} cm. If this is so there is one important fact that requires consideration. For the unseeded crystallization, the rate-controlling step in the growth of the spherulites is generally considered to be one of secondary nucleation[5]. The form of the temperature dependence is accounted for on this assumption[4,5]. The growth of the microcrystallites, however, is unlikely to proceed by a similar mechanism, and yet the temperature dependence of the seeded crystallization found in the present experiments not only takes the same form as that for the unseeded process; it also has the same value for the characteristic parameter, B (equation 4 and *Table 2*). Consequently, although it is certain that seeded crystallization involves the growth of sub-units of structure much smaller in size than the original spherulites, it is not possible at this stage to speculate with certainty on their nature.

Apart from the lower values of n, the seeded crystallization resembles the unseeded process in many ways. Thus the crystallinity at the end of the primary stage, χ_∞, is the same in both cases, as is the temperature dependence parameter, B (*Table 2*). Also, after χ_∞ is passed the subsequent secondary crystallization is the same, as can be seen from *Figure 5*. Finally, in poly(ethylene oxide), where the seeded growth can be resolved, the growth units are similar both in appearance and growth rate to the original spherulites. One important difference, however, is that seeded crystallization occurs in the presence of unmelted crystalline material whose volume is not negligible. The question thus arises as to the location of the seeds in relation to this crystalline material.

It might appear at first sight that although the contraction and expansion of the original spherulites during partial melting and seeded crystallization is excluded, a process of this nature could be occurring uniformly with the sub-units within the spherulites. This, however, is excluded by the form of equation (3), which shows that the start of each seeded crystallization is a unique state, characterized, for example, by an apparent induction period of zero rate (provided that $n \neq 1$). Thus, the state arrived at by melting to, say ten per cent crystallinity, and then crystallizing to twenty per cent, is different from that produced simply by melting directly to twenty per cent; the subsequent rate plots are not superimposable, a point which also follows from equation (3). It is of course possible that melting occurs along a different axis from that involved in subsequent growth, but it is difficult to visualize any picture which would allow space for the development of crystallinity under these conditions.

A more likely picture is one which assumes that the crystalline material remaining after partial melting is inert, and that crystallization on subsequent cooling occurs in the molten regions from seeds of negligible volume. The decrease in rate which occurs as the melting point is approached (cf. *Figure 4*) is thus accounted for on this picture by the progressive disappearance of seeds from the molten regions. The postulate of crystallization

from seeds of negligible volume, in the presence of inert unmelted material, is the one which best accounts for the observed time-dependence of the seeded process (*Figure 3*). It is also consistent with the broad melting behaviour, which suggests the presence of a range of structural units of varying temperature stability.

SUMMARY

The general picture proposed to account for the process of seeded crystallization is thus one whereby partial melting leaves seeds of negligible volume, which decrease in concentration as the melting point is approached. The rate of crystallization on subsequent cooling is determined by these seeds, and not by the bulk of the unmelted crystalline material, which remains inert. Growth develops from large numbers of seeds within the outlines of the original spherulites, and resembles in many ways the growth of the parent structures.

The authors gratefully acknowledge the financial assistance of British Petroleum Ltd for this work.

Arthur D. Little Research Institute,
Inveresk, Musselburgh,
Midlothian, Scotland

(*Received September 1962*)

REFERENCES

[1] KELLER, A., LESTER, G. R. and MORGAN, L. B. *Phil. Trans. A*, 1954, **247**, 1
[2] HOFFMAN, J. D., WEEKS, J. J. and MURPHEY, W. M. *J. Res. Nat. Bur. Stand. A*, 1959, **63**, 67
[3] PRICE, F. P. *J. Amer. chem. Soc.* 1952, **74**, 311
[4] BANKS, W., GORDON, M., ROE, R.-J. and SHARPLES, A. *Polymer, Lond.* 1963, **4**, 61
[5] MANDELKERN, L. *Growth and Perfection of Crystals*, pp 467–497. Chapman and Hall: London, 1958
[6] BANKS, W., HAY, J. N., SHARPLES, A. and THOMSON, G. *Nature, Lond.* 1962, **194**, 542
[7] BANKS, W. and SHARPLES, A. Unpublished results
[8] ZACHMANN, H. G. and STUART, H. A. *Makromol. Chem.* 1961, **41**, 148
[9] PADDEN, Jr, F. J. and KEITH, H. D. *J. appl. Phys.* 1959, **30**, 1479
[10] SHARPLES, A. and SWINTON, F. L. *Polymer, Lond.* 1963, **4**, 119
[11] SHARPLES, A. *Polymer, Lond.* 1962, **3**, 250
[12] RICHARDS, R. B. and HAWKINS, S. W. *J. Polym. Sci.* 1949, **4**, 515
[13] RHODES, M. B. and STEIN, R. S. *J. Polym. Sci.* 1960, **45**, 521
[14] HARTLEY, F. D., LORD, F. W. and MORGAN, L. B. *Phil. Trans. A*, 1954, **247**, 23

The Diffusion and Clustering of Water Vapour in Polymers

J. A. BARRIE and B. PLATT

Steady state permeation and sorption equilibrium measurements have been made on the water–polydimethylsiloxane system at 35°, 50° and 65°C, and on the water–polymethylmethacrylate system at 50°C. The results have been analysed to determine the concentration dependence of the diffusion coefficient, which in both systems is found to decrease as the concentration of water is increased. The concentration dependence is interpreted in terms of clustering of the water molecules which renders an ever increasing proportion of the overall concentration relatively immobile. A recent model which describes the polymerization of water in an inert continuum is used to evaluate the fractions of polymeric water species present in the polymer. The total flux is then regarded as the sum of the flux contributions from each polymeric species assuming that no contribution to flow occurs within a cluster. The model predicts satisfactorily the shape of the D versus C curve for water–polydimethylsiloxane but the data are not sufficiently accurate to determine whether water species higher than monomer contribute significantly to the overall flux. Satisfactory agreement is not obtained with the D versus C curve for polymethylmethacrylate and the limitations of the model are discussed.

THE diffusion coefficients of organic vapours in polymers are usually found to increase as the penetrant concentration is raised. Generally this effect has been associated with the plasticizing action of the penetrant molecule whilst more specifically Meares has interpreted this concentration dependence in terms of the variation of the segmental jumping frequency with the free volume of the polymer–penetrant mixture[1]. With water vapour as penetrant the normal concentration dependence is often less marked and in fact for polyvinyl acetate, cellulose nitrate, cellulose acetate and 6–10 nylon the diffusion coefficient has been reported as constant over an appreciable range in the concentration[2]. Even more striking is the decrease in the diffusion coefficient with concentration observed with polyethylene[3] and ethylcellulose[4] and which was attributed to the formation of clusters of water molecules within the polymer. The results of the present investigation indicate a similar concentration dependence for the diffusion coefficient of water vapour in polydimethylsiloxane and polymethylmethacrylate. A recent model proposed to account for the polymerization of water in an inert medium such as toluene or benzene provides a means of estimating the cluster size distribution[5]. Relationships derived from this theory are combined with the diffusion equation in an attempt to describe the magnitude and form of the concentration dependence of the water vapour diffusion coefficient.

EXPERIMENTAL

Polydimethylsiloxane sheets approximately 2 mm thick were supplied by Imperial Chemical Industries and were prepared from a polydimethyl-

siloxane gum crosslinked by curing with one per cent by weight of 2,4-dichlorobenzoylperoxide.

Polymethylmethacrylate films approximately 0·2 mm thick were prepared by casting from a benzene solution on a mercury surface followed by outgassing for 12 h at 120°C under high vacuum.

Sorption isotherms were obtained with the polymer sample suspended from the end of a calibrated silica spiral enclosed in a high vacuum apparatus similar to that employed by Barrer and Barrie[4].

Steady state permeation rates were measured as a function of the upstream vapour pressure which was maintained constant throughout a single determination. The effluent vapour was sorbed by a dehydrated aluminosilicate suspended from a calibrated silica spiral and the weight of water permeated in a given time in the steady state calculated. But for the fact that mercury cut-offs were used in place of stopcocks to isolate the effluent system, the apparatus was similar to that of Barrer and Barrie[4].

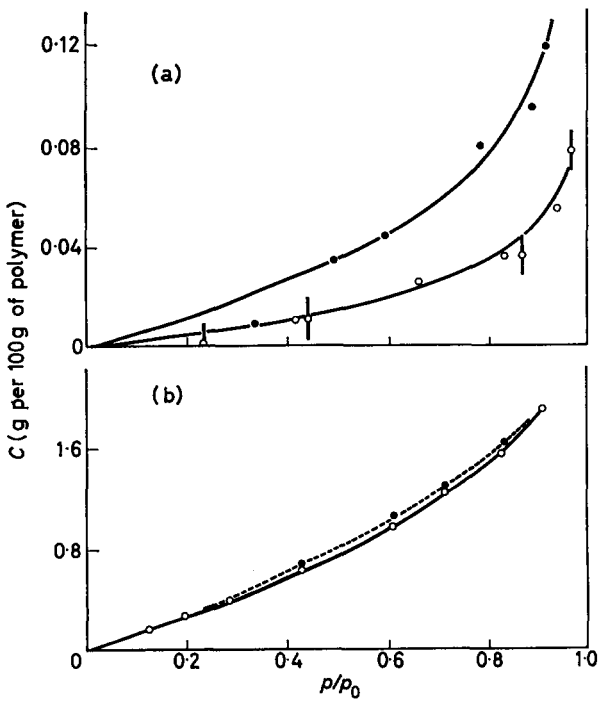

Figure 1—Sorption isotherms for water: (a) Polydimethylsiloxane: (○) 35°C, (●) 60°C; (b) Polymethylmethacrylate at 50°C: (○) sorption, (●) desorption

RESULTS

The permeation rate P is expressed as the number of grammes of water which passed in one hour across 1 cm² of polymer membrane in the steady state of flow. The permeability coefficient $\overline{P}$ is defined by Pl/p_1 where l (cm) is the membrane thickness and p_1 (cm of mercury) is the vapour

pressure at the upstream face. The concentration C is the number of grammes of water vapour sorbed by 100g of thoroughly outgassed polymer. Both C and P were obtained as functions of the upstream relative pressure p_1/p_0 as shown in *Figures 1* and *2* respectively. Plots of P versus C were then constructed of which some typical examples are shown in *Figure 3*.

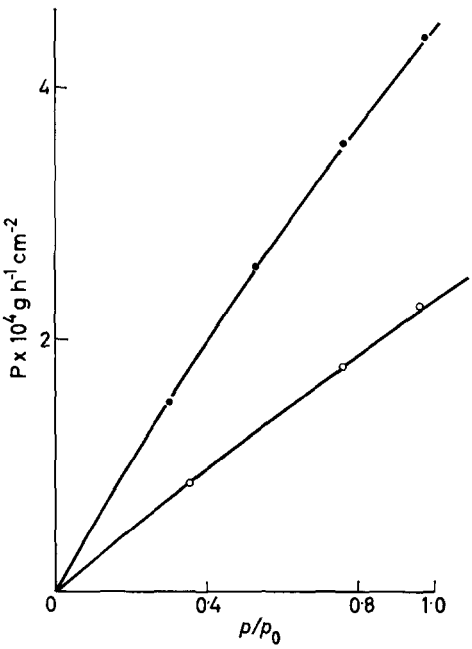

Figure 2—Dependence of the permeation rate on the relative pressure at the upstream face for polydimethylsiloxane: (○) 35°C; (●) 50°C

With the above units for P and C, and with D ($cm^2\ sec^{-1}$) the diffusion coefficient and ρ ($g\ cm^{-1}$) the density of the polymer one has for steady state flow

$$P = -36\rho D\partial C/\partial x = -D'\partial C/\partial x \qquad (1)$$

from which it follows that

$$D = (l/36\rho)\,(dP/dC) \qquad (2)$$

The concentration dependence of the diffusion coefficient is then determined from the slope of the P versus C curve at different values of the concentration.

Polydimethylsiloxane

Since the amount of water vapour sorbed by the silicone rubber was small even at high relative pressures the accuracy of the data was somewhat reduced and some indication of the error involved is shown in *Figure 1*(a). However, the shape of the isotherm is clearly defined and is typical of simple solution behaviour or of sorption systems where sorbate–sorbate interactions are relatively stronger than those of sorbate–sorbent. Within the limits of the experimental error no hysteresis was observed.

Values of the permeation rate for a given membrane were reproducible to within ±2 per cent, and for a given temperature the dependence on the relative pressure at the upstream face was given by

$$P = A\,(p_1/p_0) - B\,(p_1/p_0)^2 \tag{3}$$

and so

$$\overline{P} = \overline{P}_0 - a\,(p_1/p_0) \tag{4}$$

A, B and a are temperature dependent positive constants and $\overline{P}_0$ is the permeability coefficient at zero relative pressure. In *Table 1* are given

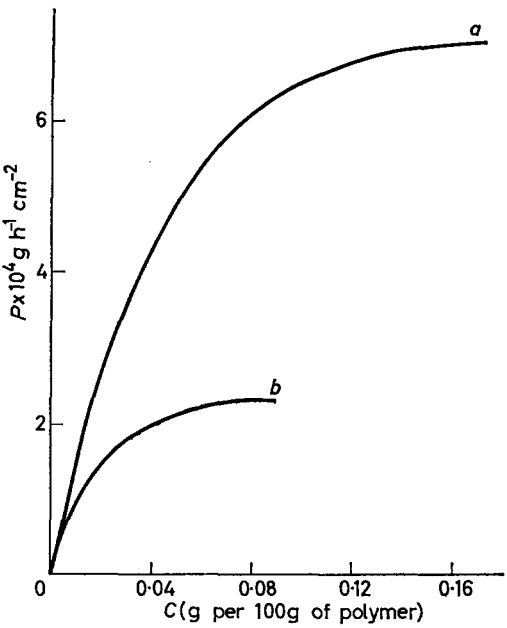

Figure 3—Dependence of permeation rate on concentration at the upstream face for polydimethylsiloxane (*a*) 65°C; (*b*) 35°C

values of $\overline{P}_0$, while in *Figures 2* and *3* the permeation rate is shown as a function of the relative pressure and of the concentration C at the upstream face respectively.

Table 1. Values of $\overline{P}_0 \times 10^5$ (g cm/cm²/h/cm Hg), $a \times 10^5$ and $D_{c=0} \times 10^5$ (cm² sec⁻¹)

T°C	$\overline{P}_0$	a	$D_{c=0}$
35	1·27	0·07	7
50	1·17	0·14	9
65	0·95	0·12	10

The most interesting feature of the data is the marked decrease in the diffusion coefficient with increasing concentration of water as indicated in *Figure 4*. Values of the diffusion coefficient at zero concentration ($D_{C=0}$) are also included in *Table 1* and may be compared with values of the order

10^{-7} to 10^{-6} ($cm^2\ sec^{-1}$) encountered with most polymers in this temperature range. The values of $D_{C=0}$ are not considered accurate enough to give a reliable estimate for the activation energy for diffusion but an approximate value of 3 kcal $mole^{-1}$ has been calculated. Relatively large diffusion coefficients have also been measured for hydrocarbon vapours in silicone rubbers and were shown to be a consequence of low energies of activation for diffusion[6].

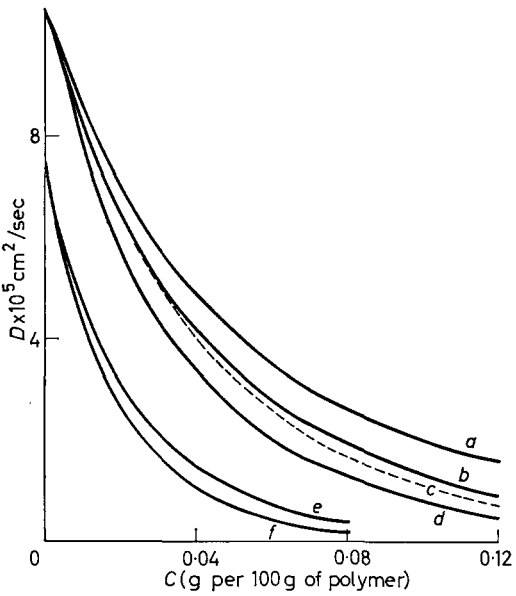

Figure 4—Concentration dependence of the diffusion coefficient for polydimethylsiloxane at 65°C: (*a*) equation (13), $C_s = 0{\cdot}18$; (*b*) equation (13), $C_s = 0{\cdot}225$ and $D_2 = D_3 = \overline{D} = 0$; (*c*) experimental; (*d*) equation (13), $C_s = 0{\cdot}18$ and $D_2 = D_3 = \overline{D} = 0$; and at 35°C: (*e*) experimental; (*f*) equation (13), $C_s = 0{\cdot}12$ and $D_2 = D_3 = \overline{D} = 0$

Polymethylmethacrylate

Sorption isotherms exhibited hysteresis but the sorption branch was reproducible provided that the sample was first outgassed and that the isotherm was determined by stepwise addition. A typical isotherm is shown in *Figure 1*(b) and it is observed that the sorptive capacity for water vapour of the polymethylmethacrylate is almost ten times that of the polydimethylsiloxane. The isotherms are similar to those reported by several investigators[7–9] and a comparison of the amounts sorbed at a relative pressure of 0·75 is made in *Table 2*. Those of Brauer and Sweeney[10] showed a similar type of hysteresis and were independent of temperature in the range 20° to 60°C.

Table 2. Comparison of C (g/100g) values at 50°C for $p/p_0 = 0{\cdot}75$

1·3*	1·3[7]	1·1[8]	1·4[9]

*This investigation.

The permeation rate was determined as a function of the relative pressure at 50°C only, and again the data were well represented by equations (3) and (4). Compared with a value of $1{\cdot}17 \times 10^{-5}$ for polydimethylsiloxane, $\overline{P}_0$ was only $7{\cdot}4 \times 10^{-7}$ even although the sorptive capacity of the poly-

methylmethacrylate was much greater. This is again a reflection of the relatively large diffusion coefficients encountered with silicone rubbers, thus at 50°C, $D_{C=0}$ for the polymethylmethacrylate is $1{\cdot}3 \times 10^{-7}$ compared with 9×10^{-5} for the polydimethylsiloxane. From *Figure 5* it is seen that the diffusion coefficient decreases almost linearly with concentration. The same system has also been studied using the sorption–desorption kinetic technique. Bueche[7] found that sorption-kinetic data yielded values of D which decreased with increasing concentration, while corresponding desorption data gave a constant D. Further the rate of desorption was faster than the corresponding

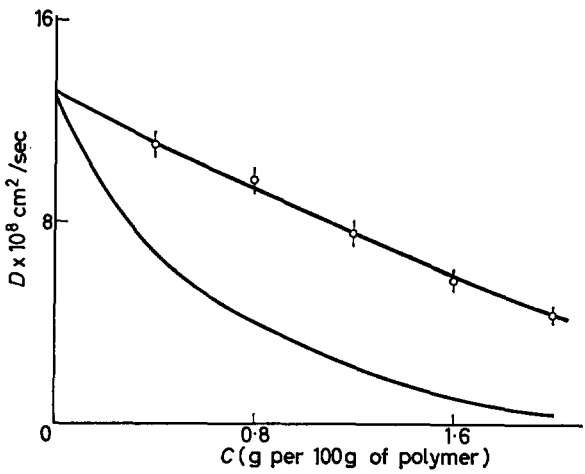

Figure 5—Concentration dependence of the diffusion coefficient for polymethylmethacrylate at 50°C: —○— experimental; ——— equation (13), $C_2=3{\cdot}0$ and $D_2=D_3=\overline{D}=0$

rate of sorption, and somewhat similar results were obtained by Thomas[8] for the same system. This behaviour is in agreement, at least qualitatively, with Crank's[11] analysis of sorption–desorption kinetics for Fickian diffusion with D decreasing as the concentration is increased. Both Bueche[7] and Thomas[8] regarded the diffusion coefficient as constant in their analyses and obtained values of approximately 4 and 5×10^{-8} respectively at 50°C. These average values are in fact much less than the corresponding value of $D_{C=0}$ (13×10^{-8}) derived from the steady-state data of this investigation.

DISCUSSION

Although diffusion coefficients which decrease with concentration of water vapour have been reported for polyethylene[3], ethylcellulose[4], polydimethylsiloxane and polymethylmethacrylate, this behaviour is not common to all polymer–water vapour systems. For example, in polyvinylalcohol[2] and cellulose[12] the diffusion coefficient increases rapidly with concentration, which is the normal concentration dependence observed with organic vapours and is attributed to the swelling or plasticizing action of the

penetrant. To explain the decrease in the diffusion coefficient with concentration it was postulated that monomeric water was the major diffusion species and that as a result of clustering the proportion of monomer decreased as the total concentration was increased[4].

Polymerization or clustering of water in polymers

In general one may expect clustering of penetrant when penetrant–penetrant interactions are stronger than those of penetrant–polymer. Rogers, Stannett and Szwarc[13] used relations developed by Zimm and Lundberg[14] to deduce that in the sorption of organic vapours by polyethylene considerable clustering of penetrant occurred.

More recently the properties of water solutions in benzene and toluene have been discussed in terms of a model which describes the polymerization of water in an inert continuum[5]. In this the water molecule is regarded as a tetrafunctional monomer in which all four hydrogen bonds are independent in the sense that the free energy of formation of any one is unaffected by the state of the others. The polymerization process is considered to be a purely random formation of hydrogen bonds and the gel point is identified with the saturation or precipitation point of the system. More specifically the weight fraction of polymeric species composed of n water molecules is given by

$$w_n = \frac{fq^{n-1}(1-q)^{fn-2n+2}(fn-n)!}{(n-1)!(fn-2n+2)!} \tag{5}$$

where $f=4$ is the functionality of the water molecules and q is the fraction of the hydrogen bonds actually formed. The saturation point of the system is defined by

$$q_c = 1/(f-1) \tag{6}$$

and the law of mass action for the breaking of a hydrogen bond may be written

$$K = C(1-q)^2/q \tag{7}$$

If C_s is the saturation concentration of water it follows $K = \frac{4}{3}C_s$.

Diffusion with cluster formation

It is assumed that diffusion of water molecules within a cluster or polymeric species is negligible and that the equilibrium distribution of equation (5) obtains in the membrane during the steady state of flow. If there is no interference between the diffusional flow of each species then

$$P = -\sum_1^n D_n' \partial C_n/\partial x = -D' \partial C/\partial x \tag{8}$$

where the subscripts $1, 2 \ldots n$ denote respectively monomer, dimer ... n-mer of water and C is the total concentration of water in the polymer. It follows that

$$D = \sum_1^n D_n \mathrm{d}C_n/\mathrm{d}C \tag{9}$$

and the quantity $\mathrm{d}C_n/\mathrm{d}C$ can be obtained from the polymerization theory

outlined above. Thus with $w_n = C_n/C$, and substituting the negative root of the quadratic equation (7) into equation (5), one obtains

$$C_n = \frac{3n!}{(n-1)!(2n+2)!} \frac{(2C+K-k)^{n-1}(k-K)^{2n+2}}{2^{3n-1}C^{3n}} \tag{10}$$

where $k=(K^2+4KC)^{1/2}$. The positive root of equation (7) was discarded since it gives $q \geqslant 1$. The quantity dC_n/dC can be evaluated from equation (10) and for monomeric species one has, since $f=4$,

$$C_1 = (k-K)^4/16C^3 \tag{11}$$

and

$$\frac{dC_1}{dC} = \frac{(k-K)^3}{16C^3}\left\{\frac{8K}{k} - 3\frac{(k-K)}{C}\right\} \tag{12}$$

Polydimethylsiloxane

Since the solubility of water in the polydimethylsiloxane is so low specific interactions between polymer and penetrant may be ruled out. A probable value of C_s was estimated by extrapolation of the isotherm data to a relative pressure of unity and at 65°C was in the range 0·15 to 0·30 weight per cent. For water in benzene at 67°C, $C_s = 0{\cdot}26$ per cent[5] and it is reasonable to assume that specific polymer–penetrant interactions are absent from the dimethylsiloxane–water system.

In the limit $C \longrightarrow 0$, $dC_1/dC \longrightarrow 1$, and $(D_1)_{C=0}$ can be identified with the experimental diffusion coefficient $D_{C=0}$, which at 65°C is $10{\cdot}5 \times 10^{-5}$. As the concentration of water is small the plasticizing effect will be slight and to a first approximation D_1 can be regarded as constant and equal to $D_{C=0}$ throughout the whole of the concentration range. An estimate of the diffusion coefficients for dimer and trimer is made by analogy with the results of Barrer and Skirrow[15] for diffusion of methane, ethane and propane in natural rubber at 40°C. The ratios of the diffusion coefficient for these three hydrocarbons were 145 : 54 : 34 which when applied to water monomer, dimer and trimer gives 10·5 : 3·6 : 2·1 for $D_1 : D_2 : D_3$ at 65°C. Polymer species of four or more water molecules are considered as having an average diffusion coefficient ($\bar{D}$) to which is assigned a somewhat arbitrary value of 1×10^{-5}. This is probably an overestimate particularly as some of the larger polymeric species may be highly branched and have relatively low diffusion coefficients. Equation (9) is now written

$$D = D_1\frac{dC_1}{dC} + D_2\frac{dC_2}{dC} + D_3\frac{dC_3}{dC} + \bar{D}\left[1 - \left(\frac{dC_1}{dC} + \frac{dC_2}{dC} + \frac{dC_3}{dC}\right)\right] \tag{13}$$

since $\sum_1^n dC_n/dC = 1$. The relative importance of the terms in equation (13) is shown in *Table 3* with $C_s = 0{\cdot}18$ at 65°C.

The contribution to the diffusion process of polymeric species with $n > 3$ becomes significant for $C/C_s > 0{\cdot}33$. However, it is emphasized that the calculations purposely overestimate these same terms and in the range of C/C_s from 0 to 0·66 a reasonable approximation may be made by considering monomeric water as the sole diffusing species. In *Figure 4* the experimental D versus C relationship at 65°C is compared with that

Table 3
$C_s = 0{\cdot}18$ at 65°C

C/C_s	$10{\cdot}5\frac{dC_1}{dC}$	$3{\cdot}6\frac{dC_2}{dC}$	$2{\cdot}1\frac{dC_3}{dC}$	$1{\cdot}0\left[1-\sum_1^3\frac{dC_n}{dC}\right]$	$D\times10^5$
0	10·5	0	0	0	10·5
0·055	7·67	0·73	0·10	0·02	8·52
0·11	5·71	0·94	0·23	0·08	6·96
0·22	3·36	0·88	0·33	0·27	4·84
0·33	2·02	0·66	0·30	0·48	3·46
0·44	1·28	0·46	0·23	0·64	2·61
0·66	0·46	0·18	0·10	0·85	1·59

predicted from equation (13) with in the one case all water species diffusing and in the other monomer only. The effect of C_s is also considered by recalculating the curve for monomer diffusion with a C_s value of 0·225. In each case the form of the D versus C curve is similar to that obtained experimentally and in this respect the theory is satisfactory, but the accuracy of the data does not enable one to distinguish between the several theoretical curves of *Figure 4*.

The D versus C curves at 50° and 35°C were similar in shape to that at 65°C, and also in *Figure 4* the data at 35°C are compared with the theoretical curve calculated assuming monomer diffusion only. Satisfactory agreement is obtained with a C_s value of 0·12 compared with the corresponding value of 0·225 at 65°C. This is in accord with the isotherm data of *Figure 1*(a) where it is clear that the sorptive capacity of the polymer increases with temperature at a given relative pressure.

Polymethylmethacrylate

In *Figure 5* the theoretical curve assuming monomer diffusion only, with $D_1 = D_{C=0} = 1{\cdot}33\times10^{-7}$ and $C_s = 3{\cdot}00$, lies well below the experimental one and although to allow for diffusion of polymeric species would minimize this difference the curvature of the theoretical line is not borne out by experiment. However, the sorptive capacity of the polymethylmethacrylate is at least ten times that of the polydimethylsiloxane which suggests that this polymer cannot be regarded as an inert continuum. This is also true for ethylcellulose the sorptive capacity of which is of the same order as that of polymethylmethacrylate.

Previous work with glassy polymers has indicated the presence of cavities[16–18] in which penetrant molecules are sorbed preferentially with little disturbance of the ambient polymer matrix. Polymerization of the water molecules may be expected to develop more freely in these cavities relative to the denser regions of the matrix where some degree of expansion would be necessary. Further, both polymethylmethacrylate and ethylcellulose contain polar groups and these, apart from increasing the sorptive capacity of the polymer, in turn may act as centres of nucleation for cluster growth. In either case, the theory can no longer be considered adequate and the distribution given by equation (5) may be considerably distorted. In addition the relatively higher sorptive capacities of these polymers could lead to significant plasticization of the matrix and an associated increase in the

diffusion coefficient with concentration. Nevertheless, the decrease in D with C observed for both of these polymers suggests that some mechanism of clustering is predominant in determining the concentration dependence of the diffusion coefficient.

The sorption isotherms of all three polymers are similar in shape to those of systems exhibiting normal solution behaviour. Isotherms of this form also obtain for systems where sorbate–sorbate interactions are stronger than those of sorbate–sorbent. If the sole mechanism of sorption were the interaction of the water molecules with a limited number of sites of interaction such as polar groups or cavities then initially a Langmuir type isotherm, eventually superseded by normal solution behaviour, should result. This is indeed so when hydrocarbon vapours are sorbed by ethylcellulose[17]. However, the isotherms with water as sorbate show no trace of Langmuir sorption unless this occurs at relatively low concentrations and apparently the water–polymer interactions are not sufficiently strong to prevent clustering, presumably around the specific sites of interaction.

The sorption isotherms and the D versus C relationships obtained by Rouse[3] for the water–polyethylene system were similar in form to those for the polydimethylsiloxane one but his data have not been analysed in terms of the cluster model in view of discrepancies in the literature solubility data which have been discussed in some detail by Klute[19]. Moreover, Yasuda and Stannett[20] have recently published data which indicated that clustering was present in ethylcellulose and rubber hydrochloride but was absent from polyethylene, polypropylene and polyethyleneterephthalate. It was suggested that the latter do not have the means of nucleation under the normal conditions of exposure and that the polyethylene of Rouse may have been oxidized sufficiently to provide centres for initiating clustering or some form of capillary condensation. Although trace catalyst or perhaps the Si–O–Si linkage may play a similar role in polydimethylsiloxane, such an explanation is less likely for the water–benzene system[5] and for the methanol–benzene system for which Caldwell and Babb[21] postulated the existence of polymeric species of methanol to account for the concentration dependence of the diffusion coefficient.

In conclusion, the proposed model for diffusion describes satisfactorily the form of the D versus C relationship for the water–polydimethylsiloxane system in which polymer–penetrant interactions are weak. The sorptive capacities of polymethylmethacrylate and ethylcellulose for water are relatively higher and these polymers can no longer be regarded entirely as an inert continuum for the water polymerization process. The theory no longer describes satisfactorily the shape of the D versus C curves even although clustering is still dominant.

This work was supported by the Ministry of Aviation and is part of an investigation of water diffusion in polymer films.

Physical Chemistry Department,
Imperial College of Science and Technology,
London, S.W.7

(Received September 1962)

REFERENCES

[1] MEARES, P. *J. Polym. Sci.* 1958, **27,** 391
[2] LONG, F. A. and THOMPSON, L. J. *J. Polym. Sci.* 1955, **15,** 413
[3] ROUSE, P. E. *J. Amer. chem. Soc.* 1947, **69,** 1068
[4] BARRER, R. M. and BARRIE, J. A. *J. Polym. Sci.* 1958, **28,** 377
[5] GORDON, M., HOPE, C. S., LOAN, L. D. and RYONG-JOON ROE. *Proc. Roy. Soc. A,* 1960, **258,** 215
[6] BARRER, R. M., BARRIE, J. A. and RAMAN, N. K. *Polymer, Lond.* 1962, **3,** 595 and 605
[7] BEUCHE, F. *J. Polym. Sci.* 1954, **14,** 414
[8] THOMAS, A. M. *J. appl. Chem.* 1951, **1,** 141
[9] KAWASAKI, K. and SEKITA, Y. *J. appl. Phys. Japan,* 1957, **26,** 678
[10] BRAUER, G. M. and SWEENEY, W. T. *Mod. Plast.* 1955, **32,** No. 9, 138
[11] CRANK, J. *The Mathematics of Diffusion,* p 276. Oxford University Press: London, 1956
[12] STAMM, A. J. *J. phys. Chem.* 1956, **60,** 83
[13] ROGERS, C. E., STANNETT, V. and SZWARC, M. *J. Polym. Sci.* 1960, **45,** 61
[14] ZIMM, B. H. and LUNDBERG, J. L. *J. phys. Chem.* 1956, **60,** 425
[15] BARRER, R. M. and SKIRROW, G. *J. Polym. Sci.* 1948, **3,** 549
[16] MEARES, P. *J. Amer. chem. Soc.* 1954, **76,** 3415
[17] BARRER, R. M., BARRIE, J. A. and SLATER, J. *J. Polym. Sci.* 1958, **27,** 177
[18] MICHAELS, A. S., VIETH, W. and BARRIE, J. A. *J. appl. Phys.* 1963, **34,** 1 and 13
[19] KLUTE, C. H. *J. appl. Polym. Sci.* 1959, **1,** 340
[20] YASUDA, H. and STANNETT, V. *J. Polym. Sci.* 1962, **57,** 907
[21] CALDWELL, C. S. and BABB, A. L. *J. phys. Chem.* 1955, **59,** 1113

Dipole Relaxation in the Crystalline Phase of Polymers—II

C. A. F. TUIJNMAN

The frequency location and temperature dependence of the dielectric losses, experimentally established in mixtures of long chain esters with paraffins and long chain ketones with polyethylene, can be satisfactorily explained if it is assumed that the chains in the crystals take part in a rotation process. Brinkman's diffusion theory for independent particles based on the two-hole model is extended to the case for polymer chains. For flexible chains several energetically different rotations are possible. It is found that the reaction rate constant is practically fully determined by the energetically most favourable rotation starting at the head or tail of the chain.

WHEN 'long-chain ketones' are dissolved in polyethylene it appears that, as regards the frequency location, over 90 per cent of the dielectric loss of the solution is comparable with the loss of a real solid solution of these molecules in crystalline paraffins[1]. This justifies the assumption that when a molten, slightly oxidized polyethylene is subjected to cooling, a number of oxidized chains will occur in the crystallites. In a previous publication[1] attention was drawn to the possibility that these crystalline chains may be responsible for the dielectric low-frequency losses in oxidized high-pressure polyethylene. The principal arguments on which this hypothesis is based are:

(*i*) the decrease of the low-frequency losses with increasing temperature, resulting in the disappearance of these losses at the crystalline melting point of the polymer;

(*ii*) the fact that the low-frequency losses at room temperature occur only if the oxidation takes place at temperatures higher than the melting point.

Upon mild oxidation at room temperature only the 'amorphous' medium and high frequency losses occur; this can be ascribed to the fact that diffusion of oxygen takes place preferably in the amorphous regions.

It is well-known that in paraffin and polyethylene the carbon atoms tend to form flat chains with parallel axes. Such a structure suggests that rotation of a chain about the longitudinal axis from a stable position 1 across a potential barrier to a stable position 2 can with good purpose be related to a relaxation process in the crystalline phase of polyethylene.

Fröhlich[2] calculated the difference ΔU between the maximum and minimum values of this potential for chains of different lengths in paraffin crystals. The experimentally found dependence of the relaxation time on the chain length could thus be reasonably accounted for by means of the formula $\tau = \text{constant} \times \exp(\Delta U / kT)$. This relation, however, still contains an unknown constant which has to be chosen so as to fit the experimental data.

Recently, however, Brinkman[3] derived an expression for the two-hole model, which for the case $\Delta U \gg kT$ permits calculation of the number of particles per unit of time diffusing from the one potential hole to the other. This makes it possible to relate the relaxation time for loose particles quantitatively to a friction parameter and to the parameters that determine the potential function.

It will be investigated in what way Brinkman's theory can be applied for describing dipole relaxation in lattice structures, as in paraffins where a chain molecule can occupy two equilibrium positions. Our aim is to indicate a general relationship between the dielectric measuring quantities, which determine the relaxation time, and the above-mentioned parameters, which are correlated with the lattice structure. Using this relationship, we shall endeavour to give a theoretical explanation of the change in frequency of the low-frequency losses with the length of polar model chains dissolved in paraffin and polyethylene, and of the influence of the temperature on the frequencies of these losses.

DIPOLE RELAXATION IN LATTICE STRUCTURES

Brinkman[3] used the two-hole model for describing diffusion of loose particles. In this model (see *Figure 1*) practically all particles are concentrated in the two minima of a potential field.

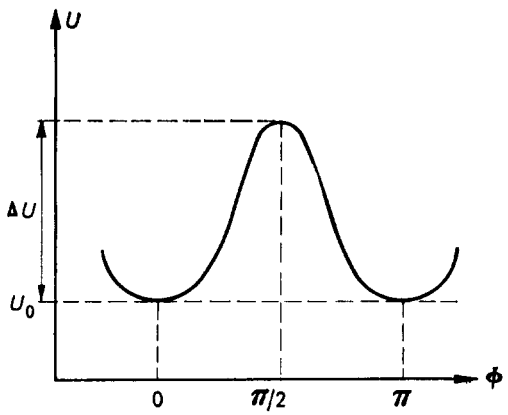

Figure 1—Two-hole model; potential energy versus angle of rotation

The variable ϕ may be, for example, a rotation angle. The particles are dispersed in a medium of a given temperature and viscosity. The energy needed for making the particles diffuse from hole 1 into hole 2 and vice versa is suppiied by the medium. An essential condition in Brinkman's approach is that $\Delta U \gg kT$. This entails that in the equilibrium condition the particle density ρ on the barrier can be practically neglected. So, when n_1 and n_2 represent the numbers of particles in hole 1 and hole 2 respectively, the following relation is valid:

$$n_1 = \int_{-\pi/2}^{+\pi/2} \rho \, d\phi; \qquad n_2 = \int_{\pi/2}^{3\pi/2} \rho \, d\phi; \qquad n_1 + n_2 = n \tag{1}$$

The restriction that the height of the barrier must be very great compared with kT furthermore permits $\rho(\phi)$ to be approximately represented by a Boltzmann distribution for each separate hole. The number of particles $w(\phi)$ diffusing from hole 1 into hole 2 per unit of time at point ϕ is, to a good approximation, described by Smoluchowski's equations:

$$\frac{\partial \rho}{\partial t} = -\frac{\partial w}{\partial \phi}; \quad w = -\frac{\rho}{\zeta}\left\{\frac{\partial U}{\partial \phi} + \frac{kT}{\rho} \cdot \frac{\partial \rho}{\partial \phi}\right\} \tag{2}$$

In the latter equation ζ represents a rotatory friction coefficient defined as the ratio between moment of force and angular velocity. Introducing the assumption that $w(\phi)$ is approximately independent of ϕ, Brinkman for a symmetric potential now derives from (2) the following relation:

$$-\mathrm{d}n_1/\mathrm{d}t = \mathrm{d}n_2/\mathrm{d}t = K(n_1 - n_2) \tag{3}$$

The quantity K in this equation has the function of a reaction constant. Its relation to the shape of the potential curve appears from the following equations:

$$K = \frac{kT}{\zeta I_- I_+}; \quad I_- = \int_{-\pi/2}^{+\pi/2} \exp(-U/kT)\,\mathrm{d}\phi; \quad I_+ = \int_0^{\pi} \exp(+U/kT)\,\mathrm{d}\phi \tag{4}$$

The integrand of I_- contributes essentially to the integral only in the hole, that of I_+ only on the barrier. At equilibrium $\mathrm{d}n_1/\mathrm{d}t = 0$ and hence, according to (3), $n_1 - n_2 = 0$. Schwarzl[4] used the formal solutions (3) and (4) for describing mechanical relaxation phenomena, paying special attention to non-linear behaviour.

Chains present in the crystalline phase of a polymer may exist in several stable energy conditions. For example, the chain molecules in paraffin crystals may occupy two equilibrium positions. To illustrate this point the unit cell of a polyethylene crystal is shown in *Figure 2* (see ref. 5). The chain

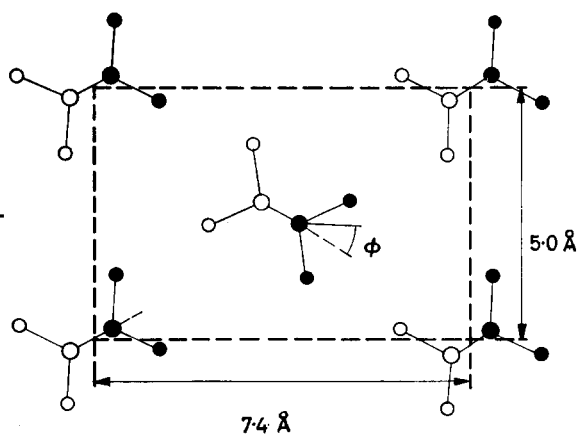

Figure 2—Unit cell of polyethylene crystal

molecules are normal to the plane of the rectangle and constitute a flat zig-zag chain the projections of which are shown. By rotation about the longitudinal axis through an angle of 180° a chain may evidently be moved from the one position into the other. We assume that if a molecule contains a carbonyl or ester group, the lattice will not be disturbed to any appreciable extent and the two levels of equal minimum energy will remain unchanged. In these positions the dipoles are oppositely directed because the carbonyl group lies in the chain plane and is arranged perpendicular to the chain axis (*Figure 3*). The system to be considered here consists of a dilute solution of such polar chains in paraffin or polyethylene crystals. The chains may differ in length, but may never be longer than the crystals in which they are incorporated.

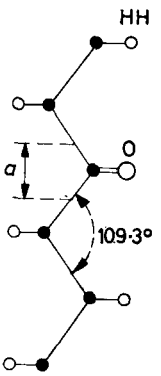

Figure 3—Polyethylene chain with carbonyl group

Straightforward application of Brinkman's theory to such a system is possible only if the chain is perfectly rigid. Only then will the function $U(\phi)$ be unique. The flexible chains, however, may move from hole 1 to hole 2 in many ways. This is a direct result of the fact that twisting is liable to occur in a flexible chain. For, in the case of twist practically the full energy needed for moving the whole chain over the barrier will be produced at the moment when the head of the chain has arrived in hole 2, irrespective of the chain length still present in hole 1. Should the movement start from the middle of the chain, the amount of energy will be about twice as large. Since the angle ϕ along the chain is normally not constant, the potential energy will hereinafter be considered as a function of $\bar{\phi}$, i.e. the average value of ϕ. The various ways along which the chain can be transferred from hole 1 to hole 2 correspond to different $U(\bar{\phi})$ functions. The minimum values of this $U(\bar{\phi})$ function for $\bar{\phi}=0$ and $\bar{\phi}=\pi$ are equal. Each transition makes its own contribution to the average value $\langle K \rangle$ of the reaction constant. The function for which $U(\bar{\phi})$ is minimum will make the largest contribution to $\langle K \rangle$.

Choosing the head of the chain as the point where the rotation is applied, one finds this function by determining for each value of the rotation angle at the point of application the chain location for which the potential energy is minimum. The effect of the energetically less favourable rotations for an arbitrary point of application on $\langle K \rangle$ can be approximately brought into

account by separately minimizing the energy of the LH and RH part by the same procedure.

For the polymer system equation (4) then changes into:

$$\langle K\rangle = \frac{kT}{\zeta}\left\langle \frac{1}{I_- I_+}\right\rangle; \quad I_- = \int_{-\pi/2}^{+\pi/2} \exp(-U/kT)\,\mathrm{d}\bar{\phi}; \quad I_+ = \int_0^{\pi} \exp(+U/kT)\,\mathrm{d}\bar{\phi} \tag{5}$$

In the next section, where the effect of the chain length on the relaxation time in crystalline polymers will be discussed, $\langle K\rangle$ will be approximately calculated following this procedure, and the influence of the energetically less favourable rotation will be considered.

So far, the system has been considered in the absence of an electric field and the equations given can be applied both to the polar and apolar chains. Application of an electric field permits the rotation process of the polar chains to be studied separately. The polar group acts as a tracer by means of which the relaxation process manifests itself as dielectric relaxation. In a static field E a new distribution of the polar chains over the two holes is set up. By dielectric relaxation is now meant the retarded adjustment of this distribution.

It will be indicated how the average relaxation time τ for our model can be related to $\langle K\rangle$ and the dielectric measuring quantities. In the polycrystalline material those crystallites are selected, whose dipoles include angles with the field direction equal to θ_i and $\theta_i+\pi$ in holes 1 and 2 respectively. If in the dilute system, one neglects the influence of other dipoles the potential energies in holes 1 and 2 are $U_0-\mu E\cos\theta_i$ and $U_0+\mu E\cos\theta_i$ respectively. In practice the field strength is such that $\mu E \ll kT$. Equation (3), which describes the rate at which deviations from equilibrium are eliminated, now becomes:

$$-\frac{\mathrm{d}n_1}{\mathrm{d}t} = \frac{\mathrm{d}n_2}{\mathrm{d}t} = \langle K\rangle\,[(n_1-n_2)-\Delta];\ n_1+n_2=n_i \tag{6}$$

where n_i represents the total number of particles with orientation i in the two holes. Under equilibrium conditions, unlike in the case where no electric field is present, there will exist a difference between n_1 and n_2. Using Boltzmann's theorem and the condition that $\mu E \ll kT$, we now find, after neglecting terms of the Δ^2 and higher orders,

$$\Delta = n_i \mu E\cos\theta_i/kT$$

and, hence, for (6)

$$-\mathrm{d}n_1/\mathrm{d}t = \langle K\rangle\,[(2n_1-n_i)-n_i\mu E\cos^2\theta_i/kT] \tag{7}$$

The contribution of the n_i dipoles to the polarization amounts to

$$P_\mu = \mu\,(2n_1-n_i)\cos\theta_i$$

Using (7), the derivative of P_μ with respect to time is found

$$\mathrm{d}P_\mu/\mathrm{d}t = 2\,\langle K\rangle\,[-P_\mu + n_i\mu^2 E\cos\theta_i/kT] \tag{8}$$

So, the rate at which the equilibrium polarization is realized upon generation

of E is fully determined by the reaction rate constant $\langle K \rangle$. This becomes clear when it is borne in mind that:

(*i*) equation (3) has been derived under the condition $\Delta U \gg kT$ and K is determined almost completely by ΔU;

(*ii*) equation (8) has been derived for the case $\mu E \ll kT$.

In equation (8) $2\langle K \rangle$ represents a reciprocal dielectric relaxation time

$$2\langle K \rangle = \langle 1/\tau \rangle \tag{9}$$

This time relates to the time the dipoles need for moving from the one hole into the other. The polarization in the holes themselves and the associated relaxation time is left out of account. The second term in the RH member of (8) represents the equilibrium polarization P_{μ_s} of the group of dipoles under consideration. The total value of P_{μ_s} in 1 cm^3 sphere in which n dipoles are present is found by averaging over all angles θ_i: $P_{\mu_s} = n\mu^2 E/3\,kT$. It is not our intention to indicate how P_{μ_s} should be related to the dielectric quantities ε and ε_∞. The problems presenting themselves here have been extensively discussed in the literature. They are related to the value of the internal field E during application of an external field E_0 and to the value of μ when allowance is made for the dipole–dipole interaction. We assume that in an alternating field where the frequency is small compared with the frequency with which the polarization in the holes is established, equation (8) remains valid. The relationship between $\langle 1/\tau \rangle$ and ω_m, i.e. the circle frequency at which ε'' [the imaginary part of $\varepsilon(i\omega)$] becomes maximum, can then be found in a simple manner. Choosing for $E(i\omega t)$ the Lorentz field $E(i\omega t) = \frac{1}{3}[\varepsilon(i\omega t) + 2] \,.\, E_0(i\omega t)$ we find the relationship

$$\langle 1/\tau \rangle [(\varepsilon_\infty + 2)/(\varepsilon + 2)] = \omega_m \tag{10}$$

By means of (5) the experimental value of $\langle 1/\tau \rangle$ can be related to the potentials $U(\bar{\phi})$ which determine the reaction constant $\langle K \rangle$.

For all the concentrations of model substances used, the ratio $(\varepsilon+2)/(\varepsilon_\infty+2)$ in equation (10) is approximately equal to 1·02, so that $\langle 1/\tau \rangle$ was put equal to ω_m.

RELAXATION TIME AND CHAIN LENGTH

$U(\bar{\phi})$ can be calculated essentially for chains of a given length incorporated in crystallites of equal or greater length. In long chains torsion will play a part, with the result that the chain is gradually moved across the potential barrier. The maximum energy needed for transferring the chain from hole 1 to hole 2 will for these chains be approximately independent of the chain length; with short chains this energy is approximately proportional to the chain length. For rotations starting from the head or tail of the chain this maximum energy, i.e. ΔU for $\bar{\phi} = \pi/2$, has been calculated by Fröhlich[2]. With a view to calculating the integrals I_- and I_+ in the expression of the average reaction constant $\langle K \rangle$, however, the whole variation of the function $U(\bar{\phi})$ for all values of $\bar{\phi}$ is important. Following Fröhlich, the chain is considered to be continuous and the distance from a given point to chain head is indicated by z_0; in a chain of m monomers of length a therefore z_0 is equal to ma. Assuming that the interaction—and twisting—energy are

proportional to ϕ^2 and $(d\phi/dz)^2$ respectively, the internal energy of the chain is found from

$$U = U_0 + \int_0^{z_0} u \, dz \tag{11}$$

where $u = \frac{1}{2}A^2 a (d\phi/dz)^2 + \frac{1}{2}B^2\phi^2/a$.

A^2 and B^2 have the dimension of an energy per monomer unit per radial square. Integration is feasible if ϕ as a function of z is known; $\phi(z)$ is found by minimizing the potential energy of the whole chain. In the case of rotation starting from the point αz_0 ($0 \leqslant \alpha \leqslant 1$) calculus of variation shows that for $(\phi)_{\alpha z_0} \leqslant \pi/2$:

(*i*) the function $\phi(z)$ in the LH interval $0 \leqslant z \leqslant \alpha z_0$ is determined by the conditions $B^2\phi = a^2A^2 \, d^2\phi/dz^2$ and $(d\phi/dz)_{z=0} = 0$.

(*ii*) the function $\phi(z)$ in the RH interval $\alpha z_0 \leqslant z \leqslant z_0$ is determined by the conditions $B^2\phi = a^2A^2 \, d^2\phi/dz^2$ and $(d\phi/dz)_{z_0} = 0$.

For the LH part of the chain with length αz_0 the following relations are valid:

$$\Delta U = \int_0^{\alpha z_0} (\Delta u) \, dz \tag{12}$$

and

$$\Delta u = \left(\frac{\partial u}{\partial \phi}\right) \Delta\phi + \frac{\partial u}{\partial (d\phi/dz)} \Delta\left(\frac{d\phi}{dz}\right) = \left(\frac{\partial u}{\partial \phi}\right) \Delta\phi + \frac{\partial u}{\partial (d\phi/dz)} \frac{d(\Delta\phi)}{dz} \tag{13}$$

Upon substitution of (13) in (12) and partial integration we find for the minimization condition:

$$\Delta U = \frac{\partial u}{\partial (d\phi/dz)} \Delta\phi \Big|_0^{\alpha z_0} + \int_0^{\alpha z_0} \left[\frac{\partial u}{\partial \phi} - \frac{d}{dz}\left(\frac{\partial u}{\partial (d\phi/dz)}\right)\right] \Delta\phi \, dz = 0$$

At the point of application αz_0 the condition $\Delta\phi = 0$ must be satisfied. At all other values of z the condition $\Delta u = 0$ is valid for all values of $\Delta\phi$, which leads to conditions (*i*). Conditions (*ii*) are derived in a similar way for the RH part of the chain with length $(1-\alpha) z_0$.

Using p as abbreviation of B/aA, we find the solutions

$$\phi_l(z) = (\phi)_{\alpha z_0} \frac{\cosh(pz)}{\cosh p\alpha z_0} \qquad \text{for } 0 \leqslant z \leqslant \alpha z_0 \tag{14a}$$

$$\phi_r(z) = (\phi)_{\alpha z_0} \frac{\cosh p(z_0 - z)}{\cosh p(1-\alpha) z_0} \text{ for } \alpha z_0 \leqslant z \leqslant z_0 \tag{14b}$$

Integrating (11) and using the two conditions yields:

$$U = U_0 + \frac{A^2 a}{2}\left[\left(\phi \frac{d\phi_l}{dz}\right)_{\alpha z_0} - \left(\phi \frac{d\phi_r}{dz}\right)_{\alpha z_0}\right]$$

$$= U_0 + \frac{AB}{2}\phi^2_{\alpha z_0} [\tanh pz_0 + \tanh p(1-\alpha) z_0] \tag{15}$$

The energy U is fully determined by the degree of twisting $d\phi/dz$ of the two parts and by the value of the rotation angle ϕ at the point of application where $\Delta\phi=0$. The final part of (15) furthermore shows that the energy is proportional to the sum of the tanh of the lengths of the two parts, i.e. proportional to tanh $(B/A)\,\alpha m$ and tanh $(B/A)\,(1-\alpha)\,m$. At a given value of ϕ_{az_0} U is minimum for $\alpha=1$, because

$$\tanh(B/A)\,m < \tanh(B/A)\,\alpha m + \tanh(B/A)\,(1-\alpha)\,m$$

Normally, when only one potential barrier has to be accounted for, the influence of the shape of the potential function is disregarded. The approximate relaxation time is then found from the following relation

$$\ln\tau \simeq \text{constant} + \Delta U/kT \tag{16}$$

In our system the most important barrier is passed when the rotation is characterized by $\alpha=1$, i.e. head or tail end as point of application. Then the chain is in a condition of maximum energy when its middle segment has arrived at $\pi/2$ and according to equation (15) with $\alpha=1$ ΔU is given by $\Delta U=AB\,(\pi^2/4)\tanh(Bm/2A)$. By dissolution of ketones of different lengths in paraffins, the slope $S_m=(\mathrm{d}\log\tau/\mathrm{d}m)_m$ can in principle be derived from dielectric loss measurements. From (16) it follows that for this slope $S_m \simeq 0{\cdot}536\,(B^2/kT)\,\mathrm{sech}^2\,(Bm/2A)$. Hence, for a given slope and a given chain length the relation between AB and B/A is approximatively given by

$$AB \simeq 1{\cdot}866\,kTS_m\,(B/A)^{-1}\cosh^2(Bm/2A) \tag{17}$$

For each value of m, $AB=\infty$ if $B/A=0$; the values of B/A for which AB is minimum satisfy $(B/A)^{-1}=m\tanh(Bm/2A)$. Our aim is to investigate whether there exists one set of values of AB and B/A for which the experimental curve of the slope S as a function of the chain length m can be calculated by means of the theory set forth in the preceding section. Should this be possible, then the curves in which AB has been plotted versus B/A for a given chain length, will intersect in one point. The significance of equation (17) is twofold:

(*i*) it indicates the shape of the AB versus B/A plots numerically obtained by applying the more exact elaborate procedure;

(*ii*) comparing the relaxation time obtained from the theory with approximate time found from (17), the influence of the less favourable rotations and the shape of the potential function can be estimated.

According to the theory of the two-hole model the slope S_m can, with the aid of equations (5) and (9), be related to the quantity $\mathrm{d}\log\langle 1/I_-I_+\rangle/\mathrm{d}m$

$$S_m = -\left(\frac{\mathrm{d}\log\langle 1/I_-I_+\rangle}{\mathrm{d}m} + \frac{\mathrm{d}\log(1/\zeta)}{\mathrm{d}m}\right) \tag{18}$$

The value of the term $\mathrm{d}\log(1/\zeta)/\mathrm{d}m$ amounts to 5 to 10 per cent of the value of S_m and may, to a good approximation, be obtained by assuming that the friction coefficient of the chain is proportional to the number of monomers: $\zeta=\zeta_0 m$. The quantity $\langle 1/I_-I_+\rangle$ can be calculated approxi-

mately by calculating $U(\bar{\phi})$ and $\bar{\phi}$ for any given point of application along the chain ($\alpha \leqslant 1$):

$$\langle 1/I_{-}I_{+}\rangle = 2\int_{0.5}^{1} \frac{d\alpha}{I_{-}I_{+}} \tag{19}$$

The equations (14) and (15) can be applied only in the range $\phi\alpha z_0 \leqslant \pi/2$. For larger angles of rotation we selected a continuous series of chain positions as represented in *Figure 4*. The value of z, for which $\phi_i(z) = \pi/2$ is here represented as z'.

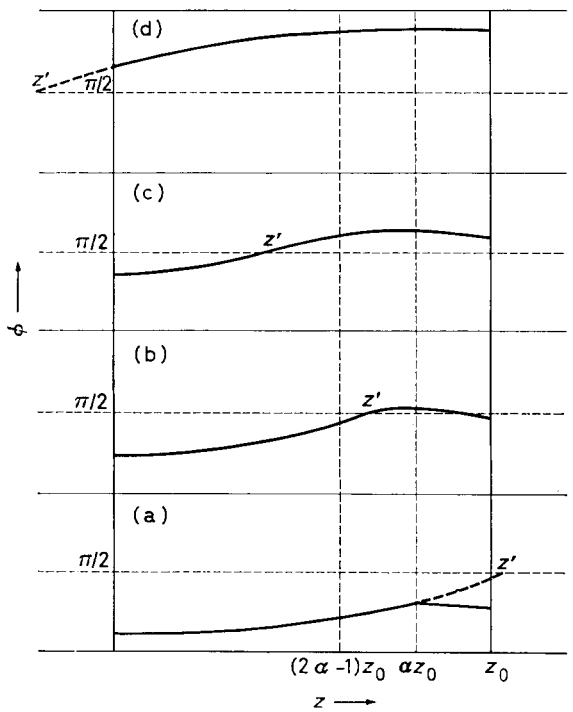

Figure 4—Series of chain positions for a rotation starting at the point αz_0

Four regions can be distinguished:

(*a*) $z' \geqslant \alpha z_0$; (*b*) $(2\alpha - 1)\, z_0 \leqslant z' \leqslant \alpha z_0$;

(*c*) $0 \leqslant z' \leqslant (2\alpha - 1)\, z_0$; (*d*) $z' \leqslant 0$.

From z' and the point of reflection of z' with respect to the αz_0 axis the chain can adjust itself freely; the condition $(d\phi/dz)_{\alpha z_0} = 0$ should then be satisfied for the regions (*b*), (*c*) and (*d*). The expressions for $U(\bar{\phi})$ and $\bar{\phi}$ in the four regions are different. In (*b*) e.g.

$$U = U_0 + \frac{\pi^2}{4}\frac{AB}{2}\left[\tanh pz' + 2\tanh p(\alpha z_0 - z') + \tanh p\{z_0(1-2\alpha)+z'\}\right]$$

$$\bar{\phi} = \frac{\pi}{2pz_0}\left[\tanh pz' - 2\tanh p(\alpha z_0 - z') + \tanh p\{z_0(1-2\alpha)+z'\} + 4p(\alpha z_0 - z'\right]$$

Using a digital electronic computer the quantity $\mathrm{d}(\log\langle 1/I_-I_+\rangle)/\mathrm{d}m$ was calculated for $m = 20$, 25, 30, 40 and 60 for a large number of values of AB and B/A. In calculating $\int(1/I_-I_+)\,\mathrm{d}\alpha$ no use was made of those values of α for which $(1/I_-I_+)_\alpha < 0{\cdot}01\,(1/I_-I_+)_{\alpha=1}$.

DISCUSSION AND EXPERIMENTAL RESULTS

Sillars[6] and Pelmore[7] performed dielectric examinations on dilute solutions of esters in paraffins. The frequencies of the maxima in ε'' for these model substances, together with those found by us on stearone ($C_{17}H_{35}COC_{17}H_{35}$) and nonapentacontanone ($C_{29}H_{59}COC_{29}H_{59}$) dissolved in low-density polyethylene, are plotted as a function of m in *Figure 5*. The values of

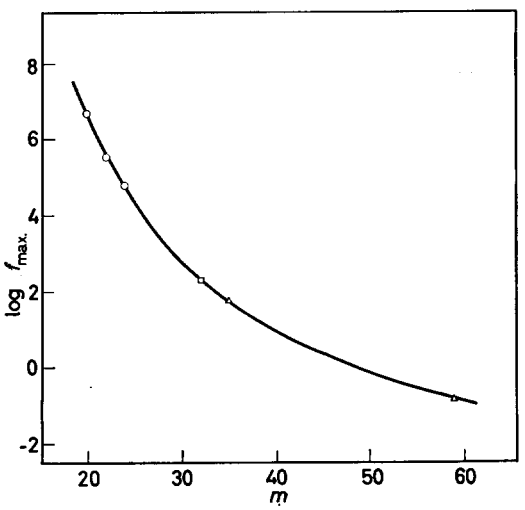

Figure 5—Frequency of maximum loss $f_{max.}$ as a function of the number of monomers m in the chain. Esters in paraffins: ○ SILLARS, R. W. *Proc. Roy. Soc. A*, 1938, **169**, 166; □ PELMORE, D. R. *Proc. Roy. Soc. A*, 1939, **172**, 502. Ketones in low-density polyethylene: △ Author

$-(\mathrm{d}\log f_{max.}/\mathrm{d}m + 0{\cdot}4343/m)$ for the various chain lengths derived from the experimental curve are marked ○ in *Figure 6*. Plotted in *Figure 7* for various chain lengths are those values of AB and B/A for which the quantity $\mathrm{d}\log\langle 1/I_-I_+\rangle/\mathrm{d}m$ calculated by means of the computer corresponds to this slope.

The curves intersect in the point: $AB = 5{\cdot}9\times10^{-13}$ erg and $B/A = 7{\cdot}3\times10^{-2}$ so that the following expressions are found for the two parameters (where mon stands for monomer unit):

$$B^2 = 4{\cdot}3\times10^{-14}\ \text{erg/mon rad}^2 \text{ and } A^2 = 8{\cdot}1\times10^{-12}\ \text{erg/mon rad}^2 \quad (20)$$

The curve in *Figure 6*, calculated by means of these values for AB and B/A, fits in well with the experimental points. The values of the energy para-

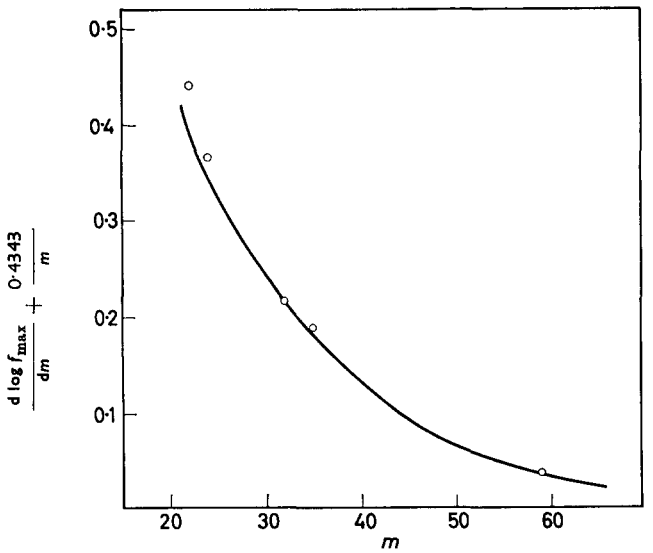

Figure 6—Calculated $\{d \log f_{max.}/dm + 0{\cdot}4343/m\}$ versus m curve; points indicated are obtained from experimental $\log f_{max.}$ versus m curve

meters found from the point of intersection of the AB versus B/A curves with the aid of the approximation formula (17) are of the same order of magnitude. *This implies that the reaction rate constant is practically fully determined by the rotation characterized by $\alpha = 1$, and that the influence of the energetically less favourable rotations can be substantially neglected.*

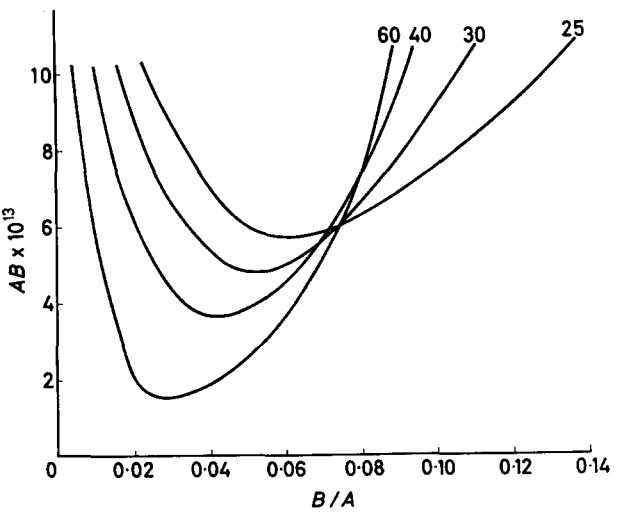

Figure 7—Values of the energy parameters AB and B/A for various chain lengths for which the calculated value of the slope $\{d \log f_{max.}/dm\}_m$ equals the experimental value

From (5), (9) and (10) it follows that

$$\omega_m \simeq (2kT/\zeta)\,\langle(1/I_-I_+)\rangle \tag{21}$$

The value of the rotatory friction coefficient ζ calculated by means of (21) with $m=35$ is $\zeta = 1{\cdot}1 \times 10^{-31}$ erg sec.

Measurement of the temperature dependence of the dispersion maximum furnished a possibility of checking the AB and B/A values found. To this end the logarithms of the frequencies for which ε'' becomes maximum with $m=35$ and $m=59$ have been plotted versus $1/T$ in *Figure 8*. The relation found is linear, which implies that the activation energy ΔH, defined by

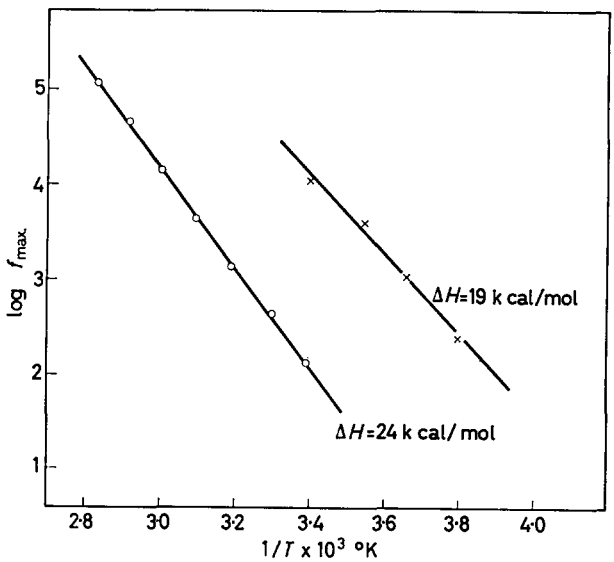

Figure 8—Log $f_{max.}$ versus $1/T$ curves: ○ low-density polyethylene plus $(C_{29}H_{59})_2$ CO; × low-density polyethylene plus $(C_{17}H_{35})_2$ CO

the equation

$$\omega_m = \text{constant} \exp(-\Delta H/kT) \tag{22}$$

is independent of the temperature.

In *Figure 9* $\log\langle 1/I_-I_+\rangle$ is shown as a function of $1/T$. The function was calculated for the values of the energy parameters given in (20) on the assumption that these values are to a first approximation independent of the temperature. Assuming that ζ is also to a first approximation independent of the temperature, the following relationship between ΔH and the slope of the curves in *Figure 9* can be derived from (21) and (22)

$$\Delta H = RT - 2{\cdot}303\,R\,\frac{\mathrm{d}\log\langle 1/I_-I_+\rangle}{\mathrm{d}\,(1/T)} \tag{23}$$

The values of ΔH calculated by means of (23) from *Figure 9* with $m=35$ and $m=59$ amount to 18·1 and 20·7 kcal/mol respectively; the effect of

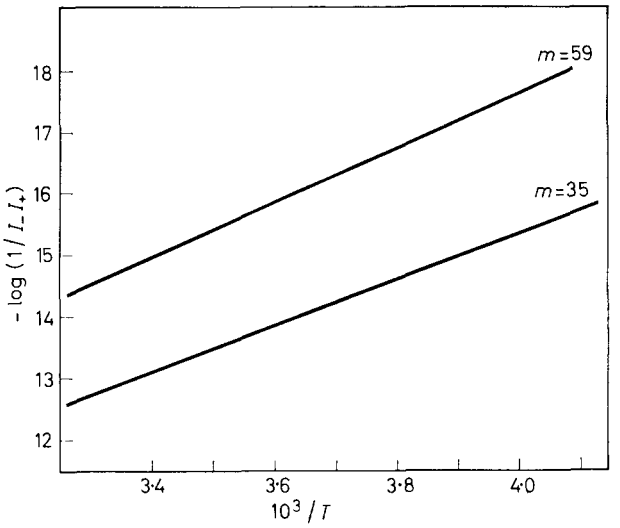

Figure 9—Calculated values of log $\langle 1/I\_I_+ \rangle$ at various temperatures

the rotations characterized by $\alpha < 1$ is slight here also; calculating ΔH by means of the equation $\Delta H \approx RT - 2{\cdot}303\, R\, \mathrm{d} \log (1/I\_I_+)_{\alpha=1} / \mathrm{d}\,(1/T)$ we find 17·9 and 20·5 kcal/mol respectively. The experimental values obtained from *Figure 8* are 19 and 24 kcal/mol respectively. Assuming $(\Delta U)_{\min.} \approx \Delta H$, then $(\Delta U)_{\min.} = AB\,(\pi^2/4) \tanh (Bm/2A)$—which determines the minimum height $(\Delta U)_{\min.}$ of the potential barrier—yields a different method of approximation for calculating ΔH. It appears that values of ΔH calculated in this way with $m = 35$ and $m = 59$ are 17·9 and 20·4 kcal/mol. Müller[5] in Table 5 of his article mentions two values of the van der Waals potential of one CH_2 group in solid paraffin calculated in different ways for a number of ϕ values; in Table 6 he gives the corresponding approximated values for the repulsion potential calculated by means of Slater's helium potential. From these data we derive for B^2 either $14{\cdot}6 \times 10^{-14}$ erg/mon rad^2 or $7{\cdot}7 \times 10^{-14}$ erg/mon rad^2.

As to A^2, we then expect a value of the order of the bond energy of one CH_2 group in the chain. This is about 80 kcal/mol, which corresponds to approximately 5×10^{-12} erg/monomer.

The values of A and B derived theoretically from the experiments with model substances are reasonable therefore, while the activation energies calculated with these values fit in well with the experimental values. The dielectric low-frequency losses in oxidized high-pressure polyethylene are related to the crystalline percentage and are probably caused by a similar motion process. The theory may probably be helpful here to explain the changes in frequency location and the amount of the losses occurring after mechanical and thermal treatments. Of late increasing interest is being taken in the existence of a more than qualitative correlation between

dielectric and mechanical losses. It is not impossible therefore that the mechanical low-frequency losses (α peak) are also produced via a chain rotation in the crystallites.

The author is indebted to Dr C. van Heerden for valuable discussions in the preparation of this paper and to Dr R. Notrot, under whose supervision the calculations with an electronic computer were made.

Centraal Laboratorium,
Staatsmijnen in Limburg,
Geleen, The Netherlands

(*Received August 1962*)

REFERENCES

[1] TUIJNMAN, C. A. F. *Polymer, Lond.* 1963, **4,** 259
[2] FRÖHLICH, H. *Proc. phys. Soc., Lond.* 1942, **54,** 422
[3] BRINKMAN, H. C. *Physica, 's Grav.* 1956, **22,** 29 and 149
[4] SCHWARZL, F. *Kolloidzschr.* 1959, **165,** Heft 1, 88
[5] MÜLLER, A. *Proc. Roy. Soc. A,* 1936, **154,** 624
[6] SILLARS, R. W. *Proc. Roy. Soc. A,* 1938, **169,** 66
[7] PELMORE, D. R. *Proc. Roy. Soc. A,* 1939, **172,** 502

Crystallization of Gutta Percha and Synthetic trans-*1,4-Polyisoprenes**

W. COOPER and G. VAUGHAN

The crystallization of gutta percha and synthetic trans-*1,4-polyisoprene has been studied by differential thermal analysis and by dilatometry. Rate constants have been obtained for crystallization from melts and for interconversion of the isomorphous forms. Synthetic polymers of the highest* trans-*1,4 content crystallize at essentially the same rate and to the same extent as do the natural polymers. The transformation of β to α crystalline forms occurs rapidly over the narrow temperature range from 53° to 63°C.*

Polymers containing appreciable amounts of the β form show some pre-crystallization at 40° to 45°C prior to melting which may amount to as much as 25 per cent of the total crystallinity. Admixture of natural rubber with trans-*polyisoprene causes a marked reduction in rate of crystallization, but the melting points and the volume fractions of gutta percha which crystallize are not reduced. The reduction in rate is ascribed mainly to an increase in the bulk viscosity of the mixture of gutta percha and rubber.*

NATURAL *trans*-1,4-polyisoprenes, gutta percha and balata, exist in two forms (α and β) in the unstressed conditions, of different melting points and with distinguishable crystalline lattices. It has been established that cooling rapidly from elevated temperatures gives the low melting (β) form which is transformed into the more stable α form on heating at temperatures close to the melting point of the β form[1]. The experimentally determined melting points obtained by rapid heating have been found to lie as much as 8°C below the equilibrium melting points[2]. More recently differential thermal analysis (DTA) has shown that the relative proportions of α and β forms depend on the rate of melting as well as on the thermal history of the sample[3]. It was also shown that synthetic *trans*-polyisoprene (TPI) behaves in essentially the same way. However, little is known of the speed of isomerization and there are also little published data on the rates of crystallization of these polymers. It is the purpose of this paper to clarify these aspects and to compare gutta percha with synthetic *trans*-polyisoprenes obtained by various coordination catalysts. In addition the influence of blending natural rubber with the gutta percha on the crystallization behaviour is examined.

EXPERIMENTAL

DTA

The equipment for this work has been described elsewhere[3]; for the present report the more sensitive apparatus with isolated cells, which requires 2 g samples, was employed.

*Paper presented at the Eleventh Canadian High Polymer Forum, Windsor, Canada, 5 to 7 September 1962.

Dilatometry

Standard U type dilatometers fitted with lower tungsten contacts were used. Samples were outgassed at 10^{-3} mm of mercury at 80° to 90°C before filling the dilatometers with mercury to a standard reference mark at 80°C. Samples of 2 to 3 g were used for the rate measurements and 0·1 to 0·2 g for the melting curves. Capillaries were 1·25 mm and 0·50 mm i.d. and bulb sizes were 10 cm^3 and 1 cm^3 respectively. Heating rate in all cases was 6°C/h. Volume changes were followed continuously using the automatic tracking device described previously[4]. Several samples of *trans*-polyisoprene, both natural and synthetic, gave an average value of 1·150 cm^3/g for the specific volume of the amorphous polymer at 80°C with an extrapolated expansion coefficient of $8{\cdot}2 \times 10^{-4}$ cm^3/g °C over the range 20° to 80°C, in good agreement with published data[1,2]. Estimates of the degree of crystallinity from dilatometric data necessitate accurate values for the densities of the two crystalline forms, obtained from electron and X-ray diffraction studies. Mandelkern[2] used the values 1·04 g/cm^3 and 1·05 g/cm^3 for the β and α forms respectively which had been proposed by Fisher[5]. However, from the cell volumes given by Fisher the densities are calculated to be 1·02(7) g/cm^3 and 1·05(6) g/cm^3. As the differences between these densities could arise from an error of one per cent in estimating unit cell dimensions (an error less than those quoted in the literature[6]), it does not seem justifiable to place too much reliance on them, and we have taken a mean value of 1·04 g/cm^3 at 20°C to apply to both forms. The coefficients of expansion for the crystalline forms of $4{\cdot}7 \times 10^{-4}$ cm^3/g °C, derived from melting curves and the estimates of crystallinity, are therefore dependent on the precision of this value.

Kinetic data are expressed in terms of the equation

$$C_t = C_\infty \{1 - \exp(-kt^n)\}$$

based on the Avrami relation[7]. C_t and C_∞ are the fractions of crystalline material after time t and after infinite time, the latter value being determined by extrapolation.

Plasticity measurements were made using the Wallace Rapid Plastimeter. The results are expressed in arbitrary units, the higher the number the higher the bulk viscosity of the material.

The following polymers were examined: Tjipetir gutta percha, three grades of balata and three synthetic *trans*-1,4-polyisoprenes distinguished by the catalysts used for their preparation

[A, VCl_3—$AlEt_3$; B, $TiCl_3$—$Al(Et)_3$ and C, VCl_3—$AlEt_3$—$Ti(OPr)_4$].

RESULTS

Melting points of isomorphous forms

The α form of gutta percha annealed at 56°C had a m.pt of 66°C. When the annealing temperature was raised the melting point progressively increased; annealed at 64°C the polymer had a melting point of 70·5°C (*Figure 1*).

The β form, obtained by rapid chilling from 80°C, had a melting point of 57°C. Annealing at 53°C resulted in a progressive increase to 60°C.

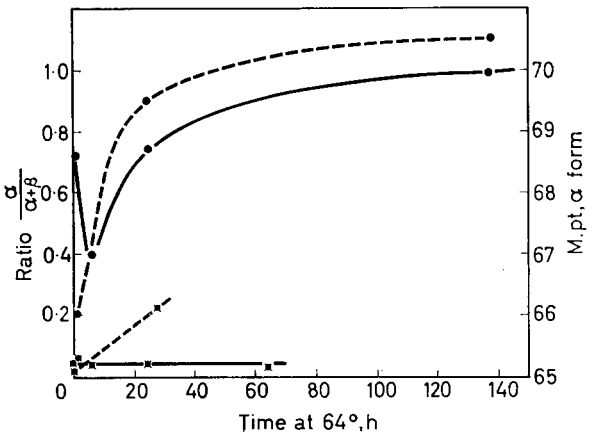

Figure 1—Change in proportions of α and β polymers (upper curves, full) and in melting points of the α form (dashed), of samples of gutta percha heated at 64°C. Initial treatment (lower curves): annealed (full), rapidly chilled (dashed)

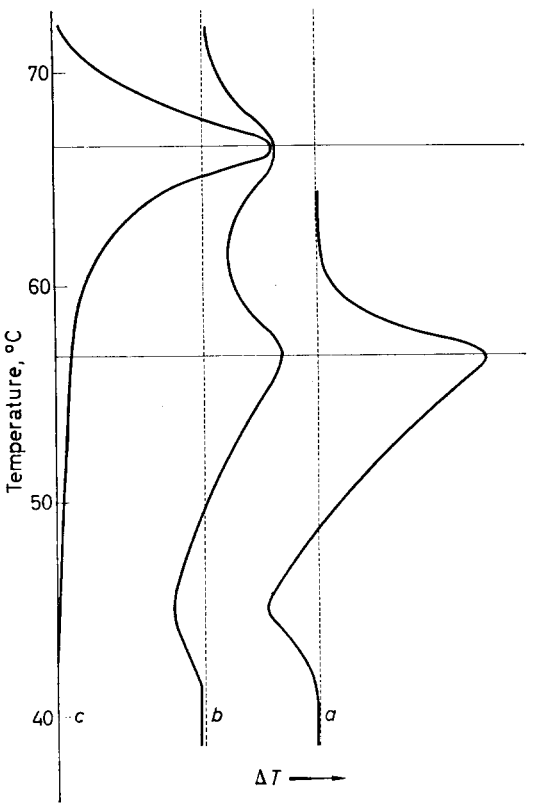

Figure 2—Differential thermograms of gutta percha: (*a*) Chilled rapidly to 0°C, (β); (*b*) Slowly cooled, (α and β); (*c*) Annealed at 58°C, (α)

(Dilatometric values were somewhat higher than those obtained by DTA, namely, 68° and 57·5°C.) In *Figures 2* and *3* is shown the dependence of crystalline form on the thermal treatment of the polymer. Blending of

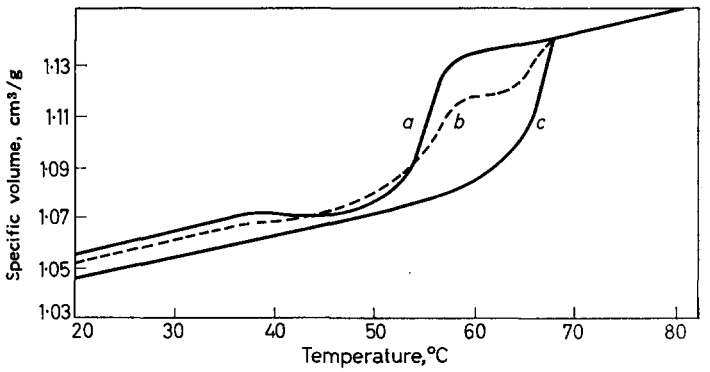

Figure 3—Specific volume/temperature curves for gutta percha: (*a*) Chilled rapidly to 0°C, (*β*); (*b*) Slowly chilled, (*α* and *β*); (*c*) Annealed at 58°C, (*α*)

natural rubber (up to 40 per cent of the mixture) with gutta percha caused no depression of melting points.

In *Table 1* are melting points (DTA) for synthetic *trans*-polyisoprenes obtained in the different crystalline forms.

Table 1. Melting points of *trans*-polyisoprenes

trans-*Polyisoprene*	*M.pt*, °C	
	α	*β*
Type A	67	—
	65·4	60·5 (also small transition at 49°C)
	—	56·5
B	65	59
	—	56·5
C	64	58 (additional transition at 52°C)

Crystallinity—Table 2 gives the crystallinities of the polymers, alone and in blends with natural rubber. In blends the crystallinity is based only on the amount of *trans*-polyisoprene present.

Table 2. Crystallinities of gutta percha, *trans*-polyisoprenes and blends with natural rubber

Polymer	% *Crystallinity*	
	α	*β**
Gutta percha	42	32 (37)
Gutta percha/Rubber 90/10 (w/w)	39	29 (37)
75/25	41	34 (37)
60/40	41	34 (36)
trans-Polyisoprene Type A	34	29 (32)
Type B	32	—
TPI–A/Rubber 75/25 (w/w)	36	—

*Numerals in parentheses refer to total crystallinity including the partial recrystallization which occurs at 40° to 45°C (see Discussion).

Table 3. Dependence of isomerization rate on annealing temperature

Annealing temp. °C	*Gutta percha*		*Half times (h) for β → α isomerization** *Gutta percha/rubber blends* 90/10	75/25	60/40	*TPI Type A*
52	—	(100)	—	—	—	15·5
54	0·5†	(5)	—	—	—	34
56	10	(0·5)	13·5	20	30	34
58	12	(1·5)	15	23	27	—
60	79	—	83	143	V. large	—
68	—	(100)	—	—	—	—

*Most of the data refer to dilatometric measurements, numerals in parentheses obtained by DTA.
†Sample incompletely molten.

Table 4. Rates of crystallization of gutta percha, *trans*-polyisoprene and blends with natural rubber

Gutta percha

Polymer composition	*Crystalliza- temp.* (°C)	*k Calc. for n=3 (t in min)*	*Experi- mental value of n*	$\tau_{1/2}$ *(min)*	*Crystallinity (on gutta percha)*
100/0	52·5	$3{\cdot}39\times10^{-9}$	3·00	593	0·35
	51·0	$1{\cdot}20\times10^{-8}$	3·00	413	0·37
	47·5	$1{\cdot}88\times10^{-7}$	3·05	177	0·35
	45·0	$1{\cdot}14\times10^{-6}$	2·74	96	0·36
	42·5	$5{\cdot}25\times10^{-6}$	3·00	54	0·37
90/10	50	$3{\cdot}39\times10^{-10}$	2·81	1270	0·39
	47·5	$2{\cdot}37\times10^{-9}$	2·84	695	0·39
	45·0	$1{\cdot}41\times10^{-8}$	3·00	365	0·38
	42·5	$1{\cdot}34\times10^{-7}$	3·50	170	0·38
75/25	50	$2{\cdot}96\times10^{-10}$	2·81	1330	0·39
	47·5	$3{\cdot}11\times10^{-9}$	3·00	620	0·40
	45·0	$2{\cdot}00\times10^{-8}$	3·00	336	0·40
	42·5	$1{\cdot}11\times10^{-7}$	3·00	183	0·38
60/40	50	$2{\cdot}87\times10^{-11}$	3·02	3180	0·39
	47·5	$3{\cdot}04\times10^{-10}$	2·76	1380	0·40
	45·0	$1{\cdot}94\times10^{-9}$	3·00	740	0·40
	42·5	$1{\cdot}80\times10^{-8}$	3·00	365	0·39
trans-Polyisoprene, type A					
100/0	50	$4{\cdot}46\times10^{-9}$	3·00	600	0·29
	47·5	$4{\cdot}66\times10^{-8}$	3·00	252	0·29
	45·0	$3{\cdot}12\times10^{-7}$	3·00	130	0·29
75/25	50	$4{\cdot}79\times10^{-11}$	3·00	2430	0·34
	47·5	$3{\cdot}89\times10^{-10}$	3·00	1215	0·34
	45·0	$3{\cdot}11\times10^{-9}$	3·00	600	0·34

Table 5. Rates of crystallization of natural *trans*-polyisoprenes

Sample	$\tau_{1/2}$ *at 40°C (min)*	$[\eta]$ *100 ml g*$^{-1}$
Tjipetir gutta percha	27	1·74
Manaos balata	46	1·54
Demerara balata	15	1·58
Aniba balata	14	1·87

Transformation of β to α form

Table 3 gives typical data for the times of half change from the β form for gutta percha, blends with natural rubber and *trans*-polyisoprene.

Samples of chilled gutta percha and gutta percha annealed at 58°C for 24 hours were stored at 64°C for varying periods. They were then rapidly chilled and examined by DTA. The changes in the proportions of α and β are shown in *Figure 1*.

Rates of crystallization

In *Table 4* are given summarized data for the different polymers and blends. Plots of $\log \{\ln 1/(1-C_t/C_\infty)\}$ against $\log t$ gave good straight lines up to 60 per cent crystallization for the blends with natural rubber and to 55 per cent with pure gutta percha. Calculation of the overall rate constant (k) was from the best line of slope 3 through the points; comparison with the actual experimental values of the gradients indicated that deviations from 3 were small. The times for half-crystallization ($\tau_{1/2}$), were obtained directly from experimental data.

Table 5 shows comparative crystallization rates of four natural *trans*-polyisoprenes (within experimental limits the crystallinities and melting points were identical). Intrinsic viscosities of the polymers (benzene, 32°C) are also given.

DISCUSSION

Melting behaviour

The melting points of the two isomorphous forms of gutta percha are in agreement with values obtained elsewhere[8]. Over the range of heating rates from 1 to 15 degrees per hour the melting points did not vary greatly, although there was a small increase at the lowest rates.

When the β form of gutta percha is heated melting starts to occur at about 40°C and is followed by some crystallization at about 42°C. The extent of the recrystallization is considerable and it can account for up to 25 per cent of the observed crystallinity (*Table 2*). It has been suggested[8] to be the result of alignment after melting of stress-distorted crystallites formed during the rapid cooling which is necessary to obtain pure β form. As would be expected, neither the stretched β form of gutta percha nor the α form of the polymer show any recrystallization before melting. If the sample is heated at 45°C and slowly cooled there is an increase in density. Remelting then occurs without any recrystallization and the whole melting transition is of β polymer (*Figure 4*). The possibility that the volume contraction (*Figure 5*) results from the collapse of voids produced in the polymer by rapid cooling (voids are produced by stretching gutta[9]) is ruled out, since DTA shows heat liberation at corresponding temperatures (*Figure 2*). The small but well defined transitions which are found on occasion with both natural and synthetic polymers are likely also to result from partial melting of disordered crystallites. Since these transitions occur over a fairly wide temperature range, and particularly as they are

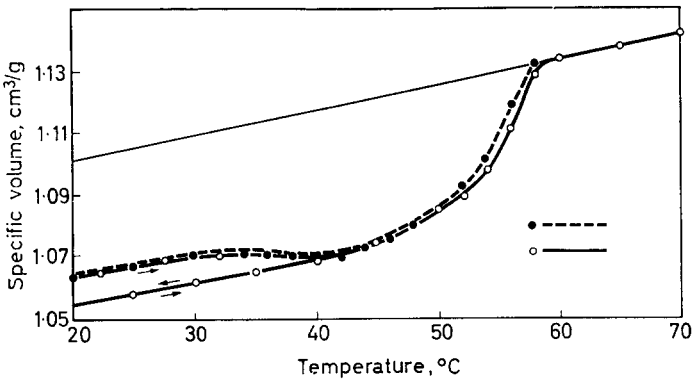

Figure 4— ——●—— Normal specific volume/temperature curve. ——○—— Sample heated to 45°C, cooled to 20°C and subsequently heated to 70°C

most frequently detected in synthetic *trans*-polyisoprene of lower steric purity, where the formation of imperfect crystallites might be expected, it would not be justified to assume the existence of other isomorphous forms. The melting point of β polymer increases from 56° to 57°C to 58° to 60°C when it is heated for long periods at 53°C; slow crystallization from the melt (such that some α polymer is produced at the same time) also results in a higher melting point. Presumably under these conditions more perfect crystallites are obtained.

The melting of α gutta percha starts at 58°C, is rapid at 62°C and is complete at 66° to 67°C. As with the β form, the melting point is unchanged over the range of heating rates used, except at the lowest rate.

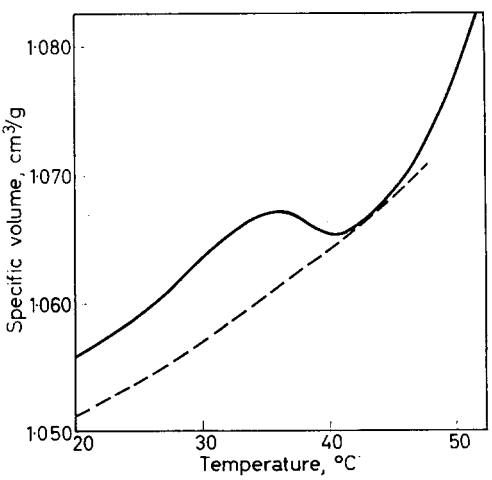

Figure 5—Precrystallization in β gutta percha (———), Annealed (– – – –)

The behaviour of TPI was parallel to that of gutta percha, and with carefully purified samples virtually identical melting points were obtained.

With synthetic polymers of somewhat lower steric purity the melting points were more dependent on the cooling conditions. Slow cooling gave higher and more sharply defined melting points. The cause of this behaviour is not clear but it is not necessarily the result of *cis*-1,4 or 3,4-monomer units in the chain, since bands corresponding to these structures have not so far been identified in the near infra-red spectra. A possible explanation is that it is due to the very high molecular weights or to branched molecules, which are characteristics of many of the synthetic polymers. Thus on mastication the amount of lower, indeterminate, melting decreases and the melting points of both forms increase (*Figure 6*).

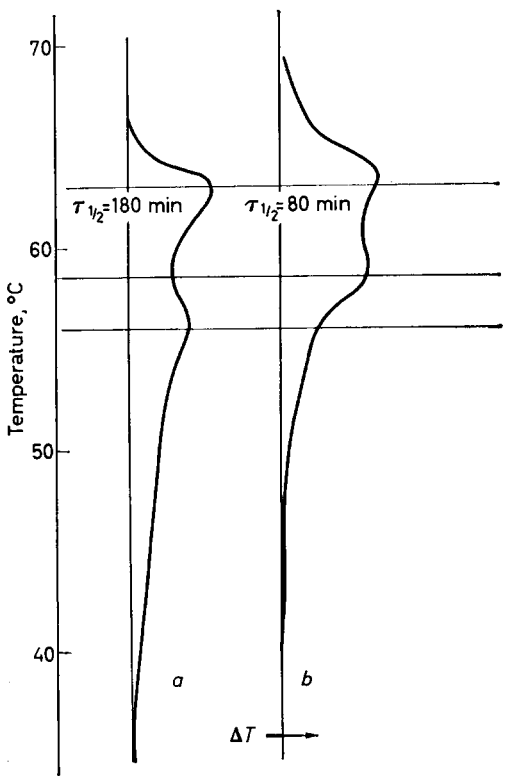

Figure 6—Effect of mastication on melting behaviour of synthetic *trans*-1,4-polyisoprene: (*a*) initial, (*b*) milled for 30 min

It had previously been observed[3] that the ratios of α to β forms were dependent on the temperature at which the sample had been heated before obtaining the differential thermograms. This was thought to be due to the presence of nuclei existing in the sample at a temperature several degrees higher than the experimental melting point. Some confirmation of this view has now been obtained from crystallization rates. Although samples of gutta percha did not show any volume change other than purely thermal expansion above 67°C, the crystallization kinetics were not reproducible unless the polymer had been melted at temperatures higher than 75°C (*Table 6*).

This is clearly the result of persistence of nuclei within the apparently molten polymer, and it is the presence or absence of these nuclei which determines the proportions of the two isomers on cooling. When heated above 80°C and cooled rapidly, the polymer consists wholly of the β form*. Annealing β polymer has no effect up to 52°C, but transformation to α polymer occurs rapidly over the range 53° to 60°C. If the α polymer is

*The earlier report[3] that some α polymer was always produced on rapid chilling referred to 10 g samples; with small samples (1 to 2 g) only the β form is detected.

Table 6. Influence of melting temperature on crystallization at 40°C of gutta percha*

Melting temp., °C	60	65	70	75	80	85
$\tau_{1/2}$, *min*	1·9	16	24	32	34	34

*Sample heated 15 min at stated temperature. Thermal equilibrium was reached in 3 to 4 min at 40°C.

heated at 66°C, some melting occurs and the β form is subsequently found after chilling; the remainder appears as α form from retained α nuclei. The proportion of α polymer and its melting point both increase as the time of heating is prolonged.

Slow cooling gives a mixture of the two forms in roughly equivalent amounts. The proportions of α and β polymers found in mixtures seems to depend on the rate of heating the sample, an increase in rate being associated with an increase in the proportion of the β form[3]. It was thought that at the lower rates some melted β form has time to recrystallize on to existing α nuclei or crystallites to give an apparent decrease in the proportion of β polymer. However, since pure β thermograms have now been obtained, even at the lowest rates of heating, the effect can only be important in the presence of some of the α form. An alternative explanation is that melting of α crystallites starts before the β form is fully molten, particularly with rapid heating rates, so that some of the less ordered α crystallites are included in the β peak.

The results obtained by dilatometry and DTA in *Table 3* for the transformation of β to α differ quite markedly, the former technique showing very much slower rates. This is not unexpected. In the former case the whole process takes place from an amorphous state at the temperature of the experiment, whereas in the latter the sample is chilled prior to DTA, and it would be expected that there would be rapid growth on existing α nuclei as the sample is cooled. α Nuclei form only near to or above the melting point of β polymer and when samples are rapidly chilled very few are produced. That some are formed, however, is shown by the fact that subsequent transformation to α polymer on annealing is faster than crystallization of polymer which has been fully melted and then cooled to the appropriate temperature. The fraction of α polymer is thus a measure of the α nuclei formed as the sample cools over the temperature range 53° to 60°C.

The crystallization of *trans*-polyisoprenes shows precisely the same features as the natural polymers.

Incorporation of rubber in gutta percha does not depress the melting points of the two forms, but it increases the fraction of the gutta which crystallizes and reduces the proportion of precrystallization when in the β form. Rubber is retained in the amorphous region of the polymer and, because of the reduction in the rate of crystallization (see below), time is available for equilibrium to be achieved. The fraction of crystalline polymer is also increased by annealing; at 45°C to give β polymer (*Figure 4*) and at 55°C to α polymer (*Table 2*). The influence of annealing or the presence of rubber on the fraction which crystallizes can be explained if less volume is excluded between crystallites as a result of reduced nucleation relative to growth[10].

The transformation of β to α polymer in blends with rubber is parallel to that of the pure polymer being in all cases much faster than corresponding crystallization from melts.

Kinetics of crystallization

(i) *Pure polymers*—The kinetic data in *Table 4* are seen to give values for n in the Avrami equation close to 3. This implies that if growth of nuclei is spherical then the number of nuclei present remains constant during crystallization[11, 12]. The dependence of the rate of crystallization of gutta percha on temperature (T) is of the right order if the literature value for the equilibrium melting point (T_m) of 74°C is accepted[2], only a slight deviation from linearity of the function $(T_m/T_m-T)^2$. $(1/T)$ versus k being observed[11, 12] (*Figure 7*). *trans*-Polyisoprene (type A) fitted the same curve if T_m was taken to be 72°C, somewhat lower than gutta percha. With synthetic *trans*-polyisoprenes there was in general considerable variation in the rates of crystallization, dependent not only on the catalyst system employed but also from batch to batch using the same catalyst. These differences ($\tau_{1/2}$ varying from 11 to 55 minutes at 40°C), as in the case of the melting characteristics, may be due to minor but undetected changes in microstructure. (It should be mentioned here that the natural polymers likewise show some variation in crystallization rate dependent on the source, *Table 3*). On mastication a branched, high molecular weight *trans*-polyisoprene (type C) of somewhat lower steric purity (97 per cent *trans*-1,4) increased not only in melting point but also in rate of crystallization (*Figure 6*).

(ii) *Blends with natural rubber*—The effect of blending natural rubber with gutta percha in reducing the crystallization rates could be attributed to three possible causes:

(*1*) a decrease in the equilbrium melting point[12, 14, 15],

(*2*) a reduction in the volume in which nucleation and crystallization can occur[10, 13], and

(*3*) a decrease in the mobility of polymer chains as a result of the high molecular weight of the blended rubber.

The first possibility can easily be shown to be inadmissible. From the data in *Figure 7* and the crystallization rate constants of the blends it is possible to calculate what the equilibrium melting points of the gutta would have to be to account for the results. The calculations are shown in *Table 7*.

A progressive decrease in melting point would be required as the rubber content increases. Experimentally it is found that the melting points are independent of rubber concentration and are the same as those of the pure polymer.

The excluded volume theory likewise fails to account for the kinetic results. The treatment of Gent[10] can be followed to calculate the influence of rubber on the extent and rate of crystallization. It can then be shown that the extent of crystallinity in the presence of rubber $(C_\infty)_r$ is related to that in its absence C_∞ by $(C_\infty)_r/C_\infty=\exp(-r)$ and the corresponding crystallization half times by $(\tau_{1/2})_r/\tau_{1/2}=\exp r/n$. So far as extent of crystallinity is concerned the agreement is fair and the theory certainly

Table 7. Calculated equilibrium melting points (°C) for gutta percha blended with rubber

Crystallization temp., °C	*Gutta percha/rubber* 100/0	90/10	75/25	60/40
50·0	$T_m = 74$	68·5	68·5	67·4
47·5	74	68·6	69·0	66·4
45·0	74	68·2	68·6	66·0
42·5	74	68·5	68·2	66·0

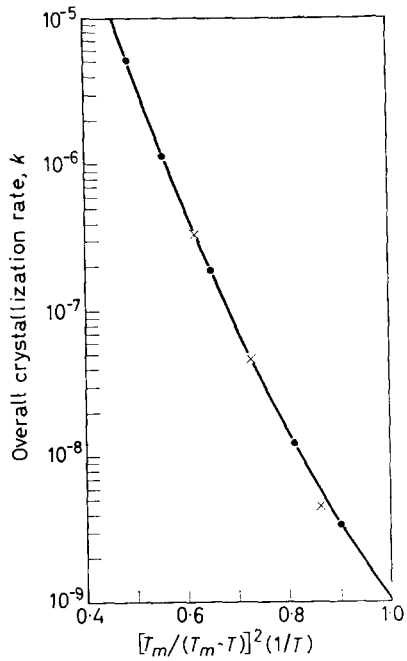

Figure 7—Variation of overall crystallization rate constants (time in minutes) with temperature. $T_m = 347$ Å (gutta percha ——●——), $T_m = 345$ Å (TPI ——×——)

predicts an increase in the fraction of gutta which crystallizes, in accordance with experiment (*Table 8*) but the retardation of crystallization is very much greater than would be calculated from this theory.

The dominant factor determining the rate of crystallization appears to be the mobility of the chain segments. It would be predicted that the higher the bulk viscosity the lower the crystallization rate and, in addition, because of the extra time available for segments to be incorporated into a crystalline lattice, there would be some increase in the degree of crystal-

Table 8. Influence of rubber on crystallinity of gutta percha

Volume fraction of gutta percha $(1-r)$	$(C_\infty)_r/(C_\infty)$ *Temperature, °C* 50	47·5	45·0	42·5	exp $(-r)$
1·000	1·000	1·000	1·000	1·000	1·000
0·904	0·963	0·991	0·956	0·948	0·905
0·758	0·799	0·851	0·833	0·785	0·787
0·610	0·643	0·681	0·699	0·663	0·677

linity. These views are supported by the data in *Table 9* where it is shown that blending 25 per cent of a liquid *cis*-polyisoprene, which increases the plasticity, also increases the rate of crystallization, whereas 25 per cent of crêpe rubber decreases the plasticity and rate of crystallization.

Table 9. Influence of plasticity on crystallization of gutta percha blends

*75/25 blends gutta/*cis*-polyisoprene*	$\tau_{1/2}$ *at 45°C (min)*	*% Crystallinity of gutta*	*Plastimeter reading*
cis-Polyisoprene $[\eta]=0{\cdot}23$	190	36	3
Masticated rubber $[\eta]=1{\cdot}5$	370	37	7·5
Crepe rubber $[\eta]\simeq 6{\cdot}0$	465	39	19
No additive	240	32	7

The authors wish to acknowledge the experimental assistance of Miss R. K. Smith and Mr J. Yardley and to thank the Dunlop Rubber Company Limited for permission to publish.

Central Research Division,
Dunlop Research Centre,
Fort Dunlop, Birmingham 24

(Received September 1962)

REFERENCES

[1] DEAN, J. N. *Trans. Instn Rubber Ind.* [*I.R.I. Trans.*] 1932, **8,** 25
[2] MANDELKERN, L., QUINN, F. A. and ROBERTS, D. E. *J. Amer. chem. Soc.* 1956, **78,** 926
[3] COOPER, W. and SMITH, R. K. *J. Polym. Sci.* 1963, **A1,** 159
[4] VAUGHAN, G., SEWELL, P. R. and HOLLINS, P. H. *Chem. & Ind.* **1960,** 1155
[5] FISHER, D. *Proc. phys. Soc., Lond.* 1953, **66,** 7
[6] FULLER, C. S. *Industr. Engng Chem.* (*Industr.*), 1936, **28,** 907 (and *Rubb. Chem. Technol.* 1937, **10,** 137)
[7] AVRAMI, M. *J. chem. Phys.* 1939, **7,** 1103; 1940, **8,** 212 and 1941, **9,** 177
[8] LEEPER, H. M. and SCHLESINGER, W. *J. Polym. Sci.* 1953, **11,** 307
[9] COOPER, W. and VAUGHAN, G. Unpublished data
[10] GENT, A. N. *J. Polym. Sci.* 1955, **18,** 321
[11] MANDELKERN, L. 'Growth and Perfection of Crystals'. *Proceedings* of an International Conference on Crystal Growth, Coopertown, New York, p. 467. Wiley: New York, 1958
[12] MANDELKERN, L. *Chem. Rev.* 1956, **56,** 903
[13] GENT, A. N. *Trans. Faraday Soc.* 1954, **50,** 521
[14] FLORY, P. J. *J. chem. Phys.* 1949, **17,** 223
[15] GORNICK, F. and MANDELKERN, L. *J. appl. Phys.* 1962, **33,** 907

Solid State Polymerization of β-Propiolactone

C. DAVID, J. VAN DER PARREN, F. PROVOOST and A. LIGOTTI

The rate of polymerization of β-propiolactone in the solid state and the molecular weight of the resulting polymer have been studied as a function of dose, dose rate, temperature, oxygen content of the monomer and initially formed polymer. Some other physical and chemical properties of the polymer are reported. The experimental results are discussed on the basis of stationary and non-stationary state mechanism.

SOLID state polymerization initiated by γ-rays has been the subject of many studies in the past few years[1–18]. In most cases, however, the exact reaction mechanism is not known and no definite proof exists about the nature of the initiating species.

This work describes the solid state polymerization of β-propiolactone between −45° and −110°C. The kinetic behaviour of this monomer is very different from that of solid vinyl monomers; the reaction rate, which is negligible at low temperature in the liquid state, becomes important in the solid state; the maximum conversion remains far below completion and shows a temperature dependence, while the molecular weight decreases when the irradiation dose increases.

Th polymerization rate and the molecular weight of the polymer have been measured as functions of the radiation dose and intensity, and the temperature and dimensions of the monomer crystals.

EXPERIMENTAL

The polymerization reaction

The monomer was dried, distilled under reduced pressure and degassed under high vacuum and its purity checked by vapour phase chromatography. The bulbs were filled and emptied under high vacuum. The polymer produced was determined by weighing. To obtain small crystals, the bulbs were rapidly cooled to −78°C; larger crystals resulted from a slow cooling process. The bulbs were kept at constant temperature in dry ice–acetone mixture or in various solids at their melting point. Irradiations were carried out with two ^{60}Co γ-ray sources with doses of 19 300 rad h^{-1} and $2{\cdot}50 \times 10^5$ rad h^{-1} respectively. The radiation dose was measured with a ferrous sulphate dosimeter and corrections were made for absorption in the cooling media.

Polymer properties

The molecular weight of the polymers was measured viscometrically and by vapour pressure osmometry in chloroform solution[19]. Titration of acid groups was carried out by dissolving the polymer in hot chloroform, adding

an equal volume of methanol (50 ml for 100 mg r polymer) and neutralizing with alcoholic potassium hydroxide (0·05 N), the equivalent point being determined with a glass electrode. Determination of double bonds was tried by three different methods described respectively by Price[20], Wys[21] and Hübl[22].

The first two methods were ineffective with double bonds having C=O groups as α-substituents. In the third method, standardization with methyl acrylate showed that only five per cent of these double bonds could be titrated. Double bond evaluation by u.v. absorption spectroscopy is not feasible because of the lack of solubility of the polymer in adequate solvents.

The i.r. spectra of polymer films were obtained with a Perkin–Elmer Infracord spectrometer. The determination of double bonds and possible β-propiolactone cyclic end groups was performed with a double-beam model 21 Perkin–Elmer spectrometer, using a ten per cent solution of the polymer in chloroform.

Nuclear magnetic resonance spectra were studied with a Varian type apparatus using a ten per cent solution of the polymer in deuterated chloroform. Electron micrographs were obtained with a Siemens type Elmiskop 1 microscope using carbon replicas and palladium shadow casting.

RESULTS

Effect of irradiation time and temperature on degree of conversion and molecular weight of polymers

The rate of polymerization, which is relatively high in the initial stage of the reaction, decreases very rapidly after an irradiation dose of about two to six megarads (*Figures 1* and *2*).

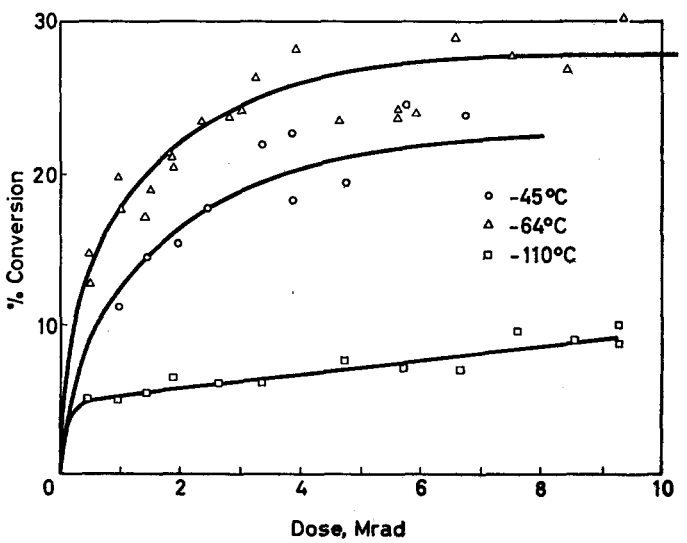

Figure 1—Percentage conversion as a function of irradiation dose in megarads (dose rate $2{\cdot}5 \times 10^5$ rad h^{-1})

The extent of reaction at constant irradiation dose increases with the temperature, except at the higher temperature (−45°C) in the vicinity of the melting point of the monomer (−35°C).

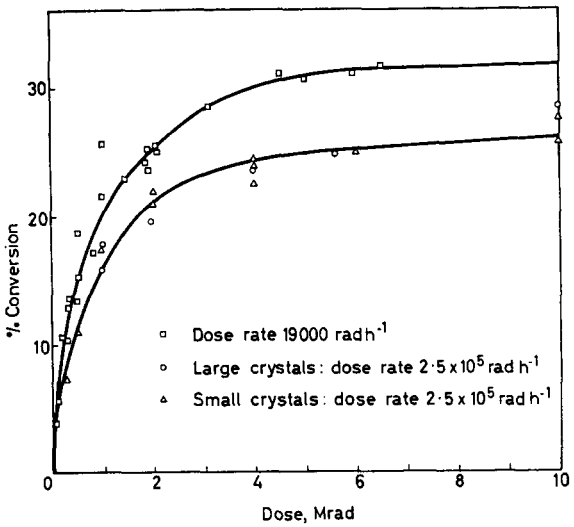

Figure 2—Percentage conversion as a function of irradiation dose in megarads at −80°C

At constant temperature, the intrinsic viscosity decreases at high conversion; at constant dose of irradiation it increases with the temperature (*Figures 3* and *4*).

Effect of intensity of irradiation

The experiments at −80°C were repeated with a dose rate of 19 300 rad h^{-1}. The extent of reaction and the intrinsic viscosity increase slightly when the dose rate decreases (*Figures 2* and *4*).

Effect of physical state

The polymerization at −45°C, which for a solid monomer proceeded to about 22 per cent, did not occur at all when the monomer was kept liquid below its fusion point. Two series of samples, one containing small and the other large monomer crystals, were irradiated under identical conditions (−78°C); no difference at all was detected in the rate of reaction, while the $\overline{DP}$ increased only slightly for the large crystals (*Figures 2* and *4*).

Effect of presence of oxygen and initially formed polymer on the polymerization

The rate of reaction and the $\overline{DP}$ of the polymers formed are not affected by the presence of oxygen. Several experiments were carried out in order to determine the influence of initial products. The monomer was irradiated in one branch of a U-shaped tube to a conversion of 21·5 per cent; the

mixture was liquefied and all volatile compounds were then distilled into the other branch which was sealed off at the central constriction. On re-irradiation the same yield was obtained. In a second experiment, the

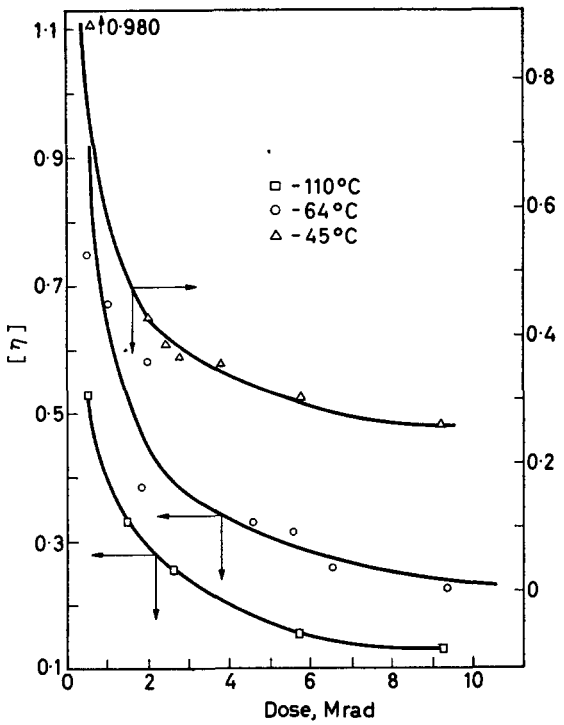

Figure 3—Intrinsic viscosity as a function of irradiation dose in megarads (dose rate: $2{\cdot}5 \times 10^5$ rad h^{-1})

monomer was polymerized to 21·5 per cent conversion, melted, recrystallized and subjected to further irradiation, which yielded only 12·5 per cent of polymer, calculated from the amount of monomer left after the second irradiation. Finally, two solutions of 25 per cent polymer in monomer were crystallized and yielded on irradiation conversions of 12·2 and 14·3 per cent respectively.

Effect of post-irradiation

An effect of post-irradiation has been observed. After an irradiation dose of 0·1 megarad at −80°C, the conversion is 2·3 per cent when the irradiation stops but increases to 5 per cent after 20 hours.

Physical and chemical properties of polymer

X-ray diffraction analysis of the polymer reveals the existence of an ordered fibre-like structure with a melting point of 92° to 93°C. The ordered fibre-like structure is confirmed by electron microscopy (*Figure 5*) of a polymer crystal. If, however, the low melting point of the monomer

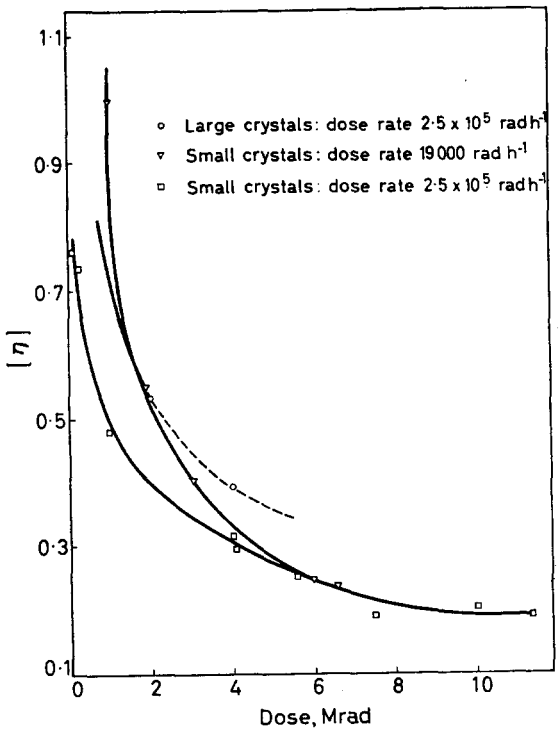

Figure 4—Intrinsic viscosity as a function of irradiation dose at −80°C

does not allow the polymerization to be followed by this method, the polyester structure was proved by i.r. spectroscopy (*Figure 6*), which showed the presence of the characteristic C=O and —C—O— bands near 1 740, 1 200 and 1 000 cm^{-1}. From nuclear magnetic spectroscopy (*Figure 7*) the same conclusions may be drawn. The values* of τ obtained for the two triplets were 7·29 and 5·54, which correspond to the $-\overset{\overset{O}{\|}}{C}-CH_2$ and $O-CH_2$ protons[23] respectively.

End groups were shown to be —COOH and $CH_2=CH-$. The number of acid groups was determined by titration with potassium hydroxide and found to be equal to the number of macromolecules. These acid end groups are formed directly during the polymerization and not by reaction of a possible ketene terminal group with a water molecule during polymer isolation. This was shown by the following experiment. A tenfold excess of absolute methanol was poured under vacuum on the polymer–monomer system after irradiation but before melting of the monomer. After 24 hours, the monomer was melted; after another 24 hours, the polymer was isolated

*$\tau = 10\,000 - 10^4\,(\Delta_{obs.} - \Delta_{TMS})/\Delta_{TMS}$.

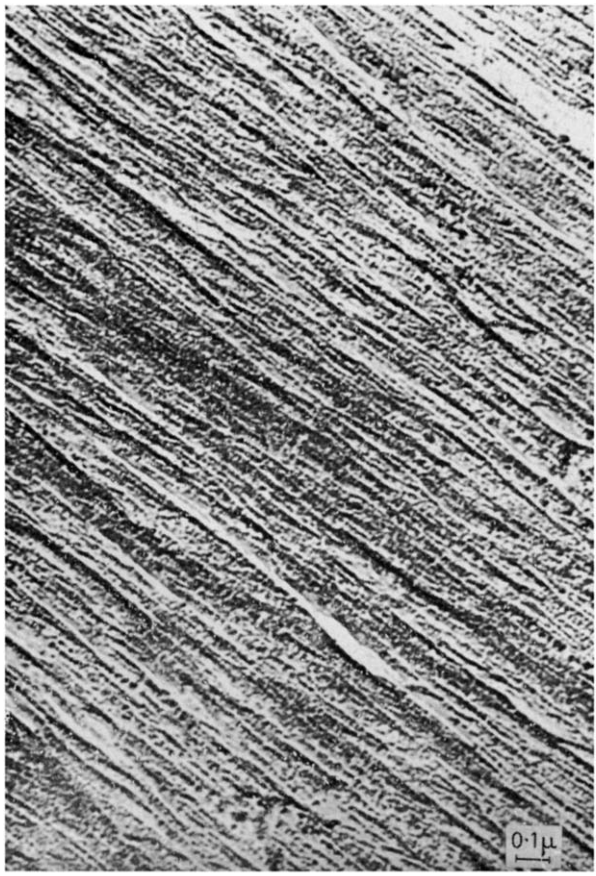

Figure 5—Electron micrograph of β-propiolactone polymer (60 000×)

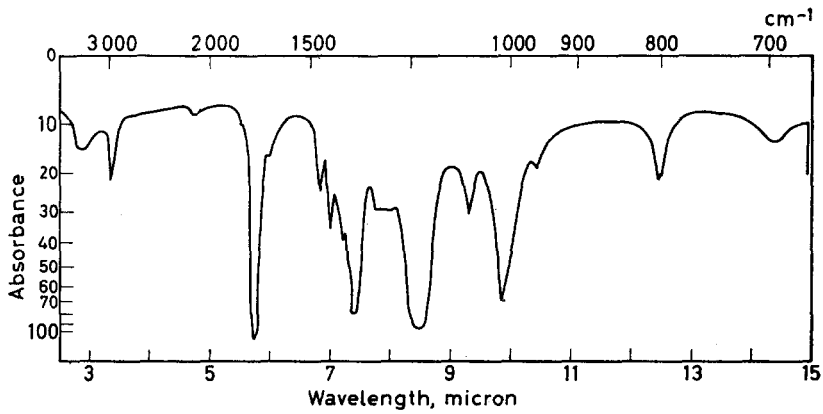

Figure 6—Infra-red spectrum of β-propiolactone polymer (film on sodium chloride)

and titrated; the same number of acid groups per molecule was found as in the usual experiment. (It should be remembered that a terminal ketene group —CH=C=O would react with a methanol molecule to give an ester group —CH_2·CO·OMe instead of the acid group formed in the presence of water.)

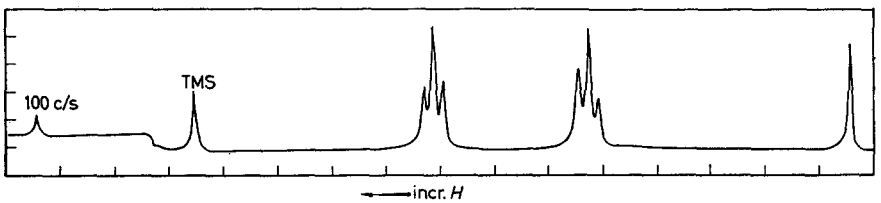

Figure 7—Nuclear magnetic spectrum of β-propiolactone polymer

Double bonds could not be determined quantitatively as explained above. The absence of terminal four-membered rings was established by i.r. spectroscopy.

An approximate relation between $[\eta]$ in dimethylformamide and $\overline{M}_n$ could be derived from measurements of the intrinsic viscosity together with number average molecular weights obtained by vapour pressure osmometry with low molecular weight polymers (irradiation doses lying between 5 and 11 Mrad). The polymer was precipitated from a hot solution of dimethylformamide into water. One obtains thus

$$[\eta] = 6{\cdot}65 \times 10^{-4} M_n^{0{\cdot}66}$$

The precipitation produces a loss in weight of 5 to 10 per cent. The variation in intrinsic viscosity after and before precipitation is never larger than 10 per cent.

DISCUSSION

As a general rule it is very difficult to determine by normal kinetic methods the exact mechanism or the nature of the reactive species in polymerizations in the solid state. However, if one assumes that the reaction is of the anionic type, since it is well known that β-lactones in solution[24] are sensitive to nucleophilic attack of anions such as OH^-, Cl^-, CH_3—COO^-, etc., the initiation may take place by interaction of an electron and a monomer molecule, resulting in scission of a proton

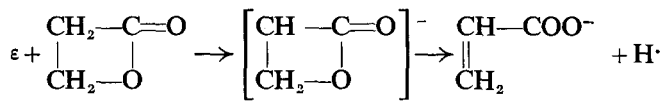

The propagation step could then be

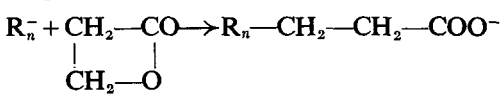

where R_n^- is the growing anionic chain.

The exothermicity of the polymerization of four-atom-ring monomers is mainly due to cyclic strain in the monomer. It has been calculated for butane[25] and measured for 3,3′-bis(chloromethyl)oxacyclobutane[26] in the liquid state. The values* were respectively 22 kcal/mole and 20·2 kcal/mole. It must be noted, however, that the differences in enthalpy and entropy associated with the two polymerization steps:

$$n\text{-}C_3H_4O_{2\,\text{solid}} \longrightarrow \text{solid polymer}$$
$$n\text{-}C_3H_4O_{2\,\text{liquid}} \longrightarrow \text{solid polymer}$$

at the same temperature are the heat and entropy of fusion of the monomer (assuming the polymers formed to be identical. These values are not known, but must be very small for cyclic compounds such as β-propiolactone in which some free rotation persists in the solid state. As an example the enthalpy and entropy of fusion are respectively 0·14 kcal/mole and 0·81 cal/deg. mole for cyclopentane, 2·006 kcal/mole and 13·9 cal/deg. mole for pentane.

From a kinetic point of view, the much higher rate of polymerization in the solid state as compared with the liquid state may be due to different factors:

(*i*) the activation energy of the propagation step may be lowered by polarizing effects of the crystalline network;

(*ii*) the lifetime of a reactive species in the solid state may be longer than in the liquid state;

(*iii*) the frequency factor may be larger due to the orientation of the monomers in the crystalline state.

On account of the low melting point of β-propiolactone, it was impossible to determine its crystallographic characteristics. The structure, however, of the very similar diketene is completely described in the literature[27]; moreover, this monomer shows the same polymerization behaviour under irradiation. From the construction of a three-dimensional model of this crystalline material, it could be demonstrated that the propagation step along the *a* axis requires very little displacement of the monomer molecules. The spatial arrangement of the monomer is such that an eventual reaction between the growing chain and the hydrogen atom of the monomer along the *b* axis may be very likely. Indeed, the occurrence of a transfer reaction, which might correspond with the abstraction of a proton as in the Perkin reaction

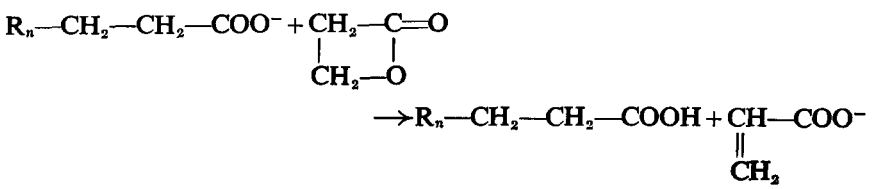

is confirmed by experimental results. From a comparison of the value of G and the $\overline{DP}$ of the polymers formed, one obtains a value greater than

*15 to 25 kcal/mole are common values for vinyl polymerization.

five for the ratio of $G_{\text{initiation}} = G/\overline{DP}$, whereas the value normally would be between 0·1 and 0·5 for the solid state*.

Another peculiar characteristic of the polymerization is the temperature dependence of the degree of conversion; this cannot be attributed to equilibrium between polymerization and depolymerization since the conversion becomes higher with increasing temperature. The intensity dependence of the maximum conversion is negligible. The data of *Figure 2* show that the maximum conversion obtained at −80°C for two dose rates of $2{\cdot}5 \times 10^5$ rad h^{-1} and 19 300 rad h^{-1} is proportional to $I^{-0{\cdot}04}$. A reaction order with respect to monomer cannot be found from the data of *Figures 1* and *2*.

A kinetic scheme involving non-steady state kinetics can qualitatively justify the most characteristic experimental results, viz. observation of a conversion, the temperature dependence and lack of intensity dependence of this maximum conversion, the decreasing mean molecular weight with increasing time of irradiation, and the impossibility of establishing a normal order of reaction with respect to the monomer. We suppose, as suggested by Ballantine for acrylamide, that the initiation takes place at active centres, probably crystal defects in solids. A true termination is excluded; the growing chain probably becomes inactive for geometrical reasons, i.e. by occupying a spatial position in which further interaction requires large displacements of the chain. Transfer is included. We define the following symbols:

S, S_0	the number of active centres at times t, 0, respectively
R	the number of growing chains at time t
M, M_0	the monomer concentrations at times t, 0, respectively
k_1, k_2, k_3, and k_4	the rate constants for initiation, termination, propagation, and transfer, respectively
Q_t	the number of primary chains appearing per unit time
Q'_t	the number of secondary chains (i.e. those resulting from transfer) appearing per unit time
$\overline{DP}$	the mean degree of polymerization
R	the solution of equation (1)

$$dR/dt = Q_t - k_2R \tag{1}$$

Since $Q_t = k_1S(t)$ and S satisfies the relation

$$dS/dt = -k_1S$$

Q_t may be written $k_1S_0\,e^{-k_1t}$ and equation (1) becomes

$$dR/dt = k_1S_0\,e^{-k_1t} - k_2R \tag{2}$$

Furthermore

$$dM/dt = -k_3RM \tag{3}$$

$$Q'_t = k_4RM \tag{4}$$

*For radical polymerization in the liquid state, the highest value found in the literature[11] is ten, and it is not demonstrated that transfer does not occur in that case.

and

$$\overline{DP} = (M_0 - M) / \int_0^t (Q_t + Q_t') \, dt \tag{5}$$

From equation (2),

$$R = \{k_1 S_0 / (k_1 - k_2)\} \, (e^{-k_2 t} - e^{-k_1 t}) \tag{6}$$

On introducing the value of R from (6) into equation (3) and integrating, one obtains:

$$-\ln \frac{M}{M_0} = \frac{k_3 S_0}{k_2} + \frac{k_1 k_3 S_0}{k_1 - k_2} \left(\frac{e^{-k_1 t}}{k_1} - \frac{e^{-k_2 t}}{k_2} \right) \tag{7}$$

For large values of t, equation (7) becomes

$$M_\infty = M_0 \exp(-k_3 S_0 / k_2) \tag{8}$$

The function $F(t) = \ln M_0 / M$ has an extremum only for $t = 0$ and $t = \infty$. Its second derivative is positive at the origin and zero when

$$t^\star = (\ln k_2 - \ln k_1) / (k_2 - k_1) \tag{9}$$

At infinity the function tends to $k_3 S_0 / k_2$. It can thus be represented by *Figure 8*. The shape of the curve does not depend upon the relative values of k_1 and k_2 which have only been supposed to be different.

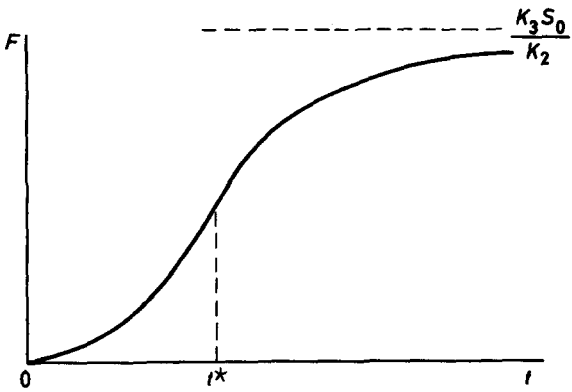

Figure 8—Shape of curve $F(t) = \ln \{M_0 / M(t)\}$

Equations (3) and (6) show that no order of reaction with respect to M can be found, since R is not constant. The maximum conversion

$$(M_0 - M_\infty) / M_0 = 1 - \exp(-k_3 S_0 / k_2)$$

is independent of the irradiation flux and dependent upon temperature through k_3 and k_2; the former, being the propagation rate constant, will have a much larger activation energy than k_2 and the maximum conversion will increase with temperature as found experimentally.

The equation obtained for the mean degree of polymerization $\overline{DP}$ is not simple. It can, however, be shown that $\overline{DP}$ decreases for large t and tends to a constant non-zero value. Replacing Q_t and Q'_t by their values in equation (3) gives

$$\overline{DP} = \frac{M_0 - M)}{S_0 (1 - e^{-k_1 t}) + (k_4/k_3)(M_0 - M)}$$

and

$$\overline{(DP)}_{t=\infty} = \frac{M_0 - M_\infty}{S_0 + (k_4/k_3)(M_0 - M_\infty)} \tag{10}$$

Consideration of the derivative of $1/\overline{DP}$ obtained from equation (10) shows that $\overline{DP}_t$ decreases for large t if and only if

$$k_1 < k_2 \{1 - u/(e^u - 1)\}$$

where

$$u = k_3 S_0 / k_2 = \ln M_0 / M_\infty \text{ by equation (8).}$$

Other mechanisms have been examined in the light of the experimental results. Non-stationary state mechanisms in which the monomer concentration does not appear in the propagation step cannot explain the decreasing molecular weight observed. The usual stationary state treatment does not hold in principle, a post-irradiation effect being observed. Special attention has, however, been paid to the stationary state mechanism proposed by Charlesby for the low temperature polymerization of isobutene 30. In this case, the following kinetic scheme applies:

initiation	rate $R_i I$
propagation	rate $k_p [XM_n]^+ [M]$
formation of inhibitor A	rate $R_a I$
unimolecular termination	rate $k_t [XM_n^+]$
termination by inhibitor	rate $k_a [XM_n^+] [A]$
chain transfer with monomer	rate $k_{tr} [XM_n^+] [M]$

This gives:—

$$\ln \left(\frac{M}{M_0}\right) = -\frac{k_p R_i}{k_a R_a} \ln \left\{1 + \frac{k_a R_a}{k_t} r\right\} \tag{11}$$

$$\frac{1}{u_1} = \frac{1}{k_p [M]} \left\{k_{tr} [M] + k_a [A] + k_t\right\} \tag{12}$$

where u_1 is the instantaneous degree of polymerization.

In the expression of $1/u_1$, the effect of radiation on the polymer may be neglected for low doses such as two to three megarads. *Figure 9* shows a good agreement between experimental and calculated values for large crystals polymerized at −80°C. Experimental results obtained at −64°C and −45°C are also fitted by equation (11). However, the agreement is not so good for small crystals at −80°C and −110°C.

This type of mechanism also explains the change of molecular weight, [M] decreasing and [A] increasing during the course of reaction. However, in order to justify the shape of the curves the inhibitor A must be formed with a very high value (larger than 30) to be efficient enough.

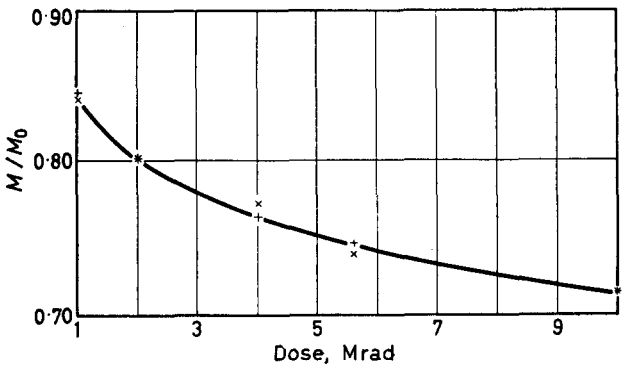

Figure 9—Large crystals polymerized at −80°C. × experimental points, + calculated points. $k_a R_a / k_t = 9{\cdot}3$, $k_p R_i / k_a R_a = 7{\cdot}4 \times 10^{-2}$

During the course of this work, a paper on the same subject appeared in the literature[29]. Our results confirm the temperature dependence of the conversion found by Hayashi and Okamura; differences, however, exist in the polymerization rates and maximum conversions, and different dependences of the degrees of polymerization conversion are reported.

We are very indebted to numerous members of C.E.N. who made this work possible through their technical assistance. We are grateful to Professor Martin from the University of Brussels who allowed us to use his infra-red installation. Also we wish to thank Professor Vanderkelen from the Rijksuniversteiteit in Ghent (Labortorium voor algem. [illegible] *en anorganische scheikunde) who obtained and studied the nuclear magnetic resonance spectra. A.L. is grateful to Euratom for financial support.*

Centre d'Etude de l'Energie Nucléaire,
Mol, Belgium

(*Received September 1962*)

REFERENCES

[1] SOBUE, H. and TABATA, Y. *J. Polym. Sci.* 1960, **43**, 459–65
[2] KARGIN, V. A., KABANOV, V. A. and ZUBOV, U. P. *Vysokomol. Soedinenıya,* 1960, **2**, 303–05
[3] FEE, J. G., PORT, W. S. and WITNAUER, L. P. *J. Polym. Sci.* 1958, **33**, 95
[4] OKAMURA, S. *et al. Third Japanese Conference on Radioisotopes, 1959,* p 165
[5] CHAPIRO, A. and STANNETT, V. *J. chem. Phys.* 1960, 35–7
[6] LAWTON, E., GRUFF, W. and BOLWIT, J. *J. Polym. Sci.* 1956, **19**, 455
[7] RESTRAINO, A. J. *et al. J. Amer. chem. Soc.* 1956, **78**, 2939
[8] BURLANT, W. and ADICOFF, A. *J. Polym. Sci.* 1958, **27**, 269
[9] COLLINSON, E. and SWALLOW, A. J. *Chem. Rev.* 1956, **56**, 471
[10] MAGAT, M. *Makromol. Chem.* 1960, **35**, 159–173

[11] BAYSAL, B., ADLER, C., BALLANTINE, D. and COLOMBO, P. *J. Polym. Sci.* 1960, **44,** 117–27
[12] ADLER, G., BALLANTINE, D. and BAYSAL, B. Symposium International de Chimie Macromoléculaire Moscou, Juin 1960
[13] ADLER, G. and REAMS, W. *J. chem. Phys.* 1960, **32,** 1698–1700
[14] MORAWETZ, H. and FADNER, R. A. *Makromol. Chem.* 1959, **34,** 162–9
[15] FADNER, T. A. and MORAWETZ, H. *J. Polym. Sci.* 1960, **45,** 475–501
[16] ADLER, G. *J. chem. Phys.* 1959, **31,** 848
[17] CHACHATY, C. *C.R. Acad. Sci., Paris,* 1960, **251,** 3857
[18] DAVID, C., GOSSELAIN, P. A. and MUSSO, G. *Bull. Soc. chim. Belg.* 1961, **70,** 583–84
[19] NEUMAYER, L. J. *Analyt. chim. Acta,* 1959, **20,** 519
[20] ST PIERRE, L. A. and PRICE, C. C. *J. Amer. chem. Soc.* 1956, **78,** 3432
[21] See PESEZ, M. et POIRIER, P. *Méthodes et Réactions de l'Analyse Organique,* p 155. Masson: Paris, 1952
[22] See KLINE, G. M. *Analytical Chemistry of High Polymers,* p 236. Interscience: New York, 1959
[23] ANDREW, E. R. *Nuclear Magnetic Resonance.* Cambridge University Press: London, 1955
[24] LACEY, R. N. *Advances in Organic Chemistry,* Vol. II, p 213. Interscience: New York, 1960
[25] DAINTON, F. S., DEVLIN, T. R. E. and SMALL, P. A. *Trans. Faraday Soc.* 1955, **51,** 111
[26] DAINTON, F. S., IVIN, K. J. and WALMSLEY, D. A. G. *Trans. Faraday Soc.* 1960, **56,** 1784
[27] KATZ, L. and LIPSCOMB, W. N. *Acta cryst., Camb.* 1952, **5,** 313
[28] CHARLESBY, A. *Radiation Effects in Materials.* Pergamon: London, 1960
[29] HAYASHI, K. and OKAMURA, S. (*a*) *Makromol. Chem.* 1961, **47,** 230; (*b*) Meeting on the Effect of Radiation on Organic Solids, Paris, July 1961
[30] CHARLESBY, A., PINNER, S. H. and WARRAL, R. *Proc. Roy. Soc. A* 1960, **259,** 386–403

*Viscosity/Molecular Weight Relation in Bulk Polymers—I**

H. P. SCHREIBER, E. B. BAGLEY and D. C. WEST

Non-Newtonian flow in polymers appears to occur only at molecular weights above M_c, the critical molecular weight above which chain entanglement is believed to occur. Studies of the non-Newtonian behaviour in systems such as poly(dimethylsiloxane) in a narrow molecular weight range ($M_c < M < 5M_c$) indicated a simple variation of the viscosity/molecular weight curve with increasing shear stress. In this work polyethylene, studied over a much wider molecular weight range ($M_c < M < 70M_c$), shows more complex behaviour, the onset of non-Newtonian flow occurring at progressively lower shear rates or shear stresses as the molecular weight increases above M_c. The dependence of melt viscosity on molecular weight becomes less pronounced as shear stress or shear rate is increased, permitting the calculation of a high shear rate at which the melt viscosity apparently becomes independent of molecular weight.

STUDY of the dependence on shear of the viscosity/molecular weight function of bulk polymers is interesting because of the light it can shed on the importance of chain entanglements in determining non-Newtonian flow of polymers. The presence of chain entanglements can be inferred from plots of viscosity against molecular weight on logarithmic scales[1,2]. In these plots two distinct portions can be defined for many polymer systems. Below a critical molecular weight M_c, the slope of the logarithmic plot is near unity. Above M_c, an abrupt transition to a power dependence in the neighbourhood of 3·5 is often noted. This transition can be attributed to the influence of polymer chain entanglements[4-6] which now begin to dominate the flow mechanism. It has been shown for several polymer systems[4,5,7,8] that the critical molecular weight for entanglement also defines the molecular weight above which non-Newtonian flow can occur, the viscosities below M_c being independent of the rate of shear.

The present work extends our earlier observations[6] on the relationship between Newtonian (zero shear) melt viscosity at 190°C and molecular weight of polyethylenes to broad ranges of shear. This work is limited to a consideration of fractionated linear (high density) polyethylenes, however, for which chain branching and molecular weight distribution effects on the bulk viscosity can be ignored. In this respect our investigation differs from the interesting studies of Porter and Johnson[5], who used conventional polyethylenes in a similar shear dependence study of the viscosity/molecular weight function for this polymer. A further difference is to be noted in the range of molecular weights of the polymer samples involved in the two studies. Porter and Johnson restrict their attention to molecular weights below about $5M_c$, whereas the molecular weight range in this work extends as far as $70M_c$. Significant extensions of the earlier work are therefore possible.

*Presented in part at 11th Canadian High Polymer Forum, Windsor, Canada, 5–7 September 1962.

EXPERIMENTAL

Phillips type linear polyethylenes were used. These were fractionated on a large scale using the coacervation technique and apparatus described by Blackmore and Alexander[9]. In a number of cases, initial fractions were refractionated to attain narrower weight distributions. Six of these refractionated samples were selected for use in defining a Mark–Houwink relation to be employed in calculations of molecular weights from intrinsic viscosity measurements. The necessary light scattering data for the calibration fractions were obtained from α-chloronaphthalene solutions of the polymers at 140°C, using a modified Bryce–Phoenix apparatus. Intrinsic viscosities in tetralin solutions at 120°C were measured by previously reported techniques[10]. Pertinent light scattering and intrinsic viscosity data are given in *Table 1*. The data closely define a relationship which is represented by the equation

$$[\eta] = 5{\cdot}24 \times 10^{-4} M^{0{\cdot}71} \qquad (1)$$

where $[\eta]$ is the intrinsic viscosity ($dl\,g^{-1}$) and M, the weight-average molecular weight, is evaluated from extrapolations to zero angle of scattering data in a broad range of incidence angles centred about 90°.

Table 1. Characterization data for calibration fractions

Fraction	*Wt av. mol. wt* $\times 10^{-5}$	$[\eta]$ $dl\,g^{-1}$	*Fraction*	*Wt av. mol. wt* $\times 10^{-5}$	$[\eta]$ $dl\,g^{-1}$
E–1	4·00	5·11	E–4	1·35	2·33
E–2	2·75	3·80	E–5	1·00	1·92
E–3	1·55	2·41	E–6	0·73	1·63

Equation (1) differs significantly from the equation given by Duch and Küchler[11] who, however, used unfractionated polyethylenes and whose $[\eta]/M$ relationship is afflicted by considerable data scatter. Subsequent molecular weight evaluation here is based on $[\eta]$ measurements and equation (1).

Ten linear polyethylene fractions were selected for use in the shear effect studies. Melt viscosities were determined using capillary viscometers which have been previously described[12]. Viscosity measurements extended over a shear rate range of less than 10^{-1} to 10^{4} sec^{-1} and a shear stress range from less than 10^{4} to 10^{7} dynes cm^{-2}, although not all samples could be studied over the entire range of variables. Limited availability of polymer samples restricted work to melt temperatures of 190°C. The same consideration made it impracticable to calculate absolute viscosities on the basis of end-correction values[12]. The apparent viscosities pertain to extrusion through capillary orifices having variable radii but constant length to radius ratios of 18·3. Repeated reversibility and reproducibility checks during an extrusion run assure a precision in the measured viscosity values of better than ±5 per cent and polymer stability under all shear rates attained in this work.

To provide a basis for comparison with viscosity data at finite shear, the apparent Newtonian (zero shear) melt viscosities of the experimental polymers were evaluated by extrapolation of low shear viscosities, using the extrapolation method described in an earlier publication[6].

RESULTS AND DISCUSSION

The molecular weights calculated from equation (1) and apparent Newtonian melt viscosities of the polyethylenes are given in *Table 2*. A logarithmic plot of the data is shown in *Figure 1*, which also shows corresponding results at a number of higher levels of shear stress. The viscosity data for *n*-alkanes in *Figure 1* are those of Doolittle[13]. The intersection of the relationships for *n*-alkanes and linear polyethylene defines the critical molecular weight for chain entanglement at $M_c = 4\,000$. Assuming

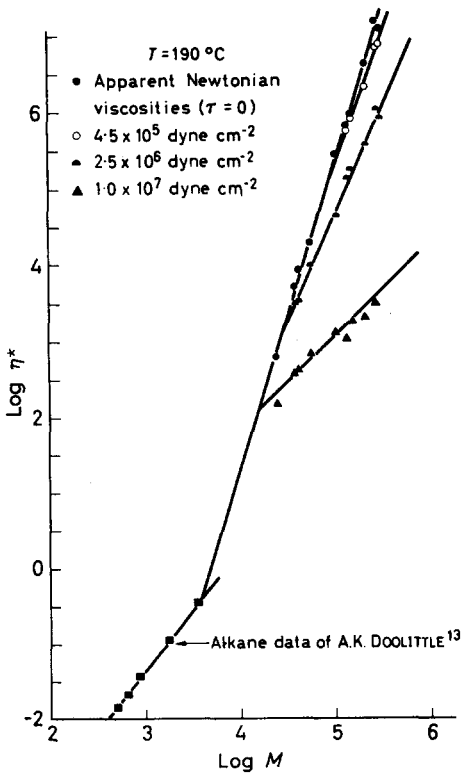

Figure 1—Melt viscosity/molecular weight function for linear polyethylenes at 190°C, showing effect of shear stress

as in previous publications[4,5,7,8], that non-Newtonian flow is associated with the loosening and slip of entanglements when a shear stress is applied to the melt, this also represents the lowest molecular weight for non-Newtonian flow in linear polyethylenes at 190°C. Porter and Johnson[5] have bracketed the M_c value between 3 300 and 8 300 at somewhat lower temperatures. They also report a slight dependence of M_c on temperature, and from their graphs the corresponding M_c value at 190°C is calculated to be approximately 5 500. This agreement with our value is surprisingly good in view of the fact that the *n*-alkane series does not, strictly speaking, represent the correct comparison sequence for the conventional, branched polyethylenes with which Porter and Johnson worked.

The Newtonian viscosity/molecular weight relation in *Figure 1* is given by

$$\log (\eta_0^*)_{190°C} = 4{\cdot}1_0 \log M - 15{\cdot}1_4 \qquad (2)$$

The slope of 4·1 is again significantly higher[6] than the 3·5 value to be expected from theory[1,2]. The reason for this is as yet not clear, although recent evidence[6,14] suggests that it may lie in the molecular weight average chosen to test the validity of the theoretical correlation.

Table 2. Characterization data for polyethylenes used in shear effect studies

Fraction	*Mol. wt from eq. (1)* $\times 10^{-4}$	*Newtonian melt viscosity at 190°C (poise)*	*Fraction*	*Mol. wt from eq. (1)* $\times 10^{-4}$	*Newtonian melt viscosity at 190°C (poise)*
f_1	2·41	$6{\cdot}17 \times 10^2$	f_6	13·2	$6{\cdot}71 \times 10^5$
f_2	3·71	$5{\cdot}16 \times 10^3$	f_7	14·4	$9{\cdot}37 \times 10^5$
f_3	4·09	$8{\cdot}80 \times 10^3$	f_8	20·5	$4{\cdot}39 \times 10^6$
f_4	5·51	$1{\cdot}95 \times 10^4$	f_9	26·2	$1{\cdot}58 \times 10^7$
f_5	10·0	$2{\cdot}82 \times 10^5$	f_{10}	28·2	$1{\cdot}30 \times 10^7$

Perhaps the most interesting feature of *Figure 1* is the manner in which extrusion at elevated shear stresses affects the viscosity/molecular weight plot. This appears to be distinctly different from the pattern of variations recorded in earlier investigations dealing with poly(dimethylsiloxane)[4], poly(isobutene)[7,8] as well as polyethylene[5]. In the earlier studies the viscosity/molecular weight relationships could be represented by a series of power law functions, all originating at the critical molecular weight M_c, the exponent decreasing with rising shear rate[15]. The corresponding power law functions in this case appear to originate at molecular weights which vary inversely with the shear stress. Because of the relatively narrow shear stress range over which a comparison of data from the experimental samples is possible, the behaviour is re-examined on the basis of varying shear rates in *Figure 2*.

To permit more detail to be shown, the coordinates in *Figure 2* are restricted to values characteristic of high polymer behaviour above M_c. An extrapolation of the *n*-alkane line defined by Doolittle's results[13] is included for comparison. The nature of the shear rate dependence of the η^*/M function is obviously analogous to that suggested by the results in *Figure 1*, the deviation from Newtonian flow behaviour occurring at successively lower molecular weights as the shear rate increases. Thus, as in the previous investigations noted, it is reasonable to regard M_c as a material constant signifying the lower limit of molecular weight for which non-Newtonian flow can be observed. For practical purposes, however, a new set of critical values is introduced to designate the initial shear rate $\dot{\gamma}_1$ (or shear stress τ_1) and the specific corresponding molecular weight M'_c (see *Figure 2*) at which initial deviations from Newtonian viscosity are actually observed. In an accompanying paper[16] a mechanism of molecular response to applied stress is suggested to provide a justification for such behaviour. For present purposes it is sufficient to note that the same basic

mechanism of decreasing importance of chain entanglements satisfactorily accounts for the results of this study as well as for the results of earlier investigations of the effects of shear on the η/M function. The distinction to be drawn between this and earlier work[4, 5, 7, 8] concerns the range of

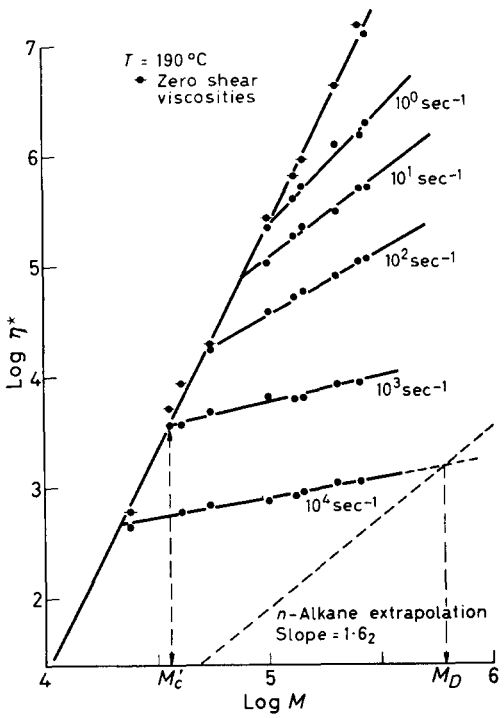

Figure 2—Melt viscosity/molecular weight function for linear polyethylenes at 190°C, showing effect of shear rate. Construction shows evaluation of M'_c *and* M_D

molecular weights involved. This is made clear in *Table 3*, which compares our apparent M_c values and maximum molecular weights with those of preceding investigations. A calculation of the apparent number of monomer units needed to allow entanglement at the given temperature is also included.

Table 3. Critical molecular weight characteristics of polymers used in shear effect studies

Polymer	M_c	*Repeat unit*	*Approx. No. of units at* M_c	*Highest M studied*	M/M_c	*Ref.*
Poly(dimethyl-siloxane) 25°C	30 000	[—Si $(CH_3)_2$—O—]	400	105 000	3·5	4
Polyisobutene 217°C	17 000	[—CH_2—C $(CH_3)_2$—]	300	71 000	4·2	8, 17
Polyethylene 190°C	4 000	[—CH_2—CH_2—]	145	< 20 000	< 5	5
Polyethylene 190°C	4 000	[—CH_2—CH_2—]	145	280 000	70	This work

Clearly, polymer samples used previously were restricted to M/M_c ratios less than about 5. In contrast, the lowest molecular weight fraction in the present work (24 000) has a higher M/M_c value (6·0) than the maximum weights involved in the corresponding earlier work also involving polyethylenes[5]. We therefore suggest that at molecular weights greater than one decade above M_c, the effectiveness of networks established by chain entanglements in the molten polymer varies more critically with molecular weight, thereby resulting in an increased shear sensitivity of the melt viscosity. For example, at molecular weights near 10^5, shear rates of about 1 sec^{-1} in our apparatus are sufficient to disrupt significantly chain couplings and result in non-Newtonian flow. At this shear rate, however, networks created in polymers with molecular weights up to about 60 000 are either more stable or less well developed and provide no detectable evidence for non-Newtonian flow with our experimental techniques. The simple shear dependence described in earlier studies therefore may apply only to molecular weights less than about a decade above the pertinent M_c, the more complex dependence coming into effect at higher molecular weights of the polymer.

Additional support for this view is inferred from the shear rate levels involved in the various studies. We have found significant deviations from Newtonian flow for some of the polyethylene samples at shear rates well below 10^{-1} sec^{-1}. By contrast, in an earlier analysis of the power law dependence of poly(dimethylsiloxane) flow[4] significant decreases in the power law are manifested mainly at shear rates above about 200 sec^{-1}. With the exception of an abrupt change in the power law function near 25 sec^{-1}, the validity of which is difficult to substantiate from the published data, the η^*/M function of this polymer is for all practical purposes independent of shear rate below 200 sec^{-1}. In the same connection, it is difficult to estimate with any accuracy the viscosity variations at low shear rates for the low molecular weight polyethylenes used by Porter and Johnson[5], but a major part of their discussion is based on data obtained in shear rate ranges above 10^3 sec^{-1}, well above the rates at which major effects are noted by ourselves.

A final point of interest in connection with *Table 3* is the calculation of the apparent number of repeating units required to constitute a chain capable of entanglement at the given temperature. This information might be used as a criterion of chain flexibility, and suggests that linear polyethylene is appreciably more flexible than polyisobutene. The data for the siloxane polymer indicate somewhat less chain flexibility than in either of the polyolefins, but of course the comparison involves a large temperature variation in this case.

In an endeavour to show whether or not the reported shear dependence of high molecular weight polyethylenes is more generally applicable to high molecular weight polymers, the literature was searched for pertinent information. The data of Spencer and Dillon[17,18] for polystyrenes lend themselves to analysis along the lines of this paper, and their results (at 200°C) were therefore used to calculate melt viscosities at zero and finite shears for some polystyrenes in the molecular weight range $8{\cdot}6 \times 10^4$

to $7{\cdot}1 \times 10^5$. The viscosity/molecular weight plot for this system is shown in *Figure 3*.

The apparent zero shear viscosity line in *Figure 3* has a slope of 3·4 in good agreement with expectations of the Bueche theory[1,2]. The shear rate dependence in this system is evidently quite analogous to that shown in *Figure 2* for polyethylenes, lending weight to the suggestion of a generally existing change in the shear dependence of the η^*/M plot at molecular weights well above M_c. The η^*/M function at 100 sec^{-1} in *Figure 3* is particularly interesting. While the higher molecular weight polystyrenes appear to define a lower index for the power function, the datum at $1{\cdot}62 \times 10^5$ molecular weight ($\log M = 5{\cdot}21$) clearly deviates from this function. It may be suggested that near this molecular weight in polystyrene, the transition between the high and low molecular weight dependence on shear of the η^*/M function takes place. The M_c value for this polymer cannot readily be defined from published data, but if the transition occurs at M/M_c ratios of not more than 10, then a lower limit of M_c for polystyrene at 200°C is of the order of 20 000*. In view of the M_c values of other polymer systems (cf. *Table 3*), this number seems not unreasonable†.

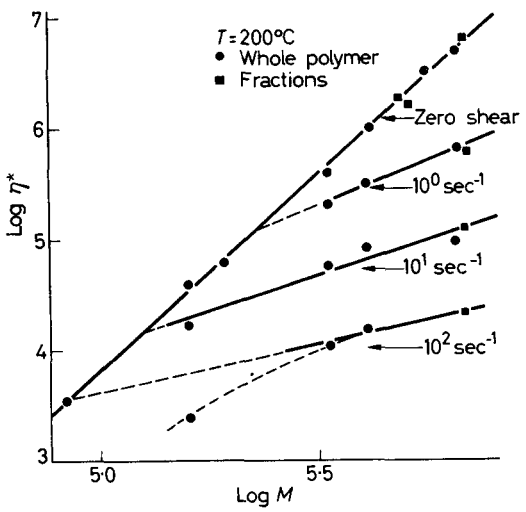

Figure 3—Melt viscosity/molecular weight function for polystyrene. Effect of shear rate at 200°C. Constructed from data of R. S. SPENCER and J. E. DILLON[17], and R. S. SPENCER[18]

Some additional information can be derived from *Figure 2*. In previous studies involving low molecular weight polymers near their respective M_c, it was shown that the slopes in the $\log \eta^*/\log M$ plots decrease with increasing shear rate toward the lower limit defined by the shear-independent portion of the function below M_c[4,5,7,8]. In the present case some of the slopes of the logarithmic η^*/M plot are clearly less than 1·62, the value characterizing the *n*-alkane data. It is then interesting to estimate the shear rate $\dot{\gamma}_t$ at which the slope in the logarithmic plot, *S*, becomes zero

*It is interesting that in a paper presented at a recent Meeting of the American Chemical Society (Washington, March 1962), Porter and Johnson report a value of about 40 000 for the M_c of polystyrene.

†Further support for the existence of a complex shear rate dependence in the η^*/M plot for polystyrene is to be found in a recent publication by J. F. RUDD (*J. Polym. Sci.* 1962. **60**, S7).

and the melt viscosity therefore becomes independent of molecular weight. For each finite shear rate below $\dot{\gamma}_t$, the minimum molecular weight for onset of non-Newtonian flow is of course the previously introduced M'_c, and this is determined as shown in *Figure 2* from the intersection with the zero shear line. Values of the slope S and M'_c for a series of shear rates are reported in *Table 4*. We also tabulate values of M'_c/M_c. These are of particular interest, for if a polymer molecule with a weight M_c is assumed

Table 4. Power law dependence and molecular weights for onset of non-Newtonian flow at varying shear rates

Shear rate $\dot{\gamma}$ (sec^{-1})	$S\left(=\frac{\mathrm{d}\log\eta^*}{\mathrm{d}\log M}\right)$	$M'_c\times10^{-4}$	M'_c/M_c
10^{-1}	3·05	10·5	26·2
10^{0}	1·97	9·6	24·0
10^{1}	1·48	7·6	19·0
10^{2}	1·12	5·4	13·5
10^{3}	0·66	3·6	9·0
10^{4}	0·34	1·8	5·5

to be sufficiently large to participate in one rheologically significant entanglement, then M'_c/M_c represents an evaluation of the minimum number of entanglements per chain needed to initiate non-Newtonian flow at the given shear rate.

Values of S and M'_c/M_c are plotted against $\log\dot{\gamma}$ in *Figure 4*. Except for some curvature at low shear rates, the well defined S versus $\log\dot{\gamma}$ relationship at $\dot{\gamma} > 1$ sec^{-1} is extrapolated to a value of $S=0$, showing $\dot{\gamma}_t \simeq 7{\cdot}5\times10^4$ sec^{-1}. Similarly, the well defined M'_c/M_c versus $\log\dot{\gamma}$ plot can be extrapolated to a ratio value of 1·0, giving a $\dot{\gamma}_t$ intercept at virtually the identical shear rate. This excellent check of the $\dot{\gamma}_t$ value can also be viewed as an independent, internal check of the M_c value determined from the apparent Newtonian viscosities in *Figure 1*.

Finally, the results in *Figure 2* can be used to predict the shear rate above which a polymer of given molecular weight will degrade. Consider the 10 000 sec^{-1} line in *Figure 2*. If this line can be extrapolated as shown, it will define a molecular weight M_D beyond which the 10 000 sec^{-1} line will lie below the extrapolation of the *n*-alkane line. Now, Porter and Johnson have shown[5] that for a given polyethylene the melt viscosity variation with shear is reversible provided the melt viscosity remains greater than that of the corresponding point on the extrapolation of the *n*-alkane line. The latter viscosity value is suggested to be the high shear limit for the polymer. At shear rates leading to lower melt viscosities, permanent viscosity losses due to shear degradation are said to occur. If the results of Porter and Johnson[5] are applicable at the higher molecular weights involved here, then M_D is the molecular weight above which shear degradation will occur at a shear rate of 10 000 sec^{-1}. In a similar manner critical molecular weights for shear degradation can be computed from *Figure 2* for any shear rate generating a η^*/M function having S less than 1·62. Thus, a diagram may be constructed showing the approximate shear rate limits within which the extrusion of a given linear polyethylene can occur with or without shear degradation.

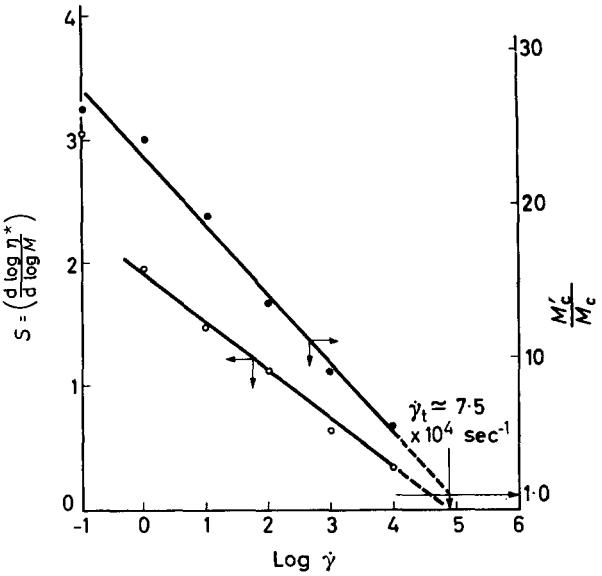

Figure 4—Power law slope S and M'_c/M_c as a function of shear rate for polyethylenes

Molecular weights for polymer degradation were calculated from the known slopes of the *n*-alkane and the appropriate $\log \eta^*/\log M$ plot at various shear rates, and the results plotted in *Figure 5*. The shaded portion indicates the molecular weight range in which most polymer samples will lie. From *Figure 4* it is evident that at 6 sec^{-1}, the slope of the logarithmic η^*/M plot is 1·62 (equal to the alkane line slope). Consequently this is the shear rate limit which must be approached asymptotically at high molecular weights in *Figure 5*. In practice, of course, it is possible that polymers with extremely high molecular weights will deviate sharply from the established η^*/M function; the diagram of *Figure 5* may therefore be inapplicable to such polymers. *Figure 5* contains a further approximation, since all

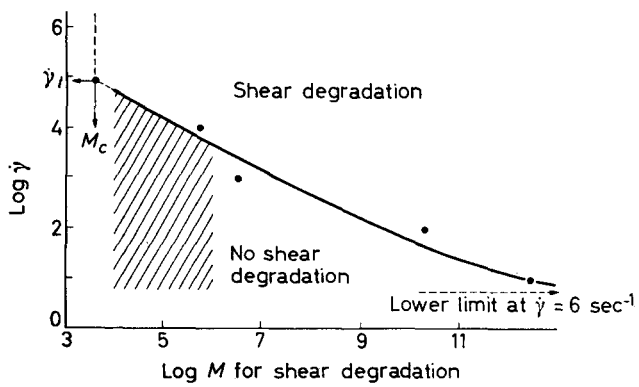

Figure 5—Suggested diagram showing area of shear degradation for linear polyethylenes extruded at 190°C

viscosity calculations are based on apparent shear rates and shear stresses, uncorrected for capillary end effects[12]. The diagram is consequently strictly applicable only to the described extrusion system, although it should constitute a reasonable approximation to a similar diagram based on absolute rheological quantities.

We wish to thank Dr H. W. Holden for the preparation of polymer fractions and Dr M. H. Waldman for light scattering measurements.

Central Research Laboratory,
Canadian Industries Ltd,
McMasterville, Quebec, Canada

(*Received October 1962*)

REFERENCES

[1] BUECHE, F. *J. chem. Phys.* 1952, **20,** 1959
[2] BUECHE, F. *J. chem. Phys.* 1956, **25,** 599
[3] FOX, T. G, GRATCH, S. and LOSHAEK, S. *Rheology,* Vol. I, Ch. 12. EIRICH, F. R. ed. Academic Press: New York, 1956
[4] BAGLEY, E. B. and WEST, D. C. *J. appl. Phys.* 1958, **29,** 1511
[5] PORTER, R. S. and JOHNSON, J. F. *J. appl. Phys.* 1961, **32,** 2326
[6] SCHREIBER, H. P. and BAGLEY, E. B. *J. Polym. Sci.* 1962, **58,** 29
[7] PORTER, R. S. and JOHNSON, J. F. *Polymer, Lond.* 1962, **3,** 11
[8] PORTER, R. S. and JOHNSON, J. F. *J. Polym. Sci.* 1961, **50,** 379
[9] BLACKMORE, W. R. and ALEXANDER, W. *Canad. J. Chem.* 1961, **39,** 1888
[10] SCHREIBER, H. P. *Canad. J. Chem.* 1961, **39,** 1557
[11] DUCH, E. and KÜCHLER, L. *Z. Elektrochem.* 1956, **60,** 218
[12] BAGLEY, E. B. *J. appl. Phys.* 1957, **28,** 624
[13] DOOLITTLE, A. K. *J. appl. Phys.* 1951, **22,** 1031
[14] BUSSE, W. F. and LONGWORTH, R. Paper Presented at Symposium on Macromolecular Chemistry, XVIII IUPAC Congress, Montreal, 1961
[15] BAGLEY, E. B. *J. appl. Phys.* 1959, **30,** 597
[16] SCHREIBER, H. P. *Polymer, Lond.* 1963, **5,** 365
[17] SPENCER, R. S. and DILLON, J. E. *J. Colloid Sci.* 1949, **4,** 321
[18] SPENCER, R. S. *J. Polym. Sci.* 1958, **5,** 591

*Viscosity/Molecular Weight Relation in Bulk Polymers—II. Onset of Non-Newtonian Flow**

H. P. SCHREIBER

The strong dependence of polymer melt viscosity on molecular weight can be attributed to the ability of polymer molecules to participate in entanglements. When unidirectional shear stress is applied, the melt viscosity reduces because of molecular motion which results in a reduced statistical requirement for segmental cooperation. Qualitative examination of polymer motion suggests that the shear stress required to reduce melt viscosity from its Newtonian flow varies inversely with molecular weight and depends on the degree of polymer polydispersity. Experiments confirm the proposed dependence of the initial shear stress for non-Newtonian flow on molecular weight, and indicate the potential use of this shear stress as a characteristic of the high molecular weight portion of the distribution in a given polymer.

THE PRECEDING paper[1] is one of several recent publications[2–4] showing that for many polymers the critical molecular weight for chain entanglement[5,6], M_c, is also the minimum molecular weight for which non-Newtonian flow behaviour is observed. Chain entanglement in polymer melts therefore seems to be a pre-requisite for the existence of non-Newtonian flow. The same publications[1–4] also show that in polymers with molecular weights greater than M_c the rate of change of melt viscosity with molecular weight becomes less pronounced at increasing levels of shear. Mechanisms involving decreasing numbers or decreasing effectiveness of chain entanglements have been proposed to explain these experimental findings.

In principle there are at least three possible ways in which the dependence on shear stress or shear rate of the viscosity/molecular weight function can be represented. These are shown by the diagrams of *Figure 1*. Diagram (a) indicates M_c to be independent of shear. At finite levels of shear, non-Newtonian flow occurs at all molecular weights above M_c, but the effectiveness of entanglements is progressively reduced at higher shear levels. This type of behaviour has been documented for poly(dimethylsiloxane)[2], polyethylene[3] and polyisobutene[4] flow, in all cases using polymer samples with molecular weights near M_c. In diagram (b), *Figure 1*, the M_c value increases with increasing shear and, in addition, the effectiveness of entanglement is reduced. While this type of variation seems reasonable, to date no experimental evidence has been presented to substantiate its existence. Diagram (c) also indicates the critical weight for chain entanglement M_c to be independent of shear, but it differs from diagram (a) in that significant evidence of non-Newtonian flow occurs at progressively lower molecular weights as the level of shear is increased. In this class of behaviour, new critical quantities are required to indicate the initial shear stress τ_1 or the initial shear rate $\dot{\gamma}_1$ for non-Newtonian flow at any $M > M_c$.

*Presented in part at 11th Canadian High Polymer Forum, Windsor, Canada, 5–7 September 1962.

This type of behaviour is documented in the accompanying paper[1] for linear polyethylenes and polystyrenes, in each case at molecular weights well in excess of M_c. With polystyrene a transition from the behaviour in diagram (a) to that in diagram (c) of *Figure 1* appears to have been found, so that

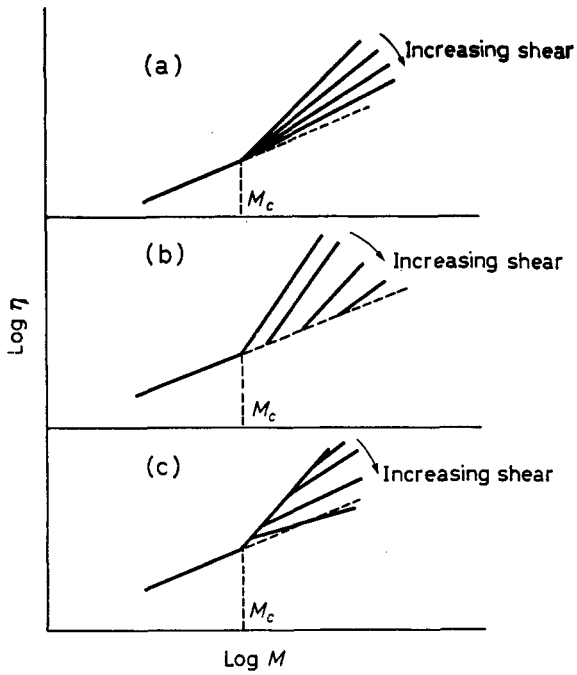

Figure 1—Possible shear dependence of viscosity/molecular weight function of polymers

high molecular weight polymers may in general conform with the latter type of variation.

In this paper a qualitative view of molecular motion in the entangled state is developed to account for a relationship of the type shown in *Figure 1*(c). In the process, the dependence of the initial shear stress for non-Newtonian flow, τ_1, on some structural variables of the polymer is indicated and the results of some experiments designed to test the proposed relationships are presented.

THEORY

For the purpose of this paper consider a polymer melt as part of a system which also includes a capillary extrusion device of known dimensions. The independent variables of this system shall be the temperature T, and the pressure drop ΔP across the extrusion device. For simplicity it is assumed that the pressure drop occurs entirely across the capillary orifice of the extrusion apparatus. For every value of ΔP_i, a proportional shear

stress gradient exists within the system, with τ_i, the maximum shear stress at the capillary wall, given by

$$\tau_i = \Delta P r / 2l \tag{1}$$

where r and l are the capillary radius and length.

Consider now a system involving any linear, monodisperse polymer with a molecular weight $M > M_c$ and at constant T above the melting temperature.

(i) $\Delta P = 0$

Random motion of polymer chains establishes a steady state in which the average number of entanglements per molecule is assumed to be proportional to M/M_c (see also preceding paper[1]). Since molecular motion in polymers is generally considered to arise from the cooperative motion of chain segments[7,8], the Newtonian melt viscosity, η_0, characterizing this steady state can be written[9]

$$\eta_0 = F_0(M)/J(\phi_s)_0 \tag{2}$$

where J is the segmental jump frequency, $(\phi_s)_0$ is the free volume of the unperturbed segment at T and F_0 is the statistical cooperation factor for segmental motion, which depends on the molecular weight of the polymer.

(ii) $\Delta P > 0$

In the new steady-state, a stress gradient is established as a result of which melt viscosity may decrease (assuming the melt is shear thinning). Viscosity changes may be formulated in terms of a partial differentiation of equation (2)

$$\frac{\partial \eta}{\partial \tau} = \frac{J(\partial F/\partial \tau) - F(\partial J/\partial \tau)}{J^2} \tag{3}$$

The primary interest here is in transitions from zero stress to shear stresses where significant evidence of non-Newtonian flow can just be detected for a given polymer. In this relatively narrow stress range the effects of melt compressibility are assumed to be minor, and the above expression is rewritten in the approximate form

$$\partial \eta / \partial \tau \simeq (1/J)(\partial F/\partial \tau) \tag{4}$$

Equation (4) indicates that the statistical factor is a measure of the potential for non-Newtonian flow in a given polymer[10], and that the melt viscosity will decrease from its upper (Newtonian) limit provided ΔP is sufficiently large to cause a significant decrease in the statistical demand for segmental cooperation to permit chain motion. Such a decrease will occur if random segmental motion is restricted and (or) if the number or effectiveness of entanglements per chain is reduced. It is possible to elaborate on this condition in terms of currently favoured concepts of macromolecular motion in stress fields. Both theory[5,6] and experiment[11] agree that an initially roughly spherical macromolecule deforms under the influence of a unidirectional stress and elongates along the axis of applied stress. Concurrently random orientation is replaced by preferential orientation in a

direction parallel to the flow axis. The segmental cooperation factor will be reduced from its maximum if these events on the molecular or larger scale also influence the near neighbour configuration of a given segment. The dependence on molecular weight of the shear stress required to cause a significant reduction in F and therefore η may be illustrated by two limiting cases.

(iii) *Infinite polymer homologue*

In this hypothetical extreme, the single molecule can fill the entire extrusion system. For any pressure drop across the system $\Delta P_i > 0$, the total stress gradient $\Delta\tau_i$ within the system also equals the effective stress gradient $\delta\tau$ acting on the single molecule; that is

$$\lim_{M\to\infty} \frac{\delta\tau}{\Delta\tau_i} = 1 \tag{5}$$

Thus, for any finite pressure drop within the system, the velocity of segmental motion within the molecule decreases from a maximum for segments at the centre of the extrusion device to zero at the capillary wall. Clearly chain entanglements (in this case intramolecular) must slip, and random segmental motion be replaced by preferential motion in the direction of applied stress. The statistical factor for cooperative segmental motion is thereby reduced, and the measured, average, viscosity of the melt must reduce from the Newtonian. Indeed, in this case the Newtonian viscosity can only be attained in the limit $\Delta P = 0$. Consequently for the condition set down in equation (5), the initial shear stress for non-Newtonian flow, τ_1, approaches zero.

(iv) *Polymer with M slightly above M_c*

In this system each molecule can, on the average, participate in only one entanglement. While there is therefore little possibility of building up an extensive entanglement network, the existence of molecular pairs does give the system a small potential for non-Newtonian flow. This potential can be realized only if the effective stress gradient $\delta\tau$ across a molecular pair is sufficiently large for disentanglement or for reducing the statistical requirements for cooperative segmental motion through orientation in the flow direction. Since in this case

$$\lim_{M\to M_c+} \frac{\delta\tau}{\Delta\tau_i} \simeq 0 \tag{6}$$

the quantity τ_1 required to achieve this condition tends to an upper limit, characteristic of the polymer.

Analysis along the above lines can be applied to polymer molecular weights intermediate between the extremes used in the illustrations but a quantitative treatment of the variation of $\delta\tau$ with molecular weight at any $\Delta\tau_i$ is difficult. A suitable form of the relationship, which satisfies the illustrated boundary conditions, can be stated, however, as

$$(\delta\tau/\Delta\tau_i) \propto (1 - M_c/M)^n \tag{7}$$

where n is considered to be an index of the effectiveness of network formation due to entanglements. Since the shear stress τ_1 varies inversely as the ratio $\delta\tau/\Delta\tau_i$, equation (7) can be written in the potentially more practical form

$$1/\tau_1 \propto (1 - M_c/M)^n \tag{8}$$

without, however, specifying the proportionality function.

Thus, the shear stress τ_1 decreases as M rises above M_c—that is, as the potential of the polymer for entanglement increases. Equation (8) is then consistent with the representation in *Figure 1*(c) of the η/M function and further suggests that there is a distinct transition in the variation of τ_1 with molecular weight from a highly sensitive form in the region $M \geqslant M_c$, to a less pronounced form of dependence at M considerably above M_c. This may account for the apparent transition in the shear dependence of the η/M function from that in *Figure 1*(a) for molecular weights[2-4] near M_c to that in *Figure 1*(c) at higher molecular weights[1].

(v) *Polydisperse systems*

In a linear, polydisperse polymer a particular τ_1 can be postulated for every member of the distribution and a range of τ_1 values therefore can be envisaged. The breadth of the range of course reflects the breadth of the molecular weight distribution. Experimentally, however, it may only be possible to define the stress for initial deviation from Newtonian flow; in general therefore the experimental τ_1 value depends on the nature of the high molecular weight end of the distribution, and the molecular weight M appearing in equation (8) will characterize an average for this part of the molecular weight distribution. The factor n in equation (8) also may be expected to depend on the breadth and shape of the molecular weight distribution.

EXPERIMENTAL

Experimental verification of the above concepts depends on the feasibility of determining the stress parameter τ_1. This involves the accuracy of melt viscosity determinations. In this work, viscosity data for whole and fractionated linear polyethylenes were obtained from capillary extrusion measurements, using the viscometer described by Bagley[12]. As in the preceding paper, apparent melt viscosities ($\eta^\star$) at 190°C uncorrected for capillary end effects, were calculated. In all cases the melt viscosities were reproducible to better than ± 5 per cent.

Determination of τ_1

Typical logarithmic plots of $\eta^\star/\tau$ are shown in *Figure 2* for fractions f_4 and f_7 (also used in the preceding work[1]). In both cases the apparent melt viscosity remains at the limiting Newtonian level ($\eta_0^\star$) over a substantial shear stress range before significant viscosity reduction is detected by the present measurements. Thereafter a steady decline in $\eta^\star$ (at an appreciably greater rate at higher M) characterizes non-Newtonian flow.

Precise definition of τ_1 from the data representation in *Figure 2* is manifestly difficult, and a less ambiguous procedure was therefore required.

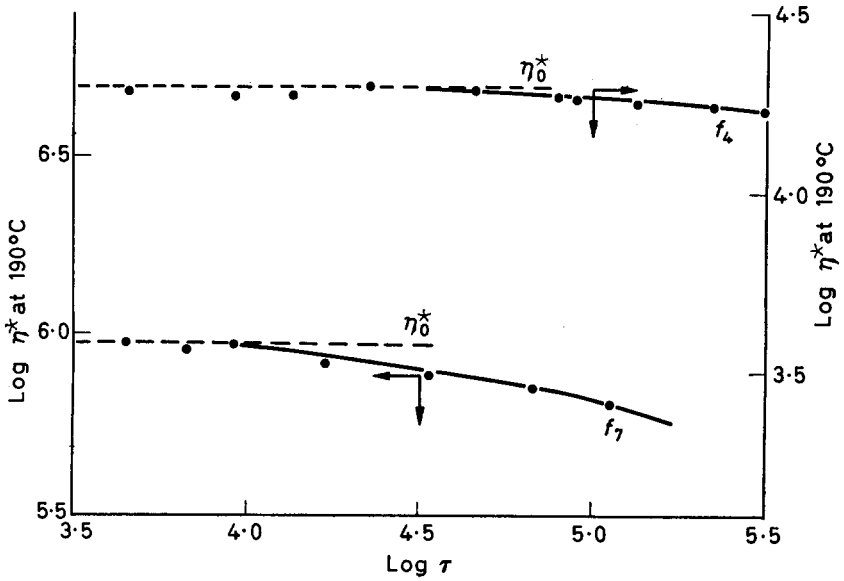

Figure 2—Typical viscosity/shear stress plot for polyethylenes in the region of Newtonian flow

A number of empirical methods can be developed to define τ_1. For present purposes, the one chosen involves a plot of $(\eta\star/\eta_0\star)^{1/2}$ versus $\log \tau$, where the apparent Newtonian viscosity, $(\eta_0\star)$, is calculated by the extrapolation method used in an earlier publication[10]. Typical examples of the plot are shown in *Figure 3* for two fractionated and one whole, linear polyethylene. Provided $(\eta\star/\eta_0\star)^{1/2} > 0{\cdot}8$, excellent linear functions are

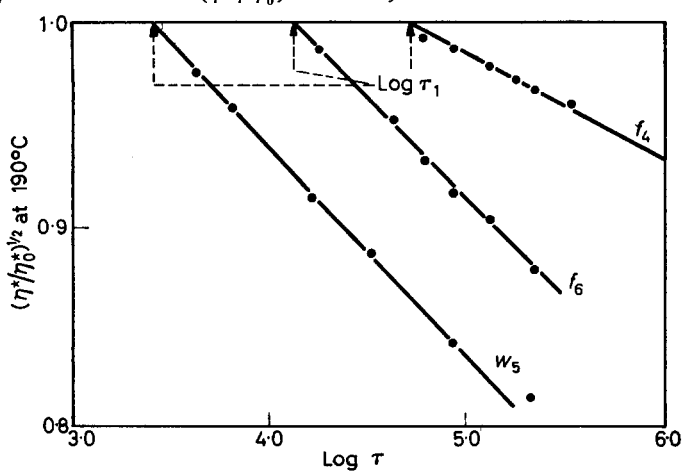

Figure 3—Plots of $(\eta\star/\eta_0\star)^{1/2}$ versus log τ for polyethylenes, showing extrapolation of log τ_1

Table 1. Molecular weight characteristics and τ_1 data for linear polyethylenes

Sample[a]	$M \times 10^{-4}$ [b]	$\Delta = \frac{M}{M_n}$ [c]	τ_1 *dyne/cm²*	$\frac{M}{M_c}$ [d]	*Average M high end of dis'n* $\times 10^{-4}$ [e]
f_1	2·41	1·9	$1{\cdot}90 \times 10^5$	6·0	—
f_2	3·71	1·6	$7{\cdot}55 \times 10^4$	9·3	—
f_3	4·09	1·7	$5{\cdot}22 \times 10^4$	10·2	—
f_4	5·51	1·9	$5{\cdot}31 \times 10^4$	13·8	—
f_5	10·0	2·2	$2{\cdot}27 \times 10^4$	25·0	—
f_6	13·2	2·9	$1{\cdot}42 \times 10^4$	33·0	—
f_7	14·4	4·3	$8{\cdot}80 \times 10^3$	36·0	18·7
f_8	20·5	7·6	$2{\cdot}86 \times 10^3$	51·3	39·1
f_9	26·2	7·9	$2{\cdot}32 \times 10^3$	65·5	46·4
f_{10}	28·2	9·6	$2{\cdot}14 \times 10^3$	70·5	91·2
w_1	25·0	13	$2{\cdot}66 \times 10^2$	62·5	212
w_2	13·0	12	$5{\cdot}28 \times 10^2$	32·5	130
w_3	12·6	13	$4{\cdot}68 \times 10^2$	31·5	139
w_4	8·20	14	$7{\cdot}10 \times 10^2$	20·5	103
w_5	5·40	7	$2{\cdot}76 \times 10^3$	13·2	43·6

(*a*) Fractions are those also described in ref. 1.
(*b*) From intrinsic viscosity measurements and eq. $[\eta] = 5{\cdot}24 \times 10^{-4}\ M^{0.71}$ derived in ref. 1.
(*c*) M_n determined from terminal vinyl group count, using infra-red spectroscopy.
(*d*) Using $M_c = 4\,000$—see ref. 1.
(*e*) From extrapolation to normalization line, *Figure 5*.

obtained which are readily extrapolated to give the desired shear stress limit, as shown. The τ_1 values so obtained are, of course, arbitrary to the extent that the method of data representation is arbitrary. Internally consistent τ_1 values are obtained, however, which suffice for current needs.

Test of equation (8)

Equation (8) indicates that a logarithmic plot of $1/\tau_1$ versus $(1 - M_c/M)$ should be linear over an appreciable range of molecular weights, with a slope equal to the 'entanglement factor', n. The polymers used to test this relationship must be chosen from a group with relatively constant degree of polydispersity, however. This follows from the suggested sensitivity of τ_1 to the high molecular weight portion of the distribution. A tabulation of molecular weight characteristics and τ_1 values for the available polyethylene samples is given in *Table 1*, where the prefixes f and w in the 'Sample' column denote fractionated and whole linear polyethylenes.

Table 1 indicates two groups of samples as suitable for the proposed test of equation (8). These are fractions f_1 to f_6 inclusive, with an apparent distribution width $\Delta \simeq 2$, as defined by the weight to number average molecular weight ratio M/M_n, and the whole polymers w_1 to w_4 with $\Delta \simeq 13$. The appropriate data are plotted in *Figure 4*. As expected from equation (8) both sets of data define good linear relationships. Also as expected, the slope n in *Figure 4* increases with the apparent breadth of the molecular weight distribution, suggesting that more effective entanglement networks can be set up in melts consisting of a broad spectrum of molecular sizes. The available data therefore substantiate theoretical expectations but they do not indicate the molecular weight limits beyond which the linearity

in the logarithmic representation of *Figure 4* breaks down. Breakdown must of course occur since at high molecular weights, where $\log(1-M_c/M)$ approaches zero, the ordinate $\log(1/\tau_1)$ tends to high positive values while at $M \simeq M_c$ the plot tends asymptotically towards an abscissa of $-\infty$.

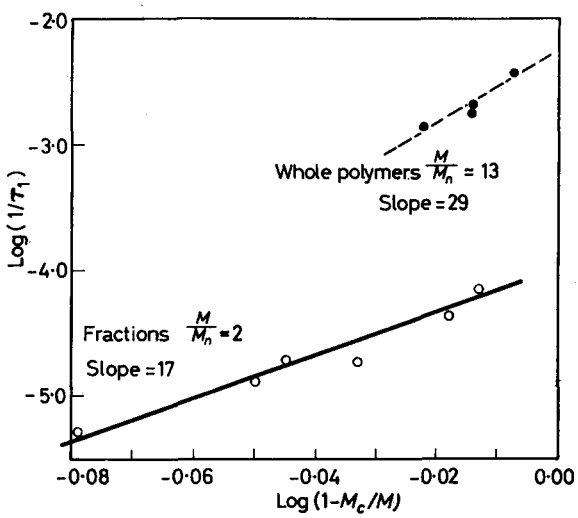

Figure 4—Experimental test of relationship between τ_1 and M_c/M, suggested by equation 8

It is therefore difficult to estimate the molecular weights associated with the high molecular weight portion of the distribution in a given polymer sample from *Figure 4*.

τ_1 and molecular weight distribution

The relationship between τ_1 and molecular weight can also be expressed empirically as

$$\log(1/\tau_1) \propto n' \log(M/M_c) \tag{9}$$

A plot based on the above statement has been used to estimate the dependence of τ_1 on the high molecular weight portion of the distribution in polydisperse linear polyethylenes, as indicated in *Figure 5* which involves coordinate values calculated from the data in *Table 1*. As in *Figure 4*, the data for the six fractions with $\Delta \simeq 2$ define a good, linear relationship. The more polydisperse fractions and the whole polyethylenes fall well off this relationship due, presumably, to the presence of molecules with higher than the given average molecular weight. Unfortunately, a quantitative statement of the polydispersity dependence of τ_1 is not feasible at this time, since no information is available regarding the shape of the distributions for the polydisperse samples. An estimate can be made nevertheless of the apparent molecular weight associated with the high end of the distribution in these polyethylenes, accepting the relationship for the six fractions with narrow distributions as a normalization function. Assuming

that this normalization function can be extrapolated as shown, horizontal lines are drawn from the datum of each polydisperse polymer sample in *Figure 5* to the intersection of an extension of the normalization line. The molecular weights computed from this intersection are entered in *Table 1*. Since the normalization procedure uses polyethylenes which themselves are slightly polydisperse, the estimated high molecular weight

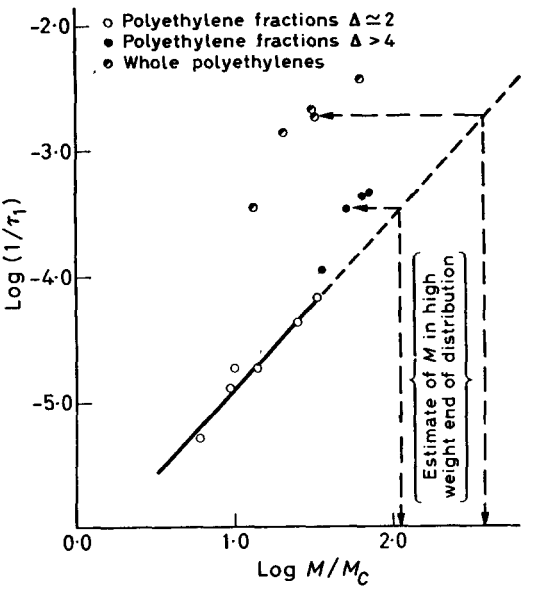

Figure 5—Alternative representation of τ_1 versus M/M_c data showing estimate of molecular weight in high end of distribution

averages in *Table 1* are to be regarded as lower limits.

Further work is planned to establish the quantitative dependence of τ_1 on molecular weight distribution and to increase the utility of this shear stress parameter by applying it to non-linear polymer systems.

I am indebted to Drs S. H. Storey and E. B Bagley for valuable discussions. I also wish to thank Dr H. W. Holden for the preparation of polymer fractions and Mr A. W. Pross for infra-red measurements. Constructive commentary by Dr Louis D. Moore Jr, Tennessee Eastman Co., is also gratefully acknowledged.

Central Research Laboratory,
Canadian Industries Ltd,
McMasterville, Quebec, Canada

(*Received October 1962*)

REFERENCES

[1] SCHREIBER, H. P., BAGLEY, E. B. and WEST, D. C. *Polymer, Lond.* 1963, **4**, 355
[2] BAGLEY, E. B. and WEST, D. C. *J. appl. Phys.* 1958, **29**, 1511
[3] PORTER, R. S. and JOHNSON, J. F. *J. appl. Phys.* 1961, **32**, 2326
[4] PORTER, R. S. and JOHNSON, J. F. *J. Polym. Sci.* 1961, **50**, 397

[5] BUECHE, F. *J. chem. Phys.* 1952, **20,** 1959
[6] BUECHE, F. *J. chem. Phys.* 1956, **25,** 599
[7] EWELL, R. H. *J. appl. Phys.* 1938, **9,** 252
[8] FLORY, P. J. *J. Amer. chem. Soc.* 1940, **62,** 1057
[9] FOX, T. G, GRATCH, S. and LOSHAEK, S. *Rheology,* Vol. I, Ch. 12. EIRICH, F. R. ed. Academic Press: New York, 1956
[10] SCHREIBER, H. P. and BAGLEY, E. B. *J. Polym. Sci.* 1962, **58,** 29
[11] MASON, S. G. and BARTOK, W. *Rheology of Polydisperse Systems,* Ch. 2. MILL, C. C. ed. Pergamon: New York and London, 1959
[12] BAGLEY, E. B. *J. appl. Phys.* 1957, **28,** 624

An Infra-red Study of the Deuteration of Cellulose and Cellulose Derivatives

R. JEFFRIES

This paper reports an infra-red study of the deuteration of cellulose and cellulose derivatives with deuterium oxide. The deuteration of the crystalline and the amorphous regions of cellulose are investigated in detail; results are obtained which suggest that the crystalline regions contain a range of degrees of perfection of the hydrogen-bonding arrangement; it is concluded that the reason for the low rate of deuteration of the crystalline regions is that the latter absorb only very small amounts of deuterium oxide. The results obtained with cellulose acetates and ethyl cellulose indicate that all the hydroxyl groups in these derivatives are readily deuterated; crystallization or orientation of the acetate films does not affect this complete exchangeability.

THIS paper describes an infra-red (i.r.) study of the OH $\longrightarrow$ OD exchange reaction in films of cellulose and cellulose derivatives. The main purpose of the work with cellulose was to extend the knowledge of the factors affecting, and the nature of, the deuteration of the crystalline and the amorphous regions. Up to the present the most detailed study of the OH $\longrightarrow$ OD exchange in cellulose is that of Mann and Marrinan[1–3]; their work established the i.r. deuteration technique as a major tool in the study of the crystalline–amorphous structure of celluloses. Since then other deuteration studies on cellulose have been reported[4–9]; some of these are referred to below. The work with the cellulose acetates and ethyl cellulose was mainly to investigate the usefulness of the i.r. deuteration technique in the elucidation of the crystalline–amorphous structure and 'accessibility' of these materials. No previous deuteration studies of cellulose derivatives have been published; several i.r. investigations which have been reported[10–13] are referred to below.

EXPERIMENTAL

Materials

The films of viscose, saponified secondary cellulose acetate and bacterial cellulose were prepared by methods previously described[1,14]; the films were 3–6μ thick when dry.

Films of five commercial secondary cellulose acetates (degree of substitution 2·3–2·4), three commercial triacetates (d.s. 2·89, 2·95 and 2·98) and one commercial ethyl cellulose (d.s. 2·5) were cast on finely ground glass plates from solutions in dry organic liquids; the solvents employed were acetone, chloroform and benzene, respectively. The thicknesses of the dry films are indicated on *Figures 6* and *8*. Linear orientation was induced in secondary acetate film by stretching it whilst swollen in 80/20 v/v methylene chloride/benzene. Both types of acetate were partially crystallized by

treatment with water at 150°C for six hours; secondary acetate was also crystallized by boiling for one hour in an aqueous solution of one per cent phenol and two per cent sodium sulphate.

AR iso-amyl acetate was used without further purification. Both *n*-butyl acetate and *n*-butyl ether (B.D.H. best grade) were fractionally distilled from drying agents.

Spectroscopic measurements and deuteration techniques

The i.r. spectra were measured on a Grubb–Parsons double-beam spectrometer, using a lithium fluoride prism for most of the work (3 700–2 300 cm^{-1}) and a rocksalt prism for a few measurements at lower frequencies. Liquids were studied with the latter enclosed between calcium fluoride plates. Polymer films were mounted in special brass cells with calcium fluoride windows; the measurements were usually made on films which had been freed from water or deuterium oxide by evacuation of the cells through a cold trap.

Deuteration of the polymer films in deuterium oxide vapour was effected, in the absence of air, with the samples mounted in the brass cells. The required vapour pressures of deuterium oxide were obtained by means of reservoirs of 99·7 per cent deuterium oxide liquid and saturated solutions of inorganic salts in deuterium oxide. Deuteration of the polymer films in liquid deuterium oxide at 25°C was effected simply by filling the brass cells with the liquid. The liquid-phase deuteration at higher temperatures was done in sealed glass tubes. The rehydrogenation of certain of the films with water was studied by techniques similar to those used for the deuteration.

RESULTS AND DISCUSSION

(A) CELLULOSE

The results below refer to the films as first dried after preparation, unless otherwise stated. Regenerated viscose film is used throughout as a typical example of the regenerated celluloses; the results with the saponified secondary acetate were very similar to those with the viscose.

(1) *Separation of the hydroxyl-stretching bands of the crystalline and the amorphous regions*

The OH $\longrightarrow$ OD exchange between cellulose and deuterium oxide is in two stages[1,2], illustrated for viscose and bacterial cellulose in *Figures 1*(a) and *1*(b): an initial rapid stage corresponding to deuteration of the amorphous regions [A to B in *Figures 1*(a) and *1*(b)] followed by a slow stage corresponding to the deuteration of crystalline cellulose. During the rapid stage a broad, featureless, absorption band, resulting from the regions where the cellulose is hydrogen-bonded in a non-regular, 'amorphous', manner, is 'removed' by the exchange reaction from the 3 600–3 000 cm^{-1} (OH-stretching) region to the 2 700–2 300 cm^{-1} (OD-stretching) region. The remaining hydroxyl band, which contains well-defined and characteristic peaks, is the result of the absorption in regions where the cellulose is hydrogen-bonded in a regular, 'crystalline' manner*. In saturated vapour

*'Amorphous' and 'crystalline' as used here, refer to the regions of cellulose thus defined in terms of i.r. absorption and hydrogen bonding.

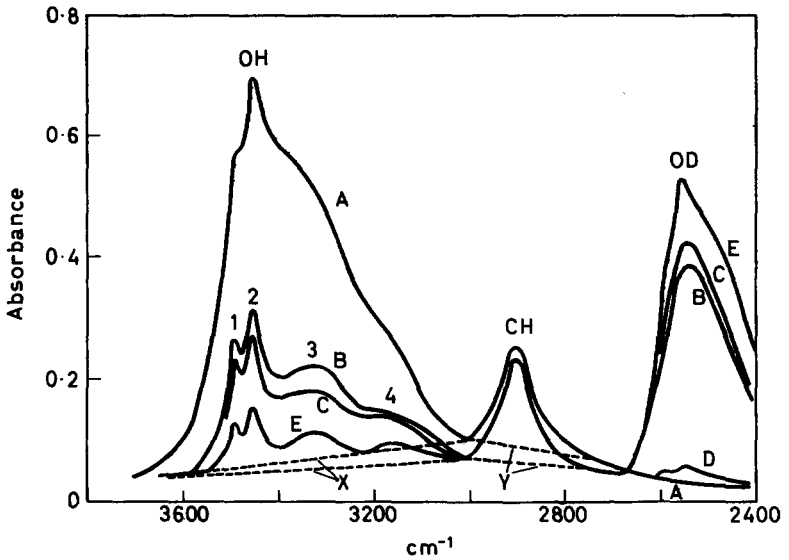

Figure 1(a)—Infra-red spectra of dry films of viscose

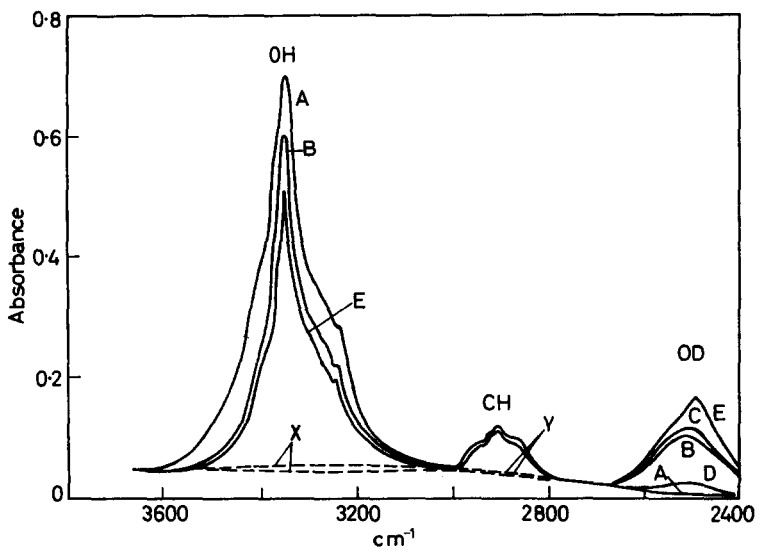

Figure 1(b)—Infra-red spectra of dry films of bacterial cellulose

Figure 1—A Undeuterated. B End of amorphous deuteration and start of crystalline deuteration (about 20 min* in saturated D_2O vapour). C Small amount of crystalline cellulose deuterated (90 min in saturated D_2O vapour). D As C, then rehydrogenated for 30 min in saturated H_2O vapour. E Deuterated for 25 days in saturated D_2O vapour

*The exact time depends upon the experimental conditions. NOTE: All treatments at 25°C.

at room temperatures this first stage of the deuteration is of 15–30 min duration, depending on the precise conditions employed. The slow second stage of the deuteration involves a slow decrease in the intensity of these 'crystalline' hydroxyl bands and the gradual appearance of the corresponding 'crystalline' OD bands superimposed on the OD band of the amorphous regions [spectra C and E in *Figures 1*(a) and *1*(b) illustrate the extent of deuteration of the crystalline regions after 90 min and 25 days, respectively, in saturated vapour at 25°C].

It is clear from the above that the difference in the rates of deuteration of the crystalline and the amorphous regions is very large. However, the exact point corresponding to the end of the deuteration of the amorphous regions and the start of the deuteration of the crystalline regions is not marked by any *very* abrupt change in the rate of decrease of the absorbance (optical density) of the hydroxyl band. A more precise determination of the change-over point can, however, be achieved as follows. The sample is treated with saturated deuterium oxide vapour for various lengths of time (in the range of, say, 10–120 min at room temperature) and after each deuteration the sample is rehydrogenated for various similar lengths of time in saturated water vapour; the amorphous regions rehydrogenate first and so the intensity of any bands from deuterated crystalline material superimposed on the OD band of the amorphous component is more clearly revealed as the intensity of the latter is progressively reduced [see, for example, the bands of deuterated crystalline material in spectra D in *Figures 1*(a) and *1*(b)]. The i.r. spectrum at the change-over from the deuteration of amorphous cellulose to the deuteration of crystalline cellulose can thus be derived.

(2) *Deuteration of the amorphous regions*

It was found that all the amorphous regions of viscose, saponified acetate, and bacterial cellulose would deuterate [i.e. spectra A to B in *Figures 1*(a) and *1*(b)] at all temperatures and at all pressures of deuterium oxide vapour, from 150°C to 25°C and from saturation to $p/p_0 = 0{\cdot}03$ at least (p is the pressure of the vapour and p_0 is the saturation pressure at the same temperature). It may thus be concluded that these regions are completely accessible to deuterium oxide liquid or vapour, and thus presumably to water liquid or vapour, over these vapour pressure and temperature ranges. The time taken for the amorphous regions to exchange at 25°C increased from about 20 min in saturated vapour (the exact time depends upon the particular experimental conditions employed) to about one day at $p/p_0 = 0{\cdot}12$ and to about four days at $p/p_0 = 0{\cdot}03$; these times decreased with increase in temperature but no systematic measurements of this have been made.

(3) *Deuteration of the crystalline regions*

(a) *Effect of pressure of deuterium oxide vapour and temperature*— In the work described below, the fraction of crystalline material deuterated during a particular treatment is calculated as the percentage decrease in the absorbance of the hydroxyl band from the absorbance corresponding to

the start of the deuteration of the crystalline regions, i.e. spectra B in *Figures 1*(a) and *1*(b). The CH band near 2 900 cm^{-1} is used as a standard of reference. With regenerated cellulose the absorbance of the hydroxyl peak 3 [*Figure 1*(a)] is used in the calculation, this peak being close to the previously recommended[2c] value of 3 360 cm^{-1}. The 'baselines' for the hydroxyl and CH bands are drawn from 3 660 cm^{-1} to 3 000 cm^{-1} and from 3 000 cm^{-1} to 2 760 cm^{-1} respectively [lines X and Y in *Figures 1*(a) and *1*(b)].

The rate of deuteration of the crystalline regions of viscose at various pressures of deuterium oxide vapour at 25°C is shown in *Figure 2*. These measurements were made on undried film, that is, film containing deuterium

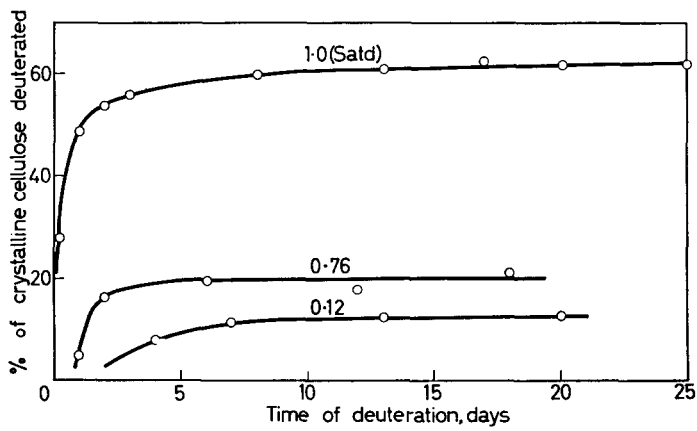

Figure 2—Rate of deuteration of crystalline regions of viscose film in deuterium oxide vapour at 25°C. The values of p/p_0 for the vapour are as marked on the curves [p is the pressure of the vapour and p_0 is the saturation pressure of the vapour at the same temperature]

oxide and with deuterium oxide vapour in the deuteration cell. It is seen that the amount of crystalline material deuterated 'levels off' after a few days at this temperature; these level-off values, though very probably not true 'equilibrium' values, are nevertheless definite enough quantities to be useful in comparing different treatments and materials. *Figure 2* shows that the rate and extent of the deuteration of the crystalline component of viscose falls off rapidly as the pressure of the deuterium oxide vapour is reduced below saturation.

Figure 3 shows that an increase in temperature increases the level-off values in liquid deuterium oxide. The lengths of treatment involved in *Figure 3* varied from 25 days at 25°C to 16 hours at 150°C, i.e. the rate of exchange of the crystalline cellulose is, as expected, dependent on temperature. The level-off value for viscose at 25°C is roughly twice the value given by Mann and Marrinan[2c]; there is good agreement, however, with their result for bacterial cellulose. Spectra E in *Figures 1*(a) and *1*(b) are the spectra of the films after deuteration to the level-off values.

(b) *The effect of deuteration of the crystalline regions of cellulose* II *samples on the shape of the hydroxyl-stretching band of these regions*— It was observed that the four hydroxyl peaks of the crystalline component of cellulose II samples [labelled 1–4 on *Figure 1*(a)] became gradually better

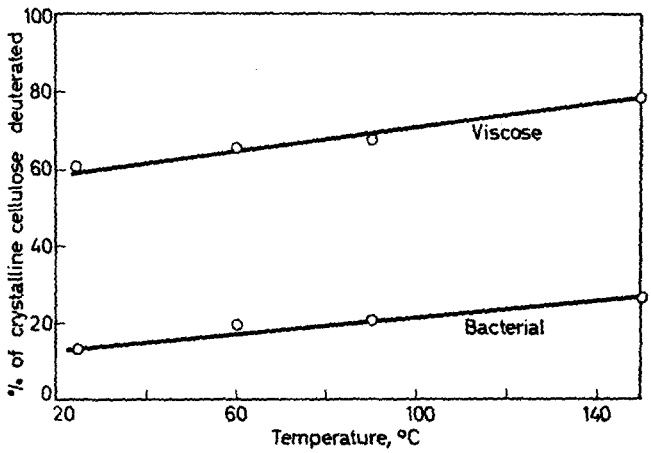

Figure 3—Effect of temperature on deuteration of crystalline regions of cellulose in liquid deuterium oxide [level-off values]

resolved as they decreased in intensity during the deuteration (the intensity of the four peaks decreased proportionally at very similar rates). A similar phenomenon was observed by Rånby *et al.*[9] in the later stages of the deuteration of crystalline cellulose with NaOD in heavy water. The results of the present experiments are illustrated for viscose in *Figure 4*; the sample of viscose is similar to the one used for *Figure 1*(a). In *Figure 4* the absorbance of each of the four hydroxyl peaks measured relative to the absorbance of the saddle point between peaks 2 and 3 is plotted against the fraction of crystalline material deuterated. In the discussion below it is sufficient to characterize the resolution of the hydroxyl band of cellulose II as the ratio of the absorbance of peak 2 to the saddle point between peaks 2 and 3; this ratio is referred to as the 'resolution index'.

As the deuteration of the crystalline regions progressed, the hydroxyl band of the portion of cellulose deuterated during each successive stage was derived by simple subtraction of the hydroxyl band before and after each stage. With the viscose used in *Figures 1*(a) and *4* it was found in this way that the resolution index obtained from these derived hydroxyl bands increased from 1·05–1·1 in the early stages of the 'crystalline' deuteration to about 2·0 in the later stages (as the deuteration of the crystalline regions approached 60 per cent). The resolution index for the crystalline material which was resistant to deuteration was 2·5 or even more.

In arriving at an explanation of the behaviour illustrated in *Figure 4* it is necessary to consider four points. *First*, it should be noted that the quantitative values in *Figure 4* and in the previous paragraph refer only

to the particular sample of viscose film used. Films prepared in different ways all showed the same *type* of behaviour as in *Figure 4*, but varied to some extent in the quantitative values obtained, i.e. in the resolution index of the hydroxyl band of the undeuterated crystalline regions and also in the increase of the index as these regions deuterated. These quantitative differences are probably due mainly to differences in the planar orientation of the films[3a]; it should, however, be emphasized that the general behaviour illustrated in *Figure 4* is not associated with, nor does it depend upon, the presence of planar orientation in the film; for instance, carefully disoriented films of regenerated cellulose showed the effect strongly. *Secondly,* the changes in resolution illustrated in *Figure 4* are independent of the change (decrease) in resolution observed when the

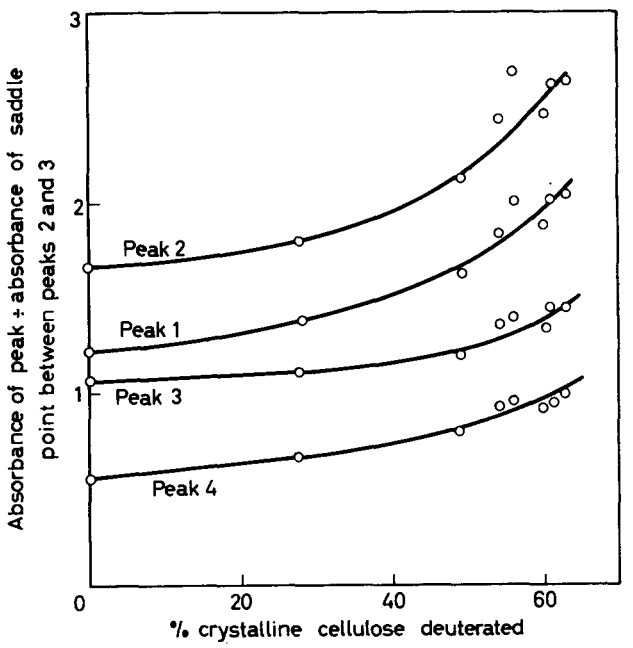

Figure 4—Effect of extent of deuteration of crystalline regions of regenerated cellulose on the resolution of the four peaks on the hydroxyl band. The deuteration was in saturated deuterium oxide vapour at 25°C

deuterium oxide is evaporated from a partially deuterated cellulose. *Thirdly,* one possible explanation of the behaviour illustrated in *Figure 4* is that amorphous regions are still being deuterated throughout the whole of the slow stage of the deuteration, the ratio of crystalline to amorphous gradually increasing as the deuteration progresses. This is thought to be unlikely since it is difficult to think of any satisfactory explanation of the very low rate of deuteration of this part of the amorphous component. *Fourthly,* the perfection of the hydrogen-bonding arrangement in the crystalline regions may gradually increase during the prolonged immersion

of the sample in deuterium oxide; such an increase in perfection would cause an increase in the resolution of the hydroxyl band. This may take place to some extent but is unlikely to be the major cause of the increases in resolution; for instance, prolonged wetting–drying treatments in water at temperatures as high as 90°C produced only comparatively small increases in the sharpness and resolution of the 'crystalline' hydroxyl band.

The most likely explanation of the increasing resolution of the hydroxyl bands as the crystalline deuteration progresses (*Figure 4*) is based on three reasonable assumptions: first, that a range of degrees of perfection of the regular hydrogen-bonding arrangement is present in the crystalline regions (the 'imperfections' may be merely distortions of the cellulose II system or they may involve hydrogen bonds of types not present in the latter system); secondly, that the resolution of the hydroxyl band of a particular part of the crystalline regions depends upon the degree of perfection of that part; thirdly, that the least perfect parts of the crystalline regions are penetrated the most readily by deuterium oxide and thus deuterate first.

(4) *The effects of wetting–drying treatments*

(a) *Crystalline regions*—Resistant OD groups are defined as OD groups which are resistant to rehydrogenation under conditions roughly similar to those of the deuteration; as would be expected, they are situated in the crystalline regions, and their formation can be attributed mainly to increases in the perfection of the crystalline regions during the wetting and drying process involved in the deuteration treatment. It would be expected that a sufficient number of wetting–drying treatments with water would 'stabilize' the cellulose and thus reduce the proportion of resistant OD groups formed in subsequent deuteration treatments. Mann and Marrinan[2a] found this to be so at room temperatures. The present work confirms this stabilization effect and this is illustrated in *Table 1*, which gives some typical values for viscose and bacterial cellulose, both unstabilized (i.e. as first dried after

Table 1. Deuteration and rehydrogenation of the crystalline regions of films of regenerated viscose and bacterial cellulose at 25°C and 90°C

Material	*Type of sample and method of deuteration**	*Temperature of deuteration and rehydrogenation*			
		25°C		90°C	
		% *deuterated*	% *resistant* OD	% *deuterated*	% *resistant* OD
Viscose	A	61	30	68	30
	B	28	7	55	5
Bacterial Cellulose	A	13	6	21	12
	B	6	3	14	5

*A—Unstabilized sample; deuterated in liquid D_2O to 'level-off' value.
B—Sample stabilized by absorption-desorption treatments at 90°C; deuterated as A.

NOTE: The values given are percentages of total crystalline component.

preparation) and stabilized by wetting–drying treatments at 90°C. The samples were first deuterated in liquid deuterium oxide at 25°C and 90°C for times necessary to give the level-off values of the deuteration and were then rehydrogenated in liquid water for two months at 25°C for the 25°C- deuterated samples and for two weeks at 90°C for the 90°C-deuterated samples. The proportion of resistant OD groups was calculated from the absorbance of the resistant OD band, measured relative to the absorbance of the OD band of the fully deuterated crystalline component. In addition *Table 1* illustrates the fact that, as might also be expected, the crystalline regions of the 90°-stabilized samples deuterate to a smaller extent than those of unstabilized samples.

The effect of wetting–drying (stabilization) treatments in increasing the perfection of the hydrogen-bonding arrangement in the crystalline regions, and also slightly increasing the amount of the latter, are revealed as increases in the resolution and intensity of the hydroxyl band of these regions.

It may be noted that the degree of deuteration of the crystalline regions was not increased to any marked extent by deuterating the sample by means of wetting–drying cycles in deuterium oxide, as compared with samples deuterated by continuous immersion in deuterium oxide. This result is in disagreement with a recent conclusion of Mason and his co-workers[5, 6].

(b) *Amorphous regions*—Stabilization (wetting–drying) treatments reduce the amount of water absorbed by celluloses[14] and much of this effect, particularly at high values of humidity, is undoubtedly due to changes in the *character* of the amorphous cellulose, rather than to the slight changes produced in its amount[2a, 14]. These changes in the amorphous structure, however, do not cause any identifiable changes in the shape of the OD band of 'amorphous-deuterated' samples, at least down to 2 300 cm^{-1}, this being the lowest frequency possible with the lithium fluoride prism. However, it is possible that stabilization treatments lead only to small increases in the low frequency tail of the band, i.e. to small increases in the number of very strong hydrogen bonds.

(5) *Mechanism of deuteration of the crystalline regions*

It is considered probable that the deuteration of crystalline cellulose involves penetration of deuterium oxide into the crystalline structure. The two alternative mechanisms, namely (*a*) the relaying of deuterons along chains of hydrogen bonds, and (*b*) the continuous disruption and reformation of the crystalline regions in the deuterium oxide–moist cellulose[5, 6], are considered to be unlikely. The low rate of deuteration of the crystalline regions, and the existence of 'level-off' values, are probably the results of one or more of the following factors: (*1*) the amount of crystalline material penetrated by deuterium oxide may increase only very slowly with time, i.e. the boundary of crystalline material penetrated by deuterium oxide moves deeper into the less accessible, more 'perfect', regions of the crystallites at a very low rate only; (*2*) hydroxyl groups hydrogen-bonded in a regular, crystalline, manner may have a low rate of H $\rightarrow$ D exchange compared with hydroxyl groups in the amorphous regions; (*3*) the concentration of deuterium oxide in the crystalline regions—particularly the more

perfect, more regularly hydrogen-bonded, regions—may be very low. Evidence that (*3*) is the most probable alternative, i.e. that (*1*) and (*2*) are unlikely to be major factors, is summarized in the following two paragraphs.

Figure 5 illustrates the rate of sorption of water vapour at 25°C by films of cellulose similar in thickness to those used in the i.r. measurements (3–5μ); four vapour pressures were studied. On the basis of the results in *Figure 5* it is reasonable to put the time required for the sorption to attain at least 98 per cent of the equilibrium value at not more than about two hours. This rapid attainment of sorption equilibrium indicates clearly that the slow and prolonged deuteration of the crystalline regions is not

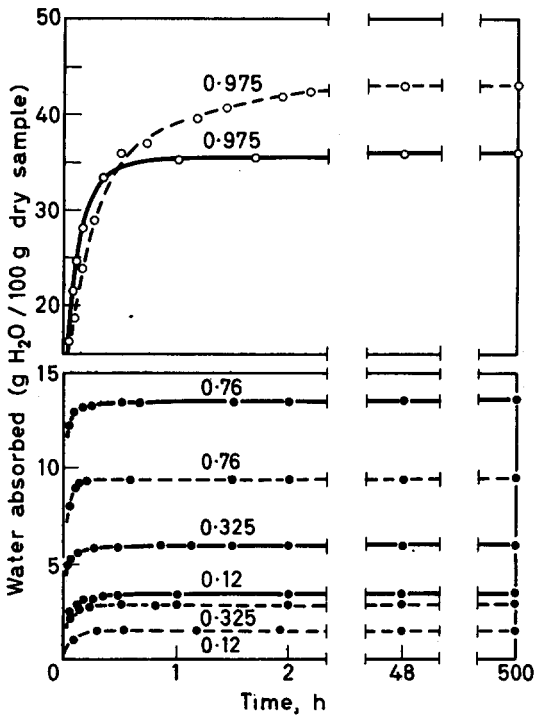

Figure 5—Rate of absorption of water vapour by cellulose films at 25°C. Full line, viscose film; dashed line, bacterial cellulose film. Values of p/p_0 as indicated

associated with any marked increase in the deuterium oxide content of these regions. This tends to eliminate (*1*) in the previous paragraph as a possible reason for the slow deuteration of the crystalline regions.

Evidence that hydroxyl groups hydrogen-bonded in the cellulose II crystalline form *will* deuterate rapidly if sufficient deuterium oxide molecules are present in the structure, i.e. that alternative (*2*) above is not a major factor, has been obtained from studying the series cellotetraose to cellopentaose. These materials can be obtained in a highly crystalline form, the X-ray diagram being of the cellulose II type[15a]; i.r. study shows[1] that the hydrogen-bonding arrangement in the crystalline regions is largely similar in character to that present in cellulose II, and that these sugars are

in fact highly 'infra-red' crystalline[16]. It has been shown[15b,16] that, despite their very high crystallinity, these sugars absorb surprisingly large amounts of water or deuterium oxide and will also deuterate rapidly and to a large extent. It seems reasonable to associate these facts, and to conclude that hydroxyl groups hydrogen-bonded in a cellulose II arrangement deuterate rapidly in the presence of adequate deuterium oxide.

(B) CELLULOSE DERIVATIVES

(1) *Acetates. The structure of the 3 500 cm^{-1} band of dry films*

Spectra H on *Figures 6*(a–c) are spectra of dry films of two of the triacetates and one of the secondary acetates. Each spectrum consists of the 3 500 cm^{-1} 'hydroxyl' band, the CH band near 2 900 cm^{-1}, and several weaker bands (probably overtone and combination bands). The 3 500 cm^{-1} band can be shown to be composed of two components and variations in the intensity and shape of the band can easily be explained in terms of these two components. The first component has a peak frequency of 3 490–3 495 cm^{-1} and is the OH-stretching vibration; this component is removed by treatment of the sample in saturated deuterium oxide vapour for several hours, with the simultaneous appearance of an OD-stretching band near 2 585 cm^{-1} superimposed on the weak bands already present in this region. Spectra D on *Figures 6*(a–c) are the spectra of deuterated

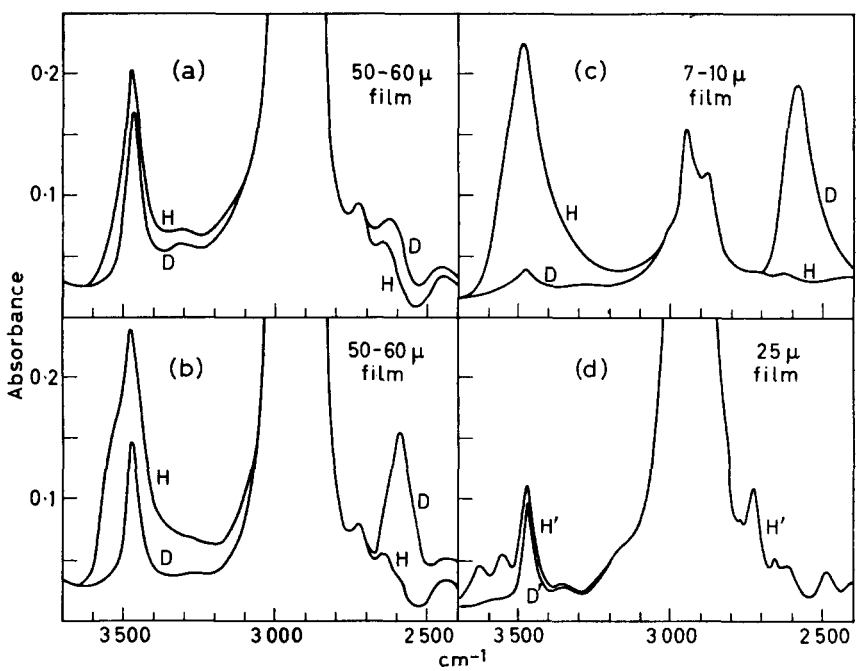

Figure 6—Infra-red spectra of films of various acetates: (*a*) Cellulose triacetate (d.s. 2·98); (*b*) cellulose triacetate (d.s. 2·95); (*c*) secondary cellulose acetate (d.s. 2·31); (*d*) iso-amyl acetate. (*a*)–(*c*): H denotes undeuterated ('hydrogen') form, dry; D is the deuterated form, dry. (*d*) H′ indicates dried with drying agents (from 'H_2O-wet'), and D′ is saturated with deuterium oxide

samples after drying. The second component of the 3 500 cm^{-1} band is not affected by any deuteration treatment, however prolonged or severe (up to 150°C, and including deuteration with the acetate in solution). This component, which is seen isolated as the sharp 3 478 cm^{-1} band in spectra D, is roughly similar in intensity for all the acetates studied and is considered to be the overtone of the carbonyl-stretching band near 1 750 cm^{-1}. This assignment of the deuteration-resistant component is supported by the close similarity of spectra D in *Figures 6*(a–c) to the spectra of simple alkyl acetates such as iso-amyl acetate [*Figure 6*(d)]; the sharp 3 468 cm^{-1} band in the spectrum of the latter is certainly the carbonyl overtone[17].

It should be pointed out here that it is difficult to be certain that the hydroxyl component of the 3 500 cm^{-1} band is *completely* removed by deuteration; a very weak deuteration-resistant hydroxyl component could well be masked by the carbonyl overtone. However, it is certain that at least 98 per cent of the hydroxyl groups in secondary acetate and 90 per cent of the hydroxyl groups in triacetate of d.s. 2·98 are readily exchanged, and there is no reason to doubt that in fact 100 per cent exchange always takes place.

The hydroxyl-stretching component of the 3 500 cm^{-1} band (obtained by subtracting the carbonyl overtone from the total band) is similar in peak frequency and shape for all the acetates studied, and also for partially deuterated samples; *Figure 7* shows that it is narrower and of a higher peak frequency than the hydroxyl band of the amorphous component of cellulose—a not unexpected result. The inset in *Figure 7* contains the hydroxyl component of the 3 500 cm^{-1} band of the three triacetates and a secondary acetate plotted as actual absorbances for equal thicknesses of film; the peak absorbance is directly proportional to the number of unesterfied hydroxyl groups in the sample.

Brown *et al.*[11] studied the absorbance of the 3 500 cm^{-1} band of cellulose acetate as a function of the hydroxyl content; a straight-line plot passing through the origin was obtained, and it was concluded that there was no appreciable contribution to the 3 500 cm^{-1} band from the overtone of the carbonyl-stretching vibration. The present work, however, shows that the intensity of the 3 500 cm^{-1} band at zero hydroxyl content (i.e. d.s. 3) will clearly have the value of the intensity of the overtone, not zero intensity. Brown *et al.*[11] suggested that the shoulder on the high frequency side of the band at about 3 550 cm^{-1} [see *Figures 6*(a) and *6*(b)] is due to some structural feature of the cellulose acetate molecule, possibly associated with free hydroxyl groups; the present work shows that the 'shoulder' is, in fact, merely the result of the superposition of a narrow overtone at 3 478 cm^{-1} on a broader hydroxyl band of peak frequency 3 490–3 495 cm^{-1}.

Gerbaux[12] measured the symmetry of the 3 500 cm^{-1} band of cellulose acetates as a function of degree of substitution; the marked changes in symmetry which he observed can readily be explained in terms of the two-component structure of the band. The small 3 472 cm^{-1} band which Gerbaux observed with fully acetylated triacetates was probably the carbonyl overtone and not the result of small amounts of water in the acetate as suggested by Gerbaux.

(2) *Acetates. Effect of crystallization and orientation on the deuteration of the cellulose acetates*

Crystallization of films of cellulose triacetate and secondary cellulose acetate, and changes in the orientation of the latter, have no effect on the subsequent deuteration of the materials, i.e. all the hydroxyl groups are readily deuterated and the spectra of the films before and after deuteration were very similar to those given for uncrystalline, unoriented, films in *Figures 6*(a–c).

(3) *Ethyl cellulose*

Since the ethyl cellulose is incompletely etherified, the dry films have a large hydroxyl absorption with a peak near 3 470 cm^{-1} (spectrum H in *Figure 8*). Deuteration of the ethyl cellulose film in saturated deuterium oxide vapour for several hours, followed by drying, removes practically all of this 3 470 cm^{-1} band and replaces it with an OD band of peak frequency near 2 570 cm^{-1} (spectrum D, *Figure 8*). After prolonged deuteration only a very weak band remains in the 3 470 cm^{-1} region, less than 20 per cent of the intensity of the carbonyl overtone observed in this

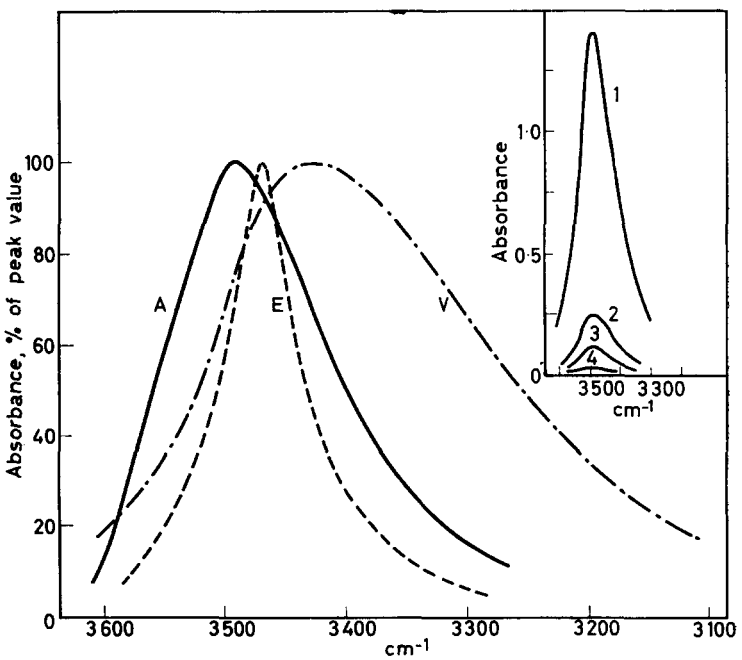

Figure 7—The hydroxyl-stretching component of the 3 500 cm^{-1} band of cellulose derivatives. A denotes cellulose acetates (d.s. 2·3 to 2·98); E, ethyl cellulose (d.s. 2·5), and V, amorphous regions of regenerated viscose film. Inset: The hydroxyl-stretching component of cellulose acetates of various degrees of substitution [equal thicknesses of film]. Curves 1, 2, 3 and 4 refer to samples of d.s. 2·31, 2·89, 2·95, and 2·98 respectively

region with the acetates. This weak band is thought to be an overtone or combination band; dibutyl ether which had been dried with sodium or washed with deuterium oxide gave a similar very weak band near 3 500 cm^{-1}. Thus it is concluded that all the hydroxyl groups in the ethyl cellulose are readily deuterated by the treatment with deuterium oxide vapour. The hydroxyl component of the 3 470 cm^{-1} band (i.e. practically all of the band) is shown in *Figure 7*; the band is seen to be considerably narrower than the hydroxyl component of the 3 500 cm^{-1} band of the cellulose acetates.

The weak bands observed near 3 200 cm^{-1} and in the region 2 650–2 350 cm^{-1} are very probably overtone and combination bands, like the similar weak bands observed with the acetates.

(4) *Accessibility of the cellulose derivatives*

It is difficult to interpret with certainty the deuteration behaviour of the cellulose derivatives, namely the complete exchangeability of the hydroxyl groups even in the 'crystalline' samples. Both X-ray and water-sorption studies[18] indicate that the 'crystallizing' treatments do in fact increase the degree of lateral order in the acetates, and so the complete OH $\longrightarrow$ OD exchange must be accounted for in one of the following ways: either the more ordered (crystalline) regions are readily accessible to deuterium oxide, so that any hydroxyl groups present in these regions will exchange rapidly,

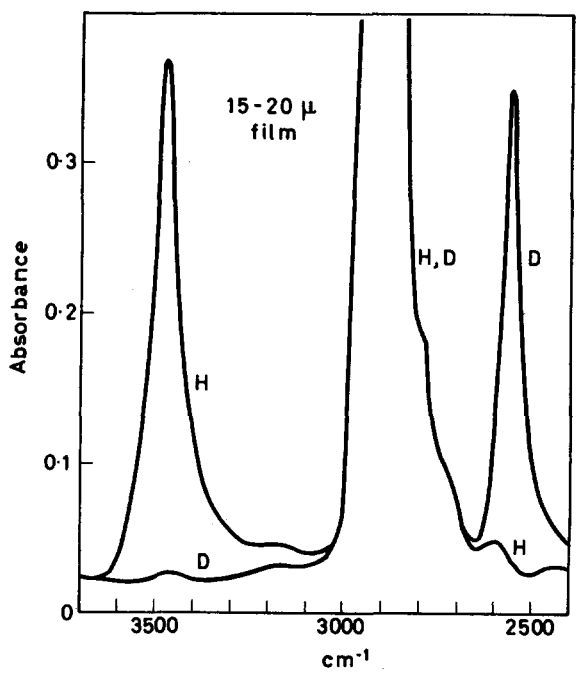

Figure 8—Infra-red spectrum of film of ethyl cellulose. H indicates undeuterated ('hydrogen') form, dry; D is the deuterated form, dry

or the more ordered regions do not include hydroxyl groups, i.e. the higher degrees of order form in hydroxyl-free regions (the deuteration technique would of course provide no information on the accessibility of such ordered regions). The latter alternative seems the more likely, since the occasional hydroxyl group must have a disorganizing effect on the chain packing and thus tend to surround itself with an 'amorphous' region. It is clear, however, that whatever the explanation of the complete OH $\longrightarrow$ OD exchange with crystallized samples, the i.r. deuteration technique is of limited value in the study of the crystalline–amorphous structure and accessibility of these cellulose derivatives.

The author is grateful to Drs S. G. Smith, H. Spedding and J. Mann for helpful discussions during the preparation of this paper.

This work was carried out partly at the British Rayon Research Association, Heald Green Laboratories, Wythenshawe, Manchester 22, and partly at the Cotton, Silk and Man-Made Fibres Research Association, Shirley Institute, Didsbury, Manchester 20.

(*Received October 1962*)

REFERENCES

[1] MARRINAN, H. J. and MANN, J. *J. appl. Chem.* 1954, **4,** 204
[2a] MANN, J. and MARRINAN, H. J. *Trans. Faraday Soc.* 1956, **52,** 481
[b] MANN, J. and MARRINAN, H. J. *Trans. Faraday Soc.* 1956, **52,** 487
[c] MANN, J. and MARRINAN, H. J. *Trans. Faraday Soc.* 1956, **52,** 492
[3a] MANN, J. and MARRINAN, H. J. *J. Polym. Sci.* 1956, **21,** 301
[b] MANN, J. and MARRINAN, H. J. *J. Polym. Sci.* 1958, **32,** 357
[4] SOBUE, H. and FUKUHARA, S. *Kogyô Kagaku Zasshi,* 1957, **60,** 320; 1960, **63,** 520
[5] LANG, A. R. G. and MASON, S. G. *Canad. J. Chem.* 1960, **38,** 373
[6] SEPALL, O. and MASON, S. G. *Canad. J. Chem.* 1961, **39,** 1934, 1944
[7] MORRISON, J. L. *Nature, Lond.* 1960, **185,** 160
[8] HIGGINS, H. G., STEWART, C. M. and HARRINGTON, K. J. *J. Polym. Sci.* 1961, **51,** 59
[9] JENNINGS, A. J., PRINS, W., HALE, R. D. and RANBY, B. G. *J. appl. Polym. Sci.* 1961, **5,** 676
[10] ROWEN, J. W., HUNT, C. M. and PLYLER, E. K. *J. Res. nat. Bur. Stand.* 1947, **39,** 133
[11] BROWN, L., HOLLIDAY, P. and TROTTER, I. F. *J. chem. Soc.* **1951,** 1532
[12] GERBAUX, R. *Bull. Soc. chim. Belg.* 1957, **66,** 382
[13] BOURIOT, P. *Bull. Inst. text. Fr.* 1961, **15,** 7
[14] JEFFRIES, R. *J. Text. Inst.* 1960, **51,** T339
[15a] MANN, J. and HERITAGE, K. J. Private communication
[b] HERITAGE, K. J. Private communication
[16] JEFFRIES, R. Unpublished results
[17] THOMPSON, H. W. and JAMESON, D. A. *Spectrochim. Acta,* 1958, **13,** 236
[18] JEFFRIES, R. *J. Text. Inst.* 1960, **51,** T441

Gamma Irradiation Polymerization of Isobutene and β-Propiolactone at Low Temperature

C. DAVID,* F. PROVOOST and G. VERDUYN

It has been shown that ionic oxides only slightly modify the rate and molecular weight for the solid state polymerization of β-propiolactone and isobutene whereas the effect is much larger in the liquid phase. Resistance measurements of the pure monomers during solid state polymerization have been made. The possibility of an ionic mechanism of polymerization according to the model proposed by Fowler is discussed to explain conductivity induced in polymers by ionizing radiation.

THE work related in this paper is part of a general fundamental study of the influence of solid additives on polymerization reactions initiated by γ-rays. The influence of ionic oxides and microporous carriers on the polymerization of ethylene and the telomerization of ethylene with carbon tetrachloride has been studied[1] at C.E.N., Mol. The cationic polymerization of isobutene in the liquid phase in the presence of ionic crystals has been investigated by Worrall and Charlesby[2] and is now being studied by us. This work showed that the presence of solid additives considerably modifies the reaction in several cases, by changing the mechanism[1] or by increasing the rate of initiation[2].

In this paper we propose to discuss the influence of various ionic oxides on polymerization in the solid phase of β-propiolactone and isobutene. The results will be compared with those obtained for the same monomers polymerized in the liquid phase. The theory of chain propagation by positive holes and electrons in the monomer and solid additive will be used to explain the mechanism. This model is identical to the one proposed by Fowler[3] to explain the conductivity obtained with ionizing radiation in insulators.

Some resistance measurements were performed on solid β-propiolactone and isobutene during irradiation; these results are compared with those obtained by us for solid water and non-polymerizable ketones and by Fowler for polymers.

Different examples of polymerization in a homogeneous solid phase have been described in the literature. These reactions are extremely intricate; no kinetic scheme given so far accounts for the reaction rate and the molecular weight of the products up to high conversion. Furthermore, the exact nature of the chain of propagation (anionic, cationic, or by radicals) has not always been established. A detailed study[4] of the solid state polymerization of β-propiolactone was made in the laboratories of C.E.N. The nature of the chain propagation is probably anionic since it was shown by Bartlett[5] that this monomer polymerizes in solution in the presence of various nucleophilic ions such as OH^-, Cl^-, CH_3^-, COO^-.

*Present address: Université Libre de Bruxelles, Service de Chimie Générale II.

POLYMERIZATION EXPERIMENTS

Experimental

The monomers were repeatedly vacuum distilled (10^{-5} mm of mercury). The oxygen content was controlled by mass spectrometry and shown to be less than 30 p.p.m. The solids were degassed at 200°C until a static vacuum of 10^{-5} mm of mercury was obtained; the methods of preparation for the different additives are given in *Table 1*. The bulbs were filled and emptied

Table 1. Preparation and characteristics of the additives

Solid	*Starting material*	*Method (ref.)*	*Additive*	*Surface, m^2g^{-1}*
NiO Ia	$NiCO_3$	Calcined at 1 000°C for 3 h	—	—
NiO Ib	$NiCO_3$	Calcined at 600°C for 6 h	—	4·78
NiO II	$Ni(NO_3)_2 . 6H_2O$	[11]	—	2·91
NiO III	$Ni(NO_3)_2 . 6H_2O + Li_2CO_3$	[11]	5% Li	1·28
NiO IV	$Ni(NO_3)_2 . 6H_2O + CrO_4(NH_4)_2$	[11]	5% Cr	1·04
ZnO I	ZnO U.C.B.	Heated at 800°C for 12 h	—	—
ZnO II	Zn	[12]	—	1·53
ZnO III	Zn	[12]	5% Li	—
ZnO IV	Zn	[12]	2·1% Cr	—
ZnO U.C.B.	ZnO	—	—	5·03

under vacuum. The quantities introduced were determined by weight for β-propiolactone and solid additives and volumetrically in the gaseous phase for isobutene. The last method was also used after irradiation, to determine the unreacted isobutene. The amount of poly-β-propiolactone formed was obtained by weighing. Irradiations were performed at liquid nitrogen temperature (−192°C) and at −78°C in an acetone–dry ice bath. The irradiation dose was determined by the ferrous sulphate method, taking a value of 15·5 for the radiochemical yield per 100 eV. Molecular weights were established by viscosity measurements at 30°C in carbon tetrachloride for polyisobutene, using the equation[2]

$$[\eta] = 2{\cdot}9 \times 10^{-4} \times M_v 0{\cdot}68$$

The viscosity of poly-β-propiolactone was measured in chloroform and in dimethylformamide. As no calibration for this polymer is available only relative values were obtained.

Results

The experimental results for the polymerization are given in *Table 2*. In calculating G_{total} (number of molecules reacted per 100 eV) only energy dissipated in the monomer was taken into account. Dividing G_{total} by the mean degree of polymerization $\overline{DP}$ gives $G_{initiation}$. $\overline{DP}$ is related to the viscosity molecular weight by the equation[2]

$$M_v = 1{\cdot}85 \times 56{\cdot}1\ \overline{DP}$$

From *Table 2* it appears that:

Table 2. Polymerization of isobutene and β-propiolactone

No.	*Dose Mrad*	*Dose rate Mrad h⁻¹*	*T°C*	*Phase*	*Additive‡ 1 g*	*Conversion percentage*	G_{total}	$G_{initial}$	[η]¶	$M \times 10^{-4}$
Polymerization of isobutene										
1 2	1	0·250	−80	Liquid	—	3·6	619	0·2	1·63	32·69
1 5	1	0·250	−80	Liquid	ZnO	87	14·961	5·8	1·50	28·93
1 x*	13·8	0·250	−192	Solid	—	1·23	15·3	0·0075	0·267	2·292
1 y†	13·8	0·250	−192	Solid	ZnO	1·62	20·2	0·017	0·185	1·322
—	—	—	−192	Solid	ZnO	0·01	—	—	—	—
Polymerization of β-propiolactone										
X 210	2	0·250	−17	Liquid	—	0·3§	20	—	—	—
X 222	2	0·250	−17	Liquid	ZnO	3·3	221	—	—	—
X 31	1	0·260	−80	Solid	—	17·6	2 358	(50‖)	0·480D 0·90 C	—
X 88	1	0·250	−80	Solid	NiO Ia	13·9	1 869	—	0·93 C	—
X 92	1	0·250	−80	Solid	NiO Ib	16·8	2 258	—	0·315D	—
X 90	1	0·250	−80	Solid	NiO II	12·2	1 637	—	0·325D	—
X 91	1	0·250	−80	Solid	NiO III	12·9	1 734	—	—	—
X 99	1	0·250	−80	Solid	NiO IV	15·5	2 075	—	—	—
X 79	0·92	0·253	−80	Solid	ZnO U.C.B.	10·7	1 567	—	0·66 C	—
X 100	1	0·248	−80	Solid	ZnO I	14·2	1 903	—	0·200D	—
X 102	1	0·248	−80	Solid	ZnO II	15·0	2 015	—	—	—
X 101	1	0·248	−80	Solid	ZnO III	14·1	1 885	—	0·140D	—
X 99	1	0·248	−80	Solid	ZnO IV	14·5	1 958	—	0·378D	—
X 66	0·72	0·255	−80	Solid	Quartz wool	14·4	2 680	—	0·100D	—

*Average of 5 measurements.
†Average of 6 measurements.
‡All ampoules contained 1 g of additive, except 1 5 which contained 0·8 g.
§Limit of precision in the experimental set-up.
‖ This abnormally high value probably indicates a very high chain transfer.
¶D denotes dimethylformamide, and C, chloroform.

(*1*) The polymerization rate of isobutene in the absence of additives is at least 20 times higher in liquid phase than in the solid phase.

(*2*) For β-propiolactone, in the absence of additive, the polymerization rate in the solid phase at −80°C is higher by a factor of 60 than in the liquid phase at −17°C.

(*3*) Zinc oxide enhances the polymerization rate of isobutene and β-propiolactone in the liquid phase by a factor of 24 for the former and of 10 for the latter.

(*4*) The presence of solid additive modifies the rate of both polymerizations in the solid phase. However, the influence is much smaller than that in the liquid phase (< 50 per cent).

Discussion

Possibility of ionic polymerization in the solid state.—It is easy to calculate that the rate of recombination of electrons and holes formed during irradiation of solid monomer is sufficiently low to give rise to an ionic polymerization. We made this calculation for monomer undergoing polymerization with help of the theory developed by Fowler to explain induced conductivity in insulators and of the experimental results obtained by the same author for polyethylene.

We briefly summarize Fowler's theory below. It is well known that ionizing radiations give rise to free electrons and an equal number of positive holes. Less than 0·1 per cent of the electrons thus ejected are fast electrons. The electrons and holes can move in an electric field giving an induced current. They can be trapped in electron or hole traps and afterwards re-excited thermally in the conduction band. The existence of a band structure in organic compounds is not obvious. However, if an electron has acquired a sufficient amount of energy by ionizing radiation to be able to move in the substance, a conduction level is said to exist. One considers the substance to be formed by atomic groups having conduction levels corresponding to different energies. The conduction levels of one atomic group can form a trap for a neighbouring atomic group. In an electric field, the electronic conductivity of insulators is taken as negligible. The study of induced conductivity and of its relaxation allowed Fowler to calculate the number of traps, holes and conduction electrons and their lifetime. This theory provides a working hypothesis for polymerization initiated by γ-radiation in the solid phase. In fact, a cationic polymerization could be initiated by a hole and an anionic polymerization could arise from an electron trapped in a monomer molecule. The chain length of the polymer in both cases has to be related to the lifetime of these electrons and holes.

We have calculated for isobutene and β-propiolactone under our experimental conditions of flux and temperature, probable values of τ_t, $\tau_{e,l}$ and $\tau_{e,p}$ which are respectively the lifetimes of holes, and of free and trapped electrons (*Table 3*). These calculations provide only an indication of the order of magnitude since the lifetimes were calculated assuming that the conductivity induced in the monomers at 20°C by a flux of 480 rad.h^{-1} is similar to that measured by Fowler in the same conditions for polyethylene.

This assumption is, however, justified by Fowler's experimental results which show that the induced conductivity for insulators depends only slightly on the chemical structure of the solid and on its crystallinity. We considered the electron mobility and the recombination rate of electrons and holes to be independent of the temperature. The values given in *Table 3* are therefore upper limits since both parameters decrease with

Table 3. Number of holes and electrons and their lifetime‡

No.	I rad h^{-1}	$T°K$	Δ	E_x eV molecule^{-1}	n cm^{-3}	$m+n$ cm^{-3}	τ_t sec	$\tau_{e,l}$ sec
1*	480	298·1	—	—	$6·0\times10^{5}$	10^{15}	$2·4\times10^{3}$	$1·4\times10^{-6}$
2	$2·5\times10^{5}$	298·1	1	—	$3·2\times10^{8}$	10^{15}	4·5	$1·4\times10^{-6}$
3		298·1	0·5	—	$1·4\times10^{7}$	$2·3\times10^{16}$	1×10^{2}	$6·2\times10^{-8}$
4		100	1	—	$3·2\times10^{8}$	10^{15}	4·5	$1·4\times10^{-6}$
5		200	1	—	$3·2\times10^{8}$	10^{15}	4·5	$1·4\times10^{-6}$
6		100	<1	0·3	$1·4\times10^{3}$	$2·3\times10^{6}$†	∞	$6·2\times10^{3}$
7		200	<1	0·3	$4·4\times10^{4}$	$7·2\times10^{13}$	$3·2\times10^{4}$	2×10^{-5}
8		100	<1	0·03	$1·4\times10^{6}$	—	1×10^{3}	—
9		200	<1	0·03	$7·9\times10^{6}$	—	$1·8\times10^{2}$	—

*Polyethylene values.
†Calculated with $\Delta=0·5$.
‡Calculated with $b=7\times10^{-10}$ cm^3 sec^{-1}.

Where I is the intensity of radiation,
T the temperature,
Δ a constant defined by $i_x \propto I^{\Delta}$ where i_x is the induced current,
E the activation energy of the conductivity process,
b the recombination coefficient of electrons and holes,
n the number of free electrons,
$n+m$ the number of holes,
τ_t the lifetime of holes and trapped electrons, and
$\tau_{e,l}$ the lifetime of free electrons.

temperature. *Table 3* shows clearly that the lifetimes of the holes and electron traps range from seconds to infinity according to flux, temperature and type of electron trap distribution. In some cases, a chain propagation induced by holes or a trapped electron must be possible. Since there is no information about the magnitude of the propagation rate constant in the solid phase, it was not possible to give quantitative values to support this hypothesis. However, it appears that the lifetime of a hole is higher by different powers of ten as compared with that of a radical or an ion in the liquid phase, 1·65 and 0·01 sec being respectively typical values in these cases[6,7]. The lifetime of a free electron, however, seems to be too short except in one case (ex ref. 6) to give rise to chain growth.

Comparison between the rates of polymerization in liquid and solid phases.—The difference in rate observed between the liquid- and solid-state reactions of β-propiolactone may arise from several factors. Thus the lifetime of a reactive species in the solid state is greater than that in the liquid state as shown in the preceding section and the activation energy of the propagation steps may be lowered by polarizing effects on the crystalline network. Further the frequency factor may be larger in the solid phase because the monomer is conveniently oriented for polymerization in the crystal. In fact, from the construction of a three-dimensional model of a diketene crystal (which shows the same polymerization behaviour as

β-propiolactone) it can be demonstrated that the propagation step along the *a* axes requires little, if any, displacement of the monomer molecules.

For isobutene and other ethylenic monomers, on the other hand, the propagation step seems to be impossible without displacement of the monomer molecules, the distance between monomer molecules in the crystal being too large. The crystallographic structure of solid isobutene is not known so that no quantitative arguments can be given in this case. For ethylene, it has been shown[8] that the nearest distance between carbon atoms in neighbouring molecules in the monomer crystal is 3·8 Å whereas it is only 1·54 Å in the polymer chain. Solid state polymerization of carbon–carbon double bonds could thus be diffusion-limited reactions and have a lower rate than in liquid phase.

Polymerization of isobutene and β-propiolactone in the liquid phase in the presence of solid additives.—The effect of zinc oxide in increasing the rate of the cationic polymerization of isobutene in the liquid phase has been discussed by Worrall and Pinner[9]. They suggested that solid additives greatly increase the rate of chain initiation because they have sites suitable for retaining electrons. Barry and Kliers[10] have recently reported an increase in the conductivity of zinc oxide after absorption of isobutene which strongly suggests the formation of positive ions at the surface. According to these authors adsorbed ions could be the initial step in the polymerization. The increase in rate, however, seems more complicated. This is now the subject of a detailed study. It is important to note that the presence of zinc oxide increases the rate of polymerization of β-propiolactone although this reaction probably proceeds by an anionic mechanism.

Polymerization in the solid phase in the presence of solid additives.—In a polymerization in the solid phase in the presence of solid additives, the band diagram of the heterogeneous solid phase corresponds to that of the monomers interrupted at many points by the diagram of the additive. The interaction between additive and monomer thus depends on the relative positions of the valence and conduction levels, and the electron traps. This depends on the nature of the solids and the temperature and cannot be established *a priori*. The increased rate during the cationic polymerization of isobutene in the presence of zinc oxide can be attributed to an increase in the initiation rate. Initiation may occur at the surface of the additive through holes created in the solid by γ-radiation. If the additive can also donate electrons, the molecular weight should decrease, and this we have actually observed.

In the polymerization of β-propiolactone, having an anionic mechanism, the decrease of rate and molecular weight can be explained by collection of electrons by the solid. In this case, the number of growing chains diminishes as does the lifetime of these chains, since the number of positive holes in the monomer does not depend on the additive.

RESISTANCE MEASUREMENTS

Experimental

The conductivity measurements were made with a V.H.R. megohmmeter

Model 31A (Electronic Instruments Ltd.) equipped with an A31A resistor unit, allowing resistance measurements from 10^7 to 10^{14} ohm cm. The samples were crystallized under high vacuum between two electrodes of 45 mm² surface area and 2 mm distant from each other. The cooling baths used were ice plus sodium chloride at −20°C, chlorobenzene at its melting point (−45°C), trichlorethylene plus carbon dioxide at −78°C and diethyl ether at −110°C. None of these cooling mixtures has a sufficiently high temperature-stability to permit high precision measurements on account of the large temperature coefficient of the dark conductivities. The results thus obtained are nevertheless correct semi-quantitatively.

Results

Figure 1 gives values of the experimental resistance obtained for β-propiolactone without additive and shows that (*i*) no important change in resistance was observed under irradiation, and (*ii*) the resistance increases during and after a 40-minute irradiation at −78°C [*Figure 1, b*] and after

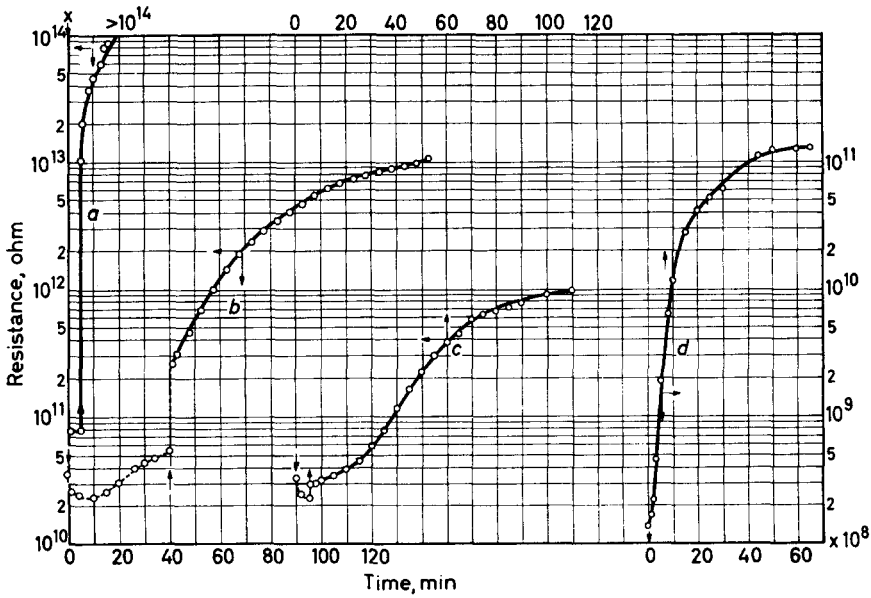

Figure 1—Electrical resistance of β-propiolactone during irradiation: *a* empty cell, *b* polymerization of β-propiolactone at *b* −78°C (40 min irradiation), *c* at −78°C (5 min irradiation), and *d* at −45°C (5 min irradiation). ↓ denotes start of irradiation, and ↑, end of irradiation

only a 5-minute irradiation at −78°C [*Figure 1, c*] or at −45°C [*Figure 1, d*]. The limiting value obtained depends on the experimental conditions.

Since the dark resistance of the isobutene sample was larger than 10^{14} ohm this monomer could not be studied. No significant change in resistance during irradiation could be observed in two non-polymerizable esters:

crystalline methyl acetate at −110°C and glassy isoamyl formate at −78°C. Solid water on the other hand shows the same type of conductivity relaxation after irradiation as the polymers studied by Fowler (*Figure 2*).

The response of the empty cell [*Figure 1, a*] is temperature independent. Caution must be applied to the interpretation of resistance measurements under irradiation when the initial resistance is not much lower than that of the irradiated empty cell. Such measurements are shown dotted on the curves.

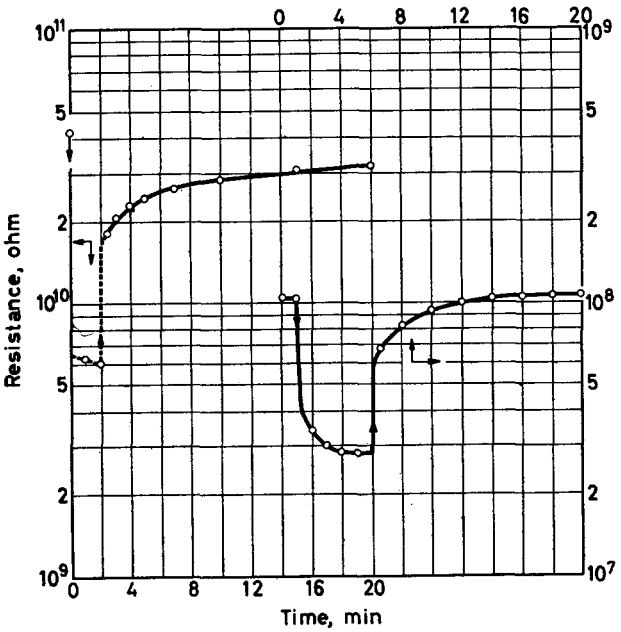

Figure 2—Electrical resistance of ice during irradiation: *a* at −80°C, *b* at −20°C. ↓ denotes start of irradiation, and ↑, end of irradiation

Discussion

Two main observations have to be discussed. First, irradiation causes no appreciable decrease in the resistance of β-propiolactone whereas in polymers[3] irradiation reduces the resistance by a factor of 10^3 to 10^4. Secondly, resistance in the polymerizing system increases during and after irradiation.

The first effect is due to the much lower dark resistance of β-propiolactone and other esters ($\simeq 10^{10}$ ohm cm at −80°C) than that of polymers ($\simeq 10^{19}$ at 20°C). If a certain number of current carriers of the same magnitude is induced in the monomer as in the polymers studied by Fowler (as must be so), no appreciable change in the resistance can be observed in the irradiated monomer.

The results obtained for ice, on the contrary, show that in this case a much larger number of current carriers ($> 10^9$ times larger than in polymer) is created, assuming equal mobilities in the two systems.

An increase in resistance during irradiation is due to the formation of polymer. After irradiation, the increase may be attributed principally to post-irradiation polymerization and perhaps in part to recombination of induced charge carriers in the partly polymerized crystal.

We are very grateful to Dr M. D'Hont, Dr V. Mathot and Dr P. Gosselain for their interest in this work.

We also wish to thank Professor S. Amelinckx, Professor Charlesby and Dr Fowler for valuable discussions.

Finally, we are very much indebted to Ir M. de Proost for access to the irradiation facilities and to Ir Ch. Jonkheere for his aid with the resistance measurements.

Centre d'Etude de l'Energie Nucléaire,
Mol, Belgium

(*Received October 1962*)

REFERENCES

[1] MECHELYNCK-DAVID, C. and PROVOOST, F. *Internat. J. appl. Radiation and Isotopes*, 1961, **10**, 191–97
[2] WORRALL, R. and CHARLESBY, A. *Internat. J. appl. Radiation and Isotopes*, 1958, **4**, 84–88
[3] FOWLER, J. F. *Proc. Roy. Soc.* 1956, **236**, 464–80
[4] MECHELYNCK-DAVID, C. *et al.*
[5] GRESHAM, T. L., JANSEN, J. E. and SHAVER, W. F. *J. Amer. chem. Soc.* 1948, **70**, 998–1004
[6] WALLING, CHEVES. *Free Radicals in Solution*, p 37. Wiley: New York, 1957
[7] COLLINSON, E., DAINTON, F. S. and GILLIS, H. A. *J. phys. Chem.* 1958, **63**, 909–16
[8] BRUNN, C. W. *Trans. Faraday Soc.* 1944, **40**, 23
[9] WORRALL, R. and PINNER, S. H. *J. Polym. Sci.* 1959, **34**, 229–40
[10] BARRY, T. I. and KLIERS, K. *Disc. Faraday Soc.* 1961, 219–29
[11] DRY, M. E. and STONE, F. S. *Disc. Faraday Soc.* 1959, **28**, 193
[12] ROMERO-ROSSI, R. and STONE, F. S. *Deuxième Congrès International de Catalyse, Paris, 1960.* Paper 72

Book Review

Sulfur Bonding

C. C. PRICE and SHIGERU OAE

Ronald Press: New York; 1962 (v+208 pp.; 6 in. by 9¼ in.), $8.00

THIS attractively written monograph, with its copious diagrams, schemes, equations and tables should not be ignored by serious students of sulphur chemistry. Its authors have attempted, with considerable success, to organize a wide variety of physical and chemical facts into a convincing account of the salient characteristics of bonds between sulphur and oxygen, carbon and other neighbouring elements. Reciprocally, it is also clear how various sulphur groupings influence chemical reactivity.

The authors have an appealing manner of taking a given concept, showing to what extent this is consistent with experimental findings, and then presenting a brief summary that the critical reader may either accept or use as a basis for further argument.

From the authors' analysis the following main points emerge. The sulphur–oxygen bonds in sulphoxides and sulphones are best represented as predominantly semi-polar bonds with rather low π-contributions; the oxygen atoms in sulphoxides seem rather more basic than those in sulphones. With reference to conjugation with electron-deficient carbon centres RS is seen to be a mild electron-releasing group though not as efficient as R_2N or RO groups. In this kind of electron-release a $3p$–$2p$ π-bond with carbon is involved. The reviewer does not agree with the authors that Me $>$ RS in conjugative electron-releasing effects. The RS group is also able conjugatively to accept electrons by making use of $3d$ orbitals to give $2p$–$3d$ π-bonds with carbon illustrated, for example, by the acidity of methylene groups joined to an alkylthio group. This electron-attracting effect is further enhanced in sulphoxides in which one also notices the unshared $3s$ electron pair being used for conjugative electron-release as in directing o–p electrophilic substitution in aromatic systems.

The electron-attracting influence is still further increased in sulphones, where the RSO_2 group is comparable to CN in many reactions. When α-carbanions are stabilized by sulphone groups it appears that the intense positive charge adjacent to C^- provides the bulk of the stabilization energy electrostatically. This is a departure from a commonly held belief that the stabilization involves rather important $2p$–$3d$ π-contributions.

The book also contains a chapter on sulphonium salts from which it is seen that R_2S— is rather similar, electrically, to RSO, and a comprehensive list of ultra-violet absorption data concerning a wide variety of organo-sulphur compounds.

If any real criticism could be levelled at this work, it is that it might have given some mention of 'kinetic sulphur-bonding', i.e. an account of sulphur atoms as both electrophilic and nucleophilic centres in substitutions.

B. SAVILLE

Notes

Proton Spin Lattice Relaxation and Mechanical Loss in Stereoregular Polymethylmethacrylates

WE HAVE measured the proton spin lattice relaxation time, T_1, as a function of temperature for three samples of polymethylmethacrylate of different tacticity. The apparatus has been described elsewhere[1]. The measurements were made at a resonance frequency, ν_r, of 21·5 Mc/s by the 180°, 90° pulse method. We have also measured the dynamic mechanical losses in the frequency region of about 200 c/s by the vibrating reed method[2]. For some of the mechanical measurements the samples were filled with 66 per cent 'Tufnit'[3]. This reduces the losses and allows the main absorption peak to be determined exactly. It can be shown to have negligible effect on the positions of tan δ maxima[3]. For lower temperatures, below the main loss region, measurements were made on the same material as used for the n.m.r. work.

The spin lattice relaxation time is expected to depend on the rate of molecular motion, $\nu_c = 1/2\pi\tau_c$, through the formula[4,5]

$$\frac{1}{T_1} = \frac{1}{1{\cdot}41\,T_{1,\min.}}\left[\frac{\nu_r/\nu_c}{1+(\nu_r/\nu_c)^2} + \frac{4\nu_r/\nu_c}{1+(2\nu_r/\nu_c)^2}\right]$$

There is a minimum of T_1 when $\nu_c = 1{\cdot}62\nu_r$; 35 Mc/s in this case. If there are several distinct molecular motions several more or less distinct T_1 minima will be observed (see *Figures 1* to *3*).

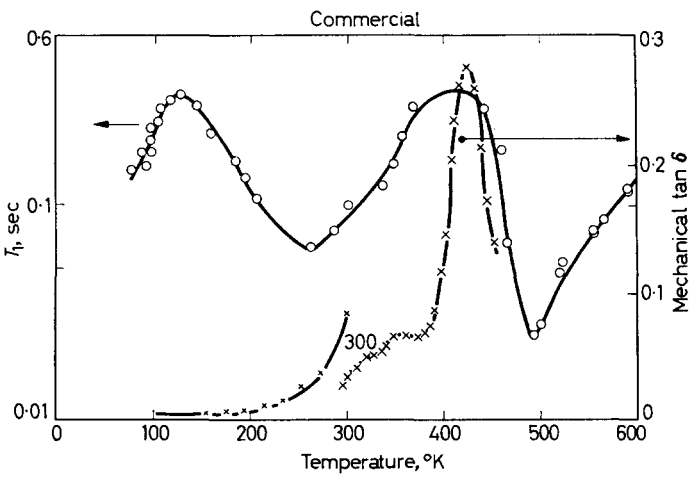

Figure 1—Proton spin lattice relaxation time at 21·5 Mc/s and mechanical loss tan δ at the frequencies indicated as a function of absolute temperature for a sample of commercial polymethylmethacrylate. The mechanical loss curve including the principal loss maximum is for material diluted with 66 per cent Tufnit. The lower temperature curve is for the pure polymer

For the mechanical measurements a peak of the mechanical loss curve means that ν_c is equal to the frequency of measurement at that temperature.

The T_1 results for commercial PMMA in *Figure 1* have been given elsewhere[6] but are included for comparison. *Figure 1* also gives mechanical measurements on the same material. This sample was free radical polymerized. It had monomer content about 0·1 per cent, Vicat softening point 123·6°C, molecular weight $>10^6$, distribution gaussian. It was 60 per cent syndiotactic as measured by n.m.r.[7]. The highest temperature minimum of T_1 and the main peak in tan δ are readily associated with the softening or

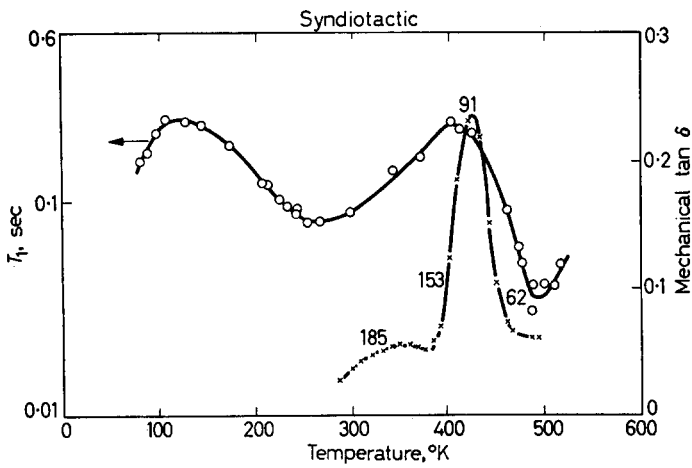

Figure 2—As *Figure 1* but for syndiotactic PMMA

α process presumed to be connected with large scale motions of the main chain. The second minimum at about 260°K has been associated by Kawai[8] and by Powles and Mansfield[6] with reorientation of the α-CH_3 group. A mechanical loss maximum due to this latter process has been observed by Bordoni[9] at about 10^4 c/s in the temperature region about 110°K Crissman, Sauer and Woodward[10] have found mechanical peaks in commercial material at 10^4 c/s at 150°K and at 45°K. However, these disappear on purification and so these and Bordoni's peak may be due to plasticizer. We did not observe any sign of a peak down to 77°K at 460 c/s. Both minima of T_1 can also be satisfactorily correlated[6] with line narrowing in the broad line proton magnetic resonance spectra which fix the temperature at which a molecular motion, ν_c, is at about 10^4 c/s. At a temperature below 90°K there must be a third minimum of T_1 and this has been associated[6,8] with the reorientation of the side chain methyl group.

The syndiotactic sample was prepared by a boron triethyl catalysed reaction under nitrogen in 100/120 petrol at −70°C. It was found by n.m.r. analysis in solution[7] to be >90 per cent syndiotactic. It was not possible to make measurements above 520°K owing to decomposition. Both the mechanical and the magnetic resonance measurements are hardly distin-

guishable from those for the commercial polymer. In particular the T_1 minima are almost at the same temperatures. This is in accord therefore with the solution n.m.r. result that the commercial material is quite syndiotactic.

The isotactic sample was prepared using ethyl magnesium bromide catalyst at 20°C. It was found by an n.m.r. calibrated infra-red analysis to contain <24 per cent atactic material. It shows a very striking change in both T_1 and $\tan\delta$, as compared with the syndiotactic material. The upper minimum in T_1 has moved down by 40°C whereas the mechanical loss peak has moved down by 75°C. If we assume that both $\tan\delta$ and T_1 in this region simply measure the rate of main chain motion we conclude that not only are the motions slower at a given temperature in the syndiotactic material but that the motions vary more rapidly with temperature. Both these effects could be ascribed to a greater hindrance to main chain reorientation in the syndiotactic as compared with the isotactic material.

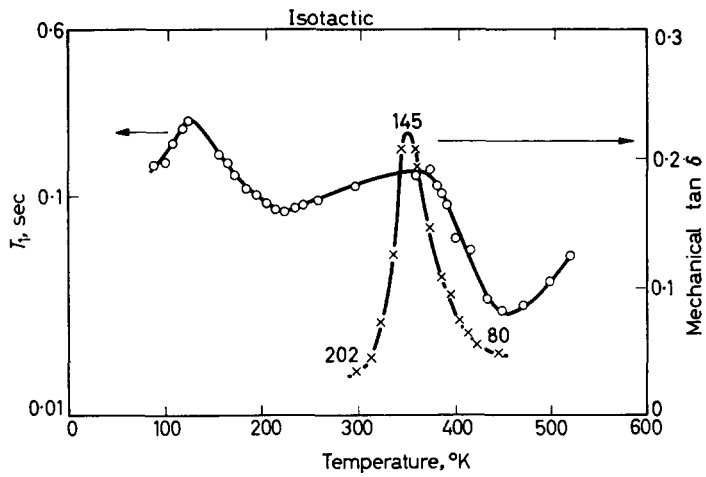

Figure 3—As *Figure 1* but for isotactic PMMA

Although the middle minimum is more shallow than in the commercial or syndiotactic material so that the position of the minimum is less exact, it also has moved down markedly in temperature, by about 40°C. It is interesting that this is just the same amount that the upper minimum moved. It is difficult to think of a mechanism which moves two different reorientation processes by the same temperature interval at different temperatures.

Odajima, Woodward and Sauer[11], from measurements of the main line narrowing in magnetic resonance, have also found commercial and syndiotactic material to be similar and that the isotactic material has a line narrowing clearly lower in temperature by about 55°C. It is interesting to compare the temperature shifts 75°, 55°, 40°C and the frequencies 10^2, 10^4, $10^{7\cdot5}$ c/s. Their[11] low temperature line narrowing, corresponding to our middle minimum in T_1, was some 15°C lower than for the commercial material both for the syndiotactic and the isotactic material. Similar results

were found by Nishioka *et al.*[12]. Our results suggest, however, that the tacticity affects quite markedly not only the main softening but also, to a rather similar extent, the ability of the α-CH_3 group to reorient. As was hoped, for this process the T_1 results show the effect of tacticity more clearly than the broad line ones.

Lower temperature measurements will be required before it can be said whether the low temperature minimum, the side chain CH_3 reorientation, is affected by tacticity.

The T_1 curves can be fitted quite well by the sum of three terms of the type given above with appropriate values of $T_{1,\min.}$ together with an activation assumption for the correlation frequencies, $\nu_c = \nu_0 \exp -\Delta E/RT$, with suitably chosen ν_0 and ΔE values. In view of our experience with a wide range of other acrylic polymers, details of which will be published shortly, we consider it unwise at present to attempt to draw conclusions from the actual shape of the T_1 curves as opposed to using the minima only.

J. G. POWLES
J. H. STRANGE
Physics Dept, Queen Mary College, Mile End Road, London, E.1
and D. J. H. SANDIFORD
Research Dept, I.C.I. Plastics Divn, Welwyn Garden City, Herts

(*Received March 1963*)

REFERENCES

[1] MANSFIELD, P. and POWLES, J. G. *J. sci. Instrum.* 1963, **40,** 232
[2] ROBINSON, D. W. *J. sci. Instrum.* 1955, **32,** 2
[3] SANDIFORD, D. J. H. and THOMAS, D. A. *Kolloidzschr.* 1962, **181,** 4
[4] BLOEMBERGEN, N., PURCELL, E. M. and POUND, R. V. *Phys. Rev.* 1948, **73,** 679
[5] KUBO, R. and TOMITA, K. *J. phys. Soc. Japan,* 1954, **9,** 888
[6] POWLES, J. G. and MANSFIELD, P. *Polymer, Lond.* 1962, **3,** 337
[7] BOVEY, F. A. and TIERS, G. V. D. *J. Polym. Sci.* 1960, **44,** 173
[8] KAWAI, T. *J. phys. Soc. Japan,* 1961, **16,** 1220
[9] BORDONI, P. G., NUOVO, M. and VERDINI, L. *Nuovo Cim.* 1961, **20,** 667
[10] CRISSMAN, J. M., SAUER, J. A. and WOODWARD, A. E. To be published
[11] ODAJIMA, A., WOODWARD, A. E. and SAUER, J. A. *J. Polym. Sci.* 1961, **55,** 181
[12] NISHIOKA, A., KATO, Y., UEKAKE, T. and WATANABE, A. *J. Polym. Sci.* 1962, **61,** S32

Primary Nucleation of Poly-3,3-bischloromethyl-oxacyclobutane Single Crystals

ACCORDING to the polymer crystallization theory of Lauritzen and Hoffman[1,2] and of Price[3], the fold period of the molecules in the primary nucleus of a polymer crystal, l_p^*, is greater than the fold period of the secondary nuclei, $\bar{l}$, which lead to the growth of the crystal. In general it is expected that $l^* > \bar{l} > \frac{1}{2}l_p^*$. If the primary nucleus has large enough lateral dimensions, one might expect to observe it in electron micrographs.

were found by Nishioka *et al.*[12]. Our results suggest, however, that the tacticity affects quite markedly not only the main softening but also, to a rather similar extent, the ability of the α-CH_3 group to reorient. As was hoped, for this process the T_1 results show the effect of tacticity more clearly than the broad line ones.

Lower temperature measurements will be required before it can be said whether the low temperature minimum, the side chain CH_3 reorientation, is affected by tacticity.

The T_1 curves can be fitted quite well by the sum of three terms of the type given above with appropriate values of $T_{1,\min.}$ together with an activation assumption for the correlation frequencies, $\nu_c = \nu_0 \exp -\Delta E/RT$, with suitably chosen ν_0 and ΔE values. In view of our experience with a wide range of other acrylic polymers, details of which will be published shortly, we consider it unwise at present to attempt to draw conclusions from the actual shape of the T_1 curves as opposed to using the minima only.

J. G. POWLES
J. H. STRANGE
Physics Dept, Queen Mary College, Mile End Road, London, E.1
and D. J. H. SANDIFORD
Research Dept, I.C.I. Plastics Divn, Welwyn Garden City, Herts

(*Received March 1963*)

REFERENCES

[1] MANSFIELD, P. and POWLES, J. G. *J. sci. Instrum.* 1963, **40,** 232
[2] ROBINSON, D. W. *J. sci. Instrum.* 1955, **32,** 2
[3] SANDIFORD, D. J. H. and THOMAS, D. A. *Kolloidzschr.* 1962, **181,** 4
[4] BLOEMBERGEN, N., PURCELL, E. M. and POUND, R. V. *Phys. Rev.* 1948, **73,** 679
[5] KUBO, R. and TOMITA, K. *J. phys. Soc. Japan,* 1954, **9,** 888
[6] POWLES, J. G. and MANSFIELD, P. *Polymer, Lond.* 1962, **3,** 337
[7] BOVEY, F. A. and TIERS, G. V. D. *J. Polym. Sci.* 1960, **44,** 173
[8] KAWAI, T. *J. phys. Soc. Japan,* 1961, **16,** 1220
[9] BORDONI, P. G., NUOVO, M. and VERDINI, L. *Nuovo Cim.* 1961, **20,** 667
[10] CRISSMAN, J. M., SAUER, J. A. and WOODWARD, A. E. To be published
[11] ODAJIMA, A., WOODWARD, A. E. and SAUER, J. A. *J. Polym. Sci.* 1961, **55,** 181
[12] NISHIOKA, A., KATO, Y., UEKAKE, T. and WATANABE, A. *J. Polym. Sci.* 1962, **61,** S32

Primary Nucleation of Poly-3,3-bischloromethyl-oxacyclobutane Single Crystals

ACCORDING to the polymer crystallization theory of Lauritzen and Hoffman[1,2] and of Price[3], the fold period of the molecules in the primary nucleus of a polymer crystal, l_p^*, is greater than the fold period of the secondary nuclei, $\bar{l}$, which lead to the growth of the crystal. In general it is expected that $l^* > \bar{l} > \frac{1}{2}l_p^*$. If the primary nucleus has large enough lateral dimensions, one might expect to observe it in electron micrographs.

In addition, the protruding portion might serve as a nucleus for the growth of an additional lamella on each side of the basal lamella.

Poly-3,3-bischloromethyloxacyclobutane crystallizes from the melt and solution in the form of lamellae. Various aspects of the structure of the single crystals and spherulites are discussed in a paper to be published shortly[4]. The crystals appear to be non-planar. The structure of the spherulites resembles that observed for polyoxymethylene[5,6]. The single crystals described in this letter were grown from a 0·1 per cent solution of Penton* 9215 in xylene by ambient cooling. (The method used was the same as that used for the Type A polyethylene crystals described in Chapter II, Section 4, of ref. 6). The number average molecular weight of this polymer is about 300 000.

More than 80 per cent of the crystals observed from the above preparation were found to have one additional, centrally located lamella on each side of the basal lamella. Sometimes the structure of the additional lamellae was complicated by spiral growths but often only the single additional lamellae would be observed (as in *Figure 1*) with spiral growths appearing elsewhere on the crystal or being absent altogether. A small percentage of the crystals were observed to have one large additional lamella and, on the opposite side, one very small lamella (*Figures 1* and *2*) while in others only one very small lamella could be observed.

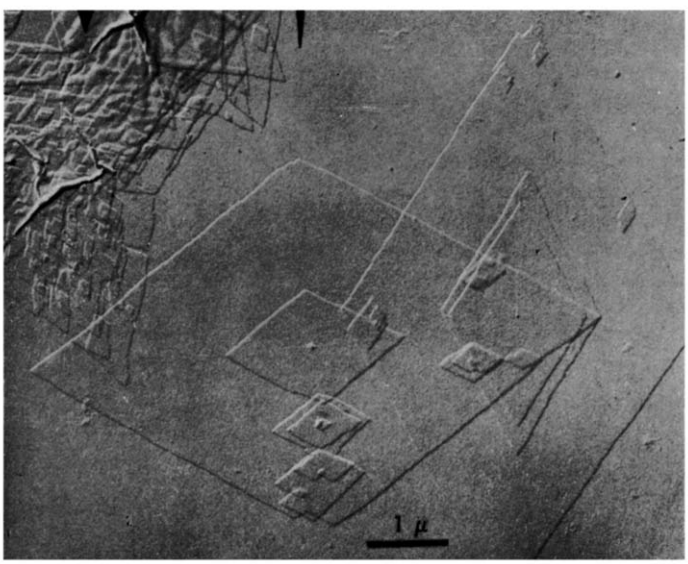

Figure 1—Single crystals of poly-3,3-bischloromethyloxacyclobutane grown from a 0·1 per cent xylene solution. The lamellae are about 30 Å thick as determined from the shadows. (Pt shadowed at $\tan^{-1} 3/12{\cdot}3$)

*Trademark of Hercules Powder Co.

On the single crystals consisting of only three lamellae the basal lamella was usually between 2·2 and 2·7 times as wide as the two additional lamellae. This latter feature suggests that their growth is diffusion controlled, each additional lamella being able to extract molecules from only about half the volume of solution from which the basal lamella can extract molecules. The fact that the additional lamellae on the two sides of the basal lamellae are of unequal size may result from the non-planar character of the crystals. Another factor in the relative size of the three lamellae would be their relative time of nucleation. The lamellae, as determined from the shadowing, are about 30Å thick on the periphery. The small angle X-ray diffraction long period from a sedimented cake of these crystals is 72Å. The cause of this discrepancy is being investigated at present. It is probably due to a change in thickness during growth, the lamellae being thinner on their periphery.

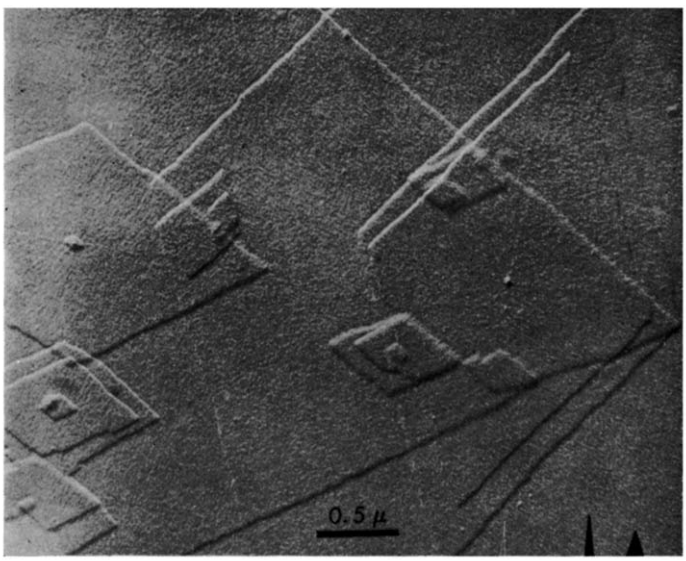

Figure 2—Central portions of two poly-3,3-bischloromethyloxacyclobutane crystals. The 'primary nuclei' are about 250 Å in diameter

A small, approximately 250Å diameter, bump can be observed in all of the crystals whose centre is not complicated by spiral growths (*Figure 2*). We attribute this bump to the primary nucleus of the crystal, which serves as the nucleus for both the basal lamella and the additional lamellae. Although we have not been able to measure its thickness, the fact that it can be observed suggests that it is more than three times as thick as the thickness of the lamellae, rather than somewhat less than twice as thick as predicted by theory[1–3]. This larger size of the primary nucleus could be a result of either a smaller value of the heat of fusion (due to numerous

defects) or a larger value of the end surface free energy (because of less perfect folds) than in the bulk of the lamella.

This work was supported by funds from the Camille & Henry Dreyfus Foundation.

P. H. GEIL*

Camille Dreyfus Laboratory,
Research Triangle Institute,
Durham, North Carolina, U.S.A.

(*Received May 1963*)

*Present address of author is Case Institute of Technology, Cleveland, Ohio, U.S.A.

REFERENCES

[1] LAURITZEN, Jr, J. I. and HOFFMAN, J. D. *J. Res. Nat. Bur. Stand. A*, 1960, **64**, 73
[2] HOFFMAN, J. D. and LAURITZEN, Jr, J. I. *J. Res. Nat. Bur. Stand. A*, 1961, **65**, 297
[3] PRICE, F. P. *J. Polym. Sci.* 1960, **42**, 49
[4] GEIL, P. H. To be published
[5] GEIL, P. H. *J. Polym. Sci.* 1960, **47**, 65
[6] GEIL, P. H. *Polymer Single Crystals.* Interscience–Wiley: New York, 1963

The Polymerization of Vinyl Ethers by Grignard Reagents

KRAY[1] has reported that treatment of vinyl ethers with Grignard reagents under nitrogen yields crystalline high molecular weight polymers. Our attempts to repeat these experiments under vacuum-line conditions, which ensured the almost complete absence of atmospheric contaminants, were unsuccessful, but polymers were obtained when small amounts of air were admitted to the system after the Grignard reagent had been formed. Further experiments, using ethyl or isobutyl vinyl ether and the Grignard reagent from *n*-butyl bromide, showed that water and nitrogen were ineffective, but that oxygen and, particularly, carbon dioxide were effective co-catalysts.

The effect of carbon dioxide was examined in more detail. The Grignard reagent, prepared in diethyl ether which was then removed, finally at $20°/10^{-5}$ mm, was treated with the monomer in cyclohexane and then, at 0°, with carbon dioxide. The molar ratios of Grignard reagent to monomer to carbon dioxide were 1·5: 100: 0·5. The containing vessel was sealed and heated at 60° to 70°C until no further change in viscosity was apparent, the reaction mixture was decomposed with aqueous ammonium chloride, and the polymer was extracted with benzene and freeze-dried. With isobutyl vinyl ether the yield and average molecular weight (determined by measurement of intrinsic viscosity[2]) varied from, respectively, 50 per cent and 900 000 after 17 h to 99 per cent and 280 000 after 6 days; with ethyl vinyl ether the maximum values were, respectively, 43 per cent and 42 000.

defects) or a larger value of the end surface free energy (because of less perfect folds) than in the bulk of the lamella.

This work was supported by funds from the Camille & Henry Dreyfus Foundation.

P. H. GEIL*

Camille Dreyfus Laboratory,
Research Triangle Institute,
Durham, North Carolina, U.S.A.

(*Received May 1963*)

*Present address of author is Case Institute of Technology, Cleveland, Ohio, U.S.A.

REFERENCES

[1] LAURITZEN, Jr, J. I. and HOFFMAN, J. D. *J. Res. Nat. Bur. Stand. A*, 1960, **64**, 73
[2] HOFFMAN, J. D. and LAURITZEN, Jr, J. I. *J. Res. Nat. Bur. Stand. A*, 1961, **65**, 297
[3] PRICE, F. P. *J. Polym. Sci.* 1960, **42**, 49
[4] GEIL, P. H. To be published
[5] GEIL, P. H. *J. Polym. Sci.* 1960, **47**, 65
[6] GEIL, P. H. *Polymer Single Crystals.* Interscience–Wiley: New York, 1963

The Polymerization of Vinyl Ethers by Grignard Reagents

KRAY[1] has reported that treatment of vinyl ethers with Grignard reagents under nitrogen yields crystalline high molecular weight polymers. Our attempts to repeat these experiments under vacuum-line conditions, which ensured the almost complete absence of atmospheric contaminants, were unsuccessful, but polymers were obtained when small amounts of air were admitted to the system after the Grignard reagent had been formed. Further experiments, using ethyl or isobutyl vinyl ether and the Grignard reagent from *n*-butyl bromide, showed that water and nitrogen were ineffective, but that oxygen and, particularly, carbon dioxide were effective co-catalysts.

The effect of carbon dioxide was examined in more detail. The Grignard reagent, prepared in diethyl ether which was then removed, finally at $20°/10^{-5}$ mm, was treated with the monomer in cyclohexane and then, at 0°, with carbon dioxide. The molar ratios of Grignard reagent to monomer to carbon dioxide were 1·5: 100: 0·5. The containing vessel was sealed and heated at 60° to 70°C until no further change in viscosity was apparent, the reaction mixture was decomposed with aqueous ammonium chloride, and the polymer was extracted with benzene and freeze-dried. With isobutyl vinyl ether the yield and average molecular weight (determined by measurement of intrinsic viscosity[2]) varied from, respectively, 50 per cent and 900 000 after 17 h to 99 per cent and 280 000 after 6 days; with ethyl vinyl ether the maximum values were, respectively, 43 per cent and 42 000.

The polymers did not show greater crystallinity than that observed for materials prepared at $-78°$ with a boron trifluoride etherate catalyst.

In another series of experiments the ethereal Grignard reagent was left in contact with carbon dioxide at one atmosphere pressure until no further absorption occurred, during which time a white precipitate separated. The ether was removed, finally at $20°/10^{-5}$ mm, before addition of the monomer (20-fold molar excess over the Grignard reagent) and cyclohexane. Polymerization was allowed to proceed at 20° until no perceptible increase in viscosity occurred. For isobuytyl vinyl ether yields of up to 97 per cent and molecular weights of about 500 000 were obtained, depending upon the time and temperature of interaction of the ethereal Grignard reagent with carbon dioxide. The most active catalyst, which caused almost complete polymerization in 3 h at 20°, was obtained by leaving the Grignard solution in contact with a carbon dioxide atmosphere at 20° for 1h; less active catalysts resulted at 0°, or when the contact time was increased. In a single experiment with ethyl vinyl ether almost complete conversion to material of molecular weight 58 000 was achieved, but methyl vinyl ether failed to polymerize. None of the monomers polymerized when diethyl ether was used as solvent.

Filtration, *in vacuo*, of the white suspension obtained by treating the ethereal Grignard reagent with carbon dioxide indicated that the ether-insoluble material was catalytically inactive, whereas the soluble material was active. Both fractions yielded *n*-valeric acid when treated with dilute sulphuric acid, but an active catalyst was not produced when the Grignard reagent was treated with a small amount of *n*-valeric acid instead of with carbon dioxide.

Since the interaction of oxygen, which is a slightly less effective co-catalyst than carbon dioxide, with the Grignard reagent is believed[3] to yield Bu^nOMgBr it was of interest to examine the co-catalytic activity of other substances which could lead to similar structures. *n*-Butanol, which would yield *n*-butane and Bu^nOMgBr, was inactive, but ethylene glycol, *n*-butanal, butanone, and propylene oxide were active, producing after several days at 70°C yields of up to 80 per cent of polymers with molecular weights of about 100 000. The last three co-catalysts would yield respectively $Bu^nPr^nCHOMgBr$, $Bu^nEtMeCOMgBr$, and $Bu^nCH_2MeCHOMgBr$ (or[4] $Bu^nCH_2MeCHOMg{\cdot}OCHMeCH_2Bu^n + MgBr_2$) by 1,2-addition, although with the carbonyl compounds products of enolization and reduction may also be formed[5].

Magnesium bromide, prepared[6] from ethylene dibromide and magnesium, was as effective as the best catalyst prepared from the Grignard reagent and carbon dioxide, but if such a species is active in the co-catalysed polymerizations it must be deactivated, possibly by complexing[7], in the original Grignard reagent, in which its presence is indicated by the formation of *n*-octane during the reaction between *n*-butyl bromide and magnesium. The picture is complicated by (*a*) the observation that a mixture of propylene oxide and magnesium bromide in the molar ratio 1·5: 1, believed[8] to yield both $BrCH_2{\cdot}MeCHOMgBr$ and $(BrCH_2{\cdot}MeCHO)_2Mg$, is a comparatively ineffective catalyst, (*b*) the heterogeneous nature of the systems, and (*c*) the

complexity[5,9] of Grignard reagents in solution, and at this stage the nature of the catalytically active species cannot be specified.

J. MALCOLM BRUCE
D. W. FARREN

Department of Chemistry,
University of Manchester

(*Received May 1963*)

REFERENCES

[1] KRAY, R. *J. Polym. Sci.* 1960, **44,** 264
[2] MANSON, J. A. and ARQUETTE, G. J. *Makromol. Chem.* 1960, **37,** 187
[3] WALLING, C. and BUCKLER, S. A. *J. Amer. chem. Soc.* 1953, **75,** 4372
[4] HUSTON, R. C. and AGETT, A. H. *J. org. Chem.* 1941, **6,** 123
[5] HOUSE, H. O. and TRAFICANTE, D. D. *J. org. Chem.* 1963, **28,** 355, and references therein
[8] STORFER, S. J. and BECKER, E. I. *J. org. Chem.* 1962, **27,** 1868
[7] KIRRMANN, A. and HAMELIN, R. *C.R. Acad. Sci., Paris,* 1960, **251,** 2990
[8] RIBAS, I. and TAPIA, E. *Chem. Abstr.* 1933, **27,** 1323, 1864
[9] STUCKY, G. D. and RUNDLE, R. E. *J. Amer. chem. Soc.* 1963, **85,** 1002
ASHBY, E. C. and BECKER, W. E. *J. Amer. chem. Soc.* 1963, **85,** 118
EVANS, D. F. and MAHER, J. P. *J. chem. Soc.* **1962,** 5125, and references therein

The Crystallinity of Stretched Gutta Percha

GUTTA PERCHA exists in two crystalline forms having melting points 56° to 64°C and 68° to 74°C and designated β and α respectively[1–5]. In a study of the crystal structures of the polymer, Fisher[3] observed that on stretching thin films a new crystalline modification was produced. This was not completely characterized owing to the presence of reflections from some β form also present in the stretched polymer, but it had similar cell constants to the normal higher-melting α isomer*. Fisher stated that the form present in the stretched polymer was distinct from the α and β modifications but always co-existed with some β structure.

In this note dilatometric measurements and X-ray data on stretched and unstretched α and β polymers are reported.

Tjipetir gutta percha was used in 1 mm unoriented sheets, and obtained as essentially pure α or β forms by well established methods[1,2]. Oriented films were prepared by machine stretching to 250 per cent or by compression moulding of thicker samples at 5 000 lb/in^2. Volume/temperature records were obtained using dilatometers and automatic recording as described elsewhere[2,6]. The heating rate was 5° to 6°C/h and samples were not heated during degassing. Densities were found from dilatometric data and by direct measurement. X-ray diffraction patterns were obtained by rotating films of the various polymers in a plane perpendicular to the

*Fisher suggested that the α modification should be called the γ form and the former designation retained for the new form claimed to be produced on stretching.

complexity[5,9] of Grignard reagents in solution, and at this stage the nature of the catalytically active species cannot be specified.

J. MALCOLM BRUCE
D. W. FARREN

Department of Chemistry,
University of Manchester

(*Received May 1963*)

REFERENCES

[1] KRAY, R. *J. Polym. Sci.* 1960, **44,** 264
[2] MANSON, J. A. and ARQUETTE, G. J. *Makromol. Chem.* 1960, **37,** 187
[3] WALLING, C. and BUCKLER, S. A. *J. Amer. chem. Soc.* 1953, **75,** 4372
[4] HUSTON, R. C. and AGETT, A. H. *J. org. Chem.* 1941, **6,** 123
[5] HOUSE, H. O. and TRAFICANTE, D. D. *J. org. Chem.* 1963, **28,** 355, and references therein
[8] STORFER, S. J. and BECKER, E. I. *J. org. Chem.* 1962, **27,** 1868
[7] KIRRMANN, A. and HAMELIN, R. *C.R. Acad. Sci., Paris,* 1960, **251,** 2990
[8] RIBAS, I. and TAPIA, E. *Chem. Abstr.* 1933, **27,** 1323, 1864
[9] STUCKY, G. D. and RUNDLE, R. E. *J. Amer. chem. Soc.* 1963, **85,** 1002
ASHBY, E. C. and BECKER, W. E. *J. Amer. chem. Soc.* 1963, **85,** 118
EVANS, D. F. and MAHER, J. P. *J. chem. Soc.* **1962,** 5125, and references therein

The Crystallinity of Stretched Gutta Percha

GUTTA PERCHA exists in two crystalline forms having melting points 56° to 64°C and 68° to 74°C and designated β and α respectively[1–5]. In a study of the crystal structures of the polymer, Fisher[3] observed that on stretching thin films a new crystalline modification was produced. This was not completely characterized owing to the presence of reflections from some β form also present in the stretched polymer, but it had similar cell constants to the normal higher-melting α isomer*. Fisher stated that the form present in the stretched polymer was distinct from the α and β modifications but always co-existed with some β structure.

In this note dilatometric measurements and X-ray data on stretched and unstretched α and β polymers are reported.

Tjipetir gutta percha was used in 1 mm unoriented sheets, and obtained as essentially pure α or β forms by well established methods[1,2]. Oriented films were prepared by machine stretching to 250 per cent or by compression moulding of thicker samples at 5 000 lb/in^2. Volume/temperature records were obtained using dilatometers and automatic recording as described elsewhere[2,6]. The heating rate was 5° to 6°C/h and samples were not heated during degassing. Densities were found from dilatometric data and by direct measurement. X-ray diffraction patterns were obtained by rotating films of the various polymers in a plane perpendicular to the

*Fisher suggested that the α modification should be called the γ form and the former designation retained for the new form claimed to be produced on stretching.

incident beam. The radial density distributions were obtained from a selenium photocell coupled to a potentiometric recorder.

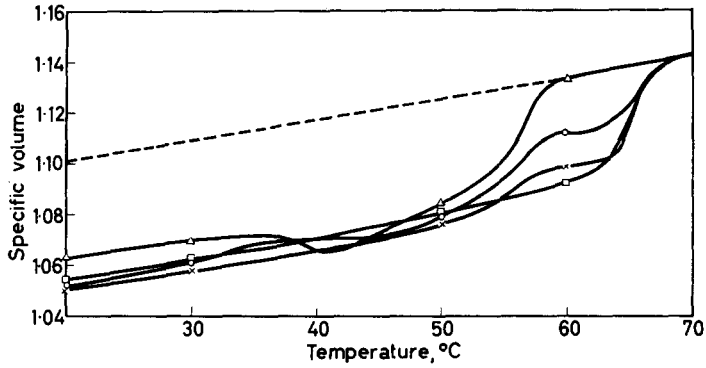

Figure 1—Specific volume/temperature curves for β polymer. Unstretched (△); unstretched and cut (○); stretched, rolled and cut (×); compressed and cut (□)

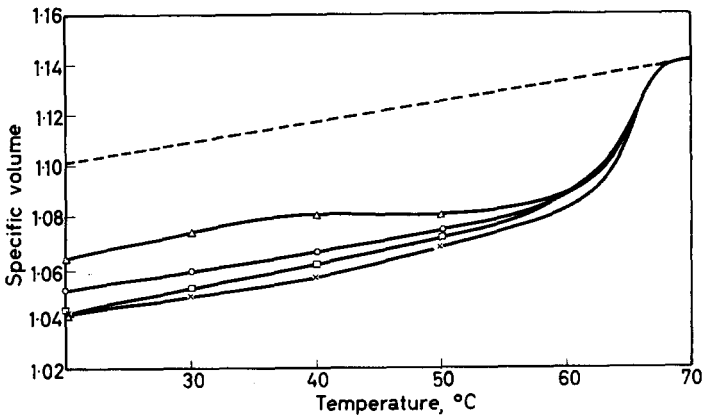

Figure 2—Specific volume/temperature curves for α polymer. Unstretched (×); stretched (△); stretched and rolled (○); compressed (□)

Tracings from continuously recorded specific volume versus temperature curves are shown in *Figures 1* and *2*, the symbols are used to distinguish the various curves and do not represent experimental points. Average densities and crystallinity data are given in *Table 1*.

Radial distribution of the X-ray diffraction patterns for stretched and unstretched α and β gutta percha are shown in *Figure 3*.

Direct diffraction patterns from non-rotated samples suggested higher levels of orientation in stretched β samples than in the stretched α forms.

Dilatometric examination of stretched β polymer shows the polymer to contain a considerable proportion of a higher melting form identical in melt point with α polymer (*Figure 1*). The annealed α polymer shows

essentially the same melting behaviour both in the stretched and the unstretched condition, and in no case was a low melting β transition observed (*Figure 2*). This is apparently contradictory to the findings of Fisher who reported that on stretching all samples reverted to a mixture of two modifications in which the β component predominated. The dilatometric data

Table 1. Average densities of gutta percha (g/cm³; 20°C/20°C)

Polymer history	*Unstretched*	*Stretched*	*Stretched and rolled*	*Compressed 5 000 lb/in²*	*Stretched, compressed 1 000 lb/in²*
α Polymer	0·956	0·947	0·962	0·959	0·953
Polymer structure high m.pt : low m.pt	100 : 0	100 : 0	100 : 0	100 : 0	100 : 0
β Polymer	0·944	0·952	0·956	0·948	—
Polymer structure high m.pt : low m.pt	0 : 100	64 : 36	64 : 36	88 : 12	—

suggest, in fact, that in the stretched condition α and β polymers are of the same form. This is not so, however, since the X-ray patterns of the stretched forms are quite different and resemble, so far as the principal reflections are concerned, their respective unstressed forms (*Figure 3*).

The recognition of β polymer from dilatometric and differential thermal

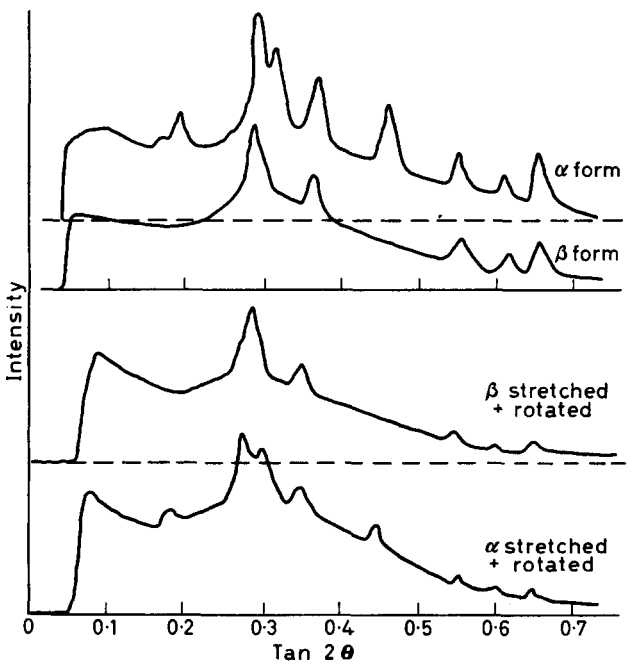

Figure 3—X-ray diffraction intensities for stretched and unstretched gutta percha

analyses is only possible when the rate of transformation of β to α structures is slow compared with the rate of heating used in the experiments. A study of the changes occurring in the X-ray diffraction patterns of oriented β polymer when heated at the rate used in the above experiments has shown that the β to α transformation takes place very rapidly without any apparent melting. The transformation in oriented samples occurs rapidly at 52°C, whereas with unoriented samples there is no change on annealing at this temperature for many hours. This increased rate of β to α transformation in oriented samples accounts for their observed high melting points. Even cutting films of β polymer with scissors introduces sufficient orientation into the polymer so that some α structure is formed during heating to melt the polymer.

The melting points and densities of stretched and unstretched polymers in *Table 1* show some anomalies. These are slight variations due to the different levels of crystallinity in the polymers but in general the densities of stretched α samples were always lower than would have been anticipated assuming no reduction in crystalline content on orientation. It was also noted that the stretched polymers were markedly opaque. This evidence suggests that voids were produced on stressing. Since the dilatometers were charged with stretched samples without heating, the voids would remain in the samples during the melting examination until the polymer softened as the melting point was approached. Voids were also observed on stretching the β polymer but, presumably as a result of its lower modulus at the yield point (1 000 lb/in^2 compared with 1 400 lb/in^2 for the α form), to a much smaller extent. Stretching the β samples eliminated the precrystallization phenomenon which has been noted[2,5] during the melting of this form.

Passing the sample through mill rolls while stretching, or subjecting the stretched material to hydrostatic pressures of 1 000 lb/in^2 eliminated most of the voids. Unstretched samples were also oriented by compression (5 000 lb/in^2) without voids being produced. With this treatment an average density increase of about 1·5 per cent occurs. All the compressed samples were more transparent than normal stretched films.

We thank the Dunlop Rubber Company for permission to publish these data.

W. COOPER
F. R. JOHNSTON
G. VAUGHAN

Chemical Research Department,
Dunlop Research Centre,
Birmingham

(Received May 1963)

REFERENCES

[1] DEAN, J. N. *Trans. Instn Rubber Ind.* 1932, **8**, 25
[2] COOPER, W. and VAUGHAN, G. *Polymer, Lond.* 1963, **4**, 329
[3] FISHER, D. *Proc. phys. Soc. Lond.* 1953, **66**, 7
[4] MANDELKERN, L., QUINN, F. A. and ROBERTS, D. E. *J. Amer. chem. Soc.* 1956, **78**, 926
[5] LEEPER, H. M. and SCHLESINGER, W. *J. Polym. Sci.* 1953, **11**, 307
[6] VAUGHAN, G., SEWELL, P. R. and HOLLINS, P. H. *Chem. & Ind., Lond.* **1960**, 1155
[7] ROBERTS, D. E. and MANDELKERN, L. *J. Res. Nat. Bur. Stand.* 1955, **54**, 167

Proton Magnetic Resonance of Polyethylene Crystals

IN A recent publication[1] proton magnetic resonance results were presented for two samples of polyethylene (Marlex 50) crystals prepared by precipitation from dilute solution. For both samples the proton resonance spectra showed a broad component or 'line' which underwent narrowing at temperatures well below the melting point for material grown from the melt. From the limited data available it appeared that the sample with the greatest low angle X-ray spacing, 120Å, underwent this narrowing process at higher temperatures than the other specimen (112Å spacing).

Measurements have now been made on a third specimen, consisting of crystals prepared at National Physical Laboratory, Teddington by Dr F. E. Karasz from a 0·1 per cent xylene solution at 90°C, found to have a low angle X-ray spacing of 144Å. Proton resonance spectra for this sample were taken in the 300° to 385°K temperature region. The peak-to-peak width of the derivative line shape (line width) is given as a function of temperature in *Figure 1*. In this figure the broad line widths reported

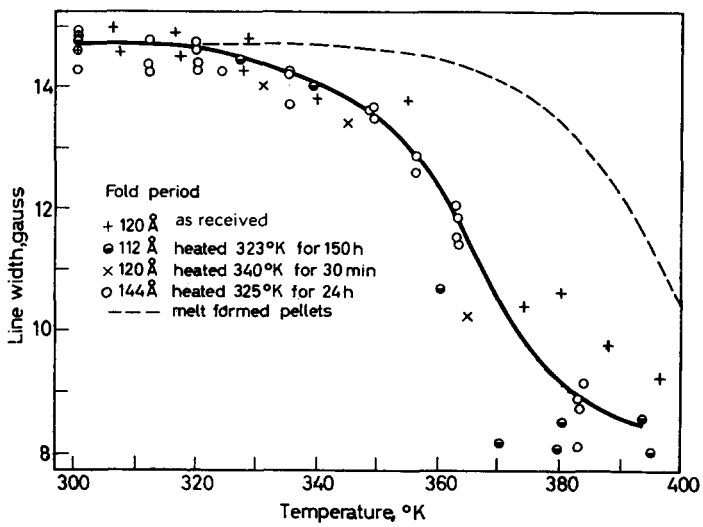

Figure 1—Line width versus temperature for polyethylene crystals with different fold periods

previously for the other two samples are also plotted. Although there is considerable scatter in these values, it is seen that the narrowing process occurs in the same temperature region regardless of low angle X-ray spacing. In addition to the broad component, a very narrow (~0·5 gauss) line of low intensity, barely distinguishable from the background noise, was observed at 300°K for both the sample in which the broad-line measurements had been made (heated to 384°K) and a sample dried for 90 h under vacuum at 315° to 325°K.

As noted earlier[1,2], the broad-line narrowing process for crystals heated at temperatures close to but below the bulk melting point and for melt formed specimens (broken line in *Figure 1*) occurs at temperatures significantly higher than for the unheated crystals. Since heating solution-grown crystals near the bulk melting point leads to an increase in the low angle X-ray spacing and the appearance of holes in the crystals[3], presumably due to a chain-unfolding process, the independence of the narrowing process on fold period for the unheated crystals was not expected. This indicates that during the unfolding process the structure is modified in some unknown way, bringing about a reduction in chain mobility in the crystalline regions.

We wish to acknowledge the support of this work by the U.S. Atomic Energy Commission and to express our gratitude to the John Simon Guggenheim Memorial Foundation for the award of a fellowship to one of us (A.E.W.) during the tenure of which this work was completed.

J. A. E. KAIL*
J. A. SAUER
A. E. WOODWARD†

Department of Physics,
Pennsylvania State University,
University Park, Pennsylvania, U.S.A.

(Received June 1963)

REFERENCES

[1] ODAJIMA, A., SAUER, J. A. and WOODWARD, A. E. *J. phys. Chem.* 1962, **66**, 718
[2] SLICHTER, W. P. *J. appl. Phys.* 1961, **32**, 2339
[3] STATTON, W. O. and GEIL, P. H. *J. appl. Polym. Sci.* 1960, **3**, 357

*Present address: Plastics Division, Imperial Chemical Industries Ltd., Welwyn Garden City, Herts.
†Present address: On sabbatical leave at Queen Mary College, University of London.

Contributions to Polymer

Papers accepted for future issues of POLYMER include the following:

The Glass Transition Temperature of Polymeric Sulphur—A. V. TOBOLSKY, W. MACKNIGHT, R. B. BEEVERS and V. D. GUPTA

Aminolysis of Polyethylene Terephthalate—H. ZAHN and H. PFEIFER

Molecular Motion in Polyethylene IV—D. W. MCCALL and D. C. DOUGLASS

A New Transition in Polystyrene, I, II, III—G. MORAGLIO, F. DANUSSO, V. BIANCHO, C. ROSSI, A. M. LIQUORI and F. QUADRIFOGLIO

Free Radical Reactions in Irradiated Polyethylene—M. G. ORMEROD

The Radiation Chemistry of Some Polysiloxanes: An Electron Spin Resonance Study—M. G. ORMEROD and A. CHARLESBY

The Mechanical Degradation of Polymers—C. BOOTH

Dynamic Birefringence of Polymethylacrylate—B. E. READ

Solution and Bulk Properties of Branched Polyvinyl Acetates I, II, III—L. M. HOBBS, V. C. LONG, G. C. BERRY and R. G. CRAIG

The Photochemical Degradation of Polyamides and Related Model n*-Alkylamines*—R. F. MOORE

Polycarbonates from the 2,2,4,4-Tetramethylcyclobutane-1,3-diols I—Preparation and Structure—Miss M. GAWLAK and J. B. ROSE

Polycarbonates from the 2,2,4,4-Tetramethylcyclobutane-1,3-diols II—Crystal Structure and Melting Behaviour—A. TURNER JONES and R. P. PALMER

The Temperature Dependence of Extensional Creep in Polyethylene Terephthalate—I. M. WARD

The Radiation Chemistry of Polymethacrylic Acid, Polyacrylic Acid and Their Esters: An Electron Spin Resonance Study—M. G. ORMEROD and A. CHARLESBY

Crystallinity and Disorder Parameters in Nylon 6 and Nylon 7—W. RULAND

Mechanism of the Ductile–Brittle Transition in Linear Polyethylene—S. STRELLA and S. NEWMAN

A Thermodynamic Description of the Defect Solid State of Linear High Polymers—B. WUNDERLICH

*Graft Copolymerization Initiated by Poly-*p*-lithiostyrene*—M. B. HUGLIN

Structure and Properties of Crazes in Polycarbonate and Other Glassy Polymers—R. P. KAMBOUR

The Crystallization of Polymethylene Copolymers; Morphology—J. B. JACKSON and P. J. FLORY

The Crystallization of Polyethylene II—W. BANKS, J. N. HAY, A. SHARPLES and G. THOMSON

Description and Calibration of an Elasto-osmometer—H. J. M. A. MIERAS and W. PRINS

Resonance-induced Polymerizations—R. J. ORR

Polypropylene Oxide I—An Intrinsic Viscosity/Molecular Weight Relationship—G. ALLEN, C. BOOTH and M. N. JONES

Viscosity/Temperature Dependence for Polyisobutene Systems: The Effect of Molecular Weight Distribution—R. S. PORTER and J. F. JOHNSON

Catalysts for the Low Temperature Polymerization of Ethylene—K. J. TAYLOR

The Effect of Tension and Annealing on the X-ray Diffraction Pattern of Drawn 6.6 Nylon—D. R. BERESFORD and H. BEVAN

CONTRIBUTIONS should be addressed to the Editors, *Polymer*, 4-5 Bell Yard, London, W.C.2.

Authors are solely responsible for the factual accuracy of their papers. All papers will be read by one or more referees, whose names will not normally be disclosed to authors. On acceptance for publication papers are subject to editorial amendment.

If any tables or illustrations have been published elsewhere, the editors must be informed so that they can obtain the necessary permission from the original publishers.

All communications should be expressed in clear and direct English, using the minimum number of words consistent with clarity. Papers in other languages can only be accepted in very exceptional circumstances.

TWELFTH CANADIAN HIGH POLYMER FORUM

The Twelfth Canadian High Polymer Forum will be held at the Cardy Alpine Inn, Ste Marguerite, Quebec, on 27 to 29 May 1964. The Forum is sponsored by the National Research Council of Canada in cooperation with the Chemical Institute of Canada, and is devoted to all aspects of Macromolecular Science.

The Forum Lecturer will be Professor Charles Sadron, director of the Centre de Recherches sur les Macromolécules, Strasbourg, France. Chairman of the Forum is Dr David A. I. Goring, Pulp and Paper Research Institute, McGill University, Montreal, Quebec.

Authors wishing to submit papers for presentation at the Forum are asked to write to the Program Chairman, Dr Leo Breitman, Research and Development Division, Polymer Corporation Limited, Sarnia, Ontario. Titles and abstracts of 200 to 300 words are required by 15 February 1964.

CRYSTALLOGRAPHIC DATA FOR VARIOUS POLMERS IV

The table containing the above data published by R. L. MILLER and L. E. NIELSEN (*J. Polym. Sci.* 1960, **44,** 391 and 1961, **55,** 643) has been revised. Any reader wishing a copy should write to the first author at Chemstrand Research Center Inc., Research Triangle Park, Box 731, Durham, North Carolina, U.S.A.

Rubber Elasticity in a Highly Crosslinked Epoxy System

D. KATZ* and A. V. TOBOLSKY

This work is a study in the field of viscoelastic and elastic behaviour of highly crosslinked systems. It was observed that epoxides crosslinked with amines have well defined transition and rubbery plateau regions. The concepts of the theory of rubber elasticity were applied to Epon 826 (Shell Chemical Company) crosslinked by four aliphatic amines (EDA, DETA, TETA, TEPA). From the measured values of the Gehman 10 sec modulus in the rubbery region the 'front factor' in the equation for rubbery networks was calculated. By use of equations that take into consideration the molecular structure of the resin derived for rubbery networks by one of the authors in an earlier work, the front factors were calculated and the agreement between the values obtained from experiments and the ones calculated is very good.

THIS work is a further study in the field of viscoelastic behaviour of highly crosslinked systems[1] with the aim of finding the correlation between the structure and properties of these systems.

Modulus/temperature measurements have shown that epoxides from the Epon series (Shell Chemical Company) crosslinked by use of polyfunctional aliphatic amines (DETA, TETA) and aromatic tertiary amines (DMP-10, DMP-30) have modulus/temperature curves similar in shape to those of crosslinked vinyl polymers, with well defined transition regions and rubbery plateau regions. As a consequence of that observation we considered the possibility of application of the concepts of the theory of rubber elasticity for the rubbery region of the epoxy resins.

The resin chosen for this work was Epon 826 (Shell Chemical Company) whose structural formula is represented by

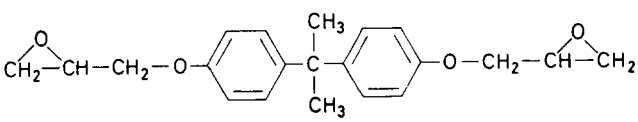

Only a small fraction of the resin is in the form of diepoxides containing one or more hydroxyl groups[2].

As crosslinking agents four aliphatic amines were used: ethylene diamine (EDA), diethylene triamine (DETA), triethylene tetramine (TETA) and tetraethylene pentamine (TEPA). Those amines being four-, five-, six- and seven-functional react with the expoxide rings giving products which are secondary alcohols, but the alcohols do not combine with other epoxides[3,4]. The products of these reactions are resins with a simple and well defined

*On leave from the Scientific Department, Israel Ministry of Defence.

structure; each amine molecule becomes a 'crosslinking bridge' for four, five, six or seven epoxy chains (depending on the amine used) and each epoxy chain is shared by two crosslinking molecules.

EXPERIMENTAL

The samples for the Gehman 10 sec modulus measurements[5] and for the specific gravity determinations were prepared by mixing the calculated and weighed amounts of the resin and amine. The mixtures were degassed and cured in aluminium foil moulds for 96 h at room temperature and for an additional hour at 140°C. In order to assure that all the epoxy rings were opened a small excess of the crosslinking agent was used (5 to 8 per cent of active hydrogen). The excess of amine does not contribute to the amount of network chains and if any is left free it can be considered as a plasticizer; it was shown in a previous work that such small amounts of plasticizer in crosslinked systems do not affect the rubbery modulus very considerably[6].

Our basic measurements were shear modulus versus temperature, using the Gehman instrument[5]. This is essentially a torsion modulus measurement, using a calibrated torsion wire coupled with the sample and measuring torsional deflection of the wire ten seconds after application of the stress. In the rubbery plateau region, the deflection is essentially independent of time. The Gehman 10 sec modulus measurements as a function of temperature are represented in *Figure 1* and the results of calculations are shown in *Table 1*. Inasmuch as the distance between epoxy chains attached

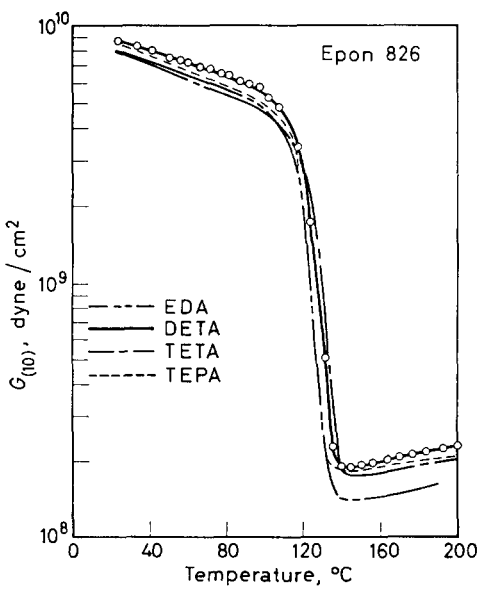

Figure 1—Ten second Gehman shear modulus versus temperature for Epon 826 resin crosslinked with four different aliphatic amines

Table 1

Amine	*Active H in amine*	*d* g/cm^3	*c* $molecules/cm^3$	(a) zc_1	(b) $zckT$
EDA	4	1·1923	$9·09\times10^{20}$	$3·018\times10^{-3}$	$1·05\times10^{8}$
DETA	5	1·1905	$7·06\times10^{20}$	$2·931\times10^{-3}$	$1·02\times10^{8}$
TETA	6	1·1899	$5·78\times10^{20}$	$2·876\times10^{-3}$	$1·00\times10^{8}$
TEPA	7	1·1885	$4·88\times10^{20}$	$2·836\times10^{-3}$	$9·90\times10^{7}$

	G $dyne/cm^2$	$\Phi=\frac{G}{zckT}$	$\overline{r_i^2}$	$\overline{r_f^2}$	$\Phi\star=\frac{\overline{r_i^2}}{\overline{r_f^2}}$
EDA	$1·43\times10^{8}$	1·36	$0·73\times10^{-14}$	$9·18\times10^{-15}$	0·78
DETA	$1·91\times10^{8}$	1·87	$0·96\times10^{-14}$	$9·18\times10^{-15}$	1·04
TETA	$1·78\times10^{8}$	1·78	$1·21\times10^{-14}$	$9·18\times10^{-15}$	1·32
TEPA	$1·87\times10^{8}$	1·88	$1·47\times10^{-14}$	$9·18\times10^{-15}$	1·62

(a) $z=\frac{1}{2}$ (Active H in amine). (b) $T=420°K$.

to the same crosslinking molecule is very small, the only flexible chains in the resin network are the epoxy chains. In the calculation of the amount of network chains per cubic centimetre the assumption is made that each molecule of amine, depending on which one was used, connects four, five, six or seven network chains, and that each network chain is shared by two molecules of the crosslinking agent. The quantity z is the number of network chains per crosslinking molecule, and z equals $\frac{4}{2}$, $\frac{5}{2}$, $\frac{6}{2}$, $\frac{7}{2}$ for the experiments made with EDA, DETA, TETA and TEPA respectively.

The equation for shear modulus from the theory of rubber elasticity is

$$G=\Phi zckT \tag{1}$$

In equation (1) G is the shear modulus, Φ is the front factor discussed below, z has been defined above, c is the number of amine molecules (crosslinking agent) per cubic centimetre, k is the Boltzmann constant, and T the absolute temperature. Subsequently we shall discuss theoretical values for the front factor which we shall denote as $\Phi\star$. Φ is to be regarded as a quantity defined by equation (1) and calculated from the experimental values of G, z, c and T. The values of Φ presented in *Table 1* were obtained in this manner, using the experimental value of G at $T=420°K$. This temperature is in the rubbery plateau region of all the polymers.

In order to correlate the properties of the resin with its structure, an attempt was made to calculate a theoretical front factor $\Phi\star$ from the dimensions of the network chains involved and to compare this value with the values obtained by calculation from experiments.

The equations used for calculation of $\Phi\star$ from the dimensions of the network chains were the ones proposed for rubber networks by one of us in his earlier work[7,8]. According to the results of this work

$$\Phi\star=\overline{r_i^2}/\overline{r_f^2} \tag{2}$$

when $\overline{r_i^2}$ is the mean square distance between network junctures in the resin and $\overline{r_f^2}$ is the mean square end-to-end length of the network chain considered as a chain in free space. In particular $\overline{r_i^2}$ was calculated for non-

interpenetrating networks where the spatially nearest crosslink is also a contiguous crosslink in the network[7]. This assumption seems to us to be applicable to this highly crosslinked epoxy system. The value for $\overline{r_i^2}$ was calculated from the equation

$$\overline{r_i^2} = \mathrm{f}(2z)/c^{2/3} \tag{3}$$

where c is the number of crosslinking molecules per cubic centimetre.

This equation was derived as follows[7]: we assume that the crosslinking molecules are distributed throughout the volume in a random fashion as is the case for an ideal gas. The formula for the probability that the jth nearest neighbour lies at a distance r from a given point in a random array

$$P_j(r)\,\mathrm{d}r = [1/(j-1)!]\,[(\tfrac{4}{3})\,\pi c r^3]^{(j-1)} \exp[-(\tfrac{4}{3})\,\pi c r^3]\,4\pi r^2 c\,\mathrm{d}r \tag{4}$$

where c is the number of points per cubic centimetre, and r is then expressed in centimetres.

The mean square value of the distance to the jth nearest neighbour is given by

$$\overline{r_j^2} = [1/(j-1)!]\,(3/4\pi c)^{2/3}\Gamma(j+\tfrac{2}{3}) \tag{5}$$

where Γ represents the gamma function.

We shall define $\overline{r_i^2}$ as the average of the mean square distance to the $2z$ nearest neighbours. In terms of equation (5), the definition is

$$\overline{r_i^2} = (1/2z)\,(\overline{r_1^2} + \overline{r_2^2} + \ldots + \overline{r_{2z}^2}) \tag{6}$$

The value for $\overline{r_i^2}$ turns out to be that given in equation (3).

The reasonability of this result is very plain. If the crosslinking points were distributed on a simple cubic lattice, the square of the distance to each of the six nearest neighbours is $c^{-2/3}$.

The value for $\overline{r_f^2}$ is obtained by analogy from the equation for the hydrocarbon chain.

$$\overline{r_f^2} = 2nl_0^2 \tag{7}$$

where n is the number of freely rotating links of fixed tetrahedral angle along the network chain and l_0 is the length of these links.

The equivalent values of n_0 and l_0 to be used in the above equation were obtained from the basic formula of the network chain.

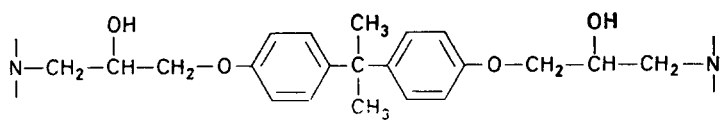

We took the value of n to be 12, with due consideration of the rigidity of each benzene ring. The average value of the 'bond length' l_0 (1·96 Å) was computed by adding up the total length of the completely linear chain from tabulated bond lengths and dividing by 12. The calculated $\overline{r_f^2}$ is $9{\cdot}18 \times 10^{-15}$ cm.

We should add that the modulus in the rubbery plateau region increases linearly with temperature but is not strictly proportional to absolute temperature.

CONCLUSIONS

(*1*) It can be clearly seen on the plots of 10 sec Gehman modulus versus temperature that all four resins have a transition region around 140°C and that they have a very definite rubbery plateau region.

(*2*) The agreement between the values for the 'front factor' obtained from experiments and the ones calculated from theory is quite good and the results show that the chains in the resin network are stretched, because the front factors are greater than unity.

Frick Chemical Laboratory,
Princeton University,
Princeton, New Jersey, U.S.A.

(*Received May 1962*)

REFERENCES

[1] TOBOLSKY, A. V., KATZ, D., THACH, R and SBHAFFHAUSER, R. *J. Polym. Sci.* 1962, **62,** 174
[2] 'Epon Resins for Structural Uses'. *Shell Tech. Bull. SC:60–39* Rev.
[3] SKEIST, I. *Epoxy Resins,* pp 23–24. Reinhold: New York, 1959
[4] LEE, H. and NEVILL, K. *Epoxy Resins, Their Application and Technology,* p 42. McGraw-Hill: New York, 1957
[5] *A.S.T.M. Standards on Rubber Products, 550,* Designation D1053–58 (1958)
[6] SHEN, M. and TOBOLSKY, A. V. Unpublished results
[7] TOBOLSKY, A. V. *Ph.D. Thesis,* Princeton University, 1944
[8] GREEN, M. S. and TOBOLSKY, A. V. *J. chem. Phys.* 1946, **14,** 80

The Glass Transition Temperature of Polymeric Sulphur

A. V. TOBOLSKY, W. MACKNIGHT, R. B. BEEVERS and V. D. GUPTA

Pure polymeric sulphur free of dissolved S_8 monomer is a semi-crystalline polymer with a T_g of 75°C. Quick-quenched (from 200°C) elastic sulphur, if maintained under conditions which prevent crystallization, is a solution of polymeric sulphur and S_8 rings, both polymer and monomer being in an amorphous state. The T_g of this plasticized polymer is −30°C.

THE most common form of elemental sulphur is rhombic sulphur whose molecules are composed of S_8 rings arranged in a rhombic crystalline lattice. Rhombic sulphur is in equilibrium with another crystalline variety, the monoclinic form, at 96°C, but the rate of the conversion is rather slow. Rhombic sulphur melts at 112·8°C, in equilibrium with S_λ. Monoclinic sulphur melts at 119·2°C to form S_λ. S_λ is a liquid composed almost entirely of S_8 molecules. When this liquid is heated to 160°C there occurs a very sharp 'transition' readily detected experimentally by an enormous increase in viscosity. Above 160°C sulphur exists as a liquid mixture of S_8 molecules together with linear polymeric species, which are in fact polymeric diradicals. The S_8 rings and the various diradical chains exist in thermodynamic equilibrium. The mathematical treatment of this equilibrium has been completely worked out[1,2], and the temperature of 160°C corresponds to a 'floor temperature,' below which no polymeric species are present in appreciable quantities[3]. As the temperature is increased above 160°C the relative proportion of polymer to S_8 monomer increases, but the average molecular weight of the polymeric fraction decreases[1].

Elastic sulphur, frequently called 'amorphous' sulphur, is prepared by quickly quenching sulphur which has been heated above 160°C, usually in the range of 200° to 250°C. The process of quick quenching temporarily freezes the equilibrium situation pertaining to the higher temperature. At 200°C the equilibrium weight fraction of polymer is 0·26. Quick quenching also temporarily freezes the amorphous physical state of the mixture of polymer and monomer which pertains to the mixture existing at the higher temperature.

The amorphous character of quick-quenched sulphur will be maintained almost indefinitely if the substance is kept below its glass transition temperature, which is approximately −30°C. This value was first obtained by Mondain-Monval[4] by following the change in specific volume with temperature. We repeated this measurement and obtained a value of −30°C as compared to the value of −29°C reported by Mondain-Monval.

When amorphous quick-quenched sulphur is heated above −30°C, there occurs a process of crystallization which becomes increasingly rapid at

higher temperatures, especially above $-10°C$. It is possible, however, by working very rapidly in the temperature range $-30°C$ to $-10°C$, to study the properties of 'amorphous' sulphur in a truly amorphous condition where it exhibits definite elastic behaviour.

It seems probable that the crystallization which occurs rapidly above $-10°C$ consists of a partial crystallization of the S_8 rings in the mixture to rhombic sulphur as well as a crystallization of the polymeric species to 'ω-sulphur'. The partially crystallized mixture is no longer elastic and no longer amorphous, though often still referred to as 'amorphous sulphur'.

The designation 'ω-sulphur' was used by Das and Gosh[5] to describe the structure of the insoluble residue left after extracting quick-quenched ('amorphous') sulphur with carbon disulphide, which removes the monomeric S_8 rings. The remaining insoluble polymer is semi-crystalline, and ω-sulphur was indeed characterized by its X-ray diagram.

Prins, Schenk and Wachters[6] determined the structure of fibrous sulphur formed by stretching 'amorphous' sulphur. The X-ray diagram indicated the presence of two modifications, 'γ-sulphur' (essentially ordered S_8 rings) and a constituent designated 'ψ'. Prins *et al.* compared the powder diffraction pattern of 'ψ' with the data of Das and Gosh on 'ω' and found the two to be essentially identical, the small differences observed being due to the stretched condition of ψ-sulphur.

Prins *et al.* also suggested that the commercially available sulphur sold under the trade name of Crystex[7] is essentially ω-sulphur. In *Table 1* the

Table 1. X-ray spacings in polymeric sulphur (Å)

	Das and Gosh (*ω-sulphur*)	*Prins* et al. (*ψ-sulphur*)	*Authors* (*Crystex*)
1.	4·50	—	4·50
2.	4·02	4·17 4·08 } Triplet 3·96	4·09
3.	3·56	3·54	3·54
4.	3·07	—	3·02
5.	2·71	—	2·75
6.	2·30	—	—
7.	2·10	—	—

line spacings obtained from an X-ray diagram of Crystex have been compared with those obtained by Das and Gosh from ω-sulphur and those of ψ-sulphur from the data of Prins *et al.* It is seen that all three correspond quite closely if account is taken of the differences that may be induced by stretching. Although Crystex is nearly pure polymeric sulphur, it was further purified by removing small quantities of S_8 monomer by extracting the commercially available sample with carbon disulphide.

It is wished to emphasize here the contrast between the structure and properties of quick-quenched elastic ('amorphous') sulphur on the one hand and pure polymeric sulphur on the other.

By quick-quenched elastic sulphur is meant the mixture of polymeric sulphur and S_8 rings which is obtained by heating sulphur to 200° to 250°C, quick quenching to $-70°C$ and maintaining both the polymer and the

dissolved monomer (S_8 rings) in a completely amorphous condition by never allowing the temperature of the mixture to rise above $-10°C$, nor to remain at any temperature above $-30°C$ for a prolonged time.

In contrast pure polymeric sulphur in the form of extracted Crystex was considered. This polymer, containing little or no dissolved monomer, is in a semi-crystalline state.

Studies were made of the specific volume versus temperature and also the modulus versus temperature of these two forms of sulphur. The modulus measurements were made ten seconds after application of load and were obtained with the Clash–Berg and Gehman torsion testing devices[9]. The specific volumes were measured by the method of immersion.

For these measurements thin rectangular bars of the quick-quenched elastic sulphur were obtained by transferring the hot (200°C) sulphur (kept in porcelain moulds) into dry ice. Crystex is obtained commercially in the form of a powder. It was press moulded into thin rectangular bars at 75° to 80°C followed by annealing for seven hours at 70°C.

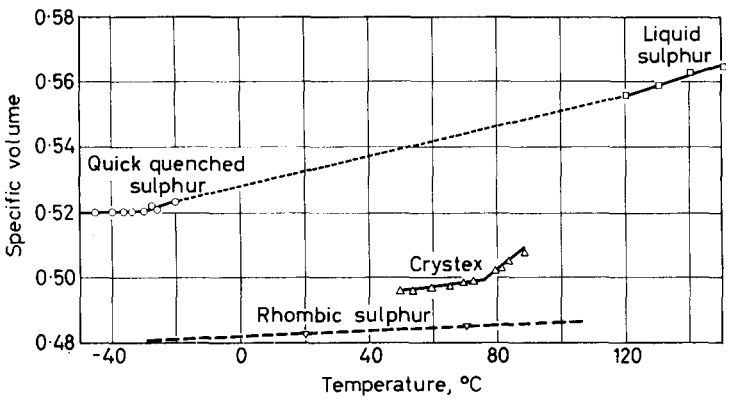

Figure 1—Specific volume versus temperature curves for quick-quenched elastic sulphur, liquid monomeric sulphur, Crystex and rhombic sulphur

Figure 1 shows the specific volume versus temperature curves of rhombic sulphur[10], liquid sulphur[11], quick-quenched (from 200°C), elastic sulphur and purified Crystex.

The specific volume versus temperature curve of the quick-quenched elastic sulphur shows a change in slope at $-30°C$, corresponding to the T_g of this dissolved mixture of polymer and monomer. It is very interesting that the specific volume versus temperature curve of liquid monomeric sulphur can be extrapolated fairly smoothly to the corresponding data for quick-quenched elastic sulphur. It has previously been shown that the density of ring molecules in the liquid phase is very close to the density of the corresponding 'infinite' linear polymer in its amorphous condition[12].

The specific volume of Crystex is much smaller than the interpolated density of amorphous sulphur rings or chains. This is consistent with the semi-crystalline nature of Crystex, which is pure polymeric sulphur. The specific volume versus temperature curve of Crystex shows a change of

slope at 75°C, corresponding to its glass transition temperature. The curve could not be carried above 90°C because at this point the transition of the polymeric sulphur to monomeric rhombic sulphur becomes rapid[7]. Sometimes in highly crystalline polymers the value of T_g is difficult to determine by specific volume measurements because the inflection on the specific volume versus temperature curve (contributed only by the amorphous regions) is not very pronounced. This was not so here; the inflection is very definite as seen in *Figure 1*.

It is assumed that if polymeric sulphur could be obtained in a wholly amorphous form, its T_g value would be the same as that determined on the semi-crystalline Crystex. This situation holds true in many other polymers.

The modulus/temperature curve of quick-quenched elastic sulphur (*Figure 2*) shows the characteristic behaviour of an amorphous polymer or a plasticized amorphous polymer. There is a glassy region of high modulus, a sharp transition region starting at T_g (−30°C), followed by a rubbery plateau region. The rubbery plateau region just barely becomes evident when unfortunately the polymer–monomer mixture begins to crystallize and the measurements become meaningless in this context.

The modulus/temperature curve of Crystex (*Figure 2*) shows a glassy region below about 75°C, followed by the beginning of a transition region.

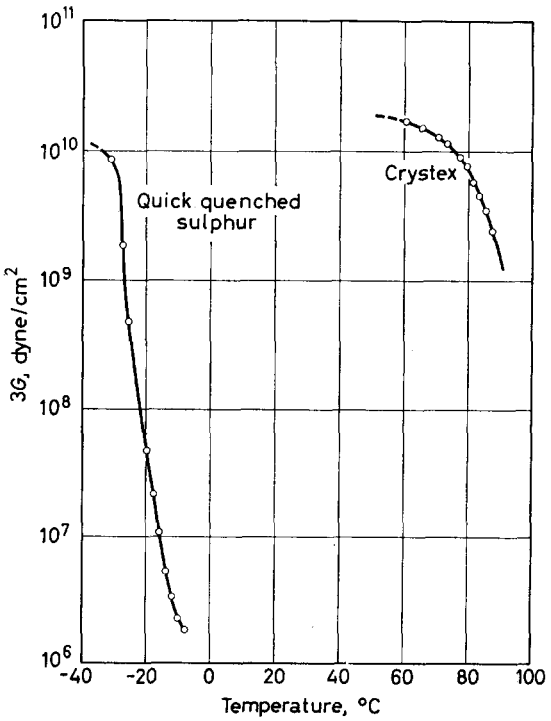

Figure 2—Modulus/temperature curves for quick-quenched elastic sulphur and for *Crystex*

In a crystalline polymer the transition region is very broad extending between T_g and the melting point T_m. Unfortunately, the melting point of polymeric sulphur cannot be determined directly, because the transition to rhombic sulphur becomes rapid above 90°C. For this reason, and because relaxation due to chemical interchange interferes with the measurement, the modulus/temperature curves for Crystex had to be terminated below 90°C.

It is concluded that pure polymeric sulphur free of dissolved S_8 monomer is a semi-crystalline polymer with a T_g of 75°C. Quick-quenched (from 200°C) elastic (or 'amorphous') sulphur, if maintained under conditions which prevent crystallization, is a solution of polymeric sulphur and S_8 rings, both polymer and monomer being in an amorphous state. The T_g of this plasticized polymer is −30°C.

Frick Chemical Laboratory,
Princeton University,
Princeton, New Jersey, U.S.A.

(*Received October 1962*)

REFERENCES

[1] TOBOLSKY, A. V. and EISENBERG, A. *J. Amer. chem. Soc.* 1959, **81,** 780
[2] GEE, G. *Trans. Faraday Soc.* 1952, **48,** 515
[3] TOBOLSKY, A. V. and EISENBERG, A. *J. Colloid. Sci.* 1962, **17,** 49
[4] MONDAIN-MONVAL, P. *Ann. Chim.* 1935, **3,** 5
[5] DAS, S. R. and GOSH, K. *Indian J. Phys.* 1939, **13,** 91
[6] PRINS, J. A., SCHENK, J. and WACHTERS, L. H. J. *Physica, 's Grav.* 1957, **23,** 746
[7] Stauffer Chemical Company, *Technical Data Sheet No. 717 Y*
[8] A.S.T.M. *Book of Standards* 1958, D 1053–58 T
[9] A.S.T.M. *Book of Standards* 1958, D 1043–51
[10] TULLER, W. N. (Ed.) *Sulfur Data Book.* McGraw-Hill: New York, 1954
[11] FEHER, F. and HELLWIG, E. *Z. anorg. Chem.* 1958, **294,** 63
[12] TOBOLSKY, A. V., LEONARD, F. and ROESER, G. P. *J. Polym. Sci.* 1948, **3,** 604

*Aminolysis of Polyethylene Terephthalate**

H. ZAHN and H. PFEIFER

By treating polyethylene terephthalate fibres with solutions of hydrazine, benzylamine, ethylenediamine, hexamethylenediamine, piperidine and aniline the following amides of terephthalic acid and oligomeric diacids have been obtained: terephthalic dihydrazide, terephthalic bis-benzylamide, bis-benzylamides of oligomers, probably dimer and pentamer, and mixtures of oligomeric bis-ethylenediamides. The existence of the latter amides has not yet been confirmed by synthesis.

IN THIS paper the following abbreviations are used:

Bz— denotes $C_6H_5CH_2$—
—T— denotes —OC—C_6H_4—CO—
—G— denotes —OCH_2CH_2O—
—Et— denotes —$HNCH_2CH_2NH$—

During investigations of the changes in fibre properties after treatment with various agents the effect of some organic bases (amines) on polyethylene terephthalate (PET) fibres was studied. These investigations seemed to be of great interest because organic amines are becoming progressively more important in the fields of surface-active agents, stabilizers, reducing agents and dyestuffs.

The recent paper by Farrow *et al.*[1] on the isolation of *N,N'*-dimethyl terephthalamide by degradation of PET with methylamine has prompted this report on similar experiments with other amines. In this paper only such experiments which were successful in isolating definite materials from the treated fibres are described. The effects on fibre properties during the treatment with organic bases have been published[2].

EXPERIMENTAL

Sample preparation

PET filaments (Diolen 100/36/7–1/2S) without delustring or other agents were washed in a solution containing 3g/l. sodium carbonate and 2g/l. non-ionic detergent (Hostapal CV) for 30 min at 60°C, rinsed with water and air dried. Before treatment the samples were dried in a drying oven at 150°C for one hour.

Degradation of the samples

Samples were degraded for 2, 4, 8, 16 and 32 hours in 10, 40 and 80 per cent w/w aqueous hydrazine hydrate (at 35°, 65° and 95°C), 10, 50 and 100 per cent benzylamine, 1, 10, 50 and 100 per cent ethylenediamine, 10, 50 and 100 per cent hexamethylenediamine, 1 and 100 per cent aniline and 100 per cent piperidine.

*XXXIII. Communication on oligomers. XXXII. Communication on oligomers *see* G. HEIDEMANN and H. ZAHN, *Makromol. Chem.* 1963, **62**, 123.

After the reaction the fibre was extracted to constant weight with dilute acetic acid (2 ml/l.) at room temperature, rinsed with distilled water and air dried.

By using the more drastic treatments, substantial amounts of the fibres were dissolved and non-fibrous (powdery) solids could be isolated from the amine solutions.

RESULTS

Hydrazine

By treating the fibres with 80 per cent w/w aqueous solution of hydrazine hydrate at 35°C for two hours or with 40 per cent solution at 65°C for four hours, a powdery substance was formed which, after washing with water in the centrifuge to neutral reaction, was recrystallized from benzyl alcohol and water. The elementary analysis of the material shows that it is terephthalic dihydrazide. For $C_8H_{10}O_2N_4$:

	C	H	N
Calc.	49·48	5·20	28·85 per cent
Found	49·60	5·47	28·43 per cent

There was no depression of the mixed melting point with the dihydrazide synthesized from dimethylterephthalate and hydrazine at 135°C in a Carius tube. The isolated and the synthetic dihydrazide gave the same X-ray powder diagram and infra-red absorption spectrum.

Benzylamine

The crystalline powders obtained from two treatments of the fibre with benzylamine (four and eight hours at 95°C) were separated as described above. They showed elementary analysis corresponding to oligomeric benzylamides of dicarboxylic acids. These dicarboxylic acids are described by Zahn and Seidel[3]. For $C_{72}H_{60}O_{22}N_2$, Bz·NH—T·(G—T—)$_5$·HN·Bz (four hours treatment):

	C	H	N
Calc.	66·20	4·60	2·15 per cent
Found	63·77	4·68	2·29 per cent

For $C_{42}H_{36}O_{16}N_2$, Bz·NH—T·(G—T—)$_2$·NH·Bz (eight hours treatment):

	C	H	N
Calc.	69·22	4·98	3·84 per cent
Found	67·72	4·94	3·39 per cent

The analysis does not enable an unambiguous identification to be made but the constitution is probably not very different from that indicated. The synthesis of the dibenzylamides of the oligomeric dicarboxylic acids is to be investigated.

On allowing the centrifugate obtained on separation of the oligomeric amides to stand for several days at room temperature, a crystalline solid precipitated and was filtered off. As the elementary analysis shows, it is terephthalic dibenzylamide. For $C_{22}H_{20}O_2N_2$:

	C	H	N
Calc.	76·73	5·85	8·13 per cent
Found	76·70	5·81	8·01 per cent

The dibenzylamide synthesized from terephthalic acid using the method of mixed anhydrides by Boissonnas[4] showed the same melting point (269°C), X-ray powder diagram and infra-red absorption spectrum as the isolated material.

Ethylenediamine

By treating the fibre for 32, 6 and 4 hours at 35°, 65° and 95°C with 100, 100 and 50 per cent ethylenediamine respectively, three different crystalline powders of low solubility which did not melt up to 360°C and became reddish coloured above 300°C were isolated in the usual way.

The material from the treatment of 32 hours at 35°C with 100 per cent amine shows, after recrystallization from dimethylsulphoxide, the same elementary analysis as an amide of an oligomeric dicarboxylic acid H·Et—T—G—T—Et·H. For $C_{22}H_{26}O_6N_4$:

	C	H	N
Calc.	59·71	5·92	12·67 per cent
Found	59·34	5·91	12·05 per cent

The other two fractions are not yet homogeneous, since the value for N increases by recrystallization. The amine–N is too low for the required formula, the main amount of N is found to be amide–N in the chain, so that it is possible that the material is an oligamide mixture.

A synthesized mono-amide of terephthalic acid and ethylenediamine behaved similarly to the products described above.

The other amines

The effects of hexamethylenediamine, piperidine and aniline were much less than those of the previously mentioned bases. From these experiments no definite products of degradation have been obtained so far.

DISCUSSION

Examination of the results obtained shows that aminolysis of PET by organic amines is accompanied by a real formation of amide bonds. The PET fibres may be degraded to oligoester-amides and, under drastic conditions, finally to diamides of terephthalic acid.

We have to thank the Hessischen Minister für Wirtschaft und Verkehr and the Arbeitsgemeinschaft Industrieller Forschungsvereinigungen (AIF), Köln (Forschungsvorhaben J 277) for their support of this work.

Deutsches Wollforschungsinstitut an der
Rheinisch-Westfälischen Technischen Hochschule Aachen,
Veltmanplatz, Aachen, Germany

(Received November 1962)

REFERENCES

[1] FARROW, C., RAVENS, D. A. S. and WARD, I. M. *Polymer, Lond.* 1962, **3,** 17
[2] PFEIFER, H. *Forschungsberichte des Wirtschafts- und Verkehrsministeriums Nordrhein-Westfalen, No. 1212,* 1963
[3] ZAHN, H. and SEIDEL, B. *Makromol. Chem.* 1959, **29,** 70
[4] BOISSONNAS, R. A. *Helv. chim. Acta,* 1951, **34,** 874

Molecular Motion in Polyethylene, IV

D. W. McCall and D. C. Douglass

The proton magnetic resonance spin-lattice and spin-spin relaxation times T_1 and T_2, have been measured for various polyethylenes as a function of temperature. Transient methods were employed. The data are discussed in terms of methyl group rotations, corresponding to T_1-minima below $-100°C$, and liquid-like molecular motions, associated with T_1 minima near $-30°C$. The importance of spin diffusion is emphasized.

This paper describes an experimental study of the proton magnetic resonance spin-lattice relaxation time, T_1, and spin-spin relaxation time, T_2, for various polyethylenes as a function of temperature.

THE MATERIALS

A Union Carbide Corporation material, designated DYNK, was chosen as a typical branched, high pressure polyethylene. Its room temperature density is about 0·92 g/cm^3 and it is thought to have 20 to 30 methyl groups per 1 000 carbon atoms. Results for DYNK were unchanged by melting the sample. A Phillips Petroleum Company polymer, Marlex-50, type 6 000, was chosen as a typical linear, low pressure material. Its room temperature density is about 0·96 g/cm^3 for the pellets as received. Results for Marlex were also unchanged on melting, subsequent cooling, and re-examination. The same Marlex linear polymer was also prepared by precipitation from 0·04 per cent xylene solution at 80°C. The crystals were allowed to settle and then filtered at 80°C. This solution crystallized material was found to be lamellar by electron microscopy. On melting and subsequent examination the relaxation time curves become indistinguishable from those for the original pellets. The Marlex material was also prepared by bulk crystallization at 150°C by application of about 2 000 atm pressure. This material has a room temperature density of about 0·99 g/cm^3. On melting (at atmospheric pressure), cooling and subsequent re-examination, this material exhibits different relaxation curves but the effect has not yet been studied in detail. Polymethylene, prepared by the gaseous decomposition of CH_2N_2, has been studied as an example of a very high molecular weight, linear polymer. The flocculent material, as received, and the same specimen studied again after melting, yielded utterly different relaxation time curves. Finally, pure n-$C_{94}H_{190}$, which was kindly made available by Professor J. A. Dixon of Pennsylvania State University, was studied for comparison. This substance gave similar relaxation curves before and after melting.

THE SPECTROMETER

The pulsed spectrometer used in this study has been described in detail previously[1,2]. The only significant alteration was the addition of a circuit

at the receiver input to reduce saturation of the receiver by the radio-frequency pulses. With this circuit, and a minor modification of the receiver gain control, recovery times of 4–7 μsec (following a 3 μsec pulse) were achieved. A typical decay curve is shown in *Figure 1*. The ordinate is proportional to the precessing nuclear moment and the abscissa is in time (10 μsec/division).

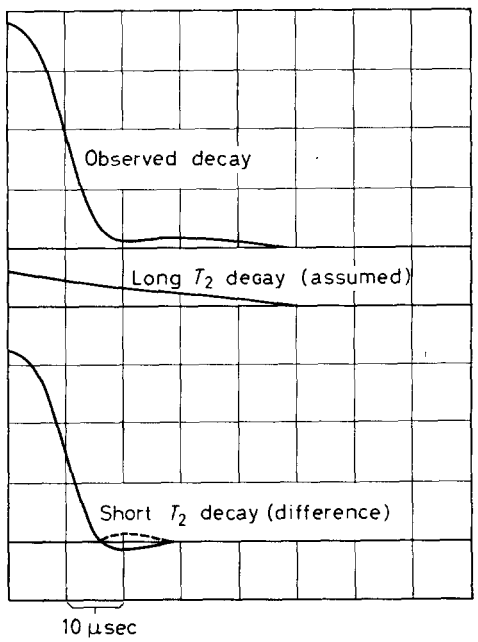

Figure 1—Schematic representation of a decay curve following a 90° pulse. The top curve is typical of those observed in polyethylene. The middle curve is an exponential decay fitted to the long time behaviour of the top curve. The bottom curve is the difference between the top and middle curves. When the negative portion is inverted (dashed portion), the bottom curve resembles the low temperature decay curves obtained experimentally. The abscissa scale is 10 μsec/division

ANALYSIS OF DATA

When the resonance absorption has a Lorentzian shape the nuclear signal following a pulse decays exponentially with a time constant T_2. T_2 is called the spin-spin relaxation time and is approximately equal to $2/\gamma\ \delta H$ where δH is the absorption resonance width and γ the gyromagnetic ratio.

In actual fact most polymers do not have Lorentzian resonances and their decay signals are not exponential. At low temperatures the decays are more nearly Gaussian corresponding to Gaussian resonance shapes. In this case the decay time is also roughly equal to $1/\gamma\ \delta H$. In fact $T_2 \sim 1/\gamma\ \delta H$ is a fundamental relation that is not dependent upon the details of the line shape because it has been shown[3], quite generally, that the decay curves are Fourier transforms of the resonance absorption shapes. Therefore, the convenient but arbitrary measure of T_2 as $t_1/\ln 2 = t_{\frac{1}{2}}/0{\cdot}692$, where $t_{\frac{1}{2}}$ is the time required for the decay signal to fall to half its maximum value, has been adopted.

Frequently the nuclear signal is a superposition of two decay curves and it is appropriate to assign two distinct T_2s. This distinction has only been made when the separation is rather obvious, that is when the two decay times differ by at least a factor of two. The problem of decomposing a

decay curve is illustrated in *Figure 1*. The observed decay (for Marlex pellets at 24°C) is shown at the top. In the middle is an exponential decay that matches the observed decay at large time values. At the bottom appears the difference signal that is similar to the low temperature signals observed for the same material. (It should be noted that the detector of the spectrometer used yields only positive signals so the negative region of *Figure 1* would appear inverted, as indicated in the dashed curve.) A 'beat' structure is often observed at low temperatures but the absorption shape that corresponds to a given decay curve is by no means obvious. It should be noted that the presence of a weak long T_2 signal increases the apparent 'beat' period.

T_1 is measured by means of a 180°–90° pulse sequence. If the 90° pulse comes a time t after the 180° pulse, and t is varied until the nuclear signal following the 90° pulse is zero, say at t_{null}, it can be shown that $T_1 = t_{\text{null}}/\ln 2 = t_{\text{null}}/0{\cdot}692$. This method has been used throughout this study. When two T_2s are appropriate it sometimes happens that two T_1s are also appropriate. This is signalled by the impossibility of adjusting the 180°–90° pulse separation to produce a zero nuclear signal after the 90° pulse (see *Figure 2*). If the signal is made zero immediately after the pulse a signal builds up later. If the later signal is made zero there is a signal immediately after the pulse. The t_{null} corresponding to the later signal is a good measure

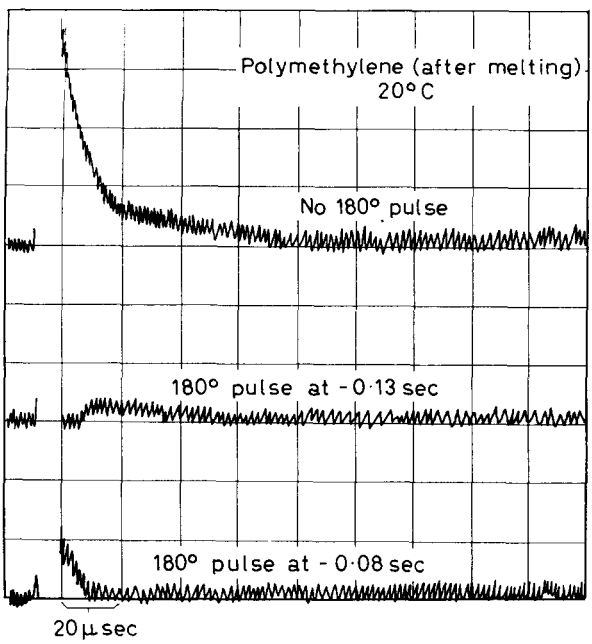

Figure 2—Typical decay curves following the 90° pulse in the T_1 measuring sequence. No 180° pulse precedes the top trace, a 180° pulse occurs at −0·13 sec in the middle trace, and a 180° pulse occurs at −0·08 sec in bottom trace. The abscissa scale is 20 μsec/division

of T_1 for the nuclei with long T_2s. However, t_{null} corresponding to the early signal is only a very approximate (sometimes even poor) measure of T_1 for the nuclei with short T_2s. In spite of this, as the T_1s are not normally too different, $T_1 = t_{null}/0{\cdot}692$ is used. In the examples reported here T_1 for the short component will be somewhat smaller than the true value.

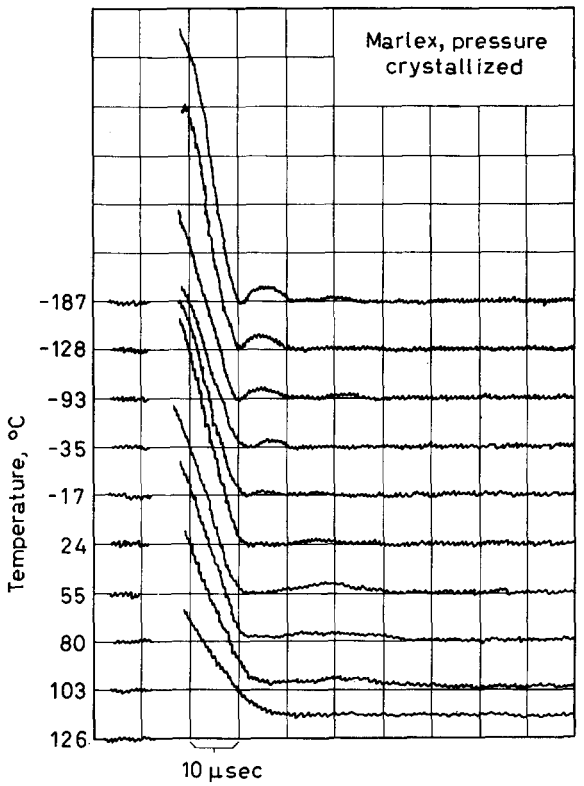

Figure 3—Oscilloscope traces of decay signals following a 90° pulse for pressure crystallized Marlex. The abscissa scale is 10 μsec/division

RESULTS AND DISCUSSION

Typical experimental decay curves are exhibited in *Figure 3*. The figures are taken from oscilloscope traces, and they are displaced vertically to distinguish the various temperatures. The trace always begins about 5 to 10 μsec before the pulse is applied. This serves to establish the baseline. The pulse is of about 3 μsec duration and an additional 4 to 7 μsec elapses before the receiver recovers. The nuclear signal then follows. It should be remembered that the detector used is such that all signals are presented as positive. Also, small signals are somewhat distorted by the 'square law' behaviour of the crystal detector used.

Rather similar decay curves are observed for all materials studied. At low temperatures a 'beat' structure is observed, which suggests that the nuclear

signal is negative in the region from about 15 to 30 μsec after the pulse (see *Figure 1*). The temperature above which the existence of 'beats' cannot be detected varies from material to material. An extremely rough estimate of this temperature is given in *Table 1*. This temperature is expected to be high when the material is highly crystalline and the crystals allow no molecular motion. However, this parameter has not been fully appreciated as yet. There is an obvious correlation of this temperature with the temperature at which one can begin to measure two T_2s (see *Table 1*).

Table 1
(Table entries are temperatures in °C)

Material	*'Beats'*	*Two T_2s*	*T_1 minima*		
DYNK	−20	−20	−130	−20	+40 (broad)
Marlex pellets	+100	+70	−140 (maybe)	−30 >	+120
Marlex (solution crystalized)	+100	+120	−120 (maybe)	−20	+120
Marlex (pressure crystallized)	+120	+100	−130 (maybe)	−30 >	+130
Polymethylene (as received)	+60	+120	< −130 (broad)	−10 >	+140
Polymethylene (after melting)	−70	−60	—	−30	—
n-$C_{94}H_{190}$	+80	>+110	−130	— >	+110

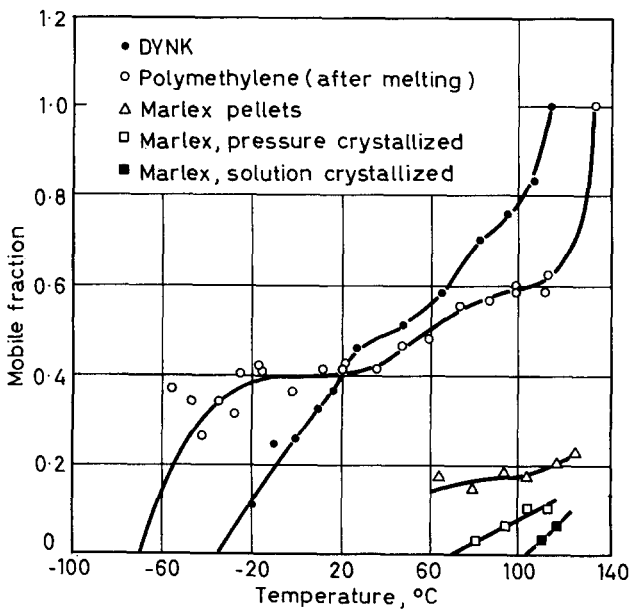

Figure 4—Mobile fractions, derived from the intercepts of the decay curves, as a function of temperature

Figure 4 exhibits the 'mobile fractions' derived from the decay curves such as those shown in *Figure 3*. 'Mobile fraction' is reported only in cases

where a definite long T_2 signal is observed and it is defined as the long T_2 intercept divided by the total decay curve intercept.

The term 'intercept' indicates the nuclear signal extrapolated to the end of the pulse. Some error is involved in this procedure but the quoted 'mobile fractions' should be good to within a few per cent. The 'mobile fraction' for Marlex pellets found here (0·15) agrees well with the 'mobile fraction' found by steady-state methods for the same material[4]. The significance of this parameter has previously been emphasized and discussed[4-6].

Relaxation time/temperature diagrams are shown in *Figures 5–11*. Considering that these materials are all solids with the same chemical structure, $(CH_2)_n$, the differences are remarkable. The T_2 curves are, in essence, reciprocal plots of the absorption width and, owing to extensive published discussions of resonance widths, T_1 results will be emphasized in this paper.

Table 1 lists temperatures for T_1 minima. It will be recalled that a T_1 minimum indicates that the motion responsible for relaxation has a correlation frequency about equal to the resonance frequency (in this case 3×10^7 c/s). Detailed examination of the curves will reveal the approximate nature of several of the temperatures listed. As it is believed that the relaxation times are strongly influenced by spin diffusion a brief digression to describe this phenomenon qualitatively follows.

The nuclear resonance experiments measure two relaxation times, T_1, the spin-lattice relaxation time, and T_2, the spin-spin relaxation time. T_1 is the characteristic time required for the nuclear spin system to transfer

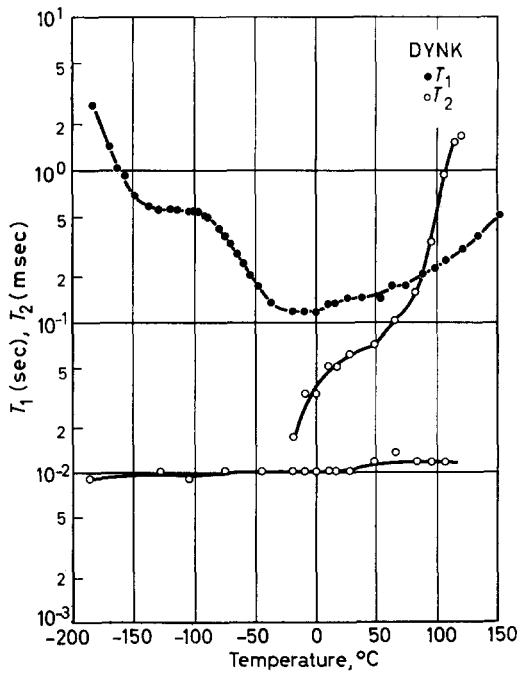

Figure 5—T_1 (sec) and T_2 (msec) for DYNK as a function of temperature

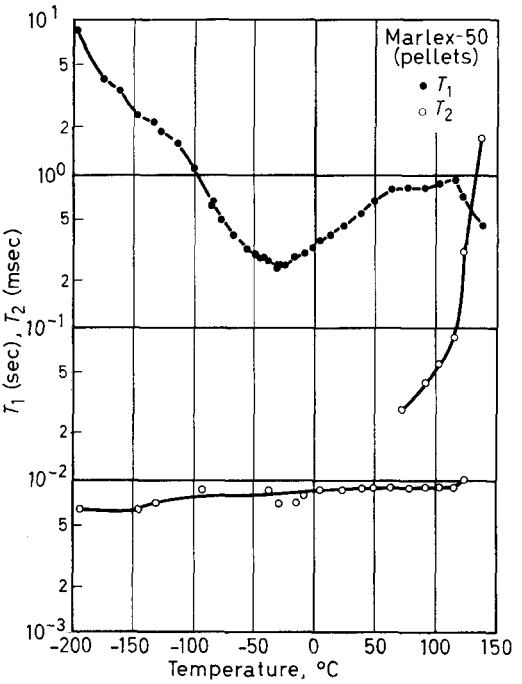

Figure 6—T_1 (sec) and T_2 (msec) for Marlex pellets as a function of temperature

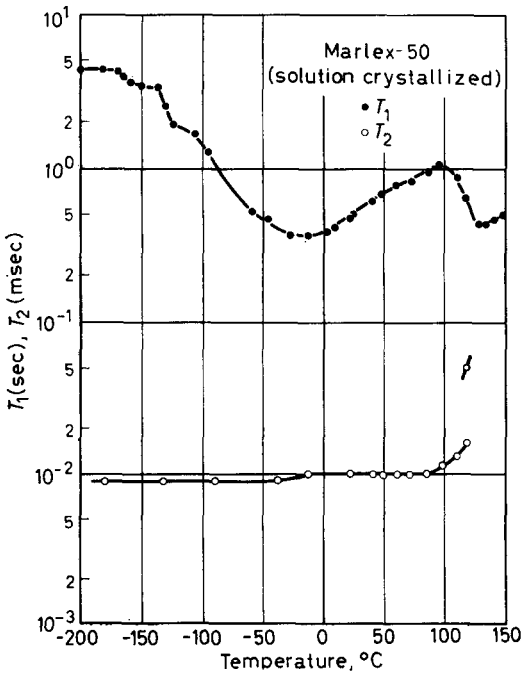

Figure 7—T_1 (sec) and T_2 (msec) for solution crystallized Marlex as a function of temperature

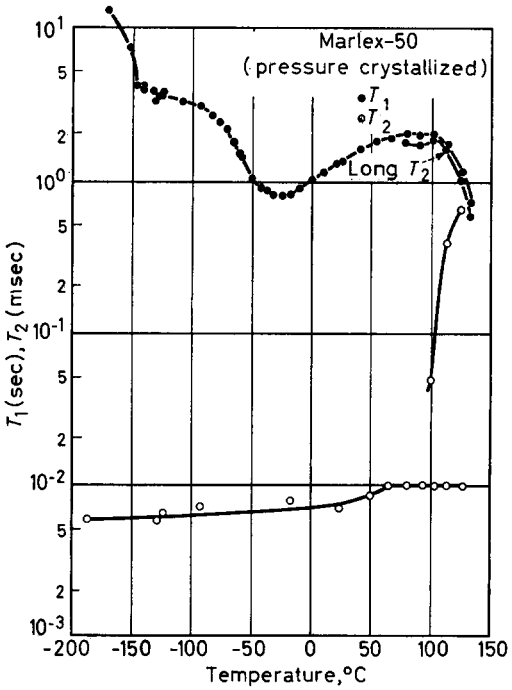

Figure 8—T_1 (sec) and T_2 (msec) for pressure crystallized Marlex as a function of temperature

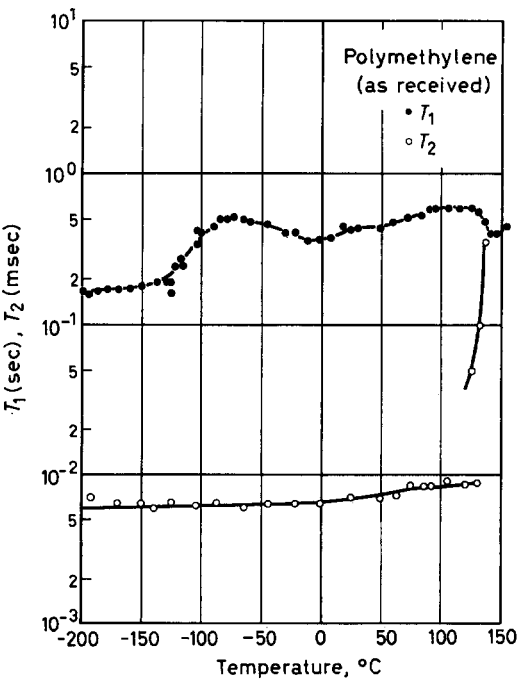

Figure 9—T_1 (sec) and T_2 (msec) for polymethylene (as received) as a function of temperature

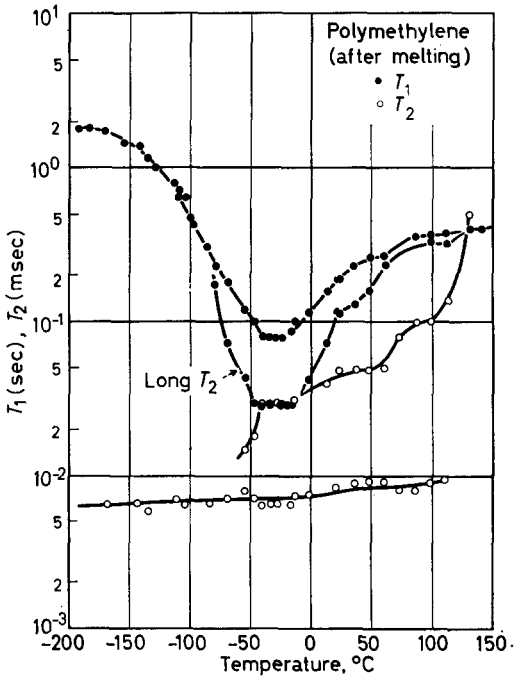

Figure 10—T_1 (sec) and T_2 (msec) for polymethylene (after melting) as a function of temperature

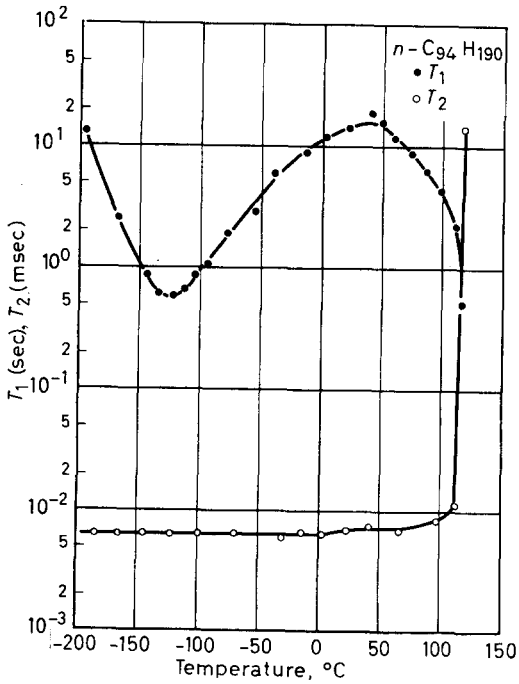

Figure 11—T_1 (sec) and T_2 (msec) for n-$C_{94}H_{190}$ as a function of temperature

energy into the thermal motions of the polymer molecules. If $T_2 \ll T_1$, as it is in polymers, T_2 represents the characteristic time for free energy to move from one part of the spin system to another. Under the condition that $T_2 \ll T_1$, energy put into the spin system by means of a radio-frequency magnetic field will remain in the spin system for a time long compared to T_2 and the possibility of energy diffusing from one region of the spin system to another before it is dissipated into the heat motion of the molecules can be visualized. In some types of molecular systems T_1 and T_2 may vary from place to place within a sample. Regions near paramagnetic impurities and lattice imperfections or segments of unusual and favourable mobility may well have very short T_1s relative to the remainder of the lattice and in these regions energy flows rapidly from the spin system into the heat motion of the sample. When this situation arises energy will flow through the spin system and be funnelled into the thermal sink through the regions with short T_1s.

This behaviour is analogous to the diffusion of molecules in a container which has a few small holes through which molecules can escape and be lost to the system. Because of the analogy between the diffusion of molecules within the container and the behaviour of energy in the spin system this phenomenon is called spin diffusion[7-9].

A more direct analogy, that has been treated in detail[7], is the case of nuclear relaxation in ionic lattices when dominated by the presence of paramagnetic impurities. Impurities can dominate T_1 even though they are present at very low concentration.

In polymers different molecular segments have different degrees of motional freedom. For these polymers, the nuclei that are able to move can exchange energy more effectively with the lattice than the fixed nuclei. However, the mobile nuclei are coupled to adjacent fixed nuclei so that the fixed nuclei can relax by transferring their energy to the mobile nuclei which, in turn, transmit the energy to the lattice. When $T_2 \ll T_1$ the number of mobile nuclei does not have to be great. That is to say, spin polarization can diffuse over relatively large distances to find a mobile molecule.

At low temperatures, i.e. below $-100°C$, the principal motion is probably methyl rotation. This motion does not involve the heavy carbon nuclei and can occur by quantum mechanical tunnelling. It is almost certainly a jump-wise rotation between potential energy minima. If there are only three minima (one for each hydrogen) they will be of equal depth and no mechanical loss will be associated with the motion. However, if there are six (or more) minima there may be two sets with different energies and mechanical loss would be anticipated.

The association of the low temperature relaxation specifically with methyl rotations is based on the following considerations. First, Slichter[10] and Kawai[11] have observed T_1 minima in the same temperature range in polymers that have methyl branches, such as polypropylene. Secondly, the n-$C_{94}H_{190}$ and DYNK exhibit almost identical T_1 curves in the low temperature range and these materials should have about the same concentration of methyl groups. Thirdly, the more linear materials show much less efficient relaxation in this region.

It is, of course, anticipated that chain ends emerging from crystal surfaces

might be subject to rather weak constraints and, consequently, be able to move at relatively low temperatures. This may provide an explanation for the very strange T_1 behaviour observed for polymethylene, as received (*Figure 9*). This material is flocculent and may have a large surface area. On the other hand, the constancy of T_2 and the persistence of the 'beats' to high temperature leads to the suggestion that only a small fraction (less than 0·1 per cent) of the molecular segments have motional freedom. These two seemingly contradictory statements are compatible provided T_1-relaxation occurs by spin-diffusion to the few mobile sites.

At higher temperatures, say about $-30°C$, liquid-like motions in the amorphous regions establish the dominant T_1-mechanism. It should be noted that n-$C_{94}H_{190}$ does not show a T_1 minimum in this region, consistent with the fact that this material has no amorphous content. Again, spin diffusion keeps T_1 for the crystalline regions almost, but not quite, as short as T_1 for the amorphous regions. In all cases the shorter T_1 is associated with the longer T_2. Actually, the measurements only point to a distribution of T_1s rather than two distinct values. Where two values are reported they indicate the rough range of T_1. Nevertheless, the shorter T_1s are associated with the longer T_2s.

It should also be noted that methyl motions at about $-130°C$ and the liquid-like motions at about $-30°C$ have reached an average frequency of 3×10^7 c/s. Thus, the liquid-like motions are to be associated with the motions responsible for the low frequency dynamic mechanical loss maxima observed below $-100°C$[12,13]. If there is a low frequency loss maximum corresponding to methyl rotation it would be expected to appear at very low temperatures. As far as is known dynamic mechanical measurements have not been carried below $-200°C$.

At temperatures above 0°C the behaviour becomes more complicated. Branched polyethylenes are known to exhibit a dynamic mechanical loss maximum near 0°C for frequencies near 10^2–10^3 c/s[13]. This loss has thus been associated with branch point motions. There is evidence for a distribution of T_1s for DYNK in the range 0° to 100°C.

At temperatures just below the melting point several of the linear specimens have T_1s that decrease with increasing temperature. This might be the result of premelting reorientations within the crystals or recrystallization phenomena of the type described by Statton and Geil[14], by Peterlin *et al.*[15] and by Slichter and Davis[16,17]. With n-$C_{94}H_{190}$, *Figure 11*, the increase is certainly the result of reorientations within the crystals. The decay curves for n-$C_{94}H_{190}$ also change shape in this region.

A type of motion that is qualitatively consistent with the magnetic resonance data may be described as follows. It must be assumed that the molecules occupy their crystallographic positions most of the time and also that the molecules can make quick reorientations (by 180° or 360°) about their long chain axes. Rotations of this sort can cause T_1 minima without greatly affecting T_2 as shown by Holcomb[18].

In closing, the results will be compared with previous measurements. Earlier measurements of T_1 versus temperature for a branched polyethylene have been reported by Wilson and Pake[19]. Their results show a pronounced T_1 minimum near $-20°C$, in agreement with the results presented herein,

but the absolute value of T_1 at the minimum is almost an order of magnitude lower than our result. Professor R. E. Norberg of Washington University, St Louis, provided a substantial amount of T_1 and T_2 data for polyethylene as measured by pulse techniques[20]. He measured the same sample used by Wilson and Pake and obtained results similar to those shown in *Figure 5*, i.e. $T_1 \sim 10^{-1}$ sec at the minimum. Wilson and Pake[19] employed steady-state saturation methods and saturation measurements of complex resonances are difficult to analyse. The authors tend to favour the pulse measurements.

The authors are indebted to their colleagues Dr W. P. Slichter and Dr S. Matsuoka for many illuminating discussions. Dr W. P. Slichter first pointed out the possible importance of spin diffusion. Professor R. E. Norberg kindly made available a considerable amount of unpublished data. They are indebted to Dr W. P. Slichter, Dr R. Salovey, Dr S. Matsuoka, and Professor J. A. Dixon for providing the materials studied.

Bell Telephone Laboratories, Inc.,
Murray Hill, New Jersey, U.S.A.

(*Received November 1962*)

REFERENCES

[1] SCHWARTZ, J. *Rev. sci. Instrum.* 1957, **28,** 780
[2] McCALL, D. W. and ANDERSON, E. W. To be published
[3] LOWE, I. J. and NORBERG, R. E. *Phys. Rev.* 1957, **107,** 46
[4] McCALL, D. W. and ANDERSON, E. W. *J. Polym. Sci.* 1963, **1A,** 1175
[5] SLICHTER, W. P. and McCALL, D. W. *J. Polym. Sci.* 1957, **25,** 230
[6] WILSON, C. W. III and PAKE, G. E. *J. Polym. Sci.* 1953, **10,** 503
[7] BLOEMBERGEN, N. *Physica, 's Grav.* 1949, **15,** 386
[8] BLUMBERG, W. E. *Phys. Rev.* 1960, **119,** 79
[9] ABRAGAM, A. *Principles of Nuclear Induction.* Oxford University Press: London, 1961
[10] SLICHTER, W. P. *Proceedings* of meeting of Division of Polymer Chemistry of American Chemical Society, p 87*, September 1962
[11] KAWAI, T. *J. phys. Soc. Japan,* 1961, **16,** 1220
[12] SCHMIEDER, K. and WOLF, K. *Kolloidzschr.* 1953, **134,** 149
[13] KLINE, D. E., SAUER, J. A. and WOODWARD, A. E. *J. Polym. Sci.* 1956, **22,** 455
[14] STATTON, W. O. and GEIL, P. H. *J. appl. Polym. Sci.* 1960, **3,** 357
[15] PETERLIN, A., KRASOVEC, G., PIRKMAJER, E. and LEVSTEK, J. Kurzmitteilung 1A3 to *I.U.P.A.C. Symposium, Wiesbaden, Germany, October 1959*
[16] SLICHTER, W. P. *J. appl. Phys.* 1960, **31,** 1865
[17] SLICHTER, W. P. and DAVIS, D. D. *J. appl. Phys.* 1963, **34,** 98
[18] HOLCOMB, D. F. and PEDERSON, B. *Bull. Amer. phys. Soc.* Ser. II, 1961, **6,** 103; *J. chem. Phys.* 1962, **36,** 3270
[19] WILSON, C. W., III and PAKE, G. E. *J. chem. Phys.* 1957, **27,** 115
[20] NORBERG, R. E. Private communication

A New Transition in Polystyrene

Part I—A Transition of Polystyrene Common to the Bulk and Molecularly Dispersed Phases

G. MORAGLIO and F. DANUSSO

Following the observation of a peculiar variation with temperature of the average radius of gyration of isotactic and atactic polystyrenes in solution and of the second virial coefficient, dilatometric observations show that critical transition phenomena undoubtedly take place both in toluene solutions and in bulk and that the transition temperature is localized between 47° and 55°C.

IN 1961 Reiss and Benoit[1] observed a peculiar variation with temperature of the average radius of gyration of isotactic and atactic polystyrenes in solution and of the second virial coefficient; both were determined by light scattering measurements. This peculiarity appeared with a maximum followed by a minimum, or vice versa, which were about 15°C apart, at different temperatures depending on the polymeric samples, between about 40° and 100°C.

The phenomenon observed might be considered as a transition of the conformational type, that is to say analogous to helix–coil shape transitions, already observed in proteins, and generally caused by changes of medium.

However, it might be a transition of a different type, occurring in the polymer on a molecular scale, but corresponding to a transition that can be observed also in the pure polymer in bulk. If this is so, and if the transition is of intramolecular type, the temperature (or the range of temperature) of transition should not be very different in bulk and in the molecularly dispersed phases of the polymer itself.

According to this hypothesis it has been investigated whether: (*a*) the transition observed by Reiss and Benoit was detectable in diluted solutions of polystyrene in toluene by dilatometry; and (*b*) the transition probably observed in the solutions occurred also in polystyrene in bulk.

In fact, a transition is actually detectable by dilatometry in both cases, provided that the accuracy of measurements is raised to about $\pm 10^{-5}$ of volume[2].

Due to the interest aroused by this topic, the results of some preliminary determinations using a capillary dilatometer with an upside-down bulb of appropriate size and with mercury as dilatometric liquid, are reported here. The heights of mercury were observed in each run systematically every twenty minutes, after heating or cooling steps of 0·5°C. *Table 1* summarizes the results of a series of runs; *Figure 1* records the nature of experimental curves of runs 5 and 10 (heights in the capillary versus temperature).

Taking into account that runs were performed at a constant, relatively high rate of heating or cooling, from the data of *Table 1* the following may be deduced:

Table 1

Run	*Polystyrene*	*Solvent (and percentage concentration of polymer)*	*Range of temperature (°C) explored*	*Transition*
1	Isotactic (fraction) M=300 000	Toluene (0·5)	43–55	Little scattering of volume data between 48° and 51° and apparent slight increase of temperature coefficient after transition
2	Isotactic (fraction) M=300 000	Toluene (0·5)	42–70	Only little scattering around 50°
3	Isotactic (fraction) M=80 000	Toluene (1·0)	42–58	Evident, critical loss of volume between 53·5° and 54·5°, permanent after transition
4	Run 3 repeated (after one night at 33°)			Small, critical loss of volume between 52·5° and 54·5°, permanent after transition
5	Run 4 repeated (after 10 days at room temperature)			Evident, critical loss of volume between 49° and 52°, permanent after transition (see *Figure 1*)
6	Atactic $\overline{M}_v$=300 000	Toluene (1·0)	42–58	Little scattering with a transitory increase of volume between 48·5° and 53°
7	Run 6 repeated (after 7 days at room temperature)			Little scattering producing a small, permanent loss of volume between 48° and 52·5°
8	Atactic $\overline{M}_v$=300 000	None	42–55	Little scattering (transitory decrease of volume followed by transitory increase) between 47·5° and 50·5°
9	Run 8 repeated (after 10 days at room temperature)			No noticeable transition phenomenon
10	Atactic $\overline{M}_v$=300 000	None	41–55	By heating: identical to run 8; by cooling: reversed transformation between 48·5° and 46°. Changes of volume by standing (see *Figure 1*: from A heating to B; from B overnight to C; cooling to D; overnight to E)

(*a*) Critical transition phenomena undoubtedly take place both in toluene solutions and in bulk in the temperature ranges explored, appearing as transitory or permanent changes of volume.

(*b*) Transition temperature (or interval of temperature) appears to be localized between about 47° and 55°C (when less evident preferably placed around 50°C), not so different for isotactic or atactic polystyrene and for toluene solutions or bulk.

(*c*) Relaxation phenomena and the smallness of volume changes make the identification of the transition and the reproducibility of the results difficult, so that no quantitative conclusions are possible as yet, which can

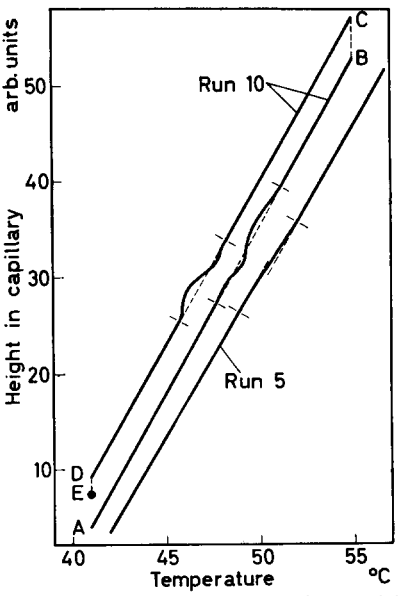

Figure 1—Results of runs 5 and 10 (*Table 1*). Heating from A to B; resting overnight from B to C; cooling to D; overnight to E

distinguish the dependence of the amplitude and of the shape of transition on the usual variables and on the steric structure of the polymer. Further extensive experiments are therefore necessary in order to obtain definitive conclusions.

Part II—A Transition of Atactic Polystyrene in Bulk

U. BIANCHI and C. ROSSI

Further experimental evidence is presented on the transition atactic polystyrene presents at about 50°C. The average value of the internal pressure has been determined and it is noted that the transition is detectable in the solid state at a temperature lower than the glass transition temperature, thus confirming the picture of an intramolecular rather than an intermolecular transition.

SOME experimental evidence has been given on a transition which atactic polystyrene should present at about 50°C. This evidence was based on measurements of end-to-end behaviour at different temperatures[1], temperature coefficient of limiting viscosity number[3], X-rays, nuclear resonance and

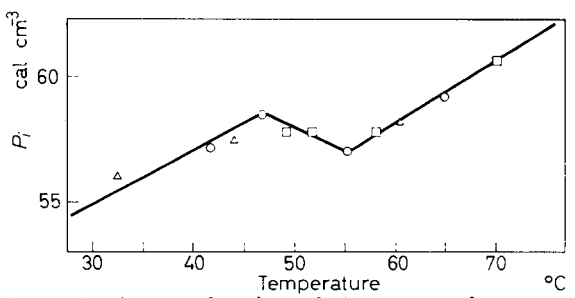

Figure 2—P_i as a function of temperature for atactic polystyrene

mechanical properties[4], expansion coefficient of polystyrene solutions (Part I of this paper) and temperature coefficient of optical density of isotactic polymer in decalin (Part III of this paper). It is apparent therefore that this transition is characteristic of the polystyrene chain, being independent of the state (bulk or solution) in which polystyrene is studied.

To confirm this point and the existence of a transition, some measurements have been recorded of internal pressure[5], $P_i\,[=(\partial U/\partial V)_T]$, on a sample of atactic polystyrene; $\overline{M}_v = 7{\cdot}4 \times 10^5$ in a temperature range 30° to 70°C. The volume of the sample was kept constant through this temperature interval. This required pressure to be increased with temperature; the initial and final conditions were ($V = V_0$, $t = 32$°C, $p = 123{\cdot}7$ atm) and ($V = V_0$, $t = 70$°C, $p = 488$ atm). P_i values are shown in *Figure 2*.

From the figure it is apparent that there is a transition in the range 47° to 55°C, which compares well with the temperature found in the above mentioned experiments. Some conclusions which can be drawn from these results are given below:

(*a*) It is confirmed that P_i is sensitive to any change of molecular arrangement in the system under examination[8]. It should be recalled, for instance, that published measurements of thermal expansion coefficient on polymer in bulk have never shown any indication of a transition at 50°C.

(*b*) The average value of P_i (*ca.* 58 cal cm^{-3}) in the temperature range explored compares well with the results obtained by Allen *et al.*[6] on the behaviour of P_i through a glass transition. P_i in the glassy state has been found to be about 40 to 50 per cent less than in the rubbery state. Whereas the above value refers to the glassy state, that reported by Allen *et al.*[7] ($P_i = 103$ cal cm^{-3}) refers to the liquid state, having been obtained by measurements on a very low molecular weight sample.

(*c*) It is very interesting to note that the transition is detectable in the solid state at a temperature lower than the glass transition temperature ($T_g = 105$°C for the molecular weight used). This should confirm the picture of an intramolecular rather than intermolecular transition.

A discussion of the significance of this conclusion in regard to a study of chain mobility below the glass temperature and a complete description of the experimental technique will appear elsewhere[7].

Part III—The Temperature Coefficient of the Optical Density in the Ultra-violet of Isotactic Polystyrene in Decalin

A. M. LIQUORI and F. QUADRIFOGLIO

The optical density of a solution of isotactic polystyrene in decalin presents some anomaly around 50°C. By integrating evidence from various sources with experimental results, the existence of some kind of thermal transition in polystyrene solutions is considered very likely.

IN Part II of this paper Bianchi and Rossi reported the variation of the internal pressure of atactic polystyrene showing evidence of a transition

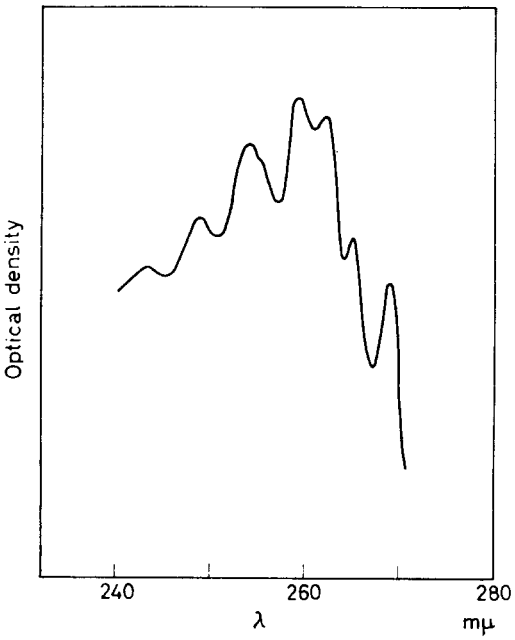

Figure 3—Ultra-violet absorption spectrum of isotactic polystyrene solution in decalin

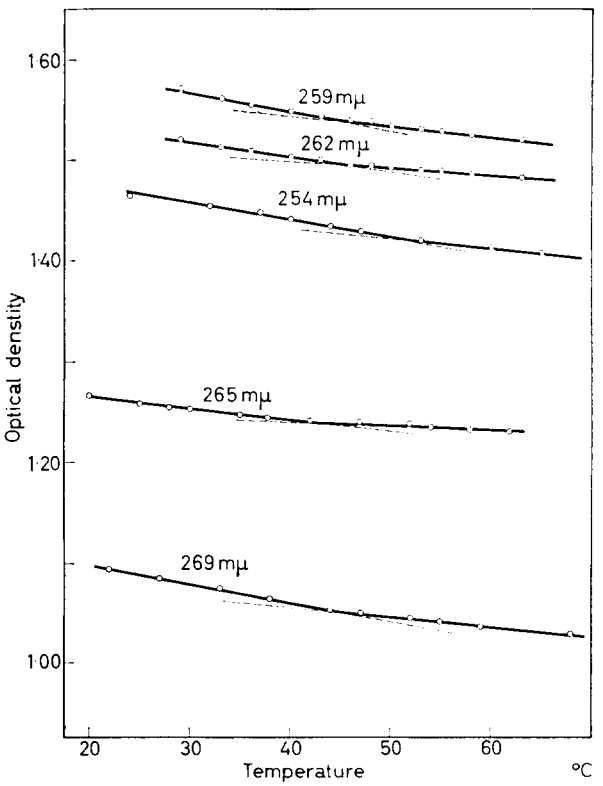

Figure 4 — Optical density at various wavelengths of isotactic polystyrene solution in decalin as a function of temperature

which apparently takes place around 50°C. It has also been observed that the optical density of a solution of isotactic polystyrene in decalin presents some anomaly around this temperature.

This effect is observable by comparison of almost all the characteristic peaks in the absorption band of the u.v. spectrum of this polymer (see *Figures 3* and *4*). With atactic polystyrene in the same solvent there is a higher degree of uncertainty in trying to locate a discontinuity.

By integrating the evidence of Bianchi and Rossi on bulk polystyrene with the various reports on polystyrene solutions quoted in Part II of this paper and with the above described results the existence of some kind of thermal transition in polystyrene solutions is considered very likely.

It should also be mentioned that very strong evidence of conformational transformations in solution has been obtained by Urazovskii and Slyusarov[8] for other polymers.

However, in order to draw definite conclusions it would be highly desirable to carry out independent measurements in various laboratories on standard samples of atactic and isotactic polystyrene.

Istituto di Chimica Industriale,
Centro Nazionale di Chimica delle Macromolecole, Sezione I, C.N.R., Politecnico, Milano, Italy
Istituto di Chimica Industriale,
Centro Nazionale di Chimica delle Macromolecole, Sezione V, C.N.R., Genova, Italy
Istituto Chimico dell'Universitá di Napoli,
Centro Nazionale di Chimica delle Macromolecole, Sezione III, C.N.R., Napoli, Italy

(*Received November 1962*)

REFERENCES

[1] REISS, C. and BENOIT, H. *C.R. Acad. Sci., Paris,* 1961, **253,** 268
[2] DANUSSO, F. Discussion in *Polymer, Lond.* 1962, **3,** 485
[3] BIANCHI, U., CUNIBERTI, C. and DELLEPIANE, G. *Ric. sci.* In press
[4] KILIAN, H. G. Discussion in *J. Polym. Sci.* 1962, **57,** 106
[5] ALLEN, G., GEE, G., MANGARAY, D., SIMS, D. and WILSON, G. J. *Polymer, Lond.* 1960, **1,** 467
[6] ALLEN, G., SIMS, D. and WILSON, G. J. *Polymer, Lond.* 1961, **2,** 375
[7] BIANCHI, U. and ROSSI, C. *Chim. e Industr.* 1963, **45,** 33
[8] URAZOVSKII, S. S. and SLYUSAROV, I. I. *Vysokomol. Soedineniya,* 1961, **3,** 420

Free Radical Reactions in Irradiated Polyethylene

M. G. ORMEROD

Different samples of the same polyethylene have been irradiated at 77°K. They were then warmed to room temperature and the decay of the free radicals in them was followed using electron spin resonance. By using samples which had different ratios of sample weight to container volume it was found that the rate of radical decay was linearly dependent on the pressure of the radiation-induced hydrogen gas above the sample. Since the number of cross-links formed was unaffected it is concluded that the hydrogen gas was increasing radical mobility.

SINCE the discovery of crosslinking in polyethylene[1], its radiation chemistry has aroused considerable interest. Recently several studies have been made using electron spin resonance (e.s.r.)[2–6]. It has been shown that irradiation produces two different free radicals—a short lived alkyl radical and a longer lived allyl radical[2]. The stability of the alkyl radical depends on the crystallinity of the sample and its pre-irradiation history[3,4]. Dole and Cracco[7] introduced deuterium above some freshly irradiated polyethylene and observed hydrogen–deuterium exchange which lasted for a time approximately equivalent to the life of the alkyl radical. They suggested that radiation-produced hydrogen reacts with the alkyl radicals and that the pressure of hydrogen above a sample would affect the radical decay rate. In this paper data are presented which confirm this suggestion and which give the dependence of radical decay rates on hydrogen pressure for a particular polyethylene.

EXPERIMENTAL

All e.s.r. measurements were made with a conventional high frequency (400 kc/s) modulation X-band spectrometer which has been fully described elsewhere[3].

The polyethylene used was a high molecular weight, high density Ruhrchemie product—RCH 1 000. It was in the form of a fine powder.

The samples were contained in glass tubes of known volume. They were irradiated at 77°K with ^{60}Co γ-rays. During irradiation the sample was in one end of the tube, and was then examined in the spectrometer in the other end. This was to avoid observing the unpaired spins in the irradiated glass. All e.s.r. measurements were made at room temperature.

The hydrogen above the samples was produced by the irradiation of the polyethylene sample. The pressures were calculated by assuming a G value of three for hydrogen formation[8] (G value is the number produced per 100 eV of absorbed radiation), and knowing the sample weight, the volume of the sample container, and the radiation dose.

Radical concentrations were determined by double integration of the derivative curve and by comparison with a coal sample which had been

calibrated against α,α′-diphenyl-β-picrylhydrazyl. The area of the spectrum obtained from an alkyl radical was related to the height of one of its outermost lines so that the alkyl radical concentration could be determined in the presence of allyl radicals.

Polymer solubilities were determined using a Soxhlet apparatus through which nitrogen gas was passed to avoid oxidation. The samples were placed in metal gauze thimbles and extracted for eight hours, and then dried in a vacuum oven.

KINETIC ANALYSIS OF THE DATA

The two major chemical changes produced in polyethylene by ionizing radiation are the formation of transvinylene double bonds and of crosslinks. It has been shown that the double bonds are formed at 77°K at which temperature the free radicals in polyethylene are stable[8]. This suggests that the radical reactions give rise to crosslinks rather than double bonds. Furthermore, Koritskii *et al.*[4] have found that for the same type of polyethylene $G_{(\text{radicals})}$ equalled twice $G_{(\text{crosslinks})}$. Their values for $G_{(\text{radicals})}$ were similar to those measured since by others[3,6].

Charlesby *et al.*[3] have studied two paraffins (n-$C_{36}H_{74}$ and n-$C_{34}H_{70}$) and an olefin (n-17-$C_{35}H_{70}$) using e.s.r. The paraffins behaved in the same way as polyethylene but the olefin showed some interesting differences. The low temperature spectrum of the olefin arose from alkyl radicals plus allyl radicals. On warming to room temperature the alkyl radical concentration decreased but the allyl radical concentration increased by a factor of about two. They interpreted this as being due to the reaction

$$—CH_2—\dot{C}H—CH_2 + —CH_2—CH{=}CH— \longrightarrow —CH_2—CH_2—CH_2— + —\dot{C}H—CH{=}CH—$$

and suggested that this was evidence for radical migration in solids. They postulated that radical migration, as suggested by Koritskii *et al.*[4], accounted for radical decay in polyethylene. The envisaged reaction was

$$—CH_2—\dot{C}H—CH_2— + —CH_2—CH_2—CH_2— \longrightarrow —CH_2—CH_2—CH_2 + —CH_2—\dot{C}H—CH_2—$$

When two radicals gain sufficient spatial proximity they combine to give a crosslink. This evidence also suggests that the allyl radicals in polyethylene are formed by the reaction of an alkyl radical with a double bond. In light of the evidence quoted above the following reaction scheme is postulated:

$$—CH_2—CH_2—CH_2— \longrightarrow —CH_2—\dot{C}H—CH_2— + H\cdot$$

$$—CH_2—CH_2— \longrightarrow —CH{=}CH— + H_2$$

$$2\,(—CH—) \longrightarrow \text{crosslink} \qquad (1)$$

$$—\dot{C}H— + —CH{=}CH—CH_2— \longrightarrow —CH_2— + —CH{=}CH—\dot{C}H— \qquad (2)$$

$$—\dot{C}H— + —CH{=}CH—\dot{C}H— \longrightarrow \text{crosslink} \qquad (3)$$

Referring to an alkyl radical (—$\dot{C}$H—) as R_1, to an allyl radical (—CH=CH—$\dot{C}$H—) as R_2, and to a double bond as U, we have the kinetic equations governing radical decay:

$$d[R_1]/dt = -k_1[R_1]^2 - k_2[R_1][U] - k_3[R_1][R_2] \quad (1')$$

$$d[R_2]/dt = k_2[R_1][U] - k_3[R_1][R_2] \quad (2')$$

Unfortunately these equations have no simple solution. However, during the early stages of the decay, $[R_2]$ will be small and reaction (3) will be comparatively unimportant. Ignoring the term $k_3[R_1][R_2]$ and assuming that [U] is constant the above equations yield the solution

$$\frac{1}{[R_1]_t} + \frac{k_1}{k_2[U]} \Big/ \frac{1}{[R_1]_0} + \frac{k_1}{k_2[U]} = e^{k_2[U]t} \quad (3')$$

This can be re-written as

$$\ln(\{1/[R_1]_t\} + a) = k_2[U]t + \text{constant} \quad (4')$$

where $a = k_1/k_2[U]$.

For all the samples $\ln(\{1/[R_1]_t\} + a)$ was plotted against t. The value of a was chosen by trial and error in each case. The slope of the straight line obtained gave $k_2[U]$. [U] was calculated by assuming a G value for double bond formation of three[8] and hence k_2 was found. The value of a was then used to calculate k_1. Owing to the large value of a, this gave a comparatively imprecise value of k_1, but as it was found that $k_2 \sim k_1 \times 10^{-2}$, during the initial part of the decay the term $k_2[U][R_1]$ could be ignored since $[U]_0 \sim [R_1]_0$. Therefore, $d[R_1]/dt = k_1[R_1]^2$ and $1/[R_1]_t - 1/[R_1]_0 = k_1 t$. A plot was also made of $1/[R_1]$ versus time from which k_1 was calculated.

From equation (2') it can be seen that $[R]_2$ has a stationary value when $[R_2] = k_2[U]/k_3$. This allows k_3 to be estimated from a plot of $[R_2]$ against time.

Points observed at zero time, i.e. measurements made at 77°K before warming to room temperature, were not plotted for two reasons. The first is that the above analysis only holds for a random distribution of radicals, and the initial distribution is probably not random, in a similar fashion to that in irradiated ice[9]. The second reason is that since radical decay is due to radical mobility[3,4], the reactions will be diffusion controlled and it has been shown that during the initial stages of a diffusion-controlled reaction the reaction constant varies with time[10]. It is assumed that the radical distribution was random and that the reaction constant had reached a steady value by the time the first room temperature reading had been taken, i.e. after two to four minutes.

EXPERIMENTAL RESULTS

Figure 1 shows the result of plotting $\ln(\{1/[R_1]\}_t + a)$ against time for three of the samples, and *Figure 2* shows plots of $1/[R_1]$ against time. Straight line plots were obtained in agreement with the above theory. All the samples studied gave similar lines. *Table 1* gives the k_1 and k_2 values for different

Table 1

Dose *Mrad*	*Hydrogen pressure* *mm* Hg	k_1 *(radical)*$^{-1}$ *g* s^{-1}	k_2 *(double bonds)*$^{-1}$ *g* s^{-1}
50	25	4×10^{-24}	3×10^{-26}
28	35	5×10^{-24}	3×10^{-26}
28	70	7×10^{-24}	5×10^{-26}
28	57	9×10^{-24}	7×10^{-26}
28	260	4×10^{-23}	2×10^{-25}
26	145	$1{\cdot}7\times10^{-23}$	1×10^{-25}
26	230	$2{\cdot}5\times10^{-23}$	$1{\cdot}5\times10^{-28}$
26	350	3×10^{-23}	2×10^{-25}
24	50	9×10^{-24}	7×10^{-26}
9	100	3×10^{-23}	2×10^{-25}

hydrogen pressures. *Figure 3* shows k_1 plotted against the hydrogen pressure. Over the range studied the points lie on a straight line, so that $k_1\times10^{-23}=1{\cdot}1p+0{\cdot}2$, where p is the hydrogen pressure, in millimetres of mercury, and k_1 is in radicals^{-1} g s^{-1}. This means that the radicals decay more rapidly in the presence of hydrogen.

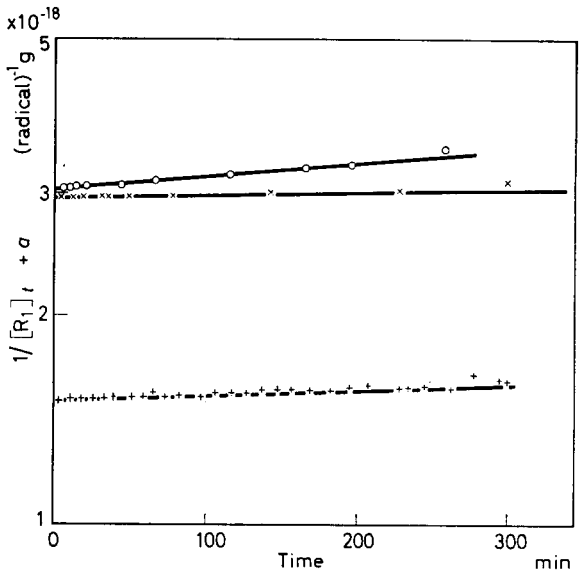

Figure 1—Decay in concentration of alkyl radicals [R_1] in polyethylene at room temperature. For description of *a*, see text. + Radiation dose 50 Mrad, hydrogen pressure 25 mm Hg, $a=1{\cdot}5\times10^{-18}$. × Radiation dose 28 Mrad, hydrogen pressure 35 mm Hg, $a=2{\cdot}9\times10^{-18}$. ○ Radiation dose 26 Mrad, hydrogen pressure 230 mm Hg, $a=3{\cdot}0\times10^{-18}$

From *Table 1* it can be seen that k_1/k_2 is constant and equals 130 ± 20. Only with the sample which had been given a dose of 50 Mrad were the data sufficiently precise to allow k_3 to be estimated. The value obtained was 2×10^{-24}.

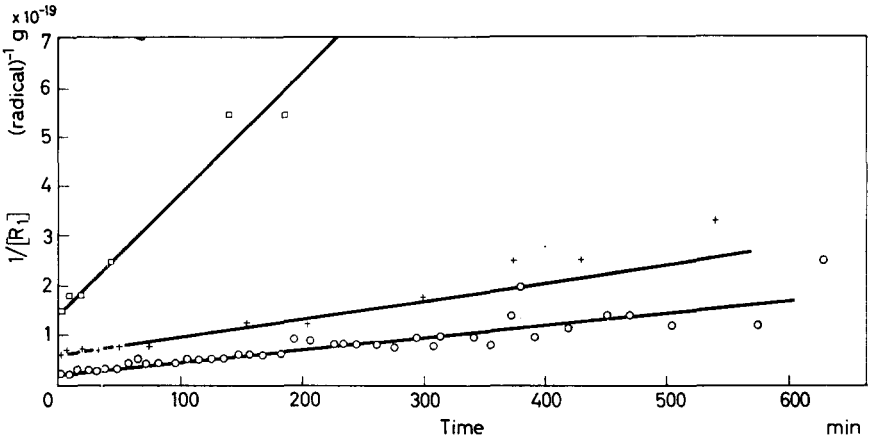

Figure 2—Decay of alkyl radicals in polyethylene at room temperature. ○ Radiation dose 50 Mrad, hydrogen pressure 25 mm Hg. + Radiation dose 28 Mrad, hydrogen pressure 35 mm Hg. □ Radiation dose 28 Mrad, hydrogen pressure 260 mm Hg

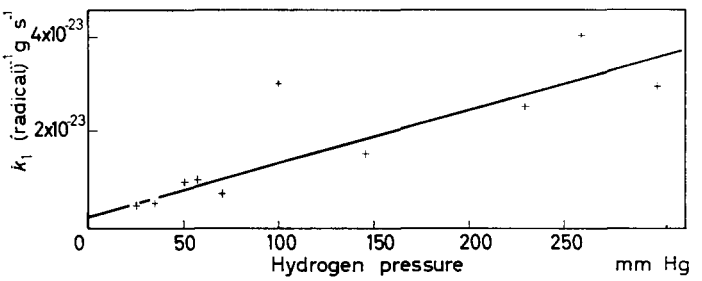

Figure 3—Second order decay constant, k_1, for alkyl radicals in polyethylene versus pressure of hydrogen gas above sample

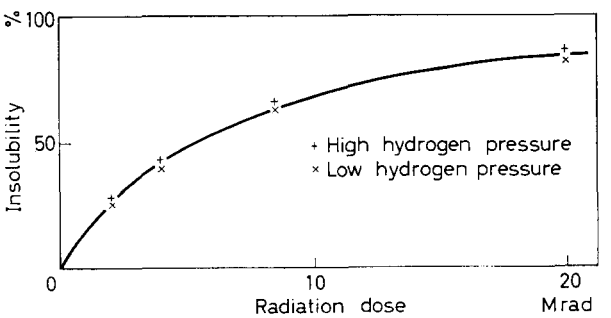

Figure 4—Polymer insolubility versus radiation dose for two samples of polyethylene in which the pressure of radiation-produced hydrogen differed by a factor of four

Measurements of solubility versus dose were made on two polyethylene samples in which the ratio of sample weight to container volume differed by a factor of four. Any differences between the two samples were within experimental error (see *Figure 4*) showing that the presence of radiation-induced hydrogen does not affect the number of crosslinks formed.

DISCUSSION

It is well known that free radicals in the solid state can travel inter- and intra-molecularly. Charlesby *et al.*[3] have followed the formation of allyl radicals from alkyl radicals in the solid olefin 17-pentatriacontene; Ormerod and Alexander[11] have observed the transfer of radicals from irradiated nucleoprotein to added cysteamine, and Henriksen and Pihl[12] have studied radical migration in glutathione. The question still remains unanswered as to how the radical can move.

This work has shown that the presence of hydrogen plays an important role in radical mobility. Dole and Cracco[7] have shown that when deuterium is introduced above an irradiated sample the following reactions occur:

$$R\cdot + D_2 \longrightarrow RD + D\cdot \tag{4}$$

$$D\cdot + RH \longrightarrow DH + R\cdot \tag{5}$$

They also found that the reaction $D\cdot + R\cdot \longrightarrow RD$ is negligible. This suggests that similar reactions occur involving hydrogen and that they offer one mechanism whereby free radicals can migrate. One drawback is that if two polymer radicals are to gain sufficient spatial proximity to combine, when reaction (4) has occurred it is to be expected that the reaction $R'\cdot + D\cdot \longrightarrow R'D$ would take place in preference to reaction (5). This would give a reduction in the amount of gas above the sample and a reduction in crosslinking—effects which are not observed. This objection can be overcome by postulating that reactions (4) and (5) do not occur separately but via a three-body complex, so that a hydrogen atom is never free to combine with a nearby free radical. The envisaged reaction is

$$R\cdot + H_2 + RH \longrightarrow [R\cdots H{-}H\cdots H{-}R] \longrightarrow RH + H_2 + R\cdot \tag{6}$$

Lawton *et al.*[6] observed radical decay although their samples were kept in a stream of nitrogen gas so that there was zero hydrogen pressure above them. Also the results presented here indicate that there is still radical decay at zero pressure. Therefore it seems that there is some second mechanism for radical mobility. This is possibly a straightforward hydrogen transfer reaction, i.e.

$$R\cdot + R'H \longrightarrow RH + R'\cdot \tag{7}$$

To summarize, the results presented here show that the presence of hydrogen has a marked effect on radical decay rates in polyethylene. It is suggested that in the absence of hydrogen, radicals can move via reaction (7) above and that this reaction is faster if a hydrogen molecule is involved, in which case a three-body complex possibly occurs as an intermediary. Similar reactions probably account for radical migration in other solid compounds.

The author thanks Professor A. Charlesby for the helpful discussions he had with him, and Mr M. R. Clay for making the solubility measurements on the irradiated polyethylenes.

Physics Branch,
Royal Military College of Science,
Shrivenham, Wiltshire

(*Received November 1962*)

REFERENCES

[1] CHARLESBY, A. *Proc. Roy. Soc. A*, 1952, **215,** 187
[2] KISELEV, A. G., MOLKUL'SKII, M. A. and LAZURKIN, YU. S. *Vysokomol. Soedineniya*, 1960, **2,** 1678
[3] CHARLESBY, A., LIBBY, D. and ORMEROD, M. G. *Proc. Roy. Soc. A*, 1961, **262,** 207
[4] KORITSKII, A. T., MOLIN, YU. N., SHAMSHEV, V. N., BUBEN, N. YA. and VOEVODSKII, V. V. *Vysokomol Soedineniya*, 1959, **1,** 1182
[5] LIBBY, D. and ORMEROD, M. G. *J. Phys. Chem. Solids*, 1961, **18,** 316
[6] LAWTON, E. J., BALWIT, J. S. and POWELL, R. S. *J. chem. Phys.* 1960, **33,** 395
[7] DOLE, M. and CRACCO, F. *J. phys. Chem.* 1962, **66,** 193
[8] CHARLESBY, A. and DAVISON, W. H. T. *Chem. & Ind.* **1957,** 232
[9] SMITH, R. C. and WYARD, S. J. *Nature, Lond.* 1961, **191,** 897
[10] WAITE, T. R. *Phys. Rev.* 1957, **107,** 463
[11] ORMEROD, M. G. and ALEXANDER, P. *Nature, Lond.* 1962, **193,** 290
[12] HENRIKSEN, T. and PIHL, A. *J. Rad. Biol.* 1961, **3,** 351

The Radiation Chemistry of Some Polysiloxanes: An Electron Spin Resonance Study

M. G. ORMEROD and A. CHARLESBY

Electron spin resonance spectroscopy was used to study the formation and behaviour of free radicals produced in some polysiloxanes by ionizing radiation. A comparison was made of the polysiloxanes with vinyl and hydrogen group substituents. At 77°K, unstable methyl radicals were observed and their subsequent reactions were studied. It was found that there are too few radicals produced at 77°K to account for the formation of crosslinks—a mechanism not involving a free radical intermediate is responsible for most of the radiation-induced crosslinking. Room temperature irradiation of a liquid polysiloxane which contained vinyl side groups produced stable free radicals. These free radicals could not be produced by low temperature irradiation and subsequent warming. This evidence indicates that the radiation chemical process in polysiloxanes differs between the glass and liquid states.

ON EXPOSING organic polymers to ionizing radiation, they either become crosslinked or suffer main chain fracture. Frequently both reactions occur simultaneously. No definite conclusion has been reached as to the mechanisms by which these reactions occur, or about the unstable intermediates formed. Usually the problem is further complicated by crystallinity and the formation of double bonds. The polysiloxane backbone, i.e.

—O—Si—O—Si—O— etc.

does not allow double bonds to be formed, and at room temperature, i.e. in the liquid state, there are no crystallinity problems. This is why these polymers are suitable for the study of the mechanisms of radiation-induced crosslinking.

Electron spin resonance (e.s.r.) has been used to study the intermediates in irradiated polysiloxanes with methyl, vinyl and hydrogen side groups. Both electron and γ-radiation was employed. The results obtained have been compared with crosslinking and gas yields given by other authors.

EXPERIMENTAL

All e.s.r. spectra were recorded using a high frequency (400 kc/s) magnetic field modulation X-band spectrometer employing a $H_{0,4}$ transmission cavity. The power level at the sample was 0·5 MW, and the amplitude of the magnetic field modulation was 2 gauss peak to peak. The magnetic field was swept through resonance at the rate of 1 gauss sec^{-1} and an integration time of 1 sec was used. All spectra are shown as the first derivative of the absorption intensity as a function of variation in magnetic field. The numbers of free radicals were determined by numerical integration of the derivative

curve and by comparison with a standard coal sample which had been calibrated against α,α'-diphenyl-β-picrylhyrazyl. Their concentration is expressed as the number present per 100 eV of absorbed energy which is the usually quoted G value.

Electron irradiations were carried out *in vacuo* using a 2 MeV 0·5 kW van de Graaff generator with a dose rate of 1 Mrad min^{-1}. It was not possible to record the e.s.r. spectra of the electron-irradiated samples until 24 hours after irradiation. During this time, the samples were kept in liquid nitrogen.

The source of gamma rays was a 2 kilocurie ^{60}Co source which gave a dose rate of 10 kilorad min^{-1}. All the samples were sealed in evacuated glass tubes. The irradiated glass tubes give rise to an additional signal but at the low sensitivity being used this signal from the glass could not be detected and was therefore ignored.

Five types of polysiloxane, which were supplied by Midland Silicones Ltd, were studied. These were 100 per cent methyl silicone

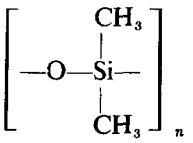

50 per cent hydrogen silicone

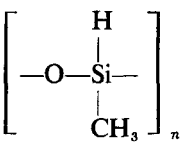

25 per cent hydrogen silicone, 25 per cent vinyl silicone

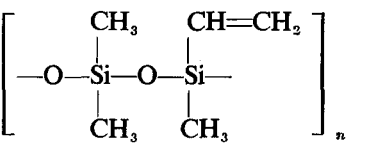

and 10 per cent vinyl silicone. They all had a viscosity of about 100 cS (molecular weight $\sim 6 \times 10^3$). In addition a sample of 100 per cent methyl silicone of viscosity 6×10^4 cS was studied (molecular weight about 10^5).

RESULTS

Low temperature spectra

After γ-irradiation to a dose of 0·3 Mrad, at 77°K and observation at this temperature immediately after irradiation, e.s.r. spectra were obtained from all the samples studied (*Figure 1*). They were basically similar to each other and to the spectrum obtained by Tsvetkov *et al.*[1] from a 100 per cent methyl silicone. They consisted of seven lines which can be divided into a quartet with a hyperfine splitting of 23 gauss (labelled '*a*'), a triplet with

a hyperfine splitting of 24 gauss (labelled '*b*') and a singlet superimposed on the centreline of the triplet (labelled '*c*'). The quartet is unstable at 77°K, as can be seen in *Figure 1*. Tsvetkov *et al.*[1] suggest that the triplet is due to radicals of the type 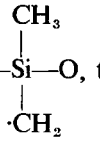 , the singlet to 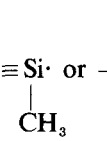 or —O·, and the quartet to ·CH_3. The radical  could either be or .

In both cases one has to postulate that the unpaired spin does not interact with the hydrogens on the methyl groups (in the case of such an interaction would occur). The interaction between an unpaired spin on a carbon atom and the hydrogen atoms on a neighbouring carbon atom is due to hyperconjugation arising from the overlap of the *p* orbital in which the unpaired spin resides and the *s* orbitals of the hydrogen atoms. The three remaining bonds of the carbon atom are sp^2 hybrids. Silicon does not form sp^2 hybrid bonds which is demonstrated by the non-existence of unsaturated silicon compounds, hence it is unlikely that an unpaired spin on a silicon atom would be in a *p* orbital. Furthermore the Si—O bond is highly polar in character and a vacant silicon *d* orbital may play an important part in the bonding which adds weight to the suggestion of Tsvetkov *et al.*[1] that the unpaired electron in this radical is localized on the silicon and oxygen atoms. These differences between silicon and carbon are sufficiently great to make reasonable the assumption that there is no interaction between the unpaired spin and the methyl group in the radical $=\dot{S}i—CH_3$. Since polydimethylsiloxane crosslinks rather than undergoes main chain scission, and it is known that ·CH_3 groups are evolved, it seems more likely that the singlet is due to .

The hydrogen silicone has a broader singlet. This could be due to the same radical in a different environment, or to a different radical—possibly

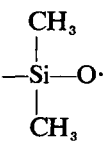

On keeping the samples at 77°K, the quartet eventually disappears completely. The remaining spectrum has been synthesized using the splittings given above and assuming a 1 : 2 : 1 intensity distribution for the

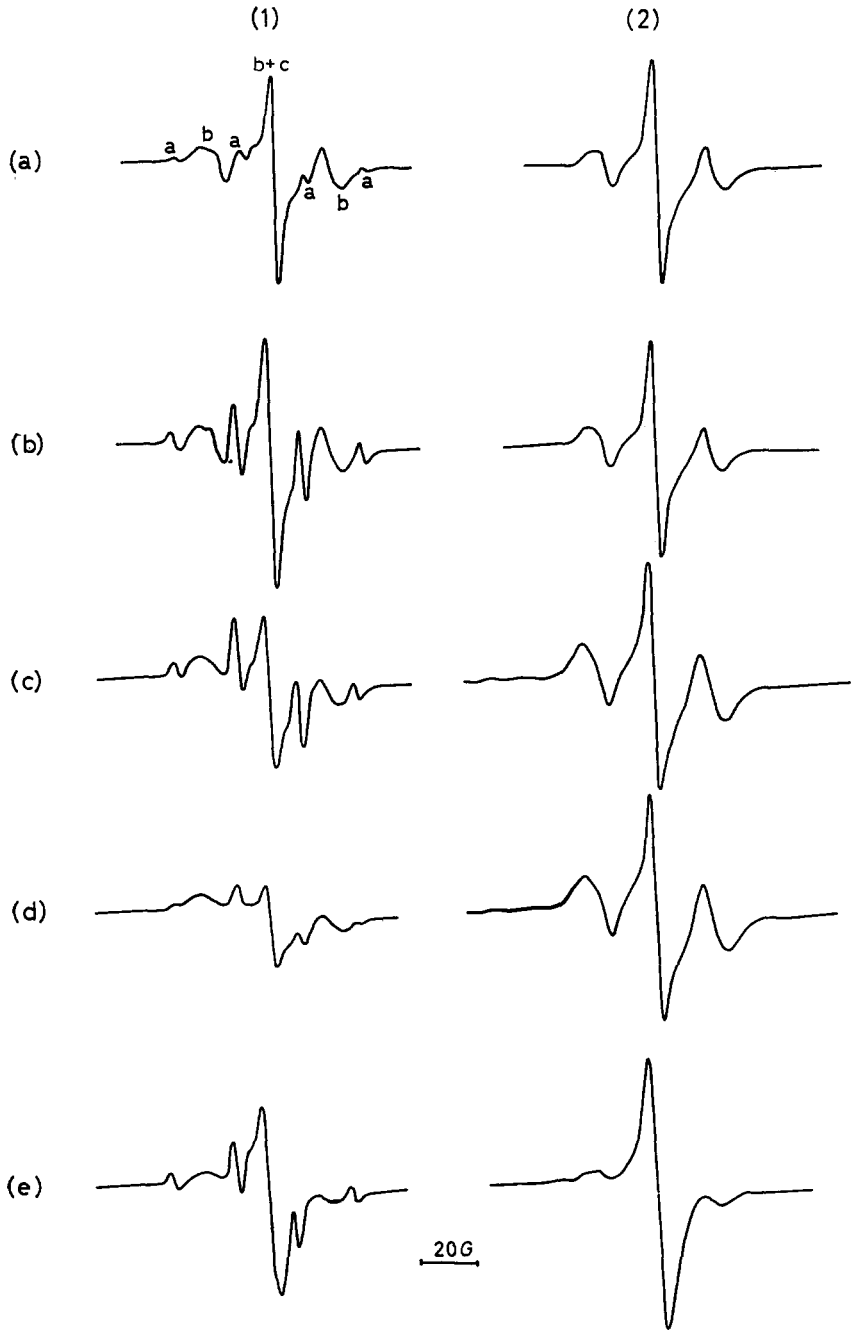

Figure 1—E.s.r. spectra of some polysiloxanes irradiated and studied at 77°K: (1) Immediately after irradiation, (2) 24 hours later; (a) 100 per cent methyl silicone (100 cS viscosity), (b) 100 per cent methyl silicone (6×10^4 cS viscosity), (c) 10 per cent vinyl silicone, (d) 25 per cent vinyl silicone, (e) 25 per cent hydrogen silicone

triplet and a Gaussian line shape. The relative intensities of the triplet and the singlet and their line widths were adjusted until a best fit to the experimental curve was obtained. The line widths finally used were 4·5 gauss for the singlet and 9 gauss for the triplet. The resulting curve is shown in *Figure 2*. The size of the triplet could be estimated by measuring the

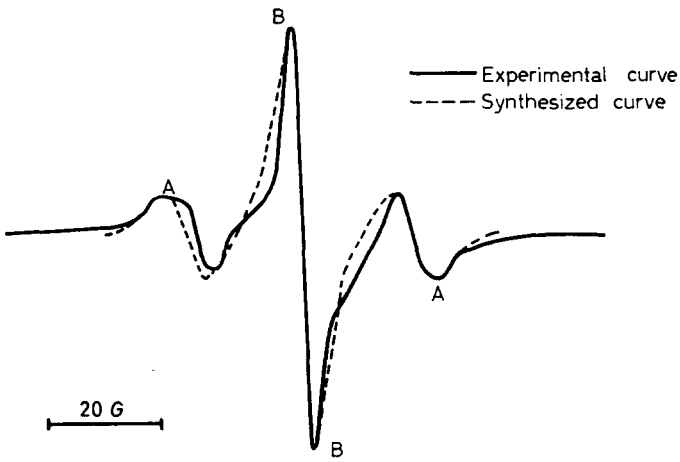

Figure 2—E.s.r. spectrum of an irradiated polysiloxane. Irradiated at 77°K and viewed after 24 hours at 77°K

Table 1. Concentrations of free radicals formed in irradiated polysiloxanes at 77°K

Type of silicone	*Radiation*	*Dose (Mrad)*	*Time after irradiation*	$G_{(rad)}$	$G_{(\cdot CH_3)}$	$G_{(-CH_2\cdot)}$	$G_{(\equiv Si\cdot)}$	$\frac{[-CH_2\cdot]}{[\equiv Si\cdot]}$
100% methyl	electron	20	24 hours	1·0	0·0	0·8	0·18	4·7
	γ	0·2	Immediately	1·0	0·1	0·7	0·2	4·4
	γ	3·0	Immediately	1·0	0·1	0·7	0·2	4·0
	γ	6·6	2 weeks	1·0	0·0	0·75	0·25	3·4
10% vinyl	electron	20	24 hours	1·0	0·0	0·85	0·15	6·1
	γ	0·3	Immediately	2·2	0·8	1·2	0·2	6·7
	γ	2·4	Immediately	0·7	0·1	0·5	0·1	6·2
	γ	2·4	5 days	0·6	0·0	0·5	0·1	7·0
25% vinyl	electron	20	24 hours	0·5	0·0	0·35	0·04	10·0
	γ	0·3	Immediately	1·3	0·3	0·9	0·1	12·5
	γ	2·4	Immediately	0·45	0·05	0·35	0·04	8·9
	γ	2·4	5 days	0·4	0·0	0·35	0·03	10·6
50% hydrogen	electron	20	24 hours	1·4	0·0	0·4	1·0	0·4
25% hydrogen	γ	0·3	Immediately	2·2	0·7	0·7	0·8	0·8
	γ	2·4	Immediately	1·2	0·1	0·4	0·7	0·6
	γ	2·4	5 days	1·0	0·0	0·3	0·7	0·5
	Absolute error			±20%	±70%	±50%	±50%	±50%
	Relative error			±10%	±40%	±10%	±10%	±20%

The ratios in the last column were calculated from the two preceding columns before the figures in these columns were rounded off.

distance marked AA, and the singlet size could then be calculated from the distance BB, after allowing for the triplet contribution. The relation

$$\text{Area of curve} \propto (\text{Peak height}) \times (\text{Line width})^2$$

was used to estimate the relative concentrations of the two radicals $\equiv Si—CH_2\cdot$ and $\equiv Si\cdot$. The $\cdot CH_3$ concentration could then be calculated from the data in *Figure 1* by subtraction. The results are summarized in *Table 1*. The values of $G_{(\text{radicals})}$ are the mean of measurements made on several samples and the errors were estimated from the scatter in these measurements.

Electron irradiation gave the same results as γ-irradiation. No methyl radicals were observed but this is to be expected since the observations were made 24 hours after irradiation. Hence it can be said that there is no noticeable radiation intensity effect.

On warming to 195°K, the radicals in all samples disappeared. The pour point for a 10^2 cS 100 per cent methyl silicone is 208°K (Midland Silicones Ltd, *Technical Data Sheet*). A 100 per cent methyl silicone of viscosity 6×10^4 cS (solidification temperature = 237°K) was also examined. The spectrum was the same as the 10^2 cS sample after irradiation and examination at 77°K, except that there were more $\cdot CH_3$ radicals present owing to their greater stability in the higher molecular weight material. The free radicals likewise disappeared on warming to 195°K. It seems the radicals are unstable at 195°K and are recombining while the material is still solid. These observations agree with those made by Zack, Warrick and Knoll[2].

On warming further to room temperature, no radicals could be observed in any of the samples.

Room temperature spectra

Samples of a 25 per cent vinyl silicone and of a 100 per cent methyl silicone were irradiated at room temperature with γ-rays. The methyl

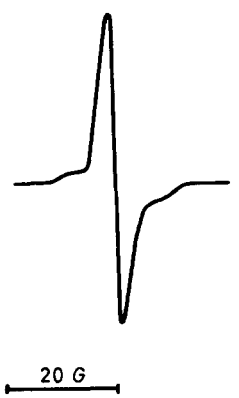

Figure 3—E.s.r. spectrum of a 100 per cent methyl silicone, irradiated and studied at room temperature. Dose = 40 Mrad

silicone gave a weak narrow singlet (*Figure 3*) which could only be detected after a dose of about 40 Mrad—beyond the dose at which the material had gelled. This singlet may be due to traces of $\equiv Si\cdot$, immobilized in the gel.

The 25 per cent vinyl silicone gave a high concentration of stable free radicals at radiation doses below the gel point, i.e. while the material was still liquid. These radicals decay slowly at room temperature, taking about 30 days for the radical concentration to drop by half. At the same time the shape of the spectrum alters (see *Figure 4*). This change in shape is probably due to the presence of two different radical species which are decaying at different rates. The radical accumulation with dose is shown in *Figure 5*. The radicals are being formed with a G value of unity.

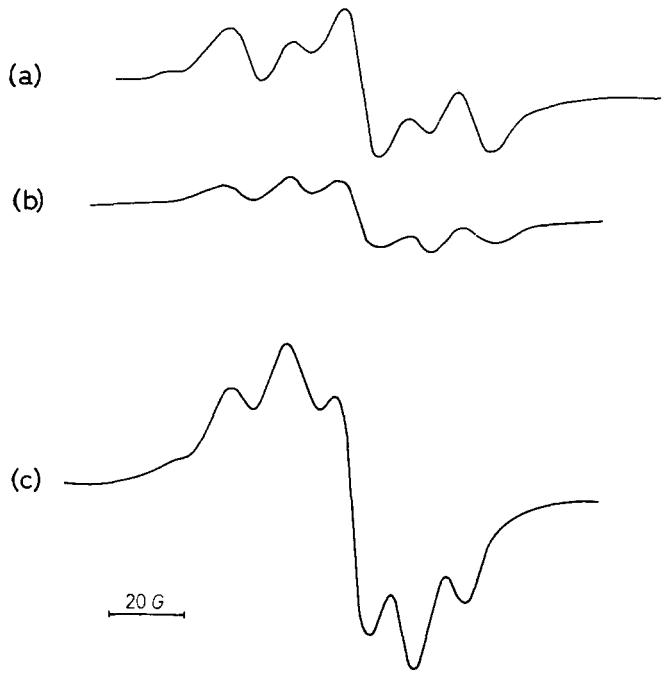

Figure 4—E.s.r. spectra from a room temperature irradiated 25 per cent vinyl silicone: (a) Dose = 4 Mrad, (b) Dose = 4 Mrad, after keeping at room temperature for 24 hours, (c) Dose = 12 Mrad

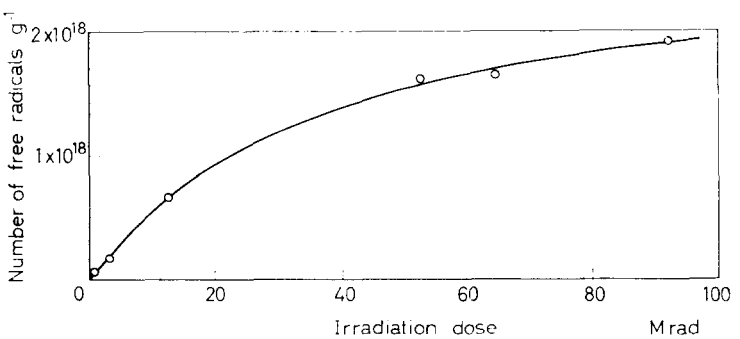

Figure 5—Radical accumulation on room temperature irradiation of a 25 per cent vinyl silicone

RADIATION CHEMISTY OF POLYDIMETHYL SILOXANES

It has been found by many workers that polydimethylsiloxane crosslinks when irradiated at room temperature. The G values for crosslinking given by different workers[2–10] are summarized in *Table 2*, from which a mean

Table 2. The G values obtained for the number of crosslinks formed by irradiation in polydimethylsiloxane

Author	*Method*	*Irradiation*	*Temperature (°C)*	*G value*
Charlesby[3]	Gelation dose (from flow)	Pile	80	3·4
	Gelation dose (from sol fraction)	Pile	80	2·9
Warrick[4]	Swelling	2 MeV electrons	20	2·8
	Elastic modulus	2 MeV electrons	20	2·3
Bueche[5]	Cryoscopy	800 kvp electrons	20	4·5
	Elastic modulus			2·3
St Pierre *et al.*[6]	Cryoscopy	800 kvp electrons	20	2·5
Barnes *et al.*[7]	Light scattering	800 kvp electrons	20	2·5
	Bubble entrapment			2·2
Charlesby[8]	Gelation dose	2 MeV electrons	150	4·7
			20	3·1
			0	2·8
			−78	2·6
Miller[9]	Gelation dose	800 kvp electrons (dose rate = 13·8 Mrad min^{-1})	300	3·2
			150	4·2
			25	3·0
			−80	2·2
			−180	1·9
		(dose rate = 0·138 Mrad min^{-1})	25	3·3
Charlesby and Garratt[10]	Gelation dose	^{60}Co γ-ray	20	2·3
	Mean value		20	2·6

value of 2·6 can be deduced. Charlesby[8] and Miller[9] have also studied the variation of $G_{(\text{crosslinking})}$ with temperature. Gel formation still results from irradiation at a low temperature when the polymer is glassy but with a lower G value; little main chain scission occurs. Replotting Charlesby's[3] and Miller's[9] solubility data according to Charlesby and Pinner's[11] method, ratios of crosslinks to scissions of 6:1 and 4:1 are found. Miller[12] and Kilb[13] give a ratio of 10:1 using other methods.

Hydrogen, methane and ethane are the gases evolved. Estimates as

to the ratio in which these gases come off in the polymer and in some models are summarized in *Table 3*. These results give a mean value of $[H_2]:[CH_4]:[C_2H_6]$ of 36:53:11 which gives a $[\cdot H]/[\cdot CH_3]$ ratio of 1·8. This average is for an extremely wide range of dose rates and other experimental conditions. The amount of gas evolved correlates well with the number of crosslinks formed at room temperature. This is to be expected since double bond formation cannot occur in silicones in an analogous way to polyethylene. However, at 90°K, gas and crosslink formation do not correlate.

Table 3. The percentage of gas evolved from a 100% methyl silicone and from some similar model compounds

Author	Charlesby[3]	Warrick[4]	St Pierre *et al.*[6]	Dewhurst and St Pierre[17]	Miller[9]
Material	Pure silicone	Cyclic tetramer	Pentamer	Hexamethyl-disiloxane	Pure silicone
Mol. wt	10^5–10^3	264	380	162	$8{\cdot}5\times10^4$
Radiation	Pile	2 MeV electrons	800 kvp electrons	800 kvp electrons	800 kvp electrons
H_2	41	34	31	28	38
CH_4	47	60	47	56	33
C_2H_6	12	4·6	22	16	29
$\dot{H}/CH_3\cdot$	1·8	1·9	1·2	1·3	1·2
$G_{(\text{total gas})}$	?	?	2·1	2·5	3·0

Author	Zack *et al.*[2]	Davison and Lloyd[16]	Charlesby and Garratt[10]	Mean value
Material	Hexamethyl-disiloxane	Pure silicone	Pure silicone	
Mol. wt	162	$6{\cdot}6\times10^3$	$2{\cdot}7\times10^4$	
Radiation	^{60}Co γ-rays	2 MeV electrons	^{60}Co γ-rays	
H_2	31	42	40	36
CH_4	69	58	57	53
C_2H_6	0	10	3	11
$\dot{H}/CH_3\cdot$	1·9	1·8	2·2	1·8
$G_{(\text{total gas})}$	1·8	1·5	2·0	2·2

At 90°K, Miller[12] found that $H_2:CH_4:C_2H_6 = 34:58:8$ $\dot{H}/\cdot CH_3 = 1{\cdot}7$ and $G_{(\text{total gas})} = 2{\cdot}8$.

Miller[9] made infra-red measurements and found that the crosslinks formed are of the types:

(i) $\equiv Si—Si\equiv$
(ii) $\equiv Si—CH_2—Si\equiv$
(iii) $\equiv Si—CH_2—CH_2—Si\equiv$

The first was not found at low temperatures. Miller also studied the effect of additives at room temperature[12] and found that oxygen can only suppress about 70 per cent of the crosslinks which would be formed *in vacuo*. However, hydrogen transfer agents, such as *n*-butyl mercaptan, were able

to suppress crosslinking completely. At the same time, ≡Si—H groups were formed showing that the reaction

$$\equiv Si\cdot + RSH \longrightarrow \equiv Si{-}H + RS\cdot$$

is occurring. The number of ≡Si—H groups thus formed is considerably larger than the number of $\cdot CH_3$ groups found in the evolved gases. This result may be due to subsequent reactions between polymer radicals and $\cdot CH_3$. After irradiation at 90°K, and subsequent warming, no ≡Si—H groups were formed in the presence of a mercaptan, although it has been shown that at this temperature both methane and ethane are evolved from the pure polymer.

In conclusion, at room temperature, radiation crosslinks a 100 per cent methyl silicone predominantly by a free radical mechanism (as Miller's work on additives has shown). The crosslinks are formed by the combination of ≡Si· and $\equiv Si{-}CH_2\cdot$ radicals. Gases are evolved with G values as follows:

$G_{(H_2)} = 0{\cdot}8$; $G_{(CH_4)} = 1{\cdot}2$; $G_{(C_2H_6)} = 0{\cdot}3$; so that $G_{(H\cdot)} = 2{\cdot}8$ and $G_{(CH_3\cdot)} = 1{\cdot}8$. $G_{(\text{crosslinks})} = 2{\cdot}6$; $G_{(\text{scission})} = 0{\cdot}4$.

DISCUSSION

100 per cent methyl silicone

There is a surprising discrepancy between the G value for radical formation (~ 1) as measured by e.s.r. and that for crosslink formation (~ 2) as measured by gel formation, for irradiations at low temperatures. For polyethylene for example no such discrepancy arises. If one assumes that two radicals form one crosslink (as with polyethylene[14]), the free radicals observed can only account for a quarter of the crosslinks produced. Since there are no double bonds present, it is difficult to envisage any form of chain reaction occurring. However, Miller's work has shown that at room temperature, crosslinking is almost certainly a free radical reaction. These facts can best be explained by making two assumptions:

(*1*) The radiation chemistry of silicones differs between the solid and liquid states.

(*2*) A mechanism not involving a free radical intermediate is responsible for three quarters of the crosslinks formed at low temperatures.

Further evidence to support assumption (*1*) will be brought forward in the discussion of the vinyl silicone results. The major crosslinking mechanism at this temperature could possibly be ionic.

The free radicals formed disappear while the polymer is still solid, i.e. at or below 195°K. This is confirmed by the 6×10^4 cS sample whose solidification temperature is 237°K. Miller has reported that no ≡Si—Si≡ crosslinks are formed by irradiation at 90°K. If we assume that radicals can migrate by hydrogen transfer (as found in polyethylene) but not by methyl transfer, then $\equiv Si{-}CH_2\cdot$ radicals are effectively mobile, but not ≡Si· Thus two ≡Si· radicals produced at a distance can only combine to give ≡Si—Si≡ in the liquid state.

Vinyl silicones

As shown by the G values in *Table 1*, the presence of vinyl groups protects polysiloxanes from radiation-induced radical formation. This is in keeping with results obtained from hydrocarbons where it was found that the presence of double bonds protects from radiation[15].

The reduction of polymer radical concentration while the methyl radicals decay indicates that they are decaying by reacting with polymer radicals—not by abstracting a hydrogen atom. (This is shown in *Table 1*.) Thus the reaction, $\cdot CH_3 + \equiv Si{-}CH_3 \longrightarrow CH_4 + \equiv Si{-}CH_2\cdot$ does not occur at 77°K, neither does the reaction

$$\cdot CH_3 + \equiv Si{-}CH{=}CH_2 \longrightarrow \equiv Si{-}\dot{C}H{-}CH_2{-}CH_3$$

The initial methyl radical concentration is larger than the $\equiv Si\cdot$ radical concentration which is surprising since both radicals are formed by the rupture of a $\equiv Si{-}CH_3$ bond. It seems unlikely that this can be accounted for by reaction between $H\cdot$ and $\equiv Si\cdot$ because the reaction $H\cdot + CH_3\cdot$ is equally likely to occur. It is possible that when a $\equiv Si{-}CH_3$ bond is broken directly by radiation the $\cdot CH_3$ group has difficulty in escaping owing to the cage effect and that only a few methyl radicals are formed this way. The rest of them could arise from the reaction

$$H\cdot + \equiv Si{-}CH_3 \longrightarrow \equiv SiH + \cdot CH_3$$

or

$$\equiv Si{-}CH_3 \text{—}\sim\!\!\!\rightarrow \equiv Si^+{-}CH_3 + e^-, \quad \equiv Si^+{-}CH_3 \longrightarrow \equiv Si^+ + \cdot CH_3$$

The $\equiv Si^+$ could then react further.

In previous polymer studies, it has been found that the spectrum obtained by irradiating at 77°K and then warming to room temperature is always qualitatively the same as that obtained from a room temperature irradiated sample. Any minor differences can be accounted for by the presence of two or more radicals of differing stabilities. None of the polysiloxanes investigated yielded an e.s.r. spectrum at room temperature after irradiation at 77°K. But the 25 per cent vinyl silicone gave a large concentration of radicals ($G \sim 1$) after a room temperature irradiation. These radicals will survive pouring the fluid from one end of a tube to the other. The spectrum from these radicals is different from that obtained at 77°K. It is to be expected that they are associated with the vinyl group but no obvious interpretation of the spectrum presents itself. This discrepancy between the behaviour of low temperature and room temperature irradiated specimens indicates that the basic radiation-induced mechanisms differ as to whether the material is solid or liquid.

It is the presence of long-lived radicals that accounts for the increase in $G_{(\text{crosslinks})}$ with time after irradiation in vinyl silicones which was observed by Davison and Lloyd[16]. The chain reaction

$$R\cdot + CH_2{=}CH{-}Si{\equiv} \longrightarrow R{-}CH_2{-}\dot{C}H{-}Si{\equiv}$$

is occurring. This can be followed in two ways. The increase in the number of crosslinks can be observed by following the increase in viscosity of the silicone fluid with time. The decrease in the number of double bonds present

can be seen spectroscopically. The free radicals present will decay by combining bimolecularly and it might be expected that the decay would be second order, but this is not found. However, the rate of diffusion of the radicals will probably decrease as the silicone fluid becomes more cross-linked and the reaction kinetics will in practice be more complicated.

We wish to thank Drs D. Libby and D. G. Lloyd in collaboration with whom some of the initial experiments were performed and Mr W. H. T. Davison for his advice.

Physics Branch,
Royal Military College of Science,
Shrivenham, Swindon, Wiltshire

(*Received December 1962*)

REFERENCES

[1] TSVETKOV, YU. D., MOLIN, YU. N. and VOEVODSKII, V. V. *Vysokomol. Soedineniya,* **1959,** No. 1, 1805
[2] ZACK, J. F., WARRICK, E. L. and KNOLL, G. *J. Chem. Engng Data,* 1961, **6,** 279
[3] CHARLESBY, A. *Proc. Roy. Soc. A,* 1955, **230,** 120
[4] WARRICK, E. L. *Industr. Engng Chem. (Industr.),* 1955, **47,** 2388
[5] BUECHE, F. *J. Polym. Sci.* 1956, **19,** 297
[6] ST PIERRE, L. E., DEWHURST, H. A. and BUECHE, A. M. *J. Polym. Sci.* 1959, **36,** 105
[7] BARNES, W., DEWHURST, H. A., KILB, R. W. and ST PIERRE, L. E. *J. Polym. Sci.* 1959, **36,** 525
[8] CHARLESBY, A. *Atomic Radiation and Polymers,* Pergamon: Oxford, 1960
[9] MILLER, A. A. *J. Amer. chem. Soc.* 1960, **82,** 3519
[10] CHARLESBY, A. and GARRATT, P. G. In press
[11] CHARLESBY, A. and PINNER, S. H. *Proc. Roy. Soc. A,* 1959, **249,** 367
[12] MILLER, A. A. *J. Amer. chem. Soc.* 1961, **83,** 31
[13] KILB, R. W. *J. phys. Chem.* 1959, **63,** 1838
[14] CHARLESBY, A., LIBBY, D. and ORMEROD, M. G. *Proc. Roy. Soc. A,* 1961, **262,** 207
[15] CHARLESBY, A. and ORMEROD, M. G. *Fifth International Symposium on Free Radicals, Uppsala,* 1961. Almqvist and Wiksell: Stockholm, 1961
[16] DAVISON, W. H. T. and LLOYD, D. G. Personal communication
[17] DEWHURST, H. A. and ST PIERRE, L. E. *J. phys. Chem.* 1960, **69,** 1063

The Mechanical Degradation of Polymers

C. BOOTH*

A sample of polyisoprene having a narrow molecular weight distribution has been degraded mechanically in several ways and the molecular weight distributions of the degradation products have been determined. From these data we conclude that chain scission occurs at a point far removed from the ends, but not necessarily near the centre, of the molecules.

WHEN polymers, or solutions of polymers, are subjected to large shear forces chain scission occurs. The experimental evidence published to date, and recently reviewed by Scanlan and Watson[1], shows quite clearly that the bonds near the ends of the polymer chain are much less likely to be broken during mechanical degradation than are the bonds nearer the centre of the chain. Moreover, theories of polymer degradation[2a, 2b] predict that the most probable place for the chain to break is at the centre. While this qualitative agreement between theory and experiment is satisfactory, the experimental results published so far do not constitute a searching test of the theoretical prediction. This is because the experimental work has been carried out on polymers with wide molecular weight distributions. In these circumstances it is difficult to interpret the differences between the original molecular weight distribution and the narrower, but still wide, molecular weight distributions of the products of mechanical degradation.

In this work polymers of very narrow molecular weight distribution, produced via anionic polymerization, have been used and the changes in molecular weight after mechanical degradation have been studied in some detail. The data reported here were obtained in a survey of several methods of degradation and suffer the drawback that the shear rates involved in the degradation processes were not held steady (nor were they measured).

EXPERIMENTAL

The techniques used in fractionating the samples by precipitation from dilute solution in toluene with methanol, in determining intrinsic viscosities in toluene at 30°C and in determining weight-average molecular weight by light scattering have been discussed in earlier papers[3]. The intrinsic viscosities quoted in this paper were measured in a Desreux–Bischoff viscometer having a shear stress of 0·3 g cm^{-1} sec^{-2}, or have been corrected to the value at that shear stress. These intrinsic viscosities were used directly in the relationship[3]

$$\eta = 2{\cdot}00 \times 10^{-4} \bar{M}_v^{0{\cdot}728} \qquad (1)$$

in order to calculate the viscosity-average molecular weight of the whole samples and the fractions.

The degradation experiments were all carried out on a single sample of polyisoprene which was prepared in hydrocarbon solution using

*Present address: Department of Chemistry, University of Manchester.

butyllithium as catalyst. The intrinsic viscosity of the freshly prepared polymer was 10·8 dl/g, but it had dropped to 10·4 dl/g after the polymer had been isolated and dried. Antioxidant 2246 was added to the polymer at a concentration of 1 part per 100 parts of rubber (1 p.h.r.).

Four distinct techniques were used to degrade the polymer: degradation in toluene solution by use of a 'Virtis 45' homogenizer (a laboratory homogenizer fitted with knife edge blades which rotate at variable speeds up to 45 000 rev/min[4]); degradation of the dry rubber in a small (i.e. 50 g rubber) internal mixer with cam style rotors which simulate the action of a Banbury mixer; degradation of the dry rubber on a laboratory micromill; degradation in toluene solution by exposure to γ-radiation. This latter experiment was carried out in order to be able to compare the molecular weight distributions obtained for the mechanically degraded samples with one measured in the same way on a sample known to have undergone random scission[5]. Details of the samples prepared by these various methods of degrading the polyisoprene are given in *Table 1*. In no experiment was any attempt made to exclude air.

Table 1. Degradation of polyisoprene

Sample	$[\eta]$ *dl/g*	*Method of degradation*
V1	3·11	In toluene solution (1·5g/100 ml) with the 'Virtis 45' homogenizer at full speed; temperature 30°–50°C; 7 p.h.r. *Ionol** antioxidant added; stirring time 2 h
V2	6·57	As V1 except 25 min stirring time
V3	8·48	As V1 except 12 min stirring time
V4	2·63	Similar conditions to V1
M1	3·15	In laboratory mixer; temperature 100°C; mixing time 1 h
MM1	2·50	On laboratory micromill; 25 g rubber; 0·005 in. gap; temperature 30°C; milling time 4 min
MM2	2·39	As MM1 except 20 g rubber
I1	2·26	In toluene solution (0·33 g/100 ml) by exposure to γ-radiation (1 megarad); 30 p.h.r. *Ionol* antioxidant added; temperature 30°C
I2	2·40	As I1

*A registered trademark of Shell Chemical Company, a Division of Shell Oil Company.

RESULTS AND DISCUSSION

The fractionation data, i.e. the weight (w_i) in grammes and the intrinsic viscosity $[\eta]_i$ in dl/g of each fraction, are given in *Table 2* together with the total weight of the fractions (Σw_i) and the weight-average intrinsic viscosity of the fractions ($\Sigma w_i[\eta]_i/\Sigma w_i$). These latter quantities give some indication of the practical efficiency of the fractionation. Integral weight

Table 2. Fractionation data

Fraction	*Orig. polymer*		*V1*		*V2*		*V3*		*M1*		*MM2*		*I1*	
	w_i	$[\eta]_i$	w_i	$[\eta]_i$	w_i	$[\eta]_i$	w_i	$[\eta]_i$	w_i	$[\eta]_i$	w_i	$[\eta]_i$	w_i	$[\eta]_i$
1	3·19	11·1	0·44	3·69	0·55	8·01	0·71	9·55	1·14	4·44	0·80	3·62	1·00	3·73
2	1·33	10·9	0·89	3·63	0·66	7·80	1·06	9·50	0·57	3·98	0·39	3·25	0·60	2·98
3	0·49	9·95	0·22	3·58	0·76	7·80	0·50	9·51	0·64	3·73	0·76	3·03	0·23	2·65
4	0·88	10·0	1·33	3·53	0·18	7·60	0·90	9·49	0·63	3·58	0·86	2·76	0·92	1·95
5	1·01	7·25	0·88	2·98	0·89	7·30	0·22	9·16	0·35	3·27	0·71	2·64	0·43	1·58
6	0·17	2·85	0·76	2·50	0·73	6·58	1·21	8·96	1·87	2·89	1·13	2·12	0·63	0·97
7	—	—	0·43	1·56	1·47	5·60	0·64	7·81	0·53	2·12	0·79	1·68	0·27	0·32
8	—	—	0·09	1·7	0·50	3·97	0·72	6·03	0·56	1·15	0·38	1·29	—	—
9	—	—	—	—	0·26	1·10	0·31	4·62	0·22	0·43	0·88	0·56	—	—
10	—	—	—	—	—	—	0·21	2·81	—	—	—	—	—	—
11	—	—	—	—	—	—	0·11	3·33	—	—	—	—	—	—
Whole sample	7·06	10·4	4·99	3·11	6·00	6·57	—	8·48	6·59	3·15	6·67	2·39	4·08	2·33
Σw_i	7·06	—	5·04	—	6·00	—	6·56	—	6·51	—	6·70	—	4·08	—
$\frac{\Sigma w_i [\eta]_i}{\Sigma w_i}$	—	10·0	—	3·10	—	6·43	—	8·26	—	3·10	—	2·31	—	2·26

distributions of molecular weights were constructed in the conventional manner[6] by plotting the cumulative weight percentage against the viscosity-average molecular weight $(\bar{M}_v)_i$ for each fraction. No effort was made to resolve the large first fraction obtained for the original polymer into further fractions since experience had shown[3] that polymers of this type gave several initial fractions of identical intrinsic viscosity. The difficulty experienced in separating anything other than this very large fraction indicated that this polymer did not differ in this respect.

Branching and crosslinking

In order to determine whether or not branching and crosslinking reactions were taking place during the degradation processes the weight-average molecular weight of some of the samples and of the two highest molecular weight fractions (denoted by Fl) were measured. These results, together with the intrinsic viscosities of the samples, are given in *Table 3*. The ratio of the measured intrinsic viscosity to that of a linear molecule of the same weight-average molecular weight [calculated by use of equation (1) and by assuming, for this purpose only, that the polymers are monodisperse]

Table 3. Branching or crosslinking in the degraded samples

Sample	$[\eta]$ *dl/g*	$\bar{M}_w \times 10^{-6}$	$[\eta]/[\eta]_l$
Original polymer	10·4	2·9	1·03
V1	2·63	0·44	1·06
M1	3·15	0·63	0·95
MM1	2·50	0·50	0·89
12	2·40	0·37	1·06
M1–F1 (12 wt %)	4·55	0·98	0·99
MM1–F1 (16 wt %)	3·89	1·4	0·65

is also given in *Table 3* where it is denoted $[\eta]/[\eta]_l$. For linear polyisoprenes of molecular weight distributions similar to those found here one would expect $[\eta]/[\eta]_l$ to be unity within the experimental error of determining $\bar{M}_w$ (i.e. ± 5 per cent to 10 per cent); for a branched polyisoprene $[\eta]/[\eta]_l$ will decrease as the amount of branching (or crosslinking) increases[7a, 7b]. It is clear that only the samples degraded on the micromill contained significant amounts of branched or crosslinked polymer. Moreover a simple calculation shows that the branched polymer is all contained in fraction 1 and so the molecular weight distribution obtained for sample MM2 is not significantly affected by this complication.

Comparison of molecular weight distributions

In order to compare the molecular weight distributions, one with another, it is convenient to plot the cumulative weight percentage against a reduced viscosity-average molecular weight for each fraction, i.e. $(\bar{M}_v)_i/(\bar{M}_v)_0$, where $(\bar{M}_v)_0$ is the viscosity-average molecular weight of the whole sample obtained from the weight-average intrinsic viscosity of the fractions. These distributions are plotted in *Figure 1*; the distribution curves for all the samples degraded by use of the 'Virtis 45' homogenizer are similar and are represented by a single curve. As a further comparison the quantities

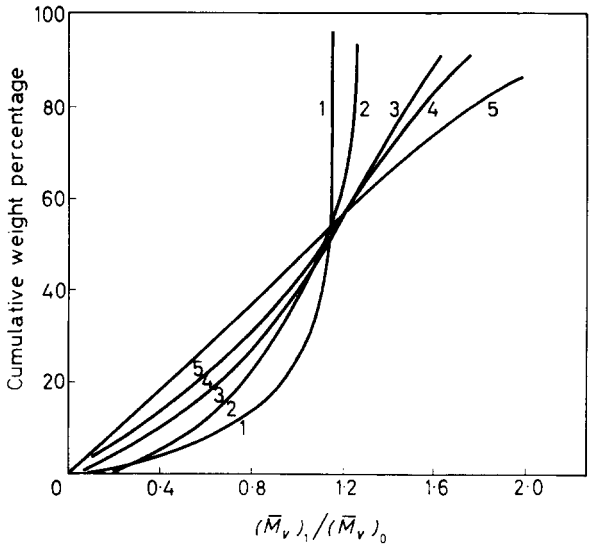

Figure 1—Reduced molecular weight distributions of original polymer (1) and of its degradation products produced by the 'Virtis 45' (2), the laboratory masticator (3), the micromill (4), and by random scission (5)

$\bar{M}_w(F)$ and $\bar{M}_z(F)$ have been calculated, i.e. the weight- and z-average molecular weights computed from fractionation data according to the following definitions:

$$\bar{M}_w(F) = \Sigma w_i (\bar{M}_v)_i / \Sigma w_i \tag{2}$$

$$\bar{M}_z(F) = \Sigma w_i (\bar{M}_v)_i^2 / \Sigma w_i (\bar{M}_v)_i \tag{3}$$

The ratios $\bar{M}_z(F)/\bar{M}_w(F)$ are listed in *Table 4*; they reflect the width of

Table 4. $\bar{M}_z(F)/\bar{M}_w(F)$ of the samples

Sample	Orig. polymer	V1	V2	V3	M1	MM2	I1
$\bar{M}_z(F)/\bar{M}_w(F)$	1·05	1·08	1·12	1·08	1·18	1·25	1·38

the weight distributions of molecular weights illustrated in *Figure 1*. The value of 1·38 obtained for the sample produced by random scission emphasizes the fact that our fractionation method was not 100 per cent efficient; one would expect $\bar{M}_z(F)/\bar{M}_w(F)$ to be somewhat nearer 1·5.

It is quite obvious, both from *Figure 1* and from *Table 4*, that the width of the molecular weight distribution of the samples increased markedly as the conditions of degradation became more severe. However, all the samples produced by mechanical degradation had much narrower molecular weight distributions than the sample produced by random scission.

The conventional integral weight distribution of molecular weights for the original polymer and for the samples degraded by use of the Virtis homogenizer are plotted in *Figure 2*. Consideration of these distributions

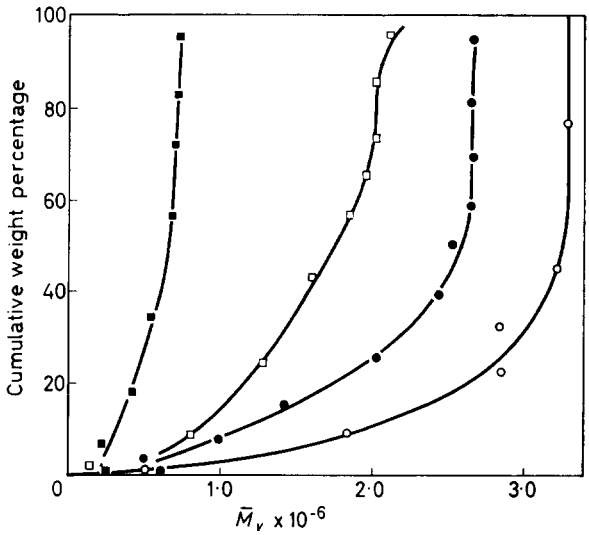

Figure 2—Molecular weight distributions of: original polymer (○), V1 (■), V2 (□) and V3 (●)

leads to the conclusion that the bond which breaks under stress is located a certain distance from the end of the chain molecule. Thus samples V2 and V3 both have narrow molecular weight distributions; that of V3 corresponds to the scission of fragments of molecular weight about $0{\cdot}6 \times 10^6$ from the high molecular weight molecules of the original polymer while that of V2 corresponds to the scission of similar fragments from V3 (or two fragments from the original polymer). There are also indications of a fraction of polymer in the region of molecular weight $0{\cdot}6 \times 10^6$ (or $[\eta] = 3$ to 4 dl/g) in the data for V2 and V3 in *Table 1*. The molecular weight distribution of V1 is less readily interpreted but is consistent with a mechanism which results in the scission of small fragments from the higher molecular weight molecules. It must be borne in mind that the 'Virtis 45' is not a constant shear rate device: quite apart from the complications of geometry, its speed is much reduced when stirring viscous solutions and we noted a considerable increase in speed as degradation proceeded. Presumably this complication will affect our results, especially when we degrade the sample to low $[\eta]$. The formation of degradation products of molecular weight $0{\cdot}2 \times 10^6$ in sample V1 is noted.

In order to ensure that the fractionation data were not grossly misleading, i.e. that the distributions of the slightly degraded polymers were in fact narrow and not mixtures of the original polymer and a lower molecular weight product of degradation (produced by scission near the centre of the molecule), top fractions were precipitated from a mixture of two polyisoprenes of differing molecular weight. The mixture was 50 wt % of the polymer used in this study ($[\eta] = 10{\cdot}4$ dl/g) and 50 wt % of a similar polyisoprene having an intrinsic viscosity of 7·3 dl/g. The fractionation data are given in *Table 5*. These results are exactly those expected for the fractionation method used (which is, of course, not completely efficient) and

Table 5. Fractionation of a mixture of polyisoprenes

Fraction	*Wt %*	$[\eta]$ *dl/g*
1	12·2	10·7
2	8·6	10·4

it is concluded that the fractionation data are significant.

As noted earlier the molecular weight distribution of the degraded polymer becomes wider as the conditions of degradation become more severe. This finding implies that the fragments severed from the chain molecules become smaller as the shear stress on the polymer increases, and the fractionation data can be presented in a way which illustrates this point more directly. The weight percentages of polymer having intrinsic viscosities less than 1·0 dl/g have been estimated and are given in *Table 6*. The amount of low molecular weight polymer increases as the severity of the conditions of degradation increases.

Table 6. Weight percentage of polymer with $[\eta] < 1{\cdot}0$ dl/g

Sample	$[\eta]$ *(dl/g)*	*Wt %*
Original polymer	10·4	0
V1	3·11	0
M1	3·15	7
MM2	2·39	11
I1	2·33	15

CONCLUSIONS

It is concluded that the mechanical degradation of a polymer leads to the scission of a bond far removed from the ends of the chain molecule but not necessarily near the centre. The fragments which can be broken from the chain decrease in length as the shear stress increases. We speculate that were our original sample of polyisoprene to be worked at constant shear rate small fragments would form initially and then, as the degradation proceeds and the shear stress decreases, the fragments would become larger and larger until the viscosity of the polymer is such that the largest molecule in the sample cannot be broken (at the centre) at the shear rate used. Some process of this nature presumably occurs during the mastication and milling of the bulk polymer. Degradation in the 'Virtis 45' under the conditions used in this work was not at constant shear rate and there is no reason to suppose that the data for sample V1 would fit this simple picture.

While these findings are pertinent to an understanding of the practice of the mechanical degradation of polymers, it is difficult to compare them with the predictions of the theories of mechanical degradation. Quite apart from the fact that the mechanical devices used in this work were not designed to produce conditions of steady shear flow, there was the additional complication that the polymer itself did not always flow smoothly. For example, it was difficult to mill the polymer and one obtained, at best, an opaque and lacy band. Similar evidence of fracture during flow was noted with the laboratory mixer; the 'Virtis 45' did not run evenly until degradation had proceeded some way. With dilute solutions of the polymer there is also the possibility of a change in the mechanism of flow as

degradation proceeds. A change in the mechanism of flow with changing molecular weight is well documented in the case of flow at or approaching zero shear rate[8] but the flow of polymers at high shear rates is not so well understood. However, it is not obvious how any of these practical defects would affect the position in the chain of the bond which breaks and it seems that there is a real discrepancy between our findings and, for example, the theoretical prediction of Bueche[2a] who concluded that the polymer chain will break at or near the centre bond under experimental conditions similar to those used in this work.

At first sight there appears to be some contradiction between the data presented here and those of Watson and co-workers[1]. However, Watson used natural rubber of intrinsic viscosity 4·4 dl/g and of wide molecular weight distribution. These features, together with their use of osmometry, make a direct comparison of the data impossible. So far as we can tell Watson's data are compatible with our conclusions.

Finally a point of practical interest. If, as we conclude, the effect of milling a high molecular weight polymer is to produce a low molecular weight polymer, it is possible that some of the physical properties of a slightly degraded polymer will differ appreciably from those of the parent polymer, especially if the molecular weight distribution of the original polymer is narrow. These would be the properties which are sensitive to the number average molecular weight of the polymer. From a practical point of view, the most important property so affected would be the apparent viscosity at high shear rate[9].

Most of the experimental work described in this paper was carried out by Mr D. G. Marsh. I would also like to acknowledge the help of Mr A. R. Bean who prepared the sample of polyisoprene used in this work, of Dr W. H. Beattie who measured the weight-average molecular weights, and of Dr G. Holden and Mr W. R. Hendricks who, respectively, masticated and milled the polymer.

Torrance Research Laboratory,
Synthetic Rubber Division of Shell Chemical Co.,
P.O. Box 211, Torrance, California

(*Received December 1962*)

REFERENCES

[1] SCANLAN, J. and WATSON, W. F. *Rubb. Chem. Technol.* 1960, **33**, 1201
[2a] BUECHE, F. *J. appl. Polym. Sci.* 1960, **4**, 101
[2b] FRENKEL, YU. I. *Acta phys.-chim. Sci. U.R.S.S.* 1944, **19**, 51
[3] BEATTIE, W. H. and BOOTH, C. *J. appl. Polym. Sci.* 1963, **7**, 507
[4] JOHNSON, W. R. and PRICE, C. C. *J. Polym. Sci.* 1960, **45**, 217
[5] BOOTH, C. and HARLAN, J. T. Unpublished work
[6] BOOTH, C. and BEASON, L. R. *J. Polym. Sci.* 1960, **42**, 81
[7a] ZIMM, B. H. and KILB, R. W. *J. Polym. Sci.* 1959, **37**, 19
[7b] KILB, R. W. *J. Polym. Sci.* 1959, **38**, 403
[8] PORTER, R. S. and JOHNSON, J. F. *Polymer, Lond.* 1962, **3**, 11
[9] COX, W. P. and BALLMAN, R. L. *J. appl. Polym. Sci.* 1960, **4**, 121

Solution and Bulk Properties of Branched Polyvinyl Acetates

Part I: Non-Newtonian Viscosity Behaviour

L. M. HOBBS* and V. C. LONG†

A series of linear and branched fractions of polyvinyl acetate of relatively narrow molecular weight distribution was prepared and characterized by solution viscosity, hydrolysis, and light scattering measurements. At a given molecular weight, the intrinsic viscosity of a branched fraction was less than that of a linear fraction. The viscosity loss which takes place after removal of branches, by hydrolysis followed by re-acetylation, is a sensitive indication of the presence of branching in polyvinyl acetate. However, the process is not quantitative because of the presence of nonhydrolysable branches in the branched polymer. Benzene solutions of linear and branched polymers above a molecular weight of about 2×10^6 were significantly non-Newtonian in character. The major factor contributing to the non-Newtonian behaviour was found to be molecular weight rather than structure. Therefore, even though the intrinsic viscosity of a high molecular weight fraction is dependent on shear rate, the ratio of the intrinsic viscosities of branched to linear fractions of the same molecular weight (a term used in the estimation of the degree of branching) is not sensitive to shear rate. Since the shear sensitivity or degree of non-Newtonian viscosity behaviour is dependent upon molecular weight, it is possible to detect the presence of branching in polymers of molecular weight greater than 2×10^6 by comparison of the shear sensitivities of branched and linear fractions of the same intrinsic viscosity.

THE work described in this paper and in parts of three further publications represents a continuation and extension of an earlier publication on the effect of branching on the viscosity of dilute solutions of polyvinyl acetate[1].

In this, the first paper of the present series, the preparation, fractionation, and characterization of linear and randomly branched polymers of vinyl acetate will be described. The fractions were characterized by dilute solution viscosity, light scattering, and hydrolysis measurements. The effect of the rate of shear upon the viscosity of dilute solutions was also observed and will be discussed in terms of the molecular weight and structure of the fractions.

The synthesis of comb-shaped branched polymers of vinyl acetate by a grafting technique is described in the second paper[2]. By that process branches of specified length and number were attached to backbone linear polymers of narrow molecular weight distribution.

A comparison of some dilute solution properties for fractions of linear, randomly branched, and the comb-shaped branched polymers is presented

*Present address: Bennettsville, South Carolina.
†Present address: E. I. du Pont de Nemours and Co., Wilmington, Delaware.

in the third paper[3]; and the effects of branching on the melt viscosity of polyvinyl acetate will be described in the fourth and final paper of this series[4].

EXPERIMENTAL

The experimental procedures and techniques employed in this study have been described in detail[1,5] and are reviewed below.

Preparation of samples

Polymerization—Five unfractionated polymers of vinyl acetate were utilized. Samples 1, 2 and 3 were described previously[1]. Samples 1, 2 and 5 were linear in structure and were prepared by similar techniques. Sample 5 was actually a combination of three batches formed at low conversion by photopolymerization at $-19°C$ with azo-bis-isobutyronitrile as the photosensitizer. The polymerization data are recorded in *Table 1*. Such conditions are reported to yield essentially linear molecules[6,7]. The fact that the intrinsic viscosities of sample 5 and two of its fractions were not significantly reduced after hydrolysis and re-acetylation, as shown in *Table 4*, is strong support of the assumption that the material is linear in structure.

Table 1. Polymerization data for the three components of sample 5

Sample No.	$[\eta]$ *(dl/g)*	% *Conversion*	*Yield* (g)	*Initiator* concentration (moles/l.* $\times 10^4$*)*
5a	2·91	4·0	38·3	2·38
5b	3·26	6·9	74·3	2·15
5c	3·33	9·5	97·3	2·08

*Ultra-violet source: 100 W mercury lamp at 30 cm.

Samples 3 and 4 were of the commercial type, prepared by the suspension polymerization method to high conversion at a relatively high temperature. Both were highly branched and high in molecular weight but entirely soluble in benzene. Both samples were prepared by Mr Wellman of the Colton Chemical Company, Cleveland, Ohio, by a technique similar to that described by Schildknecht[8]. The substantial reduction of the intrinsic viscosities of sample 4 and several of its fractions after hydrolysis and re-acetylation, as shown in *Table 4*, indicates that the material is highly branched. From the method of preparation it is considered that the branching is random in nature.

Fractionation—The samples were fractionated by the partial precipitation method using the solvent–non-solvent system of acetone–*n*-heptane[1] at $35·0° \pm 0·02°C$. The polymer concentration was 10 g/l. or less during the fractionations. After isolation, the fractions were dissolved in benzene and recovered by freeze drying. Most of the primary fractions were subjected to a second fractionation and some of these secondary fractions were subjected to an additional fractionation. A code used to designate the fractions consists of a series of digits: the first digit denotes the unfractionated sample, the second indicates the primary fraction in order of its isolation,

and the third and fourth digits have similar significance for the secondary and tertiary fractions, respectively. The fractionation data for the fractions of samples 4 and 5 are listed in *Tables 2* and *3*.

Table 2. Viscosity data for the branched fractions of sample 4 in benzene at 35°C

Fraction	$\bar{M}_w \times 10^{-6}$	$[\eta]$ (*dl/g*)	*Slope, b*	*k'*	*k'+k''*	*Yield* (*g*)
4		$3{\cdot}08_0$	3·53	$0{\cdot}37_2$	0·501	
4–1–1–1		$7{\cdot}15_0$	21·78	$0{\cdot}42_6$	0·500	2·5
4–2–1		$5{\cdot}84_5$	13·20	$0{\cdot}38_5$	0·501	3·0
4–2–2		$5{\cdot}68_0$	11·71	$0{\cdot}36_3$	0·500	6·0
4–1–1–2	12·6	$4{\cdot}82_0$	8·99	$0{\cdot}38_7$	0·502	2·5
4–3–1		$4{\cdot}77_0$	8·67	$0{\cdot}38_1$	0·502	4·3
4–3–2	3·76	$3{\cdot}79_0$	5·10	$0{\cdot}35_5$	0·501	5·0
4–2–3	6·43	$3{\cdot}50_0$	4·73	$0{\cdot}38_6$	0·502	6·0
4–4–1	2·86	$2{\cdot}97_0$	3·25	$0{\cdot}36_9$	0·499	22·5
4–4–2	1·64	$2{\cdot}26_0$	1·76	$0{\cdot}34_5$	0·498	9·0
4–3–3		$2{\cdot}23_5$	1·85	$0{\cdot}37_0$	0·502	3·0
4–5–1	1·43	$1{\cdot}96_2$	1·35	$0{\cdot}35_1$	0·499	3·5
4–5–2	0·730	$1{\cdot}48_5$	0·800	$0{\cdot}36_3$	0·501	9·0
4–4–3	0·731	$1{\cdot}38_5$	0·673	$0{\cdot}35_1$	0·500	4·8
4–5–3	0·432	$1{\cdot}10_4$	0·419	$0{\cdot}34_4$	0·500	10·0
4–5–4		$0{\cdot}71_6$	0·180	$0{\cdot}35_1$	0·501	5·2
4–6		$0{\cdot}44_5$	0·055	$0{\cdot}27_8$	0·498	9·3

Hydrolysis and re-acetylation

The procedures employed were similar to those described by Wheeler *et al.*[9] and the results are tabulated in *Table 4*. Polymer was hydrolysed by treating a methanolic polymer solution (0·75 g/dl) with ten parts of a five per cent solution of potassium hydroxide in methanol. The reaction mixture was held at 35°C for five to ten hours until the precipitation of polyvinyl alcohol was complete. The polyvinyl alcohol was separated, washed with methanol, and dried. The product was then re-acetylated by treatment with 40 ml (per gramme of polymer) of a mixture of acetic anhydride, acetic acid, and pyridine (in proportion of 15 : 5 : 1). The mixture was held at 100°C for one to two days or until the dissolution of the polyvinyl alcohol was complete. The reconstituted polyvinyl acetate was separated by pouring the reaction mixture into a large excess of water. The product was washed with water, dissolved in benzene, and recovered by the freeze-drying technique.

Viscosity measurements

The viscosity measurements were made with a modified Ubbelohde suspended level viscometer[10]. The capillary was 18·5 cm long, with an inside diameter of 0·0356 cm. Flow measurements were made at 35·0° ±0·02°C on benzene as solvent and at five solution concentrations so adjusted as to

Table 3. Viscosity data for the linear fractions of sample 5 in benzene at 35°C

Fraction	$\bar{M}_w \times 10^{-6}$	$[\eta]$ (*dl/g*)	*Slope, b*	*k'*	*k'+k''*	*Yield* (*g*)
5		$3{\cdot}41_0$	4·02	$0{\cdot}34_6$	0·499	
5–2–2		$5{\cdot}70_5$	11·39	$0{\cdot}35_0$	0·500	3·7
5–2–1	3·58	$5{\cdot}60_3$	10·86	$0{\cdot}34_6$	0·500	6·6
5–1–1		$5{\cdot}55_0$	10·50	$0{\cdot}34_1$	0·500	4·5
5–1–2		$5{\cdot}54_0$	10·93	$0{\cdot}35_6$	0·502	1·9
5–1–3		—	—	—	—	2·3
5–3–1		$5{\cdot}25_0$	9·56	$0{\cdot}34_7$	0·500	4·2
5–3–2	2·66	$4{\cdot}97_0$	8·69	$0{\cdot}35_2$	0·500	5·8
5–4–1		$4{\cdot}57_0$	7·20	$0{\cdot}34_5$	0·499	9·0
5–2–3		$4{\cdot}37_2$	6·63	$0{\cdot}34_7$	0·500	11·2
5–2–4		—	—	—	—	4·8
5–4–2	2·28	$4{\cdot}29_0$	6·46	$0{\cdot}35_1$	0·498	10·2
5–3–3		$4{\cdot}06_0$	5·69	$0{\cdot}34_5$	0·499	11·6
5–3–4		—	—	—	—	3·3
5–5–1		$3{\cdot}95_0$	5·38	$0{\cdot}34_5$	0·499	6·6
5–4–3		$3{\cdot}76_0$	4·98	$0{\cdot}35_2$	0·501	4·5
5–4–4		—	—	—	—	6·3
5–5–2	1·84	$3{\cdot}71_0$	4·80	$0{\cdot}34_9$	0·500	10·8
5–5–3		$3{\cdot}32_0$	3·82	$0{\cdot}34_7$	0·499	7·7
5–5–4		—	—	—	—	6·3
5–6–1		$2{\cdot}91_5$	2·88	$0{\cdot}33_9$	0·499	10·2
5–6–2	1·14	$2{\cdot}81_3$	2·77	$0{\cdot}35_0$	0·499	9·4
5–6–3	0·991	$2{\cdot}50_0$	2·13	$0{\cdot}34_0$	0·500	7·4
5–6–4		—	—	—	—	7·9
5–7–1		$1{\cdot}96_1$	1·30	$0{\cdot}33_9$	0·499	5·4
5–7–2	0·654	$1{\cdot}77_0$	1·01	$0{\cdot}32_2$	0·498	6·3
5–7–3		$1{\cdot}55_7$	0·810	$0{\cdot}33_4$	0·499	4·0
5–7–4	0·438	$1{\cdot}37_2$	0·629	$0{\cdot}33_4$	0·499	3·5
5–7–5		—	—	—	—	9·2

yield values of η_r in the range of 1·15 to 1·7. Values of $[\eta]$, k' and k'' were obtained from double plots[11,12] according to the expressions:

$$\eta_{sp}/c = [\eta] + k'[\eta]^2 c + \ldots \quad (1)$$

and

$$\frac{\ln \eta_r}{c} = [\eta] - k''[\eta]^2 c + \ldots \quad (2)$$

under the condition that $k' + k'' = 0{\cdot}500 \pm 0{\cdot}002$, where the symbols have their usual significance. Values of intrinsic viscosity and Huggins k' are listed in *Tables 2* and *3* for the fractions of series 4 and 5.

In addition to the viscosity measurements made under free fall conditions, the viscosities of selected linear and branched fractions were studied over a range of shear rates from about 500 to 5 000 sec^{-1}. Shear rates above that at free fall (1 920 sec^{-1} for benzene) were obtained by applying air pressure to the top of the liquid in the capillary to increase the flow rate. Shear rates below that at free fall were obtained by applying air pressure to the bottom of the liquid in the capillary to retard flow. The results were carefully examined for evidence that application of air pressure at the

bottom of the liquid in the capillary might sufficiently deform the suspended level to cause erroneous measurement. However, since plots of solvent flow time versus shear rate showed no abnormal behaviour or discontinuity, the technique was judged to be satisfactory for the purpose of this study.

The water manostat used to control the air pressure was similar to that described by Sharman *et al.*[13] with the addition of a constant-head water supply. Flow times were reproduceable to approximately $\pm 0{\cdot}2$ per cent in the shear range indicated above. A kinetic energy correction of $20/t$ was subtracted from all flow times, where t is the flow time at free fall. Consideration of the Poiseuille equation shows that the kinetic energy correction is essentially independent of shear rate[5].

The maximum rate of shear at the capillary wall was used in all correlations and was calculated by the following equation

$$D = rghd/2L\eta_0\eta_r \tag{3}$$

where r and L are the radius and length of the capillary, respectively, $\mathbf{g}$ is acceleration of gravity, h is average effective height of the driving head and d its density, η_0 is solvent viscosity, and η_r is the relative viscosity of the solution. A more precise calculation for D which accounts for non-Newtonian flow, suggested by van Oene and Cragg[14], was not used because the correction was small under the conditions of this study and would not have significantly altered the correlations. For example, the correction for one of the most non-Newtonian cases, fraction 3–3, was only 1·5 per cent. Likewise, a similar correction to η_r was omitted because the correction was small, about 1·5 per cent for fraction 3–3, compared to the observed changes in η_r.

Light scattering measurements

The light scattering measurements were made with a Brice–Phoenix light scattering photometer, model number 1410, using a cylindrical type scattering cell with flat entrance and exit windows. The measurements were made with 4 358 Å light, and methyl ethyl ketone was employed as the solvent, taking 0·080 as the value of dn/dc[15].

The scattering data were treated according to a method of Zimm[16]. Values of weight average molecular weight, $\overline{M}_w$, for selected samples are tabulated in *Tables 2* and *3*. The values of the second virial coefficient and radius of gyration will be considered in the third paper of this series[3].

RESULTS AND DISCUSSION

Characterization of fractions

Molecular weight and polydispersity—At a given molecular weight, the intrinsic viscosity of a branched fraction is lower than that of the linear polymer as shown in *Figure 1*. The weight average molecular weights of the linear fractions are related to the intrinsic viscosities in benzene at 35°C by the expression

$$\log \overline{M}_w = 5{\cdot}426 + 1{\cdot}48 \log [\eta] \tag{4}$$

The above is typical behaviour for linear and branched materials.

The polymer fractions are believed to be relatively narrow in molecular weight distribution because of the fractionation technique employed. This is particularly true of the secondary and tertiary fractions. It is realized, however, that the branched fractions must be somewhat more polydispersed because of the dependence of solubility on both molecular weight and structure.

An estimate of the degree of polydispersity was obtained for the linear fractions of series 5 from the shape of the reciprocal scattering curve of the light scattering data[17]. The ratio of $\overline{M}_w/\overline{M}_n$ averaged about 1·1 for these fractions. Although this method for estimating polydispersity is not applicable to branched polymers, the shape of the scattering envelopes of the branched fractions supports the contention that they are reasonably narrow fractions.

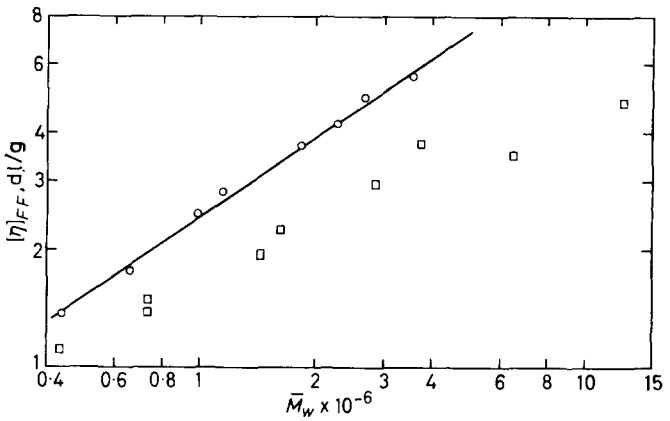

Figure 1—Intrinsic viscosity in benzene at 35°C versus weight average molecular weight: □—branched fractions, series 4; ○—linear fractions, series 5

Identification of structure by hydrolysis and re-acetylation—Branching in polyvinyl acetate that results from chain transfer mechanisms may be classified as two types. Branches attached to the backbone chain via acetate groups are of the hydrolysable type, and branches connected directly to the backbone by C—C bonds are non-hydrolysable. Both types of branching may be minimized by polymerization at low temperature and low conversion.

The decrease in intrinsic viscosity and molecular weight of the branched fractions of sample 4, *Table 4*, is a sensitive indication of the presence of hydrolysable branches, even for the lower molecular weight fractions which contain relatively few branches. The absence of a change in intrinsic viscosity of the linear polymer, sample 5, *Table 4*, establishes the absence of hydrolysable branches. Since the linear polymer was prepared at low temperature (−19°C) and low conversion (4–10 per cent) it is assumed that the material also contains no non-hydrolysable branches and is, indeed, truly linear in structure.

The presence of non-hydrolysable branches in the branched material becomes apparent when the molecular weight of the hydrolysed and re-

acetylated product calculated from $[\eta]_H$ by equation (4) is compared to the molecular weight of the same product from light scattering for fractions 4–4–2 and 4–1–1–1, *Table 4*. The fact that the measured molecular weight is greater than the calculated value is taken as evidence of non-hydrolysable

Table 4. Hydrolysis data[a, b]

Fraction	$[\eta]$	$[\eta]_H$	$(\bar{M}_w)\times 10^{-6}$	$(\bar{M}_w)_H\times 10^{-6}$
4	3·08	1·15	—	0·328
4–1–1–1	7·15	1·34	—	0·412[c]
4–2–1	5·85	1·39	—	0·435
4–4–2	2·26	1·17	1·64	0·336[d]
4–5–1	1·96	1·03	1·43	0·278
4–4–3	1·39	0·89	0·731	0·224
4–5–2	1·49	0·95	0·730	0·247
4–5–3	1·10	0·85	0·432	0·210
5	3·41	3·38	—	—
5–3–2	4·97	5·03	—	—
5–6–2	2·81	2·82	—	—

a *H* denotes properties after hydrolysis and re-acetylation.

b $(\bar{M}_w)_H$ was calculated from $[\eta]_H$ by equation (4).

c $(\bar{M}_w)_H\times 10^{-6}=0{\cdot}674$ by light scattering.

d $(\bar{M}_w)_H\times 10^{-6}=0{\cdot}408$ by light scattering.

branching. Thus, while the hydrolysis technique is a sensitive means of detecting hydrolysable linkages, it cannot be used as a quantitative means of estimating the degree of branching present in branched polyvinyl acetate.

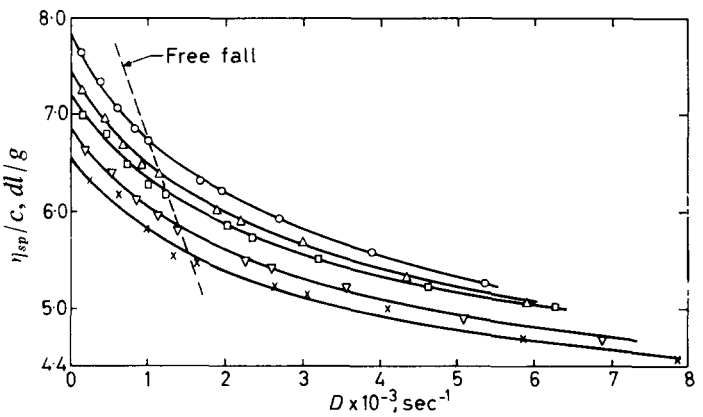

Figure 2—Reduced specific viscosity in benzene at 35°C versus rate of shear for fraction 3–3. Concentration (g/dl): ○—0·1280, △—0·1024, □—0·0853, ▽—0·0640, ×—0·0320

Non-Newtonian viscosity behaviour of dilute solutions

In studying the high molecular weight fractions, it was of interest to determine for the polyvinyl acetate–benzene system whether non-Newtonian behaviour affects the values of $[\eta]$ and k' of the Huggins equation as they are normally measured in a capillary viscometer and whether it affects the ratio of the intrinsic viscosities of branched and linear polymers, $[\eta]_B/[\eta]_L$,

of a given molecular weight, a function that is utilized in estimating the degree of branching in Part III[3] of this series of papers. Furthermore, it was desired to examine the effects of changes in shear rate upon the viscosities of linear and branched fractions as a possible means for detecting the presence of branched structures.

The viscosities of dilute solutions of selected linear and branched fractions were measured over a range of shear rates of approximately 500 to 5 000 sec^{-1}. A typical graph of the reduced specific viscosity, η_{sp}/c, versus shear rate, D, is shown in *Figure 2*. The curvature of the lines is due to the non-Newtonian character of the solutions. This curvature is large for polyvinyl acetate fractions of high molecular weight and, for a given fraction, it is somewhat greater at the higher concentrations. The straight line drawn across the curves represents the shear rates for the normal measurement at free fall, that is, at the shear rates produced in the particular viscometer with the particular solutions by gravity. Under free fall conditions, the more concentrated or more viscous solutions are subjected to relatively lower shear rates. This situation, as has been pointed out by Conrad *et al.*[18], causes an increase in the slope of the η_{sp}/c versus c plot and thus results in an increased value of k'.

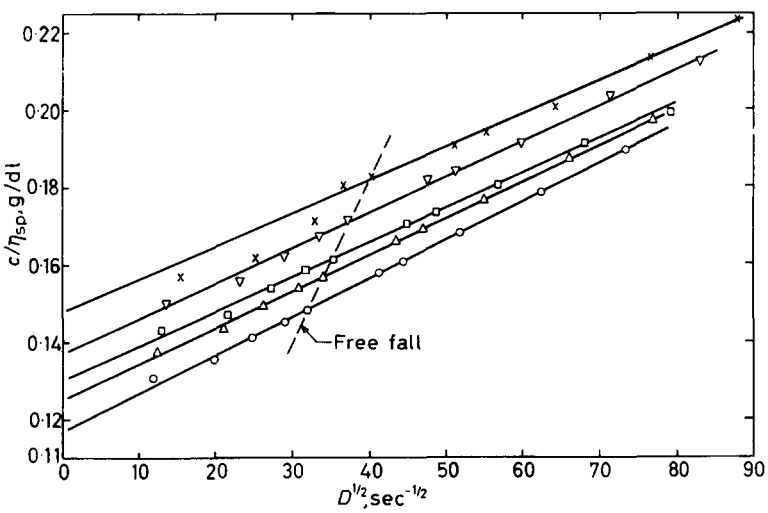

Figure 3—Reciprocal reduced specific viscosity in benzene at 35°C versus square root of shear rate for fraction 3–3. Concentration (g/dl): ○—0·1280, △—0·1024, □—0·0853, ▽—0·0640, ×—0·0320

In order to establish a reference point, Dr L. H. Cragg suggested the plot, c/η_{sp} versus $D^{1/2}$, *Figure 3*, which provides a means of extrapolation to the hypothetical condition of zero shear rate. The slopes of the lines for the several concentrations, J_c, are measures of the shear sensitivity of the solutions or the degree of their non-Newtonian character. The lines are represented by the equation

$$(\eta_{sp}/c)^{-1}_{c,D=0} = (\eta_{sp}/c)^{-1}_{c,D} - J_c D^{1/2}$$

For the low concentrations employed, it was found that J_c is a linear function

of concentration (graph not shown). Extrapolated values of $J_{c=0}$ are listed in *Table 5*. It was also observed that a plot of the shear rates at free fall condition versus concentration yielded a straight line from which the shear rate at infinite dilution under free fall was found to be 1 920 sec^{-1}, or the value calculated for the solvent. With this information, equation 5 at zero concentration becomes

$$[\eta]_{D=0}^{-1} = [\eta]_{D=1\,920}^{-1} - 1\,920^{-1/2} J_{c=0} \tag{6}$$

where $[\eta]_{D=1\,920}$ is the intrinsic viscosity determined at infinite dilution and as the shear rate approaches that of pure solvent, i.e. the usual free fall intrinsic viscosity. Thus equation (6) provides the means for estimating the intrinsic viscosity at zero shear rate from the values of the intrinsic viscosity, $[\eta]_{FF}$, as normally measured under free fall conditions. The calculated values of $[\eta]_{D=0}$, recorded in *Table 5*, are useful as points of reference in comparing

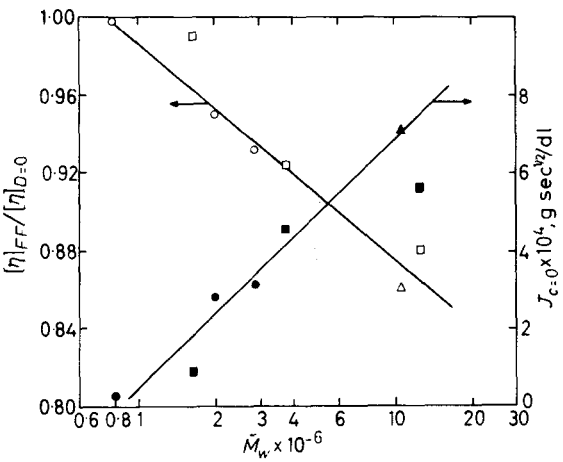

Figure 4—Shear rate sensitivity versus weight average molecular weight: ○—linear fractions, series 1 and 2; △—branched fractions, series 3; □—branched fractions, series 4

the effects of rate of shear encountered in routine measurements upon the viscosity properties of the linear and branched fractions. It is not suggested that they would be identical with results obtained by measurements at very low shear rates.

As noted in connection with *Figure 2*, the non-Newtonian character of the solutions of the high molecular weight fractions causes a marked reduction in the intrinsic viscosity and a moderate increase in k'. The degree of non-Newtonian character or shear sensitivity is reflected in $J_{c=0}$ and the ratio $[\eta]_{FF}/[\eta]_{D=0}$. These variables are plotted against $\overline{M}_w$ in *Figure 4*. It is evident that the shear sensitivity varies directly with $\overline{M}_w$ regardless of the presence of branching. Based on this information, the percentage change of $[\eta]_{FF}$ with respect to $[\eta]_{D=0}$ can be calculated. A 5 per cent decrease in the value of $[\eta]_{FF}$ occurs at a $\overline{M}_w$ of 2×10^6.

In *Figure 5*, the plot of the shear sensitivity function, $J_{c=0}$, versus Huggins k' shows the existence of a direct relationship between the two variables which, again, is insensitive to the presence of branching. Since $J_{c=0}$ is a direct function of molecular weight (*Figure 4*) it must be concluded that

Table 5. Shear dependence data

Fraction	$[\eta]_{D=0}$ (*dl/g*)	$[\eta]_{FF}$ (*dl/g*)	k'	$\overline{M}_w \times 10^{-6}$	$J_c \times 10^4$	*Concentration* (*g/dl*)
4–1–1–1	10·3	7·15	$0{\cdot}42_6$	—	9·80	0
					10·1	0·0248
					10·0	0·0372
					10·4	0·0740
3–3	6·61	5·32	$0{\cdot}42_2$	—	8·35	0
					8·70	0·0320
					9·00	0·0640
					9·22	0·0853
					9·47	0·1024
					9·72	0·1280
4–1–1–2	5·47	4·82	$0{\cdot}38_7$	12·6	5·64	0
					6·16	0·0561
					6·70	0·1121
3–4	5·19	4·47	$0{\cdot}39_8$	10·8	7·10	0
					7·90	0·0362
					7·76	0·0482
					8·12	0·0724
					8·28	0·0965
					8·84	0·1158
					9·18	0·1447
3–5	4·35	3·89	$0{\cdot}38_5$	—	6·20	0
					6·75	0·0624
					6·92	0·0936
					7·40	0·1871
4–3–2	4·10	3·79	$0{\cdot}35_5$	3·76	4·55	0
					5·10	0·0510
					5·30	0·0765
					6·10	0·1530
4–4–2	2·28	2·26	$0{\cdot}34_5$	1·64	0·9	0
					0·96	0·2451
2–1–1	5·31	4·95	$0{\cdot}35_2$	2·85	3·13	0
					3·22	0·0583
					3·30	0·1165
2–4	4·10	3·90	$0{\cdot}33_0$	2·00	2·80	0
					2·80	0·0602
					2·93	0·0904
					2·97	0·1807
1–2	2·10	2·09	$0{\cdot}32_7$	0·795	0·3	0
					0·4	0·1963
					0·5	0·2945

molecular weight makes a significant contribution to the observed value of k'. A gradual increase in k' with increasing molecular weight is seen in *Figure 6*. However, a few values of k' do lie substantially above the band

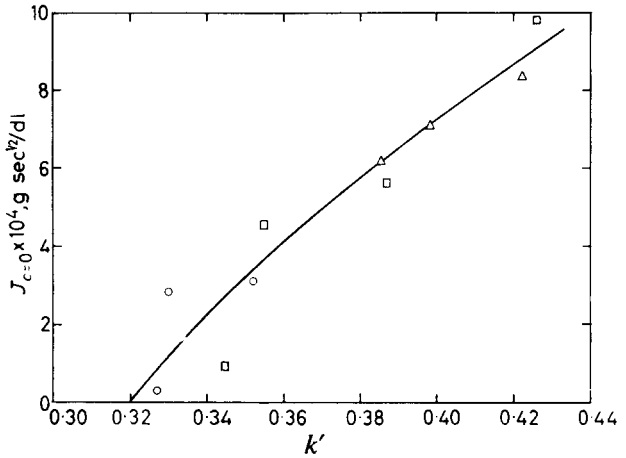

Figure 5—Shear rate sensitivity versus Huggins k': ○—linear fractions, series 1 and 2; △—branched fractions, series 3; □—branched fractions, series 4

of points in *Figure 6*, and it may be that k' is increased by certain types of molecular structure in branched polyvinyl acetate, as well as by molecular weight or non-Newtonian behaviour.

The ratio $[\eta]_B/[\eta]_L$ at a given molecular weight is useful in estimating the degree of branching, for example, by the method of Stockmayer and Fixman[19]. While the individual values of $[\eta]_B$ and $[\eta]_L$ may be reduced by measurement at shear rates other than that of zero, the ratio is little changed,

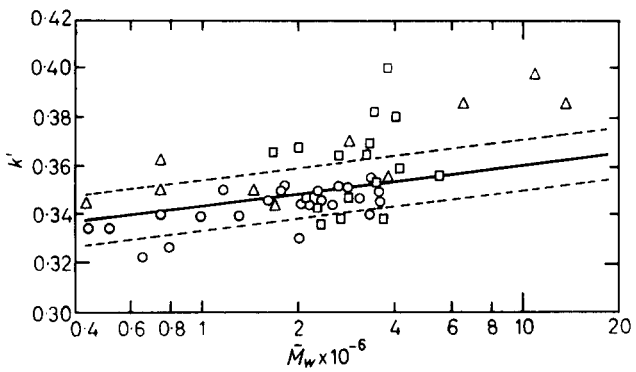

Figure 6—Huggins k' versus weight average molecular weight: ○—linear fractions, △—randomly branched fractions, □—comb-shaped branched fractions

at least for the polyvinyl acetate–benzene system of this study. This results because of the strong dependence of shear sensitivity on molecular weight as shown in *Figure 4*. Thus, the ratio $[\eta]_B/[\eta]_L$, as normally determined from measurements made under free fall conditions, will be useful for the

estimation of the degree of branching for both Newtonian and non-Newtonian solutions.

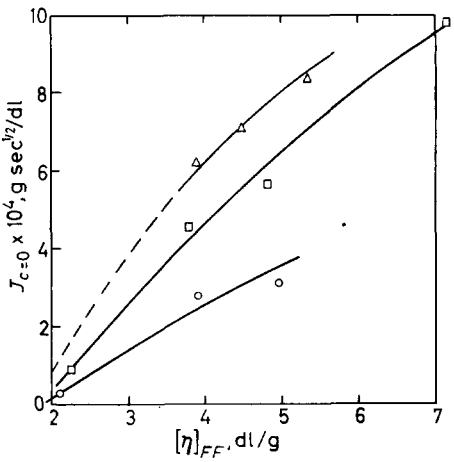

Figure 7—Shear rate sensitivity versus intrinsic viscosity in benzene at 35°C: ○—linear fractions, series 1 and 2; △—branched fractions, series 3; □—branched fractions, series 4

In *Figure 7* it may be seen that the shear sensitivity of the branched fractions increases more rapidly with $[\eta]$ than does that of the linear fractions. This is a consequence of the fact that the molecular weight of the branched fractions changes more rapidly with $[\eta]$. It would be possible, although tedious, to detect branching in polyvinyl acetate from viscosity data obtained over a range of shear rates without supplementary information regarding molecular weight. If $J_{c=0}$ for the sample of unknown structure were obtained and the $J_{c=0}$ versus $[\eta]$ curve of *Figure 7* were established for linear fractions, then the ratio of $J_{c=0}$ for the unknown to $J_{c=0}$ of the linear polymer having the same value of $[\eta]$ could be obtained. Values of the ratio greater than unity would indicate the presence of branching.

We express our appreciation to the Goodyear Tire and Rubber Company for their contribution to the Michigan Memorial–Phoenix Project which has made this work possible. We also wish to thank Professor L. H. Cragg, of the University of Alberta, and Dr J. A. Manson, of the Air Reduction Company, for helpful suggestions, and Dr C. H. Lu and Mr M. M. Gurvitch for their aid with portions of the experimental work while students at the University of Michigan.

Department of Chemical Engineering and
Michigan Memorial–Phoenix Project,
University of Michigan, Ann Arbor, Michigan

(*Received December 1962*)

REFERENCES

[1] HOBBS, L. M., KOTHARI, S. C., LONG, V. C. and SUTARIA, G. C. *J. Polym. Sci.* 1956, **22**, 123
[2] BERRY, G. C. and CRAIG, R. G. *Polymer, Lond.* In press
[3] BERRY, G. C., HOBBS, L. M. and LONG, V. C. *Polymer, Lond.* In press

[4] BERRY, G. C., HOBBS, L. M. and LONG, V. C. *Polymer, Lond.* In press
[5] LONG, V. C. *Ph.D. Thesis,* University of Michigan, 1958
[6] BURNETT, G. M., GEORGE, M. H. and MELVILLE, H. W. *J. Polym. Sci.* 1955, **16,** 31
[7] MATSUMOTO, M. and OHYANAGI, Y. *J. Polym. Sci.* 1960, **46,** 520
[8] SCHILDKNECHT, C. E. *Vinyl and Related Polymers,* pp 244–246. Wiley: New York, 1952
[9] WHEELER, O. L., ERNST, S. L. and CROZIER, R. N. *J. Polym. Sci.* 1952, **8,** 409
[10] CRAIG, A. W. and HENDERSON, D. A. *J. Polym. Sci.* 1956, **19,** 215
[11] HELLER, W. *J. Colloid Sci.* 1954, **9,** 547
[12] EWART, R. H. *Advanc. Colloid Sci.* 1946, **2,** 211
[13] SHARMAN, L. J., SONES, R. H. and CRAGG, L. H. *J. appl. Phys.* 1953, **24,** 703
[14] VAN OENE, H. and CRAGG, L. H. *J. Polym. Sci.* 1962, **57,** 209
[15] SCHULTZ, A. R. *J. Amer. chem. Soc.* 1954, **76,** 3422
[16] ZIMM, B. H. *J. phys. Colloid Chem.* 1948, **52,** 260; *J. chem. Phys.* 1948, **16,** 1093, 1099
[17] BENOIT, H., HOLTZER, A. M. and DOTY, P. *J. phys. Chem.* 1954, **58,** 635
[18] CONRAD, C. M., TRIPP, V. W. and MARES, T. *J. phys. Colloid Chem.* 1951, **55,** 1474
[19] STOCKMAYER, W. H. and FIXMAN, M. *Ann. N. Y. Acad. Sci.* 1953, **57,** 334

The Photochemical Degradation of Polyamides and Related Model N-Alkylamides

R. F. MOORE

Analogous products to those obtained from exposure of simple model N-alkylamides to u.v. light, in oxygen or under anaerobic conditions, have been sought in a concurrent investigation of the photodegradation of polyamides (chiefly 6.6 nylon) in u.v. light and sunlight. The polymer degradation has been characterized by measurement of yarn tenacity losses under different conditions, and correlation of these with changes in intrinsic viscosity, u.v. absorption and end-groups. Chemical changes occurring, detected by analysis of the hydrolysed polymer, indicate the formation of aldehyde and primary amide end-groups, and a smaller number of n-pentylamino and n-pentanoyl end-groups. The results for both N-alkylamides and polyamides, can be interpreted by postulating two types of reaction: a photolysis into both free radicals and smaller molecules, occurring at short wavelengths and independent of oxygen, and a photosensitized autoxidation, occurring at longer wavelengths, involving oxidative attack predominantly at the methylene group adjacent to the N atom of the molecule, and subsequent decomposition of the derived radical R.CO.NH.CH(O·).R′. *The more rapid loss of tenacity observed with titanium dioxide delustered yarns containing no oxidation inhibitors is due to increased photodegradation around the delustrant particles; the same products result as with bright yarns.*

EXPOSURE to sunlight under natural conditions causes a deterioration in the desirable properties of many artificial and natural textile materials. The changes which occur, which can be reproduced using artificial light, manifest themselves as a loss of strength and elasticity of the individual fibres. There is an accompanying reduction in the molecular weight of the fibre molecules, and slight changes in its chemical constitution can be detected.

The present work is confined to an investigation of the photochemical degradation of polyamide material used in the manufacture of nylon (in particular 6.6 nylon). Although from the practical point of view, the main interest lies in the degradation occurring in the presence of oxygen, a straight photolysis of the polyamide chains was also studied. To gain some insight into the type of chemical changes to be expected, a parallel investigation of the photochemical decomposition of aliphatic *N*-alkylamides of the type $H(CH_2)_mCO.NH(CH_2)_nH$ (where $m+n=11$ or 12) was also carried out.

The comparatively meagre information available in the literature on the photo-decomposition of amides has recently been augmented by a comprehensive study of the photo-oxidation of *N*-pentyl hexanamide and analogous amides[1]. With light of wavelength greater than 3 000 Å, acids, aldehydes, primary amide, carbon monoxide and dioxide were obtained; oxidative attack occurred primarily at the methylene group adjacent to the nitrogen atom of the amide molecule, resulting in peroxidation at this

point with subsequent breakdown to give an aldehyde and primary amide. Compounds of the type $RCO.NH.C(R'')_2R'$ (where R'' is alkyl) were found to be resistant to oxidation. Independent work in these laboratories has followed similar lines; however, as shorter wavelength light was not excluded, products from photolysis were also observed. *N*-acylamides have also been reported as major products of the autoxidation of *N*-alkylamides[2]. These are formed from the alternative modes of breakdown of the peroxy radical $RCO.NH.CH(OO\cdot)R'$.

Although considerable work has been published on the photodegradation of nylon[3–10], few attempts have been made to study chemical changes occurring in the polymer. Both chainbreaking and crosslinking have been shown to occur, the latter chiefly at shorter wavelengths; in the absence of oxygen, the formation of hydrogen, carbon monoxide and hydrocarbons has been observed with both 6.6[11] and 6 nylon[12]. Evidence for the role played by water is conflicting[3, 13, 14].

In the present investigation, the results from the work with *N*-alkylamides led to a search for similar products as end-groups in the cleaved polymer chains. A study was also made of the conditions under which both bright (containing nil delustrant) and delustred yarns undergo degradation as measured by loss in tenacity, and the latter was related to changes in other physical and chemical properties occurring on exposure of polyamide fibres to sunlight.

EXPERIMENTAL

Apparatus

The lamp used in experiments with artificial light was an air-cooled, 1 kW high pressure mercury vapour lamp, having a virtual point source. The light from three circular apertures in the lamp housing was focused into almost parallel beams, *ca.* 9 cm across, by water-filled quartz flasks. A fourth aperture led to a photocell actuating an integrating meter which measured the total light energy in arbitrary units on a counter. Chance glass filters were used to select various wavelengths of light.

The model amides were exposed in quartz flasks. In the experiments using artificial light, polymer film and yarn samples were exposed in gas-tight metal cells with plane windows of quartz or Pyrex.

Materials

The *N*-alkylamides, all liquid at 25°C, were prepared by reacting equivalent amounts of the aliphatic amine and carboxylic acid chloride in benzene or ether, in the presence of a slight excess of pyridine at a temperature below 30°C. The amide, after washing with dilute hydrochloric acid, ten per cent sodium carbonate solution and water, was purified twice by distillation under reduced pressure. Details are as follows:—*N*-hexylhexanamide, b.pt 108° to 111°C at 0·07 mm (found C, 72·4; H, 12·7; N, 6·9 per cent); *N*-butyloctanamide, b.pt 125° to 129°C at 0·2 mm (found C, 71·9; H, 12·6; N, 6·8 per cent); *N*-heptylhexanamide, b.pt 132° to 136°C at 0·2 mm (found C, 73·6; H, 12·6; N, 6·4 per cent); *N*-methyl-*N*-pentylhexanamide, b.pt 75° to 76°C at 0·06 mm (found C, 72·3; H, 12·9; N, 7·4 per cent); *N*-(1,1-dimethylbutyl)-hexanamide*, b.pt 81°C at 0·08 mm

*1,1-Dimethylbutylamine was prepared according to Montagne's method[15].

(found C, 72·5; H, 12·7; N, 7·0 per cent. $C_{12}H_{25}ON$ requires C, 72·3; H, 12·6; N, 7·0 per cent: $C_{13}H_{27}ON$ requires C, 73·2; H, 12·8; N, 6·7 per cent).

Hot pressed films of 6.6, 6.10, 10.6 and 6 nylons free from delustrant were used in small scale experiments involving exposure of polymer to artificial light. For larger scale sunlight exposures, hanks of bright (30 denier, 10 filament, nil titanium dioxide) and delustred (45 denier, 15 filament, 1·6 per cent titanium dioxide) multifilament nylon yarns (supplied by British Nylon Spinners Ltd) were used. The yarns for tenacity measurements were obtained by doubling or trebling low-twist yarns, twisting to 4 or 5 turns per inch and steam-setting. All delustred yarns were free of additives present in commercial yarns to reduce photodegradation[16].

Paper chromatographic analysis

Details of the methods used for the analysis of carboxylic acids and amines are as follows[17]. Using a descending method of development, the solvent for monobasic acids was butanol: 1·5 N ammonia (1:1 v/v); for dibasic acids, ethanol: water: conc. ammonia (20:4:1 v/v); and for amines, butanol: acetic acid: water (4:1:5 v/v). After drying, the sheets of Whatman No. 1 paper were sprayed respectively with bromocresol green (0·1 per cent in isopropanol) to detect monobasic acids (giving blue spots on a yellow background), with B.D.H. Universal indicator for dibasic acids (red spots on green), and with ninhydrin (0·3 per cent in butanol) for amines (purple spots for primary aliphatic amines after heating for 15 min at 80°C). Aldehyde 2,4-dinitrophenylhydrazones were chromatographed using paper impregnated with phenoxyethanol, and light petroleum as the developing solvent[18].

Exposure of N-*alkylamides to u.v. light*

In most experiments pure oxygen or nitrogen was bubbled slowly (*ca.* 0·5 l./h) through about 160 g of the *N*-alkylamide in a 200 ml quartz flask, placed about 30 cm from the lamp; the amide reached a temperature of about 40°C. Off-gases passed consecutively through two traps cooled in Drikold, Anhydrone and Carbosorb tubes, and a bubbler containing 0·01 N hydrochloric acid. In no experiment was there any indication of the absorption of basic gases by this trap. Carbon monoxide was detected using 'CO-test' tubes containing silica gel impregnated with potassium palladosulphite and estimated with iodine pentoxide[19].

The cold traps condensed a small amount of organic material and water and further volatile material was collected in them by heating the exposed amide to 150°C in a current of nitrogen. Analysis of these products by mass and i.r. spectroscopy and paper chromatography indicated a mixture of *n*-paraffins and 1-olefins, carboxylic acids and an aldehyde which was identified by paper chromatography of its 2,4-dinitrophenylhydrazone.

The bulk of exposed material was distilled under reduced pressure to give a low-boiling fore fraction (*ca.* 10 g), a large middle fraction of unchanged amide, and a residue (*ca.* 5 g). The fore fraction and residue were examined before and after acid (5 N hydrochloric) or alkaline (10 per cent

ethanolic sodium hydroxide) hydrolysis by a combination of chromatographic, i.r. and mass spectrometric techniques. The fore fraction was further separated by steam distillation to give a small distillate (*ca.* 1 g) consisting mainly of acids; from the non-volatile material, which consisted largely of unchanged *N*-alkylamide, a solid primary amide (*ca.* 1 g) was obtained by distillation and purified by crystallization. In addition, the viscous residue, on treatment with ether, sometimes yielded a small amount of solid which analysed approximately for a dimer of the parent *N*-alkylamide.

In some experiments, concentration of the gaseous products of the degradation for mass spectrometric analysis was effected by re-circulating the same oxygen through the *N*-alkylamide. (Similar analyses were obtained of the off-gases from exposures *in vacuo*.) The circulating technique was also used to compare the rates of oxygen absorption of selected model amides when exposed to light of different wavelength. The amides compared, *N*-hexyl-hexanamide, *N*-methyl-*N*-pentylhexanamide and *N*-(1,1-dimethylbutyl)-hexanamide, were chosen because of the varying number of hydrogen atoms adjacent to the nitrogen atom of the molecule.

The experiments carried out and the products obtained are summarized in *Table 1*; other details are as follows.

Exp. 1. Unknown amines from the residue hydrolysate had R_f values 0·90, 0·55, 0·39 and 0·30.

Exp. 2. The 'dimer', 0·03 g, m.pt 186° to 189°C (crystallized from ethanol: found C, 72·9; H, 11·8; N, 6·9 per cent, corresponding to an empirical formula $C_{12}H_{23\cdot1}N_{0\cdot97}O_{1\cdot04}$; mol. wt 444·5 corresponding to a C_{24} molecule) is probably two *N*-butyl-octanamide molecules crosslinked in some way. The i.r. spectrum was similar to that of the parent amide but contained additional bands at 8·25, 8·76 and 10·46μ, possibly due to a diamide. Unknown amines from the residue hydrolysate had R_f values 0·84, 0·80, 0·37 and 0·24.

Exp. 4. Mass spectrometric analysis of volatile material, b.pt 87° to 120°C at 0·15 mm, indicated masses 157, 129, 116 and 115 as parent ions. Of these, mass 157 (with a large breakdown ion, mass 142) could be due to *N*-acetylheptylamine; mass 115 was due to hexanamide while mass 129 suggests a methyl homologue of it. However, no methylamine was detected in the hydrolysate. The unknown compound of mass 116 was not *n*-hexanoic acid.

Exp. 5. Mass spectrometric analysis of material, b.pt 130° to 180°C at 11 mm, again showed masses 157, 129 and 116.

Exp. 8. During distillation of the exposed amide *ca.* 0·01 g of *n*-heptylamine was condensed in a cold trap.

Exp. 9. *N*-Butylhexanamide (100 g) was exposed in pure cyclohexane (150 ml); extraction of the solution with dilute hydrochloric acid yielded no amines. The recovered cyclohexane showed no unsaturation.

Exps. 10–12. Rates of oxygen absorption were determined for the three selected *N*-alkylamides (70 g samples in 100 ml quartz flask) in the full beam of the lamp, and with light of wavelength greater than 3 000 Å (Pyrex filter) and 3 500 Å (Chance filter OY 10) only. The comparative rates for wavelengths greater than 2 500 Å were in the order *N*-methyl-*N*-pentylhexanamide: *N*-hexylhexanamide: *N*-(1,1-dimethylbutyl) hexanamide, 2·9 : 1·5 : 1: The same order was found in the comparison of the last two amides when light of wavelengths greater than 3 000 Å and 3 500 Å was used, the ratios being 4·7 : 1 and 25 : 1 respectively. Products of the degradation included with *N*-methyl-*N*-pentylhexanamide, a non-steam volatile fraction, b.pt

94° to 142°C at 15 mm (0·55 g), which on mass spectrometric analysis showed two molecular ions at masses 129 and 142, probably due respectively to *N*-methylhexanamide and *N*-acetyl-*N*-methylpentylamine. The hydrolysate contained small amounts of methylamine and probably acetic acid.

Chemical investigation of photo-degraded nylons

Nylon films degraded in u.v. light—Films of 6.6, 6.10, 10.6 and 6 nylons were exposed in quartz-windowed cells, in atmospheres of air, nitrogen or *in vacuo*, to the full beam of the lamp for about four days. After hydrolysis of the degraded films by heating at 120°C in a sealed tube with 5N hydrochloric acid for 16 hours, products were separated into volatile and non-volatile acids and bases by a procedure of steam distillation and continuous ether extraction of the hydrolysate under acid and subsequently under alkaline conditions, and examined by paper chromatography. Controls were carried out simultaneously using unexposed films.

(*a*) 6.6 Nylon. After exposure in air at 40° to 50°C for 75 h, films were brittle, brownish in colour and no longer completely soluble in 90 per cent phenol–water; thus 1·66 g of exposed film gave 0·30 g of insoluble material and similar amounts were obtained from experiments in nitrogen and oxygen. Paper chromatographic analysis of the hydrolysate showed:

volatile acids: mostly acetic, some *n*-pentanoic and traces of butyric and propionic acids;
non-volatile acids: adipic acid only;
volatile bases: *n*-pentylamine with traces of possibly the C_1 to C_4 mono-amines;
non-volatile bases: mainly hexamethylenediamine, also traces of other substances with lower R_f values, and an unresolved streak extending to the solvent front.

The hydrolysate from unexposed film gave acetic acid, adipic acid, hexamethylenediamine and traces of *n*-pentylamine.

The analysis of the hydrolysate from films exposed *in vacuo* differed from those exposed in air only in that the amount of *n*-pentylamine was reduced and similar to that in the control.

(*b*) 6 Nylon. Analysis of the hydrolysate from films exposed in air showed the presence of (in addition to 6-aminohexanoic acid) *n*-pentanoic and acetic acid, possibly oxalic and a trace of succinic acid, and *n*-pentylamine and a small amount of a C_4 amine. The control showed acetic acid and the dibasic acids.

(*c*) 6.10 Nylon. The hydrolysate from exposed films contained besides sebacic acid and hexamethylenediamine, acetic and *n*-nonanoic acid, adipic acid and a complex mixture of unidentified dibasic acids incompletely separated on the chromatogram, *n*-pentylamine and a number of ether-insoluble non-volatile bases giving a similar pattern on the chromatogram to that observed with 6.6 nylon. The control showed acetic and adipic acids.

(*d*) 10.6 Nylon. Besides decamethylenediamine and adipic acid, acetic and *n*-pentanoic acids, with traces of butyric and propionic acids, *n*-nonylamine and traces of sundry unresolved non-volatile amines were detected in the hydrolysate.

6.6 Nylon yarn degraded in sunlight—Hanks of 30-denier bright nylon yarn were exposed to sunlight under glass for one year, while control samples were subjected to the same conditions of heat and humidity in

Table 1. Experiments involving the exposure of *N*-alkylamides to u.v. light

Exp. No.	*Model amide*	*Expl conditions*	*Time of exposure h*	*Oxygen uptake ml*	*Products*									
					Off-gases			*Hydrocarbons*[a]		n-*Aldehydes*	n-*Acids*[a, b]		n-*Amides*	*Other products*
					H_2O *g*	CO_2 *g*	CO *g*	n-*Paraffins*	*1-Olefins*		*Free*	*On hydrolysis*		
1	*N*-Hexyl-hexanamide	O_2 flow	76		0·05	0·11		Pentane	Pentene	Hexanal	**Hexanoic** Pentanoic Butyric Propionic Acetic	**Hexanoic** Acetic	Hexanamide	
2	*N*-Butyl-octanamide	O_2 flow	76		0·02	0·11	0·1	**Heptane** Hexane **Pentane**	Heptene Hexene **Pentene**	Butanal	**Octanoic** Butyric Propionic Acetic	**Octanoic** Acetic	Octanamide	'Dimer'
3	*N*-Heptyl-hexanamide	O_2 flow	76		0·03	0·08		**Hexane** Pentane Butane	Hexene **Pentene**	Heptanal	Heptanoic	**Hexanoic** Acetic	Hexanamide	
4	*N*-Heptyl-hexanamide	O_2 Circulating flow	96 97	400				**Hexane** Pentane Butane	Pentene	Heptanal	**Heptanoic** **Hexanoic** Pentanoic Butyric Propionic Acetic	**Hexanoic** Acetic	Hexanamide	*N*-acetyl-heptylamine[c] Unknown compds masses 129, 116
5	*N*-Heptyl-hexanamide	1·6% TiO_2 O_2 Circulating flow	72 72	313		0·18		**Hexane** Pentane Butane	Hexene **Pentene** Butene	Heptanal	**Heptanoic** **Hexanoic** Pentanoic Butyric Propionic Acetic		Hexanamide	*N*-acetyl-heptylamine[c] Unknown compds masses 129, 116

6	*N*-Butyl-octanamide	N_2 flow	91		0·02	0·003	0·03	Heptane	Hexene		Octanoic			
7	*N*-Butyl-octanamide	*In vacuo*	190		*d*		*d*	Heptane	Heptene **Hexene** Pentene Butene		Octanoic			'Dimer'
8	*N*-Heptyl-hexanamide	*In vacuo*	360					Pentane	Pentene		Hexanoic	Hexanoic Acetic		Heptylamine
9	*N*-Butyl-octanamide	N_2 cyclohexane	77											*f*
10	*N*-Hexyl-hexanamide	O_2 Circulating	*e*											
		(i) $\lambda > 2500$ Å	2750	353	0·14	0·04								
		(ii) $\lambda > 3000$ Å	2250	50										
		(iii) $\lambda > 3500$ Å	2400	12·9										
11	*N*-Methyl-*N*-pentyl-hexanamide	O_2 Circulating $\lambda > 2500$ Å	*e* 2275	604	0·14	0·03				Pentanal	**Hexanoic** Acetic	**Hexanoic** Acetic	*N*-methyl-hexanamide[c]	*N*-acetyl-*N*-methyl-pentylamine[c]
12	*N*-(1,1-dimethylbutyl) hexanamide	O_2 Circulating	*e*											
		(i) $\lambda > 2500$ Å	2750	200										
		(ii) $\lambda > 3000$ Å	1850	10·4	0·12	0·04								
		(iii) $\lambda > 3500$ Å	2250	0·4										

a Black type signifies the chief constituent of a group of products.
b The paper chromatographic analysis could not distinguish between formic and acetic acids; the presence of one could mask the other.
c Evidence for these compounds is only indirect.
d Detected but not measured.
e Length of exposure measured in arbitrary light integrating meter units.
f No unsaturation detected in the cyclohexane after exposure.

the dark. Before analysis it was washed thoroughly with soap and water, rinsed and dried. In addition to measurement of intrinsic viscosity and carboxyl and amine end-groups, a large scale hydrolysis of the exposed yarn (50 g) was carried out by heating under reflux in phosphoric acid (200 ml, 65 per cent w/w) in a current of nitrogen for 15 h, estimating the carbon dioxide and carbon monoxide formed. Volatile acids produced were separated by distillation in steam through a fractionating column, and estimated by titration with 0·02 N sodium hydroxide. After removal of non-volatile acids by continuous ether extraction, sodium hydroxide (350 ml, 40 per cent w/w) and methanol (350 ml) were added and volatile bases separated by distillation. Ammonia distilled with the methanol and volatile amines with the subsequent water; they were estimated separately by titration with 0·02 N hydrochloric acid. This sequence of operations was repeated with the control yarn, and also without any yarn to obtain blank measurements. The volatile acids and bases, and the impurities in the mother liquors from a crystallization of the ether-extracted non-volatile acids, were recovered for paper chromatographic analysis. The results of the analysis are given in *Table 2*.

Table 2. Analysis of bright 6.6 nylon yarn degraded by exposure to sunlight

		Degraded yarn	*Control yarn*
Carboxyl end-groups g equiv./10^6 g polymer		117	82
Amine end-groups g equiv./10^6 g polymer		20	39
Intrinsic viscosity in 90% phenol–water		0·54	0·82
On hydrolysis	Carbon dioxide g equiv./10^6 g polymer	10·2	2·3
	Carbon monoxide g equiv./10^6 g polymer	7·6	1·0
	Volatile acids g equiv./10^6 g polymer	69·2[a]	33·0[b]
	Volatile bases: methanol distillate g equiv./10^6 g polymer	85·0[c]	14·3[c]
	Volatile bases: aqueous distillate g equiv./10^6 g polymer	103·7[d]	9·2[e]

[a] Mostly *n*-pentanoic and acetic with some butyric and traces of hexanoic and propionic acids. The non-volatile acids included glutaric and succinic in addition to adipic.

[b] Acetic acid.

[c] Nessler reagent indicated ammonia.

[d] Ammonia containing 10 to 20 per cent *n*-pentylamine.

[e] Ammonia containing 2 to 5 per cent *n*-pentylamine.

Development of chemical tests on photo-degraded bright 6.6 nylon yarn— Aldehyde, peroxide and pyrrole groups were detected in bright 6.6 nylon yarn degraded by exposure to sunlight and u.v. light in air, by the application of slightly modified well-known colorimetric tests. Formation of the last grouping was due to thermal action and independent of the presence of oxygen.

The tests applied were as follows:

(*a*) For aldehyde (—CHO) groups with *o*-dianisidine[20]: on boiling 0·2 g samples of yarn for 2 min with 10 ml of a 5 per cent solution of *o*-dianisidine in acetic acid, photo-degraded samples gave a deep orange-brown solution while the blank reagent colour was pale greenish-brown.

(*b*) For carbonyl (C=O) groups with 2,4-dinitrophenylhydrazine: with a 0·7 per cent solution of the reagent in 8 N hydrochloric acid, 0·5 g yarn samples dissolved in 20 ml of the reagent solution in the cold producing different depths of orange colour depending on the degree of degradation.

(*c*) For pyrroles with Ehrlich's reagent: 0·2 g samples of yarn were dissolved in 2 ml of reagent (2 per cent *p*-dimethylaminobenzaldehyde in concentrated hydrochloric acid) and diluted with 5 ml of ethanol when a reddish-purple colour developed.

(*d*) For peroxides[21]: ammonium thiocyanate (1 g) in de-aerated methanol (50 ml), containing 1 ml 25 per cent sulphuric acid, and de-aerated formic acid (150 ml, 90 per cent w/w) was shaken with finely powdered ferrous ammonium sulphate (0·2 g) under nitrogen. Yarn samples (0·2 g) were immersed in the freshly prepared reagent (5 ml) under nitrogen, and developed a red coloration after a few minutes which persisted after dissolution of the yarn by warming.

Conditions affecting loss of tenacity and extensibility of 6.6 nylon yarn on exposure to u.v. light—Bright and delustred yarns were exposed to u.v. light under different conditions of atmosphere and humidity at different wavelengths and the resultant losses in tenacity and extensibility used to measure the amount of degradation. After exposure, yarns were conditioned overnight at 20°C and 65 per cent relative humidity prior to testing, either on a Goodbrand single thread pendulum-type machine or on a Cambridge extensometer.

The properties of the experimental yarns, from which no attempt was made to remove spinning-finish, were as follows:

60-denier bright, 20 filament, nil TiO_2: tenacity 324 g, extensibility 15·0 per cent

90-denier bright, 30 filament, nil TiO_2: tenacity 465 g, extensibility 17·8 per cent

90-denier delustred, 30 filament, 1·6 per cent TiO_2: tenacity 492 g, extensibility 19·2 per cent.

The four wavelength regions investigated were obtained by using quartz (transmitting all wavelengths) or Pyrex (above 3 000 Å) windows in the exposure cells, or by interpolating filters (OY 10, above 3 500 Å; OY 4, above 5 000 Å) in the light beam. In comparing the effect on yarn of light of different wavelengths, the periods of exposure given were inversely proportional to the amount of light transmitted by the filters, this being obtained both from actinometric measurements and by calculation from the filter transmission curves.

The results were as follows. The presence of moisture had little effect on the degradation. With bright yarn there was a small increase in the loss of strength suffered by samples exposed under dry rather than wet conditions. With delustred yarn there was little difference using all wave-

lengths of light, but above 3 000 Å a slight enhancement of degradation was observed if moisture was present. Although some loss of tenacity was observed in exposures *in vacuo* below 3 000 Å, bright and delustred yarns being degraded equally, the major part of the degradation was undoubtedly due to the presence of oxygen. The shorter wavelength light was most effective in producing loss in strength with both bright and delustred yarns which were affected equally below 3 000 Å. At higher wavelengths, delustred yarn was degraded much more rapidly than bright, being about twice as susceptible to light above 3 000 Å and about four times to light above 3 500 Å. Degradation was still appreciable with light above 5 000 Å at which wavelength bright yarn was comparatively unaffected.

The relation between loss of strength and other changes in physical and chemical properties of 6.6 nylon yarn on exposure to sunlight—A correlation between the loss of strength and changes in intrinsic viscosity, end-groups and u.v. absorption (cf. *Figure 1*) occurring on exposure of 6.6 nylon yarn to sunlight was obtained by exposing bright and delustred yarns under glass for varying periods of time and then subjecting them to analysis. For the measurements of loss of tenacity the yarns used were the 60- and 90-denier bright, and 90-denier 1·6 per cent delustred, high-twist yarns described above; for other measurements requiring larger samples, hanks of ordinary bright and delustred yarn were exposed. End-group measurements (expressed as g equiv./10^6 g polymer) comprised carboxyl*, amine†, acyl and amide; the last two were determined as the amount of volatile acids or ammonia liberated on hydrolysis, and estimated as described above.

The variation of end-groups, intrinsic viscosity, etc., with exposure time (measured in hours of daylight) and loss of tenacity is shown in *Figures 2* to *10*. In comparing graphs for bright and delustred yarns it should be

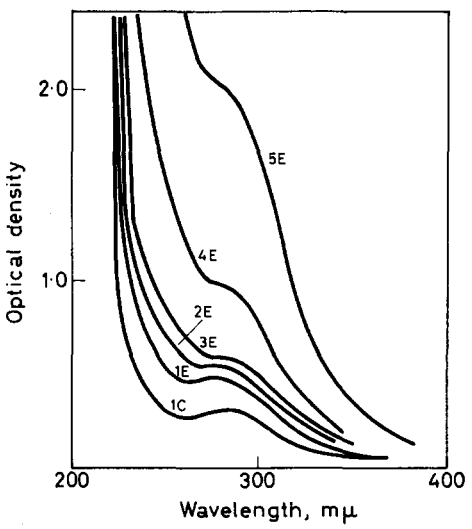

Figure 1—Ultra-violet absorption of sunlight-degraded, delustered 6.6 nylon yarns; increase with exposure time up to five months. (Delustrant removed; 1% solution in 8 N hydrochloric acid, 1 cm cell). C, control; E, exposed

*By titration in hot benzyl alcohol with 0·1 N potassium hydroxide in ethylene glycol, using phenolphthalein as indicator.

†By titration in 2:1 w/w phenol–methanol with aqueous 0·05 N hydrochloric acid, using thymol blue as indicator.

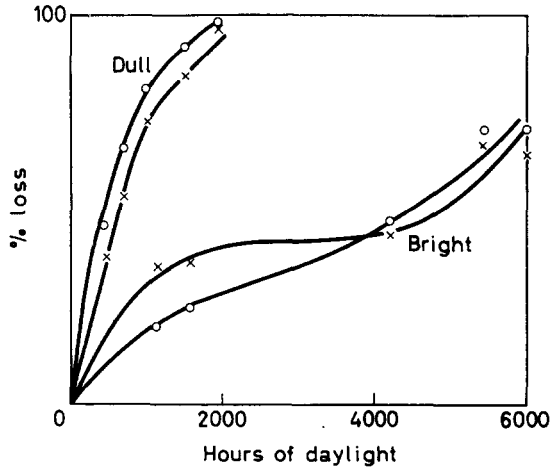

Figure 2—Variation of loss of tenacity and extensibility with exposure time for sunlight-degraded 6.6 nylon yarns (○ tenacity; × extensibility)

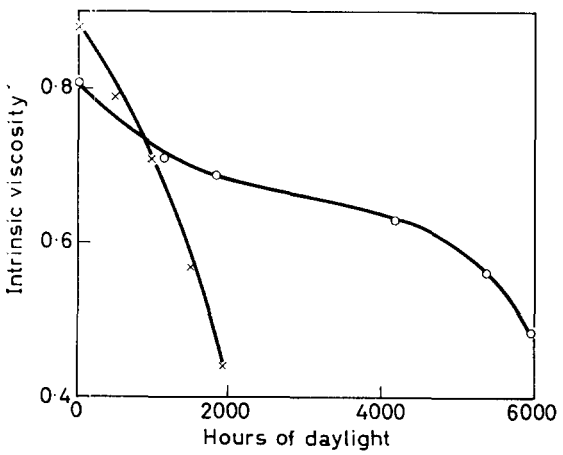

Figure 3—Variation of intrinsic viscosity in 90% phenol–water with exposure time for sunlight-degraded 6.6 nylon yarns (○ bright; × delustred)

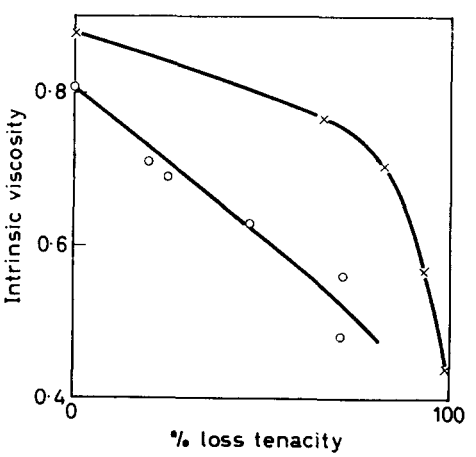

Figure 4—Volume of intrinsic viscosity with loss of tenacity (○ bright; × delustred)

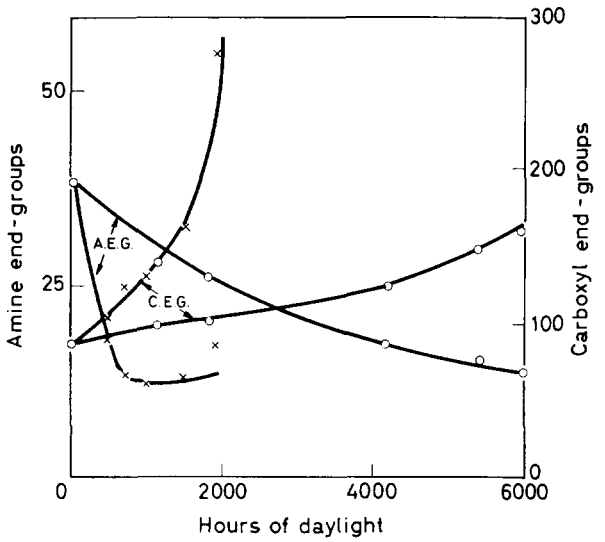

Figure 5—Variation of amine and carboxyl end-groups with exposure time for sunlight-degraded 6.6 nylon yarns (○ bright; × delustred)

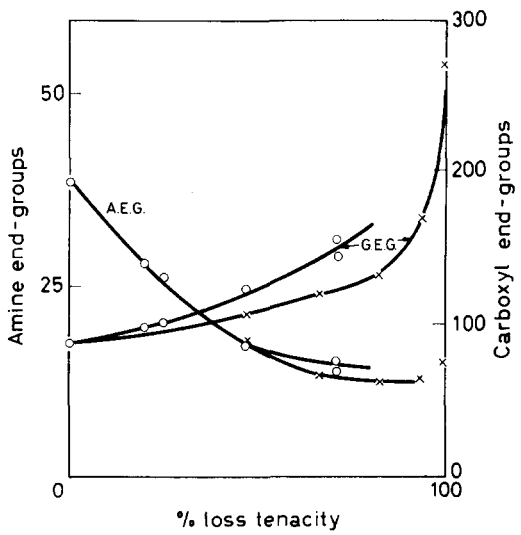

Figure 6—Variation of amine and carboxyl end-groups with loss of tenacity (○ bright; × delustred)

noted that the first 1 000 h exposure for delustred, and from 2 000 to 3 500 h for bright, was winter daylight and the rest summer; this will account for the S-shape of some of the curves for bright yarn. Also the denier of the delustred yarn was greater than that of the bright; comparison between 60- and 90-denier bright yarns indicated that the latter degraded rather more quickly. Since the tenacity measurements were carried out on specially displayed samples while other measurements were performed on less uniformly exposed yarns, the average loss of tenacity in the hank

would therefore be less than in the prepared samples, the values from which were used in plotting the curves.

The chief points to be noted from the graphs are as follows. The rate of loss of tenacity and extensibility decreased with increased exposure time,

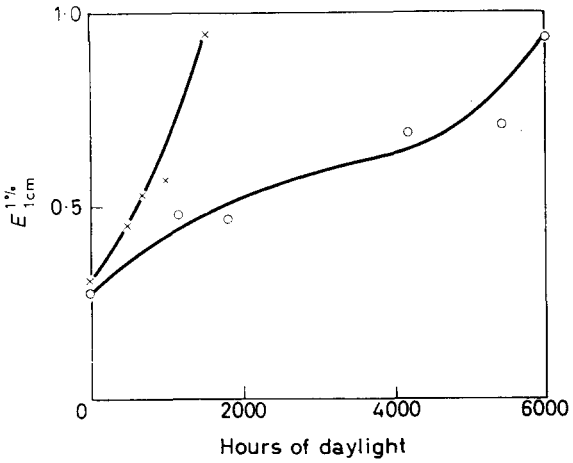

Figure 7—Variation of u.v. absorption at 280 mμ with exposure time for sunlight-degraded 6.6 nylon yarns (○ bright; × delustred; in 8N hydrochloric acid)

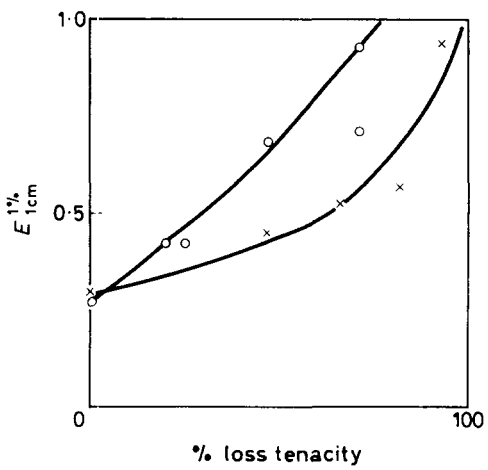

Figure 8—Variation of u.v. absorption with loss of tenacity (○ bright; × delustred)

the delustred yarn losing strength much more rapidly than the bright. This loss of strength was accompanied in both yarns by a progressive decrease in intrinsic viscosity and hence molecular weight. There was a drop in amine end-groups, which approached a constant value very quickly in the delustred yarn, and progressive increase in carboxyl end-groups, u.v. absorption, acyl and amide end-groups. In all cases the change in these properties with exposure time was more rapid with the delustred than with bright yarn. As regards loss of strength, however, the delustred yarn

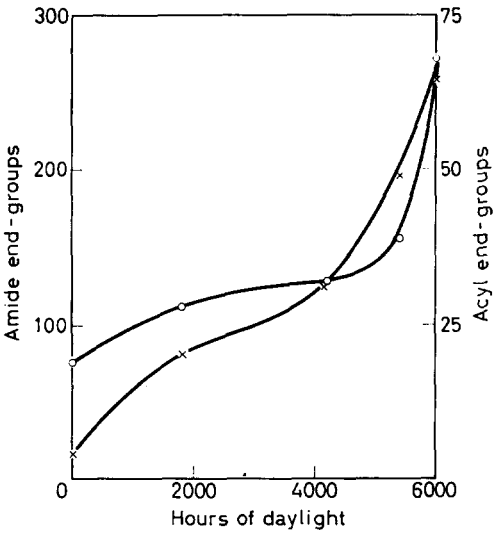

Figure 9—Variation of amide and acyl end-groups with exposure time for sunlight-degraded 6.6 bright nylon yarn (○ acyl; × amide end-groups)

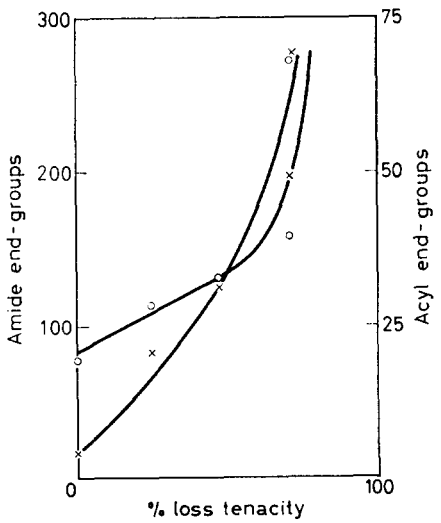

Figure 10—Variation of amide and acyl end-groups with loss of tenacity (○ acyl; × amide)

suffered rather less degradation (as characterized by changes of end-groups etc.) for the same loss of tenacity than the bright, or, conversely, for the same amount of degradation the delustred yarn lost more strength than the bright. In general the rate of degradation (i.e. chemical change as opposed to loss of tenacity) increased with exposure time.

DISCUSSION

The photodegradation of N-*alkylamides*

The products from the u.v. degradation of *N*-alkylamides differed somewhat depending on whether or not oxygen was present. It is thus possible to distinguish two types of decomposition, a photochemical oxidation, and a direct photolysis of the molecules occurring with light of somewhat shorter wavelength independently of the atmosphere.

The photolysis—The products of photolysis were carbon monoxide, water, hydrocarbons, carboxylic acids and *N*-alkylamides having different chain lengths from the parent compound; in addition there was some slight evidence for the formation of primary amine.

Although accurate bond dissociation energies are not known for all the bonds in the amide molecule, the known values indicate that the C—N bonds are probably the weakest[22] and of the two, the NH—CH_2 bond is probably somewhat weaker than the NH—CO bond the energy of which will be enhanced by the resonance energy of the amide group. However, such values are for a homolytic splitting into two free radicals whereas intramolecular fission into two complete molecules might occur more readily.

The following reaction mechanisms, involving both types of reaction can be postulated to account for the products of photolysis.

$$R.CH_2.CH_2.CH_2.CO.NH.CH_2.CH_2.R' \longrightarrow R.CH_2.CH_2.CH_2.CO. + .NH.CH_2.CH_2.R' \quad (1)$$

$$R.CH_2.CH_2.CH_2.CO. \longrightarrow R.CH_2.CH_2.CH_2. + CO \quad (2)$$

$$2R.CH_2.CH_2.CH_2. \longrightarrow R.CH_2.CH_2.CH_3 + R.CH_2.CH{=}CH_2 \quad (3)$$

$$R.CH_2.CH_2.CH_2. + XH \longrightarrow R.CH_2.CH_2.CH_3 + X. \quad (4)$$

$$R'.CH_2.CH_2.NH. + XH \longrightarrow R'.CH_2.CH_2.NH_2 + X. \quad (5)$$

$$R'.CH_2.CH_2.NH. \longrightarrow \text{polymer (?)} \quad (6)$$

$$R.CH_2.CH_2.CH_2.CO.NH.CH_2.CH_2.R' \longrightarrow R.CH_2.CH_2.CH_2.NH.CH_2.CH_2.R' + CO \quad (7)$$

$$R.CH_2.CH_2.CH_2.NH.CH_2.CH_2.R' \longrightarrow R.CH_2.CH_2.\dot{C}H_2.NH. + .CH_2.CH_2.R' \quad (8)$$

$$R.CH_2.CH_2.CH_2.CO.NH.CH_2.CH_2.R' \longrightarrow R.CH{=}CH_2 + .CH_3.CO.NH.CH_2.CH_2.R' \quad (9)$$

$$R.CH_2.CH_2.CH_2.CO.NH.CH_2.CH_2.R' \longrightarrow R.CH_2.CH_2.CH_2.CO.NH_2 + CH_2{=}CH.R' \quad (10)$$

Analogous reactions to these have been put forward by previous workers to explain photolysis in primary amides[23] and alkyl esters[24]. Which reactions occur in the photolysis of *N*-alkylamides can be deduced from the products reported in *Table 1*.

Carbon monoxide can arise through the reactions of equations (2) or (7). The former, which involves a free radical mechanism, is supported by the fact that the corresponding alkane from the radical $R.CH_2.CH_2.CH_2.$ was one of the chief hydrocarbon products. Thus *N*-butyloctanamide gave *n*-heptane, and *N*-heptylhexanamide yielded *n*-pentane. However, the evidence for the formation of amine, which should also result from this reaction, was not definite, its formation only being detected in experiment 8 and the possibility cannot be excluded that it was derived in some way by hydrolysis of the parent amide.

Hydrogen-transfer reactions of the type given by equations (4) and (5) (where XH represents a hydrogen donor, probably an *N*-alkylamide molecule) could quite easily occur in reactions in a liquid medium of essentially hydrocarbon character and should produce corresponding unsaturation. However, in experiment 9, performed in cyclohexane for the direct purpose of detecting unsaturation in the solvent, none was observed. Such conditions were also favourable for the production of amines but none was observed.

There was no evidence for the formation of carbon monoxide by the reaction of equation (7) as secondary amines of the required type were not found. Thus although the evidence is not complete, the reaction of equation (1) seems a probable one and provides a satisfactory explanation of the formation of the paraffin $R.CH_2.CH_2.CH_3$. The fate of the amino radical is undecided but seems to favour equation (6) rather than (5).

The occurrence of crosslinking reactions is evidenced by the formation of the dimer of *N*-butyloctanamide isolated in experiment 7, probably by the combination of hydrocarbon-type radicals, the amide groups being preserved intact.

There is indirect evidence for the formation of *N*-acetylamines by the reaction of equation (9) [although the experiments concerned were actually carried out in oxygen, the photolytic process of equation (9) is unlikely to be affected by this] based on the fact that in general hydrolysis of the material of somewhat lower boiling-point than the parent amide always yielded small amounts of acetic acid. In addition mass spectrometric analysis of low-boiling fractions from the experiments 4 and 5 with *N*-heptylhexanamide showed the presence of a compound of mass 157, together with a large breakdown mass of 142, corresponding to *N*-acetylheptylamine and the ion resulting from the loss of a methyl group.

The corresponding olefins from equation (9) were not found in every experiment, though 1-hexene was indeed the only olefin detected in experiment 6 with *N*-butyloctanamide under nitrogen, and the predominant one in experiment 7 with the same amide *in vacuo*. The model amides derived from hexanoic acid should yield 1-butene which was detected in some experiments. Additional olefins observed to the ones required by equation (9), were formed possibly by similar fissions occurring at other points in the molecule. In particular the formation of 1-pentene in experiments with the hexanoic amides, and 1-heptene from the octanoic ones, seems to indicate a reaction of the type of equation (11).

$$R.CH_2.CH_2.CH_2.CO.NH.R'' \rightarrow R.CH_2.CH{=}CH_2 + H.CO.NH.R'' \quad (11)$$

Formyl derivatives were never identified; hydrolysis should yield formic acid which was not distinguishable from acetic acid by the method of paper chromatographic analysis employed.

The photo-oxidation—The photo-oxidation was studied under conditions in which photolysis could still occur. The main additional products were carbon dioxide, aldehyde and primary amide with enhanced formation of water, carboxylic acids and possibly paraffinic hydrocarbons.

Previous workers have made similar observations[1,2], and attributed the formation of these products to an oxidative attack occurring predominantly

at the methylene group in the α-position to the nitrogen atom of the amide group. Assuming peroxidation to occur at that point by the reactions of equations (12) to (14), then breakdown of the derived alkoxy radical [equation (15)] can occur in several ways [equations (16) to (19)].

$$\text{R.CO.NH.CH}_2\text{.R}' + \text{X.} \longrightarrow \text{R.CO.NH.}\dot{\text{C}}\text{H.R}' + \text{XH} \quad (12)$$

$$\text{R.CO.NH.}\dot{\text{C}}\text{H.R}' + \text{O}_2 \longrightarrow \text{R.CO.NH.C(OO.)H.R}' \quad (13)$$

$$\text{R.CO.NH.C(OO.)H.R}' + \text{XH} \longrightarrow \text{R.CO.NH.C(OOH)H.R}' + \text{X.} \quad (14)$$

$$\text{R.CO.NH.C(OOH)H.R}' \longrightarrow \text{R.CO.NH.C(O.)H.R}' + \text{.OH} \quad (15)$$

$$\text{R.CO.NH.C(O.)H.R}' \xrightarrow{\text{X.}} \text{R.CO.NH.CO.R}' + \text{XH} \quad (16)$$

$$\text{R.CO.NH.C(O.)H.R}' \xrightarrow{\text{XH}} \text{R.CO.NH.C(OH)H.R}' + \text{X.} \quad (17)$$

$$\text{R.CO.NH.C(O.)H.R}' \longrightarrow \text{R.CO.NH.} + \text{OCH.R}' \quad (18)$$

$$\text{R.CO.NH.C(O.)H.R}' \longrightarrow \text{R.CO.NH.CHO} + \text{.R}' \quad (19)$$

The reactions of equations (17) and (18) can ultimately result in the same products. Thus, *N*-(1-hydroxyalkyl)-amides of the type depicted in equation (17) appear to be inherently unstable, the only compounds reported in the literature being formed by condensation of primary amides with formaldehyde[25] or chloral and its homologues[26] (attempts to extend this reaction to the higher aldehydes resulted in the formation of *N,N'*-alkylidenediamines[27,28]) and even the hydroxymethyl derivatives are decomposed slowly in water[29]. Thus the subsequent spontaneous decomposition will give the required aldehyde and primary amide. Assuming the amide radical can pick up a hydrogen atom, then these products are also derived from equation (18).

In contrast to other reports[2], the diacyl amides formed from the reactions of equations (16) and (19) were not detected. Thus acids of the type R'.COOH were not found in the hydrolysates of the degraded *N*-alkylamide fractions; similarly *N*-formylhexanamide, if present at all, contributed only a comparatively insignificant peak to the complex mass spectrum of the low-boiling fractions from experiments 4 and 5. However, there is evidence for the occurrence of the reaction of equation (19) from the hydrocarbons detected. Thus *N*-hexylhexanamide should give *n*-pentane and *N*-heptylhexanamide *n*-hexane, and both were identified in experiments with these compounds.

If the molecule XH in the above schemes represents a molecule of *N*-alkylamide, then a chain reaction is established by the reactions of equations (13) and (14), the initiation step being that in equation (1), the resultant acyl radical playing the role of the species X. in equation (12). The aldehyde (corresponding to XH) was never found although the corresponding acid was invariably detected. A possible source of this acid is from the reaction of the acyl radical with oxygen and decomposition of the resultant per-acid. The acid derived by oxidation of the aldehyde formed from the amine segment of the molecule was in general observed and will arise by a similar mechanism. Some of the carbon dioxide formed in these photo-oxidations may originate from an alternative decomposition of such

per-acids to the alkene and water[30] [equation (20)]. In general water will arise from any hydrogen abstraction reaction involving hydroxyl radicals.

$$R.CH_2.CH_2.CO.OOH \rightarrow R.CH{=}CH_2 + H_2O + CO_2 \qquad (20)$$

The reported increased stability towards photo-oxidation, as measured by the rate of oxygen uptake, conferred by substituting the H atoms of the methylene group adjacent to the N atom, in the amine segment of the molecule, with alkyl groups[1] was also found in the present work, confirming that the oxidative attack occurs predominantly at this point. The effect was less noticeable in the presence of short wavelength light when photolytic reactions also occur.

The photodegradation of polyamides

The loss of strength of nylon yarns on exposure to light is undoubtedly due to chemical degradation; thus even with slight losses of tenacity it was possible to detect chemical changes in the fibres.

For photodegration to occur the presence of oxygen is necessary at longer wavelengths whereas at shorter wavelengths it is not, conforming to the concepts of respectively a photosensitized oxidation and a photolysis[3,4]. (The presence of water vapour was found to have little or no effect.)

Hydrolysis of photo-degraded nylon yielded, with 6.6 polymer, in addition to hexamethylenediamine and adipic acid, carbon monoxide, carbon dioxide, *n*-pentanoic acid, lesser amounts of other mono-carboxylic acids, ammonia, *n*-pentylamine, lesser amounts of lower monobasic amines, and traces of higher amines of unknown constitution. In addition, as found by other workers[31], aldehyde groups could be detected in the unhydrolysed yarn. These products can be explained by proposing reactions to occur in the polyamide chain analogous to those found with the model *N*-alkylamides.

The photolysis—In the process of photolysis occurring at wavelengths below 3 000 Å, both direct scission of the polyamide chains and crosslinking should result. Evidence for the latter lies in the formation of the phenol-insoluble material produced on exposure of nylon films to the unfiltered beam from the u.v. lamp. Unfortunately the nature of the crosslinking was not disclosed by the examination of the insoluble polymer, though chemically it behaved on hydrolysis like the parent material.

The probable scissions of, for example, the 6.6 nylon chains are as follows.

$$\begin{array}{c} \sim CO.CH_2.CH_2.CH_2.CH_2.CO\sim \\ | \\ NH.CH_2.CH_2.CH_2.CH_2.CH_2.CH_2.NH\sim \end{array} \rightarrow \begin{array}{c} CO.CH_3 + CH_2{=}CH.CH_2.CO\sim \\ | \\ NH.CH_2.CH_2.CH_2.CH_2.CH_2.CH_2.NH\sim \end{array} \qquad (21)$$

$$\rightarrow \begin{array}{c} .CO.CH_2.CH_2.CH_2.CH_2.CO\sim \\ + \\ .NH.CH_2.CH_2.CH_2.CH_2.CH_2.CH_2.NH\sim \end{array} \qquad (22)$$

$$.CO.CH_2.CH_2.CH_2.CH_2.CO\sim \rightarrow CO + .CH_2.CH_2.CH_2.CH_2.CO\sim \qquad (23)$$

$$.CH_2.CH_2.CH_2.CH_2.CO\sim + XH \rightarrow CH_3.CH_2.CH_2.CH_2.CO\sim + X. \qquad (24)$$

The sequence of reactions of equations (22) to (24) thus explains the

production of *n*-pentanoic acid on hydrolysis of photo-degraded 6.6 nylon. With 6.10 and 6 nylons the corresponding products would be *n*-nonanoic acid and *n*-pentylamine, which were in fact identified. The reaction of equation (21) should produce acetic acid on hydrolysis; however, acetyl groups were already present in the undegraded polymer due to the addition of acetic acid added as stabilizer during its manufacture. There was some evidence for the accompanying unsaturated fragment insofar as traces of a C_4 acid were detected in the experiments with 6.6 nylon, and of a possible C_4 amine with 6 nylon. The fate of the amine radical end-groups in equation (22) is not known.

Due to the rigid nature of the polymer, disproportionation reactions between radicals, of the type in equation (3), are improbable. The hydrogen donor XH in equation (24) is thus most likely a methylene group in an adjacent polyamide chain.

Although photolytic reactions of this type occur only with light of short wavelength, it is interesting that *n*-pentanoic acid was detected in the hydrolysate of 6.6 nylon yarn exposed to sunlight behind glass, indicating that these reactions can occur under such conditions.

The photo-oxidation—By applying the reactions postulated for the photo-oxidation of *N*-alkylamides to the polyamide chain, the remainder of the observed products of degradation can be accounted for. With oxidative attack occurring predominantly at the methylene group adjacent to the N atom, by reactions analogous to equations (12) to (15), subsequent decomposition of the derived alkoxy radical can occur as follows.

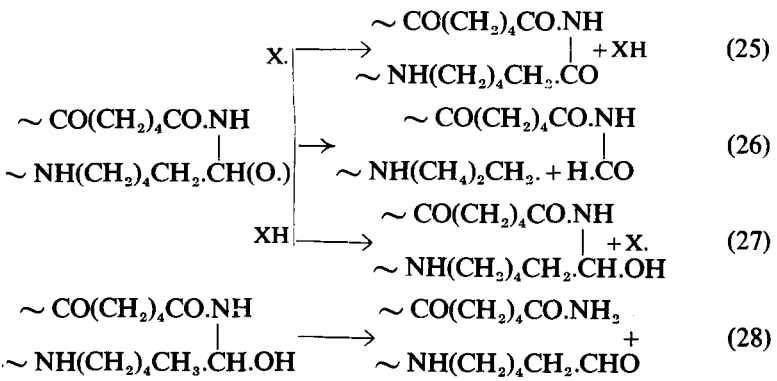

The reactions of equations (27) and (28) account for the observed production of aldehyde end-groups in the polymer, and of ammonia on hydrolysis of the corresponding amide end-groups formed. (The 6-amino-hexanal which should also be produced on hydrolysis was not detected but may have been decomposed by the method of working up.) The reaction of equation (26) will also yield ammonia on hydrolysis together with formic acid and *n*-pentylamine. Though the presence of formic acid would be obscured by the acetic acid present, small amounts of *n*-pentyl amine (less than ten per cent of the total volatile bases) were detected. (By this reaction 10.6 nylon should yield *n*-nonylamine, and 6 nylon *n*-pentanoic acid which were in fact observed.) The alternative formation

of pentylamine end-groups by photolysis of the aldehyde end-groups produced, may also occur to some extent.

Products from the reaction of equation (25) were not observed; the small amounts of 6-aminohexanoic acid to be expected on hydrolysis of photo-oxidized 6.6 nylon (or 9-aminononanoic acid from 10.6 nylon, or adipic acid from 6 nylon) were not distinguished in the complex pattern on the chromatogram. In fact their detection would not prove the occurrence of this reaction as the same products can arise by further oxidation of the aldehyde end-groups produced; this undoubtedly occurs and must account for much of the observed increase in carboxyl end-groups in the polymer.

Although these reactions are probably the predominant ones occurring in the photodegradation of polyamides, they are not the only ones. Thus hydrolysis of degraded 6.6 nylon resulted in the formation of small amounts of carbon monoxide and dioxide which probably arise by decomposition of hydroxy- or keto-acids; in addition small amounts of glutaric and succinic acids were detected. The formation of these compounds requires some oxidation to occur in the acid segment of the polyamide chain. Also the overall increase of u.v. absorption of 6.6 nylon on exposure to sunlight (*Figure 1*) is indicative of the formation of more complex groupings than those derived from the reactions described above. Discussion of these reactions has been based on the assumption, for example, that 6.6 nylon is pure polyhexamethyleneadipamide. In fact other uncharacterized groupings, associated with the absorption band at 2 800 to 2 900 Å[32], are introduced to a slight extent during manufacture by the thermal processes of polymerization and spinning. It is possible that these groupings influence the photodegradation by serving as absorbers of radiation and may provide the radical initiators required for the processes of degradation outlined above; they act as photosensitizers in increasing what, in their absence, would be a much slower reaction.

The effect of delustrant—The presence of titanium dioxide as delustrant in nylon polymer enhances the photodegradation only above 3 000 Å in the presence of oxygen and hence is connected with the photo-oxidation rather than the photolysis. No difference in chemical constitution was detected between photodegraded bright and delustred yarns. Although the rate of degradation of delustred yarns was much greater than bright, *Figures 2* to *10* indicate that relatively more chemical change occurred in bright than in delustred yarn for the same loss of tenacity. Presumably the enhanced degradation is confined to the locality of the titanium dioxide particles, and is more effective in causing tenacity loss than an equivalent amount spread more evenly as with bright yarn. The titanium dioxide thus does not appear to change the nature of the oxidation processes, but acts as a photo-sensitizer. From the practical point of view it is of considerable importance that certain additives, in particular manganous salts[16], have been found effective in limiting this photocatalytic action, and such additives are normally to be found in many delustred commercial nylon yarns.

The author is indebted to Mr A. E. Williams for the measurement and interpretation of mass spectra, and to Mr M. St C. Flett for infra-red spectra. Considerable technical assistance was given by Mr B. W. H. Terry.

Research Department, I.C.I. Ltd, Dyestuffs Division,
Hexagon House, Blackley, Manchester 9

(*Received December 1962*)

REFERENCES

[1] SHARKEY, W. H. and MOCHEL, W. E. *J. Amer. chem. Soc.* 1959, **81,** 3000
[2] LOCK, M. V. and SAGAR, F. B. *Proc. chem. Soc., Lond.* **1960,** 358
[3] EGERTON, G. S. *J. Text. Inst.* 1948, **39,** T293
[4] EGERTON, G. S. *J. Soc. Dy. Col.* 1949, **65,** 764
[5] SIPPEL, A. *Textil-Praxis,* 1952, **7,** 220
[6] SIPPEL, A. *Kolloidzschr.* 1952, **127,** 79
[7] TAKESHI HASHIMOTO. *Bull. chem. Soc. Japan,* 1957, **30,** 950 (*Chem. Abstr.* 1958, **52,** 8615)
[8] ACHHAMMER, B. G., REINHART, F. W. and KLINE, G. M. *J. appl. Chem., Lond.* 1951, **1,** 301
[9] PRATI, G. *Ann. chim. Roma,* 1958, **48,** 15 (*Chem. Abstr.* 1958, **52,** 10586)
[10] SCHWEMMER, M. *Textilrdsch.* 1956, **11,** 1, 70, 131
[11] STEPHENSON, C. V. *et al. J. Polym. Sci.* 1961, **55,** 451, 465, 477
[12] RAFIKOV, S. R. and TSI-PIN, S. *Vysokomol. Soedineniya,* 1961, **3,** 56
[13] VINEA, E. *Industr. textila, Bukarest,* 1957, **8,** 64 (*Chem. Abstr.* 1957, **51,** 15136)
[14] AGSTER, A. and HOLZINGER, O. *Textil-Praxis,* 1956, **11,** 825 (English edn. 1957, 26)
[15] MONTAGNE, M. *Ann. Chim.* 1930 (10), **13,** 116
[16] British Nylon Spinners Ltd. *Brit. Pat. No. 861, 354* (14.6.1958)
[17] BLOCK, R. J., DURRUM, E. L. and ZWEIG, G. *A Manual of Paper Chromatography.* Academic Press: New York, 2nd edn, 1958
[18] LYNN, W. S., STEELE, L. A. and STAPLE, E. *Analyt. Chem.* 1956, **28,** 132
[19] ROBERSON, E. C. *J. Soc. chem. Ind., Lond.* 1938, **57,** 39
[20] FEIGL, F. *Spot Tests in Organic Analysis,* p 210. Elsevier: Amsterdam, 5th edn, 1956
[21] WAGNER, C. D., CLEVER, H. L. and PETERS, E. D. *Analyt. Chem.* 1947, **19,** 980
[22] COTTRELL, T. L. *The Strengths of Chemical Bonds.* Butterworths: London, 1958
[23] BOOTH, G. H. and NORRISH, R. G. W. *J. chem. Soc.* **1952,** 188
[24] WIJNEN, M. H. J. *Canad. J. Chem.* 1958, **36,** 691
AUSLOOS, P. *Canad. J. Chem.* 1958, **36,** 383
[25] EINHORN, A. *Liebigs Ann.* 1908, **361,** 113
[26] LAROCCA, J. P., LEONARD, J. M. and WEAVER, W. E. *J. org. Chem.* 1951, **16.** 47
[27] NOYES, W. A. and FORMAN, D. B. *J. Amer. chem. Soc.* 1933, **55,** 3493
[28] PANDYA, K. C. and SODHI, H. S. *Proc. Indian Acad. Sci. A,* 1948, **27,** 196 (*Chem. Abstr.* 1950, **44,** 4415)
[29] ILICETO, A. *Ann. chim., Roma* 1953, **43,** 516 (*Chem. Abstr.* 1954, **48,** 6208)
[30] SWERN, D. *Chem. Rev.* 1949, **45,** 1
[31] KOICHI, KATO. *Text. Res. J.* 1962, **32,** 181
[32] LIQUORI, A. M., MELE, A. and CARELLI, V. *J. Polym. Sci.* 1953, **10,** 510

Polycarbonates from the 2,2,4,4-Tetramethylcyclobutane-1,3-diols

*Part I: Preparation and Structure**

Miss M. GAWLAK and J. B. ROSE

The preparation of a series of polycarbonates of high molecular weight from the cis- *and the* trans-*2,2,4,4-tetramethylcyclobutane-1,3-diols is described. Methods were established for determining the ratio of* trans- *to* cis- *repeat units in the polymers and the nature of an extensive side reaction producing carbon dioxide and 2,2,4-trimethyl-3-pentenal was investigated.*

POLYCARBONATES of aromatic dihydroxy compounds are well known, but very few examples of polycarbonates based entirely on alicyclic diols have been reported. A mixture of the *cis-* and *trans*-2,2,4,4-tetramethylcyclobutane-1,3-diols has recently become available commercially, and this prompted us to prepare polycarbonates, I, from these diols. At the outset of

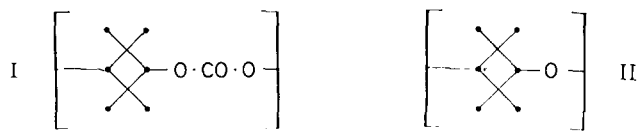

this project, two interesting possibilities were apparent: first polymers of controlled physical properties could be prepared by controlling the ratio of *cis-* to *trans*-cyclobutane units in the chain, which appeared possible because a means of separating the isomeric diols was known[2,3], and secondly polymers containing units of structure, II, might be prepared by thermal decomposition of the polycarbonates, I. There appears to be no well documented example of the preparation of polyethers by these means, but the preparation of cyclic ethers by the base catalysed pyrolysis of the cyclic carbonates or linear polycarbonates of certain 1,3-diols has been reported by Searles *et al.*[4], who have postulated the following mechanism for the reaction:

*A preliminary account of this work has been published previously[1].

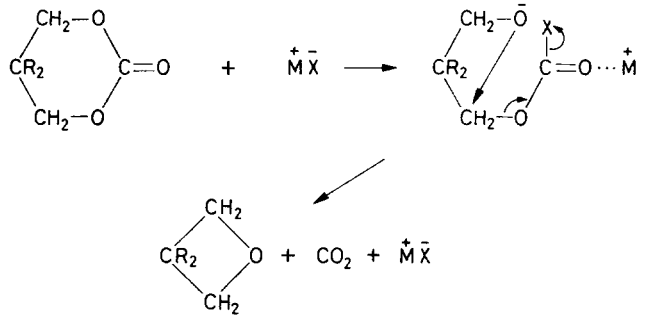

For the case of the polycarbonate, I, intramolecular reaction of the type indicated above would not be possible as too great a distortion of the normal valency angles would be required to produce a cyclic ether, so that the only ether which could be formed would be the polymeric structure, II.

This paper describes the preparation of high melting polycarbonates of known steric composition from these diols, the dependence of the physical properties of the polymers on their steric composition being described in Part II[5]. However, it was not possible to realize the conversion of the polycarbonates, I, to the polyethers, II, although an extensive side reaction producing carbon dioxide was shown to occur.

RESULTS

The polymers were prepared by base catalysed ester interchange between the diols and their bis(ethyl carbonate) esters, III, these latter compounds being prepared in good yield by base catalysed interchange between the diols and a large excess of diethyl carbonate.

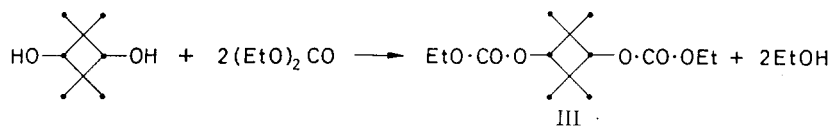

III

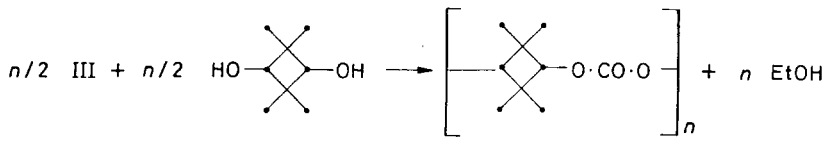

Although ester interchange between the diols and their ethyl carbonate esters readily gave polymers of high molecular weight, the yield of polymer was always less than that expected from the quantities of reagents used. It was found that carbon dioxide was evolved during the later stages of the polymerizations and that the liquid distilling from the melt contained a little ethyl carbonate and a liquid boiling at 146°C, as well as ethanol. Some solid products also distilled out of the polymerization vessel and these were shown to be unreacted starting materials.

Carbon, hydrogen and molecular weight determinations carried out on the liquid boiling at 146°C showed that it had the empirical formula

$C_8H_{14}O$. This liquid reduced ammoniacal silver nitrate, and gave a crystalline semi-carbazone and phenylhydrazone. Its infra-red spectrum was similar to that of 2,4,4-trimethylpentene-2, except that it showed a strong absorption at 1 728 cm^{-1} typical of an aldehyde type carbonyl group. Wolff–Kishner reduction of both the hydrazone and the semi-carbazone of the aldehyde gave 2,4,4-trimethylpentene-2, IV, and oxidation of the aldehyde with dichromate or with alkaline permanganate gave a mixture of products from which dimethyl malonic acid, V, was isolated. Thus, the aldehyde is 2,2,4-trimethyl-3-pentenal, VI, and its Wolff–Kishner reduction, and its oxidation occurs as follows:

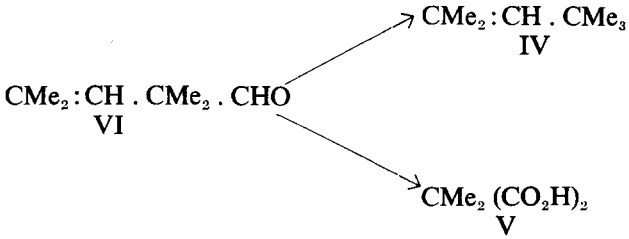

There are references[6-8] in the older literature to the preparation of an aldehyde thought to have the structure, VI, by dehydration of isobutyraldol, but no sound proof of structure was given and such physical constants that were recorded are not in agreement with ours. Since our work was completed, a new preparation of VI by acid catalysed dehydration of *trans*-2,2,4,4-tetramethylcyclobutane-1,3-diol has been reported[9], proof of structure being provided by i.r. and n.m.r. techniques, together with hydrogenation to the known saturated trimethyl pentanol. The physical constants and melting points of derivatives recorded are in agreement with those noted by us so that the structure, VI, is assigned correctly.

A number of inorganic bases were tried as catalysts and it was found that both the rate of polymerization and the extent to which decarboxylation occurred depended on the basicity of the catalyst. Weak bases, such as butyl titanate or aluminium tertiary butoxide, were poor catalysts and with these extended reaction times were required to produce polymers which were of low molecular weight. However, these catalysts caused little decarboxylation. Metallic magnesium or calcium were somewhat better, but it was not possible to obtain polymers of high molecular weight in a reasonable time without too much decarboxylation. Lithium hydride worked fairly well but tended to give more decarboxylation than did the carbonate. Potassium cyanide and potassium borohydride were powerful catalysts inducing rapid reaction at relatively low temperatures but decarboxylation occurred to such an extent that no polymer was obtained. Lithium carbonate appeared to be the best catalyst and all further polymerization experiments were carried out using this compound.

Polymerizations were carried out in two stages, the first involving reaction between the diol and its bis(ethylcarbonate) ester at atmospheric pressure and a maximum temperature of 260°C, while in the second stage the temperature was gradually raised to 280°C or above while the pressure was reduced to 0·1 mm of mercury. Results obtained by varying both the

concentration of catalyst and the final temperature of the second polymerization stage are given in *Table 1*.

Table 1. Polymerizations catalysed by lithium carbonate

10^4 [*catalyst*] (*moles*)	% *Yield*	η*	*Temperature of polymerization (2nd stage)*	*Mole % decarboxylation*
3·1	59	1·52	280–300°	15
6·2	53	1·98	280–290	16
3·1	53	1·92	280–300	16
6·2	50	2·53	280–290	22
12·4	43	2·75	280–290	26
3·1	18·7	1·4	280–330	54

*Specific viscosity for one per cent solution in chloroform at 25°C.

It appears from these results that as the conditions of polymerization become more rigorous, due either to the use of higher catalyst concentrations or higher temperatures, the degree of polymerization increases but loss of reagents due to decarboxylation also becomes greater. Eventually this loss becomes so severe that it is reflected in a decrease in the degree of polymerization. Thus, careful control of polymerization conditions was required to produce satisfactory yields of high molecular weight polymer. However, although extensive decomposition always occurred during polymerization microanalysis of the polymers for carbon and hydrogen gave values as calculated for a polycarbonate with the repeat unit I and quantitative alkaline hydrolysis gave results consistent with a polymer containing 100 ± 1 per cent of these units. The i.r. spectra of the polymers was as expected from structure I and no bands attributable to ether linkages, structure II, could be observed.

Having determined optimum polymerization conditions using intermediates derived directly from the commercially available mixture of isomeric diols, samples of the pure *cis-* and *trans-* diols were separated from the mixture by a known[3] method and their bis(ethyl carbonate) esters prepared. Polymers could then be prepared from intermediates of known steric composition. An assignment of *cis-* or *trans-* structures to the diols has been made[2] on the basis of their n.m.r. spectra. These diols have different i.r. spectra, and we have used this difference to determine the *trans-*/*cis-* ratios of their mixtures. Methanolysis of mixtures of the *cis-* and *trans-* esters, III, and of the polymers, I, followed by determinations of the *trans-*/*cis-* ratios of the diol mixtures so obtained provided a simple and convenient method of measuring the ratio of *trans-* to *cis-* repeat units in polymers made from reactants of known steric composition. Sterically pure esters, and polymers prepared from sterically pure reactants gave pure *cis-* or *trans-* diols on methanolysis, showing that no isomerization occurs during their preparation.

Details of some of the polymerizations are given in *Table 2* from which it appears that using reactants containing both *cis-* and *trans-* units, the *trans-*/*cis-* ratio in the polymers is always less than that in the respective reactants, so that during polymerization *trans-* units are eliminated from the

product more readily than *cis*-. The yields of polymers obtained ranged from 40 to 60 per cent of the theoretical, the balance of the reagents appearing either as decarboxylation products (aldehyde plus carbon dioxide) or as unreacted monomers, more diol than di-ester generally being lost in this way. It was found that the molar proportion of carbon dioxide evolved was always a little greater than that of the aldehyde but as the aldehyde was isolated by a fractional distillation procedure, which must involve some loss, it is reasonable to assume that the aldehyde and carbon dioxide are produced in equimolar quantities. This was checked by a separate experiment in which the aldehyde was isolated quantitatively as its semicarbazone, when it was found that the relative molar proportion of aldehyde to carbon dioxide was very close to 1 : 1.

Table 2. Polymerizations with reactants of known steric composition

Trans-/cis-*reactant ratio*	Trans-/cis-*ratio in polymer*	η*	% *Yield of polymer*	% *Yield of carbon dioxide*	% *Yield of aldehyde*
0/100	0/100	0·55	56	18	16
0/100	0/100	2·09	43	20	18
25/75	1/99	0·99	43	34	27
—	18/82	0·69	36	—	—
—	29/71	0·88	57	12	11
48/52	32/68	1·42	60	10	9
65/35	49/51	1·14	56	13	12
65/35	50/50	1·16	60	15	16
75/25	61/39	2·58	44	33	—
100/0	100/0	—	43	—	—

*Specific viscosity for a one per cent solution in chloroform at 25°C.

The all *trans*- polymer was insoluble in common solvents, but all the other polymers prepared, that is polymers containing up to 61 per cent of *trans*- units, dissolved in chloroform. Neither the all *trans*- polymer nor the one containing 61 per cent of *trans*- units could be moulded as they decomposed before melting, but all those containing 50 per cent or less of *trans*- units could be moulded at 265°C without reducing their solution viscosities. Thus samples of polymers containing up to 61 per cent of *trans*- units could be fabricated into thin sheet by solvent casting while those containing up to 50 per cent of *trans*- units could be compression moulded.

DISCUSSION

The polymerization occurs by base catalysed ester interchange between the diols and their bis(ethyl carbonate) esters, III, with elimination of ethanol. Polymer can also be produced, though more slowly, from the diester alone by the interchange reaction:

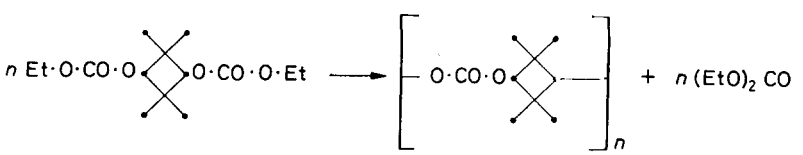

This process must occur to some extent during polycondensation of the diol with the diester, as diethyl carbonate occurs in the volatile products of this reaction. Some reactants were always lost from the melt by distillation and the proportion of diol removed in this way was usually greater than that of the diester. This is reasonable as the diol is the more volatile, and the resulting imbalance of reagents does not result in a product of low molecular weight because condensation with elimination of diethyl carbonate can occur between polymers having —O.CO.O.Et end-groups.

A very considerable loss of reagents occurs with concomitant formation of equimolar quantities of carbon dioxide and 2,2,4-trimethyl-3-pentenal. Formation of these products is considered to occur via the alkoxide ion VII according to the following type of mechanism, which is analogous to that postulated by Searles *et al.*[4] to explain the formation of olefins and aldehydes as side products during the preparation of cyclic ethers by base catalysed decomposition of cyclic carbonates.

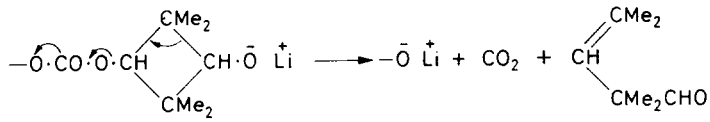

VII

Such a reaction involves no loss of functionality so that the surprising observation that polymers of high molecular weight can be formed although an extensive side reaction occurs is explained for this system. No evidence for the formation of ether linkages could be obtained so that the formation of these by an intermolecular analogue of Searle's intramolecular reaction could not be realized.

Formation of carbon dioxide and the pentenal occurs by decomposition of either *cis-* or *trans-* repeat units during the polymerization, and when both steric forms are present, i.e. when mixtures of *cis-* and *trans-* reagents are used, so that the conditions of reaction are identical for each form, the *trans-* structure undergoes reaction much more readily than the *cis-*, and this has the effect of increasing the proportion of *cis-* repeat units in the polymer melt as polymerization proceeds. Hasek *et al.*[9] have observed a similar difference in reactivity between the *cis-* and *trans-*2,2,4,4-tetramethylcyclobutane-1,3-diols, the *trans-* being dehydrated readily to the pentenal, VI, by heating with dilute sulphuric acid, whereas the *cis-*diol is unaffected by such treatment. They consider that these observations can be explained on the assumption that dehydration occurs by a concerted transannular reaction whereby one OH group is displaced by the other to form a bicyclic intermediate VIII, which is possible for the *trans-*isomer but not the *cis-*.

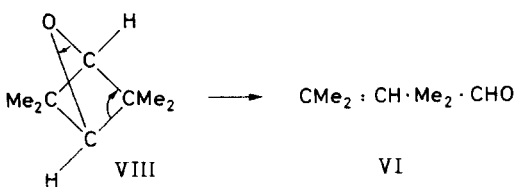

VIII VI

Decomposition of the alkoxide ion, VII, to give VI could be considered to occur in an analogous manner, provided that the existence of such a highly strained intermediate as VIII can be accepted. Formation of VIII may be less difficult than would at first sight be expected as it appears that in these polymers the cyclobutane ring is puckered[5].

EXPERIMENTAL

Intermediates

Diols—The mixed *cis-* and *trans*-2,2,4,4-tetramethyl-1,3-cyclobutane diols, obtained from Eastman Chemical Products Inc., were purified by recrystallization from toluene to give a product containing 62 per cent of the *trans-* isomer.

Separation of the isomers from the mixture was carried out as described previously[2,3] to give the pure *cis*-diol, m.pt 163° to 164°C and the pure *trans-* m.pt 149° to 150°C (Eastman Kodak report[2,3] m.pts 162·5° to 163·5°C and 148°C respectively).

Bis(ethyl carbonate) esters—These were prepared by ester interchange between the diols (1 mole) and diethyl carbonate (10 moles), the procedure being as follows. A solution of the diol in ethyl carbonate containing *ca.* 0·1 g of lithium hydride was heated to reflux under a short fractionating column and ethanol removed continuously as it was formed. When the reaction was complete, the cooled solution was filtered to remove insoluble lithium salts, and the excess diethyl carbonate distilled off at 25 mm of mercury pressure. The residue was then distilled at low pressure to obtain the *bis(ethyl carbonate)* ester, b.pt 98°/0·2 mm, in 60 to 70 per cent yield, a polymeric residue remaining behind.

Analysis of intermediates

Diols—The *trans-*/*cis-* ratio in mixtures of the diols was determined by the following method involving a comparison of their i.r. spectra with those of several known mixtures. The spectra of these mixtures (ground in Nujol and spread between rocksalt plates) were obtained and the ratio of the absorbances due to *trans*-diol (at 11·8 μ) and *cis-* (at 12·2 μ) measured in each case. A plot of these absorbance ratios against the *trans-*/*cis-* ratios gave a straight line calibration from which the *trans-*/*cis-* ratios of unknown diol mixtures could be determined by measuring their absorbance ratios.

Bis(ethyl carbonate esters)—The *trans-*/*cis-* ratio in mixtures of the esters was determined by converting them to the diols in almost quantitative yield by the following procedure and measuring the *trans-*/*cis-* ratio of the product as described above. A solution of the diethyl carbonate ester (2·88 g, 0·01 mole) in methanol (12·5 ml) containing sodium metal (0·030 g) was left to stand at room temperature for 24 h. The solution was then neutralized with 0·13 ml of glacial acetic acid, the methanol removed by distillation from a steam bath, and the residual solid sublimed under vacuum at 0·1 mm of mercury to give the mixed diols (1·3 to 1·4 g, 90 to 100 per cent yield).

The purity of the bis(ethyl carbonate) esters was determined by estimating their 'carbonate' contents by the following procedure.

About 0·3 g of ester was weighed into a Pyrex conical flask and 25 ml of 0·5 N alcoholic potash added. The solution, guarded against atmospheric carbon dioxide, was heated under reflux for one hour. The solution was then diluted to about 100 ml with distilled water, the liberated carbonate precipitated with an extremely small excess of acid-free barium chloride solution, and excess alkali determined by slow titration with standard hydrochloric acid using phenolphthalein as indicator. The strength of the alcoholic potash used was determined beforehand by titrating a 25 ml sample to which 0·5 ml of barium chloride had been added to precipitate any potassium carbonate dissolved in it. From the difference between the two titers, the amount of caustic potash used up, and hence the amount of carbonate present in the sample was calculated.

Polymerizations

Polymerizations were carried out in a cylindrical vessel heated by a 'Wood's metal' bath and fitted with a vertical capillary tube by means of which a slow stream of nitrogen could be forced through the molten reactants. This vessel was connected to a vacuum pump via a water condenser and a set of traps designed to catch the volatile materials distilling from the melt.

To carry out a polymerization, equimolar quantities of the diol, and the bis(ethyl carbonate) ester, together with a small quantity of basic catalyst, were placed in the vessel and all air removed from the apparatus by alternately evacuating and filling it with nitrogen. The reagents were then heated to a predetermined temperature at atmospheric pressure for a given time, after which the pressure was reduced gradually to 0·1 mm of mercury while the temperature was raised to complete the reaction. The polymerizations listed in *Table 2* were carried out by heating the reagents first at 240°C for 1·5 h and then at 290°C for 2 h, using 0·25 wt % of lithium carbonate as catalyst. The quantity of carbon dioxide evolved was estimated either by back-titration of the caustic soda solution in which it had been absorbed, or by measuring the volume of gas and determining its carbon dioxide content from measurements of its i.r. absorption. The liquid products from each reaction were fractionated at atmospheric pressure through a small column of high efficiency to give ethanol, b.pt 77° to 78°C, an intermediate fraction b.pt 78° to 145°C, and 2,2,4-trimethyl-3-pentenal, b.pt 145° to 146°C. Diethyl carbonate, b.pt 126° to 127°C (lit. b.pt 126°C) was separated from the mixed intermediate fractions from several polymerizations by refractionation. The solid products were removed mechanically from the apparatus and triturated with petrol ether. Almost pure diol was then filtered off, and the bis(ethyl carbonate) ester isolated by evaporation of the filtrate.

The polymers

The polymers were isolated by breaking the polymerization vessel, and freed from the catalyst residues by dissolution in chloroform followed by precipitation with methanol, a procedure which always caused some degradation, presumably by methanolysis.

Reduced viscosities $[RV]^{25°}_{1\%} = (t \text{ solution} - t \text{ solvent})/t \text{ solvent} \times C$ were determined for one per cent solutions in chloroform at 25°C.

Micro-combustion carried out on a sample of purified *polymer* gave C, 63·2; H 8·2 per cent; $C_9H_{14}O_3$ requires C, 63·5; H, 8·3 per cent. Analysis for 'carbonate content' was carried out on several polymer samples as described for the bis(ethyl carbonate) esters, except that as longer periods of heating were required an anhydrous solution of NaOEt in EtOH was used to prevent attack on the glass reaction vessel, and showed the polymers to be $100 \pm 0{\cdot}5$ per cent polycarbonates of structure I. The *trans-/cis-* repeat unit ratio for each polymer was determined by hydrolysis to the diols followed by i.r. analysis in a manner analogous to that described for the bis(ethyl carbonate) esters.

2,2,4-Trimethyl-3-pentenal

The fractionated liquid b.pt 146°C/760 mm, n_D^{20} 1·436 (Found: C, 77·4; H, 11·5 per cent. *M* (cryoscopic) 130. Calc. for $C_8H_{14}O$: C, 77·4; H, 11·4 per cent, *M*, 126), reduced ammoniacal silver nitrate solution and gave by conventional methods a *semicarbazone* (Found: C, 58·9; H, 9·9; N, 23·1 per cent. $C_9H_{17}N_3O$ requires C, 58·98; H, 9·35; N 22·9 per cent) m.pt 169° to 172°C and a 2,4-dinitrophenylhydrazone (Found: C, 55·0; H, 6·1; N, 18·2 per cent. Calc. for $C_{14}H_{18}N_4O_4$: C, 55·0; H, 5·9; N, 18·29 per cent) m.pt 143° to 144°C. Hasek *et al.*[9] record n_D^{20} 1·4357 to 1·4361 for the aldehyde and m.pt 142° to 143°C for its 2,4-dinitrophenylhydrazone.

The aldehyde, 6·3 g, was added to a solution of 12·5 g sodium in 250 ml of diethylene glycol containing 25 g of hydrazine hydrate, and this mixture heated to reflux for 20 hours. Then the volatile product was distilled off, washed with water, and dried. Fractionation at atmospheric pressure gave 1·8 g of 2,4,4-trimethylpentene-2, b.pt 104°C, n_D^{20} 1·4160: Egloff[10] records b.pt 104·5°C, n_D^{20} 1·4159.

The semicarbazone of the aldehyde, 9 g, was added to a solution of 10 g sodium in 200 ml diethylene glycol and this mixture heated to reflux for half an hour. The product was diluted with water and extracted with petrol ether (b.pt 40°C). The extract was washed with water, dried and fractionated, to give 2 g of 2,4,4-trimethylpentene-2 b.pt 104°C, n_D^{20} 1·4160.

A few millilitres of the aldehyde was heated to reflux with a solution of potassium dichromate in dilute sulphuric acid for about an hour. Then all the volatile organic products were removed by distillation and the residual aqueous liquid cooled and extracted with ether. Evaporation of the ether layer gave 0·2 g of dimethyl malonic acid m.pt 181° to 185°C decomp., (lit. m.pt 186° to 190°C decomp.) which gave by conventional means a diamide m.pt 273°C (lit. 269°C).

The help of Messrs R. J. G. Miller and B. Stay for measurement of infra-red spectra is acknowledged.

Thanks are also due to Mr D. I. Ritchie for assistance with the experimental work.

I.C.I. Ltd, Plastics Division,
Welwyn Garden City, Herts.

(*Received January 1963*)

REFERENCES

[1] GAWLAK, Miss M., PALMER, R. P., ROSE, J. B., SANDIFORD, D. J. H. and TURNER-JONES, Miss A. *Chem. & Ind.* **1962,** 1148
[2] HASEK, R. H., ELAM, E. U., MARTIN, J. C. and NATIONS, R. G. *J. org. Chem.* 1961, **26,** 700
[3] Eastman Chemical Products Inc., *Technical Brochure No. N-110* May 1960, p 20
[4] SEARLES, S., HUMMEL, S., NUKINA, D. G. and THROCKMORTON, P. E. *J. Amer. chem. Soc.* 1960, **82,** 2928
[5] TURNER-JONES, Miss A. and PALMER, R. P. *Polymer, Lond.* 1963, **4,** 525
[6] FOSSEK, W. *Mh. Chem.* 1871, **2,** 616
[7] URBAIN, P. *Bull. Soc. chim. Fr.* 1895 (3), **13,** 1048
[8] GRIGNARD, V. and ILIESCU, T. N. *C.R. Acad. Sci., Paris,* 1930, **190,** 556
[9] HASEK, R. H., CLARK, R. D. and CHAUDET, J. H. *J. org. Chem.* 1961, **26,** 3130
[10] EGLOFF, G. *Physical Constants of Hydrocarbons,* Vol. I, p 233. Reinhold: New York, 1939

Polycarbonates from the 2,2,4,4-Tetramethylcyclobutane-1,3-diols

Part II: Crystal Structure and Melting Behaviour

A. TURNER JONES and R. P. PALMER

X-ray and optical examination of a series of random copolymers of cis- *and* trans-*tetramethylcyclobutane diol carbonates ranging in composition from 100 per cent* cis- *to 100 per cent* trans- *units showed that they were well crystalline over the whole range of composition. The pure* cis- *and pure* trans- *polymers occurred in distinct crystalline forms* α *and* β *respectively, with closely related unit cells. The random copolymers with* trans- *content of 29 to 61 per cent crystallized in a third crystal form,* γ*, with a unit cell related to the* α *and* β *forms. The linear melting point versus composition curve confirmed that mixed crystal formation was occurring in this range. The chain configuration and packing of the chains in the crystallites are discussed in relation to the crystalline forms, fibre repeat units and observed melting points.*

THIS paper records the optical and X-ray data obtained in the examination of the series of polytetramethylcyclobutane carbonates prepared by Miss M. Gawlak and J. B. Rose[1] and described in Part I of these papers. The series included pure *trans-* and pure *cis-*polymers, and polymers of mixed *cis-* and *trans-* composition with *cis-/trans-* ratios of approximately 80/20, 70/30, 50/50 and 40/60 as determined by infra-red (i.r.) examination of their breakdown products (Part I). A preliminary note on this work has been published previously[2].

CRYSTALLINITY AND CRYSTAL STRUCTURE

The polymers examined are listed in *Table 1*. These were in the form of (*i*) solvent cast sheets, (*ii*) powder precipitated from methanol solution and (*iii*) specimens moulded at 220°C under 20 ton/in^2 pressure (60 seconds preheating).

Crystallinity was observed in all the polymers examined. The two pure *trans-* polymers were highly crystalline (~90 per cent) as powders as prepared. The pure *cis-* polymers were well crystalline (up to 75 per cent). The diffraction patterns of the pure *cis-* and pure *trans-* polymers were distinct and are subsequently referred to as α and β crystal forms respectively. Polymers of intermediate composition were also all obtained quite well crystalline. The 82/18 *cis-/trans-* ratio polymer showed typical *cis-* (α) crystallinity. Those in the range 71/29 to 39/61 all gave the same diffraction pattern which was different from either the α or β forms and is designated the γ form. The diffraction patterns of the α and γ forms are shown in *Figures 1* and *2*.

Table 1 shows the degree to which crystallinity was developed in the various specimens examined. The pure *trans-* polymer was insoluble in all solvents and was intractable and could not be fused or moulded into sheets. In the solvent cast sheets of the *cis-* and γ-form polymers crystallinity was

Table 1. Crystallinity, unit cell dimensions and melting points

Cis-/trans-ratio	$T_m(T_{50})$ °C	Crystallinity				Cell dimensions Å	Density, g/cm³	
		Solvent cast film	*Film heated with* MeOH	*Powder pptd from* MeOH	*Sheets moulded* 220°C		$d_{cryst.}$	$d_{meas.}$
100/0	250 (235)	good (α)	impr. (α) 75%	poor (α)		$a=9\cdot16$ $b=8\cdot22$	1·095	1·094* (good cryst.)
99/1	247	good (α)			good (α)	$a=9\cdot23$ $b=8\cdot20$		
82/18	211	mod. (α)	impr. (α)	poor (α)		$a=9\cdot15$ $b=8\cdot34$		
71/29	238	v.p. (δ)	f.g. (γ)		v.p. (δ)	$a=8\cdot68$	1·08	1·068* (poor cryst.)
68/32	235 (221)	v.p. (δ)	f.g. (γ)	poor (γ)	v.p. (δ)	$a=8\cdot70$		
51/49	246	mod. (γ)	impr. (γ)	mod. (γ)	f.g.(γ)	$a=8\cdot63$		
50/50	288, >360			mod. (γ)		$a=8\cdot61$		
39/61	329, >360	mod. (γ)	no change			$a=8\cdot55$	1·11	1·098* (mod. cryst.)
0/100	>360	v.g.† (β) ~90%				$a_0=9\cdot25$ $b_0=8\cdot28$ $\gamma_0=96\frac{1}{2}°$	~1·08	1·1†

*Solvent cast film.
†Powder as made.

f.g. Fairly good.
mod. Moderate.

v.p. Very poor.
impr. Improved.

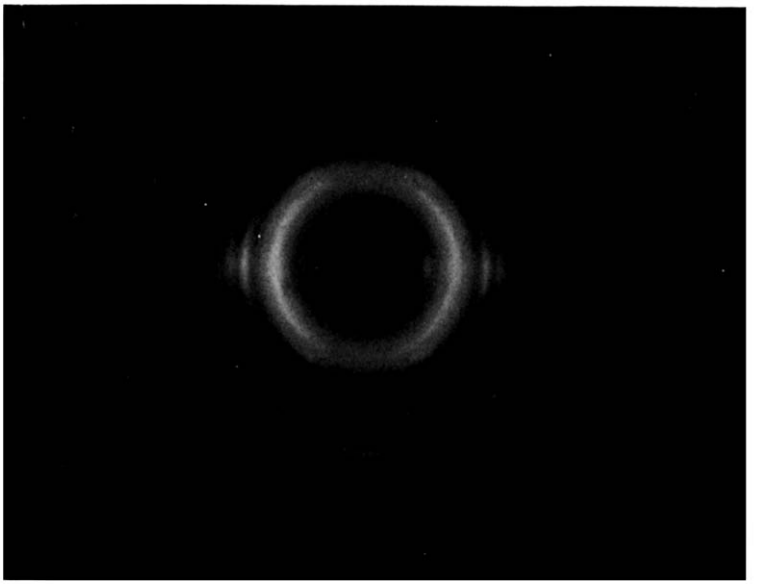

Figure 1—X-ray diffraction pattern taken with CuK$_\alpha$ radiation of a drawn fibre in the α crystalline form (fibre axis vertical)

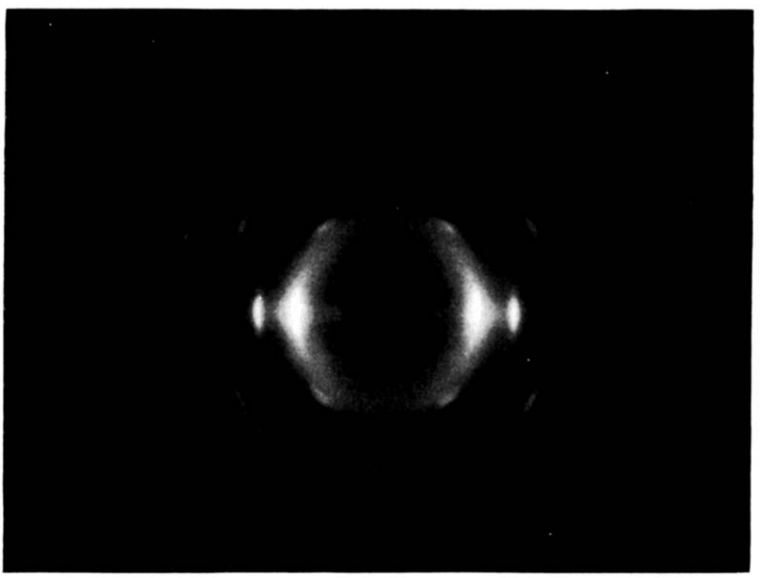

Figure 2—X-ray diffraction pattern taken with CuK$_\alpha$ radiation of a drawn fibre in the γ crystalline form (fibre axis vertical)

sometimes only poorly developed, particularly in the intermediate (γ) polymer but refluxing with methanol, in which the polymer is practically insoluble, developed the crystallinity in these specimens and improved it in specimens already moderately crystalline. Powders precipitated from methanol were usually rather poorly crystalline. Moulding from above the melting point generally tended to give very poor crystallinity but slow cooling helped to produce the normal crystal form. This 'very poor' crystallinity, whether produced after melting or by solvent casting or precipitation, was not α, β or γ crystallinity poorly developed, but a fourth 'δ' type which is characterized by a sharpening of the X-ray intensity diffracted at a d spacing of 5·5 to 5·6 Å and is probably due to a partial order and is not further considered here. The best crystallinity was produced by slow cooling specimens already crystallized in boiling methanol, from just below their respective melting points. These specimens were used for the determination of unit cell parameters (a and b axial lengths) given in *Table 1*.

The presence of good crystallinity throughout the whole range of *cis-*/*trans-* copolymer composition examined was unexpected since the polymers were believed to be random copolymers from the method of preparation. If they were block copolymers we should expect to see the characteristic pure *cis-* and pure *trans-* crystallinities in the polymer of intermediate compositions, but we do not. The presence of one crystal form only over the range 71/29 to 31/69 *cis-*/*trans-* ratio strongly suggested that mixed crystal formation was taking place over this range and that *cis-* and *trans-* units could replace each other in the lattice of the intermediate (γ) form. This was somewhat surprising in view of the very different configurations of the chains at the cyclobutane groups and is further discussed later. There was practically no change in lattice dimensions over this range. A somewhat similar situation has been found recently in *cis-*/*trans-*poly-1,4-cyclohexylene dimethylene terephthalate by Boye[3].

If mixed crystal formation were taking place as suggested we should expect to find that the three-dimensional lattice packings of the pure *cis-* and pure *trans-* crystal forms would be similar to each other and also to that of the γ form. This similarity would be expected to be reflected in the unit cell dimensions of the three forms.

Unit cell determinations

Oriented crystalline fibres were obtained from all the polymers examined except the 100 per cent *trans-* polymers, which were intractable. The fibres were drawn at temperatures between 130°C and 220°C from strips cut from solvent cast films and pressed sheets, and were annealed at constant length for half an hour to develop the crystallinity fully. The fibres were sometimes not crystalline until annealed. High orientation was obtained in all the intermediate (γ) form polymers but the *cis-* polymers could only be obtained moderately well oriented.

Unit cells were deduced for the α and γ forms as follows:

α form (*cis*-) orthorhombic

$$a = 9{\cdot}16 \text{ Å}$$
$$b = 8{\cdot}22 \text{ Å}$$
$$c = 12{\cdot}9 \pm 0{\cdot}3 \text{ Å (fibre axis)}$$
$$d_{\text{cryst.}} = 1{\cdot}10 \text{ g/cm}^3$$
$$4 \text{ monomer units/cell}$$

γ form (intermediate) tetragonal

$$a = 8{\cdot}68 \text{ to } 8{\cdot}55 \text{ Å}$$
$$c = 13{\cdot}1 \text{ Å (fibre axis)}$$
$$d_{\text{cryst.}} = 1{\cdot}08 \text{ to } 1{\cdot}11 \text{ g/cm}^3$$
$$4 \text{ monomer units/cell}$$

The sample with the *cis*-/*trans*- ratio 71/29 sometimes produced extra reflections which require a doubling of the *a* axial dimensions. The *a* axial length of the intermediate polymers varies slightly (and regularly) with composition as shown in *Table 1*. The observed densities of cast film or pressed specimens of varying crystallinity were consistent with the calculated crystalline densities within the limits of the accuracy attainable (see *Table 1*).

The two cells are very similar in dimensions and in volume; the tetragonal (γ) cell can be regarded as derived from the orthorhombic α cell by a small contraction of *a* and expansion of *b*, suggesting that the packing of the chains in the two cells is similar.

As oriented crystalline fibres could not be obtained from the β (*trans*-) form, derivation of a unit cell from the diffraction pattern of the unoriented powder was attempted. A cell was found which is consistent with the observed data and is closely related to the α and γ cells. This cell cannot be regarded as the only solution but is extremely plausible.

β form (*trans*-) monoclinic or triclinic

$$a_0 = 9{\cdot}25 \text{ Å}$$
$$b_0 = 8{\cdot}28 \text{ Å}$$
$$c = ?$$
$$\gamma_0 = 96^\circ\ 30'$$

Calc. crystalline density 1·08 g/cm³
(assuming $c = 12{\cdot}9$ Å and 4 monomer units/cell)

The relationships between the three cells are shown in *Figure 3*.

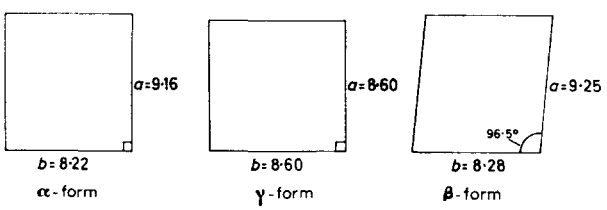

Figure 3—Relationships between cells of α, β and γ forms

The β-form cell can be regarded as derived from the α-cell by a slight deformation in the plane perpendicular to the fibre axis. The unit cell data are thus completely consistent with the idea of mixed crystal formation taking place throughout the γ-form polymer series. Moreover, based on these three cells, the angular distribution of diffracted intensity corresponds closely in the three forms—for instance the strongest reflection is the 110 reflection in all forms. This shows that the distribution of scattering matter within the unit cells is similar in the three crystal forms, in other words, that the configuration of the chains and packing of the groups is similar in the three forms. It thus appears that, in spite of the apparent difference in configuration at the dimethyl cyclobutane group of the *cis-* and *trans-* forms, the configurations of the *cis-* and *trans-* chains are not sufficiently different to cause appreciable changes in side by side packing. It follows that it is reasonable for a chain in which *cis-* and *trans-* units are randomly distributed to assume a similar chain configuration and be incorporated in a crystal lattice only slightly distorted from those of the pure *cis-* and pure *trans-* forms. It is commonly observed in crystallography that where disorder is introduced into a structure which is insufficient to disrupt crystallization completely, the crystal lattice assumes a higher symmetry than the normal crystal form. An example of this is the transition from the normal orthorhombic form to a hexagonal form which occurs in polyethylene just below the melting point. The steric irregularities present in the polycarbonate chains with random *cis-* and *trans-* units have a similar effect, and these chains pack in a tetragonal lattice with a higher symmetry than those of the α and β forms. The appearance of the γ-form diffraction pattern also suggests irregularities in chain configuration contained within a well defined basic lattice; a few very sharp reflections are present both on the equator and on the layer lines together with fuzzy reflections and streaks on the layer lines. The odd layer lines, first, third and fifth, are very weak and diffuse denoting a pseudo chain repeat of half the observed value, 6·55 Å, corresponding to one monomer unit

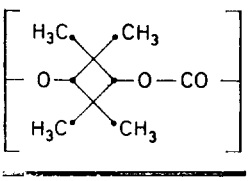

as might be expected since each unit is randomly *cis-* or *trans-*.

Chain configuration of the α, β and γ forms

Configuration at the tetramethylcyclobutane groups—Evidence from other structures suggests that the cyclobutane group in this polymer is unlikely to be planar (as in cyclobutane itself) but will be puckered in the manner shown in *Figure 4*(a). This puckering occurs in octachlorocyclobutane[4] which has eight large substituents on the four ring carbons. The tetramethylcyclobutane group has six large substituents, four of them

methyls while two of the ring carbons are joined to the rest of the polymer chain. It is therefore reasonable to assume that in this polymer tetramethylcyclobutane will be stabilized into a puckered ring. Other evidence for this from fibre repeat units is given later.

The data given in the structure determination of octachlorocyclobutane has been used in the following discussion of the chain structure of the polymer, namely:

$$C_1C_3 = 2{\cdot}20\ \text{Å} \qquad \angle O_1C_1H_1\ (=O_3C_3H_3) = 109{\cdot}4°$$

$$\angle C_1C_2C_3 = 87{\cdot}7° \qquad \text{Dihedral angle } 22°$$

Other bond angles and lengths are assumed to have their normal values namely:

C—C	1·535 Å	∠O (CO) O	109°
C—O (ether)	1·43 Å	∠C O C	111°

The methyl groups attached to C_2 and C_4 are omitted in this and subsequent figures. The angle $O_1C_1C_3$ is thus $125{\cdot}3° + 22° = 147{\cdot}3°$ and the angle $H_1C_1C_3$ is $125{\cdot}3° - 22° = 103{\cdot}3°$.

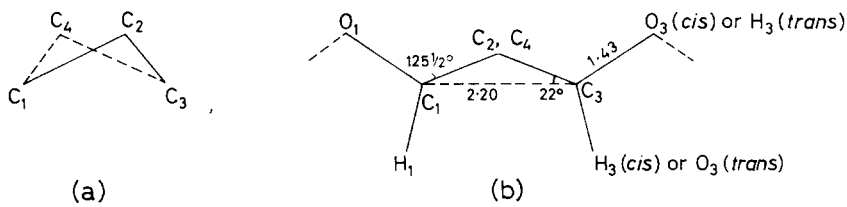

Figure 4—(*a*) Puckered cyclobutane ring. Line joining C_1C_3 is perpendicular to C_2C_4; (*b*) Section through symmetry plane of cyclobutane group containing carbon atoms C_1C_3 bonded to chain oxygen atoms of the carbonate group O_1, O_3 respectively. C_2 and C_4 are shown projected on to this plane

Stereoisomerism of cis- *and* trans- *forms*—Assuming a stabilized puckered configuration of the cyclobutane group at room temperature, there are, in addition to the stereoisomerism caused by *cis-* and *trans-* configurations themselves, stereoisomeric forms within the all *cis-* and all *trans-* configurations respectively. This arises because the *cis-* unit can take up either the A or B configuration (*Figure 5*) so that the possible chain configurations (to consider only the likely simplest ones) are —AAAA— or —BBBB— or —ABAB—. It should be noted that the A type, when O_1 and O_3 are a maximum distance apart, can be converted to the B type by simple inversion of the puckered configuration of the cyclobutane rings so that C_2 and C_4 are now on the opposite side of the line joining C_1C_3. Similarly each *trans-* unit can take up the X or Y configurations along the length of one chain giving rise to chain forms —XXXX— (=—YYYY—) and —XYXY— (effectively head-to-head and head-to-tail sequences). Here again the X configuration can be converted to the Y configuration by an inversion of the puckered configuration of the cyclobutane ring.

The observed fibre repeat units were considered in relation to possible chain configurations with the aid of scale models which permitted free rotation around bonds where permissible.

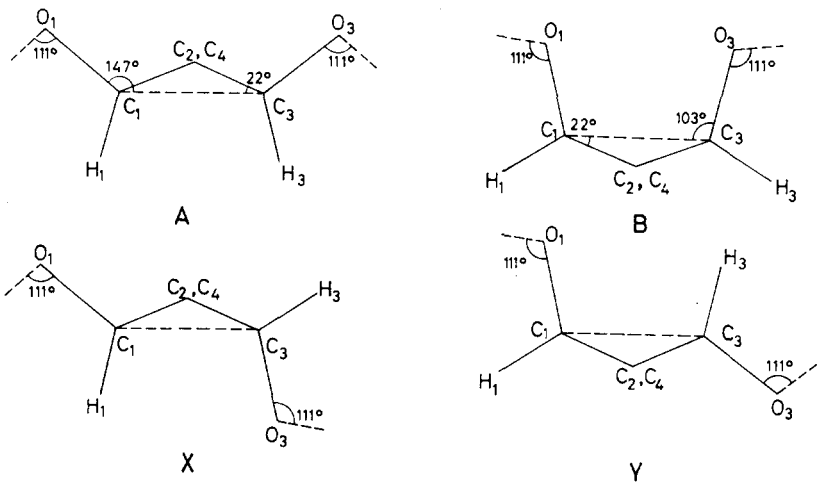

Figure 5—(A), (B) Configurations which can be taken up by *cis*- units; (X), (Y), Configurations which can be taken up by *trans*- units

cis-*form*—The fully extended chain form in the —AAAA— configuration is shown in *Figure 6* (here all atoms except C_2 and C_4 and substituents are coplanar). This has a single-monomer-unit calculated repeat of 6·9 Å (two-unit repeat = 13·8 Å). In this configuration successive monomer units lie in a straight line, owing to the fortuitous equality of the assumed angles, $O_1C_1C_3 = C_3O_2O_1' = 147°$; if these angles were not equal the chain would curve gradually and could not occur in a crystal. To achieve a straight-line succession in these circumstances, some departure from coplanarity would be required.

Similarly if the —BBBB— configuration is taken up, a fully extended planar configuration such as the above is not possible in the crystallites because the chain would be curved. Various linear regular chain configurations requiring either one or two monomer units per repeat are obtainable, however, by rotation around chain bonds. The longest two-monomer-unit repeat of these is $\sim$ 11 Å, so that since the measured repeat is 12·9 Å, the —BBBB— configuration can be excluded. We should not, in fact, expect that the chain would take up this configuration since the —BBBB— chain will have a higher energy than —AAAA—, because of the shorter distance (2·9 Å) and therefore greater repulsion between O_1 and O_3, both of which carry a small negative charge.

Using the model to consider the —ABAB— configuration, it has been shown that the maximum chain repeat (non-planar) is $\sim$ 13 Å (for two monomer units necessarily). This is therefore just possible on these grounds, but as already stated the B configuration is unlikely on energy grounds.

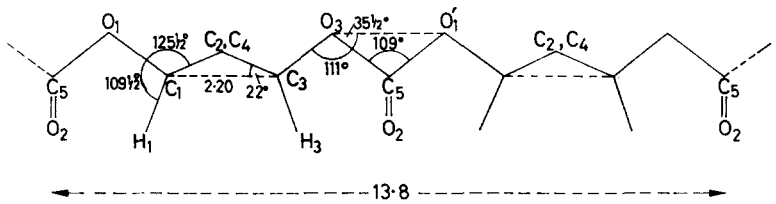

Figure 6—Fully extended chain form

It follows that we can with reasonable certainty ascribe the —AAAA— configuration to the *cis-* polymer. The shortening of the chain repeat from 13·8 Å to the observed value of 12·9 Å must result from rotation around bonds in the flexible carbonate group region. This we should expect since the planar configuration (*Figure 6*) is non-staggered. The precise configuration cannot be settled on repeat distances alone.

The maximum repeat distance calculated on a planar configuration for the cyclobutane ring is $< 6{\cdot}1$ Å ($< 12{\cdot}2$ Å for two monomer units) which provides additional evidence that the cyclobutane ring is puckered.

trans- *form*—We do not know if the *trans-* form has a single-monomer-unit repeat (—XXXX— configuration) or a two-monomer-unit repeat (either —XXXX— or —XYXY—). If the chain form adopted is —XXXX—, then by twisting around chain bonds, configurations with a single-unit repeat, in which the plane of the carbonate group makes varying angles with the average plane of the cyclobutane ring, can be envisaged, but the largest repeat distance obtainable is 6 Å which is rather short for mixed crystal formation with *cis-* units which have a repeat per monomer unit of $\sim 6{\cdot}5$ Å (α and γ forms). If alternate monomer units do not have precisely the same configuration, so that a two-unit repeat is formed, then a repeat distance of ~ 13 Å can be obtained which would be acceptable. Similarly, molecular models show that a regular repeat of ~ 13 Å can readily be obtained from the —XYXY— type chain.

Mixed crystal fo .nation—In order to obtain a sufficiently extended chain to give a repeat of 13 Å in either of these two *trans-* configurations, the line joining C_1C_3 of both cyclobutane units must lie at only a small angle to the chain axis and the rotation around chain bonds in the region of the carbonate group can only be small (i.e. the departure from a planar zigzag configuration of $C_1C_3O_3C_5O'_1C_1$ can only be small). This means that the dominating features of the chain are flattened spheres of electron density, lying with their short axes parallel to the fibre direction and equally spaced

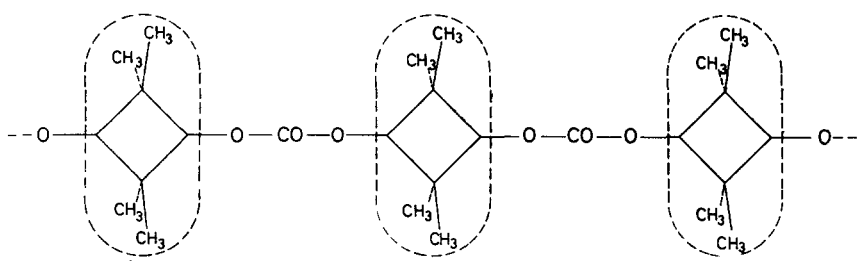

Figure 7—Diagram illustrating flattened spheres of electron density of cyclobutane groups

along the chain at intervals of $\sim 6{\cdot}5$ Å, formed by the cyclobutane rings with substituent methyl groups extending approximately perpendicular to the fibre direction. This is illustrated diagrammatically in *Figure 7*. Between every two flattened spheres lie the carbonate groups of which, in the most likely configurations, even the oxygen atom of the C=O group does not protrude beyond the methyl groups of the cyclobutane rings. These general features also apply with the *cis-* form —AAAA— (here the reduction in chain repeat from the theoretical fully extended value of $13{\cdot}8$ Å is achieved by rather greater rotations around bonds of the carbonate group). This then seems the likely explanation of why *cis-* and *trans-* units can co-crystallize, since the dominating space-filling features of the chain are these flattened spheres formed by the tetramethylcyclobutane groups. The precise configuration of the carbonate groups is not important to crystallization because they are 'sheltered' by the dimethylcyclobutane groups.

We have made chain models where *cis-* and *trans-* units are randomly disposed along the chain, and can obtain configurations where alternate dimethylcyclobutane groups are practically identically sterically disposed, giving an apparent repeat of ~ 13 Å. The average plane of the cyclobutane group between these two groups has generally to be rotated with respect to them in order to accommodate the different successive *cis-* (A) and *trans-* (X or Y) configurations. Moreover, alternate carbonate groups must have different configurations and this accounts for the apparent *two*-monomer-unit repeat, ~ 13 Å, as opposed to a single-unit repeat. It is possible, of course, that only *cis*-A and *trans*-X units are involved in the crystallization.

It is possible that randomly disposed X and Y units of the pure *trans-* polymer could be accommodated in a similar manner in the β lattice. However, the very high crystallinity of the *trans-* form suggests strongly that high steric regularity is present along the chain, namely either —XXXX— or —XYXY—.

Rates of crystallization

The relative difficulty in regaining crystallinity after melting or precipitation from solution in the *cis-* and intermediate type polymers can possibly now be explained. In the γ polymers any succession of units, e.g. *cis*-A *trans*-X *cis*-A, *cis*-A *trans*-X *trans*-Y, etc., will have a preferred configuration for crystallization, and the attainment of this configuration may involve large rotations of the dimethylcyclobutane groups around the chain direction ($\sim C_1C_3$) and this can only be attained by considerable movements in that region of the chain. Hence very slow cooling from the melt, or thermal or solvent swelling treatment of the rapidly solidified or precipitated material is necessary for crystallization. In addition, such treatment may be necessary to convert, by inversion of the puckered cyclobutane ring, *trans*-X to *trans*-Y and *cis*-B to *cis*-A, since rapid cooling may well produce a proportion of units in the *cis*-B configuration in α and γ polymers.

MELTING BEHAVIOUR

Specimens for the determination of melting points were prepared in the form of thin films between microscope slides and cover glasses by pressing

at 340°C followed by slow cooling. In some cases the specimens were treated with hot methanol to improve the crystallinity. The spherulite size ranged from 4 to 100 microns. The specimens were examined visually in a hot stage polarizing microscope with a heating rate of approximately 1°C per minute, the samples being maintained in an atmosphere of nitrogen.

The light intensity between crossed polarizers was sufficient in a few cases to allow the use of A.M.P.A., an automatic melting point apparatus developed in this laboratory. The melting curves obtained were of a simple shape and allowed both the crystalline melting point, T_m, and the T_{50} temperature, at which the room temperature response (roughly proportional to crystallinity) has dropped to half, to be obtained. The melting ranges thus determined were moderately broad. The results are given in *Table 1*.

The melting points of the α (cis-) *and* β (trans-) *forms*

The melting points of the α and β forms were 253°C and > 360°C respectively; thus, in common with many other polymers, the *cis-* form has a lower melting point than the *trans-*.

The high melting point of the *trans-* form (extrapolation suggests 420° to 440°C) is due to the existence of large essentially rigid units in a basically flexible chain. Rotation round the bonds in the carbonate group is usually very easy but in this molecule such rotation is difficult, particularly about the

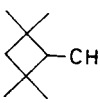

bond where the steric hindrance of the methyl groups pendant to the cyclobutane ring is powerful. In addition to this, the large tetramethyl cyclobutane units load the chain heavily. A rough quantitative treatment can be made according to the scheme proposed by C. W. Bunn[5].

The molar cohesion energy of the tetramethyl cyclobutane groups can be estimated as 3 364 calories, the value for the carbonate group depends on the nature of the adjoining groups; in diphenyl carbonate

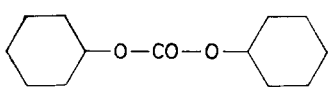

it is 1 024 cal, in diethyl carbonate $CH_3CH_2OCOOCH_2CH_3$ it is 3 390 cal whilst in di-tert-butyl carbonate $(CH_3)_3COCOOC(CH_3)_3$ it is 2 147 cal; evidently branched groups next to the carbonate exert a powerful shielding effect. Assuming that in the diphenyl carbonate some of the lowering may be due to an electronic interaction between the phenyl and carbonate groups (merely on the basis of shielding, the value for the carbonate group in between two tert-butyl groups would be expected to be lower than that for the group interposed between two phenyls) an appropriate value in the tetramethyl cyclobutane polycarbonate would therefore be about 1 500 calories. The molar cohesion energy per chemical unit is thus 4 864 calories;

each chemical unit consists of four chain units thus

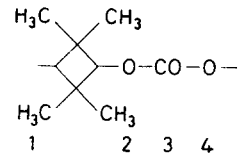

so that the cohesion energy per chain unit is 1 216 calories. According to Figure 3 of Bunn's paper 1 210 calories per chain unit would suggest a melting point for a symmetrical, streamlined aromatic polyester of about 150°C. The restricted rotation in the C—O links of the carbonate group evidently raises the melting point considerably, in fact, if the chain is considered to be composed of only two rigid units

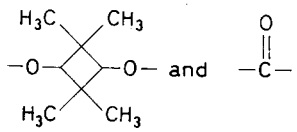

the average cohesion energy per chain unit (2 432 calories) predicts a melting point of 290° to 350°C which is nearer, but still lower than, the extrapolated value for the *trans-* form.

The lower melting point of the *cis-* form can be explained along similar lines to those for other *cis-/trans-* isomers[5]. In the *cis-* form, the 'flexible' bonds are inclined at a large angle (about 114° in the —AAAA— form) whereas in the *trans-* form the angle is much less (about 44° in either —XXXX— or —YYYY— forms). Thus similar degrees of rotation in each case will cause a much greater distortion in the *cis-* form than in the *trans-* leading to a lower melting point for the *cis-* form. The difference in melting point is, nevertheless, rather greater than would be expected for the above explanation alone.

The melting behaviour of the copolymers

The unexpected presence of good crystallinity throughout the whole range of compositions has already been referred to; the melting points also perform an unexpected trend for random copolymerization, where a minimum in melting point (or no melting point at all in the case of an amorphous composition) would be expected in the region of 50 per cent molar composition from the Flory theory[6]. Block copolymerization is ruled out, as in that case two melting points would be expected, lying near that of the pure *cis-* and pure *trans-* forms respectively. The nearly linear relationship of melting point with composition thus suggests mixed crystal formation, an interpretation confirmed by the X-ray examination. The initial drop in melting point at low *trans-* form concentrations coincides with a lowered α form crystallinity and these facts together suggest that distortions of the *cis-* crystal lattice occur in this region rather than mixed crystal formation. which is favoured at proportions greater than 20 per cent *trans-*; an increase in the *trans-* content of the mixed crystals is accompanied by an increase in

melting points. Two phases were observed at 50 and 61 per cent *trans*- but the high melting (high *trans*-) phase was present in each case only as a minor constituent so that the composition of the lower melting phase will be little different from the average value determined. No explanation can at present be advanced for the apparently low melting point of the 49 per cent *trans*-, 51 per cent *cis*- sample.

Part III of this study will be published later and will deal with the dynamic mechanical properties of these copolymers.

Thanks are due to Miss J. S. Loxley and Miss J. Bradshaw who carried out the experimental part of the X-ray work and the melting point determinations respectively.

I.C.I. Ltd, Plastics Division,
Welwyn Garden City, Herts.

(*Received January 1963*)

REFERENCES

[1] GAWLAK, Miss M. and ROSE, J. B. *Polymer, Lond.* 1963, **4,** 515
[2] GAWLAK, Miss M., PALMER, R. P., ROSE, J. B., SANDIFORD, D. J. H. and TURNER JONES, Miss A. *Chem. & Ind.* **1962,** 1148
[3] BOYE, C. A. *J. Polym. Sci.* 1961, **55,** 275
[4] OWEN, T. B. and HOWARD, J. L. *Acta cryst., Camb.* 1951, **4,** 172
[5] BUNN, C. W. *J. Polym. Sci.* 1955, **16,** 323
[6] FLORY, P. J. *J. chem. Phys.* 1949, **17,** 223

Book Reviews

Impact Phenomena in Textiles

W. JAMES LYONS

M.I.T. Press: Cambridge, Mass., 1963. (xi+180 pp.; 6¼ in. by 9½ in.), 37*s* or $5.00

THIS book would be more correctly titled, the Measurement of Impact Phenomena in Textiles. It deals mostly with measurements made by laboratory simulation of the impact phenomena under study. The book is divided into seven chapters; the first introduces the topic, the second gives an outline of the mechanical properties of real materials and the third describes methods and equipment for laboratory and other testing. A short, fourth chapter discusses theories of impact processes in yarns and fabrics and the next chapter digresses to discuss related dynamic elastic properties. The sixth chapter is concerned with the results of tests and the short final chapter discusses future possibilities. There are 119 references extending to 1962. The book has been well illustrated with both half-tone and line drawings.

It is difficult to decide at which kind of reader this book is directed. It gives an excellent account of measuring techniques, but includes many pages of very elementary elastic and viscoelastic theory that must already be known to a reader seeking knowledge of such sophisticated techniques. The reader needing the elementary theories will not find descriptions of impact phenomena. For anyone wishing to make measurements in this field, and any organization that may be faced with the need to consider impact measurements in textiles, this book is a valuable source and will rapidly earn its cost by a reduction in the time spent in searching the literature.

The reviewer notes with pleasure that the author often quotes directly from the work of others. In this way the 'flavour' of the experimental attack is recorded and there is less chance of differences arising through re-interpretation. However, there is the disadvantage that the account of the experimental work takes on the character of a list and ceases to be critical.

The repetition that arises from the long introductory chapter is irritating. This chaper is largely devoted to a condensed version of subsequent material so that, having started with the introduction, the reader is subsequently going over the same ground. On page 13 in this chapter the author has written, 'Compressive and shearing stresses play minor roles in the mechanics of textiles'. No justification for this statement is attempted; the reviewer believes it to be quite unjustifiable, but it has enabled the author to exclude any further reference to non-tensile forces. Chapter 5 on related dynamic properties is the weakest as it is not clear how related these properties are and in any case, much of the material quoted is extremely dated. Reference to polyester fibre as 'fiber V' and acrylic fibre as 'fibre A' is an unnecessary confusion arising from the early date of the results. Indeed, throughout the text, very little is done to help the reader by unifying the names of the materials tested. The U.S. Federal Code for generic names of textile fibres, whatever commercial failings it may have, has simplified the task of authors in providing simple definite terms and these could always be used with advantage. Instead we find, for example, polyester fibre called on different pages: Fiber V, Dacron, Terylene and Fortrel without any indication that these are all commercial names

for polyester fibre. The English reader is warned that the book uses an American definition of *tenacity*, i.e. load per unit linear density, not the *breaking* load per unit linear density. The reviewer deplores the introduction on page 53 of units of inches and grains.

In the interests of economy, the book has been produced from typescript but even so is priced at 37*s* in the U.K., $5.00 in the U.S.A. Pages of print of this type produce more reading strain than those of conventional types. It would help if, in editing such typescript, shorter paragraphs were made to break up the blocks of print.

K. W. HILLIER

The Physical Chemistry of Paints

P. M. FISK

Leonard Hill: London, 1963. (ix+133 pp.; 5 in. by 7½ in.), 25*s*

IN 1961 Dr Fisk published a successful *Advanced Paint Chemistry* and has followed this with the volume under review.

In the course of his small book the author deals with (among other topics) crystallography, particle size distribution, various properties of pure liquids, solutions and dispersions, surface activity, catalysis, rheology, chemical kinetics and the theory of acids and bases, equilibria, metallic corrosion, and 'light and colour'.

Each of these subjects could be (and indeed is) the subject of a large monograph, and obviously extreme compression has been practised, so that the reader tends to get a series of statements or a 'glossary of terms'—the phase rule, for example, gets about one page.

The text is generally very clearly and lucidly written, but the reviewer must doubt if this superficial treatment of so wide a field in so small a compass is of great value even to the audience of young students of paint technology to whom it is addressed.

The treatment, within the limits imposed by the author, is commonly correct enough. Two exceptions may be noted. The discussion on the metal catalysis of autoxidation on pages 61–62 is simplified much too far, and the mechanism of Fig. 45 is far from proven in such systems as occur in paint technology, the relevance of the work of Bawn on this mechanism being doubtful.

The section on the solution of polymers (page 45) seems unfortunate because it conceals the fact that by an increase in entropy a polymer can dissolve in a solvent in spite of an unfavourable (endothermic) heat of mixing. Notice of this could have led the author into a discussion of the role of entropy in the mechanical behaviour of polymers, a subject of great importance.

Lastly, although this book is called the *Physical Chemistry of Paints*, paint problems are not really discussed, and we have in effect a brief sketch of physical chemistry, a sort of Glasstone in miniature, and as said before the need for this seems doubtful.

Scientists (of whatever age and status) working in the paint industry are basically concerned with polymer science, especially in those aspects of it which impinge on physics and physical chemistry. The great need is to take a classic like Flory's *Principles of Polymer Chemistry* and show in clear and simple ways how these principles may be applied to paint technology—as they can be, and commonly are not.

for polyester fibre. The English reader is warned that the book uses an American definition of *tenacity*, i.e. load per unit linear density, not the *breaking* load per unit linear density. The reviewer deplores the introduction on page 53 of units of inches and grains.

In the interests of economy, the book has been produced from typescript but even so is priced at 37*s* in the U.K., $5.00 in the U.S.A. Pages of print of this type produce more reading strain than those of conventional types. It would help if, in editing such typescript, shorter paragraphs were made to break up the blocks of print.

K. W. HILLIER

The Physical Chemistry of Paints

P. M. FISK

Leonard Hill: London, 1963. (ix+133 pp.; 5 in. by 7½ in.), 25*s*

IN 1961 Dr Fisk published a successful *Advanced Paint Chemistry* and has followed this with the volume under review.

In the course of his small book the author deals with (among other topics) crystallography, particle size distribution, various properties of pure liquids, solutions and dispersions, surface activity, catalysis, rheology, chemical kinetics and the theory of acids and bases, equilibria, metallic corrosion, and 'light and colour'.

Each of these subjects could be (and indeed is) the subject of a large monograph, and obviously extreme compression has been practised, so that the reader tends to get a series of statements or a 'glossary of terms'—the phase rule, for example, gets about one page.

The text is generally very clearly and lucidly written, but the reviewer must doubt if this superficial treatment of so wide a field in so small a compass is of great value even to the audience of young students of paint technology to whom it is addressed.

The treatment, within the limits imposed by the author, is commonly correct enough. Two exceptions may be noted. The discussion on the metal catalysis of autoxidation on pages 61–62 is simplified much too far, and the mechanism of Fig. 45 is far from proven in such systems as occur in paint technology, the relevance of the work of Bawn on this mechanism being doubtful.

The section on the solution of polymers (page 45) seems unfortunate because it conceals the fact that by an increase in entropy a polymer can dissolve in a solvent in spite of an unfavourable (endothermic) heat of mixing. Notice of this could have led the author into a discussion of the role of entropy in the mechanical behaviour of polymers, a subject of great importance.

Lastly, although this book is called the *Physical Chemistry of Paints*, paint problems are not really discussed, and we have in effect a brief sketch of physical chemistry, a sort of Glasstone in miniature, and as said before the need for this seems doubtful.

Scientists (of whatever age and status) working in the paint industry are basically concerned with polymer science, especially in those aspects of it which impinge on physics and physical chemistry. The great need is to take a classic like Flory's *Principles of Polymer Chemistry* and show in clear and simple ways how these principles may be applied to paint technology—as they can be, and commonly are not.

Dr Fisk has considerable gifts of clarification and exposition, and if these were applied to such a project as that indicated, a more worthwhile book would emerge than that under review, and one closer in subject matter to its title.

H. S. LILLEY

Surface Chemistry. Theory and Industrial Applications
ACS Monograph 153

LLOYD I. OSIPOW

Reinhold: New York, 1962. (xiii+473 pp.; 6¼ in. by 9¼ in.), 108*s* or $13.50

DURING the last decade, some five or six authoritative works have been published on the general field of surface chemistry and it was an act of some daring to add to this list. The present volume, one of the American Chemical Society Monograph Series, 'is not intended as an exhaustive treatment of all aspects of surface chemistry, but is limited to those industrial applications in which the author has a significant experience'. Undoubtedly this volume is much less fundamental than others already published, but, even so, more than half the book (some 290 pages) concerns itself with fundamental aspects, as is shown by the relevant chapter headings: Surface Energy and Surface Tension, Physical Adsorption by Solids, Chemisorption, Electrical Phenomena at Interfaces, Insoluble Monolayers at Liquid Interfaces, Soluble Monolayers at Liquid Interfaces, Surfactants, Properties of Solutions containing Surfactants, Wetting. To cover this broad field, the author could not always start from first principles, nor develop his subject logically, so that the theoretical part of the book does not provide a coordinated account of fundamental principles. The normal reader will have to turn frequently to other works. This is particularly true of the treatment of Electrical Phenomena, which in addition demonstrates a very 'patchy' coverage. A later chapter on emulsions contains material which might with advantage have been included under Electrical Phenomena, and some (on potential energy curves) which duplicates that already treated there. The longer chapters on Properties of Solutions of Surfactants and Wetting are much freer from this type of criticism.

Chief Applications covered in the latter third of the book are Emulsions, Foams, and Detergency, the latter in particular being of especial value. Shorter chapters on Ore Flotation, Lubrication and Corrosion Inhibition indicate fields where surface chemistry is becoming increasingly important. In these latter chapters the author has gone to considerable trouble to include data on recently developed materials.

In the main, the book is well produced, though quite a few typographical errors remain, and more attention should have been given to the labelling of diagrams and to their legends, particularly where these have been adapted from other works. Occasionally the symbol appearing in the text differs from that in a diagram [e.g. page 301, n (Fig. 11·3)$\equiv m$ (text); pages 305 to 307 f (text)$\equiv \tau$ (Figs. 11·9 to 11·12)]. Some undesirable lapses in terminology occur; thus the use of the word 'emersion' (page 37 and elsewhere) for the removal of a body from a liquid, whilst technically correct, is most unwise in view of similarity with 'immersion' and to speak of a non-ionic surfactant as a 'nonionic' is somewhat unexpected in a book of this type.

As an approach to the understanding of the applications of surface chemistry the book will prove useful, but the high price will undoubtedly restrict its sale.

P. JOHNSON

Dr Fisk has considerable gifts of clarification and exposition, and if these were applied to such a project as that indicated, a more worthwhile book would emerge than that under review, and one closer in subject matter to its title.

H. S. LILLEY

Surface Chemistry. Theory and Industrial Applications
ACS Monograph 153

LLOYD I. OSIPOW

Reinhold: New York, 1962. (xiii+473 pp.; 6¼ in. by 9¼ in.), 108*s* or $13.50

DURING the last decade, some five or six authoritative works have been published on the general field of surface chemistry and it was an act of some daring to add to this list. The present volume, one of the American Chemical Society Monograph Series, 'is not intended as an exhaustive treatment of all aspects of surface chemistry, but is limited to those industrial applications in which the author has a significant experience'. Undoubtedly this volume is much less fundamental than others already published, but, even so, more than half the book (some 290 pages) concerns itself with fundamental aspects, as is shown by the relevant chapter headings: Surface Energy and Surface Tension, Physical Adsorption by Solids, Chemisorption, Electrical Phenomena at Interfaces, Insoluble Monolayers at Liquid Interfaces, Soluble Monolayers at Liquid Interfaces, Surfactants, Properties of Solutions containing Surfactants, Wetting. To cover this broad field, the author could not always start from first principles, nor develop his subject logically, so that the theoretical part of the book does not provide a coordinated account of fundamental principles. The normal reader will have to turn frequently to other works. This is particularly true of the treatment of Electrical Phenomena, which in addition demonstrates a very 'patchy' coverage. A later chapter on emulsions contains material which might with advantage have been included under Electrical Phenomena, and some (on potential energy curves) which duplicates that already treated there. The longer chapters on Properties of Solutions of Surfactants and Wetting are much freer from this type of criticism.

Chief Applications covered in the latter third of the book are Emulsions, Foams, and Detergency, the latter in particular being of especial value. Shorter chapters on Ore Flotation, Lubrication and Corrosion Inhibition indicate fields where surface chemistry is becoming increasingly important. In these latter chapters the author has gone to considerable trouble to include data on recently developed materials.

In the main, the book is well produced, though quite a few typographical errors remain, and more attention should have been given to the labelling of diagrams and to their legends, particularly where these have been adapted from other works. Occasionally the symbol appearing in the text differs from that in a diagram [e.g. page 301, n (Fig. 11·3)$\equiv m$ (text); pages 305 to 307 f (text)$\equiv \tau$ (Figs. 11·9 to 11·12)]. Some undesirable lapses in terminology occur; thus the use of the word 'emersion' (page 37 and elsewhere) for the removal of a body from a liquid, whilst technically correct, is most unwise in view of similarity with 'immersion' and to speak of a non-ionic surfactant as a 'nonionic' is somewhat unexpected in a book of this type.

As an approach to the understanding of the applications of surface chemistry the book will prove useful, but the high price will undoubtedly restrict its sale.

P. JOHNSON

Chlorine, Its Manufacture, Properties and Uses
ACS Monograph 154

Edited by JAMES S. SCONCE

Reinhold: New York, 1963. (x + 901 pp.; 6¼ in. by 9¼ in.), 200*s* or $25.00

CHLORINE has been known and its elementary character recognized for something less than 200 years. In that short span, however, the position has been reached where, in the words of the book under review, 'chlorine probably has more diverse uses than any other known chemical'. This is no extravagant claim and indeed is supported by the annual production of over five million tons in the U.S.A. and about a tenth of that amount in the U.K. Few chemists can fail to come into contact with the element or its compounds in their daily work.

Most chemists will be familiar with the series of Monographs sponsored by the American Chemical Society and the appearance of this addition to the series cannot fail to be generally welcomed. The book is a cooperative venture under the editorship of James S. Sconce who is to be congratulated on having secured the services of a panel of authors including many whose names, as well as those of the companies for whom they work, will be well known and recognized as authorities in their fields by those with any familiarity with chlorine chemistry.

It is perhaps not inappropriate that this is a very American book. Those more familiar with the picture in the Old World or in Great Britain in particular will note some interesting similarities and differences in the course of developments in production, handling and uses on the two sides of the Atlantic. The value of this broad review would, however, have been increased had more regard been paid to the developments outside the U.S.A. The early chapter on 'Production and Use Patterns' will be of universal interest, typifying as it does the growth of chemical technology in the twentieth century. By using statistics going only to to 1960, however, the impression is created that the production of ethylene oxide is still the principal use of chlorine in chemical manufacture. On the contrary the rapid development of the direct process for ethylene oxide is one of the best examples of the way in which chlorine is being ousted from its place as a reagent for the introduction of reactive groups into hydrocarbons.

Chlorine production is dealt with in an authoritative, and comprehensive manner presenting an account of modern theory and practice in the field which has not been better assembled elsewhere in the chemical literature. It is gratifying to see due prominence given to hydrochloric acid oxidation processes, for the problem of utilization of byproduct hydrochloric acid is one which must engage the attention of all who use chlorine in organic substitution reactions.

Readers of *Polymer* may, however, be expected to find greater interest in those chapters devoted to organic chlorine derivatives. Here, despite some unevenness of treatment difficult to avoid in an omnibus work of this kind, will be found assembled much useful information, not the least valuable item being the excellent bibliographies accompanying many of the articles. Like most such compilations alas these are some two years out of date due to the time-lag between preparation of an article and its publication. In the short time the book has been on the reviewer's desk he has already found it a most useful starting point for enquiries in the organic chemical field and a useful work of reference to aid his failing memory!

It is a pity, therefore, that the book has been needlessly expanded by the inclusion of matter whose right to a place in a work with this title seems

at least doubtful. In this category one includes large parts of the chapter on 'Ethylene and Propylene Oxides and Glycols' which deals in large measure with chlorine-free compounds, and much of those on 'Chlorinated Benzenes' and 'Benzene Hexachloride'. The chapter on fluorochemicals seems also an unjustifiable extension of the book particularly as this topic has been dealt with in an earlier A.C.S. Monograph. Unfortunately, in this category too must be placed the two chapters which would appear likely to be of most interest to readers of this journal, those on 'Vinyl Chloride' and 'Vinylidene Chloride'. Who, seeking information on polymer chemistry, will look in this book when so many specialist works are already available? The information in these chapters is accurate but in the nature of things, highly condensed—in fact it does not in either case differ greatly from that given in Kirk Othmer. It would have been more appropriate in the present volume to have dealt at greater length with monomer processes to the exclusion of much of the matter on polymerization and polymer processing.

Noteworthy omissions from the book which would have had some interest for polymer chemists are references to the chloroparaffins, to chlorendic acid and to methyl chloroform. The former may in part be excused on the gounds that the chloroparaffins have made less headway in the plasticizer and oil additive fields in America than they have in Europe and, more particularly, in the U.K. The other two materials are, however, fairly recent American innovations and might well have been expected to find a place in the book.

These strictures must, however, not be allowed to detract unduly from a great deal which is good. The book is commended to all chemists as at one and the same time illuminating the magnitude and importance of chlorine chemistry and providing a most valuable work of reference in this wide and still developing field.

J. H. BROWN

Diffusion and Membrane Technology

ACS Monograph 156

S. B. TUWINER

Reinhold: New York, 1963. (ix + 421 pp.; 6¼ in. by 9¼ in.), 96*s* or $12.00

THE versatility of synthetic high polymeric materials has contributed to an expanding industrial use of membranes and the publication of an ACS monograph on membrane science and technology is opportune. An understanding of the mechanism of membrane action or of the design of apparatus and plant using membrane techniques involves some familiarity with the principles of diffusion and often a knowledge of the properties of electrolytes. The author has, therefore, after a short historical introduction, used over a quarter of this monograph to present the fundamentals of diffusion in liquids and the behaviour of electrolytes. Not all of the matter in the section is relevant to the main theme of membrane structure and action, but the general reader will find much to interest and inform him in this concise treatment which is supported by over 100 references.

Chapters on membrane thermodynamics, general properties of membranes and the diffusion of ions in membranes are followed by two informative chapters on cellulosic and synthetic membranes. The main sections of

at least doubtful. In this category one includes large parts of the chapter on 'Ethylene and Propylene Oxides and Glycols' which deals in large measure with chlorine-free compounds, and much of those on 'Chlorinated Benzenes' and 'Benzene Hexachloride'. The chapter on fluorochemicals seems also an unjustifiable extension of the book particularly as this topic has been dealt with in an earlier A.C.S. Monograph. Unfortunately, in this category too must be placed the two chapters which would appear likely to be of most interest to readers of this journal, those on 'Vinyl Chloride' and 'Vinylidene Chloride'. Who, seeking information on polymer chemistry, will look in this book when so many specialist works are already available? The information in these chapters is accurate but in the nature of things, highly condensed—in fact it does not in either case differ greatly from that given in Kirk Othmer. It would have been more appropriate in the present volume to have dealt at greater length with monomer processes to the exclusion of much of the matter on polymerization and polymer processing.

Noteworthy omissions from the book which would have had some interest for polymer chemists are references to the chloroparaffins, to chlorendic acid and to methyl chloroform. The former may in part be excused on the gounds that the chloroparaffins have made less headway in the plasticizer and oil additive fields in America than they have in Europe and, more particularly, in the U.K. The other two materials are, however, fairly recent American innovations and might well have been expected to find a place in the book.

These strictures must, however, not be allowed to detract unduly from a great deal which is good. The book is commended to all chemists as at one and the same time illuminating the magnitude and importance of chlorine chemistry and providing a most valuable work of reference in this wide and still developing field.

J. H. BROWN

Diffusion and Membrane Technology

ACS Monograph 156

S. B. TUWINER

Reinhold: New York, 1963. (ix + 421 pp.; 6¼ in. by 9¼ in.), 96*s* or $12.00

THE versatility of synthetic high polymeric materials has contributed to an expanding industrial use of membranes and the publication of an ACS monograph on membrane science and technology is opportune. An understanding of the mechanism of membrane action or of the design of apparatus and plant using membrane techniques involves some familiarity with the principles of diffusion and often a knowledge of the properties of electrolytes. The author has, therefore, after a short historical introduction, used over a quarter of this monograph to present the fundamentals of diffusion in liquids and the behaviour of electrolytes. Not all of the matter in the section is relevant to the main theme of membrane structure and action, but the general reader will find much to interest and inform him in this concise treatment which is supported by over 100 references.

Chapters on membrane thermodynamics, general properties of membranes and the diffusion of ions in membranes are followed by two informative chapters on cellulosic and synthetic membranes. The main sections of

the work, however, are concerned with the use of membranes in dialysis and electro-dialysis. Here details of plant design and economics are given. From a descriptive point of view these chapters are of considerable interest to the non-specialist as well as to the chemical engineer. Other aspects of membrane science are dealt with in a rather condensed manner. It is a pity that a chapter on the permeation of membranes by gases and vapours is too short to mention the interesting phenomena of the sorption and diffusion of vapours in polymers below the glass temperature. Ultrafiltration, reverse osmosis, liquid permeation separation and fuel cells are briefly treated in another chapter. The inclusion of the large subject of biological membranes is a little surprising in a work dealing essentially with membrane technology and would more advantageously form the basis of a separate work. This section is perhaps most useful as an index to the hundred or so references quoted.

A collection of diffusion coefficients and other data are given in an appendix but the references given at the foot of pages throughout the book are not collected together and in the absence of this collection the omission of an author index is regrettable. A few errors like the upside down printing of Fig. 13.1 do not detract appreciably from the quality of the book which forms a useful addition to the ACS series of monographs.

G. S. PARK

Note

The Polymerization and Ring Strain of Enantholactam

THE kinetics of the hydrolytic polymerization of enantholactam have been followed by Skuratov and co-workers[1] by the method of differential colorimetry. These workers reported that enantholactam polymerizes more rapidly than caprolactam under the same conditions, and attributed this result to greater strain in the 8-membered ring of enantholactam. The faster polymerization of enantholactam has not been confirmed in this work, and the evidence for a similar or rather less ring strain in enantholactam than in caprolactam is discussed.

Enantholactam synthesized from cycloheptanone[2] was purified by low temperature recrystallization from hexane. Commercial caprolactam was used without further purification. Commercial capryllactam was recrystallized from cyclohexane. All the lactams were dried by distillation under reduced pressure of nitrogen before use. The polymerizations were carried out in sealed tubes under nitrogen and stopped when required by plunging the tubes into cold water. The reaction products were weighed and then extracted to constant weight with a 50-fold excess of boiling water. The weight of water insoluble material formed has been shown to be a good

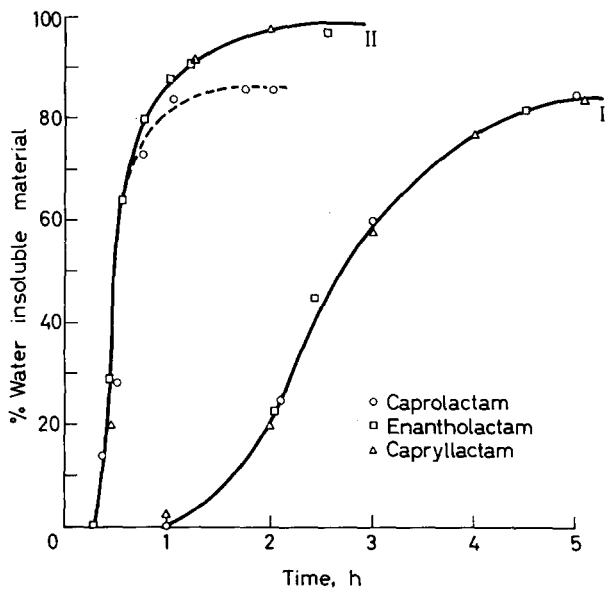

Figure 1—Water initiated polymerization of caprolactam, enantholactam and capryllactam. Curve I: temp. 230°C, 2 per cent by wt water; II: temp. 260°C, 4 per cent by wt water

approximation for the amount of polymer formed[3]. The polymerization procedure gave results reproducible to ± 3 per cent.

Figure 1 shows the results obtained at 230°C using 2 per cent by weight of water as the initiator and at 260° using 4 per cent by weight of water. It is apparent that all three lactams polymerized at the same rate up to about 70 per cent conversion. At this point the polymerization of caprolactam is slowed down as the depropagation reaction becomes increasingly important, and eventually equilibrium is established between monomer and polymer. Enantholactam and capryllactam polymerize to almost complete conversion and the depolymerization reaction is evidently insignificant for these lactams. Allowing for the effect of the depolymerization of poly caproamide the relative rates of propagation are:

$$\text{Caprolactam} > \text{Enantholactam} = \text{Capryllactam}$$

Figure 2 shows the variation in end-group concentration during the water initiated polymerization of enantholactam. The maximum in the end-group concentration corresponds approximately with the maximum rate of polymerization. The amine and carboxyl end groups on the polymers were balanced throughout the polymerization.

When 6.6 nylon salt was used as the initiator, the polymerizations did not show an induction period. The relative rates of polymerization of the lactams were the same as those found using water as the initiator.

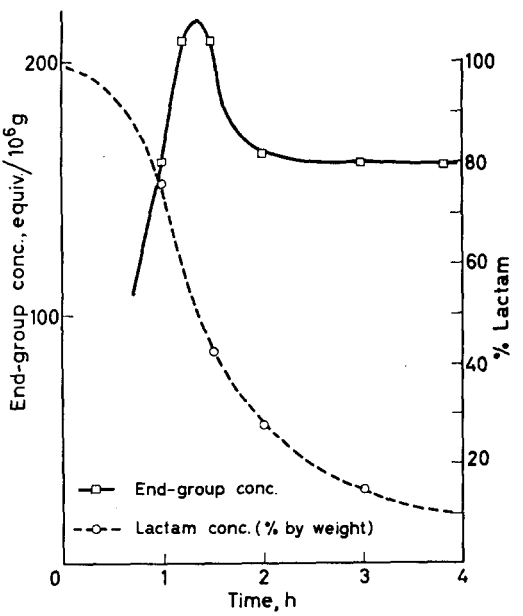

Figure 2—Variation of end-group concentration during polymerization of enantholactam by 4% (wt) of water at 230°C

DISCUSSION

The polymerization of enantholactam shows the same kinetic features, and end group behaviour, as the polymerization of caprolactam[4]. The results can be explained qualitatively in terms of the mechanism proposed by Hermans[4] for the hydrolytic polymerization of caprolactam.

Initiation

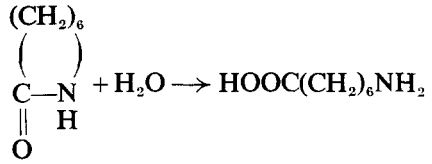

Polyaddition

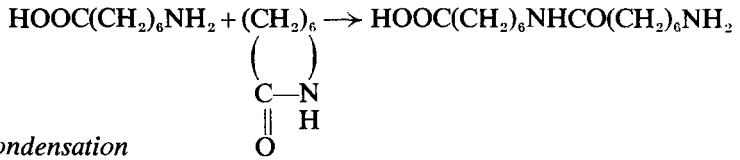

Polycondensation

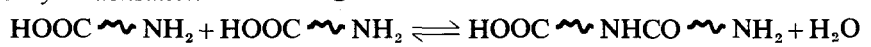

Initiation takes place by hydrolysis of the lactam. This reaction is end group catalysed, thus accounting for the autocatalytic nature of the polymerization. When 6.6 nylon salt is used as the initiator end groups are already present to catalyse the hydrolysis and no induction period is observed.

There are two propagation mechanisms: direct reaction of the lactam at the end groups and polycondensation. *Figure 2* shows that the end group concentration falls after reaching its maximum and this must be a result of the polycondensation reaction. However, Hermans[4] has shown that with caprolactam the bulk of the polymerization can be accounted for by an end group catalysed polyaddition mechanism. Studies on linear amides[5] indicate that this addition takes place at the amine end groups and is catalysed by carboxyl groups. With enantholactam and capryllactam the reverse of the initiation and polyaddition reactions need not be considered.

The polymerization involves opening the lactam ring and thus the rate of polymerization would be expected to reflect the strain in the ring. The relative rates of polymerization observed imply that there is rather less strain in the 8- and 9-membered rings than in the 7-membered ring of caprolactam. Dipole moment and infra-red studies of the lactams[6] show that the amide group has the *cis* configuration in caprolactam and enantholactam. Capryllactam contains a small proportion of *trans* configuration and the higher lactams have a completely *trans* configuration. The strain in these rings is due to the

cis *trans*

crowding of the hydrogen atoms inside the ring[7] and is sufficiently relieved in the 10-membered ring to allow the attainment of the more stable *trans* configuration found in linear amides. Thus this evidence shows that the ring strain decreases slightly in the 8- and 9-membered rings and then there is a marked fall in strain with rings of 10 members or more. This conclusion is supported by the fact that lauryl lactam (13-membered ring) polymerizes more slowly than capryllactam[8].

The difference in ring strain between enantholactam and capryllactam can also be estimated from the heats of combustion:

$$\Delta H_{\text{Enltm}} - \Delta H_{\text{Cpltm}} = \Delta H_{\text{CH}_2} + \Delta H_{\text{strain}}$$

where ΔH_{CH_2} denotes heat of combustion increment for a methylene group in a linear hydrocarbon. The difference in the heats of combustion found by Skuratov *et al.*[9]: 157·2 kcal mole^{-1} at 75°C, corresponds very closely to the heat of combustion increment for a methylene group (156·9 kcal at 75°C). Thus all the available evidence is consistent with a similar or very slightly reduced strain in enantholactam and capryllactam compared with caprolactam.

The very low equilibrium monomer contents of enantholactam and capryllactam are a result of the difficulty of forming 8- and 9-membered rings. This can be attributed to a probability factor[10]; as the chain length of the ω amino acid is increased the chances of the end groups being in a suitable configuration for intramolecular reaction are reduced.

The author wishes to thank British Nylon Spinners Ltd, for permission to publish and Mr A. Williams for practical assistance.

R. C. P. CUBBON

Research Department,
British Nylon Spinners Ltd,
Pontypool, Mon.

(*Received October 1963*)

REFERENCES

[1] SKURATOV, S. M. *et al. Dokl. Akad. Nauk S.S.S.R.* 1954, **95,** 591
[2] COFFMAN, D. D. *et al. J. Polym. Sci.* 1948, **3,** 85
[3] KRUISSIUK, CH.A., VAN DER WANT, G. M. and STAVERMAN, A. J. *J. Polym. Sci.* 1958, **30,** 67
[4] HERMANS, P. H., HEIKENS, D. and VAN VELDEN, P. F. *J. Polym. Sci.* 1958, **30,** 87
[5] WYNESS, K. G. *Makromol. Chem.* 1960, **38,** 189
[6] HUISGEN, R. *Angew. Chem.* 1957, **69,** 341
[7] HALL, Jr, H. K. *J. Amer. chem. Soc.* 1958, **80,** 6428
[8] DACHS, K. and SCHWARTZ, E. *Angew. Chem.* (Internatl Ed.), 1962, **1,** 430
[9] SKURATOV, S. M. *et al. Dokl. Akad. Nauk S.S.S.R.* 1955, **102,** 105
[10] RUZICKA, L. *Chem. & Ind.* **1935,** 2

Contributions to Polymer

Papers accepted for future issues of POLYMER include the following:

Dynamic Birefringence of Polymethylacrylate—B. E. READ

Solution and Bulk Properties of Branched Polyvinyl Acetates, II, III—G. C. BERRY, R. G. CRAIG, L. M. HOBBS and V. C. LONG

The Temperature Dependence of Extensional Creep in Polyethylene Terephthalate—I. M. WARD

The Radiation Chemistry of Polymethacrylic Acid, Polyacrylic Acid and Their Esters; An Electron Spin Resonance Study—M. G. ORMEROD and A. CHARLESBY

Crystallinity and Disorder Parameters in Nylon 6 and Nylon 7—W. RULAND

Rate Dependence of the Strain Birefringence and Ductility of Polyethylene—S. STRELLA and S. NEWMAN

A Thermodynamic Description of the Defect Solid State of Linear High Polymers—B. WUNDERLICH

Graft Copolymerization Initiated by Poly-p-lithiostyrene—M. B. HUGLIN

Structure and Properties of Crazes in Polycarbonate and Other Glassy Polymers—R. P. KAMBOUR

The Crystallization of Polymethylene Copolymers: Morphology—J. B. JACKSON and P. J. FLORY

The Crystallization of Polyethylene II—W. BANKS, J. N. HAY, A. SHARPLES and G. THOMSON

Description and Calibration of an Elasto-osmometer—H. J. M. A. MIERAS and W. PRINS

Resonance-induced Polymerizations—R. J. ORR

Polypropylene Oxide I—An Intrinsic Viscosity/Molecular Weight Relationship—G. ALLEN, C. BOOTH and M. N. JONES

Viscosity/Temperature Dependence for Polyisobutene Systems: The Effect of Molecular Weight Distribution—R. S. PORTER and J. F. JOHNSON

The Photolytic Decomposition of Poly-(n-butyl)methacrylate—J. R. MACCALLUM

Catalysts for the Low Temperature Polymerization of Ethylene—K. J. TAYLOR

The Effect of Tension and Annealing on the X-ray Diffraction Pattern of Drawn 6.6 Nylon—D. R. BERESFORD and H. BEVAN

Sequence Length Distribution and Entropy of Stereoregularity in Homopolymers of Finite Molecular Weight—A. M. NORTH and D. RICHARDSON

Orientation in Crystalline Polymers related to Deformation—Z. W. WILCHINSKY

Morphology of Polymer Crystals: Screw Dislocations in Polyethylene, Polymethyleneoxide and Polyethyleneoxide—W. J. BARNES and F. P. PRICE

Nuclear Spin-Lattice Relaxation in Polyacetaldehyde—T. M. CONNOR
The Copolymerization of Methylmethacrylate and Maleic Anhydride—A. M. NORTH and D. POSTLETHWAITE

CONTRIBUTIONS should be addressed to the Editors, *Polymer*, 4-5 Bell Yard, London, W.C.2.

Authors are solely responsible for the factual accuracy of their papers. All papers will be read by one or more referees, whose names will not normally be disclosed to authors. On acceptance for publication papers are subject to editorial amendment.

If any tables or illustrations have been published elsewhere, the editors must be informed so that they can obtain the necessary permission from the original publishers.

All communications should be expressed in clear and direct English, using the minimum number of words consistent with clarity. Papers in other languages can only be accepted in very exceptional circumstances.

A leaflet of instructions to contributors is available on application to the editorial office.

ANNOUNCEMENTS

POLYMER PHYSICS

A Meeting on Polymer Physics is to be held at the Royal Military College of Science, Shrivenham, on 1 to 3 April 1964 with a view to forming a Forum for Polymer Physics in Britain. The scientific programme will consist of half-day sessions on crystalline morphology, molecular structure, relaxation processes and visco-elasticity, and properties of solutions. Organizing committee:

G. ALLEN, Manchester
A. CHARLESBY, Shrivenham
A. KELLER, Bristol
I. M. WARD, Harrogate
D. H. WHIFFEN, Teddington

Further information may be obtained from Dr I. M. Ward, Research Department, I.C.I. Ltd, Fibres Division, Harrogate, Yorkshire.

PLASTICS AND POLYMER GROUP
SOCIETY OF CHEMICAL INDUSTRY
£50 GROUP PRIZE

The Plastics and Polymer Group has instituted an annual prize of £50 for the best paper submitted on any aspect of pure or applied polymer science. The competition is open to all British subjects under 30 years of age. Full details may be obtained from The Secretary, Plastics and Polymer Group, c/o Society of Chemical Industry, 14 Belgrave Square, London, S.W.1.

Classified Contents

Author Index

Author Index